Application of metabolomics to identify functional metabolic changes associated with *Haliotis midae* growth

Leonie Venter

orcid.org 0000-0003-0019-3722

Thesis submitted in fulfilment of the requirements for the degree *Doctor of Philosophy in Biochemistry* at the North-West University

Promoter:	Dr JZ Lindeque
Co-promoter:	Prof DT Loots
Assistant promoter:	Dr A Vosloo

Graduation May 2018

21834350

ABSTRACT

The South African abalone, “perlemoen” (as it is called locally) industry is largely based on farming with *Haliotis midae*, which has been commercially cultured in man-made shore-based systems with great success for the last 20 years. Due to the basic dynamics of abalone aquaculture being well-known, the high market value and the demand for this delicacy, this sector is commercially, the largest of all aquaculture sectors in SA. However, knowledge of abalone metabolism and the biochemical processes associated with abalone growth and development are lacking. Since maximising growth and health of abalone is the primary goal for optimising production and revenue on abalone farms, research on abalone metabolism could lead to a better understanding of their metabolic responses to specific perturbations and subsequently, to better growth. Metabolomics, one of the newest additions to the “omics” research technologies, aims to investigate the metabolism holistically, and is considered a powerful tool for new biomarker identification and better elucidation of the observed phenotypical changes associated with a perturbation.

Considering this, the effects of 1) functional and environmental hypoxia and 2) diet and abalone age as experienced within the standard farming environment, were investigated in *Haliotis midae* in this thesis. By analysing different tissue samples (adductor muscle, foot muscle, left gill, right gill, haemolymph and epipodial tissue), using a multiplatform (nuclear magnetic resonance spectroscopy, gas chromatography mass spectrometry and liquid chromatography mass spectrometry), standardised metabolomics approach, growth and metabolism of abalone could be elucidated. Univariate statistical methods were used to identify those features of significance, to which metabolite identifiers were assigned, based on well-defined identification guidelines, which were subsequently used in pathway analyses and for biological interpretation of perturbations in relation to growth of abalone.

The results show that functional and environmental hypoxia result in a metabolic imbalance in *H. midae*, with the resulting energy deficit being compensated for by phosphoarginine reserves. This initial response is later supplemented by anaerobic glycolysis, whereby glucose is converted to pyruvate, and then to lactate or opines, in order to replenish the dwindling nicotinamide adenine dinucleotides required as substrates for further adenosine triphosphate production. Furthermore, the metabolomics results also suggest that stressors such as hypoxia, causes abalone to redirect their energy utilisation towards those metabolic pathways essential to the survival of the animal, at the expense of growth. In contrast, the metabolomics analysis done on the adductor muscle samples of abalone, with comparatively good growth rates, showed that faster growing individuals utilise energy pathways and reserves (via elevated

insulin production) in such a way that they promote protein synthesis. Furthermore it is suggested that modified artificial abalone feed stimulates mitochondrial function, enabling juvenile abalone to catabolise proline for energy production, while in adult abalone, proline was utilised primarily towards improving energy production through ß-oxidation pathways.

From this metabolomics investigation, it becomes evident that abalone have well-developed metabolic mechanisms ensuring survival during periods of oxygen depletion, however, this does inhibit growth, and in the absence of such stress, the metabolism of abalone would favour protein synthesis. At this stage the reasons as to why some individuals utilise amino acid reserves more rapidly for protein synthesis, under the same growth conditions are still debatable. Furthermore, this study proves that metabolomics is an extremely valuable tool for investigating the altered metabolic processes related to growth in abalone, and hence, could be considered a valuable tool for the abalone aquaculture industry, for identifying biomarkers for growth and health monitoring.

KEYWORDS: Abalone; Aquaculture; Growth; *Haliotis midae*; Hypoxia; Metabolic response; Metabolism; Metabolomics.

ACKNOWLEDGEMENTS

A PhD is said to give you a fantastic set of transferable skills that you can take into pretty much any field imaginable. Amidst all of the skill transferring and imagining, a PhD quickly escalates into something very personal, infiltrating all aspects of your life. Nearing the end of it all, I feel extremely blessed to have had the opportunity to do something of this magnitude and even though I am still far from a biochemical expert, my personal learning curve exceeded all expectations, making this an exceptional journey; one that is now summarised in the pages that follow. This thesis is not only the result of my own hard work but also the by-product of a dedicated number of extraordinary individuals. The words “thank you” feels insignificant to truly express my gratitude, but as I will never be able to repay you, may my gratitude suffice.

To my long-suffering supervisor, **Zander**, thank you for your commitment to this study and for that matter, your commitment to my entire postgraduate study “career”. Your unrestricted supervising challenged me at times, but ensured that I am now worthy of this degree. Regardless of the situation, you always patiently assisted and kept faith in me, I wholeheartedly thank you. **Peet**, you have routinely gone beyond your call of duty for this study, so, thank you, thank you and thank you. I am beyond grateful for the time, effort and advise you invested in me personally, academically and more. I’m really going to miss your stories and the good old logic you bring to the party. I am especially thankful to you, **Andre**, for introducing me to this wonderful world of abalone and aquaculture. Your enthusiasm for all things life, new and “abaloney” just adds more value to our crazy ventures, thank you for taking a chance on this study and this student. **Prof Loots**, your work ethic and professional know-how is second to none. Thank you for making the tough calls when necessary and adding the extra bits and pieces to ensure the best possible outcomes. Your guidance added tremendous value to this study and is much appreciated.

Prof Mienie, your love and appreciation for metabolism is inspiring in itself. Prof, thank you for assisting with the formulation of concise results and the interpretation thereof, and also for tolerating my endless questions and freely sharing your wealth of knowledge. **Shayne**, the NMR sample prep and analyses were without a doubt some of the most enjoyable practical sessions. Thank you for enduring my chatting, and thank you for all of your assistance with regards to the NMR sections of this study. Thank you, **Mari**, for your timely efforts devoted to data analyses and explanations.

A special word of thanks to **HIK abalone farm**; to everyone from ground level to management, who assisted with sample collection, animal feeding, and making farm visits and the donation of animals possible, your assistance is highly appreciated. May your abalone always grow in the right direction! Thank you to all of the **sampling minions**, Andre, Sharon, Asanda, Siflo and Thabani, for providing camaraderie and assistance through countless abalone dissections.

To the staff and students at **Biochemistry**, thank you for all of your small efforts, repeated day in and day out, which accumulate to the harmony found in this department. I salute the **NWU** for creating a safe learning environment where students can flourish and dream. I also thank the **NWU postgraduate fund** for financial incentives and **Ms Valerie Viljoen** for the language editing of this thesis.

Lastly, to my **family** and **friends**, who still aren't exactly sure what an abalone is, I thank you for your unwavering support. Life doesn't stand still while completing a PhD and looking back, this task influenced you just as much as it did me (maybe even more so). Your endless love, understanding, prayers and motivation played a vital role throughout my years as PhD student. Thank you for making them memorable years. **Siblings** you mean the world to me, thanks for being a constant in all of the uncertainty that comes with this process, come what may, we can do anything! Above all, I give thanks to the **Lord**, for blessing me in abundance with talents, opportunities and truly amazing people. *"And we know that God causes everything to work together for the good of those who love God and are called according to His purpose for them."* – Romans 8:28

"I have learned that life rewards you when you live your dream. Go out and find your bliss."

– Jan Hendrik van der Westhuizen
South African Michelin-star chef

TABLE OF CONTENTS

LIST OF FIGURES

LIST OF TABLES

LIST OF ABBREVIATIONS

A:	
AA	Amino acid
ADP	Adenosine diphosphate
Ala	Alanine
AM	Adductor muscle
AMP	Adenosine monophosphate
AMPK	AMP-activated protein kinase
ANOVA	Analyses of variance
Arg	Arginine
Asp	Aspartate
ATP	Adenosine triphosphate
B:	
BCAA	Branched-chain amino acid
BSTFA	O-bis(trimethylsilyl)trifluoro acetamide
C:	
C0	L-carnitine
C2	Acetyl-L-carnitine
C3	Propionyl-L-carnitine
C4	Butyryl-L-carnitine
C5	Isovaleryl-L-carnitine
C6	Hexanoyl-L-carnitine
C8	Octanoyl-L-carnitine
C10	Decanoyl-L-carnitine
C12	Dodecanoyl-L-carnitine
C14	Tetradecanoyl-L-carnitine
C16	Hexadecanoyl-L-carnitine
C18	Octadecanoyl-L-carnitine
Ca^{2+}	Calcium
CCS	Collision cross section
CE	Capillary electrophoresis
CE	Collision energy
CHO	Carbohydrates
CID	Collision-induced dissociation
CO_2	Carbon dioxide
CoA	Coenzyme A
cox	Cytochrome *c* oxidase subunit
CV	Coefficient of variation
Cys	Cystine
D:	
D_2O	Deuterium oxide-based
DAFF	Department Agriculture Forestry Fisheries
DNA	Deoxyribonucleic acid
d-value	Practical significance
E:	
E	Epipodial tissue
e.g	Exempli gratia; for example
EH	Environmental hypoxia
EI	Electron impact
ESI	Electrospray ionisation
ETC	Electron transport chain
ETF	Electron transfer flavoprotein

F:	
F	Fragmentor
FA	Fatty acid
FA (22:6n3)	Docosahexaenoate
FA (20:5n3)	Eicosapentaenoate
FA (20:1)	Eicosenoate
FA (18:1.5n7)	Hexadecanoate
FA (18:0)	Octadecanoate
FA (18:4n3)	Octadecatetraenoate
FA (18:3n6)	Octadecatrienoate
FA (18:1n9)	Octadecenoate
FA (16:0)	Octadecynoate
FA (18:1n12)	Octadenoate
FA (18:4n3)	Otadecatetraenoate
FA (16:1)	Palmitoleate
FA (15:0)	Pentadecanoate
FA (14:0)	Tetradecanoate
$FADH_2$	Flavin adenine dinucleotide
FAME	Fatty acid methyl ester
FbF	Find by formula
FH	Functional hypoxia
Fig	Figure
FM	Foot muscle
FDR	False discovery rate
G:	
G-3-P	Glyceraldehyde-3-phosphate
GC	Gas chromatography
GC-MS	Gas chromatography mass spectrometry
GC-MSD	GC-mass spectrometry-detector
GC-TOF	GC-time of flight spectrometry
glog	Generalised logarithm
Glu	Glutamate
Gly	Glycine
GLYAT	Glycine N-acyltransferase
GTP	Guanosine triphosphate
H:	
H	Haemolymph
H^+	Hydrogen ion
H_2O	Water
H_2O_2	Hydrogen peroxide
HCl	Hydrogen chloride
HIF	Hypoxia-inducible factor
HILIC	Hydrophilic interaction liquid chromatography
His	Histidine
HP-921	Protonated hexakis phosphazine
I:	
i.e	Id est; that is
ID	Identification
Ile	Isoleucine
IMP	Inosine monophosphate
IS	Stable isotopes
ISO	International Organisation for Standardisation

K:	
KH_2PO_4	Potassium phosphate monobasic
KOH	Potassium hydroxide
L:	
LC	Liquid chromatography
LC-MS/MS	LC tandem mass spectrometry
LC-QTOF	LC quadrupole time of flight mass spectrometry
Leu	Leucine
LG	Left gill
Lys	Lysine
M:	
Met	Methionine
MFE	Molecular feature extraction
MPP	Mass Profiler Professional
MRM	Multiple reaction monitoring
MS	Mass spectrometry
MS/MS	Tandem-mass spectrometry
MSTFA	N-methyl-N-(trimethylsilyl) trifluoroacetamide
MSTUS	Mass spectrometry total useful signal
MTOR	Mechanistic target of rapamycin
N:	
n	Sample size
NaBH3CN	Sodium cyanohydridborate
NAD^+	Nicotinamide adenine dinucleotide (oxidised)
NADH	Nicotinamide adenine dinucleotide (reduced)
NADP	Nicotinamide adenine dinucleotide phosphate
NaN_3	Sodium azide
NaOH	Sodium hydroxide
NH_3	Ammonia
NMR	Nuclear magnetic resonance
NO	Nitric oxide
NWU	North-West University
O:	
O	Other
O_2	Oxygen
O_2^-	Superoxide anion
OXPHOS	Oxidative phosphorylation

P:	
P5C	Pyrroline-5-carboxylate
PCA	Principle component analysis
PEP	Phosphoenolpyruvate
pH	Potential of hydrogen
Phe	Phenylalanine
PLS-DA	Projection latent structures discriminant analysis
ppm	Parts per million
Pro	Proline
p-value	Statistical significance
Q:	
QC	Quality control
QTOF	Quadrupole-TOF
R:	
RG	Right gill
RNA	Ribonucleic acid
ROS	Reactive oxygen species
RP	Reversed-phase
S:	
SA	South Africa
Ser	Serine
T:	
TCA	Tricarboxylic acid
Thr	Threonine
TMCS	Trimethylchlorosilane
TMS	Trimethylsilyl
TOF	Time-of-flight
Trp	Tryptophan
TSP	Trimethylsilyl-tetradeuteropropionic acid
Tyr	Tyrosine
U:	
UMP	Uridine monophosphate
UPLC-IM-QTOF	Ultra-performance LC-ion mobility-QTOF
UTP	Uridine triphosphate
V:	
Val	Valine
W:	
WSRLP	Withering syndrome Rickettsiales-like prokaryote

Units:

%	Percentage
°	Degree
°C	Degrees Celsius
µg	Microgram
µL	Microlitre
g	Gram
g	Gravity constant
Hz	Hertz
L	Litre
m/z	Mass to charge
mg	Milligram

min	Minute
mL	Millilitre
mm	Millimetre
ms	Millisecond
N	Normal
psi	Pressure
r	Correlation coefficient
s	Second
V	Volt
µm	Micrometre

Symbols:

α	Alpha	↓	Decrease
ß	Beta	↑	Increase
*	Asterisk	>	Greater-than
		<	Less-than

Web servers:

AMDIS	Automated Mass Spectral Deconvolution and Identification System http://chemdata.nist.gov/mass-spc/amdis/downloads/
ChEBI	Chemical Entities of Biological Interest https://www.ebi.ac.uk/chebi/
Drug bank	DrugBank database http://www.drugbank.ca
HMDB	Human metabolome database http://www.hmdb.ca/
IUBMB	International Union of Biochemistry and Molecular Biology http://www.iubmb-nicholson.org/
KEGG	Kyoto Encyclopaedia of Genes and Genomes http://www.genome.jp/kegg/
LMSD	LIPID MAPS Structure Database http://www.lipidmaps.org
MetaboAnalyst	Tool for metabolomics analysis and interpretation http://www.metaboanalyst.ca/
METLIN	Metabolite and tandem MS database http://metlin.scripps.edu
MET-IDEA	METabolomics Ion-based Data Extraction Algorithm http://bioinfo.noble.org/download/
NIST	National Institute of Standards and Technology https://www.nist.gov/

CHAPTER 1

INTRODUCTION

“They that go down to the sea in ships; that do business in great waters; these see the works of the Lord, and His wonders in the deep.”

– Psalm 107:23-24

1.1 Background and motivation

Over the course of the last two decades, the high market value for abalone has contributed dramatically to aquaculture production globally (Lachambre *et al.*, 2017). Abalone is currently considered South Africa's most successfully produced aquaculture export product, with a 76 % share of the total value generated by the aquaculture sector. Additionally, abalone has the highest product value (US$ 30-50/kg), production volumes and contributes to the largest employment opportunities in this sector (Britz and Venter, 2016). In South African abalone, *Haliotis midae*, as is the case in most other commercially important abalone species, slow growth rates are considered one of the biggest limitations to profitability and the global commercial competitiveness of farming with this species (Venter *et al.*, 2016b). Differences in growth rates exhibited by different animals under identical environmental conditions are often assigned to unexplained variance and subsequently present a number of important research questions (Tamayo *et al.*, 2011). The methods for cultivating abalone have been investigated to the extent that most factors relating to abalone farming are generally considered to be well understood. In contrast, the knowledge of abalone metabolism and the related biochemistry associated with growth, development and feeding are not well defined (Venter *et al.*, 2016b).

A better understanding of abalone physiology, and the effects of various biotic and abiotic factors on their growth and health are considered essential to ensure successful husbandry of these animals (Hahn, 1989). In broad terms, growth is defined as an irreversible increase in mass of an organism, resulting in an increase in cell size or number (Givens and Reiss, 2002). For the most part, growth can be adequately investigated by looking at metabolism, which constitutes all chemical reactions in living cells. Metabolites or small molecules within a cell, tissue, organ, biological fluid or the entire organism, constitutes the metabolome (Lankadurai *et al.*, 2013) and are likely to contribute to the functional state of cells and additionally serve as a direct signature of biochemical activity (Patti *et al.*, 2012). Undoubtedly, the best way to understand metabolic responses within a biological system, under specific conditions, directly related to the phenotypic state, is via a metabolomics research approach (Alonso *et al.*, 2015). Metabolomic experiments typically generate large datasets of biological variables, which are subsequently used for answering biological questions and/or expansion of existing knowledge and research via new hypothesis generation (Brown *et al.*, 2005). Metabolomic studies on abalone (specifically *Haliotis midae)* are scarce and new knowledge generated on this organism using metabolomics, would undoubtedly contribute to the elucidation of the metabolic processes in abalone. In turn, these findings will lead to more efficient farming practices related to improved growth. The importance of linking farm stressors and husbandry practices to animal biology (like metabolic processes) as a means to better understand growth and mortality of

abalone, cannot be emphasised enough from a commercial farming perspective (Lachambre *et al.*, 2017). A better understanding of abalone metabolism could potentially result in identifying additional strategies to optimise growth and to identify markers for more efficient health monitoring. In this study, the focus was to investigate the intricate and somewhat unique biochemical processes of abalone, using metabolomics as the research tool of preference, in order to better understand their metabolic responses to specific perturbations and farming in general, and to relate these to growth and metabolism.

The following questions where investigated using this research theme:

- How does abalone metabolism respond to environmental hypoxia and do they rely heavily on mitochondrial energy metabolism?
- How does abalone metabolism respond to functional hypoxia and what is the impact thereof on anabolism?
- What are the metabolic differences between slow and fast growing abalone under standard farming conditions, and can the findings be used to screen/select abalone that would potentially grow faster?
- Can abalone growth be enhanced using modified artificial abalone feed, and what is the metabolic response to this feed that allows for additional growth?

1.2 Aim and objectives

The **aim** of this study was to use metabolomics as a research tool to elucidate the functional metabolic differences and responses of South African abalone (*Haliotis midae*) under standardised and challenged farming conditions, and to identify the metabolic reactions or pathways related to growth.

The **objectives** followed to accomplish this aim included:

1. A literature-based investigation of current knowledge of abalone metabolism.
2. The standardisation of both targeted and untargeted metabolomic methodologies for application to screening of the abalone metabolome.
3. Using the standardised methods in objective 2, to investigate the metabolic response of abalone following a) functional hypoxia and b) environmental hypoxia.
4. Using the standardised methods in objective 2, to investigate the metabolic differences found between a) slow and fast growing abalone housed in standard farming conditions and b) slow and fast growing abalone, consuming modified artificial abalone feed.

1.3 Structure of thesis

This thesis is a compilation of eight chapters, written specifically to comply with the requirements of the North-West University, for the completion of the degree *Philosophiae Doctor* (Biochemistry) in thesis format. For the sake of flow and focus, each of the result chapters comprise of an introduction, a materials and methods section concerned with the specific chapter, results, discussions and conclusions.

Chapter 1 provides insight into the problem of irregular growth, currently experienced in the abalone farming sector and serves as justification to the current investigation.

Chapter 2 is an overview of *Haliotis midae* physiology, metabolism, growth and the use of metabolomics as a research tool. Parts of this chapter have been published in the journal, *Reviews in Aquaculture* (as shown in Section 1.4).

Chapter 3 is a compressed overview of the study design with motivation for 1) the execution of multiple abalone experiments, 2) the use of multiple abalone tissue samples, and 3) the utilisation of numerous metabolomic approaches and platforms.

Chapter 4 serves as general materials and methods chapter, containing all of the specifications of the reagents, prepared solutions and lab equipment used, abalone sample collection and dissection, metabolite extraction procedures, and sample preparation for metabolomics analysis, instrumentation used, data processing protocols, metabolite identification procedures and pathway analysis. Parts of this chapter have been published in *Food Analytical Methods* and *Journal of Chromatography B* (as shown in Section 1.4).

Chapter 5 describes the results related to the metabolic response of abalone subjected to anaerobic stress. The metabolite information generated from functional hypoxia and environmental hypoxia experiments were further used for the construction a metabolic map of abalone metabolism. Based on these findings, the presence or absence of some metabolites during hypoxic conditions is discussed in relation to energy production in abalone. Parts of this chapter have been published in *Metabolomics* and *Biology Open* (as shown in Section 1.4).

Chapter 6 demonstrates abalone growth variation encountered during standard farming conditions and also clarifies the underlying metabolic differences between slow and fast growing abalone. Furthermore, the metabolic effects of alternative artificial abalone feed are demonstrated and discussed in terms of slow and fast growing abalone.

Chapter 7 gives a summative discussion and conclusion to the study, in addition to potential future prospects, which emanated from the results.

Chapter 8 contains the references used in this thesis.

Appendix A contains the additional results of unidentified metabolic features resulting from the experiments conducted in Chapter 5.
Appendix B contains additional metabolite comparisons of the data presented in Chapter 6.
Appendix C contains the published manuscripts of this study.
Appendix D contains the conference contributions of this study.

1.4 Outcomes of this study

The following publications originated from this study:

1) VENTER, L., JANSEN VAN RENSBURG, P. J., LOOTS, D. T., VOSLOO, A. & LINDEQUE, J. Z. 2016. Untargeted metabolite profiling of abalone using gas chromatography mass spectrometry. *Food Analytical Methods*, 9, 1254-1261.
2) VENTER, L., LOOTS, D. T., VOSLOO, A., JANSEN VAN RENSBURG, P. J, & LINDEQUE, J. Z. 2016. Abalone growth and associated aspects: now from a metabolic perspective. *Reviews in Aquaculture*, 0.1111/raq.12181.
3) VENTER, L., JANSEN VAN RENSBURG, P. J., LOOTS, D. T., VOSLOO, A. & LINDEQUE, J. Z. 2017. From untargeted LC-QTOF analysis to characterisation of opines in abalone adductor muscle: Theory meets practice. *Journal of Chromatography B*, 1071, 44-48.
4) VENTER, L., LOOTS, D. T., MIENIE, L.J., JANSEN VAN RENSBURG, P. J., MASON, S., VOSLOO, A. & LINDEQUE, J. Z. 2018. Uncovering the metabolic response of abalone (*Haliotis midae*) to environmental hypoxia through metabolomics. *Metabolomics*, doi.org/10.1007/s11306-018-1346-8.
5) VENTER, L., LOOTS, D. T., MIENIE, L.J., JANSEN VAN RENSBURG, P. J., MASON, S., VOSLOO, A. & LINDEQUE, J. Z. 2018. The cross-tissue metabolic response of abalone (*Haliotis midae*) to functional hypoxia. *Biology Open*, doi:10.1242/bio.031070.

The following conference contributions resulted from this study:

1) VENTER, L., JANSEN VAN RENSBURG, P. J., LOOTS, D. T., VOSLOO, A. & LINDEQUE, J. Z. Untargeted metabolite profiling of abalone using gas chromatography mass spectrometry. Poster presentation. Elsevier - Aquaculture cutting edge science in aquaculture conference, 23 - 26 Aug 2015 Montpellier, France.
2) VENTER, L., JANSEN VAN RENSBURG, P. J., LOOTS, D. T., VOSLOO, A. & LINDEQUE, J. Z. Metabolome temperature stress response in abalone. Poster presentation. Aquaculture

Association of Southern Africa - Aquaculture conference, 28 Sept - 2 Oct 2015, Polokwane, South Africa.

3) VENTER, L., JANSEN VAN RENSBURG, P. J., LOOTS, D. T., VOSLOO, A. & LINDEQUE, J. Z. Application of functional metabolomics to identify key metabolic changes in *Haliotis midae* due to environmental hypoxia. Oral presentation. World Aquaculture Society conference, 26 - 30 Jun 2017, Cape Town, South Africa.

4) VENTER, L., VOSLOO, A., LOOTS, D. T., JANSEN VAN RENSBURG, P. J. & LINDEQUE, J. Z. Metabolic evidence associated with faster growth observed in farmed *Haliotis midae*. Oral presentation. The 10th International Abalone Symposium, 8 - 12 May 2018, Xiamen, China.

1.5 Author contributions

Dr J.Z. Lindeque supervised all aspects of this study and together with Prof D.T. Loots, Dr A. Vosloo and Mr P.J. Jansen van Rensburg, assisted with the study design, planning, execution, thesis formulation, publications, conference proceedings, and approval of final thesis and research outputs. Dr J.Z. Lindeque assisted with general data analysis, metabolite identification and sample analysis. Mr P.J. Jansen van Rensburg assisted with method standardisation and sample analysis. Dr A. Vosloo assisted with sample collection and dissection. Prof L.J Mienie assisted with metabolic mapping of metabolites of interest and biological interpretation. Dr S.W. Mason assisted with NMR sample analysis and data processing. Ms M. van Reenen assisted with statistical analysis of the data presented in Chapter 6.

As co-author, I hereby approve and declare that my role in this study, as indicated above, is representative of my actual contribution and I hereby give my consent that this work may be published as part of the PhD thesis of Leonie Venter.

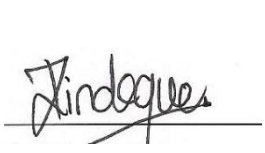

Dr J.Z. Lindeque

Prof D.T. Loots

Dr A. Vosloo

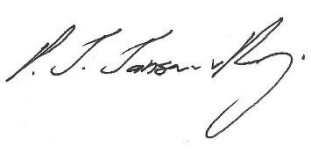

Mr P.J. Jansen van Rensburg

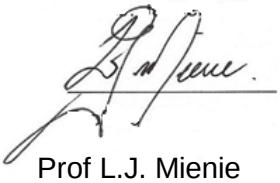

Prof L.J. Mienie

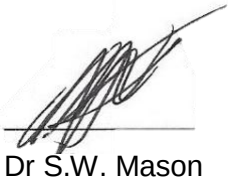

Dr S.W. Mason

Ms M. van Reenen

CHAPTER 2

OVERVIEW OF ABALONE GROWTH AND METABOLISM AND INSIGHTS INTO METABOLOMICS AS A RESEARCH TOOL

"If I were doing a PhD, I'd be doing it in Metabolomics."

– James Watson, Nobel Prize winner for DNA structure discovery

Subsections of this chapter have been published:

VENTER, L., LOOTS, D. T., VOSLOO, A., JANSEN VAN RENSBURG, P. J, & LINDEQUE, J. Z. 2016. Abalone growth and associated aspects: now from a metabolic perspective. *Reviews in Aquaculture*, 0.1111/raq.12181.

.

2.1 Introduction

To date, the methods for cultivating abalone, a marine invertebrate mollusc, have been investigated to such an extent that most factors concerning abalone farming (e.g. spawning, water temperature, formulated diets) are generally considered to be well understood. Despite this however, knowledge of abalone metabolism and the biochemical processes associated with growth, development and feeding are not. This fact becomes evident when reviewing the existing scientific literature and is further substantiated by Morash and Alter (2015): '*We are at a crucial time where understanding the mechanistic physiology of abalone will give us an advantage as the climate continues to change and farming practices become more industrialised.*', Laas and Vosloo (2010): '*Knowledge of the basic biochemical constituents of abalone under culture conditions would be a very useful tool in their management in aquaculture systems.*', and Sales and Janssens (2004): '*Evaluation of the effective use of feed ingredients in abalone feeds is not only hampered by a lack of knowledge on nutrient requirements and possible anti-nutritional factors present in some feed ingredients, but also by an effective measurement of the response to these*.' As the future of sustainable abalone aquaculture depends on optimal growth rates, the various growth mechanisms involved has become a popular research topic.

In their natural habitat, abalone are classified as opportunistic herbivorous deposit scrapers, inhabiting subtidal zones with rocky shores or kelp forests (Vosloo and Vosloo, 2006). Wild abalone populations are globally under pressure through overfishing, disease (Chang *et al.*, 2005, Wetchateng *et al.*, 2010, Macey *et al.*, 2011), ocean acidification (Byrne *et al.*, 2011) and poaching. For example, abalone populations along the coast of South Africa have been in decline since the early 1990s and are classified as depleted, mainly due to a highly organised poaching network involving divers, local middlemen and foreign syndicates (Raemaekers and Britz, 2009, De Greef and Raemaekers, 2014).

Abalone farming on the other hand serves to supply to the growing demand, without depleting the natural abalone reserves, and have shown exponential growth since the mid-1990s. South African abalone are now successfully cultured in man-made, shore-based systems, where they are increasingly grown on formulated artificial feeds (Laas and Vosloo, 2010). Due to its unique gustatory properties, special nutritional value and the safety standards that this food has to comply with, for commerce, these abalone are in high demand and of high monetary value (Øiseth *et al.*, 2013, Latuihamallo and Apituley, 2015).

To successfully culture abalone, an understanding of its physiology and the effects of various biotic and abiotic factors on the organisms growth and health are essential (Hahn, 1989). Furthermore, a better understanding of abalone metabolism could also assist in identifying potential additional strategies to optimise growth, identify markers for monitoring health and growth rates and subsequently improve abalone farm productivity.

This chapter summarises the current literature describing relevant aspects pertaining to abalone biology, feeding and nutrition, in the context of their commercial value and that of abalone farming. In order to better understand the limitations or deficiencies of current farming practices, feeding strategies and growth, it is necessary to understand abalone biology and structure, and related cellular processes, including their metabolism. Subsequently, a comprehensive overview of current literature of this organism's metabolome will also be described and further investigated in the experimental section using metabolomics. Metabolomics, is a research tool, aimed at identifying the metabolites in a biological system or sample, using various analytical techniques, and bioinformatics. Subsequently, the lack of a definite abalone metabolic design, together with the potential use of information attained through abalone metabolomics driven research, in the context of commercial abalone farms will conclude this section.

2.2 The interrelationship between structure, function and metabolism

Abalone are single-shelled marine molluscs that belong to the phylum Mollusca, the class Gastropoda, family Haliotidae and the single genus *Haliotis* (Denny and Gaines, 2007). Abalone are possibly best known for their unusual flattened shell, with the mother-of-pearl lining and the row of respiratory pores extending from the left anterior margin of the shell, closing posteriorly as growth proceeds (Kilburn and Rippey, 1982). Abalone have the typical molluscan body plan, consisting of a head-foot portion and a visceral mass portion, displaying ~180° torsion (Hickman *et al.*, 2006).

2.2.1 Head-foot portion

The head-foot section of abalone is characterised by a muscular foot structure containing a haemolymph cavity, which functions as a hydrostatic skeleton (Kilburn and Rippey, 1982, Payne and Crawford, 1989, Mgaya and Mercer, 1994, Hickman *et al.*, 2006). The large muscular foot, fills the shell opening and functions in attachment and locomotion (Leighton, 2008). From a metabolic perspective, it is interesting to note that although the foot region comprises approximately 66 % of the body mass, it receives only 27 % of the cardiac output (Jorgensen *et al.*, 1984). Poor perfusion, high glycogen reserves (Laas and Vosloo, 2010) and the diversity in

anaerobic enzymes (Gäde, 1988, O'omolo *et al.*, 2003) suggest that the foot muscle relies primarily on anaerobic glycolysis for energy generation.

2.2.2 Visceral mass portion

The visceral mass is the non-muscular metabolic region of the abalone and contains the digestive, respiratory, circulatory and reproductive organs (Kilburn and Rippey, 1982, Hickman *et al.*, 2006).

The abalone digestive system consists of a mouth, a buccal region and an oesophagus that extends posteriorly to the crop and terminate in the anus which, due to torsion, is situated dorsally to the gills. The digestive gland is closely associated with the intestine and functions in energy storage (in the form of lipids and glycogen), metabolic transformation, enzyme synthesis, gametogenesis and a protective role via antioxidant production (Carefoot *et al.*, 2000). Due to these dynamic functions, biochemical constituents of the digestive gland tissue are highly variable (Laas and Vosloo, 2010), and there have been conflicting reports of digestive gland glycogen decreasing (Carefoot *et al.*, 1993) or remaining unchanged (Sheedy *et al.*, 2015) in a response to starvation.

Aerobic metabolism of abalone is supported by gas exchange through a pair of bipectinate gills located below the shell pores. Due to shell asymmetry, the left gill is bigger than the right (Wells *et al.*, 1998a, Ragg and Taylor, 2006, Leighton, 2008). During resting conditions, the right gill is continuously perfused, and this adequately supplies to the oxygen demand. However, when oxygen demand increases, abalone are able to divert more haemolymph towards the left gill also, subsequently increasing oxygen uptake (Ragg and Taylor, 2006).

A circulatory system containing a heart, arteries, veins and various sinuses throughout the body is found in abalone, allowing haemolymph to fill and circulate through the spaces surrounding its internal organs (Hickman *et al.*, 2006, Morash and Alter, 2016). Haemocyanin of gastropods displays a reverse Bohr effect, where oxygen binds tighter at a low pH or high carbon dioxide (CO_2) partial pressure, enabling abalone to maintain oxygen saturation when clamping to surfaces (Wells *et al.*, 1998a, Morash and Alter, 2016). The structural and functional limitations of the oxygen supply system may partly explain the enhanced anaerobic capacity and diversity of the anaerobic pathways (D-lactate, opine and glucose/aspartate–succinate pathways) in abalone. As a result of the oxygen binding properties of haemocyanin, it has been suggested that the abalone circulatory system has a bias for oxygen storage instead of oxygen delivery, in scenarios where muscles are actively working (Donovan *et al.*, 1999).

It is clear that the evolutionary history of abalone has endowed them with adaptations, some quite unique, at the morphological, anatomical, biochemical and metabolic levels to suit their biology and ecology. We require a good understanding of these features as the characteristics of the farming environment may be complementary, or at odds with, the basic biology of abalone.

2.3 Abalone biology vs. growth in the farming context

Abalone have a number of traits that contribute to successful farming including: the relatively small number of adults required as broodstock, which relieves pressure on wild stocks, they have a non-feeding planktonic larval stage, they consume a relatively non-fouling algal food supply as juveniles, they have high survival rates under crowded conditions, they are relatively sedentary (hence use minimal energy for movement), and they eat plant-based food which is relatively cheap (Hahn, 1989, Fallu, 1991). Considering all of these characteristics, abalone can be considered as a model farm animal, supporting expanding industries in China, Korea, South Africa, Chile, Australia and the USA (all producing > 200 metric tonnes per annum) (Cook, 2014).

Abalone farms are found in regions with coastal water temperatures that coincide with optimal growth temperatures. Many farms have both hatcheries and on-growing facilities. The hatchery is typically divided into four divisions; each specialised to the different life cycle phases of the abalone, and includes the (i) broodstock, (ii) larvae, (iii) settlement and (iv) weaning phase. Once abalone have completed these development stages, they are moved to the farms' grow-out facility where they are tended and cared for until they reach market size (Hahn, 1989, Fallu, 1991, Troell *et al.*, 2006).

As abalone grow only two to three centimetres per year, it takes approximately 4 years in South Africa for abalone to reach a market size of approximately 80 g / 90 mm, in these intensive culture systems (Fallu, 1991, Troell *et al.*, 2006). Freezing, canning or live export to Eastern markets are the destined outcome for most farm grown abalone, ultimately contributing significantly to the country's exports and economy per annum (Vosloo and Vosloo, 2006).

To optimise growth, strict control of the farming growth environment is maintained, including water temperature (due to site selection), oxygen supply, food availability and water circulation rates (Denny and Gaines, 2007). Despite this however, and the fact that all abalone in a basket are typically the offspring of a small number of parents with very little genetic variation, individual abalone growth performance (based on size) in a hatchery is difficult to predict

between the individuals (Heath and Moss, 2009). Although regular size grading and sorting into size classes assist in better growth performance, variation in growth rates still occurs. In the end, slow-growing animals will never really catch up and fail to reach their potential maximum size, despite optimising the growth environment (Steinarsson and Imsland, 2003). Even in a good growth performing abalone group, slow growers are always present, which contribute to an increased average age of the population (Mouton and Gummow, 2011). Fallu (1991) reported that slow growth, coinciding with a decreased food utilisation, and reduced rates of meat protein and glycogen synthesis, could be reversed by treating these slow growers with insulin. A study investigating the genetic growth aspects of tropical abalone *Haliotis asinina* revealed upregulated ferritin and metallothionein in the fast-growing animals. Consequently, it was speculated that fast-growing animals have a different metabolic rate and/or a differential ingestion of copper containing feeds, making ferritin and metallothionein possible markers of improved growth in abalone (Lucas, 2007).

It can be expected that the way abalone utilise available energy strongly influences the degree of growth achieved by the end of the farming period. Abalone are known to be poikilotherms and subsequently do not utilise energy to maintain body temperature, and generally, their metabolic rate can be predicted by body size and ambient water temperatures (Fallu, 1991, Britz *et al.*, 1997). Barkai and Griffiths (1988) used a standard energy budget equation (consumption = growth rate + reproductive output + respiration + faecal losses + excretion), to determine the energy allocation pattern of *Haliotis midae*. From this study, it was found that approximately 63 % of the energy content of the consumed food is lost as faeces; 32 % expended on respiration; less than 1 % lost as excreted ammonia (NH_3); and only about 5 % of energy intake is used for growth and reproductive output (Barkai and Griffiths, 1988, Sales and Britz, 2001).

The concept of growth can be crudely summarised as the process by which ingested food gets converted to body tissue. Optimising maximum growth is top priority in the abalone farming sector (Lee, 2004, Naidoo *et al.*, 2006) and is typically measured as a correlation between shell length and live weight (Sales and Janssens, 2004). On a typical abalone farm, the grow-out phase is usually the most expensive and the longest of all the development phases, making it a priority for the farmer to get the maximum growth and hence, return on the investment spent during this phase (Fallu, 1991). Subsequently, a great deal of research has gone into the feeding of abalone, for the purpose of manufacturing high-quality feed necessary for increasing farm productivity.

2.4 Feeding of abalone in the farming context

Although abalone are generally nocturnal feeders (Fallu, 1991, Knauer *et al.*, 1995), it was reported that *H. midae* prefer to feed in the early hours of the morning, rather than at dusk (Wood and Buxton, 1996). Due to their nocturnal feeding pattern, abalone are relatively sedentary during the day, and active at night (Barkai and Griffiths, 1988). Furthermore, vigorously moving water was also reported to stimulate abalone to feed (Fallu, 1991). A feeding frequency of once a day was found sufficient when using formulated feeds (Sales and Britz, 2001), due to the fact that these foods can remain in the crop and stomach of abalone for up to 12 hours after ingestion, and subsequently released as needed (Wood and Buxton, 1996).

Abalone can be classified as opportunistic herbivores and subsequently feed on a variety of different plant-based foods, which changes throughout their development, that is their diets progress from planktonic diatoms, to sessile diatoms/algae, to attached seaweeds, etc. as they develop from free-swimming larvae, to attached, to juveniles, to adults, respectively (Sales and Britz, 2001, Troell *et al.*, 2006). When deciding on which feed best suits the farm (kelp, seaweed and/or artificial feeds), various factors are considered and include the price of the specific feed, its conversion ratio, its freshness and its accessibility. Farms are constantly investigating suitable feeding combinations and feeding formulas that will significantly improve growth rates of abalone (Troell *et al.*, 2006). To achieve maximum growth rates, the type of feed that is utilised in culture systems needs to complement the abalone digestive system (Bansemer *et al.*, 2014). Tamayo *et al.* (2011) found that in clams, high growth rates are typically achieved through a combination of faster feeding and higher digestive performance, this may be true for abalone as well.

Research carried out for the purpose of determining the exact nutrient requirements, and subsequently, optimal feed ingredients of formulated abalone feeds are complicated by the slow-feeding behaviour and growth rates of abalone (Sales, 2004). Despite this however, extensive research regarding the best feeding strategy for abalone is widely available. As the scope of this study is not to review all these findings, dietary research carried out on especially *H. midae* serve well to illustrate this point (Day and Cook, 1995, Britz, 1996a, Sales and Britz, 2001, Day and Branch, 2002, Macey and Coyne, 2005, Naidoo *et al.*, 2006, Ten Doeschate and Coyne, 2008, Robertson-Andersson *et al.*, 2011, Huddy and Coyne, 2014).

2.4.1 Formulated feeds as main diet for growing abalone

Pelletized or extruded abalone feed is usually formulated from proteins, carbohydrates, lipids, minerals and vitamins, which are held together by an alginate binder (Fallu, 1991). Abfeed™ (Marifeed Pty Ltd, Hermanus, South Africa), for instance, is formulated using fishmeal, soya bean meal, starch, vitamins and minerals consisting of about 43 % carbohydrates, 35 % protein, 10 % moisture, 6 % ash, 5 % fat and 1 % crude fibre (Troell *et al.*, 2006). A review performed by Bansemer *et al.* (2014) gives comprehensive insights into macroalgae used as abalone feed. The benefits of using formulated abalone feeds over that of fresh seaweed, macroalgae or kelp include the following: being more readily available, ease of use, easily manufactured, optimised to achieve high growth rates, has a low food conversion ratio, easily stored and transported, and its composition is not varied or dependant on a geographical location (Fallu, 1991, Fleming *et al.*, 1996). Optimising the percentage of proteins, carbohydrates, lipids and other additives in formulated abalone feed is the subject of numerous complementary and contradictory studies, and will subsequently be briefly discussed below.

2.4.1.1 Proteins

Protein is regarded as an important dietary component in abalone feed, as this is the anabolic substrate which is considered to mostly influence growth (Lee, 2004). Apart from using protein-rich ingredients including fish and abalone viscera silage, *Spirdina* spp., additional amino acids such as methionine, arginine, lysine or threonine are also added. Although sufficient amounts of protein are essential for optimum growth, amounts above a certain threshold hold no additional value (Fleming *et al.*, 1996) and simply get catabolised to free amino acids not utilised for growth (Dunstan, 2010). That said, there are, however, large discrepancies in the literature regarding the optimal levels for dietary protein intake in abalone, with the amounts reported in scientific literature to vary between 20 % and 50 % of the total nutrient intake (Fallu, 1991, Fleming *et al.*, 1996, Bautista-Teruel and Millamena, 1999, Angell *et al.*, 2012). This variation could be species dependent, and the optimal dietary protein intake for *H. midae* largely considered to be 36 % of the total nutrient intake (Robertson-Andersson *et al.*, 2011) derived mainly from fishmeal and *Spirulina* spp. (Britz, 1996b).

2.4.1.2 Carbohydrates

Research on the composition of *Haliotis* digestive enzymes revealed high concentrations of not only protease but also amylase, cellulase and alginase accompanied by comparatively low amounts of lipases, and subsequently, the conclusion was made that carbohydrates are the most important energy source for these animals (Lee, 2004). Consequently, formulated abalone feeds contain carbohydrate contents varying anything between 30 % and 60 % (Fallu, 1991, Fleming *et al.*, 1996, Sales, 2004), derived from low cost raw materials such as wheat flour,

maize flour, sodium alginate, dextrin, starch and bran (Sales, 2004). When abalone are fed a diet with insufficient amounts of carbohydrates, they utilise mostly protein, as a source, for *de novo* carbohydrate synthesis, reducing the amounts of available protein for muscle anabolism and growth (Fallu, 1991).

2.4.1.3 Lipids

Dietary lipids play an important role in the provision of energy, essential fatty acids and fat-soluble nutrients, for optimal abalone growth. The lipids in formulated abalone feeds are typically derived from fish oil, vegetable oil, lipids bound in fishmeal or a combination of these ingredients. As abalone have low dietary lipid requirements (5 %), substantiated by their low lipase activity, it is likely that lipids are still oversupplied in some formulated feeds on the market (Fallu, 1991, Fleming *et al.*, 1996, Lee, 2004).

2.4.1.4 Minerals and vitamins

In general, research on the optimal composition and levels of vitamins and minerals in abalone feed are scarce (Fleming *et al.*, 1996); however, overtime an approximation of 5 % of the total nutrient contents of formulated abalone feed was deemed sufficient to make up minerals, vitamins and other trace elements in abalone feed (Fallu, 1991). Some examples of the vitamins found in formulated abalone feeds are vitamin E (Bansemer *et al.*, 2016a), vitamin-A, vitamin-B12, vitamin-C, vitamin-D, riboflavin and biotin (Mai, 1998). Minerals used to enhance abalone feeds may include sodium, calcium (Bansemer *et al.*, 2016a), sodium chloride, zinc and potassium iodide (Tan and Mai, 2001). Many of these minerals added to the diet are considered unnecessary as abalone absorbed some of these components directly from the surrounding water (Fleming *et al.*, 1996, Sales, 2004).

2.4.1.5 Binders

Apart from the added starch which can serve as a binding agent, other binding agents are also added to formulated abalone feeds, which not only allow for the food pellets to remain intact but also serve to stabilise and prevent loss of the water soluble nutrients (Fleming *et al.*, 1996, Sales, 2004). Typically, sodium alginate is used in amounts ranging from 20 % to 45 % of the total feed weight (Fallu, 1991).

2.4.2 Inter-individual variation despite identical feeding strategies

Inter-individual variation in energy acquisition and growth exists in the same population of abalone despite similar or identical environmental conditions. These inter-individual differences, although being problematic from a farming productivity perspective, do create new opportunities

for understanding the energetics involved in growth variability, which surely is a necessity in aquaculture (Tamayo *et al.*, 2014). As previously mentioned, growth can be summarised as the conversion of ingested food to body tissue, that is the relationship between anabolism (biosynthesis) and catabolism (biodegrading) which is important for growth, and a better understanding thereof could assist in determining the optimal nutrient requirements and also possibly those factors related to abalone growth rates. In a spat of clams for instance, it was found that faster growth was related to increased energy acquisition, reduced metabolic maintenance costs and reduced growth costs in terms of the metabolism used to sustain biosynthesis (Tamayo *et al.*, 2011). The evaluation of normal metabolism includes scenarios from adaptation to starvation periods, exercise and pregnancy. Abnormal metabolism may be a consequence of abnormal hormone secretion, enzyme deficiencies, nutrient deficiencies or the actions of drugs and toxins (Murray *et al.*, 2003). However, before one can assess or measure abnormal metabolism due to any stressors, an adequate knowledge of 'normal' abalone metabolism is first required.

2.5 Basic metabolism and how we apply it to abalone

Metabolism can be seen as the sum total of all chemical changes that convert nutrients to energy and the chemical end products of cells. The synthesis of biological macromolecules and the generation of energy to drive vital functions are regarded as the two main purposes of metabolism. To achieve this balance, contrasting metabolic pathways are required as depicted in Figure 2.1. These pathways are typically divided into three categories: (i) Catabolism, (ii) Anabolism and (iii) Amphibolism. Catabolism can be broadly defined as the oxidation of complex nutrient molecules, through mostly exergonic reactions, resulting in the production of energy in the form of adenosine triphosphate (ATP). In this instance, carbohydrates, lipids and proteins are metabolised to a common intermediate molecule known as acetyl coenzyme A (acetyl-CoA). Acetyl-CoA subsequently serves as a substrate for the tricarboxylic acid (TCA) cycle, which in turn generates reduced electron carriers for ATP production via the oxidative phosphorylation (OXPHOS) system and the end products of catabolism, namely water (H_2O), CO_2 and NH_3 (Murray *et al.*, 2003, Garrett and Grisham, 2010). Anabolism on the other hand is the synthesis of complex biomolecules from simple precursors. These reactions involve the formation of new covalent bonds and an input of chemical energy to drive endergonic processes. Hence, the ATP generated during catabolism is used together with nicotinamide adenine dinucleotide phosphate (NADP) for the reductive reactions required during this process. Anabolic processes subsequently allow for the synthesis of various macromolecules including polysaccharides, lipids, proteins and nucleic acids from their sugar, fatty acid, amino acid and nitrogenous base precursors, respectively. In essence, these metabolic processes are

used to build genetic material, cells and muscle and are essential for the development, growth and maintenance thereof (Garrett and Grisham, 2010). Amphibolism is the process or those pathways that act as both catabolic and anabolic, as many metabolic intermediates are shared between the two processes (Murray *et al.*, 2003, Whitney and Rolfes, 2008, Garrett and Grisham, 2010).

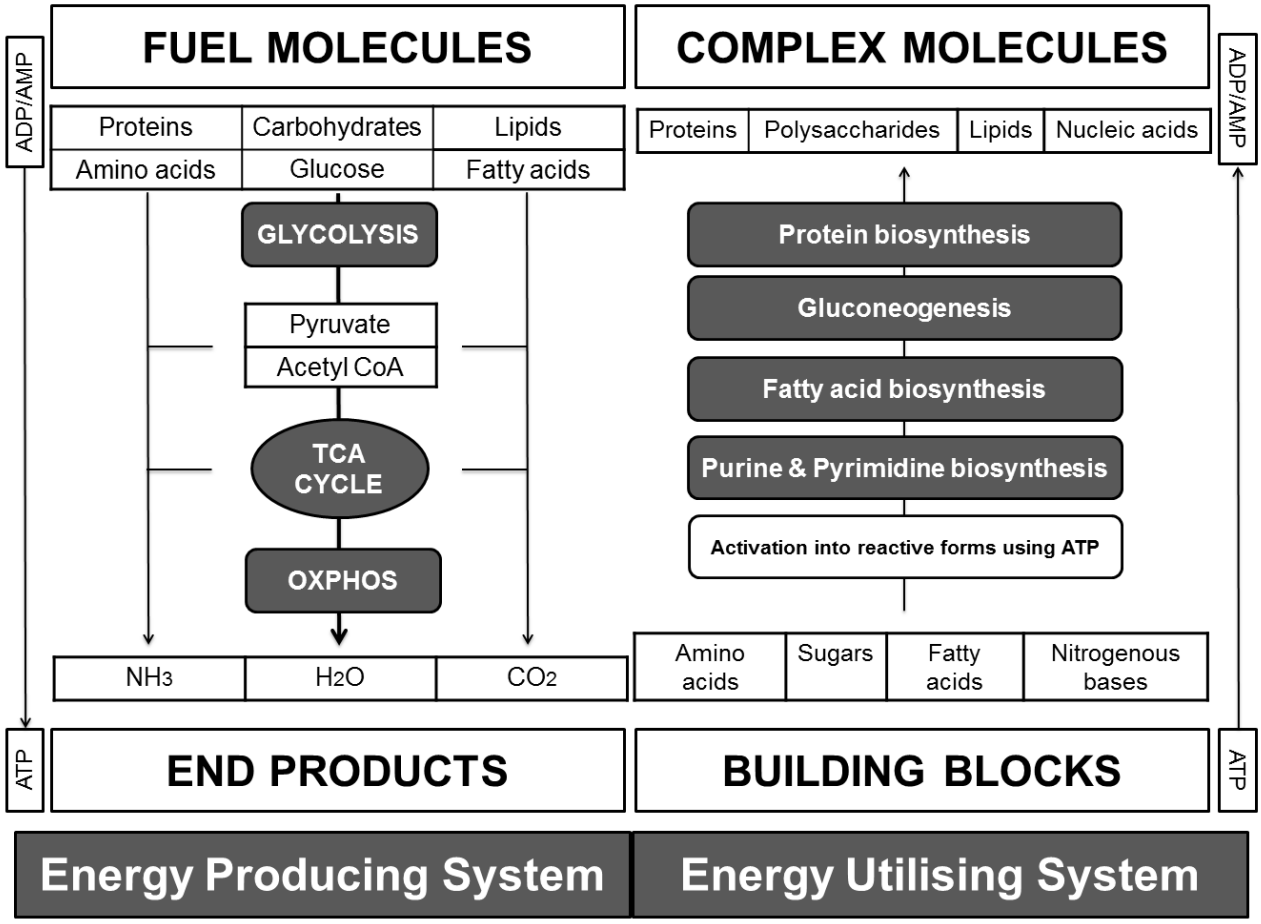

Figure 2.1: Overview of metabolism. Energy balance is maintained by both energy producing and utilising systems.

One of the unifying principles of biology is the profound similarities that exist in the major metabolic pathways when comparing different species and organisms (Garrett and Grisham, 2010). A result of this phenomenon is the scientific practices of gene prediction, functional genomics and associated software. Also, large similarities between molluscan metabolism and that of vertebrates have been reported (Ballantyne, 2004). Subsequently, it is advisable to investigate abalone metabolism in the context of what is already known from other organisms, to predict the missing puzzle pieces in abalone metabolism.

Large differences in energy expenditure associated with the metabolism of proteins, carbohydrates and lipids are found in tissues. These changes are due to the different ways proteins, carbohydrates and lipids are handled by cells and their function in cellular metabolism. Generally, proteins act as structural and functional elements in cellular metabolism, carbohydrates are used primarily for energy production, and lipids serve as the major structural elements of cell membranes (Lawrence, 2013). Abalone are capable of catabolising proteins, carbohydrates and lipids, as these are all prominently found in their diet. As a rule, abalone tissue has a low lipid content, and therefore, proteins and carbohydrates are mainly used to fuel metabolism resulting in reduced lipid metabolism (Vosloo and Vosloo, 2010). This phenomenon, and many other unique metabolic processes identified in abalone, will be discussed below.

2.5.1 Protein metabolism

The primary physiological purpose of amino acids is to serve as the building blocks for proteins. Amino acid biosynthesis requires firstly the synthesis of the correct alpha (α)-keto acid carbon skeleton for the amino acid, followed by transamination of the α-keto acid with glutamate serving as the amino donor via an aminotransferase reaction (Garrett and Grisham, 2010) Abalone essential amino acids (Arg – arginine, His – histidine, Ile – isoleucine, Leu – leucine, Lys – lysine, Met – methionine, Phe – phenylalanine, Thr – threonine, Trp – tryptophan and Val – valine) and nonessential amino acids (Ala – alanine, Asp – aspartate, Cys – cystine, Glu – glutamate, Gly – glycine, Pro – proline, Ser – serine and Tyr – tyrosine) have been confirmed in a number of studies (Fleming *et al.*, 1996, Viana *et al.*, 2007, Bae *et al.*, 2011, Latuihamallo and Apituley, 2015). Rosenblum *et al.* (2005) reported that the less metabolically active nonessential amino acids of abalone are used to maintain osmoregulation, when the levels of free amino acids are depleted. The fact that taurine has a well-established role in osmoregulation of marine invertebrate tissues (Welborn and Manahan, 1995, Fasulo *et al.*, 2012, Cappello *et al.*, 2013) further supports this observation. Apart from their possible role in osmoregulation, these essential and nonessential amino acids are typically degraded by different pathways, subsequently forming succinyl-CoA, acetyl-CoA, acetoacetate, pyruvate, α-ketoglutarate, fumarate and oxaloacetate, all of which feed into the energy production pathways (Whitney and Rolfes, 2008, Garrett and Grisham, 2010).

It is generally considered that energy production from proteins is energy expensive, and less optimal than energy acquisition from carbohydrates. To favour carbohydrates as the preferred energy source, various organisms, including abalone can catabolise, ingested proteins into their respective amino acids, peptides or protein pools (Lawrence, 2013). However, in times when energy levels are low, or carbohydrate intake is restricted, or when there is surplus of protein or amino acids in the system, protein is used as an energy source. For this to occur, protein is

catabolised into two end products: the carbon structure (without an amino group) and ammonia (Whitney and Rolfes, 2008, Garrett and Grisham, 2010). The carbon structure feeds directly into the energy generating metabolic pathways, and in aquatic animals, the ammonia is excreted, due to its toxicity (Morash and Alter, 2016). It has additionally been reported that especially during the early development phase of marine animals, protein is more readily used as an energy source (Latuihamallo and Apituley, 2015).

2.5.2 Carbohydrate metabolism

In most organisms, a large amount of cellular energy is derived from the oxidation of carbohydrates via glycolysis and the TCA cycle (Lawrence, 2013). Glycolysis consists of two phases: (i) glucose breakdown to glyceraldehyde-3-phosphate (G-3-P) molecules and (ii) the conversion of G-3-P to eventually produce two pyruvate molecules. During this process, two ATP and two nicotinamide adenine dinucleotide (NADH) molecules are the result (Garrett and Grisham, 2010). Enough evidence exists to suggest that glucose in abalone follows the traditional glycolysis route used in other organisms. A number of studies have focused on the quantification of glucose in abalone (Carefoot *et al.*, 2000, Braid *et al.*, 2005, Rosenblum *et al.*, 2005, Rosenblum *et al.*, 2006, Laas and Vosloo, 2010, Sheedy *et al.*, 2015, Zhou *et al.*, 2015, Venter *et al.*, 2016a). Also, glucose-6-phosphate was successfully measured in the shell adductor and foot muscle of *Haliotis lamellose* (Gäde, 1988), supporting glucose breakdown via glycolysis. That said, it should also be noted that no studies have been carried out to date proving the presence of the other metabolites of glycolysis, for example fructose-6-phosphate, fructose-1,6-diphosphate and dihydroxyacetone phosphate in abalone. Regardless of this shortcoming, the well-known end product of glycolysis, pyruvate (essential for opine formation, as will be discussed later), has been successfully measured in abalone (Zhou *et al.*, 2015), further supporting this suggested metabolic pathway exists in this animal.

During conditions when insufficient carbohydrates are consumed and glycogen is depleted, most organisms have the capacity for *de novo* glucose synthesis, from non-sugar carbon substrates, through a process known as gluconeogenesis (Salway, 2004). Gluconeogenesis can be seen as the reversal of glycolysis, with a few deviations. Glycolysis and gluconeogenesis are under reciprocal control, thus when the one is active, the other is inhibited (Garrett and Grisham, 2010). As glycogen has also been measured on a number of occasions in abalone (Carefoot *et al.*, 2000, Braid *et al.*, 2005, Rosenblum *et al.*, 2005, Rosenblum *et al.*, 2006, Laas and Vosloo, 2010, Zhou *et al.*, 2015), it leads us to believe that the same, or a similar metabolic pathway exists in abalone metabolism. Metazoans are known to synthesise glycogen from glucose, as a mean to store carbohydrates, resulting in a lower energy cost for glycogen synthesis when compared to protein synthesis (Lawrence, 2013).

2.5.3 Lipid metabolism

Lipids primarily play a role in growth and gonad maturation in abalone (Durazo and Viana, 2013). The synthesis of fatty acids and other lipid components in many living organisms start with malonyl-CoA, a four carbon molecule synthesised using two acetyl-CoA's, at the expense of one ATP molecule. As mentioned earlier, abalone have low lipid concentrations in their tissues, which is most likely due to a lower dependence on these compounds as an energy source, driven by the low amounts of lipid compounds present in their diets, and subsequently less lipase in their digestive tract (Laas and Vosloo, 2010). Interestingly, the primary function of n-3 and n-6 polyunsaturated fatty in abalone is to serve as substrates for structural components (Durazo-Beltrán *et al.*, 2003). Generally, the neutral lipids of abalone are only metabolised as an energy source, when protein and carbohydrates are depleted, during extended periods of fasting (Durazo and Viana, 2013).

The portion of cellular energy, utilised for lipid metabolism, is relatively low when compared to the overall costs of carbohydrates and proteins, because only a fraction of the fatty acids and sterols absorbed from the diet, undergo *de novo* lipid synthesis (Lawrence 2013). Nonetheless, when lipids are required as an energy source, they are typically metabolised to glycerol and fatty acids in the cytoplasm, and eventually form glycolysis substrate intermediates (Murray *et al.*, 2003, Whitney and Rolfes, 2008, Garrett and Grisham, 2010). The catabolism of fatty acids can proceed via a number of routes depending on the length of the acid, the number of carbons and whether they are saturated or unsaturated via a process named beta (ß)-oxidation. Most important to know is that the products of ß-oxidation are acetyl-CoA, NADH and flavin adenine dinucleotides ($FADH_2$). Equally important to note is that acetyl-CoA enters the TCA cycle, and NADH and $FADH_2$ will be used by the electron transport chain (ETC) to produce ATP (Lopaschuk *et al.*, 2010). Fatty acids ranging from C14 to C24 have been detected abalone. Studies investigating the effect of starvation, dietary composition, water temperature variation, and pre- and post-spawning cycles on abalone lipid and/or fatty acid content are present in the literature. Very few mechanistic studies investigating the breakdown of these lipids, however, have been performed, with most of the research to date focused more towards describing the varying compositions of the fatty acids during such conditions (Durazo-Beltrán *et al.*, 2004, Grubert *et al.*, 2004, Durazo and Viana, 2013, Hernández *et al.*, 2013, Wang *et al.*, 2014).

2.5.4 Nucleic acid biosynthesis

Nucleic acids [deoxyribonucleic (DNA)–ribonucleic acid (RNA)] are complex polymeric molecules, with a sequence of nitrogenous bases (or nucleotides) which encodes the genetic information necessary for biological inheritance as well as having other functions, like coding for

both structural and functional proteins (Hickman *et al.*, 2006). Nucleotides (purine: adenine and guanine and pyrimidine: thymine, cytosine and uracil) play a central role in metabolism, because they carry energy (in the form of high-energy phosphate bonds), combine cofactors of enzymes and participate in cell signalling (Salway, 2004, Garrett and Grisham, 2010). When energy levels are low, most of the ATP is in the form of adenosine monophosphate (AMP), and AMP-activated protein kinase (AMPK) is allosterically activated. Activation of AMPK signals the breakdown of proteins and lipids and shuts down biosynthesis and cell growth pathways (Garrett and Grisham, 2010). From a farming productivity perspective, it would make sense to keep the AMP levels to a minimum, ensuring AMPK is inactive and anabolic pathways function as normal. However, from a culinary point of view, it has been reported that higher AMP levels play a key role in the desired taste of abalone (Brown *et al.*, 2008). This may be a point of further investigation as both a high or low AMP content can be justified for increased productivity, and these ratios can easily be altered during stress. However, it was indicated that changes in adenylate concentrations can be detected rather rapidly following application of a stressor. In the short time, it took to remove *Haliotis iris* from substratum and freeze clamping the tissue samples, changes in adenylate muscle concentrations could already be detected and it was found that inosine monophosphate (IMP) concentrations increased due to AMP degradation (Wells *et al.*, 1998b).

2.5.5 Energy metabolism

Cellular respiration is the process whereby cells manufacture energy (ATP) using intermediates produced during catabolism. Two types of respiration occur namely: (i) aerobic (requiring oxygen) and (ii) anaerobic (absence of oxygen) respiration. In terms of the amounts of ATP produced, aerobic respiration is far more efficient than anaerobic respiration. Respiration can roughly be divided into three stages consisting of: (i) glycolysis (aerobic and anaerobic), (ii) tricarboxylic acid cycle (aerobic) and (iii) oxidative phosphorylation (aerobic) (Wardlaw and Insel, 2006), which will be discussed briefly below in the context of abalone metabolism.

2.5.5.1 Aerobic glycolysis

As described above, glycolysis is the process by which 1 x glucose molecule is metabolised into 2 x pyruvate molecules, 2 x ATP molecules, 2 x coenzyme molecules, 2 x hydrogen ions (which enter the ETC) and 2 x water molecules. In animals, the pyruvate produced is generally converted to acetyl-CoA during aerobic conditions, by means of the enzyme pyruvate dehydrogenase, and then further metabolised in the TCA cycle to produce NADH, $FADH_2$ and CO_2. Acetyl-CoA can also be used for the synthesis of fatty acids and lipids when the energy demand is met and glycogen stores are well stocked (Wardlaw and Insel, 2006, Garrett and

Grisham, 2010). As a general observation, abalone adductor–foot muscle are poorly perfused and subsequently abalone are thought to depend more strongly on anaerobic glycolysis to synthesise the required energy for this organs function of clamping to surfaces and movement (Hickey and Wells, 2003). As these animals are considered to be rather sedentary by nature, the proposed anaerobic glycolysis pathway can easily meet the lower energy demand required by the foot muscle, despite it producing comparatively less ATP than aerobic glycolysis.

2.5.5.2 Anaerobic glycolysis

Anaerobic metabolism is initiated whenever the oxygen demand exceeds the supply (Wardlaw and Insel, 2006). In abalone, anaerobic glycolysis occurs due to the adequate muscle glycogen reserves available, high activities of pyruvate reductase for generating NAD^+ and the high concentrations of arginine phosphate (Donovan *et al.*, 1999). During anaerobic conditions, such as hypoxia, the adductor muscle, mantle, digestive glands and gills of mussels have been reported to switch to anaerobic respiration in an attempt to generate ATP (Stefano *et al.*, 2015). A similar mechanism of energy production is thought to take place in abalone, because its adductor muscle, foot muscle and haemolymph (Gäde, 1988, Wells and Baldwin, 1995, Donovan *et al.*, 1999, Vosloo and Vosloo, 2006) have been reported to respond to hypoxic conditions. However, during prolonged exercise or rapid movement through well-oxygenated water, anaerobic glycolysis is localised to the foot muscle only (Donovan *et al.*, 1999). In survival scenarios where the whole animal needs to deal with anoxic (or hypoxic) situations, both the shell adductor and foot muscle were shown to uphold anaerobic metabolism (Gäde, 1988). Three main pathways are said to be responsible for energy production in marine invertebrates (including abalone) during anaerobic conditions (Fig. 2.2), namely (i) the lactate pathway, responsible for medium rates of energy production and used to maintain or increase metabolic activity; (ii) the opine pathway, which has the same function as the lactate pathway but occurs exclusively in invertebrates; and (iii) the glucose/aspartate–succinate pathway, which is used primarily for survival during anoxia (Livingstone, 1983, Lee and Lee, 2011, Harcet *et al.*, 2013).

***Lactate pathway*:** Mitochondrial respiration actively consumes electrons from NADH, produced from the oxidation of carbohydrates and other substrates (amino acids and to a lesser extent fatty acids in abalone). When mitochondrial respiration is low (due to low bioenergetics or an oxygen shortage), the ETC can no longer function optimally, and subsequently, NADH accumulates. This in turn results in a rate reduction in other important metabolic pathways due to a consequential NAD^+ shortage. It is during such times that the lactate pathway comes into play to avoid total metabolic shutdown during anaerobic conditions. Accumulating pyruvate is converted to lactate (by means of lactate dehydrogenase and coenzymes) simultaneously

oxidising NADH to NAD^+, allowing the anaerobic glycolysis pathway to function (Murray *et al.*, 2003, Whitney and Rolfes, 2008, Garrett and Grisham, 2010). Numerous mollusc (including abalone) species produce the D-isomer of lactate (and not L-lactate as in vertebrate organisms) which is said to play an important role in anaerobic energy metabolism (Cristescu *et al.*, 2008). Due to abalone's reportedly low mitochondrial activity (see Tricarboxylic acid cycle section), it can be assumed that this pathway is extremely important to this species in order to regulate NAD^+ concentrations, and to produce much needed ATP. This hypothesis is also supported by the relatively high D-lactate levels commonly found in abalone muscle samples when analysed with gas chromatography mass spectrometry (GC-MS). However, the opine pathway is perhaps a better means for supplying to the required energy demand during anaerobic conditions, as it does not result in an acidic end product.

Opine pathway: In addition to D-lactate, molluscs accumulate a multitude of end products of anaerobic glycolysis (O'omolo *et al.*, 2003), for example octopine, strombine, alanopine, tauropine, lysopine and ß-alanopine (collectively known as opines). Opine formation in invertebrates (like abalone) takes place via a cytosolic fermentation pathway, where pyruvate is coupled to an amino acid (most popularly arginine, glycine, alanine, taurine, lysine and ß-alanine) using a very specific dehydrogenase, resulting in an imino acid derivative (octopine, strombine, alanopine tauropine, lysopine and ß-alanopine, respectively) as an energy metabolism end product (Pyruvate + amino acid + NADH + $H^+ \rightarrow$ imino acid dehydrogenase $\rightarrow$ imino acid + NAD^+ + H_2O) (O'omolo *et al.*, 2003, Baldwin *et al.*, 2007, Müller *et al.*, 2012, Harcet *et al.*, 2013). The imino acid dehydrogenase in molluscs functions in a similar fashion to that of lactate dehydrogenase, resulting in the regeneration of cytoplasmic NAD^+ for usage in the G-3-P dehydrogenase reaction of glycolysis. Regardless of this substitution, the proton stoichiometry and the ATP yields remain the same (Gäde, 1988, Prosser, 1991, O'omolo *et al.*, 2003), with the synthesis of two molecules of ATP per one molecule of glucose (Livingstone, 1983, Müller *et al.*, 2012). The main advantage of the opine pathway, however, over that of the lactate dehydrogenase reaction is that the opine end products are less acidic than D-lactate, which subsequently allows for better intracellular pH regulation and osmotic pressure (Harcet *et al.*, 2013). As one amino acid is required for each opine synthesised (Müller *et al.*, 2012), a large amino acid pool in molluscs is crucial for sustaining the lower NADH:NAD^+ ratio required (Gäde, 1988). Gäde (1988), Wells *et al.* (1998b) and O'omolo *et al*. (2003) investigated opine metabolism in the adductor and foot muscles of various abalone species during anaerobic conditions, and observed an accumulation of tauropine in the adductor muscle and D-lactate in the foot muscle. The presence of tauropine dehydrogenase in the shell adductor muscle is most likely due to this muscle being more metabolically active (when compared with the foot muscle) and largely dependent on anaerobic metabolism. As the foot muscle is responsible for the slower gliding movements, it requires less energy comparatively, and hence, D-lactate

dehydrogenase alone is sufficient. Predominately, tauropine is produced during functional hypoxia and D-lactate seems to be formed during environmental hypoxia (Gäde, 1988). On the basis of these findings, it was suggested using D-lactate dehydrogenase and tauropine dehydrogenase, as indicators of anaerobic stress, rather than the measurement of glycogen reserves, which are generally more difficult to quantify accurately (Wells and Baldwin, 1995).

Glucose/aspartate–succinate pathway: This pathway is conventionally divided into (i) the glucose–succinate pathway and (ii) the aspartate–succinate pathway (with succinate being the end product of both). In essence, this pathway involves the reversal of the second half of the TCA cycle, as a mean to use accumulating reduced equivalents for the synthesis of NAD^+ and FAD. Both of these pathways are advantageous to cells rich in amino acids, typically those of marine invertebrates (Harcet *et al.*, 2013) like abalone.

Generally, the catabolism of glucose via glycolysis produces phosphoenolpyruvate (PEP), which in turn can be metabolised to pyruvate via pyruvate kinase, or to oxaloacetate by means PEP carboxykinase (Fig. 2.2) (the ratio of which varies in different species and tissues). In the presence of high amounts of reduced equivalents such as NADH and FADH, oxaloacetate can be converted to succinate and propionate through a reversed TCA cycle. The conversion of succinate to propionate results in approximately five ATP molecules, allowing the organism to survive in a lower energy state, with comparatively lower free radical production (Stefano *et al.*, 2015). Amino acids (such as aspartate) can also be used in this process, by feeding directly into the cycle via oxaloacetate. In tissues where low PEP carboxykinase activity occurs, the main precursor of succinate or propionate is aspartate. The result of these reactions is an increased ATP yield from glucose, as extra substrate-level phosphorylation reactions and an electron-transfer-coupled phosphorylation involving fumarate as the electron acceptor take place. The primary function of the glucose–succinate pathway is survival during anoxia, even though the energy efficiency of this pathway is twice that of the D-lactate or opine pathways (Livingstone, 1983, Prosser, 1991). Before the glucose–succinate pathway can become operational in marine molluscs however, a reduction in pH is required and subsequently inhibition of PEP carboxykinase and pyruvate kinase activities. This pH reduction is made possible by the accumulation of acidic end products, largely brought about by the aspartate–succinate pathway (Livingstone, 1983) as well as lactate.

Equally important to this process is the aspartate–succinate pathway, operating during the early stages of anaerobic metabolism which requires NADH (from carbohydrates) and produces alanine (Livingstone 1983). In addition to the breakdown of glycogen and arginine phosphate, the amino acid aspartate is also able to serve as a substrate for energy production during anoxia in abalone. Co-fermentation of glycogen and aspartate during anaerobic conditions are

indicated by the synchronised depletion of aspartate and accumulation of alanine and succinate in the foot and adductor muscles of abalone. However, Gäde (1988) further speculates that the lack of propionate and acetate found in abalone is an indication that abalone can tolerate anoxic conditions less well as compared to other species like blue mussels or oysters. Confirmation of this is the fact that *H. lamellose* cannot survive anoxia experiments exceeding eight hours (Gäde, 1988).

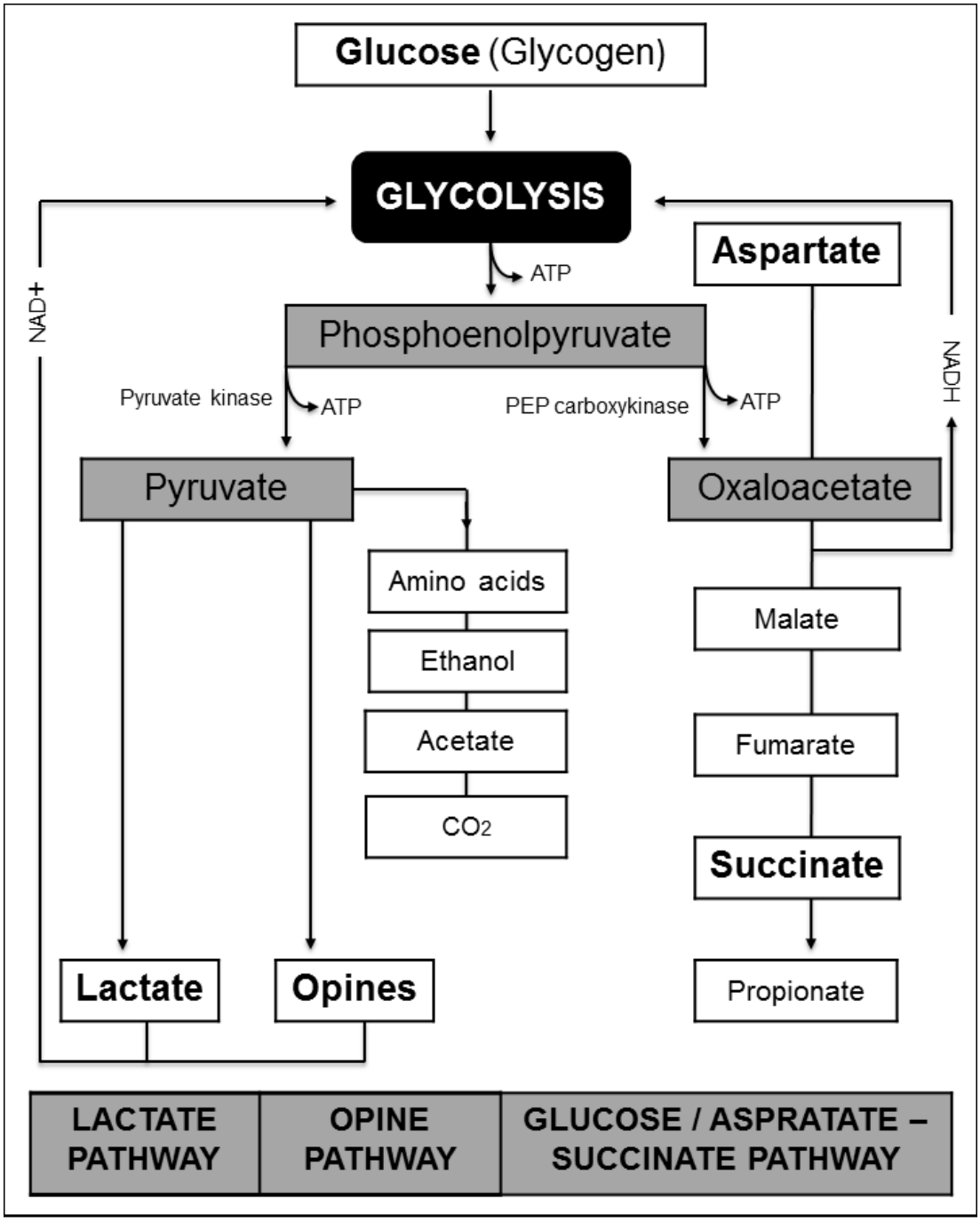

Figure 2.2: Anaerobic glycolytic routes. Typically abalone utilise the lactate pathway, the opine pathway, the glucose/aspartate–succinate pathway during anaerobic respiration for the production of energy.

2.5.5.3 Tricarboxylic acid cycle

The final pathway required for the oxidation of carbohydrates, proteins and lipids is the TCA cycle, which is a series of reactions that oxidises acetyl-CoA and reduce coenzymes, that upon re-oxidation, are linked to ATP formation (in the presence of oxygen). Briefly, the binding of oxaloacetate with a 2-carbon length acetyl-CoA molecule results in a 6-carbon compound called citrate, which initiates this process. By releasing carbons (as CO_2) during a range of reactions, the 4-carbon compound oxaloacetate forms and the process repeats itself, subsequently releasing hydrogen ions along with electrons, which are carried by the electron carriers NADH and $FADH_2$ to the ETC (Murray *et al.*, 2003, Whitney and Rolfes, 2008, Garrett and Grisham, 2010).

When investigating the effect of food restrictions on withering syndrome Rickettsiales-like prokaryote (WSRLP) infected abalone, reduced TCA cycle intermediates were detected in the foot muscle of *Haliotis rufescens* (Rosenblum *et al.*, 2005). Succinate was also found in elevated concentrations in abalone muscle in response to toxic exposure. The conversion of α-ketoglutarate to succinate is associated with aerobic respiration, resulting in an indirect increase in reactive oxygen species (ROS), and subsequently oxidative stress (Zhou *et al.*, 2015). Succinate is actually the most commonly found TCA cycle intermediate in abalone metabolism-based studies (Gäde, 1988, Sheedy *et al.*, 2015, Zhou *et al.*, 2015), which can be expected considering it presents as an anaerobic end product. It is important to note that the TCA cycle of abalone has as yet not been fully characterised, making this an important point for future research. Interestingly, a study performed by Venter *et al.* (2016) showed comparatively low organic acids to be present in various GC-MS analysed tissue samples of abalone, in comparison with their amino acid content, which is a rather unique occurrence, because these levels are usually very similar in other animal tissue samples analysed via the same approach (Lindeque *et al.*, 2013). The fact that the TCA cycle intermediates in abalone are often below the detection limits of such analytical approaches supports the hypothesis that these animals make little use of mitochondrial metabolism and most likely have fewer than expected mitochondria per cell.

2.5.5.4 Oxidative phosphorylation

During aerobic metabolism, almost all of the energy released from the oxidation of proteins, lipids and carbohydrates are made available as reducing equivalents (hydrogen ions and electrons) in the mitochondria which subsequently feeds into the ETC where they move along a redox gradient, with oxygen ultimately acting as the final electron acceptor, with the production of water and ATP (Murray *et al.*, 2003, Whitney and Rolfes, 2008, Garrett and Grisham, 2010). As a by-product of OXPHOS, mitochondria generate ROS, which is a highly regulated

procedure under normal physiological conditions. Excessive mitochondrial ROS production, during conditions of stress, or disease, or anoxia or toxin exposure, may overwhelm the repair rates, radical scavenging capacity and detoxification mechanisms of the cell, eventually causing damage to proteins, lipids and DNA, and potentially also mitochondrial defects (Wallace and Fan, 2010, Vosloo *et al.*, 2013a).

Vosloo and colleagues did extensive studies in this regard on abalone. They determined that the mitochondrial respiration efficiency was optimal at 19 °C with a 98 % oxygen exposure. This was measured by an increase in cytochrome *c* oxidase subunits 1 and 2 (*cox*1 and *cox*2) transcripts level, proposing a change in the efficiency of complex IV for preventing ROS formation. A lowered metabolic rate, however, was found at 19 °C and 126 % oxygen exposure, which is most likely due to an improvement in gaseous exchange (Vosloo *et al.*, 2013c). Furthermore, antioxidant enzyme activity (superoxide dismutase and glutathione peroxidise, specifically) was also found to be upregulated at elevated temperatures (Vosloo *et al.*, 2013b), subsequently resulting in a reduction in DNA fragmentation and protein damage at elevated oxygen consumption rates. However, at lowered oxygen consumption rates, DNA damage occurred under hypoxic and hyperoxic conditions, suggesting that the antioxidant enzymes did not prevent oxidative damage during these conditions (Vosloo *et al.*, 2013a). This shows not only the importance of oxygen control but also that of temperature in the farming scenario.

2.5.5.5 Phosphagens

Phosphagens store energy in the form of high-energy phosphate bonds, for rapid use when necessary, or for the maintenance of a favourable ATP:adenosine diphosphate (ADP) ratio (Prosser, 1991, Murray *et al.*, 2003). In vertebrates, the only available phosphagen is in the form of creatine phosphate (phosphocreatine) while in invertebrate muscle tissue, such as that of abalone, arginine phosphate (phospho-L-arginine) is the primary phosphogen used. During prolonged conditions of hypoxia, it was determined that abalone use phosphoarginine as a phosphate reservoir for ATP synthesis (Morash and Alter, 2016). Evidence also exists that abalone depend on phosphoarginine as an energy source during both environmental and functional anoxia. During periods of increased energy requirements (such as during hypoxia), energy stored as phosphoarginine is released to acceptors such as ADP, resulting in free arginine. Considering that octopine is the combination of arginine and pyruvate (in the opine pathway), it can be hypothesised that the released arginine binds pyruvate to restore NAD^+ levels for glycolysis, thereby acting in two important energy preservation pathways. Considering the importance of phosphoarginine in abalone's energy metabolism, it was proposed using the phosphoarginine:inorganic phosphate ratio, as an indicator of the energy status of the organism, rather than the change in adenylate energy charge (Viant *et al.*, 2001). Interestingly, we have

observed relatively high concentrations creatine in abalone muscle samples analysed with nuclear magnetic resonance spectroscopy (NMR) and liquid chromatography tandem mass spectrometry (LC-MS/MS). The latter suggests that abalone might also use creatine to store high-energy phosphates in addition to arginine. In the context of the abalone farm, it might be worthwhile to monitor the levels of these phosphagens, as a mean to ascertain how the energy levels in abalone vary in different farming conditions, for maximising abalone growth.

2.6 Where to from here?

Due to their relatively low energy requirements, and their hypothetically low mitochondrial activity, a number of compounds traditionally used for anabolism are also being used for energy production or to maintain NAD^+ levels in abalone. Despite the fact that in recent years there has been an increased effort to better characterise abalone metabolism, there is still much that is largely unexplained. Considering that abalone growth rates are the primary point of interest to the abalone farmer (van der Merwe *et al.*, 2011), a better understanding of abalone genetics, transcriptomics, proteomics and metabolomics would undoubtedly give clues to interventions which could optimise growth. This can be achieved through omics experiments comparing fast and slow growers, an approach previously used in oysters (Tamayo *et al.*, 2014). Considering the abalone omics research to date, van der Merwe *et al.* (2011), using transcriptomics and quantitative real-time polymerase chain reaction experiments, indicated that the genes associated with the insulin signalling pathway explain the growth variation of farmed *H. midae*. An Illumina Genome Analyzer was used to generate high-quality DNA, in order to characterise the *H. midae* transcriptome, and identified the expressed genes associated with important traits, like improved growth and disease resistance (Franchini *et al.*, 2011). Proteomic analysis carried out on the eggs produced from a hybrid abalone (*Haliotis discus hannai Ino* and *Haliotis gigantea*), and its parental lines identified 59 abalone proteins involved in energy metabolism, lipid metabolism, protein biosynthesis, electron carrier proteins, proliferation, apoptosis, signal transduction, immunity, decomposition and cytoskeletal structure (Di *et al.*, 2015).

The total number of primary metabolites found in all organisms is far less than the total number of genes, RNA transcripts and proteins present, and thus, an investigation of the genome, transcriptome and proteome alone is not considered sufficient as they do not necessarily accurately reflect the phenotype. As metabolomics is at the endpoint of the omics cascade, and the closest to the cells functional phenotype, it not only links the genotype and phenotype, but it is regarded as the final recipient of genetic information, as gene expression is ultimately reflected in changes of metabolite concentrations (Dettmer *et al.*, 2007, Tugizimana *et al.*, 2013).

2.7 Metabolomics

Metabolomics can be defined as the nonbiased identification and quantification of metabolites in a biological system, using highly selective and sensitive analytical techniques (Dunn *et al.*, 2005). Metabolites or small molecules within a cell, tissue, organ, biological fluid or the entire organism constitutes the metabolome (Lankadurai *et al.*, 2013), and are likely to contribute to the functional state of cells and serve as a direct signature of biochemical activity (Patti *et al.*, 2012). Considering this, using such an approach for investigating abalone growth patterns would undoubtedly result in a better understanding of the effects of various stressors or interventions on the abalone metabolome, possible metabolic pathways that are linked to growth and the polymorphisms influencing this.

Metabolomics analysis provides a snapshot of a biological system, hence those metabolites present at a given point in time, under a specific condition/perturbation (Tugizimana *et al.*, 2013). Depending on the aim of the study, a number of different metabolomic approaches can be used, including: 1) *targeted analysis* (where known analytes are measured in a quantitative way, each described in terms of their absolute concentrations), 2) a *semi-targeted approach* (that focuses on metabolites related to a certain class of compounds or metabolic pathway, described in terms of either absolute or relative concentrations) and 3) an *untargeted approach* (where the goal is to simultaneously measure as many metabolites as possible, with no particular focus or knowledge of the metabolites present beforehand, and described in terms of their relative concentrations) (Zelena *et al.*, 2009, Patti *et al.*, 2012, Esterhuizen *et al.*, 2017).

Even though metabolomics has emerged as a powerful research tool, there is currently no single instrument platform that can analyse all the metabolites present in a biological sample, mainly due to the vast concentration range and the diverse physical and chemical properties of the metabolites (Dettmer *et al.*, 2007). Additionally, the organism and sample type (blood, urine, tissue etc.) also contributes to the size and complexity of the metabolome (Dettmer *et al.*, 2007, Dunn *et al.*, 2011b). Thus, to achieve optimal coverage of the metabolome, it is advised that various metabolomic approaches and platforms be combined, and different samples from the same organism analysed.

2.7.1 Basic metabolomics workflow

A metabolomics experimental workflow generally consists of 1) specific sampling prerequisites determined by the experimental design, 2) sample preparation, 3) sample analysis, 4) data mining, 5) metabolite identification and 6) metabolite validation steps (Fig. 2.3). All of the steps should be carefully planned and completed in order to ensure usable datasets which can validate the experimental conclusions (Fiehn, 2002).

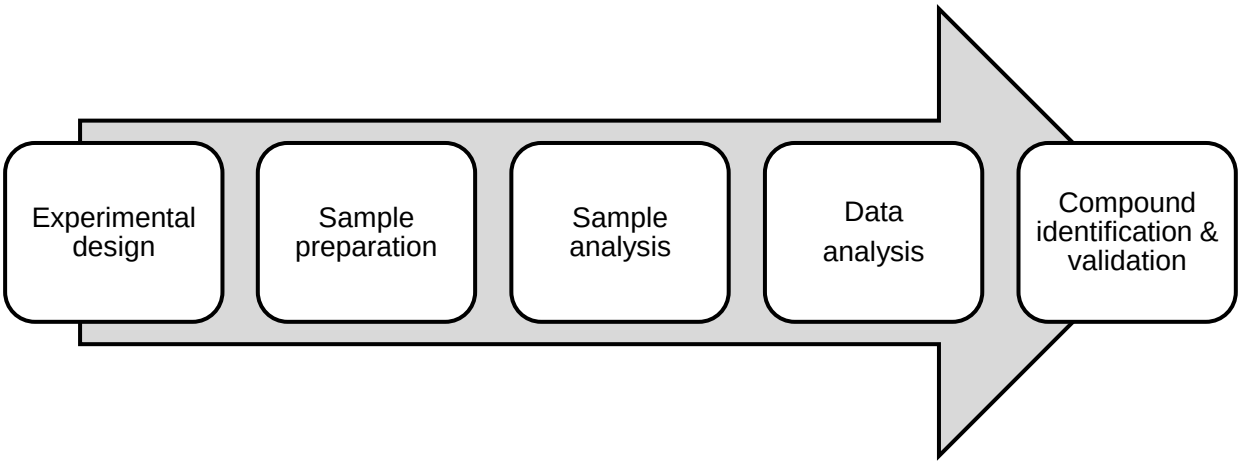

Figure 2.3: Typical metabolomics workflow. Subsequent to the experimental design and sample selection, sample preparation is performed, followed by sample analysis, data analysis and later compound of interest identification.

2.7.1.1 Experimental design

First and foremost, metabolomics experimental design, as with most other research disciplines, should ensure that the variation related to biological variance investigated, by far exceeds any variation introduced by the performance of the study (Dunn *et al.*, 2012). The selection of a model organism (e.g. abalone), a type of external stressor (e.g. temperature variations) and the mode of exposure (e.g. heating pump) are the first factors that need to be determined (Lankadurai *et al.*, 2013) in the context of relevance to the biological question. Cofounding biological, technical and experimental variability should be eliminated or kept to a bare minimum to allow optimal results (Young and Alfaro, 2016).

Part of the planning of the experimental design is also dependant on the type of samples chosen, that are best suited to answer the biological question. Sample selection is a critical step and greatly benefits from previous knowledge of the biological system under investigation. Sample selection is also dependant, however, on sample availability and practicality, considering non-invasive sample techniques and the type of analytical instrumentation available (Álvarez-Sánchez *et al.*, 2010a). The use of tissue samples for metabolomics research, allow for data generation of organ-specific metabolic fingerprints, while bio-fluids integrate the metabolic changes that occur systemically (Lin *et al.*, 2007). Cell cultures on the other hand, enable easy discrimination between extracellular and intracellular metabolites (Álvarez-Sánchez *et al.*, 2010a). Sample size is also of utmost importance, and in the case of metabolomics, large numbers of samples are beneficial to enhance statistical power, in order to ensure that even subtle differences within the subject cohort can be detected (Zelena *et al.*, 2009). Biological replicates of n = 5 is a proposed sampling measure made by the Metabolomics standards initiative (Sumner *et al.*, 2007). Also, the control and treated groups should if possible match

with regards to age, gender, size class, genetic background etc., for metabolomics research, as in the case of all other biological research disciplines, when selecting the experimental cases for sampling (Young and Alfaro, 2016).

The collection of samples should be done as quickly as possible in order to reflect the metabolic profile at the exact time of sampling. Ideally, fluid sampling or tissue dissection and sample analysis should be done simultaneously, but as it is not always possible, appropriate sample quenching and storage serves well (Álvarez-Sánchez *et al.*, 2010a). Quenching is a way of instantly halting all metabolic activity by freezing the samples with liquid nitrogen for example. Aliquoting samples at the time of sampling prevent unnecessary changes to the sample integrity induced by freeze and thaw cycles. It is also advisable to store the frozen samples at -80 ºC, preventing the recovery of enzyme activities (Lin *et al.*, 2007, Verpoorte *et al.*, 2008).

Various abalone samples, including: haemolymph (Behrens *et al.*, 2002, Malham *et al.*, 2003, Rosenblum *et al.*, 2005, Vosloo and Vosloo, 2006, Vosloo *et al.*, 2013a), muscle (Wells *et al.*, 1998b, Rosenblum *et al.*, 2005, Rosenblum *et al.*, 2006, Baldwin *et al.*, 2007, Laas and Vosloo, 2010, PÉRez-Estrada *et al.*, 2011, Vosloo *et al.*, 2013a, Venter *et al.*, 2016a, Venter *et al.*, 2017), digestive glands (Carefoot *et al.*, 2000, Rosenblum *et al.*, 2005, Rosenblum *et al.*, 2006, Laas and Vosloo, 2010, PÉRez-Estrada *et al.*, 2011), digestive organs (Garcia-Carreno *et al.*, 2003, Sheedy *et al.*, 2015), abalone eggs or larvae (Moran and Manahan, 2003), and gills (Vosloo *et al.*, 2013a, Lu *et al.*, 2016, Lu *et al.*, 2017), have successfully been used in metabolic studies. These metabolic studies, investigated the impact of: anoxia and exercise (Gäde, 1988, O'omolo *et al.*, 2003), air (Wells and Baldwin, 1995, Donovan *et al.*, 1999), starvation (Durazo-Beltrán *et al.*, 2004, Rosenblum *et al.*, 2005, Durazo and Viana, 2013, Sheedy *et al.*, 2015), toxins (Bae *et al.*, 2011, Zhou *et al.*, 2015, Lu *et al.*, 2017) and temperature fluctuations (Rosenblum *et al.*, 2006, Hooper *et al.*, 2014) to name but a few.

Regardless of the experimental samples used, it is important to analyse representative quality control (QC) samples as well, such as sample replicates, analytical replicates and method blanks (Dettmer *et al.*, 2007). Dunn *et al.* (2012) describes a quality control sample as a sample, which is the average of the composition of all samples studied. When working with abalone haemolymph, this can merely be a pooled sample, compiled from small amounts of all the individual haemolymph samples collected from the entire study population. It may also be possible to prepare a QC sample from a commercially available matrix (Want *et al.*, 2013). Typically, QC samples are extracted together with the samples selected for the particular analytical batch and analysed intermittently with these experimental samples, to evaluate and compare the quality of the analysis. The monitoring of QC data may be helpful when evaluating the analytical performance of both the analyst and the analytical platform (t'Kindt *et al.*, 2009).

Since repeatable metabolic analyses require retention time, signal intensity and mass accuracy to be stable throughout analyses, QC samples can be used to monitor these features of the analytical system, especially when analysing different sample batches. Furthermore, QC samples help to ensure conditioning of the analytical platform (Dunn *et al.*, 2012). More importantly, it allows for the filtering out of metabolites that are not reliably measured due to instability over time (in the sample vial) or when metabolites end up near the detection limit of the instrument (Dunn *et al.*, 2011a). Generally, a suitable QC sample should be injected at regular intervals to provide data, from which repeatability can be assessed (Want *et al.*, 2013, Fiehn, 2016).

2.7.1.2 Sample preparation

The sample preparation step usually involves metabolite extraction, derivatisation and resuspension, to ensure a suitable sample format for analysis using the selected analytical instrument (Wu *et al.*, 2008, Tugizimana *et al.*, 2013). Ideally, one would aim to use an extraction method that isolates only those metabolites of interest, while excluding macromolecules (such as proteins), which are of no interest for metabolomics analysis. Unfortunately, there is no single extraction method that results in the complete extraction of all metabolite classes present in a biological sample (Yang *et al.*, 2013), forcing the researcher to once again perform an extraction method that best fits the goal of the experiment (Lankadurai *et al.*, 2013). Unlike bio-fluids, tissue or cell culture samples have to be homogenised and metabolites extracted, prior to analysis. Various different techniques can be used for tissue homogenisation, including manual disaggregation of chilled tissue with scissors or manual homogenisers, cryogenically cooled pestle and mortar systems, and mechanical disruption appliances. The method of choice will be determined by the type of sample to be homogenised. Never-the-less, this is a labour intensive procedure, considered a bottleneck in the metabolomics workflow (Wu *et al.*, 2008, Want *et al.*, 2013).

A number of extraction methods are typically used to isolate free metabolites from the biological sample once it is homogenised (Kanani *et al.*, 2008). Those compounds of interest are typically divided into non-polar compounds (e.g. fatty acids), medium polar compounds (e.g. secondary metabolites) and polar compounds (e.g. amino acids) (Verpoorte *et al.*, 2008). An ideal metabolomics extraction method would need to be fast, reproducible, contain as few steps as possible and be unbiased, detecting a wide range of metabolites. Some of the methods used for extraction of compounds from biological samples include: liquid-liquid extraction, solid-phase extraction, microwave-assisted extraction and solid-phase micro-extraction (Moco *et al.*, 2007, Want *et al.*, 2013). Then again, more specific extraction approaches can also be performed

(e.g. fatty acid methyl ester, organic acid or amino acid extraction methods) depending on the group of metabolites required for investigation.

Liquid-liquid extraction strategies, based on the Bligh and Dyer's classic methanol-chloroform-water combination solvent solution, are commonly used for metabolomic investigations (Dettmer *et al.*, 2007, Wu *et al.*, 2008) and are also suitable for abalone sample extractions. This extraction approach is popular for metabolomics research applications, since it recovers both hydrophilic and hydrophobic metabolites from the sample (Lin *et al.*, 2007). Since metabolites within bio-fluids are already extra-cellular and in suspension, a simple preparation step such as protein precipitation can be used before untargeted analysis. A sample like haemolymph, for example, can be easily deproteinated using a solvent such as cold acetonitrile or methanol, followed by centrifugation (Poynton *et al.*, 2011).

Once the metabolites are extracted from the sample, it is important to ensure that they are now compatible with the analytical instrument, which will be doing the analysis. The preparation of samples for NMR analysis, for example, requires the addition of a chemical shift standard and a deuterium oxide-based (D_2O) phosphate buffer, to ensure a constant pH across all samples. The biggest drawback with the addition of aqueous buffers, is the fact that only polar metabolites will be extracted (Lankadurai *et al.*, 2013). When LC-MS is the selected technique, the extracted tissue samples can be evaporated under nitrogen and re-suspended in the mobile phase solvent used for analysis (Dettmer *et al.*, 2007). These are typically regarded as methods that require minimal sample preparation, but it should be noted, that these are usually more complex samples considering their compound composition, with high salt content which could result in ionisation suppression and interference (Álvarez-Sánchez *et al.*, 2010b). When GC-MS instruments are selected for analysis it is important to ensure that extracted compounds are in a volatile (or semi-volatile) state. Derivatisation of the sample components is often used to improve sample volatility, stability, sensitivity and selectivity and prevent reaction between the sample components and the GC system. Derivatisation is generally performed by silylation, which allows functional groups, with active hydrogen atoms to be trimethylsilylated by a silylation reagent like MSTFA/BSTFA [N-methyl-N-/bis-(trimethylsilyl) trifluoroacetamide] (Álvarez-Sánchez *et al.*, 2010b). Silylation is commonly used when analysing tissue samples or bio-fluids, due to their comprehensive chemical group coverage. To minimise the conversion reactions, such as keto-enol tautomerisation during silylation, oximation is performed prior to the silylation reaction with the use of methoxamine hydrochloride (Xu *et al.*, 2010).

2.7.1.3 Sample analysis

Before sample analysis, analytical methods should be validated and/or standardised first, in order to ensure reliability of the data. Using validated methods and appropriate quality control, it is possible to confirm the quality, reliability and consistency of the analytical results (Koek *et al.*, 2011, Naz *et al.*, 2014). Validation in itself is rather specialised, with several guidelines for both targeted and untargeted methods, as described by Koek *et al.* (2011) and Naz *et al.* (2014). Also, methods should be implemented in terms of a standard operating procedure to ensure repeatable results for comparison of experimental groups and also to allow inter-laboratory comparisons (Vuckovic, 2012, Emwas *et al.*, 2015).

A wide range of analytical platforms are currently available for metabolomics research, each has its own advantages and disadvantages. Since no individual analytical method can detect all the metabolites present in a sample, combinations of techniques are often used to maximise the information collected from the samples that were gathered (Lin *et al.*, 2006, Xu *et al.*, 2010). Multiplatform approaches, such as nuclear magnetic resonance spectroscopy (NMR), vibrational spectroscopy (infrared and Raman spectroscopy) and mass spectrometry (MS), using direct infusion or coupled to separation techniques (Dunn, 2008), are often used in a complementary manner to extend coverage of the metabolome, if available. Even though vibrational spectroscopy techniques, such as Fourier transform infrared, near/mid-infrared and Raman spectroscopy, are powerful non-destructive analytical tools, with application in a variety of biological fields (Dunn *et al.*, 2005); special focus will only be given to NMR and MS approaches in this study.

Nuclear magnetic resonance spectroscopy

Nuclear magnetic resonance is a widely used analytical technique, capable of generating structural information about chemically diverse metabolites in a non-selective way and is considered non-destructive to the sample (Lin *et al.*, 2006, Samuelsson and Larsson, 2008). Analyses of metabolites by NMR are based on the measurement of protons, by subjecting the atomic nuclei to a magnetic field and applying a specific radiofrequency pulse to change its energy state. In the presence of other nuclei, the chemical bond changes within the magnetic field and forces nuclei within a metabolite to absorb energy at a unique frequency (chemical shift), resulting in a unique spectrum (fingerprint) (Goldsmith *et al.*, 2010, Young and Alfaro, 2016). NMR requires little sample preparation and allows for absolute metabolite identification, based on the structural information provided. NMR, however, has the disadvantage of poor selectivity and sensitivity (Tugizimana *et al.*, 2013).

Mass spectrometry

Mass spectrometry is a popular choice for metabolomics experiments, since it is comparatively sensitive, and capable of generating rapid results with good metabolite quantitation and identification (Lin *et al.*, 2006, Moco *et al.*, 2007, Samuelsson and Larsson, 2008). Moreover, mass spectrometry-based experiments can be coupled to an array of separation techniques, including liquid chromatography (LC), gas chromatography (GC) and capillary electrophoresis (CE) (Samuelsson and Larsson, 2008, Viant and Sommer, 2013). The combination of such technologies enhances the selectivity of the instrument and allows for a larger coverage of the metabolome. The addition of high resolution mass spectrometers further increases the specificity by which metabolites can be detected. Commonly used mass analysers include: tandem-mass spectrometry (MS/MS), time-of-flight (TOF), quadrupole-TOF (QTOF), ion trap and Orbitrap detectors, all of which have their own pros and cons (Moco *et al.*, 2007, Patti *et al.*, 2012, Viant and Sommer, 2013).

Liquid chromatography mass spectrometry

Liquid chromatography mass spectrometry allows for the analysis of non-volatile, secondary metabolites (Tugizimana *et al.*, 2013). For liquid chromatography purposes, many different stationary and mobile phases are generally used for chromatographic separation. The principle of this technique is that the mobile phase passes through the stationary phase and separates the mixture of analytes, infused into the mobile phase via their variable interaction with the stationary phase (Wilson and Walker, 2010). The mobile phase typically consists of water, and one or more organic solvents (methanol, acetonitrile, isopropanol, tetrahydrofuran or a mixture thereof) of choice, with a mobile phase modifier, like ammonium formate, ammonium acetate, formic acid or acetic acid, typically required for improving ionisation and LC separation (Cajka and Fiehn, 2016). Similarly, many stationary phase columns are also available for LC-MS analysis (Lu *et al.*, 2008), with reversed-phase (RP), normal-phase and hydrophilic interaction liquid chromatography (HILIC) being the most popular of these (Cajka and Fiehn, 2016). Even though RP chromatography is the most widely adopted retention mechanism for the majority of analyses, it does lack the capacity to effectively retain very polar analytes. As an alternative, HILIC columns can be used when analysing polar and/or basic solutes, but also has its own set of drawbacks (Buszewski and Noga, 2012, Viant and Sommer, 2013). Analyte polarity can be overcome using various derivatisation strategies, such as butylation, to improve chromatographic retention of especially the polar metabolites, analysed on RP columns (Harder *et al.*, 2011). Mass spectrometers coupled to LC also come with a variety of ionisation sources, which are capable of generating ions from neutral metabolites in a sample, with the most common ion source used, being electrospray ionisation (ESI) (Viant and Sommer, 2013). Ionisation can be performed in either a positive or negative ion mode, but for maximum

metabolome coverage, it is advisable to utilise both (Want *et al.*, 2013). To summarise then, LC-MS offers both good sensitivity and selectivity, and is a popular choice for the discovery of unknown metabolites, due to the high mass accuracy, which can be achieved when used in combination with high resolution mass analysers and chemical standards (Young and Alfaro, 2016). Despite this, however, a drawback to LC-MS is the identification of metabolites, largely due to the complex and large number of unknowns in biological systems (Engskog *et al.*, 2016).

Gas chromatography mass spectrometry

Gas chromatography, is the most commonly used metabolomics technique, ideal for identification and quantification of small molecular metabolites (Fiehn, 2016). Gas chromatography exploits differences in the partition coefficients between a stationary liquid phase (typically a silicone grease or wax coated on the internal wall of the column) and a mobile gas phase (nitrogen, helium or hydrogen), as volatilised analytes are carried through the column by the mobile gas phase. Separated molecules then travel through a source chamber, in which hard ionisation and fragmentation of each compound occurs, which subsequently generates an electric signal in the detector. In the case of GC-MS, electron impact (EI) ionisation takes place in the ion source chamber, where a beam of electrons collides with the molecules to produce an ion, corresponding to a relative molecular mass of the compound being analysed (Wilson and Walker, 2010). When linking mass spectrometry with GC, the longstanding use of EI ionisation ensures high sensitivity, highly reproducible ionisation and high-chromatographic metabolite resolution, which are highly advantageous to compound annotation, on the basis of comparison of the generated mass spectra to that in previously generated compound libraries (Vinaixa *et al.*, 2016). GC-MS analysis is dependent on a compound being thermally stable and possessing a sufficient vapour pressure (Dettmer *et al.*, 2007). Matching spectra to these libraries should, however, be done carefully, since signal deconvolution, chemical derivatisation and column degradation may compromise accurate database matching (Vinaixa *et al.*, 2016).

To date, NMR is mostly used in the context of prior relevant abalone research (Rosenblum *et al.*, 2005, Rosenblum *et al.*, 2006, Sheedy *et al.*, 2015, Zhou *et al.*, 2015, Lu *et al.*, 2016, Lu *et al.*, 2017, Tripp-Valdez *et al.*, 2017). Very little LC-MS data for abalone samples exists, however, the work done in the current study, using LC-MS for opine analyses in abalone (Venter *et al.*, 2017), and its application for phosphoarginine analysis in abalone tissue (Viant *et al.*, 2001), justifies the application of this technique in abalone research activities. Metabolic profiling of abalone tissue extracts, using gas chromatography techniques, is relatively simple once the abalone samples have been extracted and derivatised (Venter *et al.*, 2016a). Lastly, vibrational spectroscopy techniques have also been previously applied, using near infrared

spectroscopy, to determine glycogen concentrations in the foot muscle of cultured abalone (Fluckiger *et al.*, 2011).

2.7.1.4 Data analysis

Metabolomics research generates large volumes of data in a high-throughput manner, which presents challenges if one wants to process this in the traditional manner (Lankadurai *et al.*, 2013). Therefore, any meaningful interpretation of the data requires the use of appropriate statistical tools, in order to correctly manipulate these large raw data sets, into a workable and understandable format (Issaq *et al.*, 2009). This typically includes: 1) data extraction; 2) data pre-processing and normalisation; 3) data pre-treatment and 4) statistical analysis.

Data extraction: Sample analysis, using any of the above analytical procedures, generates data which are stored as a series of chromatograms, spectra, masses, retention times, intensities, etc., collected at a given point in time or scan (Brown *et al.*, 2005, Dettmer *et al.*, 2007). The term “features” is used, as opposed to “metabolites”, when no additional verification of the specific compound has yet been done. A feature can be defined as a mass to charge (m/z) ratio at a specific retention time related to a molecular entity. Features can be detected as protonated and deprotonated ions, adduct ions, salt ions, fragment ions, dimers trimers, etc. Thus, the number of features in a sample will be more than the actual number of metabolites present once the data is processed, hence, the use of sophisticated software is required to group (deconvolute) all features belonging to the same compound. Features, however, are used as initial metabolite identifiers, and rely on exact mass searches against metabolite databases like the Human metabolome database (HMDB) or National Institute of Standards and Technology (NIST) database, in order to assign compound names to features (Do Yup Lee and Northen, 2010, Dunn *et al.*, 2011b, Dunn *et al.*, 2013).

Data extraction and data mining is initially required to gather information from raw MS data. The goal is to extract the raw data files into vectors, using a variety of software packages (Dettmer *et al.*, 2007). In the case of MS data, data extraction is generally performed using the following steps: 1) peak-picking (which allows for the detection of peaks from the baseline and background compounds), 2) deconvolution (the process that enables the separation of co-eluting peaks with their own mass spectra and retention time) and 3) alignment (resulting in the removal of shifts among samples) (Theodoridis *et al.*, 2008, Yi *et al.*, 2016). NMR strategies generally involve: 1) baseline correction (to allow for better metabolite quantification), 2) alignment (to ensure similar peaks) and 3) spectral binning (where NMR spectra is divided into regions or buckets of defined width, to allow for the determination of a fraction of the peak

intensity relative to the total signal, further reducing variation between spectra) (Craig *et al.*, 2006, Smolinska *et al.*, 2012).

Data pre-processing: Data pre-processing, can be considered the editing (compressing) of the instrument specific data into a usable size and format, while extracting the relevant analytical information for subsequent statistical analysis (Goodacre *et al.*, 2007, Nielsen *et al.*, 2010). As a starting point, uncommon variables not detected in most of the samples can be removed from the data matrix (Di Guida *et al.*, 2016), which is referred to as filtering. The type of filtering applied is dependent on the data and aim of the study. One such commonly used filtering method is "zero filtering", which permits the elimination of features with extensive missing values, thereby removing variables that contain no biological and/or statistical value prior to any statistical analysis (Venter *et al.*, 2015). An additional approach allows the filtering of features based on the coefficient of variation (CV), determined from the quality control samples (Engskog *et al.*, 2016). As a rule of thumb for untargeted analysis, features with a CV value larger than 50 % are eliminated from the data matrix (Luier and Loots, 2016). The next pre-processing step includes what has been termed "missing value replacement" (imputation). Missing values in the data typically occur if compounds in certain samples fall below the detection limit of the instrument, or if they were not measured in all of the samples consistently. Sometimes missing values result from biological origin and they can also emerge as outliers (Brown *et al.*, 2005, Steinfath *et al.*, 2008, Hrydziuszko and Viant, 2012). The software often ascribes a 'zero' to missing peaks or compounds, which is not a true reflection of the concentrations if, for example, the compound was below the detection limit. There are several options on how to handle missing values, which range from gap-filling (where the missing peak section of the chromatogram is integrated), missing value imputation (where the absent data is estimated), or missing value replacement (where the missing value is replaced with half the minimum value in the dataset or the mean or median of the metabolite concentrations over all samples) (Steinfath *et al.*, 2008, Xia *et al.*, 2009, Engskog *et al.*, 2016). The possibility of outliers should also be assessed and removed if present. Outliers are data points (samples or variables) that deviate from the distribution of the majority of the data (Goodacre *et al.*, 2007). Such outliers can be determined by simply looking at the ratio between the mean and median. Furthermore, the use of visualisation tools such as heatmaps, can allow for easy recognition of changing patterns in metabolite concentrations, which may additionally be used to indicate the presence of an outlier (Steinfath *et al.*, 2008, Xia *et al.*, 2015).

Normalisation: Data normalisation is an essential part of the data pre-processing procedure, as it warrants the removal of non-biological variation, which may occur due to intensity variations caused by technical or analytical reasons (Steinfath *et al.*, 2008, Engskog *et al.*, 2016). Calculating the relative concentrations of all compounds by comparison to the area of the

internal standard, is a popular normalisation approach (Luier and Loots, 2016). Alternatively, MS total useful signal (MSTUS) normalisation can be used, which does a compound/feature correction in accordance to the sum of all the component signals that are present in all the samples (Warrack *et al.*, 2009).

Data pre-treatment: Data pre-treatment allows the transformation of the cleaned data into a useable format for statistical analysis (Goodacre *et al.*, 2007). Data pre-treatment methods typically transform or scale the data, so that the highly abundant compounds do not overwhelm the multivariate statistical tests, and the less abundant (yet important) compounds are also given enough weight in order to be considered relevant in the statistical tests (van den Berg *et al.*, 2006, Goodacre *et al.*, 2007). These data pre-treatment steps can include: 1) centering (where the mean of each variable across the samples is subtracted), 2) scaling (where variables are divided by a scaling factor such as the standard deviation) and 3) transformation (where the variables are converted in a nonlinear way to remove heteroscedastic noise) (van den Berg *et al.*, 2006, Goodacre *et al.*, 2007). The use of generalised logarithm (glog) transformation allows an increase in the intensity of the weaker signals relative to the stronger ones, by calculating a transform parameter, which minimises the technical variance of the data (Parsons *et al.*, 2007).

Batch effect correction: As previously mentioned, metabolomic studies aim to make consistent measurements, accompanied by the minimum amount of technical variance. This is compromised during the analyses of large sample groups, where groups are separated into smaller batches, resulting in analyses of different batches on different days. Inconsistencies in the metabolite profiles analysed in the different batches may occur due to slight variation in the laboratory environment, variation to reagent composition or volumes and contaminant build-up on the analytical platform. When differences between batches occur, it is termed a “batch effect”, which is seen as the systematic, non-biological variation between the analysed sample batches within the experimental groups, due to circumstances or factors that occur during sample handling or the analytical process (Leek *et al.*, 2010, Luo *et al.*, 2010). These between-batch or within-batch effects should be corrected, prior to statistical analysis (Wehrens *et al.*, 2016), most often with the use of quality control samples. Assessment of the quality of the data is easily achieved by visualising the data generated from the QC samples, analysed via principle component analysis (PCA), where the QC samples cluster tightly together in the PCA when no batch effect is present (Want *et al.*, 2013). However, if a batch effect is detected, exploratory analyses must be carried out to identify the existence of the batch effect, followed by steps to quantify their effects (Leek *et al.*, 2010). Although, caution should be displayed when performing batch corrections, to prevent the inclusion of more unwanted variation.

Statistical analysis: The statistical methods used for studies aimed at identifying compound markers for biological interpretation, may differ from those approaches used for new biomarker discovery (Xia *et al.*, 2013). However, irrespective of the study design, both univariate and multivariate statistical methods are essential to fully explore/exploit the data.

The univariate analysis/comparison of data, allows the separate examination of each variable across the compared groups (Saccenti *et al.*, 2014). Tests such as Student's *t*-test, analyses of variance (ANOVA) or many other non-parametric equivalent tests, are commonly applied for such univariate assessments (Young and Alfaro, 2016). The Student's *t*-test is typically used to find statistically significant differences in metabolite levels between two experimental groups, with a general p-value < 0.05 (Bonferroni or False discovery rate corrected p-value), indicating that features differed significantly between groups (Lindeque *et al.*, 2015). Due to the fact that statistical significance does not necessarily imply that results are important in practice, the use of effect size (d-value) is often implemented as a measure of practical significance, which is independent of sample size, and a large difference (d > 0.8) is the desired outcome (Ellis and Steyn, 2003). Then again, for data with two influential factors, two-way ANOVA can be used to find significance in the metabolic change over time (Lindeque *et al.*, 2015).

Multivariate statistical analyses are typically used when variables need to be compared between groups, still taking into account their interactions with other variables as well (Liland, 2011). Large and complex datasets are best assessed with multivariate methods, which may include PCA, projection to latent structures discriminant analysis (PLS-DA) and other clustering methods. All of these approaches give an overview and visual representation of the data, pinpointing discriminating features responsible for sample grouping (Engskog *et al.*, 2016, Young and Alfaro, 2016). PCA is the most commonly used unsupervised multivariate test currently used in metabolomics, since it is an unsupervised statistical approach, which does not use any prior knowledge to guide the analysis (such as group labels). PCA finds the directions of maximum variance in a data set (X), while ignoring the class labels (Y), meaning that grouping of the sample scores is solely based on the similarities/differences between their metabolic profiles (Christin *et al.*, 2013, Lankadurai *et al.*, 2013, Saccenti *et al.*, 2014). PCA therefore indicates whether or not natural separation between experimental groups exists, based on the underlying differences/similarities in each sample's metabolite profile. Multivariate statistics subsequently give additional information in the form of recognition of patterns, group structures, and metabolite and sample relationships (Young and Alfaro, 2016), which univariate statistical approaches miss.

2.7.1.5 Compound identification

Currently, the biggest challenge in metabolomics is metabolite nomenclature or identification. Over the last couple of years, a number of strategies have emerged to assist with assignment of peaks and the extraction of new knowledge (Bundy *et al.*, 2009). Databases and compound libraries, such as the HMDB and Metabolite and tandem MS database (METLIN), have been created to assist in compound name allocation, by comparison of accurate mass of a detected peak to that of known compounds in the database. Once a database match is made, the possible metabolite name assigned must be confirmed by further matching MS/MS data and retention time index of the model compound, to the feature in the original sample (Patti *et al.*, 2012). However, databases do not contain experimental spectra of every possible metabolite for any given biological system, thus other computational strategies and *in-silico* fragmentation software tools are also often used for the identification of novel metabolites (Engskog *et al.*, 2016). It is further important to note that the number of detected signals is far less important for metabolomics analysis than the number of identified metabolites. If only one metabolite can be identified with certainty, it is more meaningful than a hundred unidentified signals. Keeping in mind that our current level of knowledge of those metabolites present in a sample-specific metabolome are far from complete, and that features can be related to unknown endogenous metabolites and exogenous metabolites (from diet, lifestyle, gut flora, pharmaceuticals etc.), care should be taken when building biological conclusions based only on putatively annotated metabolites (Dunn *et al.*, 2013). Furthermore, metabolites not involved in the classical function of anabolism or catabolism (i.e. epimetabolites) are largely ignored, and the discovery thereof would require high resolution-mass spectrometry accompanied by *in-silico* fragmentation prediction tools, which warrant a much more detailed identification process (Showalter *et al.*, 2017).

Currently, quantitative and alphanumerical scoring systems are being developed with the hope of adding additional confidence levels to the identified metabolites. By using such systems, a minimum score value for a confident metabolite identification can be set. In order to achieve biochemical and biological meaning from the data, accurate metabolite identification is critical (Sumner *et al.*, 2014). An alternative set of guidelines were proposed by Schymanski *et al.* (2014), where identification confidence levels are assigned to findings. In brief, low-confident identities, based only on accurate mass and isotopes patterns, are considered as a Level 5 and Level 4 identity, respectively. When fragmentation spectra can be added to the identification, a Level 3 will be assigned. Once a probable structure can be matched to information in an orthogonal library, a Level 2 identification is considered. When a reference standard (and a subsequent retention time match) can be matched to the compound of interest, the highest confidence is achieved, resulting in a Level 1 identification (Schymanski *et al.*, 2014).

2.7.1.6 Validation

Metabolomic studies are mainly performed with the aim to identify those metabolites that assist in understanding a biological process or serve as biomarkers to the perturbation. In terms of better understanding a biological mechanism, the accurate identification of metabolites is crucial in interpreting the mechanistic metabolic changes associated with the intervention or phenotype (through automated or manual pathway analysis or interpretation). For biomarker discovery, a feature or subset of features that allow maximum discrimination between the experimental groups is required, followed by performance evaluation (statistical assessment and validation of the biomarkers) and lastly, final model creation (combination of the selected features into a single test score) (Xia *et al.*, 2013).

2.7.2 Implementation of metabolomics

From an environmental science point of view, metabolomics can be utilised for biomarker discovery; disease diagnosis and monitoring; risk assessment of toxicant exposure; determination of metabolite profiles correlated with the physiological status; and characterisation of metabolic perturbations due to stress or effects of temperature, water, food availably, disease, etc. (Lin *et al.*, 2006, Bundy *et al.*, 2009, Motti, 2012). In 2006, Rosenblum *et al.* suggested that metabolomics should be further developed and integrated as a complementary tool for characterising and identifying pathological events affecting various aquatic species. It was further suggested that metabolomics could be useful in better understanding drug–host–pathogen interactions and the outcome of drug treatments in these aquatic species. Now, 10 years later, it is still believed that the potential of metabolomics research, with regards to aquaculture, has yet to be realised (Alfaro and Young, 2016). Although metabolomics as a research tool is still in its infancy stages, the use of metabolomics for aquaculture applications is highly relevant (Young and Alfaro, 2016), especially considering the well-established value chain for aquaculture products (especially abalone) currently in place, the potential to expand as the market grows and the recent advancements in metabolomics.

2.8 Conclusion

In *H. midae*, as is the case in most other commercially important abalone species, slow growth rates are the biggest obstacle for achieving profitability and global competitiveness of this species. Ongoing research into the intricate and somewhat unique biochemical processes of abalone is needed to better understand growth, which ultimately includes a better understanding of their metabolism and the factors influencing this. After a thorough study of the literature, it was determined that little is really known about the metabolism of abalone. Some important theories arose from this study, which could actually impact the farming industry

considerably – such as the hypothesis that abalone have very few mitochondria and thus low respiration rates. Subsequently, abalone rely comparatively more on other metabolic pathways for energy production, which in turn may give clues to improved feeding approaches. In that respect, a global picture of abalone metabolism, under normal and stressed conditions, is needed to predict the physiological traits associated with growth rates, body weight, food conversion efficiency, disease resistance and flesh quality, and also to optimise nutrient supply and other farming conditions. Systems biology studies, such as metabolomics on *H. midae* are generally scarce and would greatly contribute to the elucidation of these metabolic processes. Clarification of the abalone metabolome would also be considered a valuable approach to identifying biomarkers of growth, stress and health.

CHAPTER 3

STUDY DESIGN

“For many problems there is an animal on which it can be most conveniently studied.”

-The August Krogh Principle

3.1 Introduction

As previously discussed, *Haliotis midae* farming is a major contributor to the South African aquaculture sector, contributing millions of dollars to the country's exports economy. Even though abalone are cultivated under identical farming conditions, originating from homogenous genetic stocks, variation is experienced in individual abalone growth rates, justifying further research into the mechanisms related to these growth differences, especially considering the importance of this to the productivity of this very successful farming sector for South Africa. In effect, this variation in growth rates result in financial implications, as some animals will need to be taken care of for longer periods of time. Insights into the intricate and unique biochemical processes of abalone would help in finding answers to the various metabolic factors related to varied abalone growth rates. Unfortunately, there is a lack of abalone metabolism data, especially relating to the altered metabolic response as a result of a perturbation. Growth, in terms of the relationship between anabolism (biosynthesis) and catabolism (biodegrading), serves as the dominant topic in this thesis, and with this in mind, the abalone experiments conducted, abalone tissue samples collected, sample preparation methods and analytical platforms, were chosen and standardised to enable investigation into the overall metabolic mechanisms of *Haliotis midae*.

3.2 Experimental approach

In order to investigate the metabolic changes associated with abalone growth, samples were collected from *Haliotis midae* and a metabolomics research approach was used. To accomplish this it was required to: 1) standardise the metabolomics methods used; 2) perform various perturbations on the abalone in order to capture a) metabolic changes brought by anaerobic respiration and b) growth variation; 3) investigate these changes on various tissue samples; 4) determine the sample preparation methods that should be used and 5) utilise multiple analytical platforms for data collection of metabolic changes. It is noteworthy to emphasise that the possibilities pertaining to the above-mentioned factors are endless when conducting research, and even though some of the steps completed as part of this study are not the best, newest or easiest, the factors given here are chosen, based on comprehensive literature research, fit for a purpose, previous knowledge and availability of analytical equipment.

The overall experimental approach followed in this study is illustrated in Fig. 3.1, with detailed explanations of each of these experiments, documented in the relevant chapters to follow. First and foremost, method standardisations were performed to ensure compatibility of abalone samples with the in-house methods currently used for metabolomics analysis. Once methodology verifications were complete, various perturbations on abalone were conducted. The first perturbation involved exposing abalone to anaerobic stress, as it forms a significant part of their lifecycle, and subsequently determining what the impact of hypoxia would be to their metabolome, using data collected from left gill, right gill, epipodial tissue, foot muscle, adductor muscle and haemolymph samples. The second set of experiments included monitoring of farm animals relating to growth variation. Following interval sampling episodes, abalone adductor muscle samples were collected for determination of metabolic alterations experienced during the farming period. Following both sets of experiments, the animals were sacrificed, dissected and abalone tissues and haemolymph were collected and stored for later analyses. Sample preparation included homogenisation of samples to enable metabolite extraction, after which the samples were prepared to ensure compatibility with the various analytical platforms. Analytical platform analyses comprised of untargeted gas chromatography-time of flight spectrometry (GC-TOF) analysis, untargeted ultra-performance liquid chromatography-ion mobility-quadrupole time of flight spectrometry (UPLC-IM-QTOF) analysis, untargeted nuclear magnetic resonance (NMR) spectroscopy analysis, semi-targeted gas chromatography-mass spectrometry-detector (GC-MSD) analysis of fatty acid methyl esters (FAMEs), semi-targeted butyl ester liquid chromatography-quadrupole time of flight mass spectrometry (LC-QTOF) analysis and targeted butyl ester liquid chromatography-tandem mass spectrometry (LC-MS/MS) analysis. Various standardised metabolomics data clean-up and processing procedures were performed, followed by statistical analyses in order to identify which compounds varied most when comparing the experimental groups in each experiment. These metabolite markers were subsequently interpreted in the context of the biological question, in order to better understand the impact of the perturbation on the metabolism and growth of abalone.

On the basis of the workflow demonstrated in Fig. 3.1 the choice that led to the design of this study is discussed and motivated in the subsequent subsections.

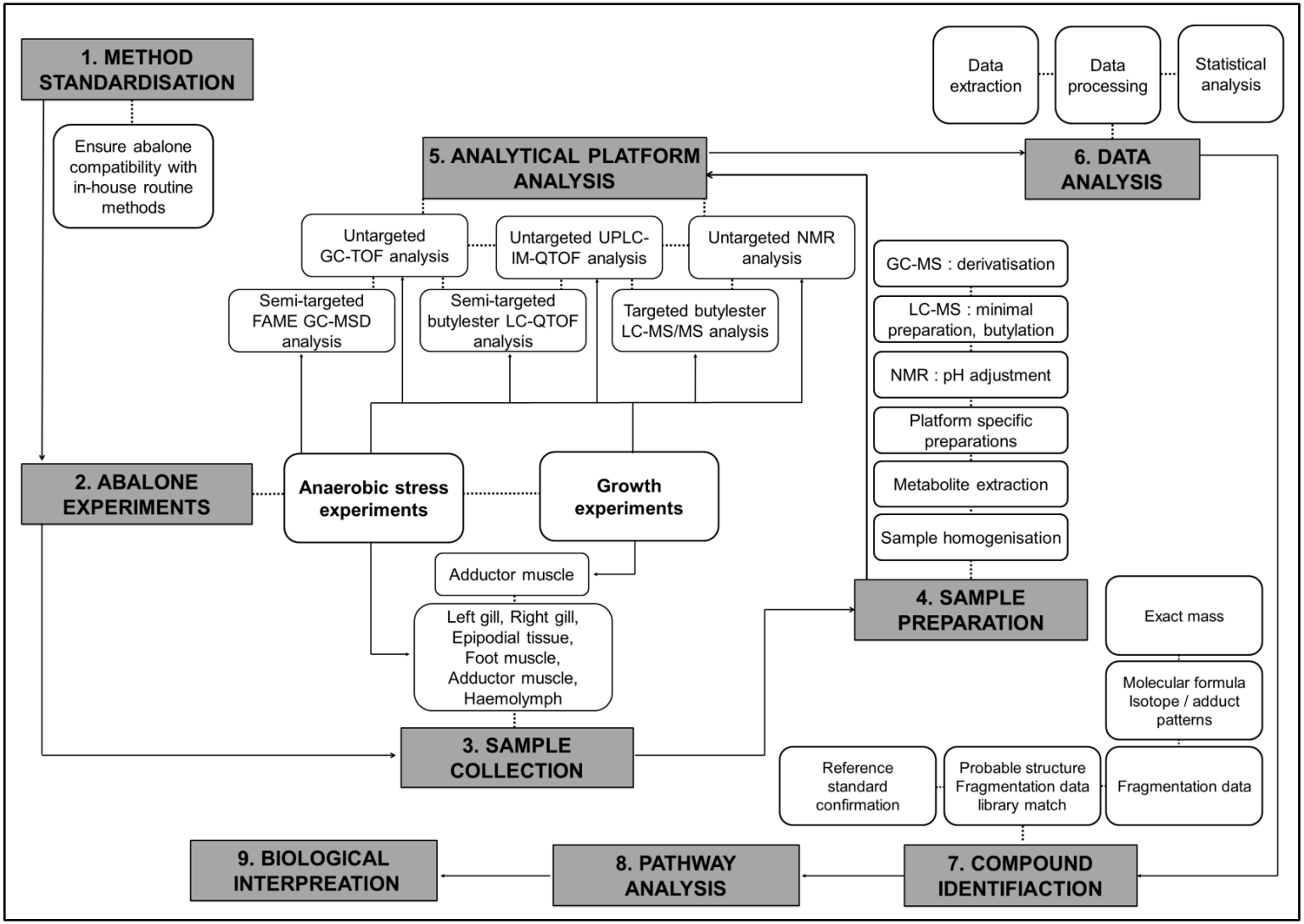

Figure 3.1: Experimental approach. Workflow followed throughout this study including: method standardisation, abalone experiments, sample collection, sample preparation, analytical platform analysis, data analysis, compound identification, pathway analysis and biological interpretation.

3.2.1 Method standardisation

The primary focus of this study was not to redevelop and validate all factors concerning metabolomics research, but to merely implement the current in-house standardised methods routinely used at the North-West University's (NWU) Metabolomics Platform. Thus, sample preparation and analytical methods were just adapted to ensure compatibility of the various abalone samples collected.

3.2.2 Abalone experiments conducted

Abalone are not only considered model farming animals (Cook, 2014), but also ideal experimental animals from a metabolomics research perspective, since most of the sample selection factors considered vital for a metabolomics experiment can be easily adhered to. Ideal sample selection for metabolomics analysis, involves collecting samples from control and treatment groups, which have the same genetic backgrounds, age, size, gender etc. (Young and Alfaro, 2016). The experiments implemented in this study enabled one to select experimental animals from the same animal breeding cohort, resulting in controls that are identical to the treatment groups, considering all possible confounding factors, with the exception of the perturbations. The anaerobic stress experiments were executed to force abalone to activate their anaerobic metabolic pathways, which were subsequently used for the construction of a "blue print" of an abalone metabolic map. The growth experiments on the other hand, served as a replica of normal farming practices, and the consequences thereof, on their metabolism. Successively, the metabolic map created from the hypoxia experiments could be used to fit metabolic findings of the farming growth experiments.

3.2.2.1 Anaerobic stress experiments

Invertebrates have the capacity to invoke unique metabolic adaptations to cope with situations of oxygen deprivation, (typically experienced when there is an increase in water temperature or a decrease in the dissolved oxygen content), by predominantly switching to metabolic pathways involved in anaerobic respiration. Since hypoxia can occur at any instance, fast and easily reverted cellular responses are required to survive such hypoxic episodes. As biochemical modifications can instantly come into effect, this forms the basis for survival during such hypoxic conditions (Bacchiocchi and Principato, 2000).

Considering the above, in this investigation, *Haliotis midae* were subjected to: 1) functional hypoxia and 2) environmental hypoxia (specifications of both experiments are given in Chapter 5). To date, no holistic investigation has been done on the metabolic adaptations used by abalone for energy production, growth and survival during anaerobic conditions and their

associated anaerobic metabolic pathways. Single point metabolic changes taking place in abalone during hypoxia (e.g. the production of D-lactate) are known and were considered when constructing a metabolic map of abalone metabolism, together with the metabolite markers detected in this metabolomics research study. This information was additionally used, to expand on the existing metabolic map of abalone.

The environmental hypoxia experiment served to demonstrate the metabolic response to the most extreme natural environmental perturbation known. During such conditions, it is expected that all available energy would become depleted, causing abalone to utilise alternative means for energy production. After exposure to environmental hypoxia, available energy is most likely utilised exclusively for survival and no longer for growth, making this the opposite metabolic response of growth. The functional hypoxia experiment is a more likely anaerobic metabolism activation method, which will in turn keep aerobic glycolysis going, as a degree of oxygen will still be present within the cell. This assessment is also required, as it serves as a metabolic state between “normal” and “extreme”, where the findings obtained by this less extreme hypoxia serves as confirmation of the environmental hypoxia experiment findings.

3.2.2.2 Growth experiments

This experiment was conducted within the standard farming parameters of HIK (Pty, Ltd, Hermanus, South Africa) abalone farm. Abalone reared under controlled hatchery conditions, were used to analyse the metabolic basis underlying inter-individual differences in growth rates. To study the inter-individual difference, a nested case-control study was designed with three sampling times (as described in Chapter 6). Briefly, abalone were sampled at a time serving as control (baseline) specimens, after which the animals were cared for in compliance with the day to day farming activities. After a four-month and eight-month time period respectively, sample collection occurred again. Sampling at the second and third time intervals included collection of animals: 1) of two different abalone ages, 2) receiving two different artificial feeds and 3) grouped into two different growth rates (i.e. slow and fast growing abalone).

Both juvenile and adult abalone were assessed to minimise any bias associated with age. It is known that younger animals have higher initial growth rates than older animals, both in terms of body mass and shell length (Laas and Vosloo, 2010). Thus, by analysing abalone of two different age groups, a better understanding of age on growth can be determined and accounted for.

Growth is undoubtedly influenced by dietary nutrients and implementation of a second feeding regime supplemented with an enhanced amino acid, which makes sense from a metabolic

perspective, considering that amino acids are predominately used for growth under normal conditions and energy production in abnormal/stressed scenarios (Venter *et al.*, 2016b). The animals receiving the modified artificial feed were compared to those on standard abalone feed, and interpretation of the metabolomics data allowed determination of growth advantages and/or survival benefits for the farm animals, supplied with the enriched feed.

Classifications of slow and fast growing abalone in these experiments were based on abalone from the same farming baskets, in order to ensure that specimens used in the comparisons had the same size at well-defined abalone grading intervals. Despite the fact that all abalone in a basket are typically the offspring of a small number of parents, who have very little genetic variation, and are selected from the stocks via grading on similar size, variation in growth rates still occurs, despite the environmental and feeding conditions being identical (Venter *et al.*, 2016b). This irregular growth rate variation is largely not understood and will be investigated using metabolomics, considering that metabolites serve as a direct signature of biochemical activity and subsequently, abalone growth. From a real-world application perspective, understanding the reasons as to why certain animals grow faster than others, and additionally their response to hypoxia, would be expected to lead to a better understanding of growth, and subsequently optimise this and abalone farm productivity. Furthermore, various markers may be identified, which additionally, can be used for monitoring growth and health in these animals, also positively influencing productivity, as early growth delays can be identified and addressed immediately.

3.2.3 Sample collection considering tissue specific functions

When conducting metabolomics experiments, some knowledge of the biological system is required for proper selection of tissues or bio-fluids, and their suitability for the given experiment and the analytical approach (Young and Alfaro, 2016). Since different tissues have specific metabolic processes, associated with their specific functions in the biological system, the choice of tissue sampled for a metabolomics investigation is strongly dependant on the aim of the experiment. Sampling of the abalone adductor muscle, foot muscle, left gill, right gill, haemolymph and epipodial tissue samples, were selected for analysis in order to accomplish the aims of this investigation (comprehensive sampling procedures are given in Chapter 4).

Following hypoxia, certain tissues may become anoxic and others not (Ellington, 1983). For this reason, a comprehensive sampling approach was followed, collecting six different tissues in the hypoxia experiments. Analyses of solely the adductor muscle were conducted on animals forming part of the growth experiments, since this is considered the sought-after part of abalone used as primary export produce. South African abalone have unique gustatory properties, and

together with their pale cream to light brown foot colour, *Haliotis midae* is regarded an important commercial species (Muller, 1986, Sales and Britz, 2001). Thus, the metabolic process influencing growth of the muscle section is of utmost interest from a farming perspective, and hence most relevant to this study.

3.2.3.1 Adductor and foot muscle

The foot region (adductor and foot muscle) constitutes about 66 % of the total body mass of abalone, and is comprised of different muscle fibre types, which are expected to have different metabolic end products (Venter *et al.*, 2016b), since they perform different functions. The adductor muscle is used to pull down the animal's shell for protection and for righting when dislodgment takes place. The foot muscle, however, is used for slow gliding movements (Gäde, 1988). The major muscle section is the sought after edible part of the abalone, commonly canned or frozen for exportation. Research on this section of abalone can be regarded as vital, as abalone are grown and cared for with the sole purpose of supplying abalone (more specifically muscle) of market size to the demanding market. The assurance of growth of the muscle section requires a number of important metabolic processes, needing to be clarified within this study.

3.2.3.2 Left and right gill tissues

Abalone have a pair of bipectinate gills located below the shell pores, but due to shell asymmetry, the left gill is larger than the right gill. The gills are capable of high oxygen extraction efficiencies and are responsible for oxygen uptake under circumstances of both normoxia and hypoxia (Ragg and Taylor, 2006, Leighton, 2008). During normoxic conditions, routine metabolism is supported by the right gill, which is continuously perfused. In hypoxic conditions, however, the left gill is recruited to enhance the surface area and oxygen uptake (Ragg and Taylor, 2006, Lu *et al.*, 2016). As the main interface between aquatic organisms and the external environment, the gills are the first line of protection against a wide range of stressors, and was reported to be more susceptible to hypoxic stresses (Lu *et al.*, 2016). Considering the importance of both gills during normal and stressed conditions, it was deemed fit to include both gill samples in this metabolomics investigation.

3.2.3.3 Haemolymph

Collection of haemolymph can potentially be used as a non-destructive sampling method to identify markers which may provide an early warning to a stressor (Hooper *et al.*, 2014, Roznere *et al.*, 2014), and can be collected from adult abalone via the pallial sinus, without any harm to the animal (Vosloo and Vosloo, 2006). Furthermore, adaptive responses to hypoxia, like acid-base balance modifications, have been reported in *H. diversicolor supertexta,* following

haemolymph investigations (Cheng *et al.*, 2004). Haemolymph also represents the exo-metabolome, as metabolic end products are released into haemolymph, which fills the spaces around organs. From here, the products can be used for respiration or simply be excreted (Ellington, 1983). The preparation of haemolymph samples for metabolomics analysis is also relatively easy when compared to muscle preparation, since no homogenisation is required. Considering all of the above, haemolymph would be considered the sample of choice, considering that collection of this sample is non-invasive, and would subsequently serve as an excellent sample for health and growth monitoring.

3.2.3.4 Epipodial tissue

The foot of abalone is surrounded laterally by the epipodium, which contains sensory tentacles enabling abalone to detect/feel its environment (Morash and Alter, 2016). It is also believed that the epipodium assist with oxygen uptake in abalone (Taylor and Ragg, 2005). Sampling of abalone epipodial tentacles, has been reported to be used successfully as part of a non-destructive tissue sampling approach in abalone (Slabbert and Roodt-Wilding, 2006), however, no metabolite information is available as yet.

3.2.4 Sample preparation

The homogenisation, metabolite extraction, derivatisation and analysis steps are identical to those used as part of the standardised metabolomics methods of the NWU, however, these methods were verified using abalone tissue samples, ensuring adequate sample size for metabolic extraction. According to the International Organisation for Standardisation (ISO) 9000 documentation (ISO, 2005), verification is merely confirmation (through objective evidence) that specified requirements have been fulfilled that are fit-for-purpose, and in this case, precise and adequate metabolite levels. Some important selected specifications regarding the metabolomics workflow will be motivated below.

3.2.4.1 Homogenisation and metabolite extraction

The techniques utilised for sample preparation strongly depend on the biological sample collected and the analytical platform used for analysis of the extracts (Young and Alfaro, 2016). It is important to note that no single extraction method can isolate all metabolites within a sample with equal efficiency (Duportet *et al.*, 2012), nor can a single analytical platform analyse all compounds. Hence, following standardisation, the methods selected for metabolite extraction in this study were deemed fit-for-purpose, precise, fast and relatively unbiased. Simultaneous homogenisation and metabolite extraction from the aforementioned tissue samples, were carried out by using the appropriate solvents and a vibration mill. A simple methanol,

chloroform, water extraction method was used for tissue metabolite extraction in this study. The reason for the biphasic extraction, was to recover both hydrophilic and hydrophobic metabolites (Dettmer *et al.*, 2007, Lin *et al.*, 2007, Wu *et al.*, 2008). This technique displays satisfactory results in terms of sample throughput, precision, extraction yield and lipid partitioning for both NMR and MS analyses (Wu *et al.*, 2008). Since metabolites in haemolymph are already in suspension (and do not require extraction from cells), a simple protein precipitation step was deemed sufficient for this purpose. Acetonitrile deprotonation was selected, as it removes proteins sufficiently without compromising the metabolite levels (Poynton *et al.*, 2011).

3.2.4.2 NMR analysis

Extracts for NMR spectroscopy analysis were re-suspended in a phosphate buffer at pH 7.4, the latter of which is important to ensure compound stability and prevent a chemical shift, subsequently resulting in more accurate matches to databases using the same pulse sequences (dependant on pH) (Beckonert *et al.*, 2007).

3.2.4.3 LC-MS analysis

The use of LC-MS enables one to use a multitude of columns, mobile phase modifiers and ionisation conditions, in both positive and negative ion modes. For tissue extracts, reverse phase columns (typically C18-bonded silica) served well to retain and separate moderately-polar and nonpolar metabolites (Want *et al.*, 2013). In this study, untargeted LC-MS analysis was conducted on a reverse phase C18 - Waters T3 column, and semi-targeted and targeted LC-MS analysis on a reverse phase C18 - SB-Aqua column. Both columns can however handle a 100 % aqueous mobile phase and are designed to also retain highly polar analytes.

For enhanced metabolome coverage during untargeted metabolomics experiments, it is advisable to perform both positive and negative electron spray ionisation (Want *et al.*, 2013). However, one would expect to detect only those metabolites containing C, H and O elements via LC-MS in negative ionisation mode, and metabolites containing C, H, O and N elements when using a positive ionisation (Want *et al.*, 2010). Hence, we used only positive electron spray ionisation in this study. The mobile phase used for the LC-MS analyses consisted of water (phase A) and acetonitrile (phase B), with the addition of 0.1 % formic acid, the latter of which enhances ionisation (Want *et al.*, 2013).

In this study, butylation was used as a derivatisation technique for semi-targeted and targeted LC-MS analysis (Venter *et al.*, 2017). Butyl ester formation at the carboxylic acid end of the amino acid is achieved by derivatisation reagents such as butanolic hydrogen chloride (HCl).

Not only does butylation allow for improved sensitivity and selectivity, but also improved chromatographic retention of polar amino acids on a C18 column (Harder *et al.*, 2011).

3.2.4.4 GC-MS analysis

The diverse physio-chemical properties of various metabolites pose a challenge to their simultaneous analysis. Subsequently, various derivatisation strategies, which chemically modify a compound to produce a new compound that has properties more conducive for analysis via a specific analytical method, are often used to overcome such difficulties (Pawliszyn, 2012). For the purpose of GC-MS analyses, derivatisation via silylation is most commonly achieved with the use of BSTFA and TMCS (Catrinck *et al.*, 2013). Subsequently, a trimethylsilyl (TMS) group is added to each hydroxyl-, or carboxyl-, amino-, or thiol- group, displacing the hydrogen in the process, which facilitates GC-MS detection due to the increased volatility of the formed compounds (Fiehn *et al.*, 2000, Kanani *et al.*, 2008, Fiehn, 2016). Also, in order to minimise conversion reactions (like keto-enol tautomerization) during silylation, an oximation reaction is used prior to silylation, using methoxamine hydrochloride (Xu *et al.*, 2010).

Furthermore, methylation of possible lipid compounds was included in the sample preparation method to yield fatty acid methyl esters (FAMEs) and allow for subsequent analyses of these fatty acids (Roberts *et al.*, 2008). Methylation of a total lipid extract was performed using a base-catalysed method, followed by silylation, oximation and GC-MS analyses (Willers *et al.*, 2016). Methylation was only included on the samples collected from the hypoxia experiments as proof of concept implementation, considering that abalone tissues are known to have low lipid contents (Vosloo and Vosloo, 2010).

3.2.5 Analytical platforms

Even though metabolomics has emerged into a powerful research tool, there is currently no single analytical instrument that can analyse all the metabolites present in a biological sample, mainly due to the vast concentration range involved, and the diverse physical and chemical properties of metabolites (Dettmer *et al.*, 2007). Thus, multiplatform approaches are necessary to extend coverage of the metabolome. Nuclear magnetic resonance spectroscopy and mass spectrometry are two of the most commonly employed analytical methods used in metabolomics (Wu *et al.*, 2008), each with their own pros and cons. NMR spectroscopy is appropriate for a wide range of metabolites (if large sample volumes for analysis are available), GC-MS is used for the analysis of volatile organic compound and derivatised metabolites belonging to the primary or central carbon metabolism, and LC-MS for the analysis of secondary metabolites and a wider range of semi-polar compounds (t'Kindt *et al.*, 2009, Zhang *et al.*, 2012). In this study, the combined used of NMR, LC-MS and GC-MS techniques were

used to detect a wide range of metabolites present in a biological sample, likely consisting of amino acids, carbohydrates, organic acids, peptides, nucleic acids, alkaloids and inorganic species etc. (Zhang *et al.*, 2012).

Metabolomics analysis provide a snapshot of a biological system and subsequently information of the metabolite concentrations in a sample at a given point in time, induced by a specific condition or perturbation (Tugizimana *et al.*, 2013). Depending on the aim of the study, a number of different metabolomics approaches can be followed to obtain this snapshot. Typically, metabolomics can be divided into targeted (hypothesis testing) and untargeted (hypothesis generating) approaches (Fiehn, 2002). Due to the lack of hypotheses or pathways to monitor growth in abalone, it was decided to make use of an untargeted metabolomics approach to answer newly formulated questions. In order to get high metabolome coverage (as well as some quality data), we incorporated different analyses including: untargeted NMR, LC-MS and GC-MS analysis, semi-targeted LC-MS analysis of butylated compounds and semi-targeted GC-MS of fatty acid methyl ester compounds, and lastly targeted LC-MS analysis of selected metabolites, especially set up and standardised for this purpose as part of the outcomes of the study.

Information describing the remaining steps included in the experimental approach (Fig. 3.1) giving details regarding data analysis, compound identification, pathway analysis and biological interpretation can be found in Chapter 4 (Sections 4.6 – 4.8).

CHAPTER 4

GENERAL MATERIALS AND METHODS

"Measure what is measurable, and make measurable what is not so."

– Galileo Galilei

Publications from this chapter:

VENTER, L., JANSEN VAN RENSBURG, P. J., LOOTS, D. T., VOSLOO, A. & LINDEQUE, J. Z. 2016. Untargeted metabolite profiling of abalone using gas chromatography mass spectrometry. *Food Analytical Methods*, 9, 1254-1261.

VENTER, L., JANSEN VAN RENSBURG, P. J., LOOTS, D. T., VOSLOO, A. & LINDEQUE, J. Z. 2017. From untargeted LC-QTOF analysis to characterisation of opines in abalone adductor muscle: Theory meets practice. *Journal of Chromatography B*, 1071, 44-48.

4.1 Introduction

In this chapter, all of the detail regarding the: 1) reagents, standards, solutions, consumables and equipment used in the various analytical experiments; 2) collection, dissection and preparation of the biological samples; 3) analytical parameters used during instrument analysis and 4) data processing methods performed, will be described. Analytical analysis included the use of: 1) untargeted nuclear magnetic resonance (NMR) spectroscopy; 2) untargeted ultra-performance liquid chromatography-ion mobility-quadrupole time of flight spectrometry (UPLC-IM-QTOF); 3) untargeted gas chromatography-time of flight spectrometry (GC-TOF); 4) semi-targeted liquid chromatography-quadrupole time of flight mass spectrometry (LC-QTOF), analysing butyl ester derivatives of the compounds in the sample extracts; 5) semi-targeted gas chromatography-mass spectrometry detection (GC-MSD), analysing fatty acid methyl ester derivatives of the compounds in the sample extracts (FAMEs) and 6) a targeted liquid chromatography-tandem mass spectrometry (LC-MS/MS) method for a defined set of abalone specific compounds.

4.2 Reagents, standards and solutions

4.2.1 Reagents and Chemicals

Honeywell (Burdick & Jackson) solvents: acetone (BJ010CS); acetonitrile (BJ015CS); chloroform (BJ049CS); hexane (BJ212CS); isopropanol (BJ323CS); methanol (BJ230CS) and water (BJ365CS) were purchased from Anatech Instruments (Pty) Ltd (Olivedale, South Africa (SA)). Agilent HP-921 (protonated hexakis (1H, 1H, 3H-tetrafluoropropoxy) phosphazine) API-TOF reference mass solution (G1969-85001) and Agilent ESI-L low concentration tuning mix (G1969-85000) were purchased from Chemetrix (Midrand, SA). Potassium hydroxide (KOH) (1050330500) was purchased from Merck Millipore, (Modderfontein, SA). Leucine enkephaline (186006013) was purchased from Microsep (Bramley, SA). Sigma-Aldrich (Kempton Park, SA) was used as supplier for: 2-acetamidophenol (A7000); acetic acid (320099); ammonium acetate (A1542); acetyl chloride (00990); 1-butanol (281549); caffeine (C0750); deuterium oxide (D_2O) (151882); formic acid (14265); methoxyamine hydrochloride (226904); methyl tricosanoate (91478); sodium azide (NaN_3) (S2002); sodium hydroxide (NaOH) (795429); nonadecanoic acid (N5252); nor-leucine (74560); O-bis(trimethylsilyl)trifluoro acetamide (BSTFA) with trimethylchlorosilane (TMCS) (33155); 3-phenylbutyric acid (116807); potassium phosphate monobasic (KH_2PO_4) (795488); pyridine (270970); 2,2,4-trimethylpentane (360066); sodium cyanohydridborate ($NaBH_3CN$) (156159); sodium pyruvate (P2256) and trimethylsilyl-2,2,3,3-tetradeuteropropionic acid (TSP) (71911). The following amino acid standards were also

purchased from Sigma-Aldrich (Kempton Park, SA): alanine (A7627); arginine (A5006); asparagine (A0884); aspartic acid (A9256); citrulline (C7629); creatinine (C4255); cysteine (C7352); cystine (C8755); N,N-dimethylglycine (D1156); N,N-dimethylphenylalanine (273910); glutamic acid (G1251); glutamine (G3126); glycine (G7126); histidine (H8000); isoleucine (I2752); leucine (L8000); lysine (L5501); methionine (M9625); ornithine (O2375); phenylalanine (P2126); proline (P0380); serine (S4500); taurine (T0625); threonine (T8625); tryptophan (T0254); tyrosine (T3754) and valine (V0500). Amino acid isotopes used included: [d]-L-arginine:HCl (DLM6038); [d5]-L-glutamic acid (DLM556); glycine N-Benzoyl (DLM7703); [d10]-L-isoleucine (DLM141); [d4]-L-lysine:2HCl (DLM2640); [d3]-methyl-L-methionine (CDLM9289); [d5]-ring-L-phenylalanine (IND625P) and [d8]-L-valine (CDNLM6817) were bought from Cambridge Isotope Laboratories, (Tewksbury, USA). The following carnitine and acylcarnitine standards and deuterated carnitine and acylcarnitine stable isotopes (IS) were supplied by Dr. H.J. ten Brink, Free University Hospital (Amsterdam, The Netherlands): L-carnitine.HCl (C0); acetyl-L-carnitine.HCl (C2); propionyl-L-carnitine.HCl (C3); butyryl-L-carnitine.HCl (C4); isovaleryl-L-carnitine.HCl (C5); hexanoyl-L-carnitine.HCl (C6); octanoyl-L-carnitine.HCl (C8); decanoyl-L-carnitine.HCl (C10); dodecanoyl-L-carnitine.HCl (C12); tetradecanoyl-L-carnitine.HCl (C14); hexadecanoyl-L-carnitine.HCl (C16); octadecanoyl-L-carnitine.HCl (C18); [methyl-d3]L-carnitine.HCl (C0_IS); [d3]acetyl-L-carnitine.HCl (C2_IS); [3,3,3-d3]propionyl-L-carnitine.HCl (C3_IS); [4,4,4-d3]butyryl-L-carnitine.HCl (C4_IS); [d9]isovaleryl-L-carnitine.HCl (C5_IS); [8,8,8-d3]octanoyl-L-carnitine.HCl (C8_IS); [10,10,10-d3]decanoyl-L-carnitine.HCl (C10_IS); [12,12,12-d3]dodecanoyl-L-carnitine.HCl (C12_IS); [16,16,16-d3]hexadecanoyl-L-carnitine.HCl (C16_IS) and [18,18,18-d3]octadecanoyl-L-carnitine.HCl (C18_IS). Alanopine, lysopine, octopine, strombine and tauropine were synthesised using the method described in Section 4.2.3.6.

4.2.2 Consumables and Equipment

The following consumables were used within this study: gloves (RLAS1GL014) and culture tubes (14 X 100 mm (G1TUB029Z-014100; 16 X 125 mm G1TUB029Z-016125) purchased from Lasec (Cape Town, SA). Eppendorf Safe lock 5 mL tubes (0030119401); safe lock micro test 2 mL tubes (0030120094); micro test 1.5 mL tubes (0030125150); Eppendorf 01-10 µL tips (0030000811), 2-200 µL tips (0030000870) and 50-1000 µL tips (0030000919) purchased from Merck Millipore, (Modderfontein, SA). Qiagen 3 mm tungsten carbide beads (69997) and 5 mm stainless steel beads (69989) were purchased from Whitehead Scientific (Pty) Ltd (Brackenfell, SA). Pasteur glass pipettes [(150 mm) (612-1701) and (230 mm) (612-1702)] were purchased from Monitoring & Control Laboratories (Pty) Ltd (Johannesburg, SA). Agilent blue screw caps (5182-0717); blue screw caps pre-slit septa (5182-5865); 250 µL pulled point glass inserts (5183-0717); 400 µL flat bottom glass inserts (518-0730) and 2 mL screw top clear vial (5182-

6106), were purchased from Chemetrix (Midrand, SA). Sigma 20 mL (Z768790) and 50 mL (SIAL0829) centrifuge tubes were purchased from Sigma-Aldrich (Kempton Park, SA). Euriso-Top (Saint-Aubin, France) supplied the 203 mm NMR tubes (508-UP8-5T). Volumetric flasks of 10 mL (GLMS2167807), 25 mL (GLMS2167814), 50 mL (GLMS2167817), 100 mL (GLMS2167824); 1 000 mL (GLMS2167854); and glass measuring cylinders of 10 mL (GINT2161808); 25 mL (GSCH2161814) and 100 mL (GSCH2161824); blue cap 100 mL (GSCH21801245), 250 mL (GSCH21801365) and 1 000 mL (GSCH21801545) Schott bottles were purchased from Glassworld and Chemical Suppliers CC (Randburg, SA). Hamilton syringes 1 000 µL (80900) and 100 µL (80600) from Separations (Pty) Ltd (Randburg, SA). Dissecting Kits, disposable scalpel blades and 1 mL syringes with needles attached, were purchased from Kampus Pharmacy (Potchefstroom, SA).

The following general laboratory and analytical equipment used, is situated at the Biochemistry department of the North-West University, Potchefstroom campus and included: AF80 Scotsman ice flaker from Scotsman Ice Systems (Pty) Ltd (Boksburg, SA); digital Ultrasonic cleaner CD-4820 from Healthcare Technologies (Cape Town, SA); eppendorf Pipettes (2-20 µL, 10-100 µL, 100-1000 µL) from Merck Millipore, (Modderfontein, SA); Heraues Multifuge X3R centrifuge and Savant SpeedVac from ThermoFisher Scientific (Germiston, SA); Hermle Labortechnik compact centrifuge from Lasec (Cape Town, SA); Mettler Toledo AB 304-S balance scale from Microsep (Bramley, SA); Retsch bench-top Mixer Mill MM 400 vibration mill from Monitoring & Control Laboratories (Pty) Ltd (Johannesburg, SA); Snijders Scientifc ultra low -86 °C freezer and 4 °C refrigerator from United Scientific (Goodwood, SA); Techne DB200/3 Dri-Block from Separation Scientifc (Honeydew, SA); Velp Scientifica infrared vortex mixer from Labex (Pty) Ltd (Edenvale, SA) and a WTW series InoLAb pH meter from Labotec (Midrand, SA). The analytical equipment used will be described in the relevant sections that follow.

4.2.3 Standards preparation

The internal standards: 2-acetamidophenol, caffeine, nonadecanoic acid, nor-leucine and 3-phenylbutyric acid were prepared separately, by dissolving 10.00 mg of the standard in 100 mL of methanol in a 100 mL volumetric flask, such that the final concentration is 100 µg/mL. These standards were prepared in sufficient amounts to ensure that enough was available for all relevant analytical applications throughout the study and were aliquoted and stored in reagent bottles at 4 °C when not in use.

4.2.3.1 NMR spectroscopy analysis

The NMR buffer solution was prepared by firstly dissolving 204.00 mg of potassium phosphate monobasic (KH_2PO_4) in 80 mL of deuterium oxide-based (D_2O) phosphate buffer using a graduated cylinder. A second mixture of about 100.00 mg TSP and 13.00 mg NaN_3 dissolved in 10 mL of D_2O was prepared in a separate volumetric flask. The latter was mixed with the aforementioned NMR buffer solution, and sonicated until fully dissolved. The pH of this mixture was adjusted to 7.4 by adding KOH to the mixture. Lastly, the solution was adjusted to 100 mL in a volumetric flask (Dona *et al.*, 2014), using D_2O and transferred to reagent bottles for usage.

4.2.3.2 UPLC-IM-QTOF analysis

Leucine encephalin (0.5 mg/L) was used as a lock mass solution and prepared by dissolving 3.00 mg of the standard in 3 mL of methanol, creating a stock solution (stock 1). A second stock solution was prepared by adding 1 mL (with a Hamilton syringe) of stock 1 to 99 mL of methanol in a separate 100 mL volumetric flask (stock 2). The working solution was prepared by adding 1 mL of stock 2 to 49 mL of methanol in a 50 mL volumetric flask, which was transferred to a reagent bottle. The sodium formate calibration reagent was prepared with a Hamilton syringe, by adding 2 mL of 10 % formic acid, 2 mL 0.1 M NaOH and 16 mL acetonitrile to a graduated cylinder (Arapitsas *et al.*, 2012). Both solutions were prepared in sufficient amounts to enable analysis of whole sample sets, using the same batch of reagents and were stored in reagent bottles at 4 °C until use.

4.2.3.3 GC-TOF analysis

Oximation reagent was prepared by dissolving 200.00 mg methoxyamine in 10 mL pyridine (decanted into a graduated cylinder), in an amber reagent bottle and sonicating the mixture until dissolved. Using a volumetric flask the external standard was prepared by dissolving 10.00 mg of methyl tricosanoate in 100 mL of 2,2,4-trimethylpentane, which was stored in a reagent bottle at 4 °C until use (Venter *et al.*, 2016a).

4.2.3.4 LC-QTOF analysis of butyl esters

A stock solution of reference mass solution was prepared with a Hamilton syringe by mixing 0.2 mL purine, 0.08 mL HP921 and 5 mL H_2O in a 1 000 mL volumetric flask, taken to volume using acetonitrile. This solution was subsequently diluted four times (with acetonitrile) to ensure that the peak abundance of the HP921 was within the working range of analysis. This preparation resulted in sufficient amounts of reference mass solution to ensure analysis of all samples in this investigation. The diluted solution was stored at room temperature in an amber reagent bottle until use.

4.2.3.5 GC-MSD analysis of FAMEs

Methanolic KOH was prepared daily before analysis of the batch analysed, by dissolving 280.00 mg of potassium hydroxide pellets in 25 mL methanol, using a volumetric flask (Lindeque *et al.*, 2013). Methoxyamine in pyridine and methyl tricosanoate in 2,2,4-trimethylpentane was prepared, as described in Section 4.2.3.3.

4.2.3.6 LC-MS/MS analysis

Stable isotopes were prepared in sufficient amounts for analysis of the complete sample sets, by individually preparing 20 µg/mL isotope mixtures in methanol (this served as stock solutions). From the stock solutions, a working reference standard mixture was prepared (in a reagent bottle), by adding each of the isotopes with a Hamilton syringe into a reagent bottle and filled to 100 mL volume using methanol, resulting in a final concentration of 2.5 µg/mL for each isotope standard. Butanolic hydrogen chloride (HCl) (3 N) was prepared by creating a 1:4 ratio of acetyl chloride and 1-butanol solution. In a flow cabinet and using a dropper, 25 % (of the final volume) acetyl chloride was slowly to 75 % (of the final volume) of 1-butanol in a glass reagent bottle placed on ice.

Analytical standards used to optimise the LC-MS/MS conditions were prepared in methanol (1.25 µg/mL). The standards were dried under a gentle stream of nitrogen at 37 °C, where-after 100 µL of freshly prepared 3 N butanolic HCl was added to the dried residue, capped and incubated at 60 °C for 60 min. After incubation, the butylated standards were dried under a gentle stream of nitrogen at 60 °C and reconstituted in 200 µL water:acetonitrile (50:50), containing 0.1 % formic acid and injected on the LC-MS/MS system for analysis.

Opines were synthesised individually by mixing equal amounts of sodium pyruvate (100 µg/mL) and the respective amino acid stock solutions (100 µg/mL previously prepared) in glass vials, followed by drying of the mixture under a gentle stream of nitrogen at 37 °C. Once fully dried, 100 µL of $NaBH_3CN$ (1 mg/mL) and 900 µL of methanol were added to each tube using a Hamilton syringe, followed by incubation at 25 °C for 60 min. The mixture was dried using nitrogen at 37 °C prior to butylation (Venter *et al.*, 2017).

4.3 Biological samples

All of the research pertaining to the perturbations and sample collection from abalone, was carried out in accordance with a Department of Agriculture, Forestry and Fisheries (DAFF) Aquaculture Research Permit (most recent is Permit No.1304476).

4.3.1 Abalone collection

Haliotis midae, used in the anaerobic stress, and growth experiments, were collected from the grow-out platform at HIK Abalone Farm (Pty) Ltd (Hermanus, South Africa). As part of day to day farming activities, the tanks were cleaned weekly and animals were provided with artificial abalone feed (Abfeed S34), or artificial abalone feed X (Abfeed X). Both feeds were purchased from Marifeed (Pty) Ltd, Hermanus, South Africa. Abfeed X had an identical formulation to Abfeed S34, but was supplemented with additional L-proline (Vosloo and Van Rensburg, 2009). Details regarding the specifications of the animals used in each experiment, along with the experimental setup, will be discussed in Chapters 5 and 6, respectively.

4.3.2 Abalone dissection

At time of sampling, selected abalone (discussed in Chapters 5 and 6) were removed from their respective holding systems, and gently patted dry with paper towels. Prior to dissection, the animals were weighed to the nearest 0.01 g and the shell lengths were measured to the nearest 0.10 mm, along the longest axis, using callipers. Abalone gender was assessed before dissection, by observing the colour of the gonad, which is a cream colour in males and a green colour in females. All animals were dissected, and six samples were collected from the animals subjected to anaerobic experiments, including haemolymph, left gill, right gill, epipodial tissue, adductor muscle and foot muscle tissue samples (Fig. 4.1), while only adductor muscle samples were collected from abalone included in the growth experiments.

Firstly, the animals were shucked using a scalpel, working rapidly from the anterior to posterior axis, cutting longitudinally through the foot between the mantle and the distal surface of the foot. Haemolymph (0.5 – 1.0 mL) was collected from the pedal sinus, using a one millilitre syringe with a 27-gauge needle and immediately transferred and stored in micro-centrifuge tubes. Epipodial tissue was cut from the left anterior of the area surrounding the abalone foot muscle using dissection scissors. Both the left and the right gill were collected, by making an incision in the mantle situated to the left side of the animal, located directly under the shell pores. The gills were carefully removed with dissection forceps from the left and right walls of the mantle cavity. A sample of the shell adductor muscle was taken using a scalpel from the ventral surface towards the central point, where the muscle attaches to the shell. The foot muscle samples were collected from the posterior side of the ventral surface, excluding sole epithelium and the majority of the mucus glands. Muscle samples to the equivalent of the volume of a micro-centrifuge tube, were sampled in small blocks using a scalpel. All samples were placed into respective micro-centrifuge tubes and snap frozen using dry ice.

The samples were transported on dry ice to the North-West University's Metabolomics Platform (Potchefstroom, South Africa) and stored at -80 ºC until sample extraction and analysis. The remaining biological waste was placed in bio-waste containers. Used needles were placed in a sharps container, and disposed of in compliance with the relevant laws and institutional guidelines as approved by the relevant institutional committees and that of the farm.

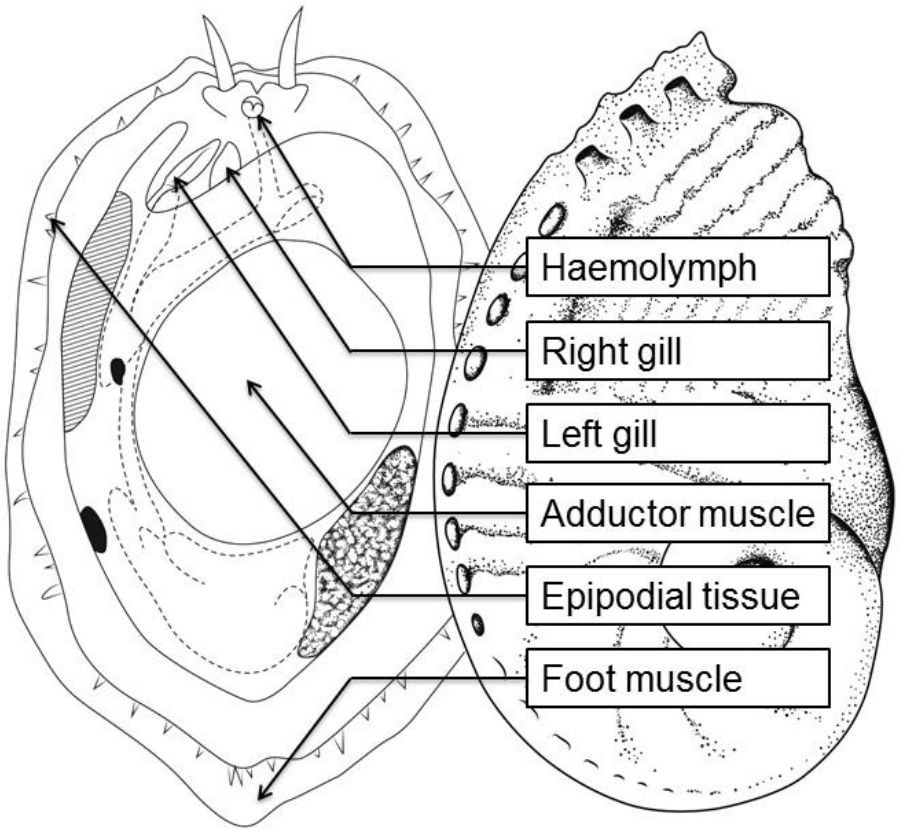

Figure 4.1: Points of interest for sample dissection. Haemolymph, right gill, left gill, adductor muscle, epipodial tissue and foot muscle tissue were dissected from each abalone collected**.**

4.4 Sample preparation for analytical platforms

4.4.1 Metabolite extraction from muscle, gills and epipodial tissue

A subsection of each sampled tissue was removed with a scalpel (while on ice), transferred into a new tube and weighed for the purpose of pre-analysis normalisation. Each sample was homogenised in bulk, where-after it was divided into five tubes for analysis on different analytical platforms (Fig. 4.2). A sample weight of 20.00 mg for the right gill tissue, 40.00 mg for the left gill tissue, 30.00 mg for the epipodial tissue and 60.00 mg for the adductor and foot muscle tissue, per sample (after homogenisation and division), were used throughout the extraction process. Tissue homogenisation was performed using the two-step method, as previously described (Lindeque *et al.*, 2013).

Using the adductor muscle tissue sample as an example, the homogenisation procedure started by adding 300.00 mg of the adductor muscle tissue (60.00 mg adductor muscle X 5 analysis), to a 5 mL safe lock micro-centrifuge tube, together with 650 µL water, 1500 µL methanol and 500 µL internal standard (2-acetamidophenol and 3-phenylbutyric acid, with a final concentration of 50 µg/mL) along with both a 3- and 7-mm stainless steel bead. Softer tissue samples like the gills were homogenised for 4 min at 25 Hz, while tougher tissue like the muscle samples were homogenised for 4 min at 30 Hz, using a Retch M400 vibration mill. The homogenate was separated from the beads, transferred to a clean tube and centrifuged at 10 000 × *g* for 5 min at 4 °C. Subsequently, the homogenate was divided into 5 aliquots containing 500 µL of sample per tube. Then 400 µL chloroform and 200 µL water was added to this and each tube was vortexed for 1 min and incubated on ice for 10 min. The samples were centrifuged at 25 000 × *g* for 10 min at 4 °C resulting in phase separation. Varying sample volumes (depending on the analytical platform used) were transferred to a screw top vial and dried under a gentle stream of nitrogen at 37 °C, together with an additional 100 µL platform-specific internal standard.

Using the extraction of the abalone adductor muscle as an example, the sample used for NMR analysis received 600 µL of the polar phase and 300 µL of the a-polar phase, and were dried together with nor-leucine and caffeine internal standards. For untargeted UPLC-IM-QTOF analysis, 400 µL of the polar phase and 200 µL of the a-polar phase were transferred and dried with nor-leucine and caffeine internal standards. For untargeted GC-TOF analysis, 400 µL of the polar phase and 200 µL of the a-polar phase were transferred and dried with nor-leucine and C19 internal standards. A volume of 60 µL polar phase and 30 µL of the a-polar phase were used for LC-MS/MS and LC-QTOF analysis, and an isotope mixture was added prior to the drying step to ensure the monitoring of a known compound for retention time comparisons between batches. For the samples used for FAME analysis, C19 internal standard and 900 µL of the a-polar phase of the tissue homogenate were dried, preceding analysis.

4.4.2 Metabolite extraction from haemolymph

Haemolymph samples were prepared by adding 100 µL of the 3-phenylbutyric acid internal standard solution to 500 µL of the collected haemolymph in micro-centrifuge tubes, followed by the addition of 1500 µL ice cooled acetonitrile (Fig. 4.2). The samples were vortexed and incubated on ice for 30 minutes, followed by centrifugation at 25 000 × *g* for 10 min at 4 °C. The supernatant was aliquoted into five screw top vials (one for each analytical instrument analysis) and, together with 100 µL of the respective internal standards, were dried under a gentle stream of nitrogen at 37 °C.

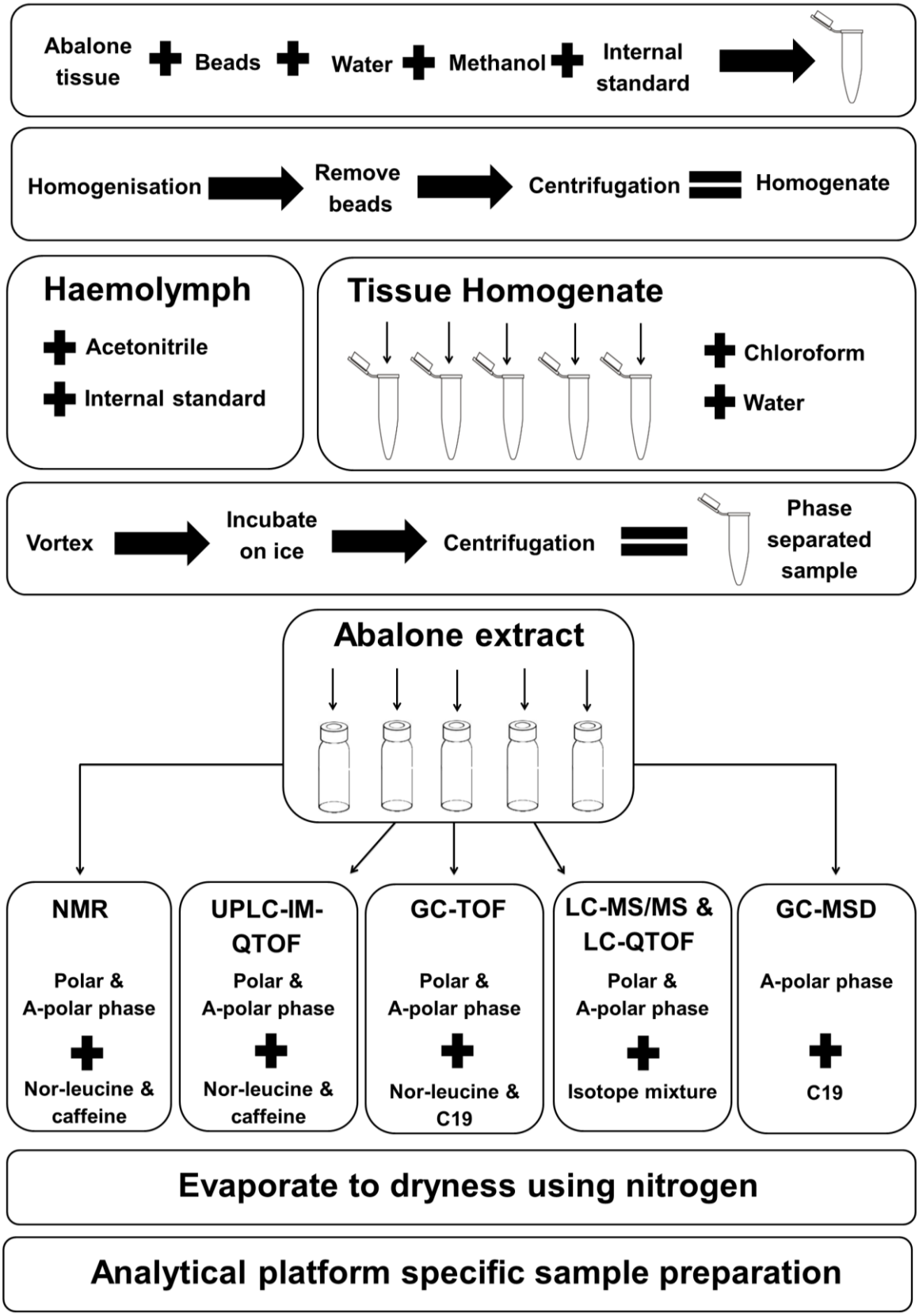

Figure 4.2: Standardised abalone extraction procedure explained. Schematic representation of the metabolite extraction procedure followed prior to analytical analyses.

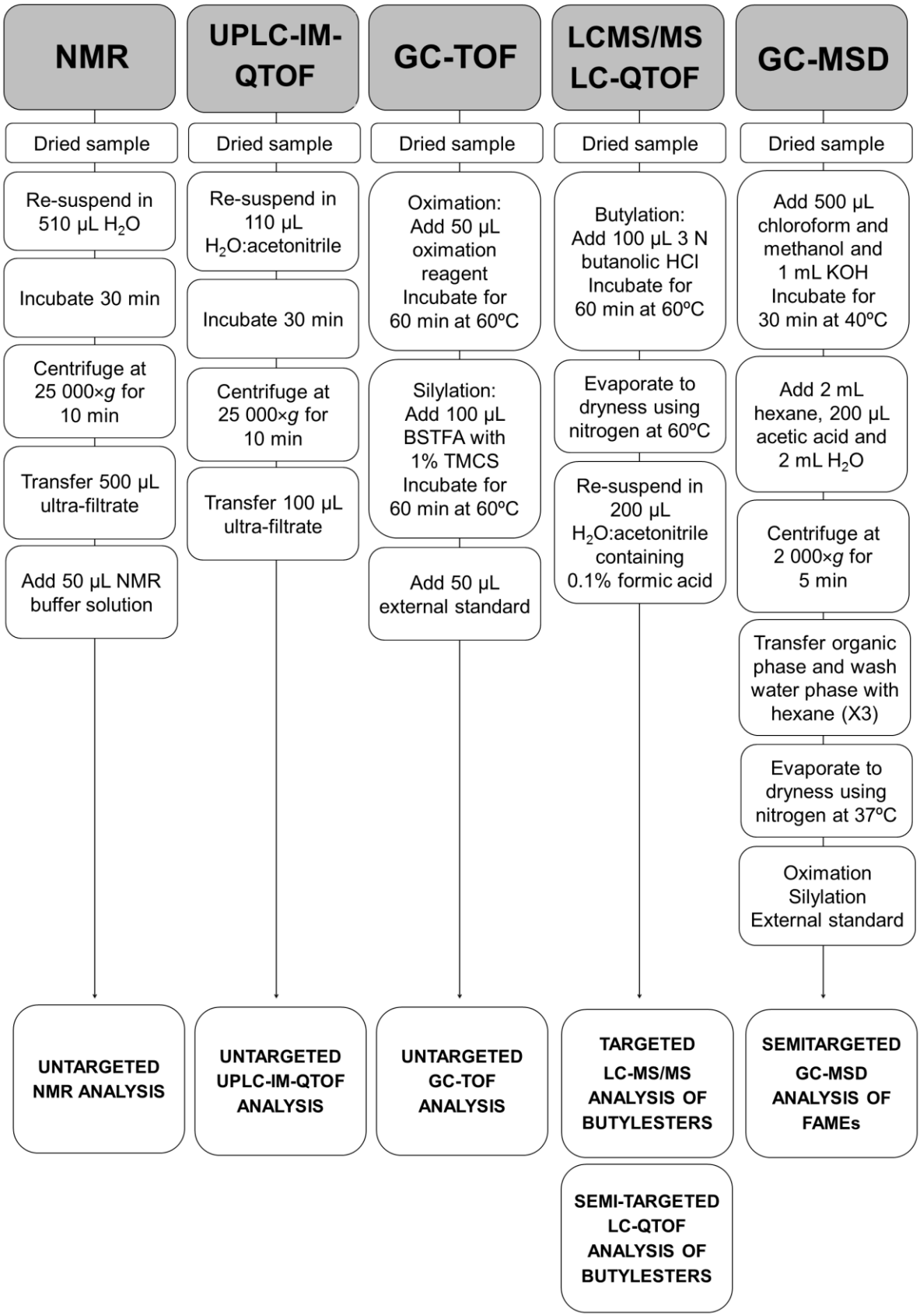

Figure 4.3: Analytical platform specific sample preparation. Schematic representation of the specific sample preparation procedures followed for each analytical platform.

4.4.3 Sample preparation for untargeted NMR spectroscopy analysis

The dried sample extracts were re-dissolved in 510 µL ultra-pure water, and were subsequently incubated at room temperature for 30 min. After the hydration step, the samples were centrifuged at 25 000 × *g* for 10 min. A volume of 500 µL of the ultra-filtrates was transferred together with 50 µL NMR buffer solution to a new tube and vortexed for 30 seconds to ensure complete homogenisation and then transferred to 5 mm NMR glass tubes (Fig. 4.3).

4.4.4 Sample preparation for untargeted UPLC-IM-QTOF analysis

Dried samples were re-suspended in 110 µL water:acetonitrile (50:50), where-after the samples were vortexed and incubated at room temperature for 30 min to ensure complete hydration. The samples were subsequently centrifuged at 25 000 × *g* for 10 min, and the supernatant (100 µL) transferred to vials for analysis (Fig. 4.3).

4.4.5 Sample preparation for untargeted GC-TOF analysis

The sample extracts prepared for untargeted GC-TOF analysis were removed from the freezer and dried under a nitrogen stream at 60 °C for 5 min, prior to oximation and silylation. A volume of 50 µL of the oximation reagent (Section 4.2.3.3) was added to the samples, where-after the samples were capped, vortexed for 1 min and incubated for 60 min at 60 °C. Once oximation was complete, the samples were cooled prior to adding 100 µL BSTFA (containing 1 % TMCS). The samples were then vortexed (1 min) and incubated for 60 min at 60 °C, after which 50 µL of the external standard (methyl tricosanoate in trimethylpentane) was added (Fig. 4.3) to monitor instrument response. The samples were subsequently transferred to glass GC vials for analysis (Venter *et al.*, 2016a).

4.4.6 Sample preparation for targeted LC-MS/MS and semi-targeted LC-QTOF analysis of butyl esters

Prior to butylation, the dried residue (stored at -80 °C) was dried again, using nitrogen at 60 °C for 5 min. To the dried residue, 100 µl 3 N butanolic HCl was added and the samples were incubated at 60 °C for 60 min. The butylated samples were then evaporated to dryness again under a stream of nitrogen at 60 °C (Fig. 4.3). The dried residue was reconstituted in 200 µL water:acetonitrile (50:50) containing 0.1 % formic acid (Venter *et al.*, 2017).

4.4.7 Sample preparation for semi-targeted GC-MSD analysis of FAMEs

The prepared dried extracts (removed from the freezer) were dried using a stream of nitrogen at 60 °C for 5 min. The samples were suspended in 500 µL chloroform and 500 µl methanol, followed by the addition of 1 mL of methanolic KOH and incubated for 30 min at 40 °C. Once the samples were cooled to room temperature, FAMEs were extracted with the addition of 2 mL hexane, 200 µL acetic acid (1 N) and 2 mL water. The samples were centrifuged for 5 min at 2 000 × *g* in order to separate the organic and water phases. The upper organic phase was recovered using a clean tube with a rubber suction teat, and the lower phase was re-extracted with 2 mL hexane, for another three cycles as described above. The pooled organic solvent phases collected, were evaporated under a gentle stream of nitrogen at 37 °C. Following the drying step, 50 µL oximation reagent was added, then vortexed for 1 min and incubated for 60 min at 60 °C. After cooling, silylation was performed by adding 50 µL BSTFA (containing 1 % TMCS) to the samples and incubated for 60 min at 60 °C (Fig. 4.3). A volume of 50 µL of the external standard was added to the sample and vortexed prior to GC-MSD analysis (Willers *et al.*, 2016).

4.4.8 Sequence and batch design

Due to the large number of samples analysed over a period of many days, the sample analysis occurred in batches. Samples from the anaerobic stress experiment were analysed on one day (hence, one batch) due to the low number of samples. The entire set of samples from the growth experiments were, however, analysed in more than one batch. Samples were assigned to batches using a randomisation equation to allocate these to the respective batches for analysis (Dunn *et al.*, 2012). Quality control (QC) samples were included in every batch by preparing a pooled mixture of the tissue that was analysed in that specific batch. These QC samples were included within the biological sample batches and treated no differently than the experimental samples. The QC samples were injected at regular intervals throughout the analytical run of the analysed batch. A test mixture of the same abalone haemolymph was prepared daily with each batch and included in every batch analysed. Furthermore, each batch started with a blank sample. For GC-MS analysis, the blank was hexane and for LC-MS analysis, the mobile phase (water, acetonitrile and 0.1 % formic acid) was used as a blank injection. For daily optimisation purposes, a test mixture (abalone tissue being analysed) was included at the start of each NMR analysis batch. A column wash and mass spectrometer wash step were included at the end of each batch analysed with LC-MS.

NMR spectroscopy: Test mixture, QC1, 10 samples, QC2, 10 samples, QC3, 10 samples, QC4, 10 samples, QC5.

UPLC-IM-QTOF: Blank, test mixture, QC1-3, 7 samples, QC4, 7 samples, QC5, 7 samples, QC6, 7 samples, QC7, column wash, MS wash.

GC-TOF: Blank, test mixture, QC1-3, 10 samples, QC4, 10 samples, QC5, 10 samples, QC6, 10 samples, QC7.

LC-QTOF: Blank, test mixture, QC1-3, 7 samples, QC4, 7 samples, QC5, 7 samples, QC6, 7 samples, QC7, column wash, MS wash.

GC-MSD: Blank, test mixture, QC1-3, 10 samples, QC4, 10 samples, QC5, 10 samples, QC6, 10 samples, QC7.

LC-MS/MS: Blank, test mixture, QC1-3, 10 samples, QC4, S11-20, column wash, QC5, 10 samples, column wash, QC6, 10 samples, QC7, column wash, MS wash.

4.5 Instrumentation

4.5.1 Proton magnetic resonance spectroscopy

Measurements by NMR spectroscopy were performed on a Bruker Advance III HD NMR spectrometer (Bruker, Karlsruhe, Germany), operating at 500 MHz ^{1}H, equipped with a triple-resonance inverse (TXI) $^{1}H(^{15}N, ^{13}C)$ probe head and x, y, z gradient coils. Automated tuning and matching, locking and shimming using the standard Bruker routines ATMA, LOCK, and TopShim were used to optimise the NMR conditions daily. The NMR spectra were acquired as 128 transients in 32 000 data points with a spectral width of 6002 Hz. The sample temperature was maintained at 27 ºC and the H_2O resonance was pre-saturated by single-frequency irradiation during a relaxation delay of 4 s, with a 90 ° excitation pulse of 8 µs, acquiring spectra at 64 scans per sample (~runtime of 8 min per sample). Shimming of the sample was performed automatically on the deuterium signal. The resonance line widths for TSP and metabolites were < 1 Hz (measurements at half the height of the peak). Fourier transformation and phase and baseline correction were done automatically. Bruker Topspin (Version 3.1) software was used for spectral data processing and Bruker AMIX (Version 3.9.12) software was used to distinguish and identify metabolites (Ellinger *et al.*, 2013, Irwin *et al.*, 2016).

4.5.2 Ultra-performance liquid chromatography – ion mobility - quadrupole time of flight mass spectrometer

A Waters Acquity UPLC system coupled via an ESI interface to a Synapt G2-Si hybrid ion mobility-MS system (supplied locally by Microsep, Bramley, South Africa), operating in W-mode and controlled by Masslynx (Version 4.1) was used for analysis. Ten µL of sample was injected and separated on a Waters HSS T3 column (2.1 x 100 mm, 1.8 µm) (Microsep, Bramley, South Africa) kept at 30 ºC, using (A) water and (B) acetonitrile both containing 0.1 % formic acid as mobile phases. The gradient used for separation included the following: 0 min 1 % (B); 0-0.2 min 1 % (B); 2-6 min 15 % (B); 6-12 min 50 % (B); 12-18 min 10 0% (B); 18-20 min 100 % (B); 20-20.20 min 1 % (B); and a post run step of 5.8 min at the final condition, subsequently making the runtime 26 min per sample. A flowrate of 0.5 mL/min was used throughout.

Mass spectrometry detection was performed with a nebulisation gas set to 650 L/min at a temperature of 500 °C, and a cone gas set to 30 L/min. The capillary voltage and cone voltage were set at 2 000 V and 30 V, respectively. The Q-TOF acquisition rate was 0.1 s, with argon used as the collision gas at a pressure of 1.025×10^{-3} psi. Data were captured in HDMS^e mode where the collision-induced dissociation (CID) energy for the first (low energy) channel was set at 0 V and those for the second (high energy) channel was set to ramp between 10 and 40 V. Collision cross section (CCS) values were automatically calculated from the ion mobility drift time based on a poly-alanine calibration. At the onset of analysis, the system was calibrated using sodium formate calibration solution to ensure mass accuracy. Accurate mass calibration of the instrument was performed at the beginning of each batch of analysis by direct infusion of a sodium formate solution (10 % formic acid: 0.1 M NaOH: acetonitrile at a ratio of 1:1:8) to ensure mass accuracy of sub 2 parts per million (ppm) for the mass range 40 to 1 000 m/z mass resolution over 14 000 FWHM. Mass drift during each run was monitored and corrected with the infusion of lock mass solution (0.5 mg/L leucine enkephaline, m/z 556.2771 for positive ion mode) at 10 µL/min flow rate.

4.5.3 Gas chromatography - time of flight mass spectrometer

A GC-TOF-system consisting of an Agilent 7890A GC (locally supplied by Chemetrix, Midrand, SA) coupled to a LECO Pegasus HT mass analyser (LECO Africa Pty Ltd, Kempton Park, SA) was used for analysis. Daily perfluorotributylamine mass and detector calibration and checks were performed to ensure optimal system performance. Chromatographic separation was performed on a Restek RXi-1MS column (30 m × 0.32 mm × 0.25 µm) (LECO Africa Pty Ltd, Kempton Park, SA). A sample volume of 1 µL was injected (using a split/split less injector) per run with a 1:20 split ratio. A 50:50 acetone and isopropanol mixture was used as needle wash

throughout analysis. The front inlet temperature was kept at 250 °C. An initial oven temperature of 80 °C was maintained for 1.0 min and then increased as follows: 10 °C/min to 150 °C at 1.50 min, 14 °C/min to 230 °C, 18 °C/min to 300 °C where it was maintained for 2 min equating to a total run time of ~20 min per sample. Hydrogen was used as carrier gas at a constant flow of 3.2 mL/min. The transfer line temperature was maintained at 225 °C and the ion source temperature at 200 °C for the entire run. Acquisition was delayed for the first 1.9 min which served as a solvent delay. Data were captured with an acquisition rate of 20 spectra (40 – 950 m/z) per second, with a detector voltage of 50 V over the daily tune voltage and electron energy of -70 V.

4.5.4 Liquid chromatography – quadruple time of flight mass spectrometer

An Agilent 1200 LC system (Chemetrix, Midrand, SA) using an injection volume of 5 µL was used for chromatographic separation. Butylated samples were separated on an Agilent ZORBAX SB-Aq C18 column (2.1 X 150 mm, 3.5 µm, Chemetrix, Midrand, SA) fitted with a guard pre-column (Phenomenex, KrudKatcher Ultra AFO 8497, Separations, Randburg, SA), at 30 ºC. The mobile phases consisted of (A) water and (B) acetonitrile both containing 0.1 % formic acid. The separation was performed using the following gradient: 0-3 min 0 % (B); 3-11 min 25 % (B); 11-30 min 100 % (B) at a flowrate of 0.25 mL/min; where-after the flowrate was increased to 0.5 mL/min to 32 min 100 % (B), and ending at 33 min 100 % (B) 0.25 mL/min along with a 10 min post-run at this condition, resulting in a runtime of 43 min per sample.

Mass spectrometry detection was performed on an Agilent 6510 QTOF mass analyser (Chemetrix, Midrand, SA) using positive electrospray ionisation with a drying gas temperature of 300 ºC, a drying gas flow of 7.5 L/min and nebuliser pressure of 30 psi. The Q-TOF was set to scan from 50 to 1 000 m/z. Both centroid and profile data were stored and the instrument set to extended dynamic range (2 GHz). The all ions MS/MS functionality was used with the following collision energies: 0, 10, 20 and 40 V using nitrogen collision gas. A reference solution containing masses 121.050873 $[M+H]^+$ and 922.009798 $[M+H]^+$ were constantly infused as accurate mass reference. Furthermore the instrument was calibrated with Agilent ESI-L low concentration tuning mix before the analysis of each batch of samples (Venter *et al.*, 2017).

4.5.5 Gas chromatography - mass spectrometer detector

An Agilent GC-MSD instrument (Chemetrix, Midrand, SA) consisting of a gas chromatograph with a split/split-less injector (250°C), equipped with an auto sampler coupled to an inert XL mass selective detector was used for analysis. The gas chromatograph was equipped with a SPB-1 column (60 m x 0.25 mm x 0.250 µm film thickness, Supelco, Sigma-Aldrich, Kempton

Park, SA) using helium as the carrier gas at a flow rate of 1.0 mL/min. A sample volume of 2 µL was injected per run with a 1:2 split ratio. The front inlet temperature was kept at 250 °C throughout the entire run. The initial oven temperature was 150 °C for 4 min, ramping to 200 °C at 4 °C/min to 250 °C at 2 °C/min, and then to 295 °C at 10 °C/min followed by a hold for 2 min, resulting in a runtime of 48 min per sample. The transfer line temperature was set to 280 °C and the source temperature at 230 °C. Acquisition was delayed for the first 5 min serving as a solvent delay. Data were captured with an acquisition rate of 3.58 spectra (40 - 450 m/z) per second, with electron energy of 70 eV used (Willers *et al.*, 2016).

4.5.6 Liquid chromatography – tandem mass spectrometer

Reverse phase liquid chromatography analyses were performed using an Agilent 1200 Infinity LC system (Chemetrix, Midrand, SA). The auto sampler's temperature was set to 4 ºC. A sample injection volume of 0.5 µL was used. Samples were separated on an Agilent SB-Aq column (2.1 X 100 mm, 1.8 µm) (Chemetrix, Midrand, SA), fitted with a guard pre-column (Phenomenex, KrudKatcher Ultra AFO 8497, Separations, Randburg, SA). The column temperature was maintained at 45 ºC. The mobile phases consisted of (A) water with 0.1 % formic acid and (B) acetonitrile with 0.1 % formic acid. The separation was performed under the following gradient conditions: 0 min 5 % (B); 0-0.2 min 5 % (B); 0.2-2 min 25 % (B); 2-7 min 25 % (B); 7-7.5 min 90 % (B); 7.5-9 min 90 % (B) all using a flowrate of 0.4 mL/min; 9-9.1 min 90 % (B); 9.1-12 min 95 % (B) and 12-12.5 min 5 % (B) the remaining gradient was executed using a flowrate of 0.5 mL/min. This final condition was maintained for 4 min as a post-run step to ensure column equilibration, resulting in a runtime of 16.5 min per sample. Mass spectrometry detection was performed on an Agilent 6410 Triple Quadrupole (Chemetrix, Midrand, SA) using positive electrospray ionisation. The drying gas temperature was set at 300 ºC with a drying gas flow of 7.5 L/min and nebuliser pressure of 30 psi.

Multiple reaction monitoring (MRM) transitions were optimised with Agilent Technologies MassHunter optimizer software (B.04.01). All of the metabolites (1.25 µg/mL) were optimised by using direct infusion. A dwell time of 45 ms was used for all metabolites investigated. All source conditions were kept at the predetermined optimum values for each metabolite. Table 4.1 summarises the optimised source and MRM conditions for each metabolite using enhanced sensitivity at an EMV of 400 displaying the monitored metabolites and isotopes (IS), the precursor and product ions (m/z) selected, the fragmentor (F) voltage and the collision energy (CE) voltage used.

Table 4.1: Multiple reaction monitoring transitions for butylated metabolites. Details pertaining metabolites of interest together with their precursor and product ions and fragmentor and collision energy voltage used.

Metabolite	Precursor Ion (m/z)	Product Ion (m/z)	F (V)	CE (V)	Metabolite	Precursor Ion (m/z)	Product Ion (m/z)	F (V)	CE (V)
C18_IS	487.5	85.1	127	32	Citruline_IS	236.2	219.1	93	8
C18	484.0	85.0	132	36	Citruline	232.2	113.1	100	5
C16_IS	459.4	85.1	127	32	Arginine_IS	235.2	74.1	108	32
C16	456.0	85.1	141	36	Arginine	231.2	70.1	93	28
C14	428.0	85.1	137	28	Phenylalanine_IS	227.2	125.1	98	20
C12_IS	403.3	85.1	142	32	Phenylalanine	222.2	120.1	80	12
C12	400.0	85.1	132	28	3Phenylbutyrate	221.2	105.0	103	24
C10_IS	375.3	85.1	137	28	C0_IS	221.2	103.1	113	20
C10	372.0	85.1	127	28	C0	218.0	103.0	123	20
Octopine	359.3	198.1	156	24	Histidine	212.1	110.1	99	16
C8_IS	347.2	85.1	132	28	Methionine_IS	209.1	107.0	99	12
C8	344.0	85.1	122	24	Methionine	206.1	104.1	60	8
Lysopine	331.4	84.1	142	28	Lysine_IS	207.0	88.0	103	20
C6	316.0	85.1	122	24	Lysine	203.2	84.1	94	20
C5_IS	311.2	85.1	112	24	Glutamine	203.1	186.0	89	8
C5	302.0	85.0	122	24	Ornithine	189.2	70.2	84	24
Cystine	297.0	151.9	89	12	Asparagine	189.1	144.0	89	8
C4_IS	291.2	85.0	80	20	Isoleucine_IS	198.2	96.1	94	12
C4	288.0	85.0	118	24	Isoleucine	188.2	86.2	80	8
C3_IS	277.2	85.0	150	30	Leucine	188.2	86.1	65	8
C3	274.0	85.0	118	24	Creatine	188.0	90.1	89	16
Alanopine	274.2	172.1	127	12	Valine_IS	182.2	80.1	94	12
Glutamic acid_IS	265.0	191.1	103	12	Valine	174.2	72.2	80	12
Glutamic acid	260.2	186.0	118	12	Threonine	176.0	74.2	84	12
C2_IS	263.2	850	100	20	Proline	172.1	70.2	80	20
C2	260.2	85.0	113	24	Serine	162.0	60.1	69	12
Tryptophan	261.2	244.0	103	8	N,N-dimethylgly	160.1	104.0	94	12
Strombine	260.2	74.0	123	24	2Acetamidophenol	152.2	110.0	79	12
Tauropine	254.1	152.0	113	16	Alanine	146.1	90.1	60	4
N,N-Dimethylphe	250.1	148.1	113	24	Glycine_IS	134.1	78.1	84	4
Aspartic acid	246.2	144.0	100	9	Glycine	132.1	76.1	55	4
Tyrosine	238.2	136.1	89	12	Taurine	126.0	85.0	98	8

4.6 Data processing

Metabolomics typically generates large volumes of data in a high throughput manner, which is difficult to process and analyse manually (Lankadurai *et al.*, 2013). Consequently, various statistical tools are used to initially manipulate these large raw data sets into a workable and understandable format (Issaq *et al.*, 2009). The steps followed to transform the data generated in this study into meaningful results, are summarised in Fig. 4.4 and included: 1) Data extraction; 2) Data pre-processing; 3) Data normalisation; 4) Data pre-treatment and 5) Statistical analysis.

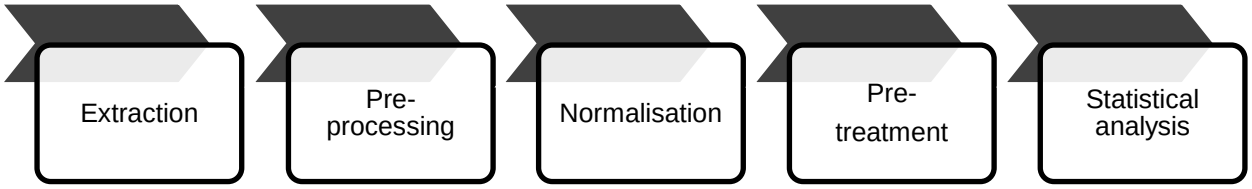

Figure 4.4: Data mining process. Steps followed to transform the data generated to a workable and understandable format.

4.6.1 Data extraction

The raw data files were extracted using various software packages in order to ensure a uniform data matrix, which was subsequently used in the data processing steps that follow. Peak detection and alignment were also performed, using the software guidelines provided by these packages. Each analytical platform contains unique software packages for data extraction and the steps followed to ensure this are presented below.

4.6.1.1 NMR spectroscopy data

Spectra were extracted and pre-processed using Bruker's Topspin NMR software (Version 3.1, Bruker, Karlsruhe, Germany), using an exponential window function (line-broadening of 0.3 Hz), and manual phase and baseline correction. Bruker AMIX (Version 3.9.12) was used for binning and quantification. The NMR spectral region representing the suppressed water signal (4.67 – 4.96 ppm) was excluded from the data matrix. A final bucket data matrix was created and scaled, relative to the total spectrum intensity, using the TSP peak as a reference. A Bruker spectral library database and an in-house pure compound database were used to identify NMR peaks (Irwin *et al.*, 2016).

4.6.1.2 UPLC-IM-QTOF data

Sample alignment, peak detection and deconvolution were performed using Progenesis QI (Nonlinear Dynamics) software, and the recommended default settings.

4.6.1.3 GC-TOF data

Data extraction, in terms of baseline subtraction, peak detection and deconvolution, were performed using ChromaTOF (LECO Africa Pty Ltd, Kempton Park, SA). The baseline tracking mode was selected with an offset of 1. The program was allowed to automatically select smoothing parameters. Peaks were detected using an expected peak width of 3 s and signal-to-

noise ratio of > 20. Also, only masses between 40 and 950 m/z were used as model ions, and any true peak had to contain five apexing masses. Compounds were identified via spectral matching to the National Institute of Standards and Technology (NIST) 2011 mass spectral library and an in-house created library (Reinecke *et al.*, 2012). A spectral match of 80 % similarity (similar to 800 in ChromaTOF) was set before a compound could be given a tentative identity. Only identities which contained at least one Si element in its formula were allowed to eliminate spectral matching of non-derivatised compounds or incorrect derivatives (Venter *et al.*, 2016a).

4.6.1.4 LC-QTOF data

Data extraction was performed using Agilent's MassHunter Qualitative software (Version B.06, Chemetrix, Midrand, SA). The find by formula function (FbF) in MassHunter was used to find features with high resolution masses and isotope patterns corresponding to the theoretical chemical formula of butylated metabolites listed in an in-house butyl ester library. Furthermore, the molecular feature extraction (MFE) algorithm was used according to Agilent's specifications to aid with data extraction. Agilent's MassHunter Mass Profiler Professional (MPP) (Version B.02.02) was used to align the data.

4.6.1.5 GC-MSD data

GC-MSD spectra were identified by spectral analysis, using the Automated Mass Spectral Deconvolution and Identification System (AMDIS, Version 2.71), the NIST 2011 mass spectral library and an in-house FAME database. A match factor of over 80 % was set. The data files created by AMDIS, together with a list of compounds found in the database, were subsequently imported into MPP where the samples were aligned to organise the compounds (Willers *et al.*, 2016). This compound list was then used as the ion-list in MET-IDEA (METabolomics Ion-based Data Extraction Algorithm) (Lindeque *et al.*, 2013), where the target peaks were reintegrated to yield a data matrix with no missing values.

4.6.1.6 LC-MS/MS data

Data was inspected with Agilent's MassHunter Qualitative software (Version B.06) for retention time drifts before quantification. Supervised peak integration was performed using Agilent's MassHunter Quantitative software (Version B.06, Chemetrix, Midrand, SA).

4.6.2 Data pre-processing

Zero filtering was performed (Venter *et al.*, 2015), stating that if a feature was detected in all of the samples of one experimental group, the feature remained in the data matrix for further analysis. Those that did not meet this criterion were removed as they do not contain any statistical value.

4.6.3 Data normalisation

In order to remove non-biological variation, the data was normalised using internal standard normalisation and mass spectrometry total useful signal (MSTUS) normalisation (Venter *et al.*, 2015, Luier and Loots, 2016). The NMR data was normalised by calculating relative concentration from the area of each compound, by comparison to that of the area of the internal standard 2-acetamidophenol, injected at a known concentration. The mass spectrometry total useful signal, was used to normalise the data by identifying component signals in the raw data set, and then summarising it to determine a total useful signal value for each sample. Each sample was then normalised with its signal value by dividing each feature's value by the total signal value and expressing it as a percentage. This was the preferred normalisation method for the data acquired via the UPLC-IM-QTOF, LC-QTOF, GC-MSD and LC-MS/MS analyses. Data from the GC-TOF analyses were normalised relative to the internal standard 3-phenylbutyric acid by calculating the relative concentration of each.

4.6.4 Data pre-treatment

The pre-treatment steps were completed, using the webserver MetaboAnalyst (3.0) (Xia *et al.*, 2015). Missing value estimation was completed, by replacing the missing (or zero) values with half of the minimum positive value in the original data. The data was further transformed, using the generalised logarithm (glog) transformation function before statistical analysis (Lindeque *et al.*, 2015).

4.6.5 Statistical analysis

After completion of data cleaning, normalisation and pre-treatment steps, the data was fit for subsequent statistical analysis. Different statistical methods were selected to determine variation between compared groups in accordance with the experimental design and the aims of the study. Details regarding the statistical analysis procedures executed on the data are described in the relevant sections in Chapters 5 and 6. In Chapter 5, Student's *t*-test and effect size calculations were used to determine which compounds displayed both statistical and

practical significance, when comparing the control and environmental- and functional hypoxia groups. In Chapter 6, two-way analysis of variance (ANOVA) and Student's *t*-test was performed with the use of MetaboAnalyst for exploratory data analysis, where-after effect size was also calculated for the relevant data. Effect size is similar to fold change (i.e. the absolute difference between the group means) but scaled to the highest standard deviation instead of the control group mean. Fold change is greatly influenced by outlier values: a group containing one high outlier metabolite value can easily increase the fold change as it looks at the differences in means. Since the standard deviation of that group would likely be high, it can be used to scale the fold change and express the differences in means as ratio of the biological variance (standard deviation). Additionally principal component analysis was also performed in Chapter 6 to visualise differences between the experimental groups.

4.7 Identification of relevant compounds

Up to this point of the data extraction and processing procedure, all compounds identified using an untargeted approach were referred to as features, with little/no attention being given to compound identity or nomenclature. The metadata, for the statistically selected features, provided by each analytical platform (accurate mass, fragmentation spectra, retention time or CCS values) were used to link the important features, to that of known compounds, by comparison to several in-house, commercial and public libraries/databases, compiled by injection and analysis of previously purchased or synthesised standards. Each identification made was ranked using the identification confidence levels previously described (Schymanski *et al.*, 2014). Briefly, low-confident identities, based only on accurate mass and isotopes patterns, are typically considered Level 5 and 4. Any identification made with the addition of fragmentation spectra are considered more accurate and noted as Level 3. By matching mass information along with orthogonal information (such as retention time or CCS values) gives the highest confidence and subsequent Level 1 or 2 annotations.

4.7.1 Identification of compounds detected with NMR spectroscopy

Metabolites found to be important using NMR analysis, were considered Level 1 identified compounds, as these metabolites were matched with spectra of authentic chemical standards complied in the library used in-house and Bruker's reference library.

4.7.2 Identification of compounds detected with UPLC-IM-QTOF

The spectra of the compounds responsible for changes between the experimental groups were subjected to the following databases: CheBI (www.ebi.ac.uk/chebi), HMDB (www.hmdb.ca), Lipid maps (http://www.lipidmaps.org), Drug bank (http://www.drugbank.ca), and an in-house library of MS/MS spectra, to find comparisons and identify the compounds. *In silico* fragmentation spectra of compounds without published spectra were generated and used within Progenesis QI to aid identification. A fragmentations score > 50 % was used as the benchmark to ascribe a possible identification to a feature. Furthermore the MS/MS fragment ions of the top features were match with Metlin (http://metlin.scripps.edu), which had to match > 3 fragments to be considered valuable. If identification was successful to this point the feature was classified with Level 3 identification.

4.7.3 Identification of compounds detected with GC-TOF

Features that differed mostly between experimental groups were identified by firstly confirming that the features were real peaks and not noise. Next the spectra of each peak of interest were match with that of the in-house library. This information was then matched with the NIST library, focusing on masses and retention index annotations. Spectral matches without retention time/index confirmation were considered Level 3 identities. Spectral and retention time/index matching resulted in a Level 1 identity.

4.7.4 Identification of compounds detected with LC-QTOF

Manual deconvolution was performed for each feature, to ensure that the fragments of the relevant features were, in fact, grouped. Once the MS/MS fragment ions were combined the formulas of features were matched to a butyl ester our in-house created library. At this stage features contained an accurate mass, formula from isotope information and MS/MS data, and were thus seen as Level 3 identified compounds.

4.7.5 Identification of compounds detected with GC-MSD

Only the FAMEs listed in the NIST 2011 mass spectral library and our in-house FAME database (constructed by reference standards) were used for identification. As a result the FAMEs found to significantly differ between the groups were classified with a Level 1 identification confidence, given their familiar elution patterns additionally. In some instances where one could not distinguish between the isomers or the structural positions of the unsaturated bonds for instance, a Level 2 identification was ascribed to the feature.

4.7.6 Identification of compounds detected with LC-MS/MS

All of the metabolites found with a *p*-value of < 0.05 and *d*-value of > 0.8 from the data obtained from the LC-MS/MS analyses were classified with a Level 1 identification confidence. As reference standards for all of these compounds were obtained and analysed prior to biological sample analysis to construct MRM transitions and retention time reference values, the identity of these metabolites are certain.

4.8 Pathway analysis and biological interpretation

The important metabolites that differed most significantly (statistically and practically), when comparing the control and experimental groups, which could be identified with a Level 1 and 2 confidences, were used for pathway analysis. The Level 3 identified compounds were used whenever they supported already affected pathways. Manual pathway analysis was performed manually using, relevant literature and online servers like Kyoto Encyclopaedia of Genes and Genomes (KEGG) and International Union of Biochemistry and Molecular Biology (IUBMB)-Nicholson, where possible. The affected metabolic pathways were used for biological interpretation of the question at hand.

CHAPTER 5

THE METABOLIC RESPONSE OF *HALIOTIS MIDAE* FOLLOWING ANAEROBIC STRESS

"Without oxygen, life on Earth would never have got beyond a slime in the oceans,
and the Earth would probably have ended its days in the sterility of Venus.
With oxygen, life has flourished in all its wonderful variety."
– Nick Lane, Oxygen – The molecule that made the World

Publications from this chapter:

VENTER, L., LOOTS, D. T., MIENIE, L.J., JANSEN VAN RENSBURG, P. J., MASON, S., VOSLOO, A. & LINDEQUE, J. Z. 2018. Uncovering the metabolic response of abalone (*Haliotis midae*) to environmental hypoxia through metabolomics. *Metabolomics*, doi.org/10.1007/s11306-018-1346-8.

VENTER, L., LOOTS, D. T., MIENIE, L.J., JANSEN VAN RENSBURG, P. J., MASON, S., VOSLOO, A. & LINDEQUE, J. Z. 2018. The cross-tissue metabolic response of abalone (*Haliotis midae*) to functional hypoxia. *Biology Open*, doi:10.1242/bio.031070.

5.1 Introduction

The key goal of intermediary metabolism is to uphold adenosine triphosphate (ATP) supply, to ensure that living cells can grow, reproduce and respond to stresses (Salway, 2004). In unstressed circumstances, basal metabolism is dominated by anabolic activity that produces macromolecules, leading to cell growth, division and repair (Garrett and Grisham, 2010). The mitochondrion is primarily responsible for the production of ATP but also plays a role in the maintenance of tissue homeostasis (Galluzzi *et al.*, 2012). However, for organisms to firstly survive hypoxic conditions, and later recover and maintain cell homeostasis, additional energy is required for managing basic survival, recovery and maintenance of cell homeostasis (Sokolova *et al.*, 2012). If homeostasis cannot be achieved, in stressed scenarios, like hypoxia, the enzyme ATP synthase starts pumping protons from the matrix in order to sustain membrane potential, resulting in an accumulation of deleterious end products (H^+) and, together with the build-up of metabolic products, causes metabolic failure and often cell death (Boutilier, 2001, Tielens *et al.*, 2002, Wilson, 2013).

Prior to this destructive outcome, however, animals can regulate their metabolism to deal with the response of cellular energetics by prioritising energy according to need, to ensure energy availability for crucial processes (Boutilier, 2001). One way of coping with low oxygen availability is by sustaining ATP production using oxygen-independent mechanisms, making the glycolytic pathway the primary source of ATP for energy-consuming reactions (oxy-regulating). Another way of survival during compromised oxygen is by reducing the cell's need for ATP production by suppressing energy-consuming reactions (oxy-conforming) (Storey, 2005). When animals fail to suppress energy need, their metabolism changes from aerobic to anaerobic respiration, which results in the utilisation of energy reserves to survive hypoxia (Le *et al.*, 2016). There are several types of hypoxia, but only two will be focused on in this study, namely functional hypoxia and environmental hypoxia.

Functional hypoxia occurs when the internal oxygen pressure falls due to intensive muscular activity (Liu *et al.*, 2014). In the wild, this type of muscle activity is likely to occur when animals are trying to escape from predators or in the pursuit of prey. In such scenarios, the rate of ATP usage by muscle is too high to be met by aerobic respiration, forcing the organism to rapidly switch to anaerobic respiration for ATP production in contracting muscles (Müller *et al.*, 2012). In a typical abalone farming environment, extreme functional hypoxia scenarios are a rare phenomenon, but functional hypoxia can be induced to a lesser extent when abalone climb and crawl for feeding purposes, or as a result of shell adhesion or repositioning after being dislodged (Morash and Alter, 2016).

Whenever ambient oxygen levels are reduced below the critical level, resulting in low or limited oxygen supply, it is referred to as environmental hypoxia (Grieshaber *et al.*, 1993, Liu *et al.*, 2014). For abalone in the wild, environmental hypoxia would manifest when the tide is low, when migration to the shore zone takes place, when there is an increase in water temperature or decrease in dissolved oxygen in rock pools. During low tide, for example, the normal gas exchange of sea water in the gills is hampered by the lack of oxygen, causing a switch to anaerobic energy metabolism to adapt to the hypoxic conditions (Müller *et al.*, 2012). In the farming context environmental hypoxia occurs due to handling practices associated with the transport of animals out of water, for example when tanks are being cleaned, or during size grading procedures and exportation (Hooper *et al.*, 2014). Moreover, oxygen depletion can also occur on farms during periods of low water flow or high water temperatures (Morash and Alter, 2016) and in the natural marine environment which severely impacts growth and survival. This was previously demonstrated when harmful algal blooms caused massive abalone stock losses in SA, attributed to anoxia (Pitcher and Calder, 2000, Mouton, 2017). Considering this, a better understanding of the biochemical response of abalone is crucial to assist with recovery or to prevent metabolic resource depletion when abalone are subjected to hypoxic episodes (Cook, 2014).

Invertebrates have well-defined anaerobic metabolic pathways capable of energy production during hypoxia (Gäde *et al.*, 1984, Gäde and Grieshaber, 1986, Fields and Storey, 1987, Gäde, 1988, Grieshaber *et al.*, 1993, Carroll and Wells, 1995, O'omolo *et al.*, 2003, Storey, 2004, Müller *et al.*, 2012, Liu *et al.*, 2014). However, current knowledge on the holistic metabolic response for energy metabolism during hypoxic conditions, and the contribution of different metabolic pathways towards the overall accumulation of anaerobic end-products in marine invertebrates, especially abalone, are scarce.

Insights into the influences of stressors like hypoxia on organism survival and prediction of their interactions can be achieved by assessment of biochemical features (Laganà *et al.*, 2014). One of the most promising tools for biochemical investigations is metabolomics, which allows for a holistic view of affected metabolic pathways due to a perturbation (Alfaro and Young, 2016). Hence, it is considered a useful tool for investigating the biochemical responses and altered metabolites induced by hypoxia. Considering that metabolomics provides comprehensive insight into naturally occurring, low-molecular-weight metabolites, a multiplatform metabolomics approach was used to investigate the metabolite profiles of *H. midae* exposed to hypoxia and included the use of: untargeted nuclear magnetic resonance (NMR) spectroscopy; untargeted ultra-performance liquid chromatography-ion mobility-quadrupole time of flight spectrometry (UPLC-IM-QTOF); untargeted gas chromatography-time of flight spectrometry (GC-TOF); semi-targeted liquid chromatography-quadrupole time of flight mass spectrometry (LC-QTOF)

analyses of butylated esters; semi-targeted gas chromatography-mass spectrometry-detector (GC-MSD) analyses of methylated fatty acids (FAMEs) and targeted liquid chromatography-tandem mass spectrometry (LC-MS/MS). The abovementioned analyses were additionally performed on numerous abalone tissue samples, to elucidate the metabolic response of the different tissues, and their interplay for ensuring optimal energy production and/or survival of abalone during hypoxia.

The aim of this Chapter was to use a multiplatform metabolomics approach to examine the metabolite changes and metabolic interactions that occur in *Haliotis midae* for energy production during moderate anaerobic stress (functional hypoxia) and extreme anaerobic stress (environmental hypoxia).

5.2 Materials and methods

Refer to Chapter 4 for a comprehensive description of abalone dissection, sample preparation, metabolomics analysis and data processing procedures used in these anaerobic stress experiments.

5.2.1 Abalone of interest

Adult abalone (*Haliotis midae* n = 18) were collected during the winter season from the same batch of animals (identical in terms of their age, growth basket and raceway) housed in the grow-out platform at HIK Abalone Farm (Pty) Ltd, situated in Hermanus, South Africa. These animals were randomly divided into three groups, namely the: 1) control group (n = 6), 2) functional hypoxia experiment group (n = 6) and 3) environmental hypoxia experiment group (n = 6). The control group had an average wet weight of 83.00 ± 8.27 g and shell length of 75.53 ± 2.05 mm, and consisted of 4 males and 2 females. The functional hypoxia group had an average wet weight of 94.33 ± 11.13 g and shell length of 79.00 ± 2.76 mm, and consisted of 2 males and 4 females. The environmental hypoxia group had an average wet weight of 95.33 ± 7.87 g and shell length of 79.33 ± 2.58 mm, and consisted of 4 males and 2 females. The specific details regarding abalone husbandry are given in Section 4.3.

5.2.2 Experimental setup

One farming raceway supplied abalone for the respective experimental groups, including: 1) control group, 2) functional hypoxia group and 3) experimental hypoxia group (Fig. 5.1). These animals were placed in a temporary farming holding system, from where animals were collected

and grouped. Control animals were removed from the system and dissected according to the procedure described in Section 4.3.2, resulting in the collection of adductor muscle, foot muscle, left gill, right gill, epipodial tissue and haemolymph samples. Additional animals were removed from the raceway and subjected to functional and environmental hypoxia (as described below), where-after dissection and sample collection followed in the same manner as that of the control group.

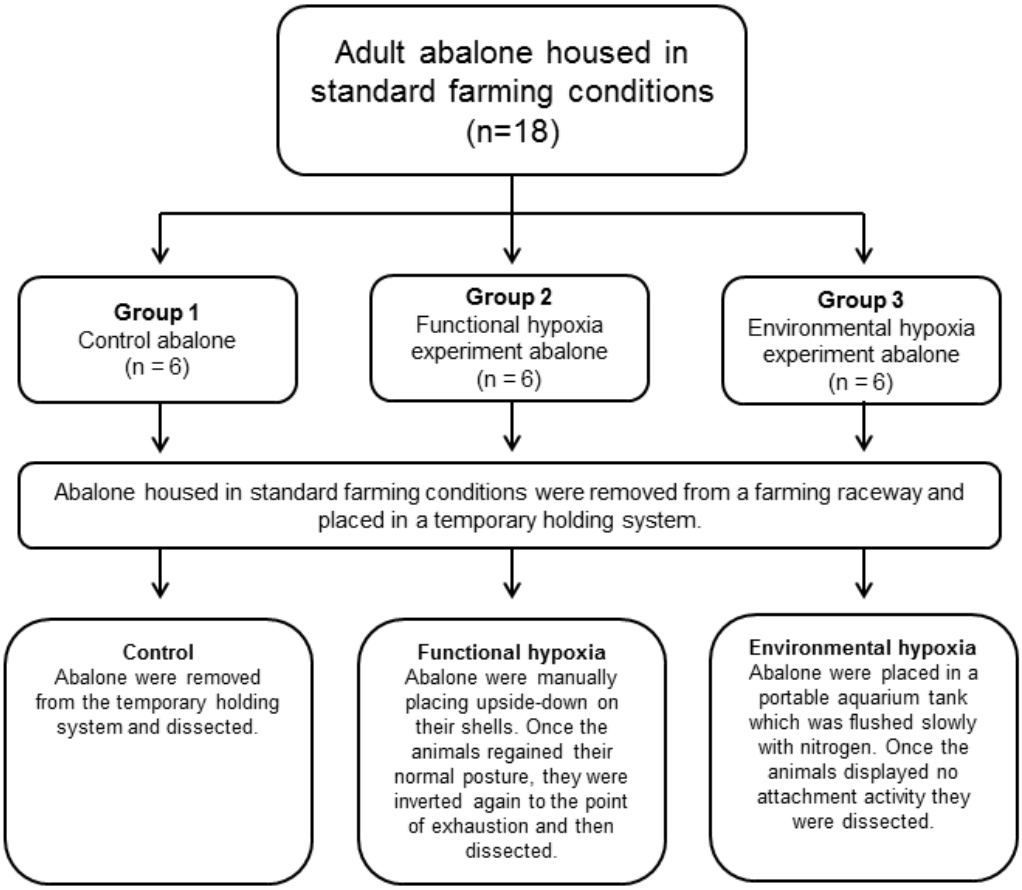

Figure 5.1: Anaerobic stress experimental design. Abalone housed in standard farming conditions were collected and divided into three groups. Group 1 served as the control group, Group 2 was exposed to a functional hypoxia experiment and Group 3 was exposed to an environmental hypoxia experiment.

5.2.2.1 Simulating functional hypoxia in *H. midae*

Abalone were removed from the temporary farming holding system and placed into a large aquarium tank with flowing seawater. In order to induce exercise, the animals were placed upside-down on their shells (O'omolo *et al.*, 2003). After relatively vigorous contractions of the shell adductor muscle, the animals eventually regained their normal posture, where-after they were immediately inverted again, this was repeated to the point where the animals were unable to upright themselves. After 18 minutes the abalone were considered exhausted and were removed from the system and dissected.

5.2.2.2 Simulating environmental hypoxia in *H. midae*

Animals were removed from the temporary farming holding system and transferred to a portable aquarium tank. Once the animals were acclimated to the experimental tank, the water surface area was covered with a polystyrene sheet that had a small opening, through which 100 % nitrogen was flushed slowly into the system (O'omolo *et al.*, 2003). Abalone were subsequently exposed to hypoxia for a period of six hours, where-after no attachment behaviour was displayed, at which point they were removed and dissected.

5.2.3 Sample preparation

The tissue samples collected from the experimental abalone were prepared using the metabolite extraction procedure described in Section 4.4.1. Metabolites from the haemolymph samples were extracted using the process described in Section 4.4.2. Furthermore, the samples were prepared in accordance to the specific metabolomic platforms used (Sections 4.4.3 – 4.4.7).

5.2.4 Sample analysis

All six samples collected, were analysed in random sequence, using the platform specifications given in Section 4.5, which included: untargeted NMR spectroscopy analyses; untargeted UPLC-IM-QTOF analyses; untargeted GC-TOF analyses; semi-targeted LC-QTOF analyses of butyl esters; semi-targeted gas GC-MSD analyses of FAMEs and targeted LC-MS/MS analyses.

5.2.5 Data processing

Data processing steps included: 1) data extraction, 2) data pre-processing, 3) data normalisation and 4) data pre-treatment methods, as described in Section 4.6.

5.2.6 Statistical analysis

Statistical analyses were performed on the data, comparing two abalone groups at a time (Fig. 5.2), in consideration of the aim of this study. Firstly, the control abalone group was compared to that of the functional hypoxia abalone group, in order to identify those metabolite markers that differed most significantly between the groups. Secondly, the control group was compared to that of the environmental hypoxia group. In each instance, the respective tissue samples collected were compared, e.g., the foot muscle samples collected from the control abalone were compared to the foot muscle samples collected from abalone that were subjected to functional hypoxia, and so on.

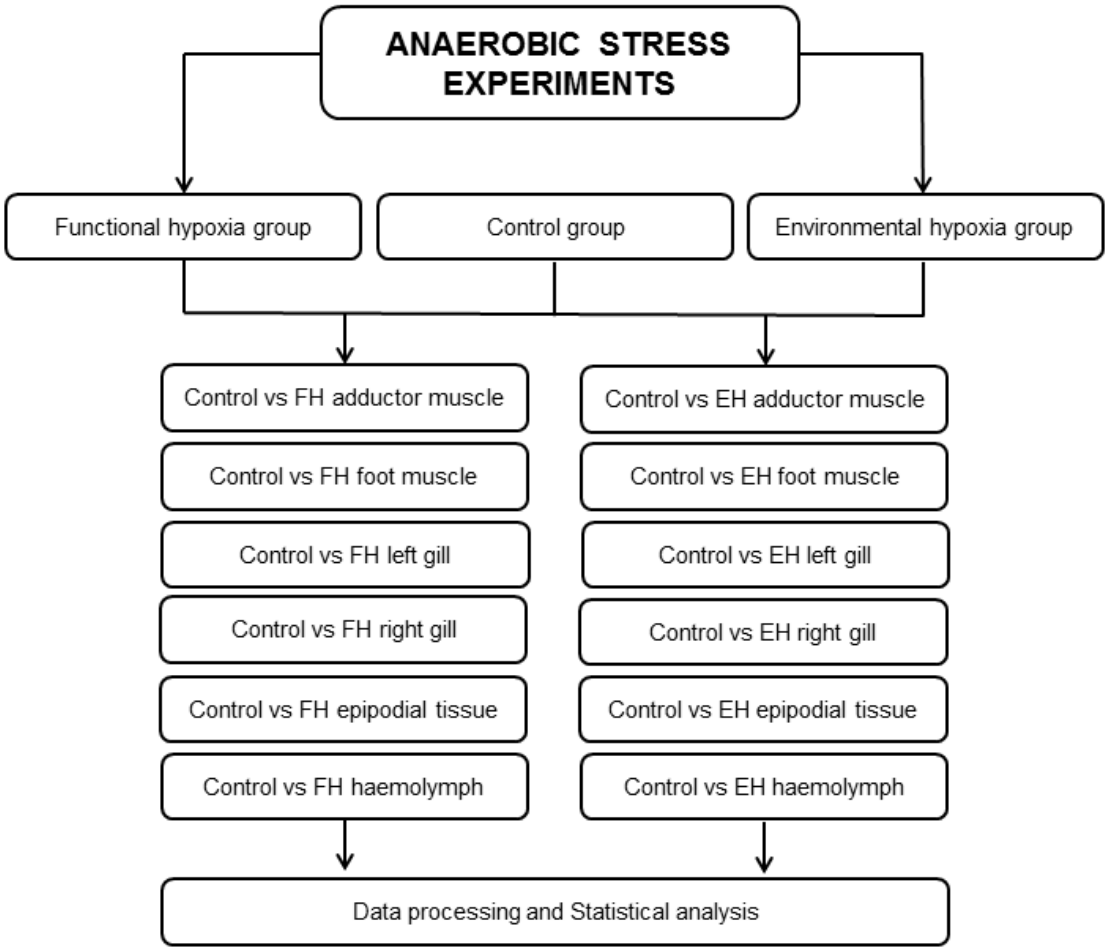

Figure 5.2: Grouping for statistical analysis purposes. Data collected from abalone serving as controls were compared to data collected from functional hypoxia (FH) and environmental hypoxia (EH) groups respectively.

The steps followed to identify relevant variation within the data and identify those metabolites with the most significant variation between the compared groups, are summarised in Fig. 5.3. The webserver MetaboAnalyst, was used for data analysis and visualisation, with special focus on outlier and batch effect confirmation (by means of a heatmap), Student's *t*-test, principal component analysis and correlation analysis (Xia *et al.*, 2015).

5.2.6.1 Batch effect evaluation

The quality of the data was firstly evaluated to ensure that technical variance from experimental factors did not affect the relevant biological variance and that the data could be used without corrections. The quality control (QC) samples analysed amongst the batch were assessed in terms of coefficient of variance percentages and visual interpretations (Wehrens *et al.*, 2016). The data were evaluated for a within batch effect using heatmaps and scatterplots (Xia *et al.*, 2012). No visible effect was seen within the datasets and thus no correction methods were applied.

5.2.6.2 Outlier detection and removal

MetaboAnalyst was used to generate a heatmap, which was subsequently used to visualise to the data and identify possible outlier samples (Xia *et al.*, 2012). No samples displayed unusually high/low compound levels, thus no samples were removed from the data matrix.

5.2.6.3 Effect of biological variation

MetaboAnalyst was additionally used to perform principal component analysis in order to determine whether a natural grouping in the data exists when considering this from a multivariate perspective (Lindeque *et al.*, 2015). Factors like gender, size and time of sample preparation were also investigated using this approach in order to confirm that the relevant biological variance in the compared groups were not influenced by these confounders. As a result, the grouping displayed visually on the PCAs did not display any favour towards possible confounding factors within the groups of interest.

5.2.6.4 Student's *t*-test

Univariate analysis was once again performed using MetaboAnalyst. Student's *t*-test was used to find significant differences in metabolite levels between the experimental groups. Features with a *p*-value < 0.05 (FDR corrected *p*-value) were considered to vary significantly between the compared groups and subsequently selected for further biological interpretation (Lindeque *et al.*, 2015). The features with a *p*-value > 0.05 were removed from the data matrix, resulting only in data with statistical significance.

5.2.6.5 Effect size

To ensure that the differences in the data, with regards to a specific variable between two groups, were large enough to have a practical significance, effect size calculations were executed on log transformed data. Effect size was calculated by determining the absolute difference between the means of the two groups divided by the maximum standard deviation of the two groups. Features with a *d*-value > 0.8 were labelled as important and remained in the data matrix for further analysis (Ellis and Steyn, 2003).

5.2.6.6 Correlation analysis

The Pearson correlation of selected metabolites in different tissues was investigated in MetaboAnalyst. Only selected metabolites involved in glycolysis, amino acid catabolism, NAD^+ recovery and detoxification were used. These include: pyruvate, alanine, arginine, glutamate, leucine, lactate, alanopine, octopine, strombine, tauropine, alanylglycine, arginylglycine and isovalerylglycine.

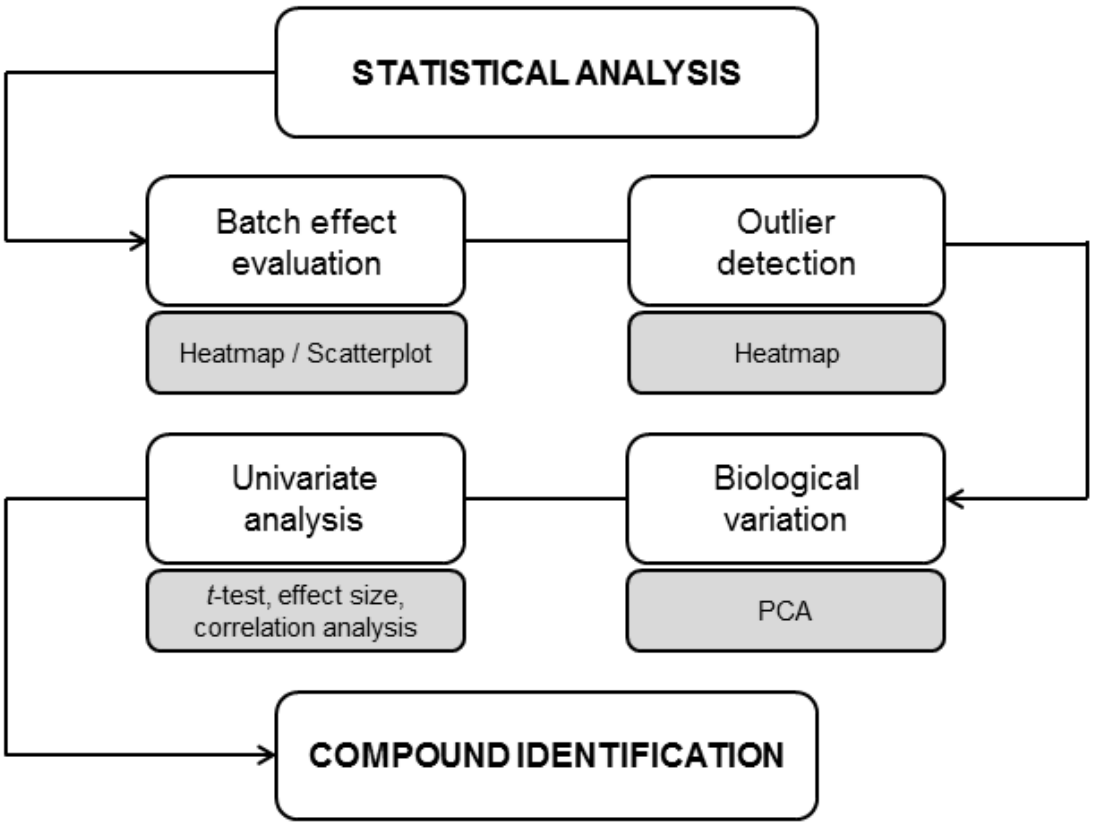

Figure 5.3: Statistical analysis workflow. Schematic representation of the steps followed as part of statistical analysis including: batch effect evaluation, outlier detection, biological variation confirmation, univariate analysis and compound identification.

5.2.7 Compound identification

Features were assigned compound (metabolite) names, using the identification confidence levels described in Section 4.7. Only compounds with Level 1, 2 and 3 identifications were considered relevant for biological interpretation.

5.3 Results and discussion

In essence, the results are the metabolic findings of abalone samples analysed with NMR, GC-MS and LC-MS platforms as described in detail in Chapter 4, and include only those metabolites, which differed most when comparing the experimental groups selected on the basis of an identification confidence Level of 1, 2 or 3, subsequent statistical significance using *t*-test ($p < 0.05$) and practical significance using effect size calculations ($d > 0.8$).

Using the adductor muscle findings as the point of departure, Tables 5.1 contains the significant metabolites from the functional hypoxia experiment, and Table 5.2 contains data generated from the environmental hypoxia experiment, both arranged in order of most significant (best *p*- and *d*-values) to least significant metabolites. Since the aim of the study was to identify and explain the variation with respect to altered metabolic response to infer biological meaning, it was not considered useful to report averages and standard deviations of the relative metabolite abundances, but rather focus on the differences in relative compound intensities between the respective groups as displayed by the increase (↑) or decrease (↓) in metabolite response. Moreover, the untargeted methods provide relative concentrations when no external calibration is used. Furthermore, the identification level assigned to the specific metabolite and the analytical platform on which the metabolite was detected is shown. It should be noted that some metabolites, such as alanine for instance, were detected on multiple analytical platforms. When this occurred, the platform with the highest identification confidence level was selected, and if duplicate metabolites were still present, the metabolite with the smallest *p*-value was then selected. The findings were also grouped into four main metabolite classes, which were discriminated in terms of convenience, metabolic reactions, and main energy producing systems. The grouping included metabolites of amino acid metabolism, carbohydrate metabolism, lipid metabolism and the remaining metabolites, belonging to all other pathways. Additionally, Tables 5.1 and 5.2 show the most significant metabolite differences detected in the adductor muscle, foot muscle, left gill, right gill, haemolymph and epipodial tissue samples.

Subsequently, the metabolite markers in Tables 5.1 and 5.2 were manually mapped on metabolic charts, focussing only on those pathways that showed significant changes induced to the abalone metabolome due to functional hypoxia (Fig. 5.4) and environmental hypoxia (Fig. 5.5). A pathway was considered important when most of the metabolites in the pathway were affected, and/or when the shared metabolites in the pathway (i.e. metabolites connected to other pathways) were considerably altered. The metabolic maps were constructed using the typical mammalian design; due to the fact that similarities exist in the major metabolic pathways when comparing different species and organisms. Non-mammalian metabolic pathways for anaerobic energy production are, however, also included. In more general terms, affected pathways in Figures 5.4 and 5.5 include: [A] sugar metabolism (Glycolysis); [B] the oxaloacetate-succinate pathway; [C] the threonine-serine-glycine metabolism; [D] sulphur containing amino acid metabolism; [E] cysteine-taurine-cysteine metabolism; [F] the pyruvate-lactate/alanine pathway; [G] aspartate-succinate pathway; [H] pyruvate-opine pathway; [I] lysine-tryptophan metabolism; [J] the glutaryl-CoA pathway; [K] branched chain amino acid metabolism; [L] ketone body metabolism; [M] propionyl-CoA pathway; [N] tricarboxylic acid (TCA) cycle; [O] alternative aspartate pathway; [P] purine and pyrimidine metabolism; [Q] urea cycle; [R] proline metabolism; [S] electron transport chain (ETC); [T] phenylalanine-tyrosine

metabolism; [U] beta(ß)-oxidation; [V] fatty acid transport pathway; and [W] fatty acid synthesis. Also included is elevated (blue) and decreased (red) metabolite abundance indicators found in abalone adductor muscle (AM), foot muscle (FM), left gill (LG), right gill (RG), haemolymph (H) and epipodial tissue (E) samples.

The discussion of these results will lead with insight into the metabolic pathways (e.g. lactate, opine, succinate and arginine pathways) anaerobically utilised by abalone to produce ATP. Next, those metabolite markers better explaining the role of how various macromolecules (carbohydrates, proteins and lipids) serve as energy substrates for survival during hypoxia will be discussed. Subsections dedicated to describing those markers and the associated metabolism related to specific amino acids, are also included. All of the above will be discussed with regards to hypoxia, and the specific hypoxic condition (i.e. functional or environmental hypoxia) will receive attention if the results deferred. Lastly, the tissue specific responses of hypoxia displayed by abalone adductor muscle, foot muscle, haemolymph, gills and epipodial tissues will also be discussed.

Table 5.1: Metabolite findings of *Haliotis midae* subjected to functional hypoxia in terms of different tissues investigated. Compounds are ordered in decreasing statistical (*p*-value) significance. Arrows indicate an increase (↑) or decrease (↓) relative to the normoxic controls. Metabolites are grouped in terms of amino acid (AA), fatty acids (FA), carbohydrates (CHO) and other (O) findings.

Adductor muscle													
Compound	**↑ /↓**	***p*-value**	***d*-value**	**ID**	**Platform**	**Group**	**Compound**	**↑ / ↓**	***p*-value**	***d*-value**	**ID**	**Platform**	**Group**
Threonine	↓	9.95E-09	9.06	1	LC-MS/MS	AA	Butyrylcarnitine (C4)	↑	2.97E-03	2.15	3	LC-QTOF	FA
Lysine	↓	1.82E-07	5.87	1	LC-MS/MS	AA	Valine	↑	5.18E-03	1.65	1	LC-MS/MS	AA
Isoleucine	↓	4.43E-07	5.45	1	LC-MS/MS	AA	Succinate	↑	7.72E-03	1.69	1	GC-TOF	CHO
Taurine	↑	3.55E-06	4.74	1	LC-MS/MS	AA	Ethanol	↓	8.70E-03	1.76	1	NMR	O
Acetylcarnitine (C2)	↑	8.37E-06	3.88	1	LC-MS/MS	FA	Hydroxysuberate	↑	2.02E-02	1.26	3	LC-QTOF	CHO
Creatine	↑	5.62E-05	3.38	1	LC-MS/MS	CHO	Uridine triphosphate	↑	2.09E-02	1.11	3	UPLC-IM-QTOF	O
Tauropine	↑	1.03E-04	2.80	1	LC-MS/MS	AA	Serine	↑	2.51E-02	1.26	1	LC-MS/MS	AA
Proline	↑	1.42E-04	2.78	1	LC-MS/MS	AA	Lactate	↑	2.61E-02	1.23	1	GC-TOF	CHO
N,N-dimethylglycine	↓	1.88E-04	2.53	1	LC-MS/MS	AA	Aminobutyrate	↑	3.58E-02	1.20	1	GC-TOF	O
Tryptophan	↓	3.30E-04	2.84	1	LC-MS/MS	AA	Adenosine	↑	3.78E-02	0.99	3	UPLC-IM-QTOF	O
Tyrosine	↑	7.47E-04	2.65	1	LC-MS/MS	AA	Glutathione	↓	4.22E-02	0.96	3	LC-QTOF	CHO
Aspartate	↓	1.45E-03	2.34	1	LC-MS/MS	AA	Octadecenoate (18:1n9)	↑	4.36E-02	1.29	1	GC-MSD	FA
Carnitine (C0)	↑	2.03E-03	2.33	1	LC-MS/MS	FA	Methionine	↓	4.46E-02	1.14	3	LC-QTOF	AA
Arginine	↑	2.10E-03	1.96	1	LC-MS/MS	AA	Leucine	↓	4.51E-02	0.85	1	LC-MS/MS	AA
Histidine	↓	2.11E-03	2.03	1	LC-MS/MS	AA	Glutamate	↑	4.96E-02	1.07	1	LC-MS/MS	AA
Glutamine	↓	2.87E-03	1.69	1	LC-MS/MS	AA							
Foot muscle													
Compound	**↑ /↓**	***p*-value**	***d*-value**	**ID**	**Platform**	**Group**	**Compound**	**↑ / ↓**	***p*-value**	***d*-value**	**ID**	**Platform**	**Group**
Tauropine	↑	3.70E-05	2.99	1	LC-MS/MS	AA	Alanine	↑	3.67E-03	1.72	1	LC-MS/MS	AA
Succinate	↑	5.22E-05	3.20	1	GC-TOF	CHO	Methionine	↓	4.01E-03	1.87	1	LC-MS/MS	AA
Leucine	↑	1.72E-04	2.60	1	LC-MS/MS	AA	Isobutyrylglycine	↑	8.23E-03	1.89	3	LC-QTOF	AA
Taurine	↑	6.67E-04	2.10	3	LC-QTOF	AA	Arginine	↓	9.40E-03	1.82	1	LC-MS/MS	AA
Propionylglycine	↑	8.57E-04	1.98	3	LC-QTOF	AA	Palmitoylcarnitine (C16)	↓	1.63E-02	1.26	1	LC-MS/MS	FA
Homoanserine	↑	1.23E-03	1.99	3	LC-QTOF	AA	Isoleucine	↑	1.78E-02	2.03	1	NMR	AA
Carnitine (C0)	↑	1.53E-03	0.80	1	LC-MS/MS	FA	Tryptophan	↑	2.45E-02	0.80	1	LC-MS/MS	AA
Lactate	↑	2.70E-03	2.55	1	NMR	CHO	Asparagine	↑	2.69E-02	1.32	1	LC-MS/MS	AA
Glutathione	↑	3.52E-03	2.09	3	LC-QTOF	CHO	Octadecenoate (18:1n9)	↑	4.36E-02	1.29	1	GC-MSD	FA
Epipodial tissue													
Compound	**↑ /↓**	***p*-value**	***d*-value**	**ID**	**Platform**	**Group**	**Compound**	**↑ / ↓**	***p*-value**	***d*-value**	**ID**	**Platform**	**Group**
Aminomalonate	↑	1.08E-19	10.61	3	LC-QTOF	CHO	Catechin	↑	5.08E-03	1.51	3	LC-QTOF	O
Proline	↑	9.00E-05	3.19	1	LC-MS/MS	AA	Oxalate	↑	7.86E-03	1.99	1	GC-TOF	CHO
Methylmalonate	↓	9.28E-05	4.90	1	NMR	CHO	Uridine	↓	8.46E-03	1.03	3	LC-QTOF	O
Homogentisate	↑	1.09E-04	1.86	3	LC-QTOF	O	Homoanserine	↑	9.24E-03	1.22	3	LC-QTOF	AA
Uridine monophosphate	↑	1.15E-04	2.05	3	LC-QTOF	CHO	Octadecatetraenoate (18:4n3)	↑	1.10E-02	1.41	1	GC-MSD	FA
Palmitoylcarnitine (C16)	↑	3.32E-04	2.73	1	LC-MS/MS	FA	Glutamate	↓	1.80E-02	1.32	1	LC-MS/MS	AA
Glutaconate	↑	3.80E-04	1.91	3	LC-QTOF	O	Phenylglycine	↑	1.80E-02	0.89	3	LC-QTOF	AA
Proline betaine	↓	1.01E-03	2.05	3	LC-QTOF	AA	Nicotinate	↓	2.41E-02	1.18	3	LC-QTOF	O
Propionylcarnitine	↓	1.03E-03	1.88	3	LC-QTOF	FA	Betaine	↓	2.58E-02	1.77	1	NMR	AA
Aminoacrylate	↓	1.19E-03	1.83	3	LC-QTOF	O	Hexadecanoate (16:0)	↓	3.01E-02	1.44	1	GC-MSD	FA
Aspartate	↓	1.41E-03	2.23	1	LC-MS/MS	AA	Pipecolate	↑	3.49E-02	0.95	3	LC-QTOF	O
Dehydroxycarnitine	↓	1.48E-03	1.75	3	LC-QTOF	FA	Rigin	↓	3.55E-02	0.88	3	LC-QTOF	O

Isovalerylglycine	↓	2.04E-03	1.65	3	LC-QTOF	AA	Lactate	↑	4.33E-02	1.13	1	GC-TOF	CHO
Taurine	↓	3.06E-03	2.79	1	NMR	AA	Glutathione	↓	4.69E-02	1.17	3	LC-QTOF	CHO
N,N-dimethylphenylalanine	↑	3.98E-03	2.10	1	GC-TOF	AA	Adenosine monophosphate	↓	4.76E-02	1.57	1	NMR	O
Carnitine (C0)	↑	4.45E-03	2.07	1	LC-MS/MS	FA	Methoxytyrosine	↑	4.78E-02	1.05	3	UPLC-IM-QTOF	O
Haemolymph													
Compound	**↑ /↓**	***p*-value**	***d*-value**	**ID**	**Platform**	**Group**	**Compound**	**↑ / ↓**	***p*-value**	***d*-value**	**ID**	**Platform**	**Group**
Glutamate	↓	1.20E-07	7.28	1	LC-MS/MS	AA	Serine	↓	3.89E-02	1.14	1	LC-MS/MS	AA
Tauropine	↑	4.62E-04	1.80	3	LC-QTOF	AA	Mannose	↑	4.72E-02	1.20	1	GC-TOF	CHO
Alanine	↑	3.60E-03	1.91	1	LC-MS/MS	AA	Octadecynoic Acid (18:1.5n7)	↑	4.72E-02	0.89	2	GC-MSD	FA
Histidine	↓	3.64E-03	2.14	1	LC-MS/MS	AA	Galactose	↑	4.95E-02	1.22	1	GC-TOF	CHO
Leucine	↑	1.22E-02	1.39	1	LC-MS/MS	AA	Lactate	↑	4.95E-02	0.80	1	GC-TOF	CHO
Palmitoylcarnitine (C16)	↑	2.25E-02	1.46	1	LC-MS/MS	FA	Eicosenoate (20:1)	↑	5.00E-02	0.98	2	GC-MSD	FA
Glutamine	↑	2.31E-02	1.40	1	LC-MS/MS	AA	Hexadecatetraenoate	↑	5.00E-02	0.81	1	GC-MSD	FA
Left gill													
Compound	**↑ /↓**	***p*-value**	***d*-value**	**ID**	**Platform**	**Group**	**Compound**	**↑ / ↓**	***p*-value**	***d*-value**	**ID**	**Platform**	**Group**
Leucine	↓	1.59E-06	5.09	1	LC-MS/MS	AA	Lactate	↑	1.94E-02	1.33	1	GC-TOF	CHO
Proline	↑	8.58E-05	2.86	1	LC-MS/MS	AA	Aminobutyrate	↑	2.15E-02	1.56	3	LC-QTOF	O
Glycine	↑	2.37E-04	2.92	1	LC-MS/MS	AA	Arginine	↑	2.37E-02	1.68	1	NMR	AA
Valine	↓	2.60E-04	2.27	1	LC-MS/MS	AA	Lysine	↑	2.37E-02	1.68	1	NMR	AA
Aminoadipate	↓	4.19E-04	2.15	3	LC-QTOF	CHO	Proline betaine	↑	2.48E-02	1.50	3	LC-QTOF	AA
Alanopine	↑	1.83E-03	1.75	1	LC-MS/MS	AA	Pyruvate	↑	2.72E-02	1.29	3	LC-QTOF	CHO
Palmitoylcarnitine (C16)	↑	6.10E-03	1.62	1	LC-MS/MS	FA	Succinate	↑	2.84E-02	1.22	1	GC-TOF	CHO
Serine	↓	7.48E-03	1.89	1	LC-MS/MS	AA	Threonine	↓	3.75E-02	1.07	3	LC-QTOF	AA
Norvaline	↓	1.12E-02	1.83	1	GC-TOF	AA	Glutamate	↑	3.88E-02	0.99	1	LC-MS/MS	AA
Tetradecanoate (14:0)	↑	1.42E-02	1.34	2	GC-MSD	FA	Pentadecanoate (15:0)	↑	4.56E-02	1.10	1	GC-MSD	FA
Phenylalanine	↓	1.43E-02	1.41	1	LC-MS/MS	AA	Palmitoleate (16:1)	↑	4.58E-02	1.16	1	GC-MSD	FA
Methionine	↓	1.49E-02	1.25	3	LC-QTOF	AA	Acetylcarnitine (C2)	↑	4.74E-02	1.15	3	LC-MS/MS	FA
Right gill													
Compound	**↑ /↓**	***p*-value**	***d*-value**	**ID**	**Platform**	**Group**	**Compound**	**↑ / ↓**	***p*-value**	***d*-value**	**ID**	**Platform**	**Group**
Leucine	↓	3.27E-09	9.71	1	LC-MS/MS	AA	Proline	↑	9.90E-04	2.49	1	LC-MS/MS	AA
Glycine	↑	7.39E-09	8.55	1	LC-MS/MS	AA	Carnitine (C0)	↑	1.64E-03	2.26	1	LC-MS/MS	FA
Aspartate	↓	2.99E-08	10.06	1	LC-MS/MS	AA	Lactate	↑	1.77E-03	2.33	1	GC-TOF	CHO
Arginine	↑	3.48E-08	12.32	1	LC-MS/MS	AA	Aminoadipate	↓	9.27E-03	1.33	3	LC-QTOF	O
Phenylalanine	↓	1.14E-07	8.79	1	LC-MS/MS	AA	Proline betaine	↑	2.12E-02	1.32	3	LC-QTOF	AA
Alanine	↑	2.69E-07	7.57	1	LC-MS/MS	AA	Isovalerylcarnitine	↓	3.02E-02	1.21	3	LC-QTOF	FA
Valine	↓	4.65E-06	3.71	1	LC-MS/MS	AA	Aminoacrylate	↓	4.19E-02	1.13	3	LC-QTOF	O
Glutamate	↓	2.83E-05	3.49	1	LC-MS/MS	AA	Octadecenoate (18:1n9)	↓	4.35E-02	1.09	1	GC-MSD	FA
Tyrosine	↓	8.52E-05	2.78	1	LC-MS/MS	AA	Threonine	↑	5.00E-02	1.14	1	NMR	AA
Serine	↑	6.90E-04	2.95	1	LC-MS/MS	AA	Homarine	↑	5.00E-02	1.20	1	NMR	CHO

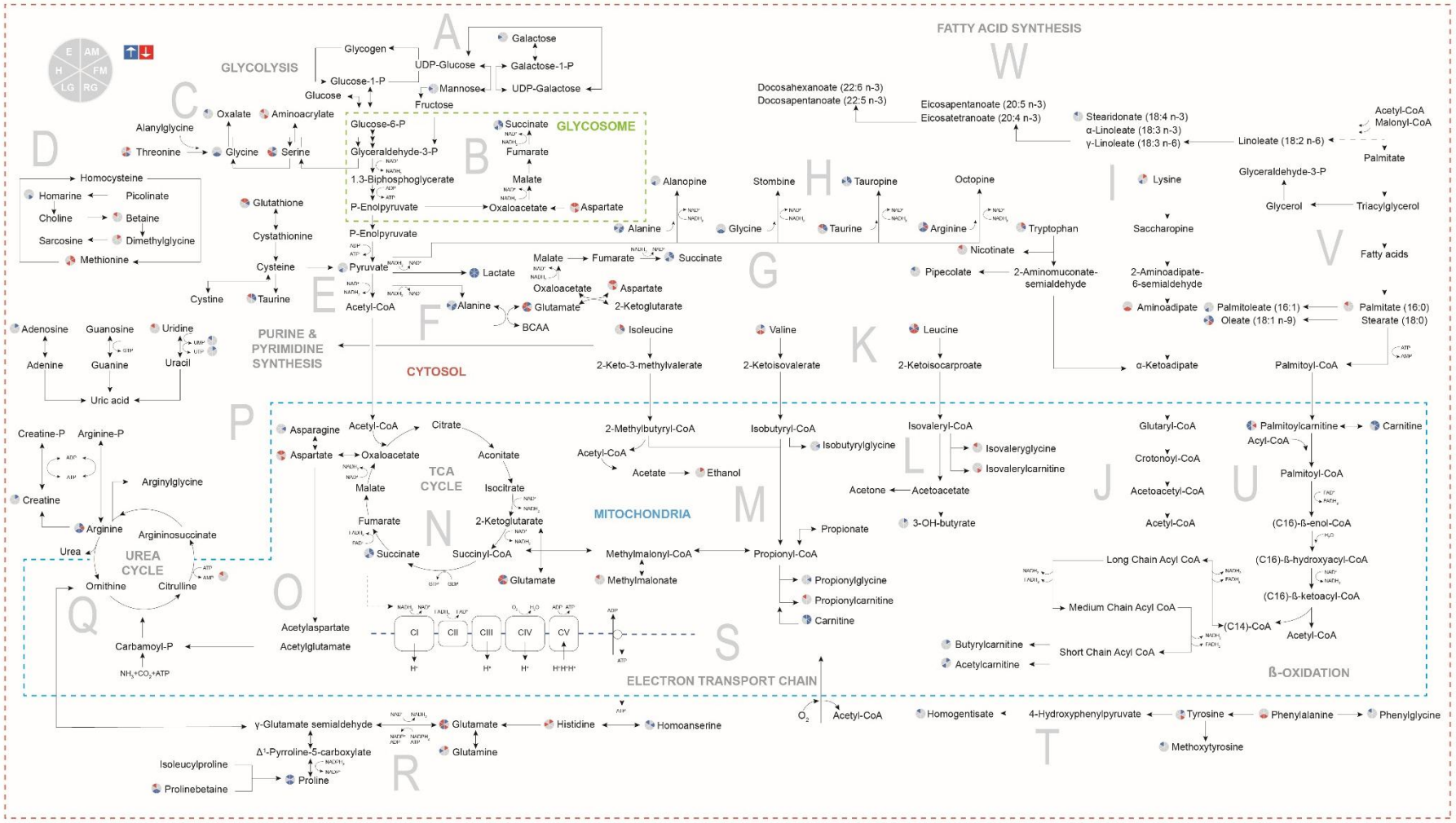

Figure 5.4: The metabolic response of *Haliotis midae* following functional hypoxia. Elevated (blue) and decreased (red) metabolite findings in abalone adductor muscle (AM), foot muscle (FM), left gill (LG), right gill (RG), haemolymph (H) and epipodial tissue (E) following functional hypoxia.

Table 5.2: Metabolite findings of *Haliotis midae* subjected to environmental hypoxia. Compounds are ordered in decreasing statistical (*p*-value) significance. Arrows indicate an increase (↑) or decrease (↓) relative to the normoxic controls. Metabolites are grouped in terms of amino acid (AA), fatty acids (FA), carbohydrates (CHO) and other (O) findings.

Adductor muscle													
Compound	**↑ /↓**	***p*-value**	***d*-value**	**ID**	**Platform**	**Group**	**Compound**	**↑ / ↓**	***p*-value**	***d*-value**	**ID**	**Platform**	**Group**
Homoanserine	↑	2.53E-22	60.62	3	LC-QTOF	AA	Palmitoylcarnitine (C16)	↓	6.34E-05	2.75	1	LC-MS/MS	FA
Arginine	↑	2.74E-20	62.40	1	LC-MS/MS	AA	Serine	↑	8.80E-05	3.42	1	LC-MS/MS	AA
Leukotriene E3	↑	3.75E-18	25.75	3	LC-QTOF	O	Isoleucine	↓	9.41E-05	2.87	1	LC-MS/MS	AA
Taurine	↑	5.26E-18	10.34	3	LC-QTOF	AA	N,N-dimethylglycine	↓	2.89E-04	2.40	1	LC-MS/MS	AA
Acetylaspartate	↓	8.36E-18	6.59	3	LC-QTOF	AA	Tauropine	↑	3.49E-04	2.23	1	LC-MS/MS	AA
Valine	↓	8.58E-18	8.41	3	LC-QTOF	AA	Lactate	↑	1.48E-03	2.07	1	GC-TOF	CHO
Glycine	↑	1.37E-17	9.56	3	LC-QTOF	AA	Tryptophan	↓	2.26E-03	2.19	1	LC-MS/MS	AA
Aminomalonate	↑	4.64E-17	11.02	3	LC-QTOF	CHO	Aminobutyrate	↑	2.78E-03	2.31	1	GC-TOF	O
Arginyl-glycine	↑	3.45E-16	34.32	3	LC-QTOF	AA	Tyrosine	↑	2.87E-03	1.73	1	LC-MS/MS	AA
Hydroxysuberate	↑	6.94E-16	31.17	3	LC-QTOF	FA	Guanosine triphosphate	↓	3.31E-03	1.76	3	UPLC-IM-QTOF	O
Chenodeoxycholate glycine	↑	1.54E-15	20.90	3	LC-QTOF	O	Butyrylcholine	↓	4.80E-03	2.01	3	UPLC-IM-QTOF	AA
Leucine	↓	1.79E-15	7.39	3	LC-QTOF	AA	N-stearoyl phenylalanine	↑	5.02E-03	1.62	3	UPLC-IM-QTOF	AA
Histidine	↑	5.52E-15	14.09	3	LC-QTOF	AA	Threonine	↓	6.60E-03	1.63	1	LC-MS/MS	AA
Aminoadipate	↑	9.43E-15	11.41	3	LC-QTOF	CHO	Proline	↑	8.30E-03	1.65	1	LC-MS/MS	AA
Alanyl-glycine	↑	9.50E-15	7.10	3	LC-QTOF	AA	Uridine	↑	8.89E-03	2.03	1	GC-TOF	O
Pipecolate	↑	1.21E-14	6.79	3	LC-QTOF	O	Cysteinyl-leucine	↓	1.00E-02	1.39	3	UPLC-IM-QTOF	AA
Carnitine (C0)	↑	1.22E-14	12.59	3	LC-QTOF	FA	Uridine triphosphate	↑	1.21E-02	1.40	3	UPLC-IM-QTOF	O
Cinnamate	↑	1.79E-14	4.13	3	LC-QTOF	O	N-stearoyl valine	↑	1.69E-02	1.43	3	UPLC-IM-QTOF	AA
Methyladipate	↑	1.95E-14	22.40	3	LC-QTOF	O	N-stearoyl taurine	↑	1.81E-02	1.34	3	UPLC-IM-QTOF	AA
Lysine	↓	1.01E-13	10.28	1	LC-MS/MS	AA	Glutamine	↑	2.35E-02	1.28	1	LC-MS/MS	AA
Glutamate	↑	2.04E-13	3.53	3	LC-QTOF	AA	Cystine	↑	2.69E-02	1.41	1	LC-QTOF	AA
Methionine	↑	1.15E-12	2.23	3	LC-QTOF	AA	Isoleucyl-threonine	↓	2.82E-02	1.43	3	UPLC-IM-QTOF	AA
Citrate	↑	4.64E-12	2.74	3	LC-QTOF	CHO	Glutathione	↓	2.85E-02	1.06	1	LC-QTOF	O
Propionylcarnitine	↑	2.19E-11	9.48	3	LC-QTOF	FA	Galactose	↑	2.86E-02	1.51	1	GC-TOF	CHO
Isobutyrylglycine	↑	8.18E-11	3.38	3	LC-QTOF	AA	Adenosine	↑	3.00E-02	1.20	3	UPLC-IM-QTOF	O
Aconitate	↑	2.36E-10	6.96	3	LC-QTOF	CHO	Ornithine	↑	3.10E-02	1.17	1	GC-TOF	AA
Propionylglycine	↑	8.60E-10	2.79	3	LC-QTOF	AA	Citrulline	↑	3.12E-02	1.29	1	GC-TOF	AA
Asparate	↓	6.30E-08	6.59	1	LC-MS/MS	AA	Glycyl-threonine	↓	3.36E-02	1.12	3	UPLC-IM-QTOF	AA
Acetylcarnitine (C2)	↑	8.81E-08	6.04	1	LC-MS/MS	FA	Adenosine monophosphate	↑	3.47E-02	1.12	3	UPLC-IM-QTOF	O
Alanine	↑	1.53E-07	7.29	1	LC-MS/MS	AA	Glycerophosphocholine	↓	4.03E-02	1.22	3	UPLC-IM-QTOF	O
Strombine	↑	2.46E-07	6.18	1	LC-MS/MS	AA	Glucose	↑	4.50E-02	1.17	1	NMR	CHO
Succinate	↑	2.72E-06	3.37	1	GC-TOF	CHO	Pyroglutamate	↑	4.56E-02	1.01	3	LC-QTOF	AA
Chenodeoxycholate	↑	3.21E-05	1.37	3	LC-QTOF	O	Ecgonine	↑	4.76E-02	1.00	3	LC-QTOF	O
Phenylalanine	↓	4.29E-05	3.44	1	LC-MS/MS	AA	Nonadecylate	↓	4.81E-02	1.08	3	UPLC-IM-QTOF	O
Hydroxy-oregnane-one	↑	5.60E-05	1.33	3	LC-QTOF	O	Octadecatrienoate (18:3n6)	↓	5.00E-02	1.04	1	GC-MSD	FA
Foot muscle													
Compound	**↑ /↓**	***p*-value**	***d*-value**	**ID**	**Platform**	**Group**	**Compound**	**↑ / ↓**	***p*-value**	***d*-value**	**ID**	**Platform**	**Group**
Succinate	↑	8.23E-06	4.22	1	GC-TOF	CHO	Adenosine monophosphate	↓	3.01E-03	2.57	1	NMR	O
Lactate	↑	7.44E-05	3.08	1	GC-TOF	CHO	Taurine	↓	3.47E-03	1.97	3	LC-QTOF	AA
Acetylglutamate	↓	9.46E-05	1.76	3	LC-QTOF	O	Glycine	↑	1.14E-02	1.45	1	LC-MS/MS	AA
Butyrylcarnitine (C4)	↑	1.38E-04	3.33	1	LC-MS/MS	FA	Glutamate	↓	1.16E-02	1.68	1	LC-MS/MS	AA
Tauropine	↑	3.12E-04	2.84	1	LC-MS/MS	AA	Phosphate	↑	1.24E-02	1.40	1	GC-TOF	O

Aminomalonate	↑	3.58E-04	1.65	3	LC-QTOF	CHO	Tryptophan	↑	1.78E-02	1.88	1	NMR	AA
Methionine	↓	6.43E-04	2.21	1	LC-MS/MS	AA	Argininosuccinate	↑	1.88E-02	1.37	3	UPLC-IM-QTOF	CHO
N,N-dimethylglycine	↑	7.02E-04	2.59	1	LC-MS/MS	AA	Aminobenzoate	↓	1.92E-02	1.48	3	LC-QTOF	O
Arginine	↓	8.34E-04	2.63	1	LC-MS/MS	AA	Proline	↑	2.67E-02	1.11	1	LC-MS/MS	AA
Aspartate	↓	1.41E-03	2.17	1	LC-MS/MS	AA	Valyl-glycine	↓	3.27E-02	0.82	3	LC-QTOF	AA
Aminoacrylate	↓	1.83E-03	2.15	3	LC-QTOF	O	Serine	↑	3.44E-02	1.16	1	LC-MS/MS	AA
Isovalerylcarnitine	↓	1.93E-03	2.22	3	LC-QTOF	FA	N-stearoyl phenylalanine	↑	3.81E-02	1.15	3	UPLC-IM-QTOF	AA
Creatine	↓	2.82E-03	1.65	1	LC-MS/MS	CHO	Ethanol	↑	3.93E-02	1.47	1	NMR	FA
Alanine	↑	2.98E-03	2.12	1	GC-TOF	AA	Ornithine	↑	4.28E-02	1.28	1	GC-TOF	AA
Epipodial tissue													
Compound	**↑ /↓**	***p*-value**	***d*-value**	**ID**	**Platform**	**Group**	**Compound**	**↑ / ↓**	***p*-value**	***d*-value**	**ID**	**Platform**	**Group**
Aminomalonate	↑	2.68E-19	9.56	3	LC-QTOF	CHO	Hexanoate	↑	2.69E-03	1.97	1	GC-TOF	O
Rignin	↑	6.39E-16	8.42	3	LC-QTOF	O	Isoleucyl-proline	↓	2.86E-03	1.60	3	LC-QTOF	AA
Lactate	↑	2.94E-09	15.5	1	GC-TOF	CHO	Homogentisate	↑	3.96E-03	1.11	3	LC-QTOF	O
Succinate	↑	9.55E-09	6.13	1	GC-TOF	CHO	Proline	↑	4.19E-03	1.80	1	LC-MS/MS	AA
Aminoacrylate	↓	1.54E-08	7.57	3	LC-QTOF	O	Glutathione	↓	5.30E-03	1.83	3	LC-QTOF	O
Alanine	↑	2.09E-06	6.52	1	GC-TOF	AA	Histidine	↑	6.61E-03	1.47	1	LC-MS/MS	AA
Acetylcarnitine (C2)	↑	7.20E-06	2.88	1	LC-QTOF	FA	Methylmalonate	↓	6.68E-03	1.99	1	NMR	CHO
Aspartate	↓	1.04E-05	4.16	1	LC-MS/MS	AA	Arginine	↑	9.74E-03	1.51	1	LC-MS/MS	AA
Glutamate	↑	2.56E-05	3.78	1	LC-MS/MS	AA	Butyrylcarnitine (C4)	↓	9.75E-03	1.31	3	LC-QTOF	FA
Strombine	↑	5.58E-05	2.62	1	LC-QTOF	AA	Palmitoylcarnitine (C16)	↑	1.17E-02	1.33	1	LC-MS/MS	FA
Leukotriene C4	↓	7.31E-05	0.87	3	LC-QTOF	O	Pipecolate	↑	1.21E-02	1.49	3	LC-QTOF	O
N,N-dimethylphenylalanine	↑	2.26E-04	3.19	1	GC-TOF	AA	Isovalerylglycine	↓	1.75E-02	1.13	3	LC-QTOF	AA
Proline betaine	↓	2.41E-04	1.94	3	LC-QTOF	AA	Docosahexaenoate (22:6n3)	↑	2.48E-02	1.32	1	GC-MSD	FA
Alanyl-glycine	↑	3.28E-04	1.02	3	LC-QTOF	AA	Isoleucine	↑	3.05E-02	1.32	1	LC-MS/MS	AA
Oxalate	↑	4.27E-04	3.43	1	GC-TOF	CHO	Octadenoate (18:1n12)	↑	4.23E-02	1.12	1	GC-MSD	FA
Cysteinyl-cysteine	↑	1.06E-03	2.03	3	UPLC-IM-QTOF	AA	Palmitate (16:0)	↓	4.44E-02	1.28	1	GC-MSD	FA
Leukotriene E3	↑	1.53E-03	1.11	3	LC-QTOF	O	Homoanserine	↑	4.58E-02	1.06	3	LC-QTOF	AA
Otadecatetraenoate (18:4n3)	↑	1.66E-03	1.87	1	GC-MSD	FA	Glycine	↑	4.98E-02	1.43	1	GC-TOF	AA
Haemolymph													
Compound	**↑ /↓**	***p*-value**	***d*-value**	**ID**	**Platform**	**Group**	**Compound**	**↑ / ↓**	***p*-value**	***d*-value**	**ID**	**Platform**	**Group**
Lactate	↑	5.56E-10	11.21	1	GC-TOF	CHO	Alanyl-glycine	↓	8.23E-03	1.84	3	LC-QTOF	AA
Alanine	↑	7.93E-08	6.99	1	LC-MS/MS	AA	Asparagine	↓	8.44E-03	1.17	3	LC-QTOF	AA
Proline	↓	1.81E-06	4.26	1	LC-MS/MS	AA	Cystine	↓	1.01E-02	1.16	3	LC-QTOF	AA
Taurine	↑	2.84E-06	4.33	1	LC-MS/MS	AA	Mannose	↑	1.18E-02	1.64	1	GC-TOF	CHO
Arginine	↓	4.17E-06	4.93	1	LC-MS/MS	AA	Pipecolate	↓	1.32E-02	1.89	3	LC-QTOF	O
Glutamine	↓	5.75E-06	4.54	1	LC-MS/MS	AA	Proline betaine	↓	1.43E-02	1.47	3	LC-QTOF	AA
Glutamate	↓	1.18E-05	3.37	1	LC-MS/MS	AA	Serine	↓	1.44E-02	1.62	1	GC-TOF	AA
Histidine	↓	2.33E-05	4.17	1	LC-MS/MS	AA	Methionine	↓	1.95E-02	1.46	1	LC-MS/MS	AA
Succinate	↑	6.98E-05	0.80	1	GC-TOF	CHO	Glycine	↓	2.05E-02	1.15	1	LC-MS/MS	AA
Aspartate	↓	7.71E-05	2.91	1	LC-MS/MS	AA	Carbamate	↓	2.19E-02	1.29	3	LC-QTOF	O
Carnitine (C0)	↑	3.30E-04	2.70	1	LC-MS/MS	FA	Valine	↓	2.72E-02	1.24	1	LC-MS/MS	AA
Ecgonine	↓	8.82E-04	2.19	3	LC-QTOF	O	Acetate	↑	2.92E-02	1.09	1	NMR	FA
Isocitrate	↑	9.51E-04	2.14	3	LC-QTOF	CHO	Phenylglycine	↑	3.56E-02	1.22	3	LC-QTOF	AA
Acetylcarnitine (C2)	↑	1.49E-03	2.47	1	LC-MS/MS	FA	Nicotinate	↓	3.72E-02	1.30	3	LC-QTOF	O
Palmitoylcarnitine (C16)	↑	1.60E-03	1.91	1	LC-MS/MS	FA	Isovalerylglycine	↓	3.73E-02	1.34	3	LC-QTOF	AA
Isovalerylcarnitine	↓	2.22E-03	1.73	3	LC-QTOF	FA	Citrate	↑	3.85E-02	1.09	3	LC-QTOF	CHO
Pyroglutamate	↓	4.29E-03	2.15	3	LC-QTOF	AA	Strombine	↓	3.94E-02	1.08	1	LC-MS/MS	AA
Tauropine	↑	5.26E-03	1.87	1	LC-QTOF	AA	Octadecanoate (18:0)	↑	3.96E-02	1.13	1	GC-MSD	FA
Isoleucine	↑	6.92E-03	1.64	1	LC-MS/MS	AA	Methylmalonate	↓	4.45E-02	1.11	1	NMR	CHO
Hexadecatetraenoate	↑	7.20E-03	1.76	1	GC-MSD	FA	Oxalate	↑	4.67E-02	1.21	1	GC-TOF	CHO
Galactose	↑	8.01E-03	1.71	3	GC-TOF	CHO							

Left gill													
Compound	**↑ /↓**	***p*-value**	***d*-value**	**ID**	**Platform**	**Group**	**Compound**	**↑ / ↓**	***p*-value**	***d*-value**	**ID**	**Platform**	**Group**
Aspartate	↓	1.23E-11	18.22	1	LC-MS/MS	AA	Methoxytyrosine	↓	1.23E-03	2.27	3	LC-QTOF	AA
Alanine	↑	2.22E-11	14.97	1	LC-MS/MS	AA	Cysteine-glutathione disulfide	↓	1.32E-03	2.11	3	LC-QTOF	O
Isoleucine	↓	1.09E-09	10.75	1	LC-MS/MS	AA	Aconitate	↑	1.94E-03	2.56	3	LC-QTOF	CHO
Glutamine	↓	9.54E-07	5.65	1	LC-MS/MS	AA	Ecgonine	↑	2.51E-03	1.77	3	LC-QTOF	O
Lysine	↓	1.77E-06	4.49	1	LC-MS/MS	AA	Asparagine	↓	2.81E-03	2.05	3	LC-QTOF	AA
Aminoacrylate	↓	1.91E-06	4.69	3	LC-QTOF	O	Threonine	↓	5.22E-03	1.60	3	LC-QTOF	AA
Glutamate	↑	2.19E-06	4.00	1	LC-MS/MS	AA	Carnitine (C0)	↓	7.57E-03	1.46	1	LC-MS/MS	FA
Lactate	↑	4.99E-06	5.43	1	GC-TOF	CHO	Butyrylcarnitine (C4)	↑	9.73E-03	1.42	3	LC-QTOF	FA
Isovalerylcarnitine	↓	5.40E-06	4.08	1	LC-QTOF	FA	Taurine	↑	1.20E-02	1.55	1	LC-MS/MS	AA
Succinate	↑	1.34E-05	4.89	1	GC-TOF	CHO	Adenosyl-ornithine	↓	1.27E-02	1.41	3	UPLC-IM-QTOF	AA
Alanopine	↑	1.68E-05	3.35	1	LC-MS/MS	AA	Leucine	↓	1.37E-02	1.52	1	LC-MS/MS	AA
Phenylalanine	↓	2.50E-05	3.58	1	LC-MS/MS	AA	Phenylglycine	↑	1.43E-02	1.63	3	LC-QTOF	AA
Proline	↑	5.01E-05	3.86	1	LC-MS/MS	AA	Betaine	↓	2.35E-02	1.68	1	NMR	AA
Valine	↓	6.14E-05	2.84	1	LC-MS/MS	AA	Carbamate	↓	2.47E-02	1.19	3	LC-QTOF	O
Homoarginine	↑	6.84E-05	3.20	3	UPLC-IM-QTOF	AA	Glutathione	↑	2.55E-02	1.30	3	LC-QTOF	O
Acetylcarnitine (C2)	↑	8.33E-05	3.10	1	LC-MS/MS	FA	Pyruvate	↑	3.55E-02	1.23	3	LC-QTOF	CHO
Adenosine	↓	9.45E-05	2.57	3	UPLC-IM-QTOF	O	Tyrosine	↓	3.85E-02	1.13	1	LC-MS/MS	AA
Serine	↓	1.03E-04	3.00	1	LC-MS/MS	AA	Methyladipate	↓	3.90E-02	0.87	3	LC-QTOF	O
Strombine	↑	1.46E-04	2.84	1	LC-QTOF	AA	Octopine	↑	4.36E-02	0.88	1	LC-QTOF	AA
Rigin	↓	1.57E-04	2.79	3	LC-QTOF	O	Arginine	↑	4.98E-02	0.94	1	LC-MS/MS	AA
Palmitoylcarnitine (C16)	↑	5.42E-04	2.68	1	LC-MS/MS	FA	Tauropine	↑	4.99E-02	1.15	1	LC-QTOF	AA
Proline betaine	↓	8.29E-04	2.08	3	LC-QTOF	AA	Docosahexaenoate (22:6n3)	↓	1.33E-01	0.80	1	GC-MSD	FA
Glycine	↑	1.23E-03	2.45	1	LC-MS/MS	AA							
Right gill													
Compound	**↑ /↓**	***p*-value**	***d*-value**	**ID**	**Platform**	**Group**	**Compound**	**↑ / ↓**	***p*-value**	***d*-value**	**ID**	**Platform**	**Group**
Alanine	↑	1.03E-11	14.96	1	LC-MS/MS	AA	Taurine	↑	1.51E-04	2.87	1	LC-MS/MS	AA
Isoleucine	↓	6.62E-10	12.90	1	LC-MS/MS	AA	Glycine	↑	2.60E-04	2.42	1	LC-MS/MS	AA
Tauropine	↑	1.85E-09	8.96	1	LC-MS/MS	AA	Succinate	↑	2.63E-04	2.68	1	GC-TOF	CHO
Aspartate	↓	5.08E-09	7.55	1	LC-MS/MS	AA	Acetylacetone	↑	6.31E-04	2.24	3	UPLC-IM-QTOF	FA
Glutamine	↓	8.51E-09	7.33	1	LC-MS/MS	AA	Adenine	↓	2.64E-03	1.69	3	UPLC-IM-QTOF	FA
Oleoyl glycine	↓	2.35E-07	1.16	3	UPLC-IM-QTOF	AA	Alanyl-lysine	↑	3.62E-03	1.32	3	UPLC-IM-QTOF	AA
Proline betaine	↓	2.56E-07	5.73	3	LC-QTOF	AA	Valine	↓	7.52E-03	1.68	1	LC-MS/MS	AA
Arginine	↑	3.81E-07	5.45	1	LC-MS/MS	AA	Choline	↑	8.99E-03	2.07	1	NMR	AA
Proline	↑	5.42E-07	5.38	1	LC-MS/MS	AA	Citrate	↑	9.13E-03	1.64	3	LC-QTOF	CHO
Isovalerylcarnitine	↓	1.02E-06	4.68	3	LC-QTOF	FA	Threonine	↑	1.02E-02	1.93	1	NMR	AA
Aminoacrylate	↓	4.46E-06	3.91	3	LC-QTOF	O	Palmitoylcarnitine (C16)	↑	1.13E-02	1.70	1	LC-MS/MS	FA
Strombine	↑	5.32E-06	4.99	1	LC-QTOF	AA	Sarcosine	↑	1.14E-02	1.74	3	LC-QTOF	CHO
Carnitine (C0)	↓	5.41E-06	4.69	1	LC-MS/MS	FA	Adenosine monophosphate	↑	1.38E-02	1.71	1	NMR	O
Acetylcarnitine (C2)	↑	1.39E-05	4.34	1	LC-MS/MS	FA	Serine	↓	2.80E-02	1.48	1	LC-MS/MS	AA
Lactate	↑	2.06E-05	3.45	1	GC-TOF	CHO	Isovalerylglycine	↑	3.46E-02	1.04	3	LC-QTOF	AA
Glutamate	↑	3.26E-05	3.23	1	LC-MS/MS	AA	Ecgonine	↑	3.55E-02	1.15	3	LC-QTOF	O
Picolinate	↑	4.25E-05	3.43	3	LC-QTOF	O	Acetate	↑	3.74E-02	1.50	1	NMR	O
Alanopine	↑	6.83E-05	3.14	1	LC-MS/MS	AA	Eicosapentaenoate (20:5n3)	↓	4.83E-02	1.09	1	GC-MSD	FA
Histidine	↓	9.44E-05	3.32	1	LC-MS/MS	AA							

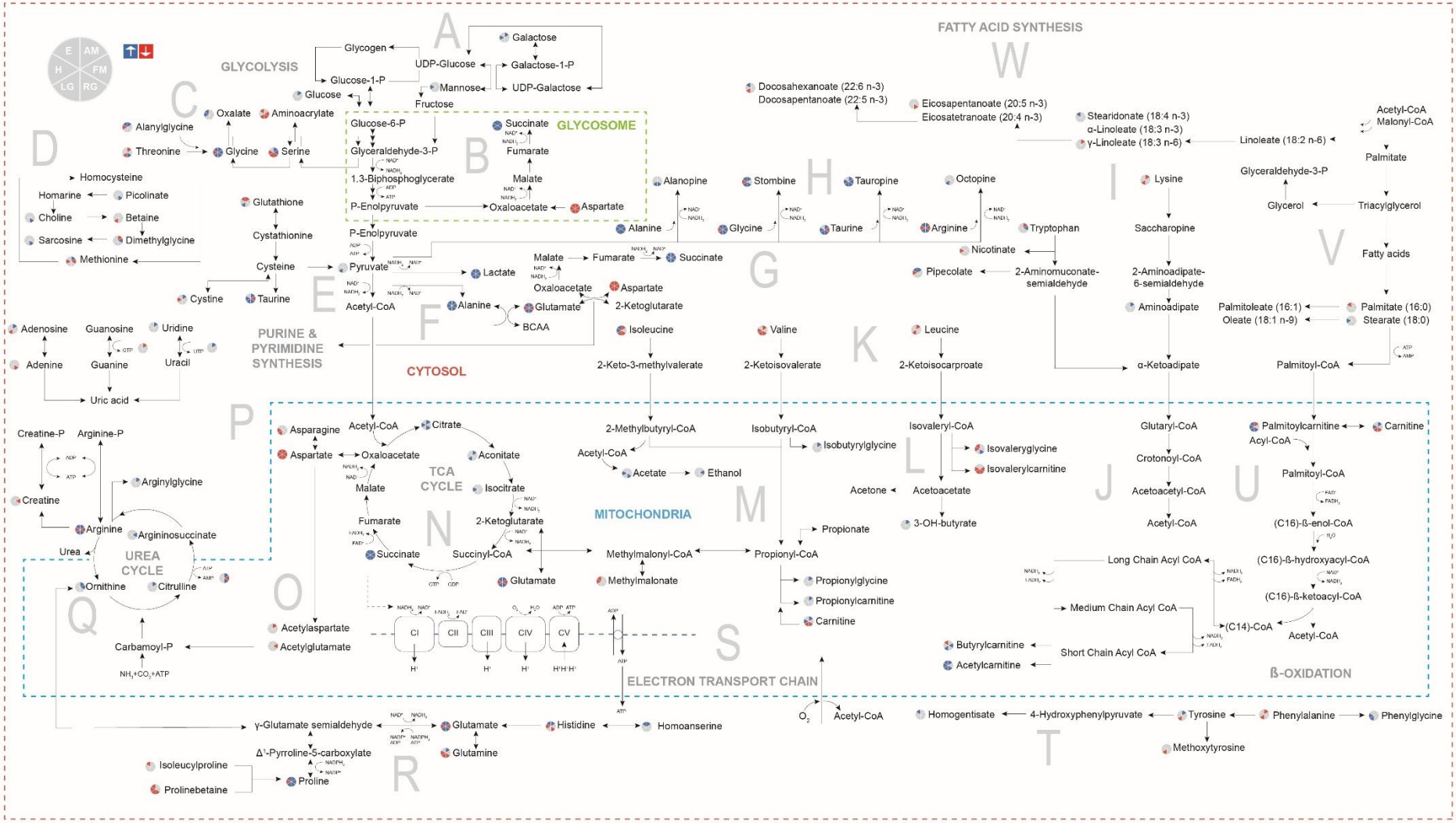

Figure 5.5: The metabolic response of *Haliotis midae* following environmental hypoxia. Elevated (blue) and decreased (red) metabolite findings in abalone adductor muscle (AM), foot muscle (FM), left gill (LG), right gill (RG), haemolymph (H) and epipodial tissue (E) following environmental hypoxia

5.3.1 Metabolic pathways involved in NAD^+ recovery and ATP production during anaerobic respiration

It is already well-known that substrate-level-phosphorylation serves as an alternative route for ATP production when mitochondrial respiratory activity become inadequate (Feala *et al.*, 2009). Based on results of Figs. 5.4 and 5.5, *H. midae* utilises substrate-level-phosphorylation in terms of: 1) phosphagen breakdown (Pathway Q) and 2) anaerobic glycolysis (Pathways B, F and H), for energy production during functional and environmental hypoxia.

5.3.1.1 Phosphagen breakdown

Typically, abalone use phosphoarginine as the primary phosphagen for instant energy liberation (Grieshaber *et al.*, 1993). However, the presence of creatine in the abductor and foot muscle of hypoxic abalone, suggests that energy production also occurs via phosphocreatine metabolism during such conditions. In Fig. 5.4 (Pathway Q), the contribution of arginine and creatine towards the production of phosphoarginine and phosphocreatine for ATP production in the adductor muscle, is proposed during episodes of muscle work, considering the elevated levels of these metabolites detected in this investigation. Interestingly, however, exposing abalone to environmental hypoxia resulted in reduced levels of arginine and creatine levels in the foot muscle samples (Fig. 5.5), which is most likely due to the further breakdown pathways being up-regulated in this tissue sample. The other tissue samples analysed (epipodial tissue, adductor muscle and the gills), displayed similarly to the abductor muscle sample, showing elevated levels of arginine during the environmental hypoxia, as one would commonly encounter when phosphoarginine is hydrolysed to drive the synthesis of ATP directly from the phosphorylation of adenosine diphosphate (ADP), resulting in the release of free arginine and ATP (Garrett and Grisham, 2010).

5.3.1.2 Glycolytic ATP production

The elevated levels of lactate, opines, succinate and alanine detected in *H. midae* (Tables 5.1 and 5.2), suggest that these metabolites and their associated pathways are involved in the regeneration of cytoplasmic nicotinamide adenine dinucleotide (NAD^+) for usage in the glyceraldehyde-3-phosphate dehydrogenase reaction of glycolysis (Pathway B) (Figs. 5.4 and 5.5). Since NAD^+ feeds into the glycolysis pathway, it enables both the phosphoglycerate kinase and pyruvate kinase reactions to synthesise ATP directly from the phosphorylation of ADP (Garrett and Grisham, 2010). The three complementary glycolytic pathways: 1) glucose-lactate pathway, 2) glucose-opine pathway and 3) glucose/aspartate-succinate pathway, involved in NAD^+ recovery in the abalone *H. midae* (Figs. 5.4 and 5.5), will be evaluated individually below in terms of the findings presented in Tables 5.1 and 5.2.

Glucose-pyruvate-lactate conversion

Elevated pyruvate was detected in the left gill during functional hypoxia (Table 5.1), as well as during environmental hypoxia (Table 5.2), albeit more severe when one takes *d*-value into account. In an attempt to avoid metabolic shutdown and allow continued glycolysis during hypoxia, pyruvate is converted to lactate, oxidising NADH (reduced form) to NAD^+ (oxidised form) (Whitney and Rolfes, 2008). Elevated lactate levels were found in all of the abalone tissues investigated (adductor muscle, foot muscle, left gill, right gill, haemolymph and epipodial tissue), following functional and environmental hypoxia. During prolonged anaerobic metabolism, lactate synthesis will eventually exceed the clearance thereof, resulting in a reduction in intracellular pH (Green and Storey, 2016), which in turn further limits the contribution of ATP homeostasis over long periods of anaerobic stress. In order to prevent acidification, an increase in cell buffer capacity is subsequently required (Garrett and Grisham, 2010), which is partially accomplished in *H. midae* by the production of alanine and opines (discussion to follow). Furthermore, the conversion of pyruvate to lactate is easily reversible when the NADH:NAD^+ ratio decreases, typically as abalone recover from hypoxic stress, and therefore plays an important role in the short-term regulation of ATP production via anaerobic glycolysis. Confirming the observations in this study, elevated lactate in various other abalone species, after exposure to stressors such as anoxia (Gäde, 1988, O'omolo *et al.*, 2003), air exposure (Wells and Baldwin, 1995), wave action (Wells *et al.*, 1998b), starvation (Sheedy *et al.*, 2015), toxins (Zhou *et al.*, 2015) and thermal and hypoxic stress (Lu *et al.*, 2016, Tripp-Valdez *et al.*, 2017) demonstrates that abalone utilise this conversion of pyruvate to lactate as a survival mechanism when aerobic respiration is compromised.

Glucose-pyruvate-opine conversion

Opines, another group of anaerobic end-products, were produced in *H. midae* (Figs. 5.4 and 5.5) by the condensation of pyruvate and various amino acids in the presence of NADH and H^+, to yield an opine product, NAD^+ and H_2O (Sato *et al.*, 1993). Although elevated levels of alanine, glycine, taurine and arginine were detected, following both hypoxic scenarios, tissue specific accumulation of alanopine, strombine, tauropine, and octopine levels were more noticeable in the environmental hypoxic group (Table 5.2). A trend between the specific opines formed and their associated amino acids, can be seen following environmental hypoxia (Fig. 5.5 - Pathway H). Elevated levels of alanine were also accompanied by an elevation in alanopine in the left and right gill samples. Reduced levels of glycine were accompanied by a reduction in strombine in the haemolymph. Taurine was seen to be elevated in the adductor muscle, gills and haemolymph samples analysed, and tauropine was elevated in the adductor muscle, gills and haemolymph samples. Octopine was elevated in only the left gill samples, which also corresponded to the elevated levels of arginine in the same sample. These results not only

indicate the extent of the hypoxic stress induced during the environmental hypoxia experiment, but also abalones' dependence on these opine pathways for energy production during anaerobic conditions. Similar associations between opines and their corresponding amino acids, were also recognised in other animals, where the production of opines following environmental hypoxia vary in correspondence to the variability in amino acids (Kreutzer *et al.*, 1989).

The synthesis of opines during functional hypoxia (Fig. 5.4, Table 5.1) was less pronounced in the abalone investigated in this study, as only alanopine (left gill) and tauropine (in the highest concentrations in the foot muscle, adductor muscle and then also the haemolymph samples) was produced. Interestingly, no octopine (formed from the condensation of pyruvate and arginine) was detected in *H. midae* exposed to functional hypoxia (Pathway H), despite arginine availability in these tissues. This is most likely due to the low enzyme activity of octopine dehydrogenase in this species (O'omolo *et al.*, 2003), or the role of the phosphoarginine and arginine flux to replenish ATP pools during the initial phase of functional hypoxia (Grieshaber *et al.*, 1993). These results suggest that functional hypoxia (Table 5.1) is not severely anaerobic enough for *H. midae* to require octopine synthesis. It has previously been reported, that octopine formation only occurs during recovery from functional anaerobiosis in most *Pecten* species (Gäde *et al.*, 1984). Following physical activity, octopine dehydrogenase was, however, detected in *H. kamtschatkana* (Donovan *et al.*, 1999) and *H. midae* (O'omolo *et al.*, 2003) without allowing some time for recovery.

Interplay between lactate and opines in abalone

Contrary to previous research reporting elevated concentrations of lactate and tauropine in both the adductor and foot muscles in the abalone *H. lamellosa* (Gäde, 1988), *H. discus hannai* (Sato *et al.*, 1991), *H. iris* (Baldwin *et al.*, 1992) and *H. midae* (O'omolo *et al.*, 2003) after functional hypoxia (Table 5.1), this study identified the highest concentrations of lactate and tauropine in the analysed foot muscle samples. Previous reports speculate that the shell adductor muscle is the main source of tauropine production during exercise, as it enables the animal to re-attach itself after becoming dislodged. In fact, a fivefold increase in the adductor muscle tauropine was reported in *H. kamtschatkana*, leading to the argument that anaerobic glycolysis supplies some of the much needed energy required in the adductor muscle, in contrast to that of the foot muscle, which primarily produces energy aerobically (Donovan *et al.*, 1999). The fact that lactate was elevated in all of the tissues investigated in our study, while tauropine was only elevated in half of the investigated tissues, following functional hypoxia (Fig. 5.4), suggests a gradual and progressive requirement for ATP during prolonged exposure to hypoxia. This is plausible since lactate is produced via a single metabolic conversion (pyruvate + lactate dehydrogenase = lactate), and subsequently produced rather fast in response to a

hypoxic onslaught. If functional hypoxia persists, however, the energy requirement would consequently be expected to surpass the amount of NAD^+ produced via lactate alone, and hence the synthesis of these intermediates via alternative/additional processes like the tauropine pathway for instance. Abalone tissue is known to contain high concentrations of taurine [the most abundant amino acid in abalone (Baldwin *et al.*, 1992)], traditionally used for osmoregulation, but the high amounts of taurine can also be used for the production of tauropine, which assists with osmoregulation amongst other things. It seems probable that opine formation does not proceed in a specific order or preference, but the particular opine formed is dependent on which amino acids are available for use, via these anaerobic energy supply mechanisms. This line of thought is confirmed by previous data collected from *Sipunculus nudus* muscle samples, where at a high glycolytic flux, only the opine dehydrogenases, which were present at high levels of activity, catalysed the formation of an end product (Kreutzer *et al.*, 1989). An interesting observation made in *Lolliguncula brevis,* is that once an anaerobic threshold has been reached, the simultaneous accumulation of different metabolites takes place, as well as a decrease in phosphagens, indicating limited oxygen supply to the mitochondria and the onset of anaerobic metabolism in the cytosol and mitochondria (Pörtner, 2002). Once *H. midae* achieves an anaerobic threshold, the possibility exists that multiple opines may be produced if the extent of the functional hypoxia requires it, but at the current energy state of the functional hypoxia experiment in this study, however, the need for multiple opines cannot be justified, as sufficient ATP is still being produced using the other anaerobic systems.

In this study environmental hypoxia resulted in elevated levels of both lactate and tauropine, in both the adductor and foot muscle samples analysed. Other studies previously done, focusing on opine and lactate metabolism in the adductor and foot muscle of *H. lamellosa* (Gäde, 1988) and *H. midae* (O'omolo *et al.*, 2003), following exposure to environmental hypoxia, indicated isolated elevations of tauropine in the shell adductor muscle and lactate in the foot muscle, but no elevations of both in the same tissue. One should, however, keep in mind that the analytical platforms used in the present study are far more sensitive than the traditional enzyme-linked reactions previously used. With that said, lactate was, detected in comparatively higher levels in the foot muscle, while tauropine was more abundant in the adductor muscle of *H. midae* (Table 5.2), corresponding to the isolated findings of Gäde (1988) and O'omolo *et al.* (2003). The production of predominately lactate (but also tauropine), in the foot muscle of *H. midae* during hypoxia, is an expected outcome since this low cost metabolic reaction is expected to take place in a less metabolically active tissue. During episodes of environmental hypoxia, abalone would require limited movement resulting in even less activity required by the foot muscle. On the other hand, the presence of tauropine and lactate (in lower levels) in the adductor muscle during environmental hypoxia demonstrates a continued dependence on the adductor muscle

for metabolic activity (Gäde, 1988). The finding of accumulated lactate and tauropine in both muscle tissue samples, analysed in *H. iris* (Baldwin *et al.*, 1992, Behrens *et al.*, 2002), *H. kamtschatkana* (Donovan *et al.*, 1999) and *H. australis* (Wells and Baldwin, 1995), adds to the findings of the present study. Furthermore, elevated levels of lactate and tauropine were previously reported in the haemolymph of *H. iris* (Behrens *et al.*, 2002) and the gill samples of *H. midae* (O'omolo *et al.*, 2003). It should be mentioned that both lactate and tauropine were elevated in majority of the tissues investigated in this study (Fig. 5.5), highlighting their importance as anaerobic metabolic end products.

Glucose/aspartate-succinate conversion

Environmental hypoxia resulted in reduced aspartate, accompanied by elevated concentrations of alanine and succinate in all of the tissues investigated (Table 5.2, and Fig. 5.5), indicating activation of the glucose/aspartate-succinate glycosomale-based pathway, and subsequently elevations of NAD^+, at the expense of NADH (Pathway B). Functional hypoxia showed the same response, however, in far less tissues (Table 5.1 and Fig. 5.4). A synchronised depletion of aspartate, accompanied by elevations in alanine and succinate in the foot and adductor muscles of other abalone, were also previously reported in response to anoxia (Gäde, 1988), confirming our findings. Succinate is the end product of the glucose-succinate pathway (Pathway B), the aspartate-succinate pathway (Pathway G) and the TCA cycle (Pathway N), during conditions of anaerobic ATP production in abalone. The metabolic fate of succinate, however, is not entirely known, and it may simply accumulate and then later be reused in gluconeogenesis when aerobic respiration occurs again, and/or be used by the mitochondria where it can be converted to propionate or arginine.

5.3.2 The involvement of carbohydrate metabolism during hypoxia

Various sugar-based metabolites, including galactose, mannose (both hypoxic conditions) and glucose (environmental hypoxia only), were generally seen to be elevated in *H. midae,* following hypoxic exposure (Figs. 5.4 and 5.5). Glycolysis and interconnected carbohydrate pathways use several sugar substrates (Pathway A) for energy production. These pathways become more important during hypoxia when anaerobic energy production is required, resulting in the up-regulation of gluconeogenesis and the release of carbohydrates from glycogen stores and glycoproteins (Roznere *et al.*, 2014). This can lead to elevated carbohydrate metabolites, as seen in abalone, which also depends more heavily on glycolysis for anaerobic energy production to survive hypoxia.

During environmental hypoxia elevations in the TCA cycle intermediates (Pathway N), citrate, aconitate, isocitrate and succinate, were detected (Table 5.2). On closer investigation, these increases suggest down-regulation of the TCA cycle via isocitrate dehydrogenase, which is responsible for the conversion of isocitrate to α-ketoglutarate, as a means to prevent metabolic energy waste (Garrett and Grisham, 2010). The aforementioned redox imbalance (due to reduced NAD^+) is a major contributor to this down-regulation and the accumulation of the aforementioned intermediates. Fortunately, however, alternative substrates, such as glutamate, can still be used to synthesise the much needed α-ketoglutarate and down-stream TCA cycle intermediates very effectively (Boardman *et al.*, 2016) during hypoxia, preventing total TCA cycle shutdown. Furthermore, production of NAD^+ through the lactate and opine pathways, also ensure that some functionality of the TCA cycle is retained, despite electron carriers ($NADH_2$ and $FADH_2$) not flowing to the electron transport chain (Pathway S). The functional hypoxia results (Fig. 5.4) suggest that sufficient substrates were still available from glycolysis for normal TCA cycle functioning and aerobic ATP supply via the electron transport chain. As the intermediates of the TCA cycle (excluding succinate) were not detected as decreased or increased following functional hypoxia, it can be said that abalone initially depend on aerobic mechanisms for ATP supply and only later require anaerobic ATP production, as demonstrated by the production of lactate, opines and succinate.

Once again, the fundamental role of succinate during hypoxia in abalone becomes apparent when one considers this in the context of the TCA cycle (Tables 5.1 and 5.2). Further confirmation of this, is the elevated levels of succinate detected in oxygen stress scenarios and subsequent oxidative stress in shellfish (Young *et al.*, 2016). However, considering the role of succinate as an end product of anaerobic glycolysis, it is more likely indicative of the mechanisms of anaerobic energy production. Succinate has also previously been shown to stabilise the alpha subunit of hypoxia inducible factor, which further supports the latter hypothesis. Furthermore, the accumulation of succinate in a biological system, has been indicated to result in a shift in metabolism towards glycolysis, and also lactate synthesis, via the activation of transcription genes which downregulate oxidative phosphorylation (Young *et al.*, 2017).

5.3.3 The involvement of protein metabolism during hypoxia

Of all the detected compound classes, proteins (amino acid subgroup) are the group of metabolites most changed by both functional and environmental hypoxia (Tables 5.1 and 5.2). During low energy states (for example during hypoxic conditions), the adenosine monophosphate (AMP):ATP ratio increases, and allosterically activates AMP activated protein kinase (AMPK), which subsequently signals the catabolism of proteins (and lipids), and

inhibition of anabolism and cell growth (Venter *et al.*, 2016b), hence, all available energy is channelled towards survival. Considering the elevated levels of AMP detected in the right gill and adductor muscle samples (Pathway Q), in combination to the elevated amino acid concentrations in these and other tissues, it becomes apparent that protein catabolism (Fields, 1983), plays a very important survival role during hypoxia. Since the amino acid changes affected multiple metabolic pathways, the findings will be discussed in the context of the impact of hypoxia on specific amino acids or groups of related amino acids.

5.3.3.1 Insight into ketogenic- and glucogenic amino acids

Several glucogenic amino acids (alanine, arginine, glycine, proline and serine) were elevated in the right gill tissue samples analysed in the functional hypoxic group (Fig. 5.4). In the environmental hypoxic group, however, the glucogenic amino acids (arginine, glutamate, glutamine, glycine, histidine, methionine, proline and serine) were predominantly elevated in the adductor muscle (Fig. 5.5). Typically, during stressed conditions, glucogenic amino acids are converted to alanine via the transamination of pyruvate (Pathway F) (Salway, 2004). The elevation in alanine and pyruvate detected in hypoxic *H. midae*, further attests to this, as well as the elevated glutamate detected, synthesised by transamination of α-ketoglutarate (Fig. 5.5). The elevated concentrations of alanine, synthesised in abalone during anaerobic conditions, is a key survival response, as it assists in: 1) the buffering of H^+ ions (generated with the production of lactate and opines), 2) regulation of intracellular osmotic pressure and 3) serves as a substrate for alanopine production (Fujimori and Abe, 2002, Garrett and Grisham, 2010, Müller *et al.*, 2012). Previously, elevated concentrations of alanine were also seen in *H. diversicolor,* after exposure to a toxin stressor that induced an anaerobic state (Lu *et al.*, 2017), confirming the current results. The elevated concentrations of glycine and methionine induced by environmental hypoxia in the muscle samples of *H. midae* in this experiments, were also previously reported (Lu *et al.*, 2016). Additionally elevated serine (Pathway C) concentrations were detected, not previously reported after environmental hypoxia, which is also an important energy substrate, since serine can be deaminated to form pyruvate (Salway, 2004).

Aspartate, asparagine, glutamate and glutamine are well-known metabolic fuels during anaerobic conditions (Storey, 2005). Functional hypoxia (Fig. 5.4) resulted in reduced aspartate in epipodial tissue, adductor muscle and the right gill, and elevated asparagine concentrations in the foot muscle. Environmental hypoxia on the other hand (Fig. 5.5) resulted in reduced concentrations of both aspartate (all tissues investigated) and asparagine (haemolymph and left gill). In both hypoxic scenarios, glutamate was increased in the adductor muscle and left gill samples analysed. The reduced aspartate levels can be explained by an induced demand for this amino acid, to serve as a substrate for TCA cycle intermediates during hypoxia (Pathway

O), as previously indicated for *Apostichopus japonicus* (Prathomya *et al.*, 2017). Furthermore, aspartate is also used for the synthesis of glutamate, and a number of other metabolic amino acid substrates, as well as energy production (Shao *et al.*, 2015). Glutamate (Pathways N and R) is an active intermediate of amino acid metabolism, closely associated with the TCA cycle. As previously mentioned, amination of α-ketoglutarate produces glutamate, which can in turn be further aminated to yield glutamine. Glutamine may serve as a nitrogen store, lowering ammonia toxicity during hypoxia (Venter *et al.*, 2016b). Protein degradation is also a common occurrence during hypoxia, also contributing to the elevated concentrations in glutamate and many other amino acids (Boardman *et al.*, 2016), as can be seen in Tables 5.1 and 5.2. Reduced histidine concentrations were detected in the haemolymph samples of hypoxic *H. midae* (Figs. 5.4 and 5.5), corresponding to the reduction of glutamate in the haemolymph. Histidine is typically metabolised to glutamate with the removal of one carbon group (Salway, 2004). Altogether, the findings following hypoxia illustrates the importance of glutamate, which can be re-synthesised for usage by other amino acids during stress (Reggiani and Bertani, 2003).

Proline has a number of functions in marine invertebrates, but as functional and environmental hypoxia (Figs. 5.4 and 5.5) resulted in significantly increased proline concentrations in the adductor muscle, left gill, right gill and epipodial tissue samples of *H. midae*, the function here is ascribed to upregulated proline synthesis (via the glutamate pathway R or ornithine pathway Q) or a reduced proline catabolism. Interestingly, an observation previously made in plants, is that during periods of dehydration, their proline anabolism pathways are activated, while the proline catabolism pathways will be repressed. When rehydration occurs, these pathways return to normal (Hayat *et al.*, 2012). Proline is thought to: prevent dehydration; function as molecular chaperon, stabilising the structure of proteins; maintain protein integrity and enhance the activities of different enzymes. Also the accumulation of proline buffers cytosolic pH and maintain cell redox status, while protecting against the damaging effects of reactive oxygen species (ROS) (Hochachka *et al.*, 1973, Hayat *et al.*, 2012, Vosloo *et al.*, 2013b) (Tables 5.1 and 5.2). Further evidence for this is in the green-lipped mussel, where elevated proline levels were associated with anaerobic metabolism, as a result of temperature stress (Dunphy *et al.*, 2015). Furthermore, after one month of L-proline supplemented diet feeding trial, *H. midae* that were subjected to oxygen and temperature stress, still displayed an increased mass, suggesting some benefit for the animal despite the stressed conditions (Vosloo *et al.*, 2013b).

Of the amino acids that are only ketogenic, leucine and lysine were detected in lower levels in the adductor muscle and left gill after exposure to environmental hypoxia (Table 5.2 and Fig. 5.5). Similarly, functional hypoxia (Table 5.1 and Fig. 5.4) resulted in reduced leucine levels in the adductor muscle and gill samples, while lysine was only reduced in the adductor muscle

samples. Although not a lot has been described about amino acids leucine and lysine in these invertebrates, both are considered essential for vertebrate species. It can only be assumed that this is the same for these invertebrates, which means that the supply thereof is limited to external consumption and/or internal protein stores. The results of this investigation support this hypothesis, since the concentrations of these and many other essential amino acids can be associated to the extent of hypoxia. Considering the up-regulated fatty acid oxidation and increased use of carnitine (Li *et al.*, 2009) during hypoxic conditions, it is also reasonable to assume that lysine is actively used to synthesise carnitine (Pathway J), which may contribute to the reduced lysine detected. Furthermore, leucine (Pathway K) and the other branched-chain amino acids (BCAA) (isoleucine and valine), are substrates for gluconeogenesis under conditions of high ATP demand (Mason *et al.*, 2015), explaining the reduced leucine in abalone during hypoxia. The BCAA leucine and isoleucine were reduced in the analysed adductor muscle samples analysed, while valine was elevated, following functional hypoxia (Fig. 5.4). Conversely, elevated BCCAs were reported in the gills of *H. diversicolor* and *H. fugens,* following hypoxia and thermal stress (Lu *et al.*, 2016). During periods of extended exercise (functional hypoxia), BCAAs are used as carbon skeletons in gluconeogenesis and alanine synthesis in order to prevent lactate accumulation (Layman, 2002). Following environmental hypoxic stress (Fig. 5.5), the BCAAs were decreased in both the adductor muscle and left gill samples, illustrating the severity of environmental hypoxia, which resulted in depletion of these essential amino acids.

5.3.3.2 Arginine, the urea cycle and products of protein degradation and glycine conjugation

The involvement of arginine for the synthesis of phosphoarginine and ATP during hypoxia (Morash and Alter, 2016) has already been discussed. However, since arginine showed the most significant increase in concentration (*d*-value of 62.40) in the adductor muscle of *H. midae* after exposure to environmental hypoxia (Table 5.2), its involvement in connected pathways cannot be ignored. Likewise, a markedly elevated level of arginine (*d*-value of 12.32) was also detected in the right gill after functional hypoxia. Significantly elevated concentrations of ornithine and citrulline were found in the adductor muscle following environmental hypoxia (Fig. 5.5), while elevated arginosuccinate was found in the foot muscle. This result implicates the urea cycle (Pathway Q) of abalone in maintaining the nitrogen/ammonia balance with increased amino acid catabolism. Abalone have the capacity to acquire vast amounts of amino acids, which can be utilised for energy production during hypoxia, after deamination and the release of ammonia. A small portion of ammonia may be used for the synthesis of non-essential amino acids; however, the majority of the ammonia is excreted, either as pure ammonia or urea, by means of the urea cycle. In this cycle, arginine is typically converted to ornithine, and urea is released into the circulation (Schmidt-Nielsen, 2007). Previous literature on *H. laevigata*

indicated that these organisms are extremely sensitive to ammonia exposure, which results in dramatically reduced growth and nutrient uptake (Harris *et al.*, 1998). Thus, the urea cycle in abalone plays an important role during stressed conditions like hypoxia. In standard farming conditions, it was reported that energy loss in the form of ammonia excretion is negligible in *H. midae*, accounting for less than 1 % of consumption (Barkai and Griffiths, 1988), however, this is likely to be significantly more during hypoxia. Accumulated arginine detected in the gill and hepatopancreas samples of *H. fulgens,* not only confirms that arginine plays a vital role in ammonia detoxification but also suggests that high rates of protein degradation occur in abalone subjected to hypoxia (Tripp-Valdez *et al.*, 2017).

Various cell types, in many animal species, use arginine to generate nitric oxide (NO), via NO synthases, which subsequently results in vasodilation and increased muscle perfusion and oxygen supply (Wingrove and O'Farrell, 1999, Tischner *et al.*, 2007). Citrulline is produced as a by-product of this reaction, which can in turn be recycled back to arginine (Guoyao and Morris, 1998). As both arginine and citrulline were elevated in the adductor muscle of *H. midae* (following environmental hypoxia, Fig. 5.5), it suggests that abalone may be trying to compensate for the lack of oxygen during hypoxia via the production of NO, and subsequently, an increased muscle perfusion for improved oxygen delivery to the hypoxic tissue seems possible.

The results in Table 5.2 indicate that several dipeptides (arginyl-glycine, alanyl-glycine alanyl-lysine, cysteinyl-cysteine, isoleucyl-threonine, phenyl-glycine, valyl-glycine) were drastically increased in the group of abalone subjected to environmental hypoxia (Fig. 5.5). The occurrence of dipeptides in cellular fluids can be largely ascribed to incomplete protein digestion. These peptides also play a key role in cell signalling, which may further modulate specific metabolic reactions. Although smaller variations for other peptides such as alanylglycine and isovalerylglycine were seen, arginylglycine (*d*-value 34.32) showed a drastic increase in the adductor muscle of *H. midae* after exposure to environmental hypoxia. The synthesis of this dipeptide might be dependent on a dipeptide synthase enzyme, however, no literature supporting the existence of such an enzyme could be found. Secondarily, arginylglycine can be considered as a reservoir for arginine, for the production of phosphoarginine during hypoxia, as arginylglycine can be converted to arginine (and *vice versa*). When abalone are exposed to hypoxic conditions, increased arginine is produced for the purpose of fuel for phoshoarginine, but when conditions return to normal, the excess arginine can be stored in the form of arginylglycine, ultimately serving as an energy sufficient mechanism to reduce the excessive arginine produced during hypoxia. Interestingly, the elevated alanylglycine and arginylglcyine correspond with elevated alanine and arginine levels. For examples: alanine levels in the epipodial tissue correlates with the alanylglycine levels (r = 0.86)

in the environmental hypoxia group, while they do not correlate in the control groups; arginine levels in the adductor muscle moderately correlates (r = 0.6) with arginylglycine levels in the environmental groups while no correlation was found in the controls; and the lower isovalerylglycine level corresponds to lower BCAA levels which suggest that these dipeptides may be a product of the glycine conjugation pathway.

It is well-known that various states of organic aciduria produce high amounts of different acyl-CoA's in humans, which in turn serve as substrates for glycine N-acyltransferase (GLYAT), and subsequently the synthesis of glycine conjugates (Loots *et al.*, 2005). Considering that acyl-transferase enzymes can conjugate glycine to a variety of different accumulated amino acids (Badenhorst *et al.*, 2014), the role of glycine conjugation in detoxifying accumulating intermediates and maintaining coenzyme A levels seems highly probable in abalone, based on our findings (Figs. 5.4 and 5.5, Pathways L and M), however, additional evidence to confirm such activities in abalone could not be found.

5.3.3.3 Amino acids and other organic osmolytes

Osmolytes altered by hypoxia included: various non-essential amino acids (alanine, arginine, asparagine, aspartate, cysteine, glutamate, glutamine, glycine, proline, serine and tyrosine), opines, taurine, homarine (detected only in the functional hypoxia experiment), choline, betaine, dimethylglycine and sarcosine. This suggests a change in the osmotic regulation of abalone when exposed to oxygen-poor environmental hypoxia (Tables 5.1 and 5.2 and Figs. 5.4 and 5.5). Taurine, for example, has been reported to be more related to osmoregulation than to energetics (Tripp-Valdez *et al.*, 2017). Likewise, the elevated concentrations of the less metabolically active non-essential amino acids are believed to maintain osmoregulation in abalone (Rosenblum *et al.*, 2005). Moreover, elevated opine levels also ensure that the intracellular osmotic pressure is maintained, via pH regulation (Harcet *et al.*, 2013).

An increased concentration of the osmolyte homarine (an endogenously synthesised hetero-aromatic quaternary ammonium compound) was detected in the right gill sample of abalone subjected to functional hypoxia in this experiment (Table 5.1, Fig. 5.4), which is most likely synthesised via methylation of picolinate or via metabolism of glycine and succinyl-CoA (Netherton and Gurin, 1982). The exact role of hormarine in abalone metabolism is still unknown despite it being elevated in *H. iris* muscle tissue, after exposure to wave action (Wells *et al.*, 1998b), the foot muscle tissue and digestive glands of stunted and diseased *H. rufescens* (Viant *et al.*, 2003) and digestive gland and foot muscle tissue of Rickettsiales-like-prokaryote infected *H. rufescens* (Rosenblum *et al.*, 2005). Homarine has previously indicated assistance with osmoregulation and trans-methylating, and exhibits morphogenetic activity, which may

influence cell proliferation and differentiation (Rosenblum *et al.*, 2005). The elevated levels of homarine detected in the right gill of *H. midae* after exposure to functional hypoxia in this experiment, supports the notion of its osmoregulatory function, since this tissue will be the first to be influenced by oxygen deprivation. The various metabolic down-stream intermediates of homarine metabolism (choline, betaine, dimethylglycine and sarcosine, Pathway D) were also elevated by the hypoxia, further confirming this observation.

The elevated concentrations of choline and sarcosine that were detected in the right gill of *H. midae* after environmental hypoxia (Table 5.2), may serve as part of its first defence function, protecting the animal against endogenous biomolecules, following environmental stressors (Zotti *et al.*, 2016). Evidence for this is seen in zebra fish, where elevated concentrations of choline was attributed to an altered glycerophospholipid metabolism, induced by a disturbance in their cellular membranes (Watanabe *et al.*, 2015). Furthermore, elevated concentrations of both sarcosine and choline were reported in abalone, after vibrio infection (Lu *et al.*, 2017). Additionally, in this current investigation, betaine (Pathway D) concentrations were reduced in the epipodial tissue of the functional hypoxia group (Fig. 5.4) and in the left gill of the environmental hypoxia group (Fig. 5.5). Betaine is reported to prevent osmotic stress in aquatic organisms via conversion to trimethylamine oxide, of which the latter plays an important role in animals that need to survive in saltwater environments (Velasquez *et al.*, 2016). Moreover, betaine can be converted to trimethylamine and eventually trimethylamine oxide, which is also a well-known osmolyte, previously detected in the tissue of various organisms after exposure to environmental stress (Hovagimyan and Gerig, 2005). A combination of trimethylamine oxide, betaine and sarcosine were reported to contribute to intracellular osmolarity in marine invertebrates (Wilbur and Hochachka, 2016). Considering this, the elevated levels of the aforementioned osmolytes in *H. midae,* following hypoxic exposure, are most likely produced for the purpose of maintaining intracellular osmolarity. The betaine, derived from choline, can also be oxidised to dimethylglycine and subsequently, glycine (Sheedy *et al.*, 2015). In the abalone tissue samples analysed in the current investigation, dimethylglycine was reduced in the adductor muscle samples (Figs. 5.4 and 5.5), since it is most likely converted to glycine (which was detected in abundance in this tissue). Proline betaine is also a well-known osmolyte (Hayat *et al.*, 2012) and is detected in elevated concentrations in the gills of abalone after functional hypoxia (Table 5.1), but in reduced levels in the gills of the environmental hypoxia group (Table 5.2), and can also be used to produce proline, another osmolyte (Liang *et al.*, 2013).

5.3.4 The involvement of lipid metabolism during hypoxia

Considering the metabolite markers described in Tables 5.1 and 5.2, and the metabolic charts of Figures 5.4 and 5.5, very few lipid metabolites were altered during functional and

environmental hypoxia, suggesting that cellular energy utilisation from lipid metabolism is limited (Pathway W). This was expected, since only a fraction of the fatty acids and sterols absorbed from the diet undergo *de novo* lipid synthesis (Venter *et al.*, 2016b).

The most apparent changes in the fatty acid profile of *H. midae,* after the functional hypoxia experiment (Fig. 5.4), were the elevated concentrations of palmitoleate (C16:1) in the left gill, and oleate (C18:1 n-9) in the muscle and haemolymph samples (Pathway V). In *H. discus hannai* Ino and *H. diversicolor,* C18:1 n-9 was reported as the predominant fatty acid, released from lipids for ß-oxidation (Lou *et al.*, 2013, Li *et al.*, 2015). Furthermore, the total lipid profiles (FAMEs analyses) in this experiment did not show vast differences in the ratios of fatty acids, which are built into lipids after hypoxia and, can be expected given the homogenous (pre-hypoxic) farming conditions during which lipid synthesis was most active. However, the release of fatty acids from lipids for energy production did not substantially influence the amounts of bound fatty acids, which was rather surprising, but highly likely due to the relatively low lipid stores previously reported to occur in abalone tissue (Vosloo and Vosloo, 2010). The types and amounts of both free and bound fatty acids detected in *H. midae* after environmental hypoxia (Fig. 5.5), varied when comparing different tissues. Previous elucidation of the lipid and fatty acid profile of *H. rubra* and *H. laevigata* confirmed this tissue specific fatty acid profiles (Grubert *et al.*, 2004). Reduced concentrations of bound docosahexaenoate (C22:6 n-3), eicosapentaenoate (C20:5 n-3) and octadecatrienoate (C18:3 n-6) were found in the left gill, right gill and adductor muscle samples, respectively. This suggests a higher fatty acid release rate (lipolysis) during hypoxia. On the other hand, the epipodial tissues contained higher amounts of bound C22:6 n-3 and octadecatetraenoate (C18:4 n-3) fatty acids, accompanied by lower levels of free palmitate, suggesting a lack of lipolysis activity. In *H. fulgens,* elevated concentrations of C22:6 n-3 and C20:5 n-3 were detected in the muscle tissue following starvation stress (Durazo-Beltrán *et al.*, 2004). These fatty acids (C22:6 n-3 and C20:5 n-3) were reduced in the gills of *H. midae* after hypoxic stress (Fig. 5.5), suggesting the usage of these metabolites as an energy source.

The fatty acylcarnitines in *H. midae* that were most affected (regardless of hypoxic exposure) included: carnitine, acetylcarnitine, butyrylcarnitine and palmitoylcarnitine. In the functional hypoxia group (Fig. 5.4), these findings were predominantly elevated, which can be used as substrates for increased ß-oxidation activity (Pathway U), resulting in the production of more acetyl-CoA for TCA cycle usage and eventually ATP production via oxidative phosphorylation (the typical response in the presence of oxygen). This again demonstrates that abalone subjected to functional hypoxia utilises aerobic respiration for a large part before depending on anaerobic mechanisms for energy. In the environmental hypoxia group (Fig. 5.5), these fatty acylcarnitines were still largely increased, however a number of decreases were also observed

in some tissues, demonstrating depletion thereof at the current energy status. The regulation of ß-oxidation (Pathway U) was also affected resulting in elevated levels of fatty acids (such as palmitoleate) and their associated fatty acylcarnitines. Furthermore, it should be mentioned that the carnitine conjugation of these accumulating fatty acids also plays a role in detoxification.

Marine molluscs have adapted to very little reliance on fatty acid and ketone body metabolism for energy (Stuart and Ballantyne, 1996), and based on evidence in Tables 5.1 and 5.2, and Figures. 5.4 and 5.5, amino acids are predominantly used for ATP production, especially during hypoxia. Despite this, however, invertebrate molluscs are known to produce acetate and propionate as metabolic end products of glycogen catabolism during prolonged periods of oxygen deprivation (Grieshaber *et al.*, 1993). Although propionate was not detected by any of the analytical procedures used in this study, which is to be expected since it is a highly volatile fatty acid, and requires specific extraction procedures including a liquid-liquid extraction procedure using diethyl ether (Adorno *et al.*, 2014), it was previously reported to occur in samples of *Mytilus edulis,* about ten hours after exposure to hypoxia (De Zwaan *et al.*, 1991). Acetate on the other hand, was in fact found to be elevated in the analysed right gill and haemolymph tissues (Table 5.2, Fig. 5.5). Previously, increased concentrations of acetate were detected in *H. diversicolor supertexta,* after a toxin perturbation, resulting in an imbalance in lipid homeostasis (Zhou *et al.*, 2015). The increased concentrations of acetate in this investigation can, however, be attributed to the production of ketone bodies (Pathway M, L), which are an important source of fuel for energy for many tissues not requiring the complexation with fatty acid binding proteins (Garrett and Grisham, 2010). In endothermic organisms, increased synthesis of ketone bodies are indicative of fats being used for energy (Roznere *et al.*, 2014), however in the *H. midae* (which are ectothermic organisms) the elevation in metabolites hydroxybutyrate and the pressor of acetoacetate, homogentisate (Pathway T), suggested a degree of energy production via fatty acid catabolism during environmental hypoxia.

5.3.5 Other metabolic findings

Apart from the main frame-work of metabolism driven by amino acids, carbohydrates and lipids, as described above, other metabolic pathways were also affected by hypoxia in the abalone. Generally, these “other” metabolites occur in far lower concentrations and display far lower levels of significance (Tables 5.1 and 5.2). The altered nucleotide metabolites adenosine, adenine, uridine, guanosine triphosphate (GTP), uridine triphosphate (UTP) and uridine monophosphate (UMP) (for example, Pathway P), suggest a continued build-up and breakdown of various intermediates for energy maintenance and survival. The altered nicotinate (Pathway I), suggests adaptation to the pyrimidine nucleotide synthesis pathways (Young *et al.*, 2017)

and subsequently the redox state of the hypoxic abalone. It would be expected, that hypoxia in abalone would result in a fluctuation of the redox reactions, in order to produce sufficient NAD^+ for glycolytic use. Furthermore, the altered pyrimidines induced by hypoxia further substantiate the reduced nicotinate in this study. Additionally, nicotinate can also be synthesised from tryptophan metabolism, the latter of which can serve as a respiratory fuel and can also be used as a precursor for the synthesis of NAD^+ and $NADP^+$ (Salway, 2004).

Using the same route, aminoadipate (an intermediate in the lysine pathway, elevated in abalone adductor muscle of the environmental hypoxic abalone and reduced in the gills following functional hypoxia), can also serve in the synthesis of acetyl-CoA (Pathway J). Changes to aminoadipate correlate with a switch in cellular respiration, where oxidative phosphorylation no longer serves as the primary energy source (Young *et al.*, 2017), which is typically induced during environmental hypoxia in the current study, where the mitochondria can no longer be used for energy production. In fact aminoadipate has previously been recognised as one of the components identified in a biosignature for respiratory chain deficiencies (Smuts *et al.*, 2013), which implicates this metabolite with irregular electron flow and energy production. Furthermore, the increased concentrations of aminomalonate and aminobutyrate, known products of protein catabolism, were induced by the hypoxia. Additionally, increased aminomalonate has also been previously associated with errors in protein synthesis and oxidative damage to amino acid residues in protein. Pyroglutamate was detected in the functional hypoxia group (increased in adductor muscle and decreased in haemolymph), originating non-enzymatically from glutamate, glutamine and gamma-glutamylated peptides (Noto *et al.*, 2014). The occurrence of pyroglutamate at the N-terminus of many peptides and proteins deems this metabolite a contributor to protein activity and stability (Kumar and Bachhawat, 2012). In light of hypoxia, the presence of pyroglutamate can be attributed to protein degradation, but decreased glutathione levels (Pathway E) are likely to secondarily result in increased production of pyroglutamate, which is typically depicted here, where abalone adductor muscle showed decreased glutathione but increased pyroglutamate following exercise (Fig. 5.4), largely due to the fact that glutathione and associated metabolism strives to protect cells from oxidative and other stressors, scavenging free radicals amongst other things. It also partakes in cell redox maintenance (Maher, 2005), influencing metabolite levels to different extents in different abalone tissues.

5.3.6 Abalone tissue specific responses and interplay

A general observation was that the adductor muscle, followed by the gills, the foot muscle, epipodial tissue and lastly the haemolymph, displayed the most metabolic alterations after exposure to functional hypoxia (Fig. 5.4, Table 5.1). On the other hand, during environmental hypoxia (Fig. 5.5, Table 5.2), the largest metabolic effects were seen in the adductor muscle,

followed by the epipodial tissue, then the left and right gill, the foot muscle and lastly, the haemolymph. The results indicated that *H. midae* tissue displays a diverse response to hypoxia, most likely attributed to the varying functionality and metabolism associated with the various organs from which the tissue was sampled. Additionally, much like higher organisms, certain metabolites are shuttled between various different organs and tissues (e.g. from hypoxic tissue to regions that have access to oxygen), where they can be more appropriately utilised. An example of this in higher animals is the lactate shuttle between fatigued muscles and liver. Each tissue function, in terms of hypoxia, will briefly be discussed.

5.3.6.1 Muscle

During functional hypoxia, both the adductor and foot muscle predominantly displayed metabolic alterations due to inhibition of mitochondrial metabolism and fatigue (Fig. 5.4). This demonstrates the reliance of abalone muscle on oxygen for energy metabolism, despite its capacity for anaerobic metabolism, as confirmed in previous experiments on *H. lamellose* (Gäde, 1988). In this investigation, the adductor muscle of *H. midae* showed more metabolites in elevated concentrations during environmental hypoxia, with the foot muscle in contrast, showing greater numbers of decreased metabolites (Fig. 5.5). During environmental hypoxia, the large adductor muscle utilises muscle phosphagen and glycogen reserves in order to fuel anaerobic glycolysis, which relies on regenerated cytoplasmic NAD^+ via pyruvate reductases (Donovan *et al.*, 1999). On the other hand, since the foot muscle can be considered less metabolically active, there is limited accumulation of metabolites due to metabolic shutdown. In fact, it is also possible that many metabolites can be depleted during extreme hypoxia. This was also previously seen in the analysed foot muscle samples collected from *H. rufescens,* following starvation stress (Rosenblum *et al.*, 2005). Since the adductor and foot muscle together, contribute to about 66 % of the total abalone body mass (Jorgensen *et al.*, 1984), it is expected that large differences will be reflected in the muscles, ultimately resulting in the production of different metabolic end products, responsible for different functions in abalone (Venter *et al.*, 2016b).

5.3.6.2 Gills

The fact that the abalone left gill is additionally used during hypoxic conditions in order to enhance surface area and oxygen uptake (Ragg and Taylor, 2006), is shown very aptly during this investigation, where the left gill was the only tissue in which octopine was produced during environmental hypoxia (Table 5.2 and Fig. 5.5). Octopine is produced from accumulated arginine, likely due to phosphoarginine breakdown to produce energy. Furthermore, larger differences were seen in the left gill during environmental hypoxia when compared to that of the right gill. With the accumulation of arginine in the adductor muscle during environmental

hypoxia, it can also be reasoned that the left gill was recruited to assist with energy production and clearance of arginine. Since the gills are proximal to the immediate environment (and oxygen) it can be speculated that numerous metabolites are shuttled to the gills during hypoxia. Thus, the elevated metabolites detected in the gills may subsequently result from the gills' elevated metabolic rates and/or uptake of shuttled metabolites. The idea that metabolites are shuttled to and from the gills are supported by the correlation of specific metabolites found in the gills (especially the left gill) and other tissues during hypoxia, e.g. in the environmental hypoxic group, alanine levels in the left gill correlated with the levels in the haemolymph (r = 0.82), which was not found in the control group. The same correlation was also found for lactate (r = 0.80) and several other accumulated metabolites. On the other hand, the right gill metabolites indicated a slightly higher increase in the altered metabolite concentrations than the left gill did during functional hypoxia (Table 5.1, Fig. 5.4), adding reason to the idea that functional hypoxia causes an increased oxygen demand, still easily met by the right gill, which is perfused at a constant rate. The right gill showed the largest increase in arginine, most probably generated for rapid energy production via phosoarginine, to meet this demand. Again, it can be speculated, that numerous metabolites are shuttled to the gills during functional hypoxia as it is proximal to the immediate environment and oxygen.

5.3.6.3 Epipodial tissue

Prior literature pertaining to the biochemistry and physiology of abalone epipodial tissue is rather scarce, but the results of this study suggest that the epipodial tissue has similar metabolic profiles to the other tissues investigated. This is rather surprising since it makes up only 0.8 % of the abalone's body weight (Jorgensen *et al.*, 1984). It should also be noted that the analyses of the epipodial tissue resulted in far more unidentified compounds after exposure to both functional and environmental hypoxia (unknowns not reported). It has been hypothesised that the epipodial tissue plays a role in oxygen uptake (Taylor and Ragg, 2005). Hence, it might be possible that metabolites from the muscles could be shuffled to the epipodial tissue during hypoxia, as with the gills. Again, this was seen with the correlation of metabolite levels between the tissues. Leucine and alanopine levels in the epipodial tissue and haemolymph, correlated (r = 0.83 and 0.78 respectively) with the environmental hypoxic group, while these levels did not correlate with the control group. Alanopine, in the epipodial tissue, also correlated moderately with that in the foot muscle (r = 0.73). Although it is possible that other factors contribute to this covariance, the involvement of metabolite shuttles cannot be dismissed. The aforementioned metabolic similarity of epipodial tissue to the muscle tissue analysed, also allows for an important opportunity for non-destructive sampling for health screening, without critical damage to the animal (Wasko *et al.*, 2003, Slabbert and Roodt-Wilding, 2006).

5.3.6.4 Haemolymph

Of all the samples studied, the least number of metabolites were detected in the haemolymph (Tables 5.1 and 5.2) during both hypoxic conditions, and of the detected metabolites, most were elevated following functional hypoxia (Fig. 5.4). As described above, during functional hypoxia, the elevated energy demand results in the elevated release of metabolites from stores that are shuttled between various organs. During extreme hypoxia, such as environmental hypoxia (Fig. 5.5) induced in this study, these stores may become depleted, resulting in reduced metabolite concentrations in the systemic fluid. Additionally, reduced pH and/or increased free ammonia could also influence metabolite channels and pumps. Considering this, the role of haemolymph as a sample for analysing metabolic end-products, like ammonia, becomes apparent. Metabolic end products produced during hypoxic conditions may be released into the haemolymph and absorbed by other tissues (organs), which are able to oxidise these products (metabolic shuttle), e.g. the metabolic profiles detected in the hepatopancreas (which receives large haemolymph volumes) of *H. fulgens* confirms the transport function of haemolymph (Tripp-Valdez *et al.*, 2017). This was indeed the case according to the correlation analysis performed. As in the previous sections, the concentrations of many compounds in the different tissues correlate with the haemolymph concentrations, which highlight its transport/shuttle function that links the different tissues. Subsequently, haemolymph represents the exo-metabolome, since it contains metabolite information of how the intracellular metabolic network influences its external environment (by the uptake of extracellular metabolites and secretion of intracellular metabolites) (Dunn, 2008). One of the end products of anaerobic respiration is lactate, which is known to cause a drop in extracellular and intracellular pH, resulting in a disturbed acid-base balance during hypoxia. It has been suggested that abalone haemolymph has very limited pH buffering capacity, and is subsequently prone to metabolic acidosis during hypoxia (Morash and Alter, 2016). However, it is important to note that haemocyanin of gastropod haemolymph displays a reverse Bohr Effect, where oxygen binds tighter at a low pH or higher CO_2 partial pressure. This enables abalone to maintain oxygen saturation when clamping to surfaces during hypoxic conditions (Wells *et al.*, 1998a).

5.4 Conclusion

Considering all of the above, the results demonstrate that functional and environmental hypoxia created a metabolic imbalance in *H. midae*, with compromised energy levels, skewed NAD^+:NADH ratio and the accumulation of metabolites and toxic end products, such as ammonia. In response to the imbalances, the metabolism shifts to more catabolic processes in order to correct the energy and redox imbalances, and subsequently limits growth. Based on the accumulation of different metabolic end products, shown in Tables 5.1 and 5.2, and

demonstrated in Figures 5.4 and 5.5, there are several metabolic responses which ensure these animals survive when oxygen supply is inadequate. Due to the large amounts of arginine detected, it can be deducted that these animals have large phosphoarginine pools able to regenerate ATP at the onset of hypoxia. Thereafter, energy production is continued via anaerobic metabolic pathways, associated with the breakdown of glycogen, proteins and lipids. For efficient anaerobic metabolism and energy production, recovery of NAD^+ is crucial, which is predominantly achieved by the conversion of pyruvate to lactate, the conversion of pyruvate to opines, and the conversion of glucose and aspartate to succinate. It is also clear that *H. midae* utilises all of the main metabolite classes e.g. proteins (amino acids), carbohydrates (glucose) and lipids (fatty acids), to contribute to ATP production as hypoxia alters metabolism from aerobic to anaerobic respiration.

It is apparent from the results that different tissues undergo different metabolic changes during hypoxia (Tables 5.1 and 5.2). Since the gills are known to be the first line of defence against hypoxia, and the sole supporter of gas exchange, the metabolic changes during oxygen deprivation most likely start here, progressively resulting into changes to the haemolymph, the muscles and then lastly, the epipodial tissue. The muscle being the largest of these organs and most directly affected by hypoxia, showed the most prominent metabolic changes. Both adductor and foot muscles were seen to produce various anaerobic intermediates associated with metabolic pathways producing NAD^+ for glycolytic ATP production.

Although abalone have the capacity to survive hypoxic episodes, hypoxia remains responsible for significant losses in aquaculture (Le *et al.*, 2016) and has a negative effect on growth (Morash and Alter, 2016). Considering this, a clear understanding of the bioenergetics of abalone metabolism is fundamental for optimising productivity in abalone farming and also in order to manage their performance in an aquaculture system. Since hypoxia is only an episodic occurrence on abalone farms, the likelihood of recovery thereafter is good, considering abalone have various metabolic pathways to manage these changes adequately. However, reference ranges for abalone metabolic markers are non-existing, making it impossible to monitor recovery after episodes of hypoxia. This investigation brings to the forefront the metabolic changes occurring in abalone after functional and environmental hypoxia. Special focus on certain intermediate and/or end-products of these metabolic changes, and establishing defined concentration ranges for normality and certain stressors in the future, may serve well to monitor and assess abalone health on abalone farms, which is something still lacking in the aquaculture industry (Fasulo *et al.*, 2012, Alfaro and Young, 2016). Nonetheless, every good idea sprouts from somewhere, and the application of metabolomics as a research tool in this study, demonstrates that abalone have remarkable metabolic processes, enabling them to manage hypoxic stress.

CHAPTER 6

ELUCIDATING GROWTH CHALLENGES OF FARMED *HALIOTIS MIDAE*

"Now! Now, cried the Queen. Faster! Faster!"

– Lewis Carrol, Through the Looking Glass

Subsections of this chapter have been submitted for publication:

VENTER, L., LOOTS, D. T., MIENIE, L.J., VOSLOO, A., JANSEN VAN RENSBURG, P. J. & LINDEQUE, J. Z. 2018. Characterising the metabolic differences related to growth variation in farmed *Haliotis midae*. *Aquaculture*, Submitted.

VENTER, L., VOSLOO, A., LOOTS, D. T., MIENIE, L.J., JANSEN VAN RENSBURG, P. J. & LINDEQUE, J. Z. 2018. Effect of proline enriched abalone feed on selected metabolite levels of slow growing adult *Haliotis midae*. *Aquaculture Research*, Submitted.

6.1 Introduction

The production of farmed abalone in South Africa has emerged into a noteworthy aquaculture sector, which is currently dominated by China and Korea. Approximately 20 abalone aquaculture farms in SA are operational, with only four operating grow-out facilities with land-based raceway systems, one sea-cage farm and two ranching operations to fulfil international demand (Britz and Venter, 2016, Probyn *et al.*, 2017). Typically, in the grow-out facility, recirculating tanks and/or offshore barrels and cages are used (Mau and Jha, 2017). Farms using recirculating tanks operate on flow-through systems, where seawater is pumped ashore. The seawater undergoes filtration and then reticulates through the tanks before flowing back to sea by gravity.

Biosecurity measures are also in place, so that the water flowing to and from the farm is not harmful to the environment. Since the tanks are cleaned regularly to ensure hygiene, and cultivated animals require daily feeding, health and husbandry of abalone, is a labour intensive and rather costly practice (Fallu, 1991, Troell *et al.*, 2006). Formulated artificial feeds have emerged on abalone farms as a popular feeding alternative to fresh seaweed, allowing farmers to use feeds with specific protein, carbohydrate, lipid, vitamin and mineral contents, for optimised growth (Venter *et al.*, 2016b, Probyn *et al.*, 2017). Over time, research and development of abalone farming has resulted in improved pellet diets, health management and husbandry conditions (Kaiser *et al.*, 2017). Various conditions affecting husbandry, such as water temperature, stocking densities, ammonia and oxygen saturation levels, the handling and transportation of animals and their dietary needs are now controlled within narrow parameters to prevent the occurrence of stressors, which are known to produce higher disease susceptibilities (or mortalities) and reduced abalone growth (Sales and Britz, 2001, Morash and Alter, 2016, Lachambre *et al.*, 2017). Even though these factors are standardised and uniform for all the animals on the farm, abalone from the same spawning batch do not all achieve market size (± 80 g / 90 mm) within the assigned four year farming period (Venter *et al.*, 2016b). This slow and variable growth of abalone is one of the biggest problems that abalone farmers currently face. Shortening this growth duration and eliminating the variability in these growth rates would indeed reduce production costs and increase turnover in the long run (Ten Doeschate and Coyne, 2008).

Considering this, elucidating those genetic and/or epigenetic factors that play a role in growth variability is urgently needed. Since abalone in one basket are typically the offspring of a small number of parents, their genetic background is considered homogenous. However, variable growth rates are often seen in the same basket of animals, which suggests that there may be some genetic variance still playing a key role even if epigenetic factors (like temperature, feed,

oxygen supply, etc.) are uniform. Genetic control is, however, applied over energy utilisation and growth efficiency parameters in a number of molluscs species (Ibarrola *et al.*, 2017), but within-individual variance is yet to be eliminated. It is thought that genetic variance is affected by age and is susceptible to epigenetic factors, such as diet. Subsequently, important questions arise such as, “Does the growth rate of younger abalone vary more than the older animals?”; “How does diet influence this occurrence?”; “Can a dietary intervention close the gap between fast and slow growing abalone?” The answers may be provided by studying the interaction of these factors (growth rate, age and feed) from a metabolic perspective.

Morash and Alter (2016) reviewed a number of studies comparing abalone that were classified into different age groups, and found no clear definitions or criteria for classifying abalone into juvenile and adult life stages (Morash and Alter, 2016). The term juvenile is generally used to classify abalone as soon as the formation of the first respiratory pore takes place (approximately 10 mm) (Hahn, 1989). At a length of about 70 mm, abalone typically start to spend their adult life in more open sea areas when living in the wild (Fallu, 1991), but in farming terms, animals are classified as young adults when an initial shell length of 40 mm is achieved (Shipton and Britz, 2001). In order to enhance growth at both of these life stages, it is important to comply with the dietary requirements of these animals as determined by the requirements of the life phase and size (Kruatrachue *et al.*, 2004).

Abalone formulated feeds were reported to promote superior growth rates when compared to growth results achieved from natural diets and also reduced weight loss during animal processing procedures (Green *et al.*, 2011). The locally manufactured Abfeed™ (Marifeed Pty Ltd, South Africa) is the preferred formulated feed for SA abalone (Troell *et al.*, 2006). However manipulations of Abfeed are commonly performed in research studies to investigate abalone growth (Venter *et al.*, 2016b) or to provide additional health benefits to the animal (Vosloo and Van Rensburg, 2009).

Irrespective of the feeding strategy, genetic variation in abalone shell length and wet weight is a well-known occurrence (Difford *et al.*, 2017), however, inter-individual variation (differences in growth rate shown by different individuals under identical environmental conditions) is often assigned to unexplained variance, receiving less research attention (Tamayo *et al.*, 2011). Research on mussels using optimised feeding conditions, indicated that a varied capacity to absorb and ingest food was the main determinant responsible for the observed variance in growth rates (Tamayo *et al.*, 2016).

The high commercial value of abalone ensures that research on various aspects of their biology remains relevant. By focussing on biochemical indicators of metabolic activity, researchers are

able to link metabolic pathways to processes important for survival, reproduction or growth (Dahlhoff, 2004). This in effect could further result in new insights into metabolic pathways of abalone, explaining variance in the observed growth rates. Since metabolomics generate data associated directly with immediate cellular functioning and the physiological states of an organism (Kim *et al.*, 2016), it is a useful tool for studying the metabolism of abalone grown during standard farming conditions. Also, metabolomics has been applied to the investigation of the metabolic characteristics of food resources associated with environmental and genetic factors (Kim *et al.*, 2016). In the current investigation, a metabolomics approach was used to indicate and better describe the metabolic variation associated with slow and fast growing abalone. A multiplatform metabolomics approach, including: untargeted nuclear magnetic resonance (NMR) spectroscopy; untargeted ultra-performance liquid chromatography-ion mobility-quadrupole time of flight spectrometry (UPLC-IM-QTOF); untargeted gas chromatography-time of flight spectrometry (GC-TOF); semi-targeted liquid chromatography-quadrupole time of flight mass spectrometry (LC-QTOF) and targeted liquid chromatography-tandem mass spectrometry (LC-MS/MS), were used to analyse abalone adductor muscle samples collected from animals of two different age classes, at three different time intervals, receiving two different abalone diets. Furthermore, at time of collection the animals were divided into two growth classes, based on growth performance observed prior to dissection.

This was done in order to address the following aims: 1) assess the metabolic differences when comparing slow and fast growing abalone consuming Abfeed; 2) determine the metabolic differences induced by Abfeed X, and 3) assess the metabolic differences between slow and fast growing abalone consuming Abfeed X.

6.2 Materials and methods

Information regarding the procedures used for abalone dissection, sample preparation, analysis and data processing can be viewed in Chapter 4. However, prior to the above mentioned, the following experimental setup and sample collection processes were performed.

6.2.1 Experimental setup and abalone details

The abalone growth experiment was conducted on-site at HIK Abalone Farm (Pty) Ltd, situated in Hermanus, South Africa between February 2015 and October 2015. After the initial sample collection, sampling took place after four months and again after eight months following grading practices implemented within the farming setup (Fig. 6.1). The study was conducted on animals classified into two age classes: juvenile (approximately 20 months of age and 29 g; 54 mm in

size) and adult (approximately 27 months of age and 65 g; 71 mm in size) animals. The same cohort of animals were monitored for the duration of the experiment allowing day to day farming activity to continue and size grading to continue as per normal at the predetermined intervals.

Within each age class, subsets of animals were subjected to two different feeding regimes. The first feeding regime was to use the standard artificial abalone feed (Abfeed S34) (Marifeed (Pty) Ltd, Hermanus, South Africa), and the second, a continuous supply of Abfeed X (Vosloo *et al.*, 2013b), which had an identical formulation to Abfeed S34, but was supplemented with 10 gram proline per kilogram dry feed (produced for research purposes by Marifeed). At time of sampling (time 0 - Feb 2015; time 4 - Jun 2015; time 8 - Oct 2015), animals were further divided into two growth classes e.g. slow growers and fast growers, based on their weight and length. Abalone were defined as a slow grower if the animal was visibly smaller than other abalone in the same sampling basket at an identical life stage. Then again abalone was defined as a fast grower if a larger size was visibly seen in an individual amongst animals from the same sample basket at the same life stage. Altogether this study consisted of three experimental factors (time, age and diet) and one resultant factor (growth). Adductor muscle samples were dissected in accordance to the procedure described in Section 4.3.2.

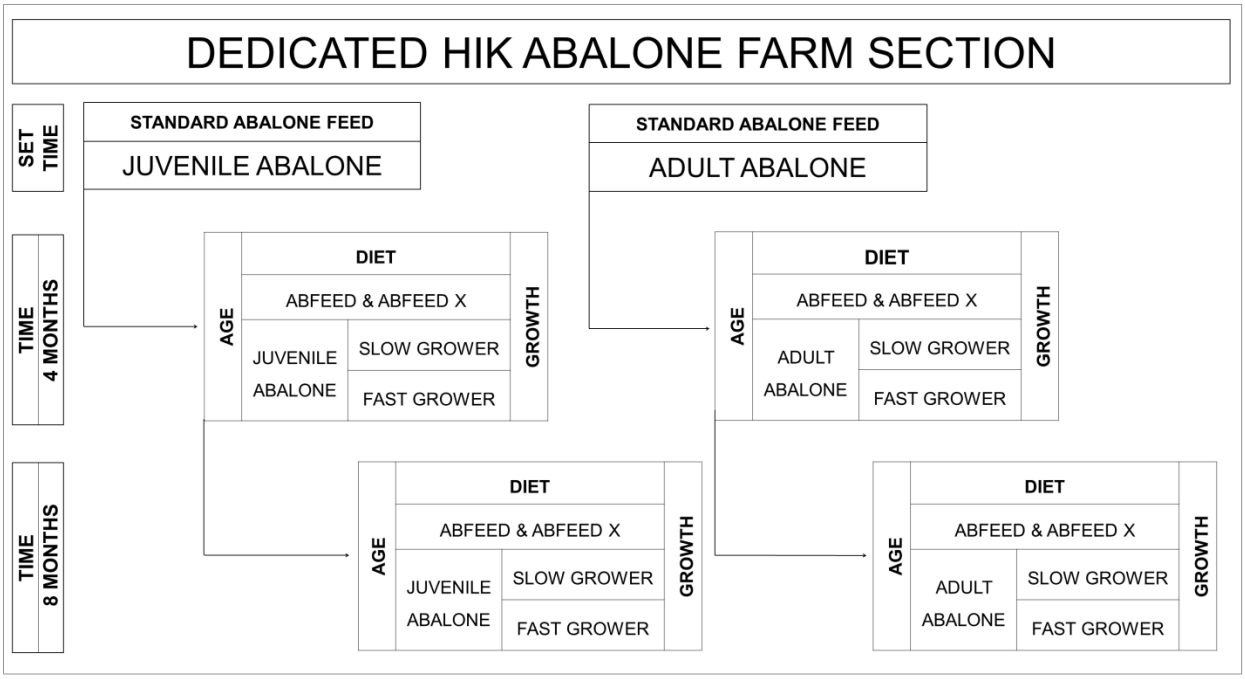

Figure 6.1: Farm based experimental design. Representative juvenile and adult abalone cohorts were used over an eight month period. Once initial samples were collected (set time), the cohorts were split into two different diet groups for the remainder of the growth trial. Fast and slow growing abalone of each age and diet group was collected after four and eight months.

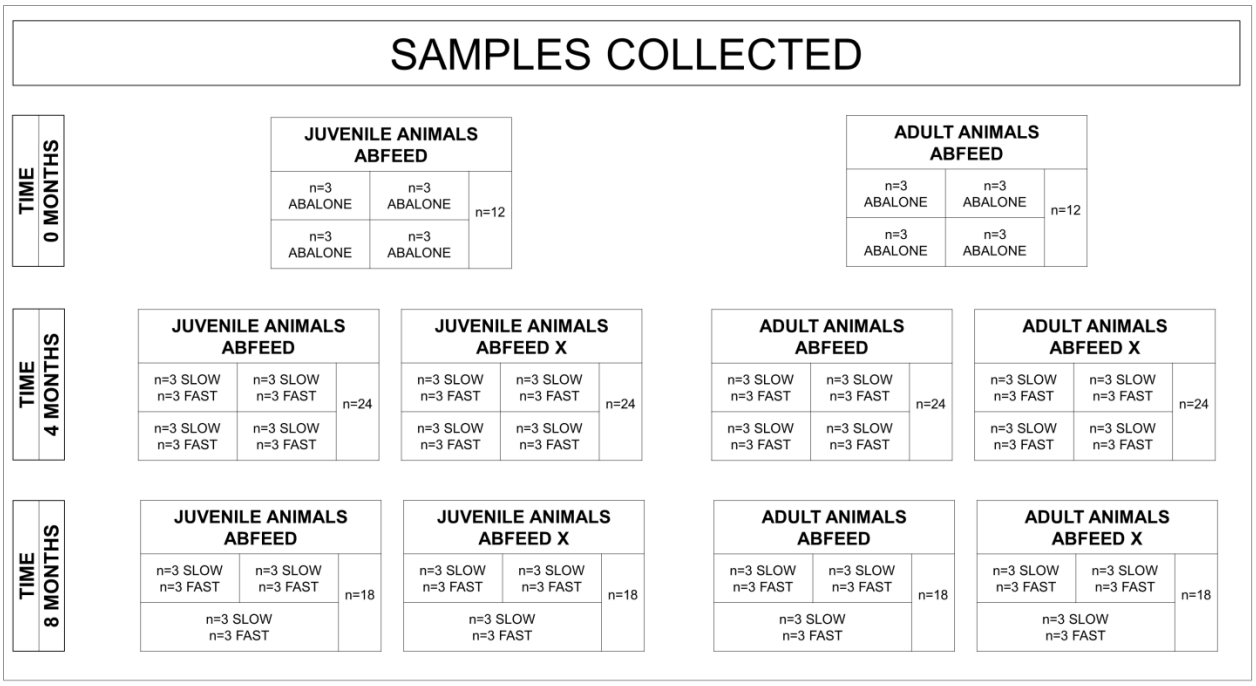

Figure 6.2: Abalone sample collection at three time intervals. Juvenile and adult abalone were collected at the first sampling time received Abfeed. After four and eight months of growth juvenile and adult animals were classified as slow and fast growing animals, collected from groups receiving Abfeed and Abfeed X respectively.

Using the dedicated farming raceways housing juvenile and adult abalone grown on Abfeed (Fig. 6.2, Table 6.1), three animals were collected from four baskets positioned closest to the water flow inlet (n = 12 juveniles; n = 12 adults). The juvenile animals had an average wet weight of 28.78 ± 5.89 g; and shell length of 54.40 ± 4.08 mm. Gender could not be determined by the examination of the gonads at this stage due to the fact that the animals had not reached sexual maturity by the time of sampling. In 6 male and 6 female adult abalone collected the average wet weight was 65.30 ± 4.30 g; and the shell length was 70.70 ± 2.09 mm at the first sample collection time.

After four months (time = 4) of farming, three slow and three fast growing animals that were fed with Abeed (Fig. 6.2, Table 6.1), were collected from the four baskets closest to the water flow inlet (n = 12 juvenile, slow growing animals; n = 12 juvenile, fast growing animals; n = 12 adult, slow growing animals; n = 12 adult, fast growing animals). The Abfeed groups consisted of: 3 male and 9 female, juvenile, slow growing abalone, with an average wet weight of 31.20 ± 8.42 g and shell length of 55.00 ± 6.76 mm; 6 male and 6 female, juvenile, fast growing abalone with an average wet weight of 56.50 ± 9.11 g and shell length of 66.50 ± 3.55 mm; 6 male and 6 female, adult, slow growing abalone with an average wet weight of 81.50 ± 9.80 g and shell length of 75.40 ± 2.98 mm; and lastly 6 male and 6 female, adult, fast growing abalone with an average wet weight of 99.00 ± 10.11 g and shell length of 80.20 ± 3.31 mm. This sampling was

repeated at four months for the collection of animals that were fed with Abfeed X (n = 12 juvenile, slow growing animals; n = 12 juvenile, fast growing animals; n = 12 adult, slow growing animals; n = 12 adult, fast growing animals). The Abfeed X groups consisted of: 5 male and 7 female, juvenile, slow growing abalone with an average wet weight of 36.30 ± 8.30 g and shell length of 56.40 ± 4.47 mm; 5 male and 7 female, juvenile, fast growing abalone with an average wet weight of 59.80 ± 4.13 g and shell length of 67.10 ± 1.51 mm; 10 male and 2 female, adult, slow growing abalone with an average wet weight of 83.00 ± 11.00 g and shell length of 74.60 ± 1.53 mm; 7 male and 5 female, adult, fast growing abalone with an average wet weight of 119.80 ± 37.58 g and shell length of 84.40 ± 8.91 mm.

Table 6.1: Abalone sampling measures. Average wet weight and shell length measures of abalone collected at three sampling intervals, consuming Abfeed or Abfeed X, with size, gender and growth rate groupings.

Feed	Size	Gender		Growth rate	Average wet weight (g)	Shell length (mm)
		Male	Female			
First sampling time: T0						
Abfeed	Juvenile	Not determined		No differentiation	28.78 ± 5.89	54.40 ± 4.08
	Adult	6	6		65.30 ± 4.30	70.70 ± 2.09
Second sampling time: T4						
Abfeed	Juvenile	3	9	Slow	31.20 ± 8.42	55.00 ± 6.76
	Juvenile	6	6	Fast	56.50 ± 9.11	66.50 ± 3.55
	Adult	6	6	Slow	81.50 ± 9.80	75.40 ± 2.98
	Adult	6	6	Fast	99.00 ± 10.11	80.20 ± 3.31
Abfeed X	Juvenile	5	7	Slow	36.30 ± 8.30	56.40 ± 4.47
	Juvenile	5	7	Fast	59.80 ± 4.13	67.10 ± 1.51
	Adult	10	2	Slow	83.00 ± 11.00	74.60 ± 1.53
	Adult	7	5	Fast	119.80 ± 37.58	84.40 ± 8.91
Third sampling time: T8						
Abfeed	Juvenile	4	5	Slow	42.10 ± 7.91	62.40 ± 3.50
	Juvenile	3	6	Fast	86.20 ± 8.55	77.00 ± 3.86
	Adult	4	5	Slow	85.70 ± 8.47	79.80 ± 1.56
	Adult	5	4	Fast	124.00 ± 11.50	87.90 ± 3.38
Abfeed X	Juvenile	6	3	Slow	48.80 ± 6.55	64.30 ± 2.21
	Juvenile	4	5	Fast	82.40 ± 12.94	76.90 ± 3.39
	Adult	5	4	Slow	90.40 ± 9.89	79.70 ± 2.11
	Adult	6	3	Fast	121.30 ± 10.62	88.10 ± 2.36

After an additional 4 months of abalone farming (8 months from time 0; time = 8) three slowing growing abalone and three fast growing abalone (consuming Abfeed), from three farming baskets positioned closest to the water flow inlet (Fig. 6.2, Table 6.1), were collected (n = 9 juvenile, slow growing animals; n = 9 juvenile, fast growing animals; n = 9 adult, slow growing animals; n = 9 adult, fast growing animals). The Abfeed groups consisted of: 4 male and 5 female, juvenile, slow growing abalone with an average wet weight of 42.10 ± 7.91 g and shell length of 62.40 ± 3.50 mm; 6 male and 3 female, juvenile, fast growing abalone with an average

wet weight of 86.20 ± 8.55 g and shell length of 77.00 ± 3.86 mm; 4 male and 5 female, adult, slow growing abalone with an average wet weight of 85.70 ± 8.47 g and shell length 79.80 ± 1.56 mm; 5 male and 4 female, adult, fast growing abalone with an average wet weight of 124.00 ± 11.50 g and shell length of 87.90 ± 3.38 mm. Repeated sampling (time 8) was done collecting animals consuming Abfeed X abalone feed (n = 9 juvenile, slow growing animals; n = 9 juvenile, fast growing animals; n = 9 adult, slow growing animals; n = 9 adult, fast growing animals). The Abfeed X groups consisted of: 6 male and 3 female, juvenile, slow growing abalone with an average wet weight of 48.80 ± 6.55g and shell length of 64.30 ± 2.21 mm; 5 male and 4 female, juvenile, fast growing abalone with an average wet weight of 82.40 ± 12.94 g and shell length of 76.90 ± 3.39 mm; 5 male and 4 female, adult, slow growing abalone with an average wet weight of 90.40 ± 9.89 g and shell length of 79.70 ± 2.11 mm; 6 male and 3 female, adult, fast growing abalone with an average wet weight of 121.30 ± 10.62 g and shell length of 88.10 ± 2.36 mm.

6.2.2 Sample preparation

Adductor muscle samples were prepared using the metabolite extraction procedure described in Section 4.4.1. The samples collected were prepared in accordance to the specific metabolomics platforms used (Sections 4.4.3 – 4.4.6).

6.2.3 Sample analysis

The collected samples were analysed using the platform specifications given in Section 4.5, which included NMR, UPLC-IM-QTOF, GC-TOF, LC-QTOF and LC-MS/MS platforms.

6.2.4 Data processing

Data were processed as described in Section 4.6, including data extraction, pre-processing, normalisation and data pre-treatment methods.

6.2.4.1 Batch effect evaluation

The samples forming part of this experiment were analysed over a minimum of 5 days and a maximum of 8 days, depending on the analytical instrument and method used. As a result, a batch effect occurred within the data generated by the UPLC-IM-QTOF and LC-QTOF platforms. The NMR, GC-TOF and LC-MS/MS data displayed no batch effects when evaluated, using PCA score plots and QC sample assessments. For both the UPLC-IM-QTOF and LC-QTOF dataset, a batch correction step was implemented by auto-scaling each batch separately.

These auto-scaled matrices were combined and descaled by multiplying each variable with the maximum of the standard deviations of the two batches (Wagner *et al.*, 2007).

6.2.5 Statistical analyses

Univariate statistical analyses were used to identify biological meaningful variables for the purpose of identifying the metabolite markers best describing the variation between the groups, in the context of the aforementioned three main research aims. Additionally, multivariate statistical analyses were used to visualise these differences.

6.2.5.1 Univariate analysis

Two-way analysis of variance (ANOVA) was used in an exploratory manner to determine the influence of age and time on the growth rate of abalone. This was done separately for each diet group. The data was then statistically blocked (Xu and Goodacre, 2012) to study the metabolic differences between fast and slow growing abalone, after considering the influence of the other factors. In order to achieve the latter, Student's *t*-test and effect size calculations were used. The data were log transformed before analysis, ensuring a more normal distribution (using MetaboAnalyst). A feature was considered statistically significant when a p-value < 0.05 (false discovery rates [FDR] corrected p-value) was achieved (Lindeque *et al.*, 2015). The effect size of each univariate comparison was also determined to complement the *t*-test findings. A d-value was calculated from the logged data by determining the absolute difference between the means of the two groups, divided by the maximum standard deviation of the two groups. A variable was considered of practical significance when it displayed a d-value > 0.8 (Ellis and Steyn, 2003).

6.2.5.2 Multivariate analysis

Principal component analysis was performed in MetaboAnalyst in order to visualise the differences between the experimental groups (Lindeque *et al.*, 2015). The data was pre-treated by performing a missing value imputation and log transformation. Scatter plots of the PCA scores were plotted with 95 % confidence ellipses to more effectively indicate grouping.

6.2.5.3 Statistics workflow

Statistical analyses were performed in three parts (Fig. 6.3) addressing each of the three aims separately, in order to determine those metabolites differing statistically when comparing: 1) slow and fast growing abalone on Abfeed, 2) the metabolic changes induced by Abfeed X, and 3) slow and fast growing abalone on Abfeed X. The latter can only be interpreted when the effect of Abfeed X is understood, thereby forming the link between the tests.

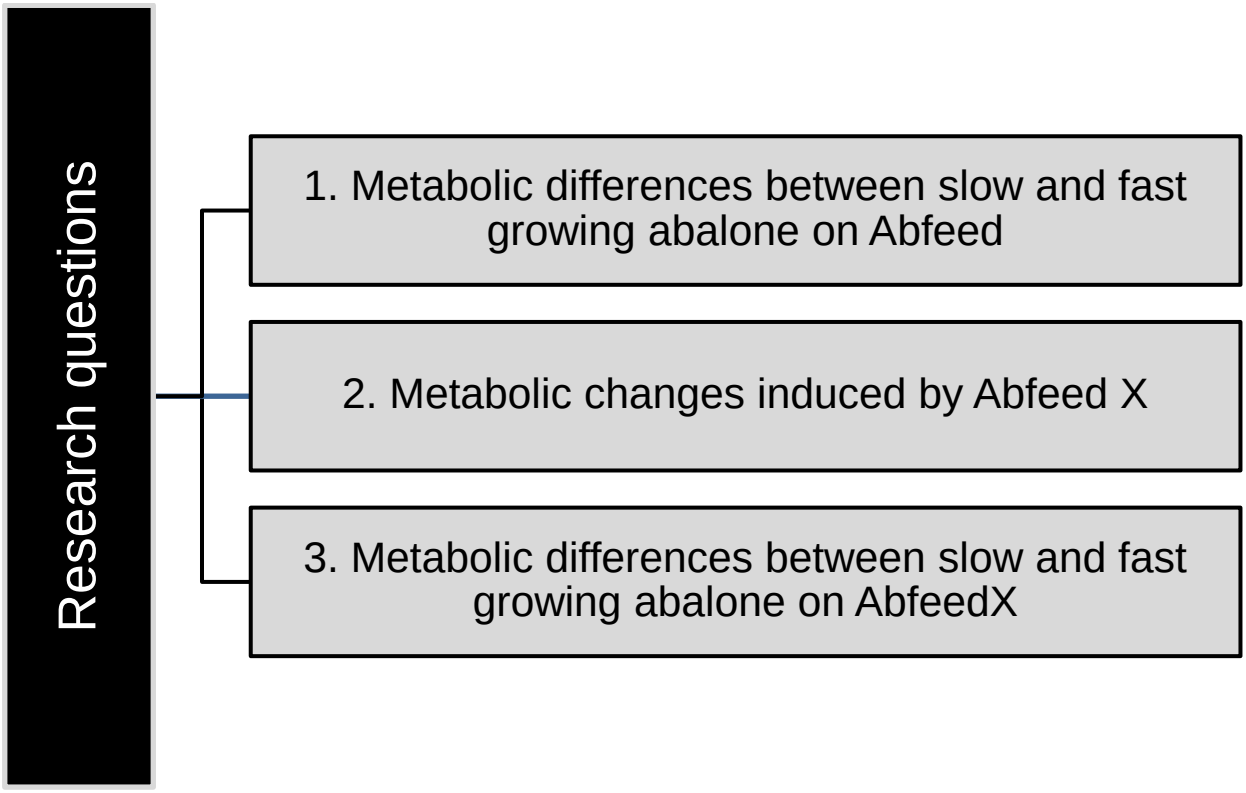

Figure 6.3: Statistical analysis based on three research questions. Statistical analyses were performed in three parts, investigating: 1) metabolite markers characterising slow and fast growing abalone fed Abfeed; 2) metabolite markers characterising abalone fed Abfeed X and 3) metabolite markers characterising slow and fast growing abalone fed Abfeed X.

6.2.5.3.1 Metabolite markers characterising slow and fast growing abalone fed Abfeed

In order to determine the metabolic differences when comparing slow and fast growing abalone grown on standard abalone feed (Abfeed), during standard farming conditions, it was initially necessary to determine the influence of various experimental factors, such as time of sampling and age of the animal on the observed growth rate variation. A two-way ANOVA was used to assess the influence of time of sampling and abalone age (Fig. 6.4), while ignoring (pooling) the resultant factor. The follow-up tests then focused on the resultant factor, as dictated by the two-way ANOVA results. The order of evaluation was as follows: A) age vs. time, comparing juvenile and adult abalone collected from time points 0, 4 and 8; B) growth rate vs. time, comparing slow and fast growing abalone collected at 4 and 8 months; C) growth rate vs. size, comparing juvenile and adult, slow and fast growing abalone sampled at 8 months. A one-way ANOVA (*t*-test) was then used to evaluate the differences between D) slow vs. fast growing abalone, consuming Abfeed, from time point 8.

A) AGE VS. TIME	ABFEED		
	JUVENILE	ADULT	
	n = 12	n = 12	TIME 0
	n = 24	n = 24	TIME 4
	n = 18	n = 18	TIME 8

B) GROWTH VS. TIME	ABFEED	
SLOW GROWTH	n = 24	TIME 4
FAST GROWTH	n = 24	
SLOW GROWTH	n = 18	TIME 8
FAST GROWTH	n = 18	

C) GROWTH VS. AGE	ABFEED		
	JUVENILE	ADULT	
SLOW GROWTH	n = 9	n = 9	TIME 8
FAST GROWTH	n = 9	n = 9	

D) SLOW VS. FAST	ABFEED	
SLOW GROWTH	n = 18	TIME 8
FAST GROWTH	n = 18	

Figure 6.4: Assessment of experimental factors relating to abalone consuming Abfeed. To determine how slow and fast growing abalone fed on Abfeed differed, experimental factors were blocked in order to establish which factors had the largest influence on the differences observed. This was achieved by comparing A) age and time, B) growth and time, C) growth and age variables and D) slow and fast growing abalone.

6.2.5.3.2 Metabolite markers characterising abalone fed Abfeed X

The effect of Abfeed X on the metabolism of abalone over time was investigated using two-way ANOVA (A). The metabolic changes induced by Abfeed X after 8 months were also compared between juvenile and adult abalone (B) to evaluate the contribution of age. Following this Student's *t*-test was used to identify statistical significant features from C) abalone fed Abfeed and Abfeed X after 8 months of feeding administration (Fig. 6.5).

A) DIET VS. TIME		
ABFEED	ABFEED X	
n = 24		TIME 0
n = 48	n = 48	TIME 4
n = 36	n = 36	TIME 8

B) DIET VS. SIZE				
ABFEED		ABFEED X		
SMALL	LARGE	SMALL	LARGE	
n = 18	n = 18	n = 18	n = 18	TIME 8

C) ABFEED VS ABFED X		
ABFEED	ABFEED X	
n = 36	n = 36	TIME 8

Figure 6.5: Assessment of Abfeed X. Assessment of metabolic changes related to feeding using Abfeed X, relied on comparisons between A) diet and time and B) diet and age resulting in a one-way comparison between C) abalone consuming Abfeed and Abfeed X.

6.2.5.3.3 Metabolite markers characterising slow and fast growing abalone fed Abfeed X

To determine how slow and fast growing abalone receiving Abfeed X differed metabolically from each other, two-way ANOVA was used to find significant features in terms of: A) growth vs. age, comparing juvenile and adult, slow and fast growing abalone. Age was then assessed independently using Student's *t*-test to find metabolic differences between B) juvenile, slow and fast growing abalone and C) adult, slow and fast growing abalone (Fig. 6.6).

A) GROWTH VS. AGE	ABFEED X		
	JUVENILE	ADULT	
SLOW GROWTH	n = 9	n = 9	TIME 8
FAST GROWTH	n = 9	n = 9	

B) JUVENILE SLOW VS. FAST	ABFEED X	
	JUVENILE	
SLOW GROWTH	n = 9	TIME 8
FAST GROWTH	n = 9	

C) ADULT SLOW VS. FAST	ABFEED X	
	ADULT	
SLOW GROWTH	n = 9	TIME 8
FAST GROWTH	n = 9	

Figure 6.6: Assessment of experimental factors relating to abalone consuming Abfeed X. Metabolic differences between slow and fast growing abalone consuming Abfeed X were determined by comparing A) growth and age experimental groups, allowing assessment of B) juvenile slow and fast growing abalone and C) adult slow and fast growing abalone.

6.2.5.4 Compound identification

Statistically and practically significant features were assigned compound (metabolite) names, using the identification confidence levels described in Section 4.7. Only compounds with Level 1, 2 and 3 identification were considered relevant for biological interpretation.

6.2.5.5 Pathway analysis

Manual pathway analysis was done, focussing on those metabolite markers indicated in Tables 6.2 – 6.5 contributing to the metabolic pathways where the largest observed differences in the relevant experimental group, when compared to the control group, was observed (as indicated by the increase [↑] or decrease [↓]). From the results it becomes evident that amino acid metabolism pathways account for the most significant variation between the compared groups.

6.3 Results and discussion

The main objective of this study was to elucidate the metabolic differences occurring when comparing slow and fast growing abalone. The influence of various contributing factors (such as diet and age) was also investigated over time, albeit as secondary objectives. Consequently, as mentioned earlier, the data were processed and the results are discussed in three subsections namely: 1) Metabolite markers characterising slow and fast growing abalone fed Abfeed; 2) Metabolite markers characterising abalone fed Abfeed X and 3) Metabolite markers characterising slow and fast growing abalone fed Abfeed X. Only those metabolites with both statistical ($p < 0.05$) and practical ($d > 0.8$) significance, and with an identification confidence Level of 1, 2 or 3, were used for biological interpretation and are discussed below.

6.3.1 Metabolite markers characterising slow and fast growing abalone fed Abfeed

In order to assess the underlying metabolic differences occurring when comparing slow and fast growing abalone receiving standard abalone feed (Abfeed) during normal farming conditions, it was necessary to determine the influence of the experimental factors time, age and growth. This was limited to the group of abalone consuming Abfeed only.

6.3.1.1 The contribution of age and time as experimental factors

The contribution of abalone age and time of sampling was investigated using a two-way ANOVA. The number of features that were significantly influenced by these factors is shown in the Venn diagram in Fig. 6.7. As predicted, the abundance of a relatively large number (128) of features varied significantly over time, irrespective of age. The concentrations of only nine

features were significantly different when comparing the juvenile and adult abalone, independent of sampling time, while the majority of the other significantly different features showed overlapping patterns and interactions when considering abalone age and sampling time.

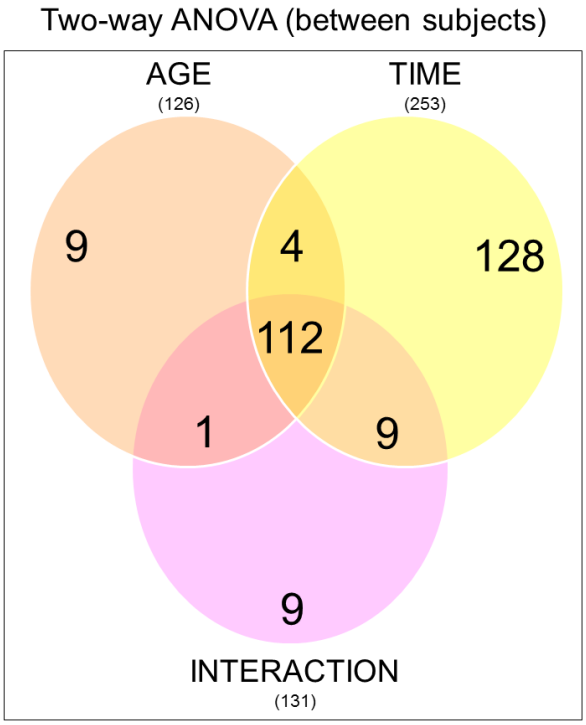

Figure 6.7: Venn diagram of important features significantly influenced by abalone age and sampling time for the group consuming Abfeed. Two-way ANOVA identified 126 features significant in the age group and 253 features significant in the sampling time group, with 131 interacting features between the two groups.

At the onset of the growth trial, a control group of abalone were sampled, following a fixed farm grading procedure, which allowed the collection of animals with well-defined farming data. The size grading procedure ensured that all the animals were of similar age and size at the onset of the experiment (time 0). Since visible size differences were observed after 8 months (related to the differences in growth rate), it is expected that the sampling time would contribute greatly to the variance in the data. This can be attributed to the fact that an 8 month time period passed from the first to the last sampling, resulting in an absolute growth rate for juvenile abalone of 60.55 ± 23.29 g wet weight/8 months and 62.91 ± 7.84 mm shell length/8 months, and an absolute growth rate for adult abalone of 96.66 ± 21.38 g wet weight/8 months and 75.01 ± 4.60 mm shell length/8 months as determined by the average weight (or shell length) of the samples collected at time 8 and 0, divided by the number of experimental months (Wang *et al.*, 2016). Additionally, a study by Laas and Vosloo (2010) indicated that in abalone, the concentrations of muscle glucose, lipids and proteins were significantly altered by abalone age (Laas and Vosloo,

2010). It was also reported that seasonal changes have a significant influence on the biochemical composition of *H. midae* (Laas and Vosloo, 2010), which additionally explains the significant effect that the time of sampling had on the metabolome differences observed in this study. The current investigation captured summer, autumn and winter (Feb – Aug in SA) fluctuations, explaining the variation observed in our investigation over the course of 8 months.

Abalone age has also been reported to have a significant effect on the biochemical composition and export performance of *H. midae* (Laas and Vosloo, 2010). Furthermore, significant differences were observed when comparing the biochemistry of one and two year old *H. laevigate*, correlated to their dietary protein intake (Stone *et al.*, 2013). An overview of the data in the current investigation (Fig. 6.7) indicates that the metabolism of juvenile and adult abalone is in fact very similar (excluding minor interacting changes). Since it is not within the scope of this study to assess the metabolic differences occurring when comparing juvenile and adult abalone, the juvenile and adult abalone sample data was analysed without differentiating the age of the animals, enabling the evaluation of metabolic differences between slow and fast growing abalone on a larger cohort of samples.

6.3.1.2 The contribution of sampling time on growth rate and related metabolic differences

Considering that the study was done over a duration of 8 months, it was essential to determine whether or not the metabolic differences detected when comparing the slow and fast growing abalone consuming Abfeed, had to be studied at one time point or whether the data for sampling time 4 and 8 could be pooled (if the metabolite levels were uniformly different at both sampling points). Time 0 was not considered for this purpose, since no growth differences were recorded at this sampling time. Hence, the influence of time (4 and 8 months) and growth rate (slow and fast growing abalone) on the data were assessed using two-way ANOVA. The number of features that were significantly influenced by these factors is shown in the Venn diagram in Fig. 6.8.

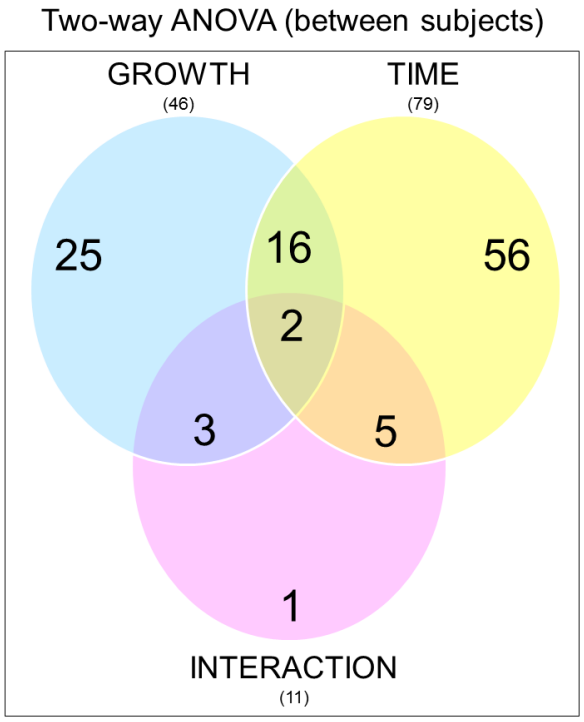

Figure 6.8: Venn diagram of important features significantly influenced by growth rate and sampling time. Two-way ANOVA identified 46 features significant in the growth group and 79 features significant in the sampling time group, with 11 interacting features between the two groups.

The concentrations of 25 features differed significantly when comparing the slow and fast growing abalone irrespective of time. However, sampling time once again showed to have the greatest influence on the data, with 56 features significantly differing when comparing T4 and T8, regardless of growth rate. Sampling time 8 was selected in order to determine which metabolites differed most significantly when comparing slow and fast growing abalone. This decision is based on the assumption that metabolic differences between slow and fast growing abalone would increase over time. Abalone growth (size) is the most important outcome for the abalone farming sector (Venter *et al.*, 2016b). Hence, in the context of the current investigation, assessing the data at time point 8 seems the most obvious time point for assessing the metabolite data comparisons between the fast and slow growing abalone. Resultantly, all the metabolic differences shown when comparing fast and slow growing abalone were done using the data collected from abalone at the sampling time point of 8 months.

6.3.1.3 Determining the effect of age on the observed growth rate at time 8

Although it was concluded that abalone age does not contribute much to the variance in the data, it was none-the-less still decided to test this again on the selected time window using the later comparisons. Hence, the effect of abalone age on the metabolic differences detected when comparing slow and fast growing abalone after 8 months of growth (on Abfeed), were studied

using a two-way ANOVA. As seen in Fig. 6.9, growth contributed 31 significant features, abalone age contributed 22 significant features, and 23 features showed interaction between the compared groups.

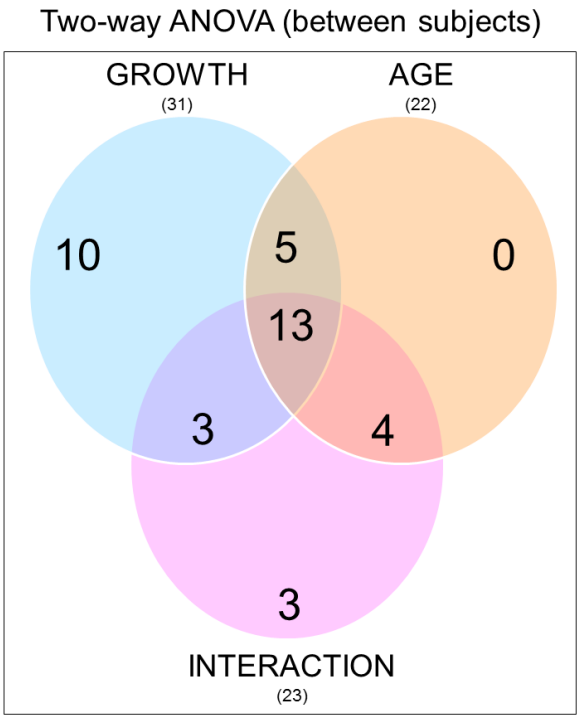

Figure 6.9: Venn diagram of important features significantly influenced by growth rate and age. Two-way ANOVA identified 31 features significant in the growth group with 22 features significant in the abalone age group, and 23 interacting features between the two groups.

The results of Fig. 6.9 illustrates that growth had the largest contributing amount of features (10) irrespective of abalone age. Independent age findings resulted in no significant features when comparing slow or fast growing, juvenile and adult abalone. Interestingly, abalone age is the only trait actively selected in terms of production from a genetic perspective (Dale-Kuys *et al.*, 2017), which from a metabolic perspective does not add real value when trying to find differences between slow and fast growing abalone consuming Abfeed. The results of this section once again confirms that abalone age can be regarded as one experimental factor that results in no differentiation between juvenile and adult animals when assessing growth tempo of abalone consuming Abfeed.

6.3.1.4 Assessing metabolic differences between slow and fast growing abalone consuming Abfeed

The most significant features differentiating the slow and fast growing abalone consuming Abfeed were determined using univariate analyses. Since the effect of abalone age to the metabolite variance in this current data set is negligible, the age groups at time 8 months were pooled before Students *t*-test and effect size analyses were performed. The features with significant ($p < 0.05$), and practical ($d > 0.8$) differences between slow and fast growing animals, are shown in Table 6.2. Of these 24 features, only 19 were confidently identified and thus used for biological interpretation. The data listed as "unknowns" represents the mass to charge ratio of the found features at a specific retention time in minutes. Table 6.2 also indicates the features in terms of increased (↑) or decreased (↓) metabolite concentrations in the fast growing abalone group, relative to the slow growing group. Metabolite classes such as amino acids (AA), carbohydrates (CHO), fatty acids (FA) and other metabolites (O) are indicated in the table along with the analytical platform used for analysis and level of identification.

Table 6.2: Significant metabolites detected in fast growing abalone consuming Abfeed. Compounds detected in adductor muscle samples are in order of most significant findings. An increase (↑) or decrease (↓) in metabolite abundance relative to slow growing (control) abalone is also indicated.

Compound	Direction fast growers	*p*-value <0.05	*d*-value >0.8	Metabolite class	Platform	ID level
Glycine	↓	1.69E-14	3.07	AA	LC-MS/MS	1
Glutamate	↑	1.49E-12	3.27	AA	LC-MS/MS	1
N,N-dimethylglycine	↓	3.18E-12	2.87	AA	LC-MS/MS	1
Carnitine (C0)	↓	4.20E-10	2.29	FA	LC-MS/MS	1
Phenylalanine	↑	5.03E-09	2.21	AA	LC-MS/MS	1
Lysine	↑	8.61E-08	1.86	AA	LC-MS/MS	1
Tauropine	↓	1.54E-07	1.63	CHO / AA	LC-MS/MS	1
Arginine	↓	3.90E-06	1.61	AA	LC-MS/MS	1
Aminobenzoate	↓	5.16E-06	1.31	O	LC-QTOF	3
Picolinate	↓	4.16E-05	1.37	O	GC-TOF	1
Dehydroxycarnitine	↓	1.43E-04	1.22	FA	LC-QTOF	3
Ornithine	↓	1.67E-04	1.39	AA	LC-MS/MS	1
Alanine	↑	3.62E-04	1.22	AA	LC-MS/MS	1
Aminomalonate	↓	5.63E-04	1.15	AA	GC-TOF	1
Acetylcarnitine (C2)	↓	6.14E-04	0.92	FA	LC-MS/MS	1
Tryptophan	↓	9.63E-04	1.01	AA	LC-MS/MS	1
Threonine	↑	3.73E-03	0.92	AA	LC-MS/MS	1
Alanopine	↓	4.41E-03	0.80	CHO / AA	LC-MS/MS	1
Tyrosine	↑	6.14E-03	0.80	AA	LC-MS/MS	1
3-Isoxazolidinone	↓	1.72E-06	1.88	-	GC-TOF	-
Unknown1_13.69 min@213.1715 m/z	↓	1.04E-05	1.66	-	LC-QTOF	-
Unknown2_0.64 min@385.2906 m/z	↑	1.20E-05	1.36	-	UPLC-IM-QTOF	-
Unknown3_0.58 min@94.0654m/z	↓	6.85E-05	1.12	-	UPLC-IM-QTOF	-
Unknown4_0.95 min@138.0561m/z	↓	7.28E-05	1.07	-	UPLC-IM-QTOF	-

A multivariate assessment of the univariate selected features of Table 6.2 is given in the PCA score plots in Fig. 6.10, constructed with 95 % confidence regions. The PCA score plot (A) shows clear differentiation between the slow growing and the fast growing abalone, which indicates an additional covariance between the univariate metabolite markers. Closer

examinations also revealed that two sub groups could be seen in the fast growing group, which can be ascribed to the subtle variation in the metabolite profiles when comparing juvenile and adult fast growing abalone (Fig. 6.10 B). These differences are however less evident in the slow growing abalone group. The observed differences between the age groups can be linked to the degree by which metabolites differ between slow and fast growing abalone in the juvenile and adult abalone, and not due to the occurrence of novel metabolites.

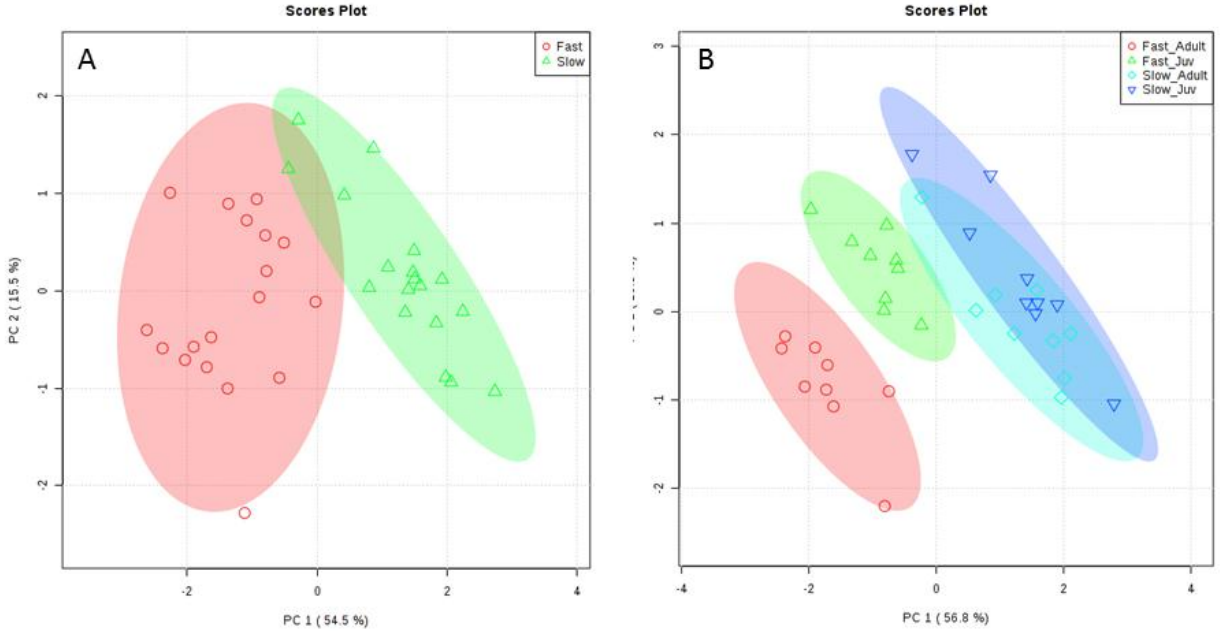

Figure 6.10: Principal component analysis of slow and fast growing abalone on Abfeed. A plot of PC1 versus PC2 of slow and fast growing abalone (A) and juvenile and adult, slow and fast growing abalone (B), showing differentiation of the groups because of variation in their metabolite profiles.

The significant metabolite markers indicated in Table 6.2, were subsequently used to create a schematic representation of those metabolic pathways favouring faster abalone growth. All of the main known energy production metabolic pathways are included in Fig. 6.11, with significantly altered metabolites depicted by an increase (↑) or decrease (↓) in metabolite abundance. Broadly interpreted, glycolysis, the TCA cycle, the electron transport chain (ETC), the urea cycle and ß-oxidation are influenced, accompanied by the upregulation in those metabolic pathways associated with insulin synthesis, all of which suggests comparatively elevated levels of protein synthesis in the faster growing abalone group.

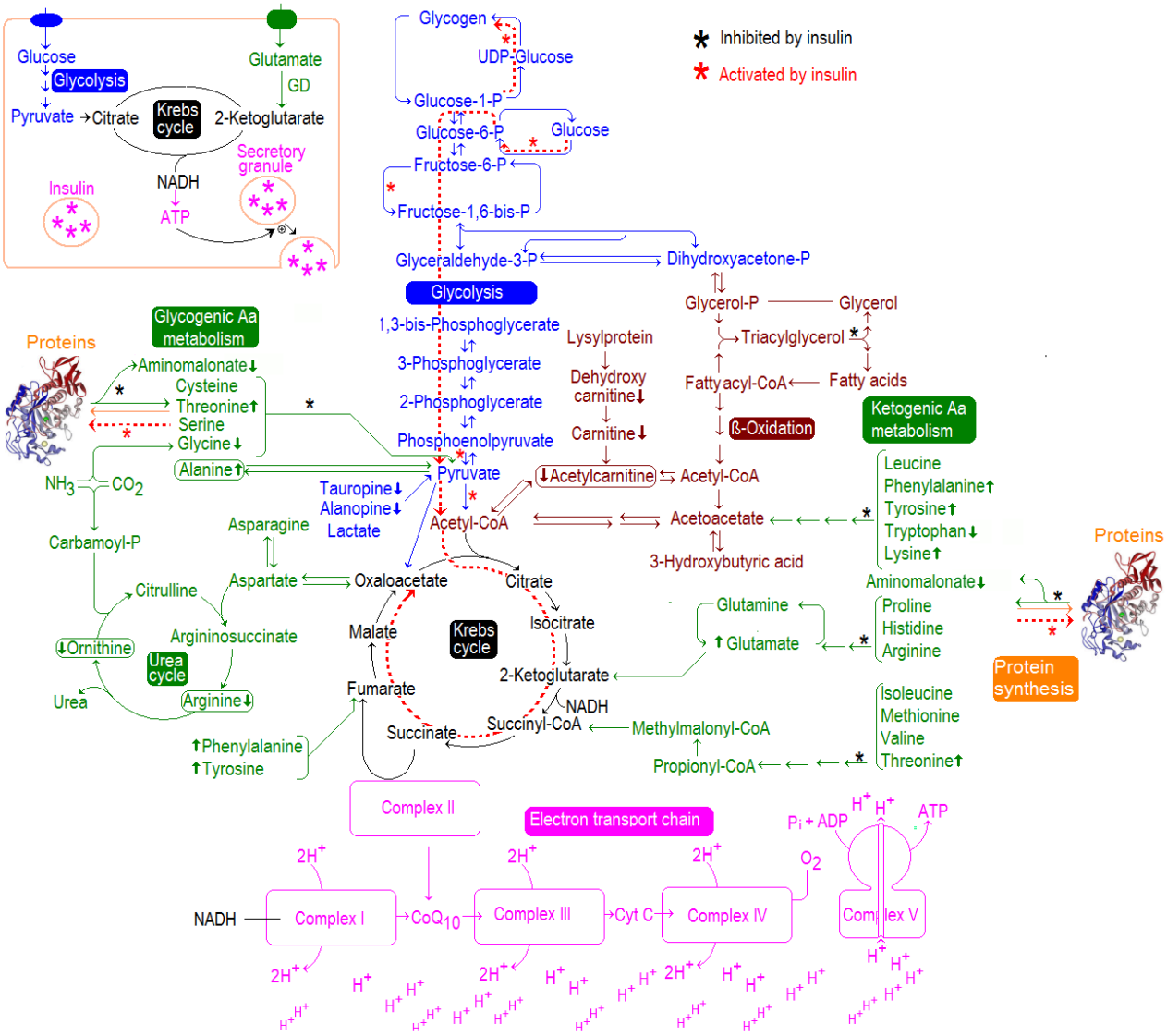

Figure 6.11: Metabolite profile of fast growing *H. midae* consuming standard abalone feed. The metabolites affected throughout carbohydrate (blue), amino acid (green) and fatty acid (brown) metabolic pathways are indicated by an increase (↑) or decrease (↓) in metabolite abundance as compared to the slow growing abalone group.

The results in Table 6.2 and Fig. 6.11, indicates that differentiation between fast and slow growing abalone consuming Abfeed, are predominantly related to amino acid metabolism. However, a few carbohydrate intermediates and fatty acid metabolites were also significantly altered. Glycine, N,N-dimethylglycine, carnitine, tauropine, arginine, aminobenzoate, picolinate, dehydroxycarnitine, ornithine, aminomalonate, acetylcarinitine, tryptophan and alanopine were all significantly reduced in the faster growing abalone group comparatively, while glutamate, phenylalanine, lysine, alanine, threonine and tyrosine were elevated. Interestingly, this is almost the exact opposite profile to what was seen in the adductor muscle of animals exposed to hypoxic conditions in the previous chapter. Glycine, carnitine, tauropine, arginine, ornithine, aminomalonate and acetylcarnitine, were significantly elevated in abalone exposed to hypoxic

conditions. Similarly, phenylalanine, lysine and threonine were depleted after hypoxia (Chapter 5). Since the amino acid profiles of the slow growing abalone correspond to that of the animals exposed to hypoxic conditions, it can be reasoned that mitochondrial function in these animals is slightly impaired. Impaired mitochondrial function results in lower energy levels and perhaps the use of alternative energy producing pathways to sustain basal energy levels. Hence, instead of using amino acids purely for anabolic activity, the slow growing abalone may require amino acids for catabolic pathways related to energy production.

In comparison Fig. 6.11 reflects that faster growing abalone consuming Afbeed used central carbohydrate metabolism as their main route for energy production, as indicated by a normal glycolysis, TCA cycle and ETC activity (demonstrated by the additional dashed red arrow running through the carbohydrate breakdown pathways). Due to the lack of increased and/or decreased metabolite markers detected in these pathways, it can be deducted that sufficient carbohydrate sources were available to ensure adequate ATP production during standard farming conditions. However, the elevated alanine (the transaminase product of pyruvate) detected, suggests that pyruvate is being synthesised more rapidly in the fast growers (Salway, 2004). Furthermore, alanine can potentially be used for osmoregulation (Fujimori and Abe, 2002), gluconeogenesis (Emery, 2015), transamination (Wu, 2009) and the promotion of insulin secretion (Dixon *et al.*, 2003). The opines, tauropine and alanopine traditionally formed via condensation of taurine and alanine with pyruvate respectively, during anaerobic conditions (Venter *et al.*, 2017), was subsequently detected in reduced concentrations in the faster growing abalone, when directly compared to the opines in slower growing abalone, suggesting a redox imbalance in the slow growers.

The major component of the abalone diet are carbohydrates, corresponding to their natural diets, which is mainly algae (Mau and Jha, 2017). It was confirmed that green-lip abalone utilise carbohydrates obtained from their diet as their main energy source (Bansemer *et al.*, 2016b) (confirmed in our results for *H. midae*). For the most part, energy availability for physiological functions are rather limited, thus, as soon as this energy is spent, on maintenance or recovering from stress, even less energy is available for growth. For the abalone farmer, this means that the abalone take longer to achieve market size (Morash and Alter, 2016). Due to the prevention/limiting/absence of major stressors during standard farming conditions, the abalone sampled for this investigation would potentially be able to use a larger portion of available energy and amino acids for growth and protein synthesis, as opposed to catabolism.

Protein degradation (catabolism) is accompanied by an increase in the urea cycle metabolites, and elevations in ammonia (Murray *et al.*, 2003, Hildebrandt *et al.*, 2015). Since glutamate (and glutamine) can be converted to aspartate (and asparagine) which in turn feeds into the urea

cycle (Griffin and Bradshaw, 2017), these may also be considered good indicators of increased amino acid catabolism when increased (Watford, 2003). Furthermore, aminomalonate has previously been identified as a constituent of proteins (Copley *et al.*, 1992), hence, elevated levels of this amino acid may also be a marker of protein degradation. Considering this, the metabolites related to these pathways indicated in Table 6.2 and Fig. 6.11, suggest that protein synthesis is elevated in the fast growing abalone comparatively; supporting the presence of relatively reduced ornithine and arginine in the urea cycle and reduced glycine, which also feeds to this cycle, and additionally the reduced levels of aminomalonate.

Acylcarnitines are metabolite intermediates considered important for the monitoring fatty acid metabolism (Reuter and Evans, 2012) and acetylcarnitine is a particularly major representative of anabolic and catabolic cellular metabolic pathways (Maldonado *et al.*, 2016). The production of acetylcarnitine is determined firstly by acetyl-CoA, the end product of glycolysis, synthesised from pyruvate via pyruvate dehydrogenase (Garrett and Grisham, 2010). Acetylcarnitine can also be synthesised via ß-oxidation of fatty acids (Longo *et al.*, 2016). In Fig. 6.11 and Table 6.2, carnitine, dehydroxycarnitine and acetylcarinitine were significantly reduced in the fast growing abalone comparatively, attesting to low fatty acid activity in faster growing abalone. This suggests that faster growing abalone required less energy via catabolic fatty acid metabolism since elevated carnitines would result in more fatty acids being available within the mitochondria, for usage in the ß-oxidation process when energy is needed (Longo *et al.*, 2016). Considering this, sufficient mitochondrial activity is concluded from this result in faster growing abalone since elevated levels of acetyl-CoA, would result in elevated carnitine production, which is associated with mitochondrial abnormalities (Smuts *et al.*, 2013).

In faster growing abalone, glycine is one of the metabolite with the largest variance detected. Glycine is known to play a crucial role in the methylation of proteins and DNA, due to its link to one-carbon metabolism (Wu, 2009). Glycine is also the basic building block in the biosynthesis of heme, purines, creatine, glutathione and uric acid (Yuan *et al.*, 2012). Furthermore, due to its structure, glycine is also abundantly used in the synthesis of various structural proteins, like collagen for instance, with every third position of the triple helical portion of the α-chain of collagen (the major component of connective tissue) being a glycine residue (Murray *et al.*, 2003). Because of its abundance in proteins, glycine levels are seen to be elevated during conditions of elevated protein catabolism (as seen in the environmental hypoxia experiment in the previous chapter). Lower glycine levels could thus imply that protein catabolism was lower in the fast growing abalone; or even that they have enhanced protein anabolic activity which results in the depletion of free glycine pools.

In summary, the elevated alanine levels associated with increased glycolytic activity, the reduced urea cycle activity, and the reduced aminomalonate, suggests reduced amino acid catabolism, and confirmation of this reduced catabolic state are the reduced carnitines supporting less need for fatty acid catabolism in the fast growing abalone. Consequently, it appears that fast growing abalone consuming Abfeed, predominantly use their central carbon metabolism for energy production during standard farming conditions. Amino acids and fatty acids are subsequently directed more towards anabolic pathways. Considering this metabolic profile, the role of insulin comes into question, as it results in glycogen, protein and lipid synthesis upon release. Taking into consideration that insulin has been found in multiple abalone studies related to growth (Morse, 1984, Fallu, 1991, van der Merwe *et al.*, 2011, Li *et al.*, 2012), the role of insulin in faster growing abalone consuming Abfeed is an important factor to consider.

Various neurotransmitters, nutrients and other hormones, are associated with elevated insulin secretion (Newsholme *et al.*, 2007). Additionally, an increase in ATP production, stimulates the release of insulin, as well as several amino acids, like glutamine, alanine and glutamate (of which the latter two were found in elevated levels in the fast growing abalone) (Newsholme *et al.*, 2007). Based on the metabolic profile of faster growing abalone (Fig. 6.11), it is speculated that these individuals can stimulate the release of insulin at a faster rate, or that released insulin results in a greater response. In a previous study done on *H. midae,* van der Merwe *et al.* (2011) indicated upregulation of various genes associated with insulin signalling in faster growing abalone, which is confirmed though our investigation. The role of insulin in the context of the results becomes apparent when investigating the site where insulin activates glycolysis, stimulating key glycolytic enzymes (indicated by the red asterisk (*) in Fig. 6.11). Insulin additionally promotes glycogenesis via glucose-6-P and the subsequent dephosphorylation and activation of glycogen synthase (Murray *et al.*, 2003, Garrett and Grisham, 2010). Perhaps, of even greater importance in the context of the results in Fig. 6.11, is the role of insulin in the activation of protein synthesis and inhibition of protein catabolism, considering the amino acids detected in the fast growers as previously described. The presence of amino acids and/or insulin activates the cell-signalling pathway involving the mechanistic target of rapamycin (MTOR) complex that primarily regulates protein synthesis (Urschel *et al.*, 2014, Wu *et al.*, 2014).

6.3.2 Metabolite markers characterising abalone fed Abfeed X

A follow-up question of this study is whether Abfeed X (an amino acid enriched diet) influences the metabolic differences between slow and fast growing abalone. Does Abfeed X enhance differences between slow and fast growing abalone, or does it close the gap between the

different growing abalone by allowing slow growing animals to grow more like fast growing animals? In order to interpret this influence, it is favourable to reveal and understand the effect of Abfeed X on the metabolism.

6.3.2.1 The contribution of diet and time as experimental factors

As depicted in the study design, all of the animals at time 0 were fed on exactly the same diet, hence it seems logical that the sampling time will have a rather large impact on the metabolite variance due to the introduction of an alternative diet from this point onwards. Nevertheless, a two-way ANOVA was used to confirm this prediction. The results from these tests are shown in Fig. 6.12.

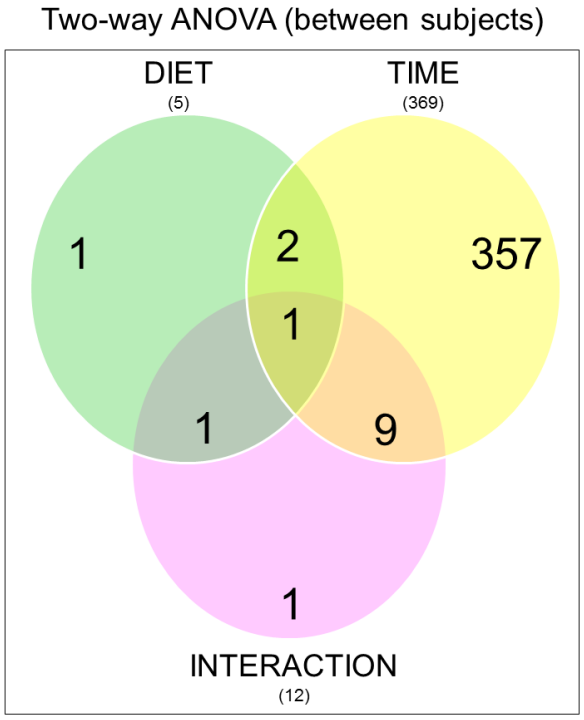

Figure 6.12: Venn diagram of important features significantly influenced by diet and time. Two-way ANOVA identified 5 features significantly varying in the diet group and 369 features significant in the time group, with 12 interacting features between the two groups.

Figure 6.12 clearly demonstrates that time had a large effect on the metabolite data generated with 357 features being significantly altered between the time points irrespective of diet. The metabolic changes induced by the dietary intervention are expected to augment the longer the animals are exposed to it. This is especially true for muscle tissue, which has comparatively slower turnover time for nutrients when compared to that of blood for instance. This principle is seen when investigating the tissue-specific biochemical responses during anoxia and recovery in the channelled whelk. Within a recovery period, the gills and ventricle samples of the whelk cleared accumulated end products within 6 hours, while the foot and radular retractor showed

little to no changes in this period (Eberlee and Storey, 1988) confirming different metabolic rates between tissues. Considering observations such as these, it was decided to only focus on the diet-induced changes at 8 months. Furthermore, the differences in weight and length of animals on Abfeed vs Abfeed X, were more pronounced after 8 months (compared to 0 and 4 months), supporting this decision. In the Abfeed X fed group, the absolute growth rate determined between time 0 and time 8 months was 61.97 ± 19.21 g wet weight/8 months and 63.83 ± 6.55 mm shell length/8 months for juvenile abalone and an absolute growth rate of 97.68 ± 18.20 g wet weight/8 months and 75.05 ± 4.58 mm shell length/8 months for adult abalone. It is clear that 8 months of abalone growth resulted in significant weight gain amongst the animals consuming Abfeed X, similarly to those consuming the standard Abfeed diet.

6.3.2.2 The contribution of diet and age as experimental factors

The effect of diet (Abfeed vs. Abfeed X) and age (juvenile vs. adult) on the metabolic variance seen at T8 were investigated with a two-way ANOVA.

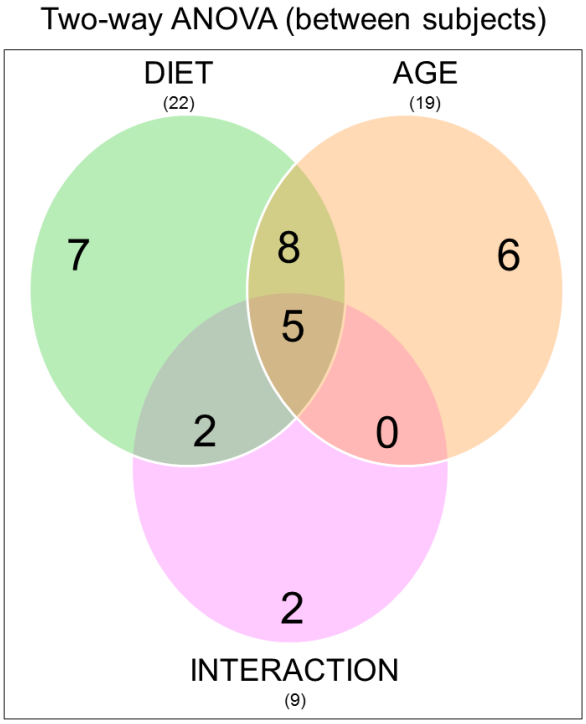

Figure 6.13: Venn diagram of important features significantly influenced by diet and age. Two-way ANOVA identified 22 features significant in the diet group and 19 features significant in the abalone age group, with 9 interacting features between the two groups.

Figure 6.13 indicates that diet and age contributed equally to the variance in the data. The abundance of six features varied when comparing the juvenile and adult abalone irrespective of diet. Likewise, the concentration of seven features was significantly altered in all abalone fed

Abfeed X, irrespective of age. Although age and diet showed some interaction, only the effect of diet, that was uniform between the ages, were of interest to provide a simplified explanation of the metabolic changes.

6.3.2.3 The metabolic changes in abalone induced by Abfeed X compared to that of abalone consuming Abfeed

Based on phenotypic evaluations of growth, no prominent differences in terms of shell length and animal weight were seen after 8 months when comparing abalone consuming Abfeed to Abfeed X (Fig. 6.14). None-the-less, since metabolomics is the endpoint of the "omics cascade" and is the closest to the functional phenotype of the cell (Dettmer *et al.*, 2007), the metabolome of these two groups were compared to investigate any further phenotypic changes, which may be induced in abalone consuming Abfeed or Abfeed X.

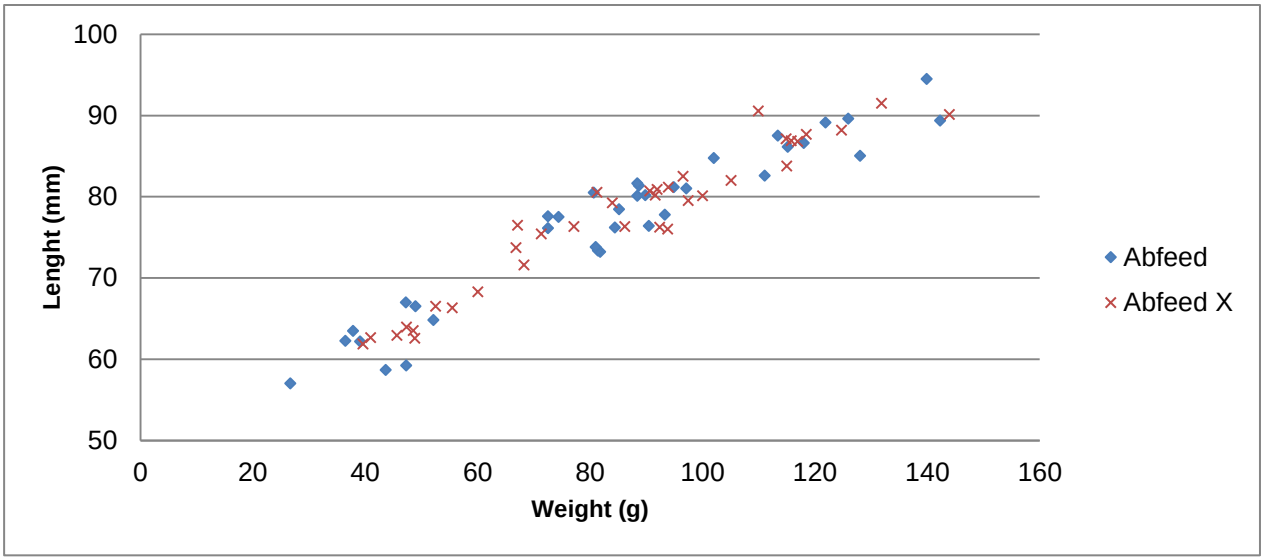

Figure 6.14: Scatterplot of abalone size after eight months of growth receiving Abfeed and Abfeed X artificial feeds. This plot reflects *H. midae* growth as a measure of shell length and wet weight after eight months of farming where animals were fed Abfeed and Abfeed X abalone diets.

Table 6.3 represents the metabolic findings of adductor muscle samples collected from abalone consuming Abfeed and Abfeed X abalone feeds. The findings are restricted to features with $p < 0.05$ and $d > 0.8$ as determined by univariate analysis. A total of 14 metabolites were significantly different when comparing the Abfeed and Abfeed X animals' metabolite data. Table 6.3 also indicates which of the respective metabolites displayed increased (↑) or decreased (↓) metabolite concentrations in the Abfeed X abalone group, relative to the Abfeed group. The amino acid (AA), carbohydrate (CHO), and fatty acid (FA) metabolite classes, the analytical platform used for analysis and level of identification is also indicated in the table.

Table 6.3: Significant metabolites detected in abalone consuming Abfeed X. Metabolites detected in abalone adductor muscle are in order of most significant findings, indicated by an increase (↑) or decrease (↓) in metabolite abundance relative to abalone consuming Abfeed.

Compound	Direction Abeed X group	*p*-value <0.05	*d*-value >0.8	Metabolite class	Platform	ID level
Proline	↑	2.12E-17	2.27	AA	LC-MS/MS	1
Tauropine	↑	7.84E-17	2.10	CHO / AA	LC-MS/MS	1
Alanine	↓	3.74E-10	1.36	AA	LC-MS/MS	1
Alanopine	↓	1.03E-09	1.60	CHO / AA	LC-MS/MS	1
Tryptophan	↓	1.09E-09	1.33	AA	LC-MS/MS	1
Taurine	↓	1.23E-09	1.26	AA	LC-MS/MS	1
Methionine	↓	2.72E-09	1.33	AA	LC-MS/MS	1
Glutamate	↓	1.29E-08	1.31	AA	LC-MS/MS	1
Aspartate	↓	4.31E-08	1.45	AA	LC-MS/MS	1
Asparagine	↑	7.73E-06	1.02	AA	LC-MS/MS	1
Lysine	↓	2.20E-05	1.04	AA	LC-MS/MS	1
Glycine	↑	2.41E-05	0.81	AA	LC-MS/MS	1
Histidine	↓	3.69E-05	0.84	AA	LC-MS/MS	1
Tyrosine	↓	5.21E-04	0.80	AA	LC-MS/MS	1

The metabolite markers indicated in Table 6.3 were assessed using multivariate analysis, resulting in the PCA score plot shown in Fig. 6.15. The PCA score plot shows clear separation between the Abfeed and Abfeed X experimental groups. Principle component 1 shows the largest variation in the data (46.8 %), which represents the relevant biological variance i.e. the inter-group variance. Principle component 2 explains the second largest variation in the data (20 %), which represents the intra-group variance. The Abfeed group shows more variance with subgroupings visible, also the Abfeed X group shows an inclining towards additional grouping.

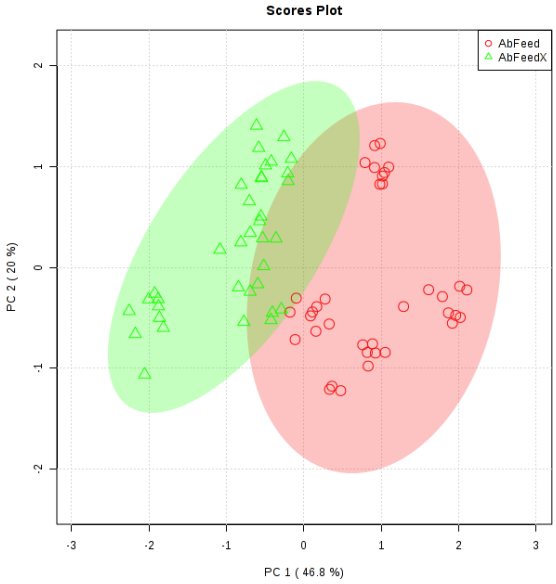

Figure 6.15: Principal component analysis of abalone consuming Abfeed and Abfeed X respectively. A plot of PC 1 versus PC 2 of abalone subjected to Abfeed and Abfeed X, shown with 95 % confidence ellipses.

From Table 6.3 it is apparent that the concentrations of proline, tauropine, asparagine and glycine in the adductor muscle of abalone fed Abfeed X, were significantly higher as compared to the abalone group receiving standard Abfeed, while the concentrations of alanine, alanopine, tryptophan, taurine, methionine, glutamate, aspartate, lysine, histidine and tyrosine were significantly lower in comparison, in the Abfeed X group.

Studies previously determined which amino acids are classified as essential and which as non-essential in abalone species *H. midae* and *H. rufescens* (Allen and Kilgore, 1975, Sales and Britz, 2003). Considering this, the non-essential abalone amino acids altered by Abfeed X in this study, included: alanine, aspartate, glutamate, glycine, proline and tyrosine, and the essential amino acids altered included: histidine, lysine, methionine and tryptophan. For the largest number of affected amino acids, a decrease in metabolite response was experienced in the Abfeed X group. Based on the findings indicated in Table 6.3, it is evident that the non-essential amino acids in muscle samples were mostly altered by Abfeed X, rather than the essential amino acids.

Tauropine (elevated) and alanopine (reduced) were the only opines seen to be significantly altered by the Abfeed X formulation. It is widely accepted that opines have an important physiological role in the maintenance of cytoplasmic redox balance during anaerobic glycolysis in muscle tissues of molluscs (Sato *et al.*, 1991), as extensively described in the previous chapter. However, the amino acid profiles indicated in Table 6.3, do not fit the metabolic profile typically experienced during anaerobic conditions (Venter *et al.*, 2016b), with the exception of the elevated tauropine (the fact that taurine is reduced attests to the fact that taurine is utilised to synthesise tauropine synthesis).

Of the amino acid changes in the Abfeed X group (Table 6.3), the most predominant change is reflected by the large elevated levels of proline detected in the muscle tissue of *H. midae.* This is to be expected since the Abfeed X formulation is Abfeed with added L-proline at a concentration, previously indicated to protect abalone against dehydration during live export (Vosloo *et al.*, 2013b). The importance of proline in numerous organisms has been widely demonstrated to play an important role in cell structure, metabolism and protein synthesis (where the requirement of proline for whole-body protein synthesis was reported to be the greatest amongst all amino acids), nutrition, wound healing, anti-oxidative reactions and immune responses (Wu *et al.*, 2011). Furthermore, proline was found to protect proteins from damage, due to its ability to act as a free radical scavenger and subsequently, protect the peptide backbone of proteins (Vosloo *et al.*, 2013b).

The physiological importance of amino acids as components of protein building blocks and substrates for the synthesis of molecules (Wu *et al.*, 2014) is well described in prior literature, where amino acids are used for dietary supplementation. The addition of lysine, methionine, threonine and tryptophan to plant-based feeds (which lack these components) for many fish species, is considered a cost effective approach to supplement-lacking amino acids (Li *et al.*, 2009). It has also been shown in pigs and poultry, that a diet supplemented with lysine, tryptophan and methionine/cysteine, improves tissue protein synthesis and growth (Wu *et al.*, 2014). Furthermore, a diet supplemented with L-proline was shown to significantly increase the growth rates in young mammals and chickens (Vosloo *et al.*, 2013b).

Artificial feeds are formulated to ensure a diet with higher protein content (Troell *et al.*, 2006). Proteins (amino acids) are considered the most important dietary component in abalone feed, required for optimised growth of the organism. However, the exact inclusion ratio of the respective individual protein (amino acid) sources for ensuring optimal abalone growth rates, are still unknown (Mau and Jha, 2017). Dietary protein is an expensive component of artificial feeds, but ensures additional nutritional value (Bansemer *et al.*, 2014), which will be assessed in terms of metabolic functioning in the succeeding section of this chapter.

6.3.2.4 Growth comparisons of juvenile and adult abalone on Abfeed and Abfeed X

Abalone growth is generally justified as a correlation between shell length and live weight, and following regression coefficients of average length and weight gain, growth rate can be determined (Sales and Britz, 2001, Sales and Janssens, 2004). To determine whether the diets experimented with in this study showed any growth benefit, the weight and length measurements collected after 8 months of abalone farming were used to construct the boxplots depicted in Figures 6.16 and 6.17. In both instances the weight (and length) measured in juvenile (Fig. 6.16) and adult (Fig. 6.17) abalone on Abfeed were compared to the findings of animals on Abfeed X, with special focus on fast and slow growing abalone. Faster growing abalone were larger than slow growing abalone irrespective of diet (as found with two-way ANOVA). Interesting, however, no statistical difference in weight or length were found between the diet groups in this experiment, which is clear in Figures 6.16 and 6.17.

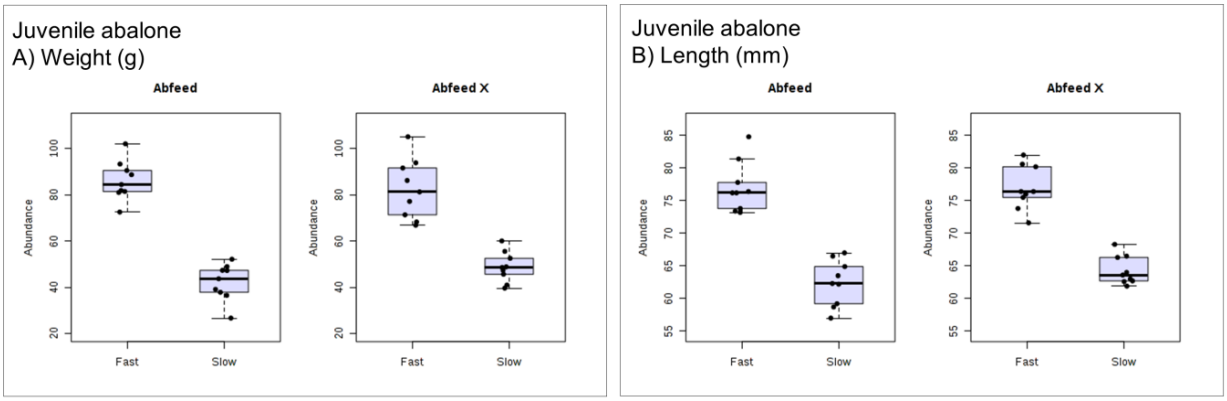

Figure 6.16: An overview of weight and length boxplots of juvenile abalone. The weight (A) and length (B) of juvenile abalone after 8 months of growth displayed in terms of fast and slow growing individuals consuming Abfeed and Abfeed X abalone diets, respectively.

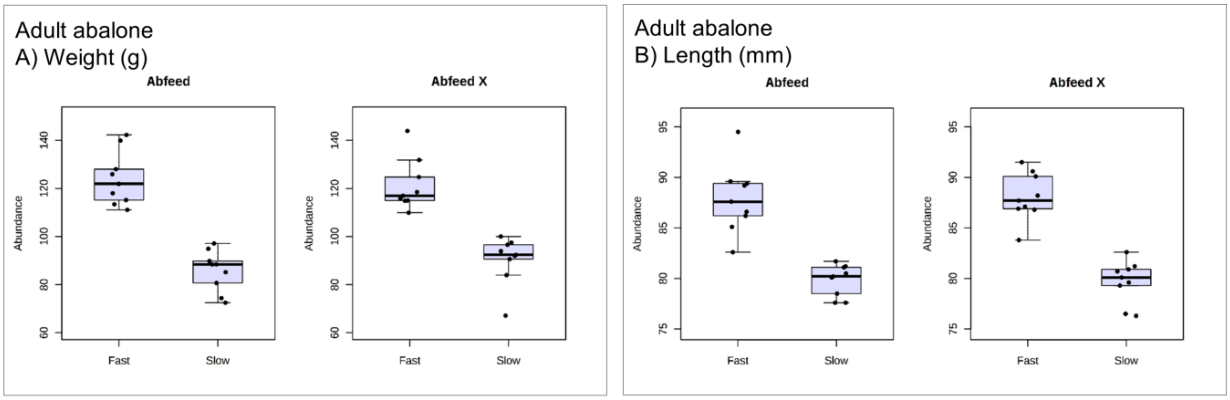

Figure 6.17: An overview of weight and length boxplots of adult abalone. The weight (A) and length (B) of adult abalone after 8 months of growth displayed in terms of fast and slow growing individuals consuming Abfeed and Abfeed X abalone diets, respectively.

Farm data collected from 48 baskets of abalone consuming Abfeed and Abfeed X, respectively, showed significant mass gain in Abfeed X individuals when compared to Abfeed individuals (unpublished data). A mean mass difference of 60 ± 26.2 g/basket/month for juvenile abalone and a difference of 122 ± 24.5 g/basket/month for adult abalone were calculated (personal communication 2016, Matt Naylor, Production and Research manager HIK Abalone Farm). This indicates that feed supplementation offers production level benefits and understandings of metabolic underpinnings of these benefits are important for future directed feed improvements. This is, however, not the observation in the current investigation, largely based on the fact that the results of Chapter 6 are based on data obtained from 72 abalone (36 juveniles and 36 adults) collected from various sampling baskets, resulting in a different view of what was achieved when doing macro analysis at production level. Nonetheless, the aim was to reflect metabolic differences between abalone consuming Abfeed and Abfeed X relating to growth in this study, as will be discussed below.

6.3.3 Metabolite markers characterising slow and fast growing abalone fed Abfeed X

As previously mentioned, an objective of this study was to determine the metabolic differences when comparing slow and fast growing abalone consuming Abfeed X. With the effect of Abfeed X on the metabolism now known, differences in the response of slow and/or fast growing abalone can be interpreted more convincingly. Since the effect of the diet was more pronounced after 8 months, along with the maximal differences in growth after 8 months, it was decided to study the animals collected at time point 8 in order to compare results. However, it was still deemed necessary to once again determine the effect of abalone age in this sub-group.

6.3.3.1 The contribution of growth and size as experimental factors

In order to determine the influence of Abfeed X on the metabolic changes occurring when comparing slow and fast growing abalone, it was again necessary to determine whether abalone age influences the comparisons when using the samples collected after 8 months of feeding, using the Abfeed X diet. The Venn diagram in Fig. 6.18 indicates that 15 features were significantly different concerning the growth, 17 related to age and 17 features showed interaction between the two groups.

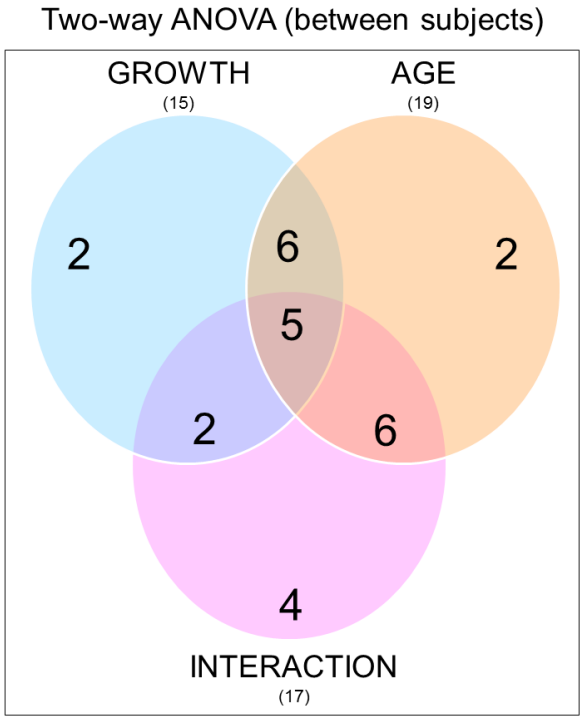

Figure 6.18: Venn diagram of important features based on the growth and age experimental groups consuming Abfeed X. Two-way ANOVA identified 15 features significant in the growth group and 19 features significant in the age group, with 17 interacting features between the two groups.

From Fig. 6.18, it is apparent that abalone age in the Abfeed X experimental group has a lager influence on the compared slow and fast growing abalone groups than initially found in the Abfeed group. Both growth and abalone age resulted in 2 significant features irrespective of the other factor. This finding is also partially demonstrated in the PCA shown in Fig. 6.15, where the Abfeed and Abfeed X comparisons were made. Considering this, in order to determined how slow and fast growing abalone consuming Abfeed X differ from one another metabolically, abalone age had to be assessed individually. Previous research on *H. tuberculata,* emphasised the importance of size/age specific grouping, stating that the sorting of abalone with respect to their size/age, improves production as growth of small individuals are increased when they are cultured with same-size counterparts (Mgaya and Mercer, 1994). Furthermore, former research using *H. iris,* suggested selecting faster growing animals for farming, since they perform better on average pertaining to growth outcomes, as when compared to those of a the smaller grade (Heath and Moss, 2009). Considering this, slow and faster growing abalone consuming Abfeed X was compared in terms of juvenile and adult groups, respectively.

6.3.3.2 Assessing metabolic differences between slow and fast growing juvenile abalone consuming Abfeed X

Univariate analyses (*t*-test and effect size) were used to find significant metabolic differences when comparing slow and fast growing juvenile abalone subjected to the Abfeed X diet. Table 6.4 summarises the 18 metabolites with significant values ($p < 0.05$ and $d > 0.8$) identified with a Level 1 confidence. Table 6.4 also indicates which of the respective metabolites displayed increased (↑) or decreased (↓) metabolite concentrations in the fast growing juvenile abalone group, relative to the slow growing juvenile group. Amino acid (AA), carbohydrate (CHO), fatty acid (FA) metabolite classes, the analytical platform used for analysis and level of identification is also indicated in the table.

Table 6.4: Significantly altered metabolites in the fast growing juvenile abalone consuming Abfeed X. Metabolites are listed in order of most significant *p*-value, indicated by an increase (↑) or decrease (↓) in metabolite response relative to slow growing abalone. All of the findings resulted in confident identification and compound nomenclature.

Compound	Direction fast growers	*p*-value <0.05	*d*-value >0.8	Metabolite class	Platform	ID level
Glycine	↓	1.49E-09	5.13	AA	LC-MS/MS	1
Aspartate	↑	1.62E-08	4.58	AA	LC-MS/MS	1
Serine	↓	1.68E-08	3.98	AA	LC-MS/MS	1
Tyrosine	↓	2.51E-08	4.29	AA	LC-MS/MS	1
Histidine	↓	3.38E-07	3.89	AA	LC-MS/MS	1
Creatine	↑	4.04E-07	3.39	CHO	LC-MS/MS	1
Arginine	↑	9.16E-07	2.91	AA	LC-MS/MS	1
Strombine	↑	1.57E-06	3.30	CHO / AA	LC-MS/MS	1
Taurine	↓	8.92E-06	2.74	AA	LC-MS/MS	1
Tryptophan	↓	6.82E-05	1.88	AA	LC-MS/MS	1
Ornithine	↑	7.33E-05	2.05	AA	LC-MS/MS	1
Threonine	↓	1.24E-04	1.78	AA	LC-MS/MS	1
Valine	↓	1.72E-03	1.73	AA	LC-MS/MS	1
Carnitine (C0)	↑	1.85E-03	1.42	FA	LC-MS/MS	1
N,N-dimethylglycine	↑	2.20E-03	1.38	AA	LC-MS/MS	1
Glutamine	↑	6.33E-03	1.40	AA	LC-MS/MS	1
Acetylcarnitine (C2)	↑	7.12E-03	1.10	FA	LC-MS/MS	1
Asparagine	↓	1.08E-02	1.19	AA	LC-MS/MS	1

Multivariate analysis using the univariate selected metabolites given in Table 6.4, resulted in the PCA indicated in Fig. 6.19. The PCA score plot shows clear grouping between the slow and fast growing juvenile abalone abductor muscle metabolites, accounting for 74.6 % of the variance in PC 1. The fast growing abalone group showed larger within group variation when compared to the slow growing abalone group, accounting for 7.9 % of the variance in PC 2. No further visible outliers or subgroupings are shown in Fig. 6.19. The score plot also shows that the covariance of these metabolites discriminates between the fast and slow growing animals (which could be used for classification in future studies).

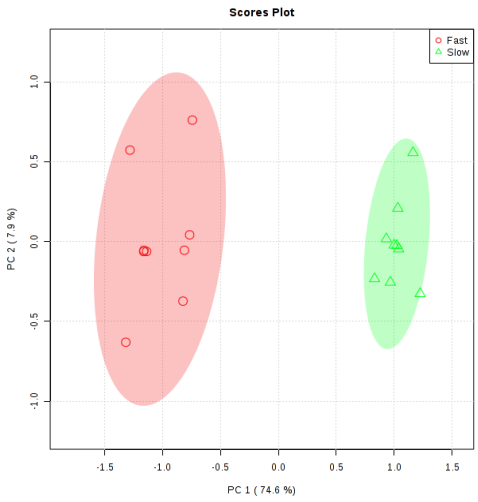

Figure 6.19: Principal component analysis of slow and fast growing juvenile abalone consuming Abfeed X. Plots of PC 1 versus PC 2 of significant metabolites concerning growth detected in juvenile abalone.

The metabolic differences found between the slow and fast growing juvenile abalone (Table 6.4) were interpreted with the effect of the diet in mind. This was made easier with visualisation of the metabolite concentrations in box plots. Proline together with the top metabolite in Table 6.4 is shown in Fig. 6.20, (with additional metabolites displayed in Appendix B). As discussed in Section 6.3.2.3 Abfeed X increased proline concentrations in both slow and fast growing abalone as seen in Fig. 6.20. Based on this observation proline displayed no favour towards growth, keeping growth rate similar in juvenile abalone. Whether this indicates that the slow growing abalone utilised proline more, to aid their growth, is questionable seeing the minor weight and length increases (Fig. 6.16). When focusing on glycine fast growing abalone on Abfeed had reduced glycine concentrations which were elevated by the consumption of Abfeed X, creating a metabolite profile that is similar to that of the slow growing group. The metabolic relevance of these observations will be discussed in conjunction with the metabolic map in Fig. 6.21.

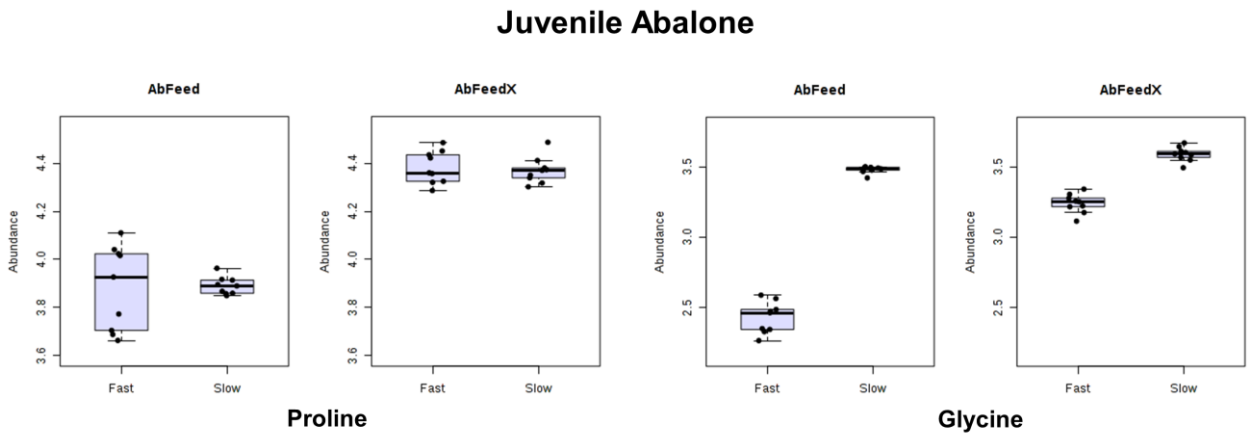

Figure 6.20: Boxplots of proline and glycine detected in juvenile abalone. Relative metabolite abundance of proline and glycine as detected in fast and slow growing juvenile abalone consuming Abfeed and Abfeed X diets respectively.

Using the muscle metabolite profile (Table 6.4) associated with the metabolic response of fast growing juvenile abalone consuming Abfeed X, a metabolic map was created as shown in Fig. 6.21. Metabolites of affected metabolic pathways are displayed as an increased (↑) or decreased (↓) metabolic response relative to the slow growing juvenile abalone. An influx of proline demonstrates catabolism thereof to power the TCA cycle and the urea cycle with ß-oxidation partially assisting with acetyl-CoA production, allowing additional amino acids to be used for protein synthesis.

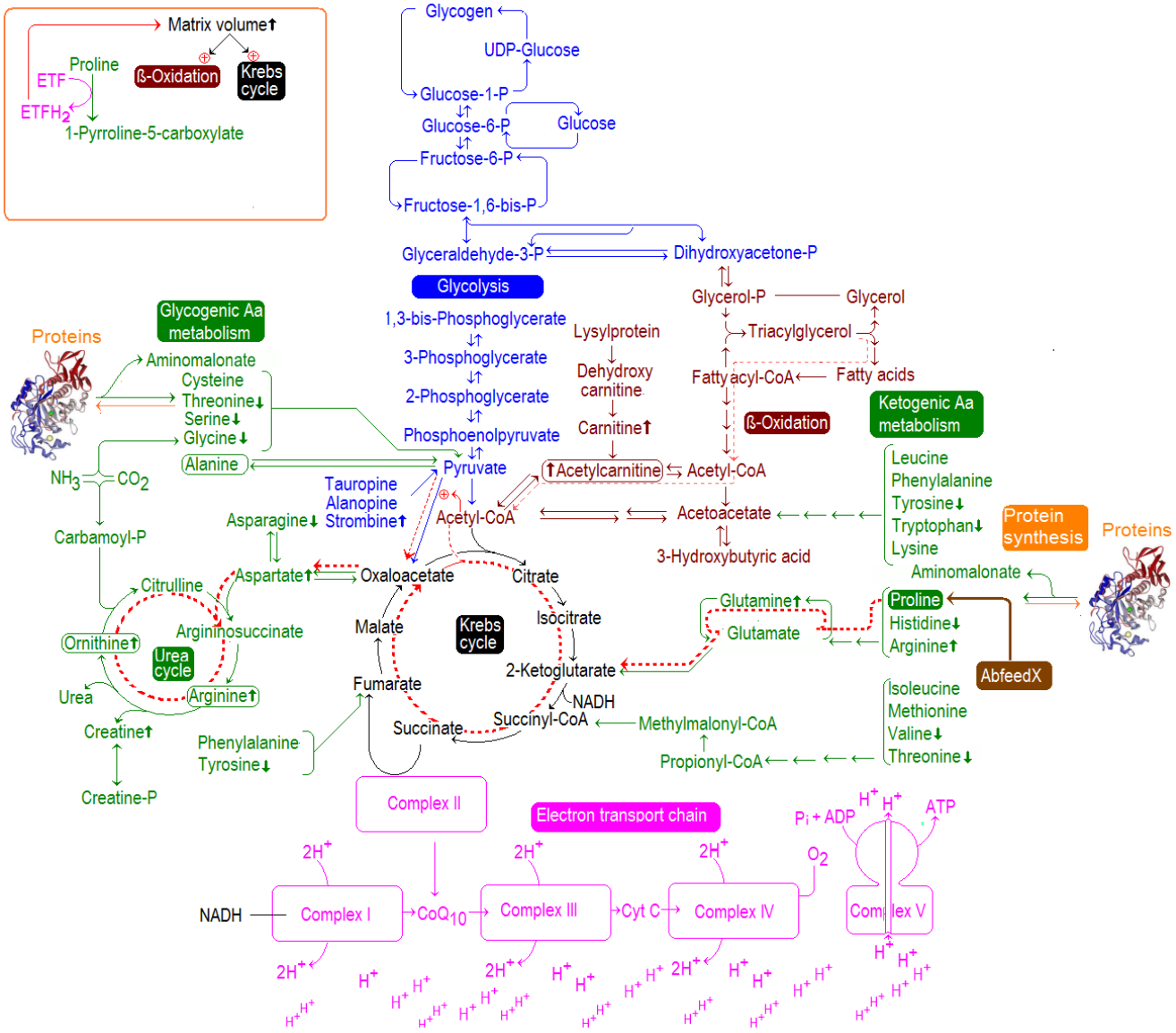

Figure 6.21: Metabolic profile of fast growing juvenile *H. midae* consuming Abfeed X. The metabolites affected throughout carbohydrate (blue), amino acid (green) and fatty acid (brown) metabolic pathways are indicated by an increase (↑) or decrease (↓) in metabolite abundance directly compared to slow growing juvenile abalone.

The metabolite profile of fast growing juvenile abalone consuming Abfeed X (Table 6.4, Fig. 6.21) affected amino acid, carbohydrate and fatty acid intermediates, displaying increases concerning: aspartate, creatine, arginine, strombine, ornithine, carnitine, N,N-dimethylglycine, glutamine and acetylcarnitine. Then again glycine, serine, tyrosine, histidine, taurine, tryptophan, threonine, valine and asparagine reflected decreases in metabolite concentration. Interestingly, this profile is almost the exact opposite of that seen in the fast growing abalone on the control diet, implying that Abfeed X closed the gap between the slow and fast growing abalone (albeit on metabolome level).

Abfeed X is enriched with proline, as mentioned before, ensuring that this group of abalone receive additional proline when compared to their Abfeed counterparts. In effect, both slow and fast growing juvenile abalone have proline supplied from a dietary source for metabolic use, driving energy production as seen in Fig. 6.21. Ultimately, no difference in proline was seen between fast and slow growing animals, but the catabolism of proline is suggested in the faster growing abalone group as indicated by the red dotted line. The increase in glutamine resulting from proline catabolism, an observation also previously made in *Staphylococcus aureus to* facilitate gluconeogenic reactions (Halsey *et al.*, 2017), ensures glutamate production to replenish α-ketoglutarate levels in the TCA cycle following deamination (Brosnan, 2000), in faster growing abalone. Glutamine is a highly abundant amino acid in cells (Salway, 2004) with important roles in peptide, protein, purine and pyrimidine synthesis, protein turnover regulation through mTOR signalling, involvement in proline metabolism and serving as a precursor for glutamate production (Wu, 2009). The use of glutamate as substrate to drive the ETC has been associated with marine gastropods for aerobic ATP production (Sheedy *et al.*, 2015), supporting the use thereof in abalone for ATP production. As part of regulatory functioning the TCA cycle allows oxaloacetate to be converted to aspartate (and *vice versa*) (Newsholme *et al.*, 2003). With additional proline catabolised, higher glutamine production is initiated ensuring glutamate production and conversion to the TCA cycle, subsequently resulting in increased aspartate production, as seen in Fig. 6.21. The decrease seen in asparagine further ensures increased aspartate formation as hydrolysis of asparagine yields aspartate (Garrett and Grisham, 2010).

The faster growing juvenile abalone utilise aspartate to produce arginosuccinate, and with that the production of arginine is stimulated, which cleaves to urea and ornithine, and also causes creatine production (Salway, 2004), of which increased metabolite concentrations were observed as summarised in Table 6.4. The catabolism of proline releases an amino group which supports the production of ammonia resulting in urea production and increased urea cycle intermediates. This is typically the image seen in abalone when subjected to hypoxic conditions (Morash and Alter, 2016). However, instead of phosphoarginine and phosphocreatine being broken down as an ATP source, it seems probable that the increased intermediates will be converted to these phosphate sources to fill stores.

Additional proline in the mitochondria supports ß-oxidation, resulting in increased concentrations of carnitine and acetylcarnitine in fast growing abalone. As minor increases were observed in carnitines, it can be speculated that juvenile abalone do not store large amounts of lipids. Muscle lipid concentrations measured in younger *H. midae* showed no significant temporal changes (Laas and Vosloo, 2010), supporting the hypothesis of the current investigation. Furthermore, acetylcarnitine enables acetyl-CoA production which also assists

with TCA functioning and ATP production via the ETC in abalone during standard farming conditions.

Numerous amino acids (asparagine, threonine, serine, glycine, tryptophan, histidine and valine) showed decreased concentrations, which supports the fact that sufficient ATP was present and the notion of protein synthesis for animal growth, despite some of the controversial findings. Glutamine is a great source of mTOR activation (Zhai *et al.*, 2015), supporting increased protein synthesis in faster growing animals. The metabolite profile created by fast growing juvenile abalone also suggests that carbohydrates are used for gluconeogenesis to produce glycogen, which is actively referred to as a major storage form of energy in abalone tissue (Laas and Vosloo, 2010). Gluconeogenesis is typically associated with an increase in oxaloacetate (as seen here) (Murray *et al.*, 2003). In the event of abalone experiencing stress, glycogen reserves will be broken down to serve as an energy source during anaerobic respiration (Baldwin *et al.*, 1992, O'omolo *et al.*, 2003). Amongst other things, the unaffected alanine concentrations in the faster growing animals and the decreases in threonine, serine and glycine (which can be utilised for pyruvate production) corresponds to the reduced use of glucose via glycolysis in Fig. 6.21.

6.3.3.3 Assessing metabolic differences when comparing slow and fast growing adult abalone consuming Abfeed X

The metabolic differences detected when comparing the adult muscle metabolite profiles of slow and fast growing abalone consuming Abfeed X are given in Table 6.5. Based on univariate analyses (Student's *t*-test and effects size evaluations), all of the selected features showed a $p < 0.05$ and $d > 0.8$, while having an indentification confidence Level of 1, 2 or 3. Of the 19 detected features, 18 could be assigned metabolite identities. Table 6.5 also indicates which of the respective metabolites displayed increased (↑) or decreased (↓) metabolite concentrations in the fast growing adult abalone group, relative to the slow growing adult group. The metabolite classes amino acid (AA), carbohydrate (CHO), fatty acid (FA), the analytical platform used for analysis and level of identification is also indicated in the table.

Table 6.5: Significantly altered metabolites in the fast growing adult abalone consuming Abfeed X. From most to least significant findings, the compounds detected are displayed by increasing (↑) or decreasing (↓) metabolite abundance relative to slow growing abalone in terms of amino acid (AA), fatty acid (FA) and carbohydrate (CHO) metabolite findings.

Compound	Direction fast growers	*p*-value <0.05	*d*-value >0.8	Metabolite class	Platform	ID level
Histidine	↑	6.54E-13	9.12	AA	LC-MS/MS	1
Ornithine	↓	2.58E-09	5.05	AA	LC-MS/MS	1
Acetylcarnitine (C2)	↑	1.08E-07	3.45	FA	LC-MS/MS	1
Tryptophan	↓	5.57E-07	2.82	AA	LC-MS/MS	1
Carnitine (C0)	↓	5.25E-06	2.89	FA	LC-MS/MS	1
Arginine	↓	9.75E-06	2.23	AA	LC-MS/MS	1
Glycine	↓	8.98E-05	1.87	AA	LC-MS/MS	1
Creatine	↓	1.21E-04	2.33	CHO	LC-MS/MS	1
Asparagine	↓	1.55E-04	2.30	AA	LC-MS/MS	1
N,N-dimethylglycine	↑	7.37E-04	1.70	AA	LC-MS/MS	1
Tauropine	↑	8.58E-04	1.61	CHO / AA	LC-MS/MS	1
Leucine	↑	9.06E-04	1.76	AA	LC-MS/MS	1
Alanopine	↓	2.54E-03	1.50	CHO / AA	LC-MS/MS	1
Tyrosine	↑	2.80E-03	1.55	AA	LC-MS/MS	1
Threonine	↓	4.85E-03	1.41	AA	LC-MS/MS	1
Proline	↑	5.18E-03	1.26	AA	LC-MS/MS	1
Alanine	↓	6.69E-03	1.19	AA	LC-MS/MS	1
Lysine	↑	1.85E-02	1.15	AA	LC-MS/MS	1
Analyte X	↓	1.25E-04	1.79	-	GC-TOF	-

Principle component analysis (Fig. 6.22) of the signifant features between slow and fast growing adult abalone consuming Abfeed X showed grouping of the fast and slow growing abalone groups. The total amount of variance explained by the first two PCs was 84.4 % of which PC 1 accounted for 68.2 % and PC 2 accounted for 16.2 %. For adult abalone, the slow growing abalone group showed more with-in group variance than the fast growing group, showing the exact opposite than the PCA done on juvenile abalone. Fig. 6.22 shows no furher visible outliers or subgroupings.

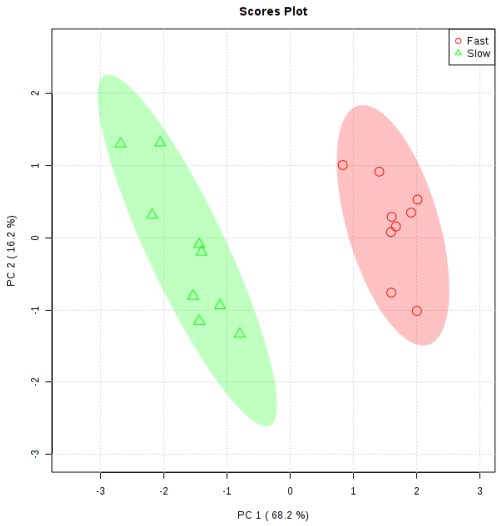

Figure 6.22: Principal component analysis of slow and fast growing adult abalone consuming Abfeed X. Plots of PC 1 versus PC 2 of significant metabolites concerning growth detected in adult abalone.

The metabolic differences found between the slow and fast growing adult abalone (Table 6.5) were also interpreted with the effect of the diet in mind (Fig. 6.23), using the top metabolite of Table 6.4, histidine and proline (additional metabolites displayed in Appendix B). Again the adult abalone showed higher concentrations of proline in the Abfeed X group, with proline being more elevated in the fast growing group. Abfeed X proved to have no influence on the faster growing abalone, but resulted in lower concentrations of histidine in the slow growing group. This result supports the idea of increased protein synthesis in the faster growing individuals which will be elaborated on when discussing Fig. 6.24.

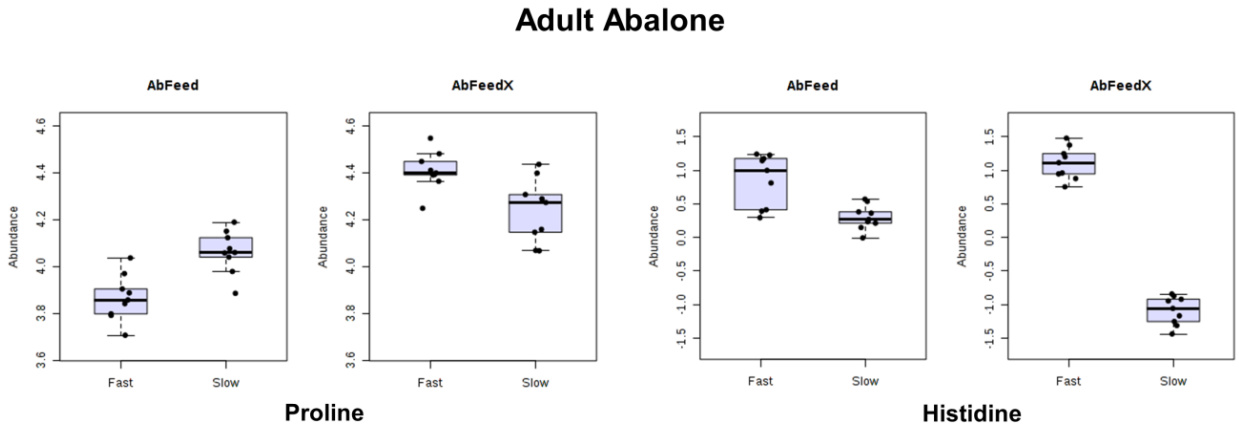

Figure 6.23: Boxplots of proline and histidine detected in adult abalone. Relative metabolite abundance of proline and histidine as detected in fast and slow growing adult abalone consuming Abfeed and Abfeed X diets respectively.

Altered metabolite concentrations of fast growing adult abalone found in Table 6.5 were used to formulate a metabolic map (Fig. 6.24) displaying these differences in terms of increase (↑) or decrease (↓) metabolites when compared to slow growing adult abalone. Again, predominantly amino acid metabolism was affected in fast growing abalone, with fatty acid and carbohydrate metabolism also being influenced.

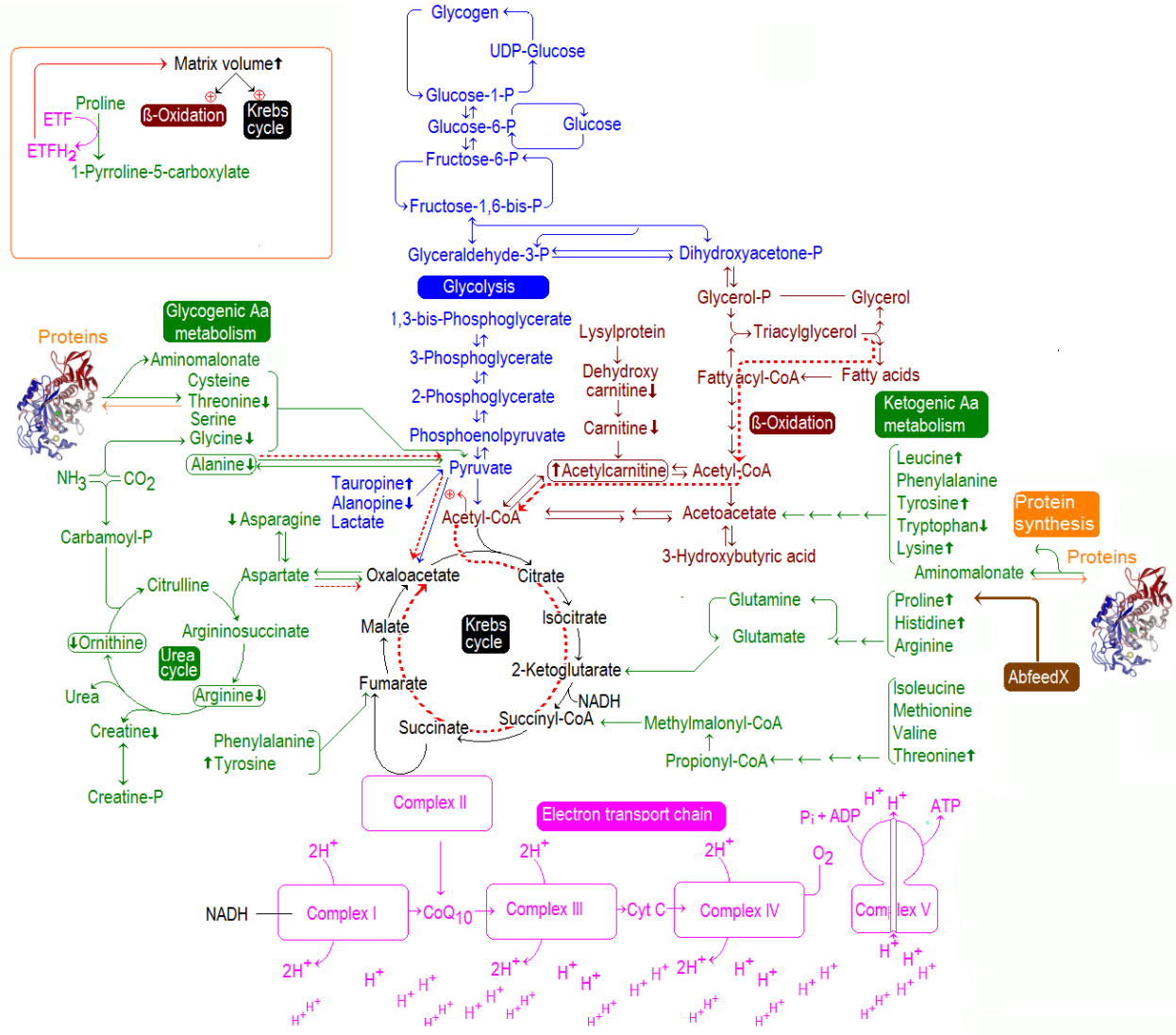

Figure 6.24: Metabolic profile of fast growing adult *H. midae* consuming Abfeed X. The comparative concentrations of those metabolites significantly different in the carbohydrate (blue), amino acid (green) and fatty acid (brown) metabolic pathways of the fast growing adult abalone, are indicated by an increase (↑) or decrease (↓) in comparison to that slow growing adult abalone group.

Analysis of adult abalone revealed that the metabolite profile (Table 6.5, Fig. 6.24) of faster growing animals consuming Abfeed X, had higher concentrations of histidine, acetylcarnitine, N,N-dimethylglycine, tauropine, leucine, tyrosine, proline and lysine, accompanied by reduced concentrations of ornithine, tryptophan, carnitine, arginine, glycine, creatine, asparagine, alanopine, threonine and alanine. This profile corresponds to that seen in the fast growing animals on Abfeed, except for acetylcarnitine, tauropine, tyrosine, proline, tryptophan and threonine. Furthermore, this profile is also opposite to that seen during hypoxia, indicating the domination of anabolic pathways when proline is added to the standard Abfeed diet.

The metabolism of fast growing adult abalone on the Abfeed X diet, is speculated to be dominated by ß-oxidation (fatty acid catabolism), considering the elevated concentrations of

acetylcarnitine produced from acetyl-CoA, comparatively. Based on a dietary lipid investigation conducted on *H. iris,* it was concluded that lipids do not significantly affect the growth of this abalone species (Tung and Alfaro, 2012). The metabolic profile of faster growing *H. midae* also supports this, as lipids were shown to be used to sustain energy production, allowing amino acids to be used for growth. The activation of fatty acid catabolism in this study is potentially made possible by the working of proline, which stimulates mitochondrial activity. Although no literature supporting this in abalone could be found, evidence for this has previously been reported in other species. Bumblebees, for example, can oxidise proline to benefit their respiratory capacity (Teulier *et al.*, 2016). Research done on plants show that during stress, proline and lipid metabolism share dual roles (Shinde *et al.*, 2016), suggesting that proline has the ability to upregulate ß-oxidation, subsequently resulting in elevated acetylcarnitine and a reduction in alanine, as seen from this metabolomics experiment (Fig. 6.24). Furthermore, adult abalone have the capacity to accumulate lipid stores, suggesting an increased dependence on ß-oxidation for energy production in adult *H. midae* (Laas and Vosloo, 2010). Since the slow and fast growing animals were of the same age, one can assume that the tissue lipid concentrations were very similar. Although both groups consumed a proline-enriched diet, an increase in proline was detected in the faster growing group suggesting that proline had an insignificant effect on the mitochondria of the slower growing animals, hinting to impaired mitochondrial activity in this group, comparatively.

The reduced urea cycle intermediates, ornithine, arginine and the by-product creatine, supports the notion of comparatively less amino acid (proline specifically) catabolism, and elevated protein synthesis in the faster growing abalone group. This is further supported in Table 6.5, by the elevated concentrations of the amino acids leucine, tyrosine, lysine and histidine. Amino acid synthesis is dependent on substrate availability, the developmental stage of the organism, environmental factors, species etc. (Wu *et al.*, 2014), making it impossible at this stage to speculate which amino acids are used for protein synthesis.

Again, as was the case for the juvenile animals on Abfeed X, minimal glucose sources were being catabolised, making gluconeogenesis the preferred pathway in faster growing abalone. Gluconeogenesis produces glucose from non-carbohydrate precursors (Murray *et al.*, 2003), like glycerol, which is the main regulatory metabolite of this process in faster growing animals, and subsequently, more amino acid availability for muscle anabolism.

6.3.3.4 Hypothesised mechanism by which proline stimulates faster growth in abalone

With the juvenile abalone almost giving the opposite metabolic profile of the adults on Abfeed X, it suggests that although both juvenile and adult groups (Figs. 6.21 and 6.24) use proline for energy production, it occurs via two very different mechanisms. The results propose that juvenile abalone catabolise proline directly for energy, while in adult abalone, proline stimulates fatty acid breakdown for energy production requirements, which makes sense considering that only adults have enough fatty acid stores accumulated over time to allow for this. The different hypothetical roles of proline in the two abalone groups are supported by literature on proline metabolism, as shown in Fig. 6.25. Two lines of proline activity will be discussed with the first focusing on the contrition of proline in the regulation of ß-oxidation and, the second will briefly highlight the action of proline during hypoxia.

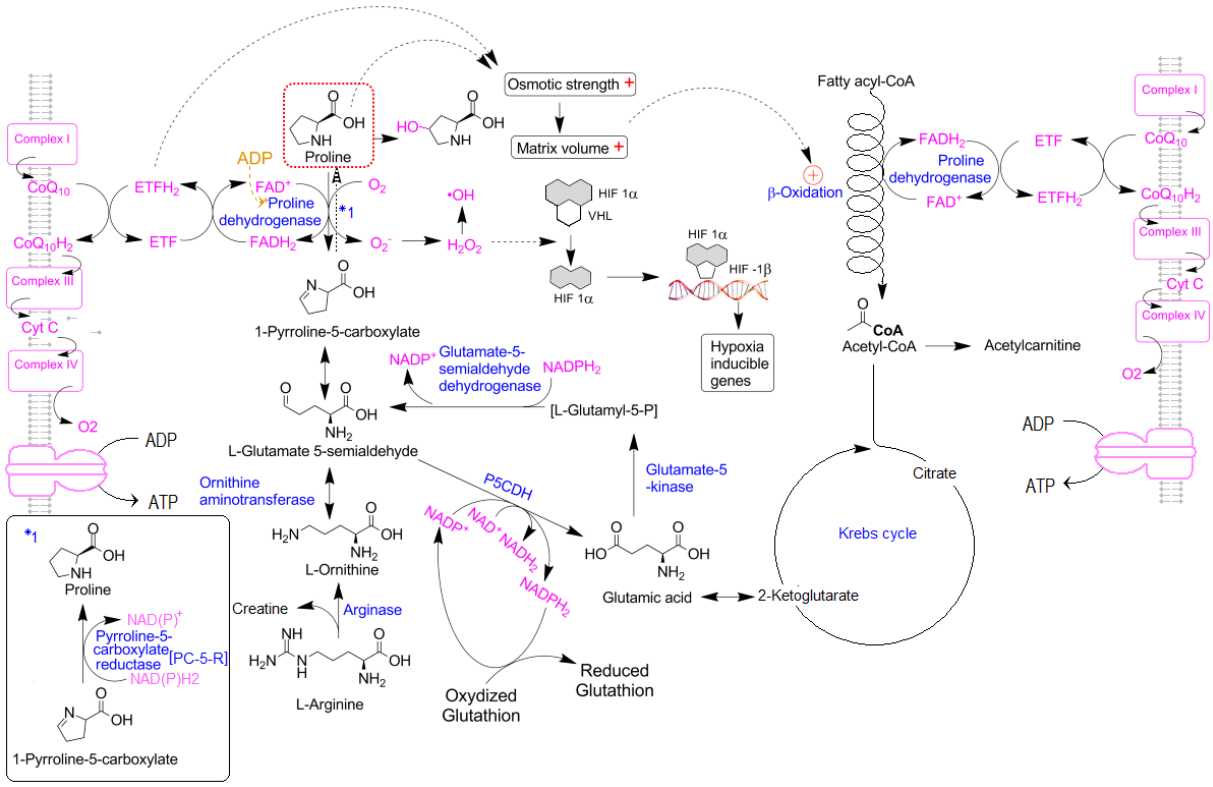

Figure 6.25: Mechanistic insights into proline metabolism. Proline enhances mitochondrial activity by stimulating cellular osmotic stress which supports increased fatty acid catabolism resulting in energy production and proline activates hypoxia inducible genes which play a protective role during hypoxia.

When proline is oxidised to pyrroline-5-carboxylate (P5C), proline dehydrogenase transfers reducing equivalents to the ETC (Krishnan *et al.*, 2008). Together with the subsequent activation of electron transfer flavoprotein (ETF), P5C has been found to be beneficial to the maintenance of osmotic stress and redox balance (Pérez-Arellano *et al.*, 2010). While the conversion of proline to P5C supplies electrons to the ETC (Teulier *et al.*, 2016), the reactions of ETF (together with increased proline) appear to have an effect on cell volume, affecting the

osmotic strength of cells, accompanied by an increase in cytoplasmic calcium (Ca^{2+}) (Halestrap, 1987). From Fig. 6.25, it seems viable that the comparatively faster growing abalone utilised the abundant proline to elevate osmotic capacity, and subsequently increase the cell matrix volume, as the mitochondrial oxidation of proline has been found to enhance osmotic swelling (Ballantyne and Moyes, 1987). With an increased matrix volume, increased rates of ß-oxidation would be expected, as was previously shown to occur in liver cells stimulated by Ca^{2+} (Halestrap, 1987), this in turn would explain the elevated ß-oxidation/fatty acid catabolism and the resulting elevated acetyl-CoA production, TCA cycle intermediates, and energy production.

It is well known that proline accumulation in plants occurs in response to osmotic stress, temperature variations, nutritional deficits, bacterial pathogens and heavy metals (Pérez-Arellano *et al.*, 2010), an additional important function of proline, is the protection of cells against hydrogen peroxide (H_2O_2) induced stress (Krishnan *et al.*, 2008). As a result of H_2O_2 production hypoxia-inducible factors (HIF) can also be activated in response to hypoxia, making HIF a master regulator of oxygen homeostasis (Bell and Chandel, 2007). Thus the action of proline to activate HIF may be beneficial to abalone encountering hypoxic stress, following deeper investigation thereof.

Considering the above in the context of the results, proline is a key regulator of biochemical and physiological processes in cells, acting as a signalling molecule, a source of P5C and free radical production, and a cellular energy status sensor (Wu *et al.*, 2011). Furthermore, the slow growing abalone seem to have a comparatively impaired mitochondrial function, which dietary proline is not able to resolve. The general belief that abalone use carbohydrates more efficiently than lipids as an energy source (Ju *et al.*, 2016) requires further assessment, since supplementation of the abalone diet with proline in this study, suggests that abalone use what is metabolically available or dominantly present for energy production. Environmental conditions like water temperatures and oxygen levels are frequently influenced on abalone farms making this a highly likely culprit of unsatisfactory abalone growth (Alter *et al.*, 2017). Keeping this in mind, the administration of proline might be crucial to ensure that especially juvenile abalone survive episodes of environmental stressors, as older *H. midae* have been reported to handle stress better (Laas and Vosloo, 2010).

6.4 Conclusion

This investigation proves that metabolomics can be used to detect metabolic differences occurring between slow and fast growing abalone. The evaluation of faster abalone growth in relation to Abfeed (Table 6.2 and Fig. 6.11), revealed that these individuals use glycolysis as

their primary energy-producing mechanism, with a subsequent reduction in their urea cycle intermediates, reduced levels of aminomalonate and reduced fatty acids, which support the notion that insulin is driving protein synthesis in these animals. Direct comparisons between Abfeed and Abfeed X revealed no clear metabolic variation, however, it did confirm elevated proline uptake in abalone consuming Abfeed X (Table 6.3). Abfeed X also induced age-specific variation, which was not seen in the animals on the control diet. The metabolic differences between slow and fast growing juvenile abalone on Abfeed X (Table 6.4 and Fig. 6.21), suggests that the faster growing abalone group catabolise proline for energy production, via the TCA cycle (via α-ketoglutarate) resulting in sufficient electron supply to the ETC and subsequently, increased aspartate and urea cycle intermediates. In addition, the observed reduction in the concentrations of most other amino acids in the comparatively faster growing group, suggests elevated protein synthesis. The metabolite profile of faster growing adult abalone on Abfeed X (Table 6.5 and Fig. 6.24), suggests that proline allows for better use of ß-oxidation of stored fatty acids as the main energy source, confirmed by the resulting reduction in urea cycle intermediates and comparatively more amino acids for protein synthesis in the faster growing abalone.

These findings and the hypotheses can at this point be confirmed, using a more targeted analytical method such as multiple reaction monitoring of affected metabolites. In addition, the use of stable isotope labelling would be beneficial in the understanding of metabolic flux in known and unknown pathways (Creek, 2013). If, for example, fatty acids, glucose and proline were labelled with an isotope, it would allow for additional insights into the breakdown of these metabolites, subsequently providing information as to exactly how these substrates are used within the metabolic network, and confirmation of which metabolic pathways are stimulated during their breakdown. It is perhaps equally important to investigate the involvement of the mitochondrion in the different growth rates, as energy production and insulin functioning are directly associated with this organelle.

South African abalone have the premium position as a luxury product delicacy, which needs to be maintained. Consequently, abalone farms are constantly required to diversify their products, and ensure that abalone flavour, texture and size satisfies the market (Britz and Venter, 2016). The driving force to produce first-class abalone to an international market warrants the research done. In the words of Mau and Jha (2017): “The current supply of farmed abalone outweighs wild harvested abalone, which is remarkable considering there is still so much research that can be carried out to improve aquaculture production.”

CHAPTER 7

CONCLUSIONS AND FUTURE PROSPECTS

”Beauty in things exists in the mind which contemplates them.”

– David Hume, Essays on Tragedy

7.1 Introduction

In South Africa, the locally produced abalone, *Haliotis midae*, is an economically important aquaculture species, favoured internationally for its large size and organoleptic properties (Difford *et al.*, 2017). However, before animal exportation becomes a reality, a number of farming obstacles are encountered, of which slow and irregular growth rates are said to be the largest. Research initiatives ranging from improved diet formulations, probiotic additives, system designs and water quality, to genetic improvement (Macey and Coyne, 2005, Troell *et al.*, 2006, Vlok *et al.*, 2016), have been implemented to improve animal growth. Up to now, research focusing on abalone metabolism and metabolic pathways related to growth, has been lacking, creating a prime opportunity for this study (Chapter 2). Metabolomics allows for non-biased identification and quantification of metabolites in a biological system (Brown *et al.*, 2005) and was applied in this study with a view to contribute to the prediction, monitoring and improvement of abalone growth. A number of different techniques based on this approach (Chapter 4) were successfully applied to assess abalone encountering hypoxic stress (Chapter 5). Similarly, this approach was highly suitable to assess farm animals consuming standard and modified artificial abalone feed (Chapter 6).

This study was a collaborative effort merging two distinct research fields, which in the end provided new dimensions of appreciation and understanding of both abalone aquaculture and metabolomics. As a first time investigation, this study **aimed to utilise metabolomics as a research tool to clarify functional metabolic differences and responses related to *Haliotis midae* growth**, based on predefined “real-life” farming encounters. As the fields of abalone and metabolomics are immense, no single study can be comprehensive in both aspects, and this thesis makes no such claim. However, the selective coverage of important and relevant questions resulted in a compelling overview of original contributions. Presented as conclusion, is a scientific summary of the main findings of the chapters of this thesis, along with their relevance to the original objectives and limitations encountered in this study. Preceding the recommendations aimed at future work, concluding observations will be clarified. Furthermore, the practical implications for metabolomics on abalone are added to this concluding chapter to serve as valuable guidance for interested parties of the aquaculture sector.

7.2 General discussion of objectives and accomplishments

Studies of this nature have not been conducted previously for South African abalone and as such, have increased our knowledge of the metabolism of *Haliotis midae.* In view of the aim, the subsequent **objectives** were put forward in this study.

7.2.1 A literature-based investigation of current knowledge of abalone metabolism.

Despite the vast body of literature available on abalone, aspects associated with the functioning of their metabolism are poorly recognised. The literature overview given in Chapter 2 was constructed to summarise metabolites detected in abalone as a means to determine functioning of metabolic processes in terms of abalone growth. With special focus given to abalone diets and the ingredients used to formulate it, it was possible to assign main metabolite classes to feeding components and speculate on how it would be metabolised. Using the typical mammalian metabolic design and single end-point findings previously made in abalone, it was possible to pinpoint factors relating to the uptake and breakdown of protein, carbohydrate and lipid metabolic compounds. Overall, the catabolic reactions used for the production of energy were apparent, but the anabolic reactions utilising energy were obscure. Using the available scientific literature and observations made in invertebrates in general, a basic metabolic plan for abalone was produced. This in effect, highlighted the need for metabolic research in abalone to confirm pathways that were predicted from literature. This investigation also confirms the need of metabolomics as a research tool to assist with identification and confirmation of general abalone metabolic systems, e.g. confirmation of the TCA cycle intermediates. From this accumulated knowledge, it becomes evident that similarities exist in major metabolic pathways, but invertebrates like abalone possess unique metabolic processes, which required special focus for concrete deductions in this study.

7.2.2 The standardisation of both targeted and untargeted metabolomic methodologies for screening of the abalone metabolome.

A comprehensive metabolomics approach utilising NMR, LC-MS and GC-MS platforms has not been previously performed on abalone, which in effect limits discoveries of certain metabolite classes and compounds, hampering a global view of abalone metabolism. Here a multiplatform metabolomics approach was used to extend coverage of the abalone metabolome. As presented in Chapter 4 all of the steps required for sample preparation and analyses were standardised to ensure compatibility of various abalone tissues with multiple analytical platforms. Furthermore, these standardised methods are now implemented within the framework of The National Metabolomics Platform of The Centre for Human Metabolomics (hosted by the NWU). This is the first study to report the use of untargeted LC-MS and GC-MS techniques for investigating abalone. The untargeted use of GC-MS enabled the detection of predominantly energy metabolism compounds, while targeted and untargeted LC-MS analyses allowed for the monitoring of acylcarnitines, amino acids and opines.

To date, the use of mass spectrometry has not been linked to opine detection in abalone. As a result of distinct metabolite identification efforts, the methodology utilised in this study makes mass spectrometric detection of opines a reality. Traditional identification and quantification thereof relies on laborious enzyme linked reactions using enzymes purified from abalone itself. Now the untargeted detection, identification and quantification of abalone opine products completed the metabolomics research cycle, where these metabolites are incorporated into a targeted LC-MS/MS method. This was a crucial achievement of this study, which ultimately enabled the connection of opines to the metabolite profile of abalone, creating a more comprehensive result. The practical significance of this enables quantitative monitoring of opines in any abalone tissue to monitor the anaerobic responses of abalone in reaction to stressors and general farming practices.

The use of epipodial tissue and haemolymph samples as non-destructive sampling methods have been previously executed on abalone without critical damage to the animal. With that being said, the current study included the use of epipodial tissue and haemolymph samples as a demonstration that metabolomics analysis can be performed on these samples. In effect, these samples added great value to the abalone metabolic plan. Haemolymph for one resulted as a clear shuttle system between tissues (organs) transporting metabolites to regulatory sites. Then again, the epipodial tissue showed a similar response to other tissues creating an important opportunity as a non-destructive sampling initiative for health screening and for repeated sampling to monitor individuals.

The results achieved with the methods described in Chapter 4 were successfully applied to the investigations of Chapters 5 and 6, as described below.

7.2.3 Investigating the metabolic response of abalone following functional and environmental hypoxia.

As a first step to investigate the metabolic response to hypoxic stress, hypoxia had to be induced. This was successfully completed in accordance with institutional ethical guidelines, following the procedures set out by O'omolo *et al.* (2003). From an ethical viewpoint, multiple tissues were dissected as the animals would be sacrificed for research regardless, resulting in the collection of six abalone tissues, each with its own research potential. This is the first study reporting the metabolic response of *H. midae* epipodial tissue in response to hypoxia. In addition hypoxic stress of *H. midae* has not been previously investigated with metabolomics.

Abalone adductor muscle tissue proved to yield the most metabolites from this hypoxic study. However, analyses of the foot muscle, left gill, right gill, epipodial tissue and haemolymph also resulted in unique findings, contributing to the overall metabolic view depicted in Chapter 5. This study further showed that *H. midae* is metabolically similar to other abalone species with the adductor and foot muscles highly dependent on anaerobic metabolism for energy production and the left gill only operational during extreme episodes of oxygen need.

In compliance with previous studies done on abalone subjected to functional and environmental hypoxia, increases in D-lactate, tauropine, arginine and succinate were detected in multiple abalone tissues. However the results generated from Chapter 5 are the first attempt at a global view of abalone metabolic changes due to hypoxia. This enabled the construction of a metabolic map, uniquely designed for abalone metabolism, highlighting the response displayed by *H. midae* after subjection to functional and environmental hypoxia. All of the main metabolic pathways e.g. glycolysis, TCA cycle, urea cycle and ß-oxidation (together with the complete list of affected metabolic pathways found in Chapter 5) were confirmed to be operational in abalone during episodes of oxygen deprivation. Uniquely, the results reflected the presence of multiple opines on a metabolic map and a number of important dipeptide compounds.

Although insights into the response to hypoxia does not support an understanding of metabolic pathways responsible for growth, it directly reflects the opposite thereof, emphasising how the abalone metabolism ensures energy production for survival which should ideally have been focused towards anabolic systems, with growth in mind. Thus Chapter 5 serves as a negative control of growth. In contrast, Chapter 6 proposes metabolic reactions in the absence of stress, creating a positive control reflecting growth.

7.2.4 Investigating the metabolic differences found between slow and fast growing abalone housed in standard farming conditions and those of animals consuming modified artificial abalone feed.

A successful growth trial was conducted for a period of 8 months, consistent with daily abalone farming procedures as implemented by HIK abalone farm (Chapter 6). Based on the experimental design of this study, it was possible to elucidate the influence of sampling time, abalone age and abalone feed on the metabolome of *H. midae*.

From this growth trial it was further possible to successfully distinguish between slow and fast growing abalone on a metabolic level, something not previously done on *H. midae.* Within this classification it was possible to link the faster growth rate observed in abalone consuming standard abalone feed with the action of insulin which stimulates protein synthesis. This

metabolomics observation provides functional support using other omics techniques where increased growth in abalone was previously connected to insulin. The enrichment of standard abalone feed with the amino acid proline (producing Abfeed X) made it possible to assess the mechanisms utilised by proline catabolism to stimulate mitochondrial activity, something that is well-known in plants, but has not been depicted in abalone as yet. Abfeed X shows the potential to protect abalone from stressful conditions like hypoxia. The metabolic profile of faster growing abalone consuming Abfeed X also favoured protein synthesis although proline was not the driver of this process.

This study leads to the question of whether slower growing abalone may have impaired mitochondrial function. Carbohydrate, lipid and protein metabolic pathways were found to be affected in slower growers, but no clear obstructions that are generally associated with inborn errors of metabolism were observed, leaving the ETC as the next possible site for malfunction. However this is speculative and requires additional confirmation.

As untargeted metabolomics research can be classified as hypothesis-generating, this study generated new possibilities for why some abalone grow faster, which now require additional verification.

7.3 Critical assessments of this study

Although the objectives of this study were achieved in full, the study is not without its limitations. The latter were taken into consideration during data interpretation and can be summarised as follows:

- Metabolite identification was addressed in accordance with the identification confidence levels proposed by Schymanski *et al.* (2014), but still required matching to several in-house, commercial and public libraries/databases. As a result of the limited experimental fragmentation spectra (used for spectral matching) available in databases, the majority of the features detected by UPLC-IM-QTOF analyses could not be used for biological interpretation due to insignificant metabolite identification. The data generated by LC-QTOF analyses also resulted in spectral data which were difficult to identify. Fortunately, since the samples analysed here were butylated, it was easier to match the features to theoretical chemical formulae of butylated metabolites listed in an in-house butyl ester library.
- A shortcoming from these experiments was the number of animals (n = 6) exposed to hypoxia. Even though the abalone had a uniform genetic background resulting in a rather

homogeneous cohort, additional sample numbers may have resulted in greater statistical power, as variation was apparent when assessing grouping differences of some metabolites. Then again the number of replicates used here falls into the proposed sampling measures of the Metabolomics Standards Initiative.

- A number of assumptions were made while constructing abalone metabolic charts which need confirmation through flux analysis of labelled compounds. For example the metabolite association between arginine and phosphoarginine was speculated in this study, based on literature that phoshoarginine is the main phosphagen in abalone, even though this metabolite was not specifically detected.
- The limited number of markers detected that can be used to distinguish between slow and fast growing abalone complicated interpretation, resulting in hypothesised metabolism associated with faster growing individuals. If more central carbon metabolites are monitored, a better understanding of the mechanisms present in faster growing abalone will be possible.
- The classification of fast and slow growing abalone in the current investigation was only based on weight and length measurements making it subjective. By using cut-off values or more specific measures of growth rates, the classification of fast and slow individuals would be more precise.

7.4 Concluding observations

Multiple metabolomic approaches were implemented to study the functional metabolic changes associated with *H. midae* growth, in effect, the catabolic and anabolic metabolic reactions regulating *H. midae* growth metabolism were investigated. From the catabolic reactions implemented by *H. midae,* it becomes clear that abalone catabolise proteins for additional energy production when subjected to hypoxia, resulting in increased urea cycle intermediates and anaerobic end-products. From the anabolic reactions implemented by *H. midae* it can be concluded that abalone consuming standard abalone feed use carbohydrate-based metabolism to support acetyl-CoA production via glycolysis, and *H. midae* consuming proline-enriched abalone feed use ß-oxidation as the main generator of acetyl-CoA. In both cases, acetyl-CoA is then metabolised in the TCA cycle, resulting in ATP production via the ETC. With adequate energy being produced, abalone in standard farming conditions channel amino acid subunits and excess energy towards protein synthesis resulting in muscle growth, the ultimate aim of the farming endeavour.

The ideal metabolic profile of farmed abalone will firstly need to maintain an adequate level of energy turnover, preferably fuelled by carbohydrate sources, where glycolysis will produce

acetyl-CoA for the TCA cycle, resulting in ATP production from the ETC. Secondly, these farmed abalone need to store lipid reserves, which can assist with additional ATP production. Thirdly, farmed abalone require adequate amino acid sources to support protein synthesis. Anaerobic end-products need to be absent in this ideal profile of farmed abalone and urea cycle intermediates should be reduced, emphasising that amino acid catabolism is suppressed in favour of protein synthesis.

From this study it can be concluded that untargeted metabolomics can be applied to investigate functional metabolic changes of *H. midae*, introducing directions where targeted analyses should be implemented to confirm proposed metabolic responses relating to faster abalone growth.

7.5 Future recommendations

Based on the work presented in this thesis, the following recommendations can be viewed as new research initiatives toward future developments regarding the use of metabolomics to investigate abalone metabolism.

- The biological replicates used as part of a metabolomics experiment should be determined by power analyses to ensure that sufficient statistical analyses can be conducted on the data collected. With the data available from this study (and the biological variation determined), it is now possible to perform such analyses for related studies.
- Having gained some insights into abalone metabolism it is strongly recommended to substitute the crude sample extraction methods used with more precise sample clean-up/extraction methods (e.g. liquid-liquid extractions), which will be beneficial for instrument sensitivity and metabolite identification.
- The assessment of metabolites correlating to faster growing abalone should be investigated in other abalone tissues e.g. haemolymph or epipodial tissue to firstly evaluate if results similar to the muscle findings are achieved and secondly to get a non-destructive sampling method in place for routine analyses focused at growth monitoring.
- Growth differences should be established at an earlier and later sampling time to allow assessment of the current findings and to determine from what time point changes are expressed at metabolic level.
- Long term hypoxic exposures would allow for assessment of abalone during and after recovery periods to confirm when metabolites return to normal metabolic values after subjection to functional and environmental hypoxia.

- The profile created by an alternative hypoxia inducing factor like the presence of algal blooms might have been of more value from an abalone farming perspective as this is an occurrence which is becoming more common on SA abalone farms (Mouton, 2017). Dinoflagellates cause disruption of the integrity of the gill, which in effect hampers abalone oxygen uptake, creating a hypoxic state which warrants investigation.
- The literature-based protective mechanisms of proline should be investigated in abalone consuming a proline enriched abalone feed during stressed conditions.
- Regardless of the results achieved a number of metabolic pathways are still assumed to be operational due to the presence of a few selected metabolites. This requires confirmation, and may be achieved by using, for example, Agilent's metabolomics dynamic MRM database and method. This would allow for routine targeted analysis of more than 215 central carbon pathway metabolites enabling the detection of amino acids, TCA cycle intermediates, carboxylic acids, nucleobases, nucleosides, phosphor-sugars and fatty acids (Sartain, 2016).
- Future research should in particular focus on establishing metabolite concentration reference ranges of abalone in standard farming conditions, where-after these findings can be used to determine if specific metabolic levels are abnormally high or low in response to stress for example.
- Insight into the number of mitochondria per abalone cell is something which also warrants additional research. Typically a Seahorse XFe analyser can be used to do bioenergetic flux (mitochondrial respiration and glycolysis) analysis, however this requires either freshly isolated mitochondria from tissues or primary cultures (myoblasts).

7.6 Abalone aquaculture take home message

The field of metabolomics, which enables the comprehensive and systematic identification and quantification of small molecules within a biological sample at a given point in time (Bujak *et al.*, 2015), is one with limited introduction in the abalone aquaculture sector. Despite the potential of metabolomics for abalone farming, there is a need to get parties within the South African abalone industry interested, before the outcome of metabolomics can be implemented on abalone farms. As soon as the power of metabolomics as a research tool to satisfy farming needs is realised, it will be possible to implement routine samplings, which can be analysed to evaluate the condition of farmed abalone, or any other question at hand. Following the use of metabolomics to investigate abalone in this study, it can be reported that abalone tissues, including: muscle, haemolymph, gills and epipodial tissue (tested here), mucus, urine, shell, larvae, eggs, digestive organs and digestive gland (evident from literature) can successfully be analysed by metabolomic techniques, creating numerous possibilities.

The most important question that needs answering when deciding to do metabolomics analysis is whether you know what you are looking for. If the answer is “yes”, targeted analysis is the way to go, using LC-MS or GC-MS technologies. In brief, if the answer is “no”, then untargeted metabolomics incorporating NMR, GC-MS or LC-MS techniques will be the starting point. Sample preparation is required to extract metabolites from the surrounding medium, which may include tissue homogenisation or protein precipitation procedures. When using NMR spectroscopy, sensitivity is a problem which would require one to use large sample volumes. Prior to NMR analysis, a buffer solution is added to the sample to adjust the sample pH. The use of GC-MS techniques generally necessitates the sample to be volatile, thus derivatisation should be implemented. Prior to using LC-MS techniques, a number of analytical variables like the column, the mobile phase, ionisation mode etc. need to be assessed.

Metabolomics is a specialised science, which would necessitate the abalone industry to collaborate with an academic or research institution. This will ensure sufficient infrastructure, experienced laboratory personnel and specialists accustomed to the operating procedures of the analytical platforms, and biostatisticians accustomed to the handling of metabolomics data. However, this will only be a starting point; where-after a metabolomics-based service to the industry may include weekly routine analysis on high-end analytical platforms. Alternatively, the findings of a respective question may result in a small list of markers, which can be transferred and refined to point of use tests that can be implemented on farms following validation. Such tests can include lateral flow devices (e.g. pregnancy tests) or dipstick approaches (e.g. urinary tract infection detection) (Trivedi *et al.*, 2017).

Currently, metabolomics is largely used as a research laboratory-based tool, which needs to move out to the industry. However, prior to the move out of academia it is important to translate the potential of metabolomics into everyday farming questions to find practical solutions, which warrants the use thereof in the abalone aquaculture sector.

CHAPTER 8

REFERENCES

”Science is built up with facts as a house is with stones. But a collection of facts is no more a science than a heap of stones is a house.”

– Jules Henri Poincare

ADORNO, M. A. T., HIRASAWA, J. S. & VARESCHE, M. B. A. 2014. Development and validation of two methods to quantify volatile acids (C2-C6) by GC/FID: Headspace (automatic and manual) and liquid-liquid extraction (LLE). *American Journal of Analytical Chemistry,* 5, 406.

ALFARO, A. C. & YOUNG, T. 2016. Showcasing metabolomic applications in aquaculture: A review. *Reviews in Aquaculture,* doi:10.1111/raq.12152.

ALLEN, W. V. & KILGORE, J. 1975. The essential amino acid requirements of the red abalone, *Haliotis rufescens*. *Comparative Biochemistry and Physiology Part A: Physiology,* 50, 771-775.

ALONSO, A., MARSAL, S. & JULIÀ, A. 2015. Analytical methods in untargeted metabolomics: State of the art in 2015. *Frontiers in Bioengineering and Biotechnology,* 3, 1-20.

ALTER, K., ANDREWARTHA, S. J., MORASH, A. J., CLARK, T. D., HELLICAR, A. D., LEÓN, R. I. & ELLIOTT, N. G. 2017. Hybrid abalone are more robust to multi-stressor environments than pure parental species. *Aquaculture,* 478, 25-34.

ÁLVAREZ-SÁNCHEZ, B., PRIEGO-CAPOTE, F. & DE CASTRO, M. L. 2010a. Metabolomics analysis I. Selection of biological samples and practical aspects preceding sample preparation. *Trends in Analytical Chemistry,* 29, 111-119.

ÁLVAREZ-SÁNCHEZ, B., PRIEGO-CAPOTE, F. & DE CASTRO, M. L. 2010b. Metabolomics analysis II. Preparation of biological samples prior to detection. *Trends in Analytical Chemistry,* 29, 120-127.

ANGELL, A. R., PIROZZI, I., DE NYS, R. & PAUL, N. A. 2012. Feeding preferences and the nutritional value of tropical algae for the abalone *Haliotis asinina*. *PloS One,* 7, e38857.

ARAPITSAS, P., SCHOLZ, M., VRHOVSEK, U., DI BLASI, S., BARTOLINI, A. B., MASUERO, D., PERENZONI, D., RIGO, A. & MATTIVI, F. 2012. A metabolomic approach to the study of wine micro-oxygenation. *PLoS One,* 7, e37783.

BACCHIOCCHI, S. & PRINCIPATO, G. 2000. Mitochondrial contribution to metabolic changes in the digestive gland of *Mytilus galloprovincialis* during anaerobiosis. *Journal of Experimental Zoology Part A: Ecological Genetics and Physiology,* 286, 107-113.

BADENHORST, C. P. S., ERASMUS, E., VAN DER SLUIS, R., NORTJE, C. & VAN DIJK, A. A. 2014. A new perspective on the importance of glycine conjugation in the metabolism of aromatic acids. *Drug Metabolism Reviews,* 46, 343-361.

BAE, J. H., YOON, S. H. & LIM, S. Y. 2011. A comparative of heavy metal contents and biochemical characteristics of Japanese (*Haliotis discus*) and Korean abalone (*Haliotis discus hannai*). *Food Science and Biotechnology,* 20, 273-276.

BALDWIN, J., ELIAS, J., WELLS, R. & DONOVAN, D. 2007. Energy metabolism in the tropical abalone, *Haliotis asinina* Linné: Comparisons with temperate abalone species. *Journal of Experimental Marine Biology and Ecology,* 342, 213-225.

BALDWIN, J., WELLS, R., LOW, M. & RYDER, J. 1992. Tauropine and D-lactate as metabolic stress indicators during transport and storage of live paua, New Zealand Abalone, *Haliotis iris*. *Journal of Food Science,* 57, 280-282.

BALLANTYNE, J. S. 2004. Mitochondria: Aerobic and anaerobic design—lessons from molluscs and fishes. *Comparative Biochemistry and Physiology Part B: Biochemistry and Molecular Biology,* 139, 461-467.

BALLANTYNE, J. S. & MOYES, C. D. 1987. The role of divalent cations and ionic strength in the osmotic sensitivity of glutamate oxidation in oyster gill mitochondria. *Journal of Experimental Biology,* 130, 203-217.

BANSEMER, M. S., QIN, J. G., HARRIS, J. O., DUONG, D. N., CURRIE, K.-L., HOWARTH, G. S. & STONE, D. A. 2016a. Dietary inclusions of dried macroalgae meal in formulated diets improve the growth of greenlip abalone (*Haliotis laevigata*). *Journal of Applied Phycology,* 28, 3645-3658.

BANSEMER, M. S., QIN, J. G., HARRIS, J. O., HOWARTH, G. S. & STONE, D. A. 2014. Nutritional requirements and use of macroalgae as ingredients in abalone feed. *Reviews in Aquaculture,* 5, 1-15.

BANSEMER, M. S., QIN, J. G., HARRIS, J. O., SCHAEFER, E. N., WANG, H., MERCER, G. J., HOWARTH, G. S. & STONE, D. A. 2016b. Age-dependent response of digestive enzyme activities to dietary protein level and water temperature in greenlip abalone (*Haliotis laevigata*). *Aquaculture,* 451, 451-456.

BARKAI, R. & GRIFFITHS, C. 1988. An energy budget for the South African abalone *Haliotis midae* Linnaeus. *Journal of Molluscan Studies,* 54, 43-51.

BAUTISTA-TERUEL, M. N. & MILLAMENA, O. M. 1999. Diet development and evaluation for juvenile abalone, *Haliotis asinina*: Protein/energy levels. *Aquaculture,* 178, 117-126.

BECKONERT, O., KEUN, H. C., EBBELS, T. M., BUNDY, J., HOLMES, E., LINDON, J. C. & NICHOLSON, J. K. 2007. Metabolic profiling, metabolomic and metabonomic procedures for NMR spectroscopy of urine, plasma, serum and tissue extracts. *Nature Protocols,* 2, 2692-2703.

BEHRENS, J. W., ELIAS, J. P., TAYLOR, H. H. & WEBER, R. E. 2002. The archaeogastropod mollusc *Haliotis iris*: Tissue and blood metabolites and allosteric regulation of haemocyanin function. *Journal of Experimental Biology,* 205, 253-263.

BELL, E. L. & CHANDEL, N. S. 2007. Mitochondrial oxygen sensing: regulation of hypoxia-inducible factor by mitochondrial generated reactive oxygen species. *Essays in Biochemistry,* 43, 17-28.

BOARDMAN, L., SØRENSEN, J. G., KOŠTÁL, V., ŠIMEK, P. & TERBLANCHE, J. S. 2016. Chilling slows anaerobic metabolism to improve anoxia tolerance of insects. *Metabolomics,* 12, 176.

BOUTILIER, R. G. 2001. Mechanisms of cell survival in hypoxia and hypothermia. *Journal of Experimental Biology,* 204, 3171-3181.

BRAID, B. A., MOORE, J. D., ROBBINS, T. T., HEDRICK, R. P., TJEERDEMA, R. S. & FRIEDMAN, C. S. 2005. Health and survival of red abalone, *Haliotis rufescens*, under varying temperature, food supply, and exposure to the agent of withering syndrome. *Journal of Invertebrate Pathology,* 89, 219-231.

BRITZ, P. & VENTER, S. 2016. Aquaculture Review: South Africa. *World Aquaculture,* 47, 19-28.

BRITZ, P. J. 1996a. Effect of dietary protein level on growth performance of South African abalone, *Haliotis midae*, fed fishmeal-based semi-purified diets. *Aquaculture,* 140, 55-61.

BRITZ, P. J. 1996b. The suitability of selected protein sources for inclusion in formulated diets for the South African abalone, *Haliotis midae*. *Aquaculture,* 140, 63-73.

BRITZ, P. J., HECHT, T. & MANGOLD, S. 1997. Effect of temperature on growth, feed consumption and nutritional indices of *Haliotis midae* fed a formulated diet. *Aquaculture,* 152, 191-203.

BROSNAN, J. T. 2000. Glutamate, at the interface between amino acid and carbohydrate metabolism. *The Journal of Nutrition,* 130, 988S-990S.

BROWN, M., DUNN, W. B., ELLIS, D. I., GOODACRE, R., HANDL, J., KNOWLES, J. D., O'HAGAN, S., SPASIĆ, I. & KELL, D. B. 2005. A metabolome pipeline: From concept to data to knowledge. *Metabolomics,* 1, 39-51.

BROWN, M. R., SIKES, A. L., ELLIOTT, N. G. & TUME, R. K. 2008. Physicochemical factors of abalone quality: A review. *Journal of Shellfish Research,* 27, 835-842.

BUJAK, R., STRUCK-LEWICKA, W., MARKUSZEWSKI, M. J. & KALISZAN, R. 2015. Metabolomics for laboratory diagnostics. *Journal of Pharmaceutical and Biomedical Analysis,* 113, 108-120.

BUNDY, J. G., DAVEY, M. P. & VIANT, M. R. 2009. Environmental metabolomics: a critical review and future perspectives. *Metabolomics,* 5, 3-21.

BUSZEWSKI, B. & NOGA, S. 2012. Hydrophilic interaction liquid chromatography (HILIC)—a powerful separation technique. *Analytical and Bioanalytical Chemistry,* 402, 231-247.

BYRNE, M., HO, M., WONG, E., SOARS, N. A., SELVAKUMARASWAMY, P., SHEPARD-BRENNAND, H., DWORJANYN, S. A. & DAVIS, A. R. 2011. Unshelled abalone and corrupted urchins: Development of marine calcifiers in a changing ocean. *Proceedings of the Royal Society of London B: Biological Sciences,* 278, 2376-2383.

CAJKA, T. & FIEHN, O. 2016. Increasing lipidomic coverage by selecting optimal mobile-phase modifiers in LC–MS of blood plasma. *Metabolomics,* 12, 34.

CAPPELLO, T., MAUCERI, A., CORSARO, C., MAISANO, M., PARRINO, V., PARO, G. L., MESSINA, G. & FASULO, S. 2013. Impact of environmental pollution on caged mussels *Mytilus galloprovincialis* using NMR-based metabolomics. *Marine Pollution Bulletin,* 77, 132-139.

CAREFOOT, T. H., QIAN, P.-Y., TAYLOR, B. E., WEST, T. & OSBORNE, J. 1993. Effect of starvation on energy reserves and metabolism in the Northern abalone, *Haliotis kamtschatkana*. *Aquaculture,* 118, 315-325.

CAREFOOT, T. H., TAYLOR, B. E. & LAND, S. 2000. Use of isolated digestive-gland cells in the study of biochemical and physiological processes in gastropod molluscs. *Comparative Biochemistry and Physiology Part A: Molecular & Integrative Physiology,* 125, 497-502.

CARROLL, J. L. & WELLS, R. M. 1995. Strategies of anaerobiosis in New Zealand infaunal bivalves: Adaptations to environmental and functional hypoxia. *New Zealand Journal of Marine and Freshwater Research,* 29, 137-146.

CATRINCK, T. C. P. G., AGUIAR, M. C. S., DIAS, A., SILVÉRIO, F. O., FIDÊNCIO, P. H. & DE PINHO, G. P. 2013. Study of the reaction derivatization glyphosate and aminomethylphosphonic acid (AMPA) with N, O-bis (trimethylsilyl) trifluoroacetamide. *American Journal of Analytical Chemistry,* 4, 647.

CHANG, P. H., KUO, S. T., LAI, S. H., YANG, H. S., TING, Y. Y., HSU, C. L. & CHEN, H. C. 2005. Herpes-like virus infection causing mortality of cultured abalone *Haliotis diversicolor supertexta* in Taiwan. *Diseases of Aquatic Organisms,* 65, 23-27.

CHENG, W., LIU, C.-H., CHENG, S.-Y. & CHEN, J.-C. 2004. Effect of dissolved oxygen on the acid–base balance and ion concentration of Taiwan abalone *Haliotis diversicolor* supertexta. *Aquaculture,* 231, 573-586.

CHRISTIN, C., HOEFSLOOT, H. C., SMILDE, A. K., HOEKMAN, B., SUITS, F., BISCHOFF, R. & HORVATOVICH, P. 2013. A critical assessment of feature selection methods for biomarker discovery in clinical proteomics. *Molecular & Cellular Proteomics,* 12, 263-276.

COOK, P. A. 2014. The worldwide abalone industry. *Modern Economy,* 5, 1181-1186.

COPLEY, S. D., FRANK, E., KIRSCH, W. M. & KOCH, T. H. 1992. Detection and possible origins of aminomalonic acid in protein hydrolysates. *Analytical Biochemistry,* 201, 152-157.

CRAIG, A., CLOAREC, O., HOLMES, E., NICHOLSON, J. K. & LINDON, J. C. 2006. Scaling and normalization effects in NMR spectroscopic metabonomic data sets. *Analytical Chemistry,* 78, 2262-2267.

CREEK, D. J. 2013. Stable isotope labeled metabolomics improves identification of novel metabolites and pathways. *Bioanalysis,* 5, 1807-1810.

CRISTESCU, M. E., INNES, D. J., STILLMAN, J. H. & CREASE, T. J. 2008. D-and L-lactate dehydrogenases during invertebrate evolution. *BMC Evolutionary Biology,* 8, 1-10.

DAHLHOFF, E. P. 2004. Biochemical indicators of stress and metabolism: Applications for marine ecological studies. *Annual Review of Physiology,* 66, 183-207.

DALE-KUYS, R., VERVALLE, J., ROODT-WILDING, R. & RHODE, C. 2017. Genetic association analysis of candidate loci under selection with size in the South African abalone. *Aquaculture International,* 25, 1197-1214.

DAY, E. G. & BRANCH, G. M. 2002. Influences of the sea urchin *Parechinus angulosus* (Leske) on the feeding behaviour and activity rhythms of juveniles of the South African abalone *Haliotis midae* Linn. *Journal of Experimental Marine Biology and Ecology,* 276, 1-17.

DAY, R. W. & COOK, P. 1995. Bias towards brown algae in determining diet and food preferences: The South African abalone *Haliotis midae*. *Marine and Freshwater Research,* 46, 623-627.

DE GREEF, K. & RAEMAEKERS, S. 2014. South Africa's illicit abalone trade: An updated overview and knowledge gap analysis. *TRAFFIC. Cambridge, UK*.

DE ZWAAN, A., CORTESI, P., VAN DEN THILLART, G., ROOS, J. & STOREY, K. 1991. Differential sensitivities to hypoxia by two anoxia-tolerant marine molluscs: A biochemical analysis. *Marine Biology,* 111, 343-351.

DENNY, M. W. & GAINES, S. D. 2007. *Encyclopedia of tidepools and rocky shores*, Univ of California Press.

DETTMER, K., ARONOV, P. A. & HAMMOCK, B. D. 2007. Mass spectrometry-based metabolomics. *Mass Spectrometry Reviews,* 26, 51-78.

DI, G., LUO, X., HUANG, M., CHEN, J., KONG, X., MIAO, X. & KE, C. 2015. Proteomic profiling of eggs from a hybrid abalone and its parental lines: *Haliotis discus hannai* Ino and *Haliotis gigantea*. *Animal Genetics,* 46, 646-654.

DI GUIDA, R., ENGEL, J., ALLWOOD, J. W., WEBER, R. J., JONES, M. R., SOMMER, U., VIANT, M. R. & DUNN, W. B. 2016. Non-targeted UHPLC-MS metabolomic data processing methods: A comparative investigation of normalisation, missing value imputation, transformation and scaling. *Metabolomics,* 12, 93.

DIFFORD, G., VLOK, A., RHODE, C. & BRINK, D. 2017. Heritability of growth traits in South African Abalone (*Haliotis midae* L.) using the 'internal reference'method. *Aquaculture,* 468, 451-457.

DIXON, G., NOLAN, J., MCCLENAGHAN, N., FLATT, P. & NEWSHOLME, P. 2003. A comparative study of amino acid consumption by rat islet cells and the clonal beta-cell line BRIN-BD11-the functional significance of L-alanine. *Journal of Endocrinology,* 179, 447-454.

DO YUP LEE, B. P. B. & NORTHEN, T. R. 2010. Mass spectrometry–based metabolomics, analysis of metabolite-protein interactions, and imaging. *Biotechniques,* 49, 557.

DONA, A. C., JIMÉNEZ, B., SCHÄFER, H., HUMPFER, E., SPRAUL, M., LEWIS, M. R., PEARCE, J. T., HOLMES, E., LINDON, J. C. & NICHOLSON, J. K. 2014. Precision high-throughput proton NMR spectroscopy of human urine, serum, and plasma for large-scale metabolic phenotyping. *Analytical Chemistry,* 86, 9887-9894.

DONOVAN, D., BALDWIN, J. & CAREFOOT, T. 1999. The contribution of anaerobic energy to gastropod crawling and a re-estimation of minimum cost of transport in the abalone, *Haliotis kamtschatkana* (Jonas). *Journal of Experimental Marine Biology and Ecology,* 235, 273-284.

DUNN, W. B. 2008. Current trends and future requirements for the mass spectrometric investigation of microbial, mammalian and plant metabolomes. *Physical Biology,* 5, 011001.

DUNN, W. B., BAILEY, N. J. & JOHNSON, H. E. 2005. Measuring the metabolome: Current analytical technologies. *Analyst,* 130, 606-625.

DUNN, W. B., BROADHURST, D., BEGLEY, P., ZELENA, E., FRANCIS-MCINTYRE, S., ANDERSON, N., BROWN, M., KNOWLES, J. D., HALSALL, A. & HASELDEN, J. N. 2011a. Procedures for large-scale metabolic profiling of serum and plasma using gas chromatography and liquid chromatography coupled to mass spectrometry. *Nature Protocols,* 6, 1060-1083.

DUNN, W. B., BROADHURST, D. I., ATHERTON, H. J., GOODACRE, R. & GRIFFIN, J. L. 2011b. Systems level studies of mammalian metabolomes: the roles of mass spectrometry and nuclear magnetic resonance spectroscopy. *Chemical Society Reviews,* 40, 387-426.

DUNN, W. B., ERBAN, A., WEBER, R. J., CREEK, D. J., BROWN, M., BREITLING, R., HANKEMEIER, T., GOODACRE, R., NEUMANN, S. & KOPKA, J. 2013. Mass appeal: Metabolite identification in mass spectrometry-focused untargeted metabolomics. *Metabolomics,* 9, 44-66.

DUNN, W. B., WILSON, I. D., NICHOLLS, A. W. & BROADHURST, D. 2012. The importance of experimental design and QC samples in large-scale and MS-driven untargeted metabolomic studies of humans. *Bioanalysis,* 4, 2249-2264.

DUNPHY, B. J., WATTS, E. & RAGG, N. L. 2015. Identifying thermally-stressed adult green-lipped mussels (*Perna canaliculus* Gmelin, 1791) via metabolomic profiling. *American Malacological Bulletin,* 33, 127-135.

DUNSTAN, G. 2010. A simple model for the determination of the relative utilization efficiency of protein by blacklip abalone *(Haliotis rubra* Leach). *Aquaculture Nutrition,* 16, 1-12.

DUPORTET, X., AGGIO, R. B. M., CARNEIRO, S. & VILLAS-BÔAS, S. G. 2012. The biological interpretation of metabolomic data can be misled by the extraction method used. *Metabolomics,* 8, 410-421.

DURAZO-BELTRÁN, E., D'ABRAMO, L. R., TORO-VAZQUEZ, J. F., VASQUEZ-PELÁEZ, C. & VIANA, M. A. T. 2003. Effect of triacylglycerols in formulated diets on growth and fatty acid composition in tissue of green abalone (*Haliotis fulgens*). *Aquaculture,* 224, 257-270.

DURAZO-BELTRÁN, E., VIANA, M. A. T., D'ABRAMO, L. R. & TORO-VAZQUEZ, J. F. 2004. Effects of starvation and dietary lipid on the lipid and fatty acid composition of muscle tissue of juvenile green abalone (*Haliotis fulgens*). *Aquaculture,* 238, 329-341.

DURAZO, E. & VIANA, M. T. 2013. Fatty acid profile of cultured green abalone (*Haliotis fulgens*) exposed to lipid restriction and long-term starvation. *Ciencias Marinas,* 39, 363-370.

EBERLEE, J. C. & STOREY, K. B. 1988. Tissue-specific biochemical responses during anoxia and recovery in the channeled whelk. *Journal of Experimental Marine Biology and Ecology,* 121, 165-176.

ELLINGER, J. J., CHYLLA, R. A., ULRICH, E. L. & MARKLEY, J. L. 2013. Databases and software for NMR-based metabolomics. *Current Metabolomics,* 1, 28-40.

ELLINGTON, W. R. 1983. The recovery from anaerobic metabolism in invertebrates. *Journal of Experimental Zoology,* 228, 431-444.

ELLIS, S. & STEYN, H. 2003. Practical significance (effect sizes) versus or in combination with statistical significance (*p*-values): Research note. *Management Dynamics: Journal of the Southern African Institute for Management Scientists,* 12, 51-53.

EMERY, P. W. 2015. Basic metabolism: protein. *Surgery (Oxford),* 33, 143-147.

EMWAS, A.-H., LUCHINAT, C., TURANO, P., TENORI, L., ROY, R., SALEK, R. M., RYAN, D., MERZABAN, J. S., KADDURAH-DAOUK, R. & ZERI, A. C. 2015. Standardizing the experimental conditions for using urine in NMR-based metabolomic studies with a particular focus on diagnostic studies: a review. *Metabolomics,* 11, 872-894.

ENGSKOG, M. K., HAGLÖF, J., ARVIDSSON, T. & PETTERSSON, C. 2016. LC–MS based global metabolite profiling: The necessity of high data quality. *Metabolomics,* 12, 1-19.

ESTERHUIZEN, K., VAN DER WESTHUIZEN, F. H. & LOUW, R. 2017. Metabolomics of mitochondrial disease. *Mitochondrion,* doi: 10.1016/j.mito.2017.05.012.

FALLU, R. 1991. *Abalone farming,* Oxford, Fishing news books.

FASULO, S., IACONO, F., CAPPELLO, T., CORSARO, C., MAISANO, M., D'AGATA, A., GIANNETTO, A., DE DOMENICO, E., PARRINO, V. & PARO, G. L. 2012. Metabolomic investigation of *Mytilus galloprovincialis* (Lamarck 1819) caged in aquatic environments. *Ecotoxicology and Environmental Safety,* 84, 139-146.

FEALA, J. D., COQUIN, L., ZHOU, D., HADDAD, G. G., PATERNOSTRO, G. & MCCULLOCH, A. D. 2009. Metabolism as means for hypoxia adaptation: Metabolic profiling and flux balance analysis. *BMC Systems Biology,* 3, 91.

FIEHN, O. 2002. Metabolomics–the link between genotypes and phenotypes. *Plant Molecular Biology,* 48, 155-171.

FIEHN, O. 2016. Metabolomics by gas chromatography–mass spectrometry: Combined targeted and untargeted profiling. *Current Protocols in Molecular Biology*, 30.4. 1-30.4. 32.

FIEHN, O., KOPKA, J., TRETHEWEY, R. N. & WILLMITZER, L. 2000. Identification of uncommon plant metabolites based on calculation of elemental compositions using gas chromatography and quadrupole mass spectrometry. *Analytical Chemistry,* 72, 3573-3580.

FIELDS, J. H. 1983. Alternatives to lactic acid: Possible advantages. *Journal of Experimental Zoology Part A: Ecological Genetics and Physiology,* 228, 445-457.

FIELDS, J. H. & STOREY, K. B. 1987. Tissue-specific alanopine dehydrogenase from the gill and strombine dehydrogenase from the foot muscle of the cherrystone clam *Mercenaria mercenaria* (Linn.). *Journal of Experimental Marine Biology and Ecology,* 105, 175-185.

FLEMING, A. E., VAN BARNEVELD, R. J. & HONE, P. W. 1996. The development of artificial diets for abalone: A review and future directions. *Aquaculture,* 140, 5-53.

FLUCKIGER, M., BROWN, M. R., WARD, L. R. & MOLTSCHANIWSKYJ, N. A. 2011. Predicting glycogen concentration in the foot muscle of abalone using near infrared reflectance spectroscopy (NIRS). *Food Chemistry,* 126, 1817-1820.

FRANCHINI, P., VAN DER MERWE, M. & ROODT-WILDING, R. 2011. Transcriptome characterization of the South African abalone *Haliotis midae* using sequencing-by-synthesis. *BMC Research Notes,* 4, 59.

FUJIMORI, T. & ABE, H. 2002. Physiological roles of free D-and L-alanine in the crayfish *Procambarus clarkii* with special reference to osmotic and anoxic stress responses. *Comparative Biochemistry and Physiology Part A: Molecular & Integrative Physiology,* 131, 893-900.

GÄDE, G. 1988. Energy metabolism during anoxia and recovery in shell adductor and foot muscle of the gastropod mollusc *Haliotis lamellosa*: Formation of the novel anaerobic end product tauropine. *The Biological Bulletin,* 175, 122-131.

GÄDE, G., CARLSSON, K.-H. & MEINARDUS, G. 1984. Energy metabolism in the foot of the marine gastropod *Nassa mutabilis* during environmental and functional anaerobiosis. *Marine Biology,* 80, 49-56.

GÄDE, G. & GRIESHABER, M. K. 1986. Pyruvate reductases catalyze the formation of lactate and opines in anaerobic invertebrates. *Comparative Biochemistry and Physiology Part B: Comparative Biochemistry,* 83, 255-272.

GALLUZZI, L., KEPP, O., TROJEL-HANSEN, C. & KROEMER, G. 2012. Mitochondrial control of cellular life, stress, and death. *Circulation Research,* 111, 1198-1207.

GARCIA-CARRENO, F., DEL TORO, M. N. & SERVIERE-ZARAGOZA, E. 2003. Digestive enzymes in juvenile green abalone, *Haliotis fulgens*, fed natural food. *Comparative Biochemistry and Physiology Part B: Biochemistry and Molecular Biology,* 134, 143-150.

GARRETT, R. & GRISHAM, C. 2010. Biochemistry. *Brooks Cole Cengage Learning, Boston USA.* Belmont, CA : Brooks Cole, Cengage Learning.

GIVENS, P. & REISS, M. 2002. *Human biology and health studies,* Cheltenham, United Kingdom, Nelson Thornes Ltd.

GOLDSMITH, P., FENTON, H., MORRIS-STIFF, G., AHMAD, N., FISHER, J. & PRASAD, K. R. 2010. Metabonomics: A useful tool for the future surgeon. *Journal of Surgical Research,* 160, 122-132.

GOODACRE, R., BROADHURST, D., SMILDE, A. K., KRISTAL, B. S., BAKER, J. D., BEGER, R., BESSANT, C., CONNOR, S., CAPUANI, G. & CRAIG, A. 2007. Proposed minimum reporting standards for data analysis in metabolomics. *Metabolomics,* 3, 231-241.

GREEN, A. J., JONES, C. L. & BRITZ, P. J. 2011. The protein and energy requirements of farmed South African abalone *Haliotis midae* L. cultured at optimal and elevated water temperatures. *Aquaculture Research,* 42, 1653-1663.

GREEN, S. R. & STOREY, K. B. 2016. Regulation of crayfish, *Orconectes virilis*, tail muscle lactate dehydrogenase (LDH) in response to anoxic conditions is associated with alterations in phosphorylation patterns. *Comparative Biochemistry and Physiology Part B: Biochemistry and Molecular Biology,* 202, 67-74.

GRIESHABER, M., HARDEWIG, I., KREUTZER, U. & PÖRTNER, H.-O. 1993. Physiological and metabolic responses to hypoxia in invertebrates. *Reviews of Physiology, Biochemistry and Pharmacology.* Springer.

GRIFFIN, J. W. & BRADSHAW, P. C. 2017. Amino acid catabolism in Alzheimer's disease brain: friend or foe? *Oxidative Medicine and Cellular Longevity*, doi.10.1155/2017/5472792.

GRUBERT, M. A., DUNSTAN, G. A. & RITAR, A. J. 2004. Lipid and fatty acid composition of pre-and post-spawning blacklip (*Haliotis rubra*) and greenlip *(Haliotis laevigata*) abalone conditioned at two temperatures on a formulated feed. *Aquaculture,* 242, 297-311.

GUOYAO, W. & MORRIS, S. M. 1998. Arginine metabolism: Nitric oxide and beyond. *Biochemical Journal,* 336, 1-17.

HAHN, K. O. 1989. *Handbook of culture of abalone and other marine gastropods,* Boca Raton, FL, CRC Press inc.

HALESTRAP, A. P. 1987. The regulation of the oxidation of fatty acids and other substrates in rat heart mitochondria by changes in the matrix volume induced by osmotic strength, valinomycin and Ca2+. *Biochemical Journal,* 244, 159-164.

HALSEY, C. R., LEI, S., WAX, J. K., LEHMAN, M. K., NUXOLL, A. S., STEINKE, L., SADYKOV, M., POWERS, R. & FEY, P. D. 2017. Amino acid catabolism in *Staphylococcus aureus* and the function of carbon catabolite repression. *mBio,* 8, e01434-16.

HARCET, M., PERINA, D. & PLEŠE, B. 2013. Opine dehydrogenases in marine invertebrates. *Biochemical Genetics,* 51, 666-676.

HARDER, U., KOLETZKO, B. & PEISSNER, W. 2011. Quantification of 22 plasma amino acids combining derivatization and ion-pair LC–MS/MS. *Journal of Chromatography B,* 879, 495-504.

HARRIS, J. O., MAGUIRE, G. B., EDWARDS, S. & HINDRUM, S. M. 1998. Effect of ammonia on the growth rate and oxygen consumption of juvenile greenlip abalone, *Haliotis laevigata* Donovan. *Aquaculture,* 160, 259-272.

HAYAT, S., HAYAT, Q., ALYEMENI, M. N., WANI, A. S., PICHTEL, J. & AHMAD, A. 2012. Role of proline under changing environments: A review. *Plant Signaling & Behavior,* 7, 1456-1466.

HEATH, P. & MOSS, G. 2009. Is size grading important for farming the abalone *Haliotis iris*? *Aquaculture,* 290, 80-86.

HERNÁNDEZ, J., DE LA PARRA, A. M., LASTRA, M. & VIANA, M. T. 2013. Effect of lipid composition of diets and environmental temperature on the performance and fatty acid composition of juvenile European abalone (*Haliotis tuberculata* L. 1758). *Aquaculture,* 412, 34-40.

HICKEY, A. J. & WELLS, R. M. 2003. Thermal constraints on glycolytic metabolism in the New Zealand abalone, *Haliotis iris*: The role of tauropine dehydrogenase. *New Zealand Journal of Marine and Freshwater Research,* 37, 723-731.

HICKMAN, C. P., ROBERTS, L. S., LARSON, A., OBER, W. C. & GARRISON, C. 2006. *Integrated principles of Zoology,* New York, McGraw-Hill: International.

HILDEBRANDT, T. M., NESI, A. N., ARAÚJO, W. L. & BRAUN, H.-P. 2015. Amino acid catabolism in plants. *Molecular Plant,* 8, 1563-1579.

HOCHACHKA, P. W., FIELDS, J. & MUSTAFA, T. 1973. Animal life without oxygen: Basic biochemical mechanisms. *American Zoologist,* 13, 543-555.

HOOPER, C., DAY, R., SLOCOMBE, R., BENKENDORFF, K. & HANDLINGER, J. 2014. Histopathology and haemolymph biochemistry following anaesthesia and movement in farmed Australian abalone (*Haliotis rubra* × *Haliotis laevigata*). *Aquaculture,* 422, 202-210.

HOVAGIMYAN, K. G. & GERIG, J. T. 2005. Interactions of trimethylamine N−oxide and water with cyclo-alanylglycine. *The Journal of Physical Chemistry B,* 109, 24142-24151.

HRYDZIUSZKO, O. & VIANT, M. R. 2012. Missing values in mass spectrometry based metabolomics: An undervalued step in the data processing pipeline. *Metabolomics,* 8, 161-174.

HUDDY, R. J. & COYNE, V. E. 2014. Detection and localisation of the abalone probiotic *Vibrio midae* SY9 and its extracellular protease, VmproA, within the digestive tract of the South African abalone, *Haliotis midae*. *PloS One,* 9, e86623.

IBARROLA, I., HILTON, Z. & RAGG, N. L. 2017. Physiological basis of inter-population, inter-familiar and intra-familiar differences in growth rate in the green-lipped mussel *Perna canaliculus*. *Aquaculture,* 479, 544-555.

IRWIN, C., VAN REENEN, M., MASON, S., MIENIE, L. J., WESTERHUIS, J. A. & REINECKE, C. J. 2016. Contribution towards a metabolite profile of the detoxification of benzoic acid through glycine conjugation: An intervention study. *PloS One,* 11, e0167309.

ISO, B. 2005. 9000: 2005 Quality management systems. Fundamentals and vocabulary. *British Standards Institution,* 58.

ISSAQ, H. J., VAN, Q. N., WAYBRIGHT, T. J., MUSCHIK, G. M. & VEENSTRA, T. D. 2009. Analytical and statistical approaches to metabolomics research. *Journal of Separation Science,* 32, 2183-2199.

JORGENSEN, D., WARE, S. & REDMOND, J. 1984. Cardiac output and tissue blood flow in the abalone, *Haliotis cracherodii* (Mollusca, Gastropoda). *Journal of Experimental Zoology,* 231, 309-324.

JU, Z. Y., VILJOEN, C., HUTCHINSON, P., REINICKE, J., HORGEN, F. D., HOWARD, L. & LEE, C. S. 2016. Effects of diets on the growth performance and shell pigmentation of Pacific abalone. *Aquaculture Research,* 47, 4004-4014.

KAISER, H., ERASMUS, B. & NAYLOR, M. 2017. Behavioural responses of farmed South African abalone *Haliotis midae* L. to disturbances caused by husbandry procedures. *Aquaculture International,* 25, 21-29.

KANANI, H., CHRYSANTHOPOULOS, P. K. & KLAPA, M. I. 2008. Standardizing GC–MS metabolomics. *Journal of Chromatography B,* 871, 191-201.

KILBURN, R. & RIPPEY, E. 1982. *Sea shells of Southern Africa,* Johannesburg, Macmillan South Africa.

KIM, S., KIM, J., YUN, E. J. & KIM, K. H. 2016. Food metabolomics: from farm to human. *Current Opinion in Biotechnology,* 37, 16-23.

KNAUER, J., HECHT, T. & BRITZ, P. 1995. A note on the feeding behaviour and growth of juvenile South African abalone, *Haliotis midae*, fed on an artificial weaning diet. *South African Journal of Science,* 91, 91-93.

KOEK, M. M., JELLEMA, R. H., VAN DER GREEF, J., TAS, A. C. & HANKEMEIER, T. 2011. Quantitative metabolomics based on gas chromatography mass spectrometry: Status and perspectives. *Metabolomics,* 7, 307-328.

KREUTZER, U., SIEGMUND, B. R. & GRIESHABER, M. K. 1989. Parameters controlling opine formation during muscular activity and environmental hypoxia. *Journal of Comparative Physiology B: Biochemical, Systemic, and Environmental Physiology,* 159, 617-628.

KRISHNAN, N., DICKMAN, M. B. & BECKER, D. F. 2008. Proline modulates the intracellular redox environment and protects mammalian cells against oxidative stress. *Free Radical Biology and Medicine,* 44, 671-681.

KRUATRACHUE, M., SAWATPEERA, S., CHITRAMVONG, Y., SONCHAENG, P., UPATHAM, E. & SANGPRADUB, S. 2004. Comparative growth performance of early juvenile *Haliotis asinina* fed various artificial diets. *Journal of Shellfish Research,* 23, 197-204.

KUMAR, A. & BACHHAWAT, A. K. 2012. Pyroglutamic acid: throwing light on a lightly studied metabolite. *Current Science,* 102, 288-297.

LAAS, A. & VOSLOO, A. 2010. Exploring basic biochemical constituents in the body tissues of South African abalone *Haliotis midae* reared in shore-based mariculture systems. *African Journal of Marine Science,* 32, 55-63.

LACHAMBRE, S., HUCHETTE, S., DAY, R., BOUDRY, P., RIO-CABELLO, A., FUSTEC, T. & ROUSSEL, S. 2017. Relationships between growth, survival, physiology and behaviour - A multi-criteria approach to *Haliotis tuberculata* phenotypic traits. *Aquaculture,* 467, 190-197.

LAGANÀ, G., BARRECA, D., GIACOBBE, S. & BELLOCCO, E. 2014. Anaerobiosis and metabolic plasticity of *Pinna nobilis*: Biochemical and ecological features. *Biochemical Systematics and Ecology,* 56, 138-143.

LANKADURAI, B. P., NAGATO, E. G. & SIMPSON, M. J. 2013. Environmental metabolomics: An emerging approach to study organism responses to environmental stressors. *Environmental Reviews,* 21, 180-205.

LATUIHAMALLO, M. & APITULEY, D. 2015. Amino acid and fatty acid of abalone *Haliotis Squamata* cultured in different aquaculture systems. *Procedia Food Science,* 3, 174-181.

LAWRENCE, J. M. 2013. *Sea urchins: Biology and ecology*, Academic Press.

LAYMAN, D. K. 2002. Role of leucine in protein metabolism during exercise and recovery. *Canadian Journal of Applied Physiology,* 27, 646-662.

LE, D. V., ALFARO, A. C., RAGG, N. L., HILTON, Z. & KING, N. 2016. Aerobic scope and oxygen regulation of New Zealand geoduck (*Panopea zelandica*) in response to progressive hypoxia. *Aquaculture,* 463, 28-36.

LEE, A.-C. & LEE, K.-T. 2011. The enzyme activities of opine and lactate dehydrogenase in the gills, mantle, foot, and adductor of the hard clam *Meretrix lusoria*. *Journal of Marine Science and Technology,* 19, 361-367.

LEE, S.-M. 2004. Utilization of dietary protein, lipid, and carbohydrate by abalone *Haliotis discus hannai*: A review. *Journal of Shellfish Research,* 23, 1027-1030.

LEEK, J. T., SCHARPF, R. B., BRAVO, H. C., SIMCHA, D., LANGMEAD, B., JOHNSON, W. E., GEMAN, D., BAGGERLY, K. & IRIZARRY, R. A. 2010. Tackling the widespread and critical impact of batch effects in high-throughput data. *Nature Reviews. Genetics,* 11, 733.

LEIGHTON, P. 2008. Abalone hatchery manual. *In:* ROBINSON, G. & MCGOWAN, N. (eds.) *Aquaculture explained.* Aquaculture Technical Section, Aquaculture Development Division, Dun Laoghaire.

LI, M., MAI, K., AI, Q., HE, G., XU, W., ZHANG, W., ZHANG, Y., ZHOU, H. & LIUFU, Z. 2015. Effect of dietary lipid on the growth, fatty acid composition and Δ5 *Fads* expression of abalone (*Haliotis discus hannai* Ino) hepatopancreas. *Journal of Ocean University of China,* 14, 317-324.

LI, N., ZHANG, Z., ZHANG, L., WANG, S., ZOU, Z., WANG, G. & WANG, Y. 2012. Insulin-like growth factor binding protein 7, a member of insulin-like growth factor signal pathway, involved in immune response of small abalone *Haliotis diversicolor*. *Fish and Shellfish Immunology,* 33, 229-242.

LI, P., MAI, K., TRUSHENSKI, J. & WU, G. 2009. New developments in fish amino acid nutrition: Towards functional and environmentally oriented aquafeeds. *Amino Acids,* 37, 43-53.

LIANG, X., ZHANG, L., NATARAJAN, S. K. & BECKER, D. F. 2013. Proline mechanisms of stress survival. *Antioxidants & Redox Signaling,* 19, 998-1011.

LILAND, K. H. 2011. Multivariate methods in metabolomics–from pre-processing to dimension reduction and statistical analysis. *Trends in Analytical Chemistry,* 30, 827-841.

LIN, C. Y., VIANT, M. R. & TJEERDEMA, R. S. 2006. Metabolomics: Methodologies and applications in the environmental sciences. *Journal of Pesticide Science,* 31, 245-251.

LIN, C. Y., WU, H., TJEERDEMA, R. S. & VIANT, M. R. 2007. Evaluation of metabolite extraction strategies from tissue samples using NMR metabolomics. *Metabolomics,* 3, 55-67.

LINDEQUE, J. Z., HIDALGO, J., LOUW, R. & VAN DER WESTHUIZEN, F. H. 2013. Systemic and organ specific metabolic variation in metallothionein knockout mice challenged with swimming exercise. *Metabolomics,* 9, 418-432.

LINDEQUE, J. Z., JANSEN VAN RENSBURG, P. J., LOUW, R., VAN DER WESTHUIZEN, F. H., FLORIT, S., RAMÍREZ, L., GIRALT, M. & HIDALGO, J. 2015. Obesity and metabolomics: Metallothioneins protect against high-fat diet-induced consequences in metallothionein knockout mice. *Omics: A Journal of Integrative Biology,* 19, 92-103.

LIU, C., SHIN, P. & CHEUNG, S. 2014. Comparisons of the metabolic responses of two subtidal nassariid gastropods to hypoxia and re-oxygenation. *Marine Pollution Bulletin,* 82, 109-116.

LIVINGSTONE, D. 1983. Invertebrate and vertebrate pathways of anaerobic metabolism: Evolutionary considerations. *Journal of the Geological Society,* 140, 27-37.

LONGO, N., FRIGENI, M. & PASQUALI, M. 2016. Carnitine transport and fatty acid oxidation. *Biochimica et Biophysica Acta (BBA)-Molecular Cell Research,* 1863, 2422-2435.

LOOTS, D. T., ERASMUS, E. & MIENIE, L. J. 2005. Identification of 19 new metabolites induced by ab normal amino acid conjugation in isovaleric acidemia. *Clinical Chemistry,* 51, 1510-1512.

LOPASCHUK, G. D., USSHER, J. R., FOLMES, C. D., JASWAL, J. S. & STANLEY, W. C. 2010. Myocardial fatty acid metabolism in health and disease. *Physiological Reviews,* 90, 207-258.

LOU, Q. M., WANG, Y. M. & XUE, C. H. 2013. Lipid and fatty acid composition of two species of abalone, *Haliotis discus hannai* Ino and *Haliotis diversicolor* Reeve. *Journal of Food Biochemistry,* 37, 296-301.

LU, J., FENG, J., CAI, S. & CHEN, Z. 2017. Metabolomic responses of *Haliotis diversicolor* to organotin compounds. *Chemosphere,* 168, 860-869.

LU, J., SHI, Y., WANG, S., CHEN, H., CAI, S. & FENG, J. 2016. NMR-based metabolomic analysis of *Haliotis diversicolor* exposed to thermal and hypoxic stresses. *Science of The Total Environment,* 545, 280-288.

LU, W., BENNETT, B. D. & RABINOWITZ, J. D. 2008. Analytical strategies for LC–MS-based targeted metabolomics. *Journal of Chromatography B,* 871, 236-242.

LUCAS, T. 2007. *Investigating genetic and molecular aspects of growth of the tropical abalone Haliotis asinina.* PhD Thesis PhD Thesis. The University of Queensland

LUIER, L. & LOOTS, D. T. 2016. Tuberculosis metabolomics reveals adaptations of man and microbe in order to outcompete and survive. *Metabolomics,* 12, 1-9.

LUO, J., SCHUMACHER, M., SCHERER, A., SANOUDOU, D., MEGHERBI, D., DAVISON, T., SHI, T., TONG, W., SHI, L. & HONG, H. 2010. A comparison of batch effect removal methods for enhancement of prediction performance using MAQC-II microarray gene expression data. *The Pharmacogenomics Journal,* 10, 278.

MACEY, B., CHRISTISON, K. & MOUTON, A. 2011. *Halioticida noduliformans* isolated from cultured abalone (*Haliotis midae*) in South Africa. *Aquaculture,* 315, 187-195.

MACEY, B. & COYNE, V. 2005. Improved growth rate and disease resistance in farmed *Haliotis midae* through probiotic treatment. *Aquaculture,* 245, 249-261.

MAHER, P. 2005. The effects of stress and aging on glutathione metabolism. *Ageing Research Reviews,* 4, 288-314.

MAI, K. 1998. Comparative studies on the nutrition of two species of abalone, *Haliotis tuberculata* L. and *Haliotis discus hannai* Ino.: VII. Effects of dietary vitamin C on survival, growth and tissue concentration of ascorbic acid. *Aquaculture,* 161, 383-392.

MALDONADO, C., GUEVARA, N., QUEIJO, C., GONZÁLEZ, R., FAGIOLINO, P. & VÁZQUEZ, M. 2016. Carnitine and/or acetylcarnitine deficiency as a cause of higher levels of ammonia. *BioMed Research International,* 2920108.

MALHAM, S. K., LACOSTE, A., GELEBART, F., CUEFF, A. & POULET, S. A. 2003. Evidence for a direct link between stress and immunity in the mollusc *Haliotis tuberculata*. *Journal of Experimental Zoology Part A: Comparative Experimental Biology,* 295, 136-144.

MASON, S., VAN FURTH, A. M., MIENIE, L. J., ENGELKE, U. F., WEVERS, R. A., SOLOMONS, R. & REINECKE, C. J. 2015. A hypothetical astrocyte–microglia lactate shuttle derived from a 1H NMR metabolomics analysis of cerebrospinal fluid from a cohort of South African children with tuberculous meningitis. *Metabolomics,* 11, 822-837.

MAU, A. & JHA, R. 2017. Aquaculture of two commercially important molluscs (abalone and limpet): Existing knowledge and future prospects. *Reviews in Aquaculture*, doi: 10.1111/raq.12190.

MGAYA, Y. D. & MERCER, J. P. 1994. A review of the biology, ecology, fisheries and mariculture of the European abalone *Haliotis tuberculata* Linnaeus 1758 (Gastropoda: Haliotidae). *Biology and Environment: Proceedings of the Royal Irish Academy*, 285-304.

MOCO, S., VERVOORT, J., MOCO, S., BINO, R. J., DE VOS, R. C. & BINO, R. 2007. Metabolomics technologies and metabolite identification. *TrAC Trends in Analytical Chemistry,* 26, 855-866.

MORAN, A. L. & MANAHAN, D. T. 2003. Energy metabolism during larval development of green and white abalone, *Haliotis fulgens* and *H. sorenseni*. *The Biological Bulletin,* 204, 270-277.

MORASH, A. J. & ALTER, K. 2016. Effects of environmental and farm stress on abalone physiology: Perspectives for abalone aquaculture in the face of global climate change. *Reviews in Aquaculture,* 8, 342-368.

MORSE, D. E. 1984. Biochemical and genetic engineering for improved production of abalones and other valuable molluscs. *Aquaculture,* 39, 263-282.

MOTTI, C. 2012. Environmental Marine Metabolomics: From Whole Organism System Biology to Ecosystem Management. *Journal of Marine Science Research & Development,* 2, 110.

MOUTON, A. 2017. Red tide devastates South African abalone farms. *Aquaculture Magazine.* Jun/July ed. Guadalajara, Mexico: Design Publications International Inc.

MOUTON, A. & GUMMOW, B. 2011. The occurrence of gut associated parasites in the South African abalone, *Haliotis midae*, in Western Cape aquaculture facilities. *Aquaculture,* 313, 1-6.

MÜLLER, M., MENTEL, M., VAN HELLEMOND, J. J., HENZE, K., WOEHLE, C., GOULD, S. B., YU, R.-Y., VAN DER GIEZEN, M., TIELENS, A. G. & MARTIN, W. F. 2012. Biochemistry and evolution of anaerobic energy metabolism in eukaryotes. *Microbiology and Molecular Biology Reviews,* 76, 444-495.

MULLER, S. 1986. Taxonomy of the genus Haliotis in South Africa. *Transactions of the Royal Society of South Africa,* 46, 69-77.

MURRAY, R., GRANNER, D. K., MAYES, P. & RODWELL, V. 2003. *Harper's illustrated Biochemistry,* New York, McGraw-Hill.

NAIDOO, K., MANEVELDT, G., RUCK, K. & BOLTON, J. J. 2006. A comparison of various seaweed-based diets and formulated feed on growth rate of abalone in a land-based aquaculture system. *Journal of Applied Phycology,* 18, 437-443.

NAZ, S., VALLEJO, M., GARCÍA, A. & BARBAS, C. 2014. Method validation strategies involved in non-targeted metabolomics. *Journal of Chromatography A*.

NETHERTON, J. & GURIN, S. 1982. Biosynthesis and physiological role of homarine in marine shrimp. *Journal of Biological Chemistry,* 257, 11971-11975.

NEWSHOLME, P., BENDER, K., KIELY, A. & BRENNAN, L. 2007. Amino acid metabolism, insulin secretion and diabetes. *Biochemical Society Transactions,* 35, 1180-1186.

NEWSHOLME, P., LIMA, M., PROCOPIO, J., PITHON-CURI, T., BAZOTTE, R. & CURI, R. 2003. Glutamine and glutamate as vital metabolites. *Brazilian Journal of Medical and Biological Research,* 36, 153-163.

NIELSEN, N. J., TOMASI, G., FRANDSEN, R. J., KRISTENSEN, M. B., NIELSEN, J., GIESE, H. & CHRISTENSEN, J. H. 2010. A pre-processing strategy for liquid chromatography time-of-flight mass spectrometry metabolic fingerprinting data. *Metabolomics,* 6, 341-352.

NOTO, A., FANOS, V., BARBERINI, L., GRAPOV, D., FATTUONI, C., ZAFFANELLO, M., CASANOVA, A., FENU, G., DE GIACOMO, A. & DE ANGELIS, M. 2014. The urinary metabolomics profile of an Italian autistic children population and their unaffected siblings. *The Journal of Maternal-Fetal & Neonatal Medicine,* 27, 46-52.

O'OMOLO, S., GÄDE, G., COOK, P. & BROWN, A. 2003. Can the end products of anaerobic metabolism, tauropine and D-lactate, be used as metabolic stress indicators during transport of live South African abalone *Haliotis midae*. *African Journal of Marine Science,* 25, 301-309.

ØISETH, S. K., DELAHUNTY, C., COCHET, M. & LUNDIN, L. 2013. Why is abalone so chewy? Structural characterization and relationship to textural attributes. *Journal of Shellfish Research,* 32, 73-79.

PARSONS, H. M., LUDWIG, C., GÜNTHER, U. L. & VIANT, M. R. 2007. Improved classification accuracy in 1-and 2-dimensional NMR metabolomics data using the variance stabilising generalised logarithm transformation. *BMC Bioinformatics,* 8, 234.

PATTI, G. J., YANES, O. & SIUZDAK, G. 2012. Innovation: Metabolomics: The apogee of the omics trilogy. *Nature Reviews Molecular Cell Biology,* 13, 263-269.

PAWLISZYN, J. 2012. *Comprehensive sampling and sample preparation: Analytical techniques for scientists,* Oxford, UK, Academic Press.

PAYNE, A. I. & CRAWFORD, R. J. 1989. *Oceans of life: Off southern Africa,* Cape Town, Vlaeberg Publishers.

PÉREZ-ESTRADA, C. J., CIVERA-CERECEDO, R., HERNÁNDEZ-LLAMAS, A. & SERVIERE-ZARAGOZA, E. 2011. Growth and biochemical composition of juvenile green abalone Haliotis fulgens fed rehydrated macroalgae. *Aquaculture Nutrition,* 17, e62-e69.

PÉREZ-ARELLANO, I., CARMONA-ÁLVAREZ, F., MARTÍNEZ, A. I., RODRÍGUEZ-DÍAZ, J. & CERVERA, J. 2010. Pyrroline-5-carboxylate synthase and proline biosynthesis: From osmotolerance to rare metabolic disease. *Protein Science,* 19, 372-382.

PITCHER, G. & CALDER, D. 2000. Harmful algal blooms of the southern Benguela Current: A review and appraisal of monitoring from 1989 to 1997. *African Journal of Marine Science,* 22, 255-271.

PÖRTNER, H. O. 2002. Environmental and functional limits to muscular exercise and body size in marine invertebrate athletes. *Comparative Biochemistry and Physiology Part A: Molecular & Integrative Physiology,* 133, 303-321.

POYNTON, H. C., TAYLOR, N. S., HICKS, J., COLSON, K., CHAN, S., CLARK, C., SCANLAN, L., LOGUINOV, A. V., VULPE, C. & VIANT, M. R. 2011. Metabolomics of microliter hemolymph samples enables an improved understanding of the combined metabolic and transcriptional responses of *Daphnia magna* to cadmium. *Environmental Science & Technology,* 45, 3710-3717.

PRATHOMYA, P., PRISINGKORN, W., JAKOVLIĆ, I., DENG, F.-Y., ZHAO, Y.-H. & WANG, W.-M. 2017. 1H NMR-based metabolomics approach reveals metabolic alterations in response to dietary imbalances in *Megalobrama amblycephala*. *Metabolomics,* 13, 17.

PROBYN, T., PRETORIUS, M., SEANEGO, K. & BERNATZEDER, A. 2017. Characterisation of water quality in effluents of land-based abalone farms in the Western Cape, South Africa. *Aquaculture Environment Interactions,* 9, 87-102.

PROSSER, C. L. 1991. *Comparative animal physiology, environmental and metabolic animal physiology,* Hoboken, New Jersey, John Wiley & Sons.

RAEMAEKERS, S. J. P. N. & BRITZ, P. J. 2009. Profile of the illegal abalone fishery (*Haliotis midae*) in the Eastern Cape Province, South Africa: Organised pillage and management failure. *Fisheries Research,* 97, 183-195.

RAGG, N. L. & TAYLOR, H. H. 2006. Heterogeneous perfusion of the paired gills of the abalone *Haliotis iris* Martyn 1784: An unusual mechanism for respiratory control. *Journal of Experimental Biology,* 209, 475-483.

REGGIANI, R. & BERTANI, A. 2003. Anaerobic amino acid metabolism. *Russian Journal of Plant Physiology,* 50, 733-736.

REINECKE, C. J., KOEKEMOER, G., VAN DER WESTHUIZEN, F. H., LOUW, R., LINDEQUE, J. Z., MIENIE, L. J. & SMUTS, I. 2012. Metabolomics of urinary organic acids in respiratory chain deficiencies in children. *Metabolomics,* 8, 264-283.

REUTER, S. E. & EVANS, A. M. 2012. Carnitine and acylcarnitines. *Clinical Pharmacokinetics,* 51, 553-572.

ROBERTS, L. D., MCCOMBIE, G., TITMAN, C. M. & GRIFFIN, J. L. 2008. A matter of fat: An introduction to lipidomic profiling methods. *Journal of Chromatography B,* 871, 174-181.

ROBERTSON-ANDERSSON, D., MANEVELDT, G. & NAIDOO, K. 2011. Effects of wild and farm-grown macroalgae on the growth of juvenile South African abalone *Haliotis midae* Linnaeus. *African Journal of Aquatic Science,* 36, 331-337.

ROSENBLUM, E., VIANT, M., BRAID, B., MOORE, J., FRIEDMAN, C. & TJEERDEMA, R. 2005. Characterizing the metabolic actions of natural stresses in the California red abalone, *Haliotis rufescens* using 1H NMR metabolomics. *Metabolomics,* 1, 199-209.

ROSENBLUM, E. S., TJEERDEMA, R. S. & VIANT, M. R. 2006. Effects of temperature on host-pathogen-drug interactions in red abalone, *Haliotis rufescens,* determined by 1H NMR metabolomics. *Environmental Science & Technology,* 40, 7077-7084.

ROZNERE, I., WATTERS, G. T., WOLFE, B. A. & DALY, M. 2014. Nontargeted metabolomics reveals biochemical pathways altered in response to captivity and food limitation in the freshwater mussel *Amblema plicata*. *Comparative Biochemistry and Physiology Part D: Genomics and Proteomics,* 12, 53-60.

SACCENTI, E., HOEFSLOOT, H. C., SMILDE, A. K., WESTERHUIS, J. A. & HENDRIKS, M. M. 2014. Reflections on univariate and multivariate analysis of metabolomics data. *Metabolomics,* 10, 361-374.

SALES, J. 2004. Abalone. *Aquafeeds: Formulation and Beyond,* 1, 23-26.

SALES, J. & BRITZ, P. 2001. Research on abalone (*Haliotis midae* L.) cultivation in South Africa. *Aquaculture Research,* 32, 863-874.

SALES, J. & BRITZ, P. 2003. Apparent and true availability of amino acids from common feed ingredients for South African abalone (*Haliotis midae* L.). *Aquaculture Nutrition,* 9, 55-64.

SALES, J. & JANSSENS, G. 2004. Use of feed ingredients in artificial diets for abalone: A brief update. *Nutrition Abstracts and Reviews: Series B,* 74, 13-21.

SALWAY, J. G. 2004. *Metabolism at a glance,* Guildford, John Wiley & Sons.

SAMUELSSON, L. M. & LARSSON, D. J. 2008. Contributions from metabolomics to fish research. *Molecular BioSystems,* 4, 974-979.

SARTAIN, M. 2016. *The Agilent metabolomics dynamic MRM database and method* [Online]. Santa Clara, California, USA. Available: https://www.agilent.com/cs/library/technicaloverviews/public/5991-6482EN.pdf.

SATO, M., TAKEUCHI, M., KANNO, N., NAGAHISA, E. & SATO, Y. 1991. Characterization and physiological role of tauropine dehydrogenase and lactate dehydrogenase from muscle of abalone, *Haliotis discus hannai*. *Tohoku Journal of Agricultural Research,* 41, 83-95.

SATO, M., TAKEUCHI, M., KANNO, N., NAGAHISA, E. & SATO, Y. 1993. Distribution of opine dehydrogenases and lactate dehydrogenase activities in marine animals. *Comparative Biochemistry and Physiology Part B: Comparative Biochemistry,* 106, 955-960.

SCHMIDT-NIELSEN, K. 2007. *Animal physiology: Adaptation and environment,* New York, Cambridge University Press.

SCHYMANSKI, E. L., JEON, J., GULDE, R., FENNER, K., RUFF, M., SINGER, H. P. & HOLLENDER, J. 2014. Identifying small molecules via high resolution mass spectrometry: Communicating confidence. *Environmental Science and Technology,* 48, 2097-2098.

SHAO, Y., LI, C., CHEN, X., ZHANG, P., LI, Y., LI, T. & JIANG, J. 2015. Metabolomic responses of sea cucumber *Apostichopus japonicus* to thermal stresses. *Aquaculture,* 435, 390-397.

SHEEDY, J. R., LACHAMBRE, S., GARDNER, D. K. & DAY, R. W. 2015. 1H-NMR metabolite profiling of abalone digestive gland in response to short-term starvation. *Aquaculture International,* 24, 503-521.

SHINDE, S., VILLAMOR, J. G., LIN, W.-D., SHARMA, S. & VERSLUES, P. E. 2016. Proline coordination with fatty acid synthesis and redox metabolism of chloroplast and mitochondria. *Plant Physiology,* 172, 1074–1088.

SHIPTON, T. & BRITZ, P. 2001. The effect of animal size on the ability of *Haliotis midae* L. to utilize selected dietary protein sources. *Aquaculture Research,* 32, 393-403.

SHOWALTER, M. R., CAJKA, T. & FIEHN, O. 2017. Epimetabolites: Discovering metabolism beyond building and burning. *Current Opinion in Chemical Biology,* 36, 70-76.

SLABBERT, R. & ROODT-WILDING, R. 2006. Non-destructive sampling of juvenile abalone using epipodial tentacles and mucus: Method and application. *African Journal of Marine Science,* 28, 719-721.

SMOLINSKA, A., BLANCHET, L., BUYDENS, L. M. & WIJMENGA, S. S. 2012. NMR and pattern recognition methods in metabolomics: from data acquisition to biomarker discovery: a review. *Analytica Chimica Acta,* 750, 82-97.

SMUTS, I., VAN DER WESTHUIZEN, F. H., LOUW, R., MIENIE, L. J., ENGELKE, U. F., WEVERS, R. A., MASON, S., KOEKEMOER, G. & REINECKE, C. J. 2013. Disclosure of a putative biosignature for respiratory chain disorders through a metabolomics approach. *Metabolomics,* 9, 379-391.

SOKOLOVA, I. M., FREDERICH, M., BAGWE, R., LANNIG, G. & SUKHOTIN, A. A. 2012. Energy homeostasis as an integrative tool for assessing limits of environmental stress tolerance in aquatic invertebrates. *Marine Environmental Research,* 79, 1-15.

STEFANO, G., MANTIONE, K., CASARES, F. & KREAM, R. 2015. Anaerobically functioning mitochondria: Evolutionary perspective on modulation of energy metabolism in *Mytilus edulis*. *Invertebrate Survival Journal,* 12, 22-28.

STEINARSSON, A. & IMSLAND, A. K. 2003. Size dependent variation in optimum growth temperature of red abalone (*Haliotis rufescens*). *Aquaculture,* 224, 353-362.

STEINFATH, M., GROTH, D., LISEC, J. & SELBIG, J. 2008. Metabolite profile analysis: from raw data to regression and classification. *Physiologia Plantarum,* 132, 150-161.

STONE, D. A., HARRIS, J. O., WANG, H., MERCER, G. J., SCHAEFER, E. N. & BANSEMER, M. S. 2013. Dietary protein level and water temperature interactions for greenlip abalone *Haliotis laevigata*. *Journal of Shellfish Research,* 32, 119-130.

STOREY, K. B. 2004. Adventures in oxygen metabolism. *Comparative Biochemistry and Physiology Part B: Biochemistry and Molecular Biology,* 139, 359-369.

STOREY, K. B. 2005. *Functional metabolism: Regulation and adaptation,* Hoboeken, New Jersey, John Wiley & Sons.

STUART, J. & BALLANTYNE, J. 1996. Correlation of environment and phylogeny with the expression of β-hydroxybutyrate dehydrogenase in the mollusca. *Comparative Biochemistry and Physiology Part B: Biochemistry and Molecular Biology,* 114, 153-160.

SUMNER, L. W., AMBERG, A., BARRETT, D., BEALE, M. H., BEGER, R., DAYKIN, C. A., FAN, T. W.-M., FIEHN, O., GOODACRE, R. & GRIFFIN, J. L. 2007. Proposed minimum reporting standards for chemical analysis. *Metabolomics,* 3, 211-221.

SUMNER, L. W., LEI, Z., NIKOLAU, B. J., SAITO, K., ROESSNER, U. & TRENGOVE, R. 2014. Proposed quantitative and alphanumeric metabolite identification metrics. *Metabolomics,* 10, 1047–1049.

T'KINDT, R., MORREEL, K., DEFORCE, D., BOERJAN, W. & VAN BOCXLAER, J. 2009. Joint GC–MS and LC–MS platforms for comprehensive plant metabolomics: Repeatability and sample pre-treatment. *Journal of Chromatography B,* 877, 3572-3580.

TAMAYO, D., AZPEITIA, K., MARKAIDE, P., NAVARRO, E. & IBARROLA, I. 2016. Food regime modulates physiological processes underlying size differentiation in juvenile intertidal mussels *Mytilus galloprovincialis*. *Marine Biology,* 163, 131.

TAMAYO, D., IBARROLA, I., URRUTIA, M. B. & NAVARRO, E. 2011. The physiological basis for inter-individual growth variability in the spat of clams (*Ruditapes philippinarum*). *Aquaculture,* 321, 113-120.

TAMAYO, D., IBARROLA, I., URRUTXURTU, I. & NAVARRO, E. 2014. Physiological basis of extreme growth rate differences in the spat of oyster (*Crassostrea gigas*). *Marine Biology,* 161, 1627-1637.

TAN, B. & MAI, K. 2001. Zinc methionine and zinc sulfate as sources of dietary zinc for juvenile abalone, *Haliotis discus hannai* Ino. *Aquaculture,* 192, 67-84.

TAYLOR, H. & RAGG, N. 2005. The role of body surfaces and ventilation in gas exchange of the abalone, *Haliotis iris*. *Journal of Comparative Physiology B,* 175, 463-478.

TEN DOESCHATE, K. & COYNE, V. 2008. Improved growth rate in farmed *Haliotis midae* through probiotic treatment. *Aquaculture,* 284, 174-179.

TEULIER, L., WEBER, J.-M., CREVIER, J. & DARVEAU, C.-A. 2016. Proline as a fuel for insect flight: enhancing carbohydrate oxidation in hymenopterans. *Proceedings of the Royal Society of London. Series B, Biological Sciences,* 283, 20160333.

THEODORIDIS, G., GIKA, H. G. & WILSON, I. D. 2008. LC-MS-based methodology for global metabolite profiling in metabonomics/metabolomics. *Trends in Analytical Chemistry,* 27, 251-260.

TIELENS, A. G., ROTTE, C., VAN HELLEMOND, J. J. & MARTIN, W. 2002. Mitochondria as we don't know them. *Trends in Biochemical Sciences,* 27, 564-572.

TISCHNER, R., GALLI, M., HEIMER, Y. M., BIELEFELD, S., OKAMOTO, M., MACK, A. & CRAWFORD, N. M. 2007. Interference with the citrulline-based nitric oxide synthase assay by argininosuccinate lyase activity in Arabidopsis extracts. *The FEBS Journal,* 274, 4238-4245.

TRIPP-VALDEZ, M. A., BOCK, C., LUCASSEN, M., LLUCH-COTA, S. E., SICARD, M. T., LANNIG, G. & PÖRTNER, H. O. 2017. Metabolic response and thermal tolerance of green abalone juveniles (*Haliotis fulgens:* Gastropoda) under acute hypoxia and hypercapnia. *Journal of Experimental Marine Biology and Ecology,* 497, 11-18.

TRIVEDI, D. K., HOLLYWOOD, K. A. & GOODACRE, R. 2017. Metabolomics for the masses: the future of metabolomics in a personalized world. *New Horizons in Translational Medicine,* 3, 294-305.

TROELL, M., ROBERTSON-ANDERSSON, D., ANDERSON, R. J., BOLTON, J. J., MANEVELDT, G., HALLING, C. & PROBYN, T. 2006. Abalone farming in South Africa: An overview with perspectives on kelp resources, abalone feed, potential for on-farm seaweed production and socio-economic importance. *Aquaculture,* 257, 266-281.

TUGIZIMANA, F., PIATER, L. & DUBERY, I. 2013. Plant metabolomics: A new frontier in phytochemical analysis. *South African Journal of Science,* 109, 01-11.

TUNG, C. H. & ALFARO, A. C. 2012. Alternative protein sources in artificial diets for New Zealand's black-footed abalone, *Haliotis iris*, Martyn 1784, juveniles. *Journal of the World Aquaculture Society,* 43, 1-29.

URSCHEL, K., ESCOBAR, J., MCCUTCHEON, L. & GEOR, R. 2014. Insulin infusion stimulates whole-body protein synthesis and activates the upstream and downstream effectors of mechanistic target of rapamycin signaling in the gluteus medius muscle of mature horses. *Domestic Animal Endocrinology,* 47, 92-100.

VAN DEN BERG, R. A., HOEFSLOOT, H. C., WESTERHUIS, J. A., SMILDE, A. K. & VAN DER WERF, M. J. 2006. Centering, scaling, and transformations: improving the biological information content of metabolomics data. *BMC Genomics,* 7, 142.

VAN DER MERWE, M., FRANCHINI, P. & ROODT-WILDING, R. 2011. Differential growth-related gene expression in abalone (*Haliotis midae*). *Marine Biotechnology,* 13, 1125-1139.

VELASQUEZ, M. T., RAMEZANI, A., MANAL, A. & RAJ, D. S. 2016. Trimethylamine N-oxide: The good, the bad and the unknown. *Toxins,* 8, 326.

VENTER, L., JANSEN VAN RENSBURG, P., LOOTS, D. T., VOSLOO, A. & LINDEQUE, J. Z. 2016a. Untargeted metabolite profiling of abalone using gas chromatography mass spectrometry. *Food Analytical Methods,* 9, 1254-1261.

VENTER, L., JANSEN VAN RENSBURG, P. J., LOOTS, D. T., VOSLOO, A. & LINDEQUE, J. Z. 2017. From untargeted LC-QTOF analysis to characterisation of opines in abalone adductor muscle: Theory meets practice. *Journal of Chromatography B,* 1071, 44-48.

VENTER, L., LINDEQUE, Z., JANSEN VAN RENSBURG, P., VAN DER WESTHUIZEN, F., SMUTS, I. & LOUW, R. 2015. Untargeted urine metabolomics reveals a biosignature for muscle respiratory chain deficiencies. *Metabolomics,* 11, 111-121.

VENTER, L., LOOTS, D. T., VOSLOO, A., JANSEN VAN RENSBURG, P. & LINDEQUE, J. Z. 2016b. Abalone growth and associated aspects: Now from a metabolic perspective. *Reviews in Aquaculture,* 0.1111/raq.12181.

VERPOORTE, R., CHOI, Y., MUSTAFA, N. & KIM, H. 2008. Metabolomics: back to basics. *Phytochemistry Reviews,* 7, 525-537.

VIANA, M. T., D'ABRAMO, L. R., GONZALEZ, M. A., GARCÍA-SUÁREZ, J. V., SHIMADA, A. & VÁSQUEZ-PELÁEZ, C. 2007. Energy and nutrient utilization of juvenile green abalone (*Haliotis fulgens*) during starvation. *Aquaculture,* 264, 323-329.

VIANT, M. R., ROSENBLUM, E. S. & TJEERDEMA, R. S. 2001. Optimized method for the determination of phosphoarginine in abalone tissue by high-performance liquid chromatography. *Journal of Chromatography B: Biomedical Sciences and Applications,* 765, 107-111.

VIANT, M. R., ROSENBLUM, E. S. & TJEERDEMA, R. S. 2003. NMR-based metabolomics: A powerful approach for characterizing the effects of environmental stressors on organism health. *Environmental Science & Technology,* 37, 4982-4989.

VIANT, M. R. & SOMMER, U. 2013. Mass spectrometry based environmental metabolomics: A primer and review. *Metabolomics,* 9, 144-158.

VINAIXA, M., SCHYMANSKI, E. L., NEUMANN, S., NAVARRO, M., SALEK, R. M. & YANES, O. 2016. Mass spectral databases for LC/MS-and GC/MS-based metabolomics: State of the field and future prospects. *Trends in Analytical Chemistry,* 78, 23-35.

VLOK, A. C., DIFFORD, G. F., RHODE, C. & BRINK, D. 2016. An assessment of hatchery cohort growth rates of South African abalone, *Haliotis midae*, across four commercial environments. *Journal of the World Aquaculture Society,* 47, 658-666.

VOSLOO, A., LAAS, A. & VOSLOO, D. 2013a. Differential responses of juvenile and adult South African abalone (*Haliotis midae* Linnaeus) to low and high oxygen levels. *Comparative Biochemistry and Physiology Part A: Molecular & Integrative Physiology,* 164, 192-199.

VOSLOO, A. & VAN RENSBURG, L. 2009. Uses of amino acid and amino acid supplements thereof. U.S. patent 20090272328, filed Sep 19, 2006 and issued Nov 5, 2009.

VOSLOO, A. & VOSLOO, D. 2006. Routes of water loss in South African abalone (*Haliotis midae*) during aerial exposure. *Aquaculture,* 261, 670-677.

VOSLOO, D., VAN RENSBURG, L. & VOSLOO, A. 2013b. Oxidative stress in abalone: The role of temperature, oxygen and L-proline supplementation. *Aquaculture,* 416, 265-271.

VOSLOO, D. & VOSLOO, A. 2010. Response of cold-acclimated, farmed South African abalone (*Haliotis midae*) to short-term and long-term changes in temperature. *Journal of Thermal Biology,* 35, 317-323.

VOSLOO, D., VOSLOO, A., MORILLION, E. J., SAMUELS, J. N. & SOMMER, P. 2013c. Metabolic readjustment in juvenile South African abalone (*Haliotis midae*) acclimated to combinations of temperature and dissolved oxygen levels. *Journal of Thermal Biology,* 38, 458-466.

VUCKOVIC, D. 2012. Current trends and challenges in sample preparation for global metabolomics using liquid chromatography–mass spectrometry. *Analytical and Bioanalytical Chemistry,* 403, 1523-1548.

WAGNER, S., SCHOLZ, K., SIEBER, M., KELLERT, M. & VOELKEL, W. 2007. Tools in metabonomics: An integrated validation approach for LC-MS metabolic profiling of mercapturic acids in human urine. *Analytical Chemistry,* 79, 2918-2926.

WALLACE, D. C. & FAN, W. 2010. Energetics, epigenetics, mitochondrial genetics. *Mitochondrion,* 10, 12-31.

WANG, H.-X., QIN, L., WANG, Y., ZHOU, D.-Y., SONG, S., WANG, X.-S. & ZHU, B.-W. 2014. Effects of heating conditions on fatty acids and volatile compounds in foot muscle of abalone *Haliotis discus hannai* Ino. *Fisheries Science,* 80, 1097-1107.

WANG, Q., YANG, C., DU, X., LIU, X., SUN, R. & DENG, Y. 2016. Growth performance and biochemical composition of juvenile pearl oyster *Pinctada martensii*. *Aquaculture International,* 24, 995-1005.

WANT, E. J., MASSON, P., MICHOPOULOS, F., WILSON, I. D., THEODORIDIS, G., PLUMB, R. S., SHOCKCOR, J., LOFTUS, N., HOLMES, E. & NICHOLSON, J. K. 2013. Global metabolic profiling of animal and human tissues via UPLC-MS. *Nature Protocols,* 8, 17-32.

WANT, E. J., WILSON, I. D., GIKA, H., THEODORIDIS, G., PLUMB, R. S., SHOCKCOR, J., HOLMES, E. & NICHOLSON, J. K. 2010. Global metabolic profiling procedures for urine using UPLC–MS. *Nature Protocols,* 5, 1005-1018.

WARDLAW, G. M. & INSEL, P. M. 2006. *Perspectives in nutrition,* New York, McGraw-Hill Higher Education.

WARRACK, B. M., HNATYSHYN, S., OTT, K.-H., REILY, M. D., SANDERS, M., ZHANG, H. & DREXLER, D. M. 2009. Normalization strategies for metabonomic analysis of urine samples. *Journal of Chromatography B,* 877, 547-552.

WASKO, A. P., MARTINS, C., OLIVEIRA, C. & FORESTI, F. 2003. Non-destructive genetic sampling in fish. An improved method for DNA extraction from fish fins and scales. *Hereditas,* 138, 161-165.

WATANABE, M., MEYER, K. A., JACKSON, T. M., SCHOCK, T. B., JOHNSON, W. E. & BEARDEN, D. W. 2015. Application of NMR-based metabolomics for environmental assessment in the Great Lakes using zebra mussel (*Dreissena polymorpha*). *Metabolomics,* 11, 1302-1315.

WATFORD, M. 2003. The urea cycle: Teaching intermediary metabolism in a physiological setting. *Biochemistry and Molecular Biology Education,* 31, 289-297.

WEHRENS, R., HAGEMAN, J. A., VAN EEUWIJK, F., KOOKE, R., FLOOD, P. J., WIJNKER, E., KEURENTJES, J. J., LOMMEN, A., VAN EEKELEN, H. D. & HALL, R. D. 2016. Improved batch correction in untargeted MS-based metabolomics. *Metabolomics,* 12, 1-12.

WELBORN, J. & MANAHAN, D. 1995. Taurine metabolism in larvae of marine invertebrate molluscs (Bilvalvia, Gastropoda). *Journal of Experimental Biology,* 198, 1791-1799.

WELLS, R. M. & BALDWIN, J. 1995. A comparison of metabolic stress during air exposure in two species of New Zealand abalone, *Haliotis iris* and *Haliotis australis:* Implications for the handling and shipping of live animals. *Aquaculture,* 134, 361-370.

WELLS, R. M., BALDWIN, J., SPEED, S. R. & WEBER, R. E. 1998a. Haemocyanin function in the New Zealand abalones *Haliotis iris* and *H. australis*: Relationships between oxygen-binding properties, muscle metabolism and habitat. *Marine and Freshwater Research,* 49, 143-149.

WELLS, R. M., MCSHANE, P. E., LING, N., WONG, R. J., LEE, T. O. & BALDWIN, J. 1998b. Effect of wave action on muscle composition, metabolites and growth indices in the New Zealand abalone, Paua (*Haliotis iris*), with implications for harvesting and aquaculture. *Comparative Biochemistry and Physiology Part B: Biochemistry and Molecular Biology,* 119, 129-136.

WETCHATENG, T., FRIEDMAN, C. S., WIGHT, N. A., LEE, P.-Y., TENG, P. H., SRIURAIRATTANA, S., WONGPRASERT, K. & WITHYACHUMNARNKUL, B. 2010. Withering syndrome in the abalone *Haliotis diversicolor supertexta*. *Diseases of Aquatic Organisms,* 90, 69-76.

WHITNEY, E. & ROLFES, S. R. 2008. *Understanding Nutrition,* Belmont, California, Cengage Learning.

WILBUR, K. M. & HOCHACHKA, P. W. 2016. *The Mollusca: Environmental Biochemistry and Physiology,* New York, Academic Press.

WILLERS, C., VAN RENSBURG, P. J. J. & CLAASSENS, S. 2016. Can a metabolomics-based approach be used as alternative to analyse fatty acid methyl esters from soil microbial communities? *Soil Biology and Biochemistry,* 103, 417-428.

WILSON, D. F. 2013. Regulation of cellular metabolism: Programming and maintaining metabolic homeostasis. *Journal of Applied Physiology,* 115, 1583-1588.

WILSON, K. & WALKER, J. 2010. *Principles and techniques of biochemistry and molecular biology*, Cambridge university press.

WINGROVE, J. A. & O'FARRELL, P. H. 1999. Nitric oxide contributes to behavioral, cellular, and developmental responses to low oxygen in Drosophila. *Cell,* 98, 105-114.

WOOD, A. & BUXTON, C. 1996. Aspects of the biology of the abalone *Haliotis midae* (Linne, 1758) on the east coast of South Africa. Feeding biology. *South African Journal of Marine Science,* 17, 61-68.

WU, G. 2009. Amino acids: metabolism, functions, and nutrition. *Amino Acids,* 37, 1-17.

WU, G., BAZER, F. W., BURGHARDT, R. C., JOHNSON, G. A., KIM, S. W., KNABE, D. A., LI, P., LI, X., MCKNIGHT, J. R. & SATTERFIELD, M. C. 2011. Proline and hydroxyproline metabolism: implications for animal and human nutrition. *Amino Acids,* 40, 1053-1063.

WU, G., BAZER, F. W., DAI, Z., LI, D., WANG, J. & WU, Z. 2014. Amino acid nutrition in animals: protein synthesis and beyond. *Annual Review of Animal Biosciences* 2, 387-417.

WU, H., SOUTHAM, A. D., HINES, A. & VIANT, M. R. 2008. High-throughput tissue extraction protocol for NMR-and MS-based metabolomics. *Analytical Biochemistry,* 372, 204-212.

XIA, J., BROADHURST, D. I., WILSON, M. & WISHART, D. S. 2013. Translational biomarker discovery in clinical metabolomics: An introductory tutorial. *Metabolomics,* 9, 280-299.

XIA, J., MANDAL, R., SINELNIKOV, I. V., BROADHURST, D. & WISHART, D. S. 2012. MetaboAnalyst 2.0—a comprehensive server for metabolomic data analysis. *Nucleic Acids Research,* 40, W127-W133.

XIA, J., PSYCHOGIOS, N., YOUNG, N. & WISHART, D. S. 2009. MetaboAnalyst: A web server for metabolomic data analysis and interpretation. *Nucleic Acids Research,* 37, W652-W660.

XIA, J., SINELNIKOV, I. V., HAN, B. & WISHART, D. S. 2015. MetaboAnalyst 3.0—making metabolomics more meaningful. *Nucleic Acids Research,* 43, 251-257.

XU, F., ZOU, L., ONG, C. N., ZOU, L., ONG, C. N. & ONG, C. N. 2010. Experiment-originated variations, and multi-peak and multi-origination phenomena in derivatization-based GC-MS metabolomics. *TrAC Trends in Analytical Chemistry,* 29, 269-280.

XU, Y. & GOODACRE, R. 2012. Multiblock principal component analysis: an efficient tool for analyzing metabolomics data which contain two influential factors. *Metabolomics,* 8, 37-51.

YANG, Y., CRUICKSHANK, C., ARMSTRONG, M., MAHAFFEY, S., REISDORPH, R. & REISDORPH, N. 2013. New sample preparation approach for mass spectrometry-based profiling of plasma results in improved coverage of metabolome. *Journal of Chromatography A,* 1300, 217-226.

YI, L., DONG, N., YUN, Y., DENG, B., REN, D., LIU, S. & LIANG, Y. 2016. Chemometric methods in data processing of mass spectrometry-based metabolomics: A review. *Analytica Chimica Acta,* 914, 17-34.

YOUNG, T. & ALFARO, A. C. 2016. Metabolomic strategies for aquaculture research: A primer. *Reviews in Aquaculture,* doi: 10.1111/raq.12146.

YOUNG, T., ALFARO, A. C. & VILLAS-BÔAS, S. G. 2016. Metabolic profiling of mussel larvae: Effect of handling and culture conditions. *Aquaculture International,* 24, 843-856.

YOUNG, T., KESARCODI-WATSON, A., ALFARO, A. C., MERIEN, F., NGUYEN, T. V., MAE, H., LE, D. V. & VILLAS-BÔAS, S. 2017. Differential expression of novel metabolic and immunological biomarkers in oysters challenged with a virulent strain of OsHV-1. *Developmental & Comparative Immunology,* 73, 229-245.

YUAN, J., KARIMI, A., ZORNES, S., GOODGAME, S., MUSSINI, F., LU, C. & WALDROUP, P. 2012. Evaluation of the role of glycine in low-protein amino acid-supplemented diets. *Journal of Applied Poultry Research,* 21, 726-737.

ZELENA, E., DUNN, W. B., BROADHURST, D., FRANCIS-MCINTYRE, S., CARROLL, K. M., BEGLEY, P., O'HAGAN, S., KNOWLES, J. D., HALSALL, A. & HUSERMET CONSORTIUM 2009. Development of a robust and repeatable UPLC−MS method for the long-term metabolomic study of human serum. *Analytical Chemistry,* 81, 1357-1364.

ZHAI, Y., SUN, Z., ZHANG, J., KANG, K., CHEN, J. & ZHANG, W. 2015. Activation of the TOR signalling pathway by glutamine regulates insect fecundity. *Scientific Reports,* 5.

ZHANG, A., SUN, H., WANG, P., HAN, Y. & WANG, X. 2012. Modern analytical techniques in metabolomics analysis. *Analyst,* 137, 293-300.

ZHOU, J., CHEN, B. & CAI, Z. 2015. Metabolomics-based approach for assessing the toxicity mechanisms of dibutyl phthalate to abalone (*Haliotis diversicolor supertexta*). *Environmental Science and Pollution Research,* 22, 5092-5099.

ZOTTI, M., DE PASCALI, S. A., DEL COCO, L., MIGONI, D., CARROZZO, L., MANCINELLI, G. & FANIZZI, F. P. 2016. 1 H NMR metabolomic profiling of the blue crab (*Callinectes sapidus)* from the Adriatic Sea (SE Italy): A comparison with warty crab (*Eriphia verrucosa*), and edible crab (*Cancer pagurus*). *Food Chemistry,* 196, 601-609.

APPENDIX A

UNKNOWN FEATURE DATA

”The human world is a mess. Life under the sea is better than anything they got up there.”

– Sebastian, The Little Mermaid

Unidentified significant features resulting from functional and environmental hypoxia

Features found to be significant ($p < 0.05$ and $d > 0.8$) from the functional hypoxia (Table A1) and environmental hypoxia (Table A2) experiments conducted on *H. midae* as described in Chapter 5. The respective features have all been assigned a Level 3 identification based on the fact that fragmentation spectra were also obtained together with an accurate mass. Additional library matches did not result in confidant findings, resulting in uncertainty of the listed compounds. In the tables below each significant feature is shown as an "unknown" together with the tentative identification made by the respective analytical platform. In Table A1 the first 11 unknowns were found by LC-QTOF analysis and the remaining 95 features by UPLC-IM-QTOF analysis. In Table A2 unknown 1 to 10 was detected by LC-QTOF analysis and unknown 11 to 149 by UPLC-IM-QTOF analysis. Furthermore the tables show the *p*- and *d*-values calculated with a positive *d*-value indicating an increase and a negative d-value a decrease in metabolite response when compared to the control group. Also the abalone tissue in which the feature was detected is shown in terms adductor muscle (AM), foot muscle (FM), haemolymph (H), epipodial tissue (E), left gill (LG) and right gill (RG) findings.

Table A.1: Unknown findings of *H. midae* subjected to functional hypoxia

Feature	*p*-value	*d*-value	Tissue	Feature	*p*-value	*d*-value	Tissue
Unknown 1 - Palmitoleoyl Ethanolamide	3.22E-08	3.72	H	Unknown 54 - DG(20:1(11Z)/15:0/0:0)	2.39E-02	1.41	FM
Unknown 2 - Lithocholate 3-O-glucuronide	5.70E-04	-2.02	RG	Unknown 55 - CPA(18:0/0:0)	2.47E-02	-1.30	E
Unknown 3 - Catechin	5.08E-03	1.51	E	Unknown 56 - Panaxynol linoleate	2.56E-02	1.21	RG
Unknown 4 - Deoxyuridine	8.46E-03	-1.03	E	Unknown 57 - PC(16:0/2:0)	2.60E-02	1.08	RG
Unknown 5 - Chenodeoxycholic acid	9.02E-03	1.23	H	Unknown 58 - Lucidenic acid K	2.67E-02	0.91	E
Unknown 6 - Amion-deoxythimidine glucuronide	1.08E-02	-1.28	AM	Unknown 59 - N-oleoyl GABA	2.70E-02	1.17	E
Unknown 7 - D-Erythro-imidazole-glycerol-phosphate	1.40E-02	-1.61	AM	Unknown 60 - Octanal propyleneglycol acetal	2.70E-02	1.15	RG
Unknown 8 - Deoxysepiapterin	2.98E-02	-1.50	AM	Unknown 61 - LysoPC(O-18:0)	2.71E-02	1.17	E
Unknown 9 - 12(13)Ep-9-KODE	3.01E-02	1.07	F	Unknown 62 - LysoPC(20:2(11Z,14Z))	2.74E-02	-1.18	E
Unknown 10 - Testosterone glucuronide	3.07E-02	-1.28	AM	Unknown 63 - Dihydrodeoxy-8-epiaustdiol	2.76E-02	-1.12	AM
Unknown 11 - Dihydro-trihydroxy-leukotriene B4	3.34E-02	-0.86	RG	Unknown 64 - Norecasantalal	2.88E-02	1.03	RG
Unknown 12 - Phytosphingosine	7.12E-05	2.55	LG	Unknown 65 - Cucurbitacin S	2.93E-02	1.25	AM
Unknown 13 - Cer(d16:1/17:0)	1.09E-04	1.86	E	Unknown 66 - LysoPC(P-18:0)	2.95E-02	1.08	RG
Unknown 14 - Cer(d16:1/17:0)2-Hydroxyacorenone	7.29E-04	2.44	E	Unknown 67 - PE(17:2(9Z,12Z)/16:0)	2.97E-02	1.41	FM
Unknown 15 - Cer(d16:1/17:0)alpha-Tocopherol succinate	7.57E-04	2.05	E	Unknown 68 - N1,N10-Dicoumaroylspermidine	3.01E-02	1.18	E
Unknown 16 - Cer(d16:1/17:0)	7.83E-04	0.84	E	Unknown 69 - TG(18:4(6Z,9Z,12Z,15Z)	3.01E-02	-1.07	E
Unknown 17 - Cer(d16:1/17:0)PF 1163B	2.06E-03	-2.07	E	Unknown 70 - PE(19:0/20:5(5Z,8Z,11Z,14Z,17Z))	3.05E-02	-1.30	FM
Unknown 18 - Cer(d16:1/17:0)4-hydroxy-8-sphingenine	2.09E-03	1.80	RG	Unknown 71 - Lucidumol A	3.07E-02	-0.91	E
Unknown 19 - Cer(d16:1/17:0)PC(20:5(5Z,8Z,11Z,14Z,17Z)/21:0)	2.35E-03	-1.83	RG	Unknown 72 - (E)-Piperolein A	3.08E-02	-1.12	AM
Unknown 20 - Endoxifen	3.15E-03	-1.98	RG	Unknown 73 - LysoPE(16:0/0:0)	3.14E-02	-1.02	E
Unknown 21 - FS4 toxin	3.25E-03	1.82	RG	Unknown 74 - Robustocin	3.21E-02	-1.19	E
Unknown 22 - PC(20:5/0:0)	3.26E-03	1.87	RG	Unknown 75 - Persicaxanthin	3.27E-02	1.05	RG
Unknown 23 - 13-(beta-D-glucosyloxy)docosanoate	4.01E-03	-1.71	E	Unknown 76 - DG(15:0/20:0/0:0)	3.30E-02	1.17	FM
Unknown 24 - 12-Hydroxy-12-octadecanoylcarnitine	4.73E-03	-1.38	E	Unknown 77 - NK154183B	3.30E-02	-1.23	RG
Unknown 25 - PE(O-18:1(9Z)/0:0)	5.42E-03	-1.58	AM	Unknown 78 - (5Z)-4,4-difluorovitamin D3	3.30E-02	0.88	AM
Unknown 26 - LysoPC(20:0)	5.82E-03	1.58	RG	Unknown 79 - PE(15:0/22:5)	3.41E-02	1.16	LG
Unknown 27 - 3-hexaprenyl-4,5-dihydroxybenzoate	6.64E-03	-1.62	E	Unknown 80 - [8]-Shogaol	3.48E-02	1.22	RG
Unknown 28 - PE(22:6(4Z,7Z,10Z,13Z,16Z,19Z)/16:0)	6.99E-03	-1.49	FM	Unknown 81 - LysoPE(0:0/22:5(4Z,7Z,10Z,13Z,16Z))	3.53E-02	1.12	FM
Unknown 29 - 2-(2-Hydroxy-4-methylphenyl)-3-pentanone	7.38E-03	1.38	E	Unknown 82 - PC(20:5(5Z,8Z,11Z,14Z,17Z)	3.64E-02	-0.97	LG
Unknown 30 - 4,5-Dimethyl-2-octylthiazole	7.76E-03	-1.72	E	Unknown 83 - Zedoarol	3.79E-02	-0.89	RG
Unknown 31 - Boviquinone 4	8.11E-03	1.52	RG	Unknown 84 - PC(O-18:0/22:5(4Z,7Z,10Z,13Z,16Z))	3.80E-02	-1.16	RG
Unknown 32 - PC(P-18:0/14:1(9Z))	1.17E-02	-1.42	RG	Unknown 85 - PG(18:2(9Z,12Z)/18:0)	3.83E-02	-1.03	LG
Unknown 33 - N-nonadecanoyl	1.22E-02	-1.57	RG	Unknown 86 - Prostaglandin E2 ethanolamide	3.87E-02	1.08	RG
Unknown 34 - PC(18:0/18:3(6Z,9Z,12Z))	1.23E-02	-1.26	FM	Unknown 87 - Oxprenolol	3.90E-02	1.01	RG
Unknown 35 - Persicaxanthin	1.27E-02	1.43	FM	Unknown 88 - PA(20:5(5Z,8Z,11Z,14Z,17Z)/0:0)	4.25E-02	1.12	RG

Unknown 36 - Kaempferol 3,7,4'-tri-O-sulfate	1.33E-02	1.27	E	Unknown 89 - PC(P-16:0/18:4(6Z,9Z,12Z,15Z))	4.30E-02	-1.01	RG
Unknown 37 - Panaxatriol	1.49E-02	-1.45	E	Unknown 90 - 3-O-Sulfogalactosylceramide	4.35E-02	1.03	LG
Unknown 38 - C20 phytosphingosine	1.55E-02	-1.32	FM	Unknown 91 - PE(P-18:0/22:4(7Z,10Z,13Z,16Z))	4.35E-02	-1.12	FM
Unknown 39 - 20-Trihydroxy-leukotriene-B4	1.67E-02	0.78	E	Unknown 92 - beta-Boswellic acid acetate	4.36E-02	0.95	E
Unknown 40 - Fumigaclavine B	1.67E-02	-1.41	E	Unknown 93 - LysoPC(20:2(11Z,14Z))	4.37E-02	-1.21	AM
Unknown 41 - PS(20:2(11Z,14Z)/0:0)	1.68E-02	1.30	FM	Unknown 94 - Fencamfamine	4.37E-02	-1.04	E
Unknown 42 - LysoPC(P-18:0)	1.71E-02	-1.25	E	Unknown 95 - PC(20:0/15:0)	4.38E-02	1.07	RG
Unknown 43 - PC(18:1(9Z)	1.74E-02	1.35	AM	Unknown 96 - Perindoprilat glucuronide	4.44E-02	0.98	AM
Unknown 44 - PE(20:0/15:0)	1.78E-02	1.19	RG	Unknown 97 - PC(15:0/20:0)	4.47E-02	-0.94	RG
Unknown 45 - LysoPE(0:0/18:3(9Z,12Z,15Z))	1.87E-02	-1.04	E	Unknown 98 - PC(16:1(9Z)/P-18:1(11Z))	4.55E-02	-0.92	RG
Unknown 46 - Persicachrome	1.89E-02	-1.02	RG	Unknown 99 - 2-hydroxydesipramine	4.62E-02	-0.94	RG
Unknown 47 - LysoPC(18:2(9Z,12Z))	1.91E-02	-1.09	E	Unknown 100 - Phosphoglycolic acid	4.68E-02	1.17	AM
Unknown 48 - Carpaine	1.96E-02	1.18	RG	Unknown 101 - PI(16:0/16:0)	4.70E-02	-1.28	FM
Unknown 49 - PC(21:0/20:5(5Z,8Z,11Z,14Z,17Z))	2.03E-02	-1.44	RG	Unknown 102 - PE(16:1(9Z)/20:0)	4.73E-02	1.26	FM
Unknown 50 - LysoPE(0:0/20:5(5Z,8Z,11Z,14Z,17Z))	2.09E-02	1.09	RG	Unknown 103 - LysoPE(0:0/18:1(9Z))	4.80E-02	1.17	FM
Unknown 51 - CDP-DG(18:0/18:0)	2.30E-02	-1.30	AM	Unknown 104 - 5-Methylthioribose	4.83E-02	0.94	E
Unknown 52 - PA(22:6(4Z,7Z,10Z,13Z,16Z,19Z)	2.35E-02	-1.40	FM	Unknown 105 - azinphos-methyl	4.86E-02	1.04	FM
Unknown 53 - Netilmicin	2.35E-02	-1.00	E	Unknown 106 - PC(o-20:0/18:3(9Z,12Z,15Z))	4.89E-02	-1.17	RG

Table A.2: Unknown findings of *H. midae* subjected to environmental hypoxia

Feature	*p*-value	*d*-value	Tissue	Feature	*p*-value	*d*-value	Tissue
Unknown1 - 12(13)ep-9-KODE	3.24E-16	15.06	AM	Unknown76 - Melleolide K	1.72E-02	1.41	E
Unknown2 - Chenodeoxycholic acid glycine conjugate	1.54E-15	20.90	AM	Unknown77 - emtricitabine	1.75E-02	1.47	E
Unknown3 - Chenodeoxycholic acid	3.21E-05	1.37	AM	Unknown78 - xanthurenic acid 8-O-sulfate	1.77E-02	-1.39	AM
Unknown4 - Hydroxy-oregnane-one	5.60E-05	1.33	AM	Unknown79 - Sterebin G	1.78E-02	1.81	E
Unknown5 - Dihydro-trihydroxy-leukotriene	7.31E-05	-0.87	E	Unknown80 - LysoPC(18:1(9Z))	1.83E-02	-1.19	E
Unknown6 - Isopentenyladenine	7.20E-03	-1.62	LG	Unknown81 - 2-Hydroxyacorenone	1.84E-02	1.65	E
Unknown7 - Arachidyl carnitine	1.69E-02	1.65	H	Unknown82 - Isolimonic acid 16->17-lactone	1.85E-02	0.81	RG
Unknown8 - 2-Isopropyl-3-oxosuccinate	2.73E-02	1.37	H	Unknown83 - 13-(beta-D-glucosyloxy)docosanoate	1.85E-02	-1.41	E
Unknown9 - Ecgonine	3.55E-02	1.15	RG	Unknown84 - (3S)-3-[(2S)-2-amino-3-hydroxybutyl]pyrrolidin-2-one	1.86E-02	-1.50	AM
Unknown10 - Oxomethylthiobutanoate	3.58E-02	-1.03	RG	Unknown85 - Cyclohexaneundecanoic acid	1.94E-02	-1.36	FM
Unknown11 - (5Z)-4,4-difluorovitamin D3	1.33E-08	6.25	AM	Unknown86 - 7a,12a-Dihydroxy-5b-cholestan-3-one	1.95E-02	-1.24	E
Unknown12 - Lauroyl diethanolamide	1.30E-07	5.51	LG	Unknown87 - 2,3-Pentanedione	1.95E-02	1.27	AM
Unknown13 - DG(18:2n6/0:0/20:5n3)	4.19E-06	-1.12	E	Unknown88 - Cefoxitin	2.01E-02	1.24	AM
Unknown14 - 2-aminohexadecanoic acid	3.00E-05	3.33	RG	Unknown89 - 6-beta-hydroxymedroxyprogesterone	2.04E-02	-1.53	FM
Unknown15 - N-Hexadecanoylpyrrolidine	4.07E-05	1.58	E	Unknown90 - 4,5-Dimethyl-2-octylthiazole	2.09E-02	-1.22	E
Unknown16 - Taurochenodeoxycholate-7-sulfate	7.42E-05	1.96	E	Unknown91 - LysoPC(20:2(11Z,14Z))	2.11E-02	-1.27	AM
Unknown17 - Octadecanamide	1.42E-04	2.46	RG	Unknown92 - Oxprenolol	2.27E-02	0.79	E
Unknown18 - 5-amino-5-deoxy-3-dehydroshikimic acid zwitterion	1.66E-04	-2.96	AM	Unknown93 - Polycartine B	2.34E-02	1.38	AM
Unknown19 - Calendic acid	1.81E-04	-2.49	RG	Unknown94 - (S)-Edulinine	2.35E-02	-1.29	FM
Unknown20 - 2-amino-5-oxohexanoate	1.81E-04	-2.59	AM	Unknown95 - Ganglioside GM2 (d18:1/26:0)	2.41E-02	0.89	E
Unknown21 - Traumatic acid	3.27E-04	2.26	RG	Unknown96 - LysoPC(P-18:1(9Z))	2.54E-02	1.30	FM
Unknown22 - hydroxypropoxy]-1,2,3,4-tetrahydro-1-naphthol(1+)	4.82E-04	0.83	E	Unknown97 - juniperic acid	2.55E-02	-1.40	AM
Unknown23 - alpha-Tocopherol succinate	5.60E-04	2.43	E	Unknown98 - Gingerglycolipid C	2.63E-02	-1.17	AM
Unknown24 - Bacteriorubixanthinal	8.30E-04	-2.28	FM	Unknown99 - Annoglabasin A	2.70E-02	-1.12	E
Unknown25 - Fenoldopam	9.81E-04	2.10	RG	Unknown100 - PE(12:0/22:2(13Z,16Z))	2.71E-02	-1.22	RG
Unknown26 - 22-hydroxy-23,24,25,26,27-pentanorvitamin D3	1.03E-03	-1.77	E	Unknown101 - LysoPE(18:0/0:0)	2.73E-02	-1.12	AM
Unknown27 - alpha-Carboxy-delta-decalactone	1.34E-03	2.04	RG	Unknown102 - CPA(18:1(9Z)/0:0)	2.75E-02	-1.04	E
Unknown28 - dienestrol	1.68E-03	-2.00	AM	Unknown103 - Armillane	2.77E-02	-1.07	AM
Unknown29 - beta-penteic acid	1.79E-03	1.96	FM	Unknown104 - Ginsenoside F2	2.77E-02	-1.27	FM
Unknown30 - Annoglabasin E	1.81E-03	-1.54	AM	Unknown105 - PS(17:0/18:2(9Z,12Z))	2.79E-02	-1.29	RG
Unknown31 - CDP-DG(18:0/18:0)	1.89E-03	-1.82	AM	Unknown106 - AS 1-5	2.84E-02	-1.12	FM
Unknown32 - Phytosphingosine	2.59E-03	1.63	RG	Unknown107 - AICAR	2.85E-02	1.28	E
Unknown33 - dihydrochanoclavine-I aldehyde	2.71E-03	-2.17	AM	Unknown108 - Dodecanedioylcarnitine	2.87E-02	-1.20	FM
Unknown34 - PE(19:0/20:5(5Z,8Z,11Z,14Z,17Z))	2.91E-03	-1.75	FM	Unknown109 - Gymnodimine	2.89E-02	1.26	RG
Unknown35 - alpha-hydroxycholestanol	3.10E-03	1.55	LG	Unknown110 - Mirtazapine	2.90E-02	0.94	E
Unknown36 - Phosphoglycolic acid	3.12E-03	1.79	AM	Unknown111 - (S)-2,3,4,5-tetrahydropyridine-2-carboxylate	2.92E-02	-1.31	FM
Unknown37 - Lucidenic acid K	3.20E-03	1.27	E	Unknown112 - 1-Octene	2.94E-02	-1.27	AM
Unknown38 - 2-Keto-6-aminocaproate	3.24E-03	1.64	E	Unknown113 - PE(P-16:0/13:0)	2.95E-02	1.27	RG
Unknown39 - DG(15:0/20:0/0:0)	3.60E-03	2.02	FM	Unknown114 - Panaxynol linoleate	3.00E-02	1.13	RG
Unknown40 - 12-Hydroxy-12-octadecanoylcarnitine	4.10E-03	-1.31	E	Unknown115 - PE(19:0/14:0)	3.01E-02	-1.17	AM
Unknown41 - Guggulsterone	4.35E-03	-1.57	FM	Unknown116 - PE(P-16:0e/0:0)	3.10E-02	-0.99	AM
Unknown42 - DG(20:4(5Z,8Z,11Z,14Z)	4.50E-03	-1.71	E	Unknown117 - LysoPE(0:0/20:0)	3.16E-02	-0.95	E
Unknown43 - LysoPC(17:0)	4.66E-03	-1.39	E	Unknown118 - DG(15:0/0:0/20:5n3)	3.23E-02	0.91	E
Unknown44 - Acrimarine I	4.87E-03	1.44	E	Unknown119 - PE(22:2(13Z,16Z)/16:0)	3.26E-02	1.01	RG
Unknown45 - p-Hydroxyphenobarbital	5.02E-03	-1.68	AM	Unknown120 - decaethylene glycol	3.32E-02	-1.25	AM
Unknown46 - beta-Boswellic acid acetate	5.05E-03	1.59	E	Unknown121 - Gentamicin	3.33E-02	-0.97	E
Unknown47 - Pseudomonine	5.06E-03	-1.71	AM	Unknown122 - PE(15:0/15:0)	3.35E-02	-1.02	FM
Unknown48 - PC(12:0/18:1(9Z))	5.99E-03	-1.46	FM	Unknown123 - 2-Oxomelatonin	3.52E-02	-1.31	AM
Unknown49 - PE(O-18:1(9Z)/0:0)	6.04E-03	-1.86	AM	Unknown124 - PE(15:0/18:1(9Z))	3.62E-02	-1.01	FM
Unknown50 - N-nonadecanoyl5-1-phosphocholine	6.31E-03	-1.75	RG	Unknown125 - PE(P-20:0/22:4(7Z,10Z,13Z,16Z))	3.66E-02	1.03	LG
Unknown51 - 4'-N-desmethylolanzapine	6.68E-03	-1.80	AM	Unknown126 - 5-Methylcytidine	3.73E-02	-1.16	LG

Unknown52 - sulfacetamide(1-)	6.96E-03	1.55	E	Unknown127 - PE(19:0/18:3(9Z,12Z,15Z))	3.87E-02	-0.99	FM
Unknown53 - 7-Pentacosanone	7.72E-03	1.27	H	Unknown128 - Muricatin C	3.87E-02	1.08	LG
Unknown54 - LysoPE(15:0/0:0)	7.89E-03	-1.06	RG	Unknown129 - Aristolodione	3.88E-02	-1.32	AM
Unknown55 - LysoPE(0:0/18:1(9Z))	8.37E-03	-1.42	AM	Unknown130 - Sulfated Dihydromenaquinone-9	3.89E-02	1.21	RG
Unknown56 - CPA(18:0/0:0)	8.65E-03	-1.41	E	Unknown131 - Iophendylate	3.92E-02	-1.08	AM
Unknown57 - Lucidumol A	9.50E-03	-1.16	E	Unknown132 - Phytanic acid	3.95E-02	-1.20	AM
Unknown58 - Citronellyl anthranilate	9.72E-03	-1.46	AM	Unknown133 - Netilmicin	4.04E-02	-0.90	E
Unknown59 - 1-Hexadecanol	1.03E-02	1.43	LG	Unknown134 - N1,N10-Dicoumaroylspermidine	4.05E-02	-1.21	RG
Unknown60 - PE(18:4(6Z,9Z,12Z,15Z)/12:0)	1.07E-02	-1.48	LG	Unknown135 - PE(22:6(4Z,7Z,10Z,13Z,16Z,19Z)/16:0)	4.09E-02	-0.99	FM
Unknown61 - DG(15:1(9Z)/	1.12E-02	-1.60	E	Unknown136 - PS(22:2(13Z,16Z)	4.13E-02	-1.32	FM
Unknown62 - 2-(2-Hydroxy-4-methylphenyl)-3-pentanone	1.13E-02	1.29	E	Unknown137 - Muricatenol	4.23E-02	-1.14	E
Unknown63 - N-Palmitoylsphingosine	1.30E-02	-1.45	E	Unknown138 - Momordicilin	4.28E-02	-1.21	E
Unknown64 - legionaminic acid	1.31E-02	-1.46	LG	Unknown139 - PE(22:2(13Z,16Z)/15:0)	4.34E-02	-1.12	FM
Unknown65 - Jasmolone	1.34E-02	-1.43	E	Unknown140 - PS(20:3(8Z,11Z,14Z)/18:0)	4.42E-02	1.21	RG
Unknown66 - 4-hydroxy-8-sphingenine	1.36E-02	1.46	RG	Unknown141 - Calycanthidine	4.57E-02	-1.01	FM
Unknown67 - LysoPE(18:1(11Z)/0:0)	1.36E-02	-1.10	E	Unknown142 - N-methylmorpholine N-oxide	4.60E-02	-0.95	RG
Unknown68 - MG(20:0/0:0/0:0)	1.41E-02	1.03	LG	Unknown143 - LysoPC(18:2(9Z,12Z))	4.61E-02	-0.86	E
Unknown69 - 1-deoxymethyl-3-dehydrosphinganine	1.42E-02	1.37	E	Unknown144 - Endoxifen	4.62E-02	-1.12	RG
Unknown70 - LysoPC(14:0)	1.44E-02	-1.49	AM	Unknown145 - LysoPC(P-16:0)	4.66E-02	-0.95	E
Unknown71 - DG(16:1n7/0:0/18:4n3)	1.53E-02	1.31	LG	Unknown146 - Dideoxymycobactin	4.69E-02	-0.92	LG
Unknown72 - 5-Methylthioribose	1.55E-02	1.24	E	Unknown147 - Nonadecylic acid	4.81E-02	-1.08	AM
Unknown73 - PE(20:2(11Z,14Z)/13:0)	1.66E-02	-1.34	AM	Unknown148 - Riesling acetal	4.83E-02	-0.99	E
Unknown74 - 5-Thymidylic acid	1.66E-02	-1.33	AM	Unknown149 - 17-O-acetylajmaline	4.88E-02	-0.94	LG
Unknown75 - 9r,13r-Opda	1.71E-02	-1.37	RG				

APPENDIX B

ADDITIONAL GROWTH TRIAL METABOLITE COMPARISONS

”Metabolites, after all, are the ultimate molecular arbiters of biological function."

– Jeffrey Perkel, The Scientist

Metabolite comparisons in juvenile and adult, fast and slow growing abalone fed with Abfeed and Abfeed X diets

In conjunction with the results given in Chapter 6 the following list of metabolites are viewed in terms of differences between slow and fast growing abalone consuming Abfeed and Abfeed X in juvenile and then adult abalone. In Figure B.1 the metabolites related to the glycolysis pathway, acetylcarnitine, alanine and tauropine are displayed. In Figure B.2 glutamine, glutamate and proline used as precursors to the TCA cycle are seen. Lastly in Figure B.3 selected urea cycle metabolites arginine, ornithine and creatine are viewed.

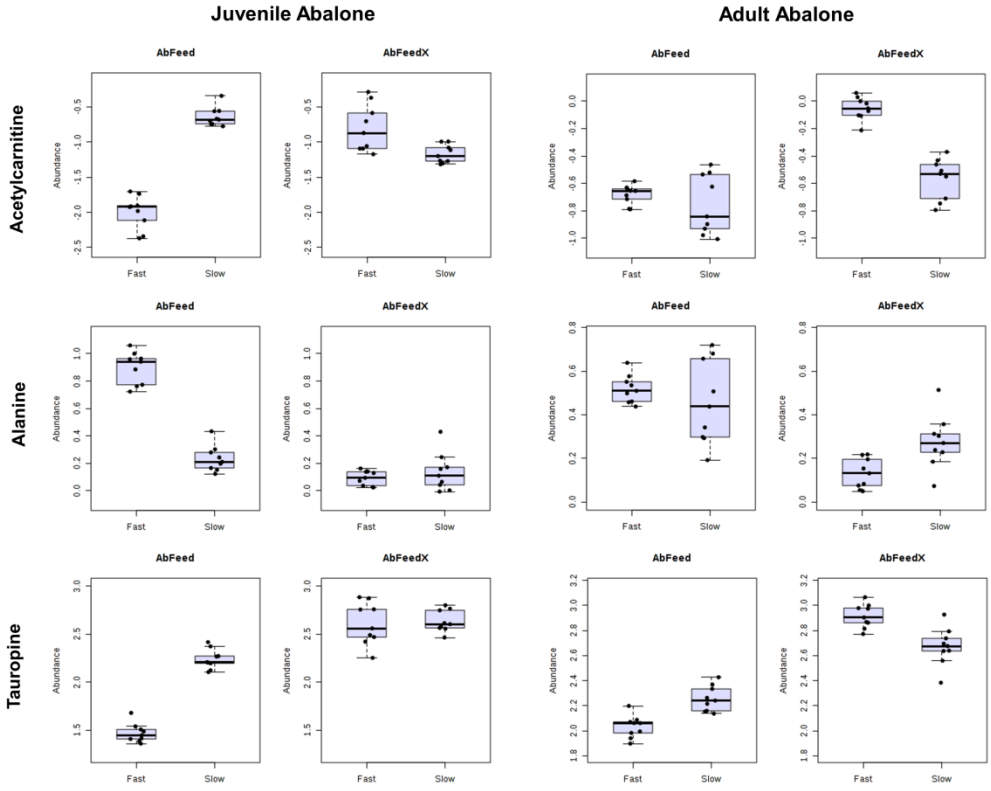

Figure B.1: Boxplots of acetylcarnitine, alanine and tauropine detected in juvenile and adult abalone. Relative metabolite abundance detected in fast and slow growing abalone consuming Abfeed and Abfeed X.

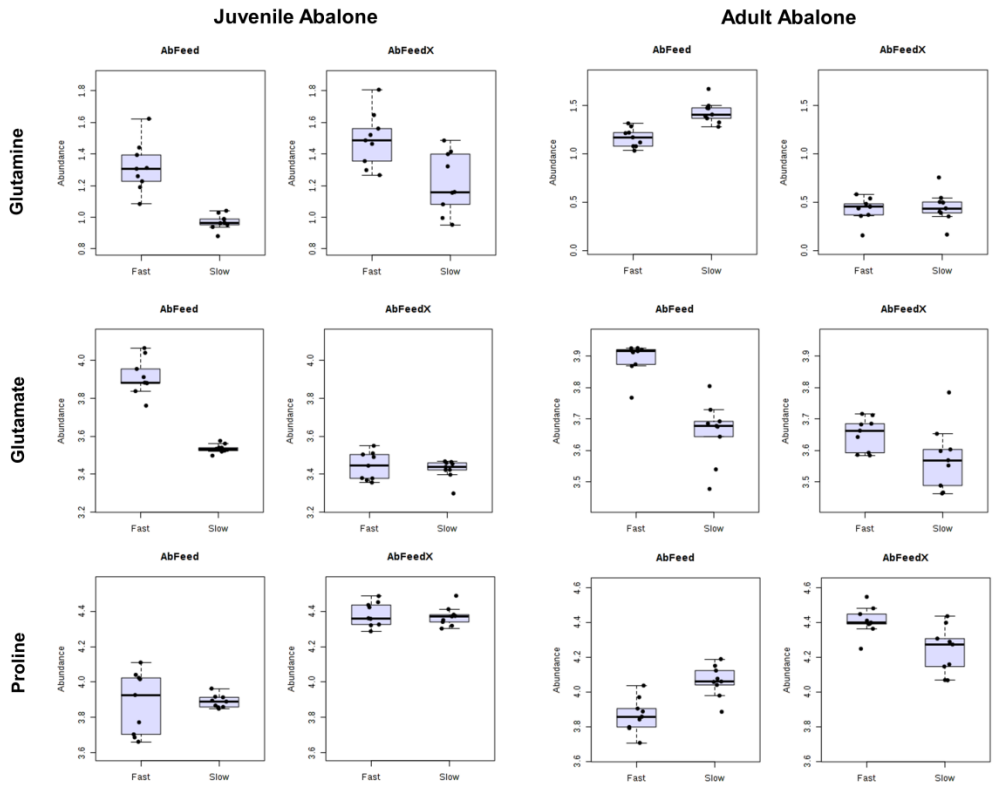

Figure B.2: Boxplots of the glutamine, glutamate and proline detected in juvenile and adult abalone. Relative metabolite abundance detected in fast and slow growing abalone consuming Abfeed and Abfeed X.

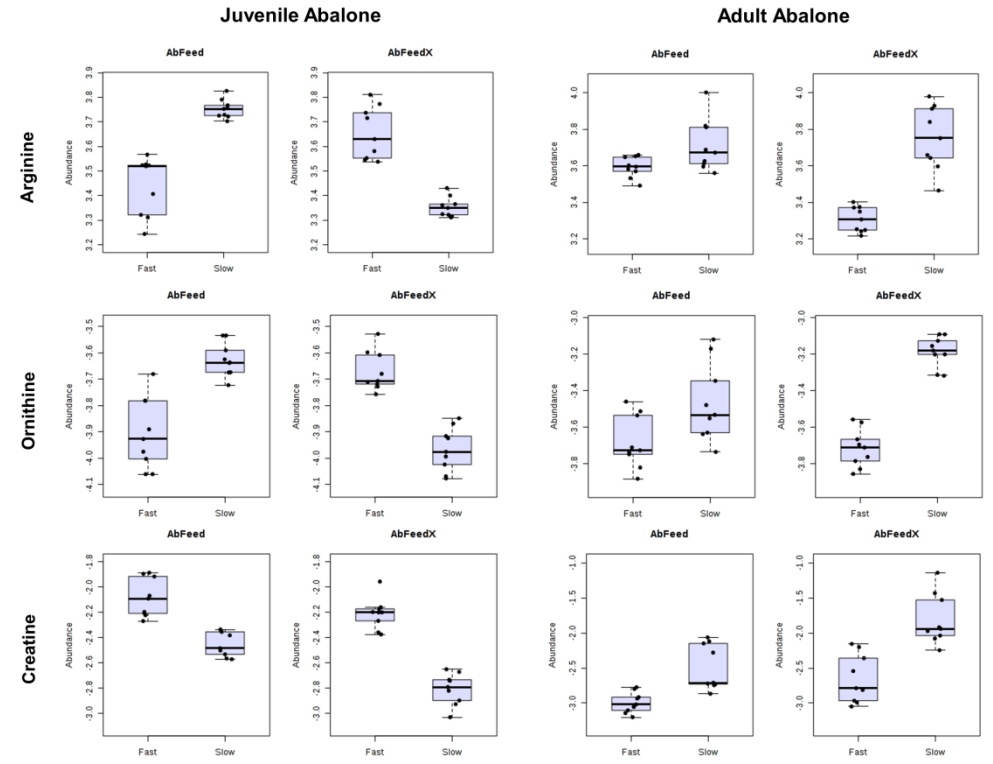

Figure B.3: Boxplots of the arginine, ornithine and creatine detected in juvenile and adult abalone. Relative metabolite abundance detected in fast and slow growing abalone consuming Abfeed and Abfeed X.

APPENDIX C

PUBLICATIONS

Application of metabolomics to identify functional metabolic changes associated with *Haliotis midae* growth

Chapter		Publications
Chapter 1	Introduction	N/A
Chapter 2	Literature	1 X Published
Chapter 3	Study design	N/A
Chapter 4	General materials and methods	2 X Published
Chapter 5	Metabolic response to anaerobic stress	2 X Published
Chapter 6	Elucidating farm growth of abalone	2 X Submitted
Chapter 7	Conclusion	N/A
Chapter 8	References	N/A

”Imagination is more important than knowledge. For while knowledge defines all we currently know and understand, imagination points to all we might yet discover and create.”

– Albert Einstein

Food Anal. Methods (2016) 9:1254–1261
DOI 10.1007/s12161-015-0285-5

Untargeted Metabolite Profiling of Abalone Using Gas Chromatography Mass Spectrometry

Leonie Venter[1] · **Peet Jansen van Rensburg**[1] · **Du Toit Loots**[1] · **Andre Vosloo**[2] · **Jeremie Zander Lindeque**[1]

Received: 24 April 2015 / Accepted: 7 August 2015 / Published online: 5 September 2015

Abstract Abalone meat is a delicacy worldwide, fetching high prices and a valuable source of income for the many countries farming and exporting this commodity. The quality of abalone is based on its unique sensory properties and an analytical metabolomics method for determining the compounds related to this would serve as a valuable tool for ensuring quality and consumer satisfaction. Metabolomics is a promising "omics" tool which can be applied towards this goal; however, widely applicable parameters for the evaluation of an untargeted gas chromatography mass spectrometry (GC-MS) metabolomic approach is still lacking. GC-MS is a popular and suitable metabolomics method due to its high separation power, reproducible retention times, and selective mass detection. The aim of this study was to establish a reliable untargeted GC-MS method for analyzing firstly a standard compound mixture consisting of 10 compounds representing various compound classes and secondly applying the method in an untargeted manner to abalone muscle samples. Using a standard compound mixture with a concentration range of 1 to 100 μg/mL, the limit of detection (LOD) ranged between 0.01 and 3.30 μg/mL, the limit of quantification (LOQ) resulted in values between 0.02 and 9.49 μg/mL, the accuracy determined was <1.5 μg/mL, and the precision displayed a coefficient of variance (CV) <25 %. When evaluating the method in terms of biological samples harvested, the repeatability and intermediate precision showed CV values <50 % for most compounds measured, allowing application of this method for metabolite profiling of abalone to answer important biological questions.

Keywords Abalone · Metabolomics · GC-MS · Untargeted metabolite profiling

Introduction

Abalone are single-shelled marine mollusks that are cultured in man-made shore-based systems at high stocking densities, yielding tons of abalone exports globally per annum (Laas and Vosloo 2010; Troell et al. 2006). The foot muscle of abalone is a highly sought after seafood delicacy (Roodt-Wilding 2007), with the quality of this food being determined by the texture, flavor, and appearance of the meat (Brown et al. 2008). Freezing, canning, or live export to Eastern markets are the destined outcome for farm-grown animals, ultimately contributing millions of dollars to South Africa's exports and economy (Vosloo and Vosloo 2006). Because it takes approximately 4 years for abalone to reach market size in South Africa, research and monitoring are important in ensuring the financial sustainability of aquaculture operations. Studying the metabolome and monitoring selected metabolite markers related to health or quality of the abalone meat would be a logical approach to this, considering that the metabolome (as opposed to the proteome or genome) is closest to its functional phenotypic properties.

From a food science perspective, the metabolism of animal muscle at the time of death is crucial for controlling the quality and taste of the meat (Rammouz et al. 2010). For instance, adenosine monophosphate and various free amino acids influence taste, and the collagen content affects texture and palatability of abalone muscle (Brown et al. 2008; Chiou and Lai

✉ Leonie Venter
2183450@nwu.ac.za

[1] Human Metabolomics, North-West University, Potchefstroom Campus, Private Bag X6001, Potchefstroom 2520, South Africa

[2] School of Life Sciences, University of KwaZulu-Natal, Private Bag X54001, Durban 4000, South Africa

2002). Considering that the abalone market does selection and pricing of production on the basis of the abovementioned quality criteria, information on which chemical components mostly influence marketable aspects of meat quality would offer significant advantage to the industry. In addition, markers that can aid in routine health and condition monitoring to ensure optimal growth of farmed animals over the 4-year farming period would be of significant commercial interest. The post-genomic technique of metabolomics could provide these necessary new insights into abalone growth and muscle content. Despite the recent advances in metabolomics and associated analytical instruments, there is still no information to date describing the use of GC with MS for monitoring the primary metabolism of abalone, especially not in the context of a global or untargeted approach.

Gas chromatography mass spectrometry (GC-MS) has been used since the 1950s and is still regarded as one of the most used metabolomics techniques today (Viant and Sommer 2013). GC coupled to time of flight (TOF) MS and two-dimensional GCXGC-MS is increasingly being used for metabolomics research since instruments like these allows better deconvolution and offer high sensitivity, peak resolution, and reproducibility (Verpoorte et al. 2008; Xu et al. 2010). Unlike nuclear magnetic resonance spectroscopy, mass spectrometric analyses require metabolites to be either in solution or in the gaseous phase. This means that metabolites in cells or tissue samples have to be extracted into a solution for subsequent derivatization, separation, and analysis (Kanani et al. 2008). This is typically done by homogenizing tissue in appropriate buffer or solvent where after reagents and solvents of differing polarities are added (Saric et al. 2012). Keeping in mind that no single extraction method can isolate every metabolite within a sample, the extraction method of choice needs to be selected and tested based on the goal of the experiment at hand (Lankadurai et al. 2013).

In this paper, we present an untargeted GC-MS-based metabolite profiling method in abalone muscle, which includes standardized homogenization, extraction, derivatization, and GC-MS analysis parameters. Due to the untargeted nature of this method and impracticality to report calibration curves for all the metabolites found in the primary metabolism, the method reported here was evaluated by using two sample sets as suggested by Koek et al. (2011) and Naz et al. (2014). A standard compound mixture consisting of 10 compounds, representing key metabolite classes normally screened for by GC-MS, covering a wide range of retention times was used to evaluate method accuracy, precision, concentration range, linearity, limit of detection (LOD), and limit of quantification (LOQ). Method repeatability and intermediate precision were evaluated using two abalone muscle sample sets. Considering that the method should also be fit for purpose (Koek et al. 2011), the two abalone samples were used to evaluate intra-group and inter-group variance using multivariate statistics.

Materials and Methods

Reagents and Chemicals

Chloroform (Honeywell, Burdick & Jackson, cat # BJ049CS), hexane (Sigma-Aldrich, cat # 296090), methanol (Honeywell, Burdick & Jackson, cat # BJ230CS), methoxyamine hydrochloride (Aldrich, cat # 226904), O-bis(trimethylsilyl)trifluoro acetamide (BSTFA) with trimethylchlorosilane (TMCS) (Fluka, cat # 33155), pyridine (Sigma-Aldrich, cat # 270970), and water (Honeywell, Burdick & Jackson, cat # BJ365CS) were used as general reagents. 2-Acetamidophenol (Aldrich, cat # A7000), nonadecanoic acid (Sigma, cat # N5252), norleucine (Fluka, cat # 74560), and 3-phenylbutyric acid (Aldrich, cat # 116807) were used as internal standard reagents. Methyl tricosanoate (Fluka, cat # 91478) dissolved in 2,2,4-trimethylpentane (Sigma, cat # 360066) was used as an external standard reagent. The standard compound mixture consisted of the following compounds: cholesterol (Sigma, cat # C8667), cysteine (Sigma, cat # C7880), glucose (Fluka, cat # G0350500), heneicosanoic acid (Fluka, cat # 2363715), malic acid (Sigma, cat # M8304), proline (Fluka, cat # P335000), ribose (Fluka, cat # 83860), serine (Fluka, cat # 84960), succinic acid (Fluka, cat # 14080), and tryptophan (Fluka, cat # 73223).

Sample Collection and Preparation

Standards

One mg/mL stock solutions of all the standards in the standard compound mixture (containing the 10 standards mentioned in Section 2.1) were prepared and kept at 4 °C. These stocks were subsequently used to prepare the concentration range sample dilution set or working internal and external standard solutions. Standard samples were prepared in duplicate with the following concentrations: 0, 0.5, 1, 5, 10, 30, 70, and 100 μg/mL. Internal standards were added to the standard compound mixture to a final concentration of 50 μg/mL. The standard compound mixture was treated in an identical manner to that of the biological samples, i.e., it went through the entire extraction and derivatization process as mentioned in "Sample Extraction" and "Oximation and Silylation" sections, prior to analysis.

Biological Samples

South African abalone, *Haliotis midae*, were obtained from the grow-out platform at HIK Abalone Farm (Pty) Ltd. situated in Hermanus, South Africa. Columellar muscle was sampled from the foot muscle after shucking the animals, followed by freezing using dry ice and storage at −80 °C until use. Two abalone sample sets, known as groups A and B (consisting of

five replicates) were created by taking five pieces of muscle from each of the abalone, as described below.

Sample Extraction

Five samples of approximately 50 mg of frozen abalone tissue were cut from each of the abalone muscle samples using a scalpel. Metabolite extraction was performed using the two-step method as previously described (Lindeque et al. 2013). Briefly, the 50 mg tissue samples were placed into separate Eppendorf tubes, followed by the addition of 560 μL methanol, 200 μL water, 60 μL of the internal standard solution (with a final concentration of 50 μg/mL), and a 3- and 7-mm stainless steel bead (QIAGEN, 69989, 69990), followed by homogenization of the samples for 4 min at 30 Hz using the Retch M400 vibration mill. Subsequently, 180 μL chloroform was added to the samples, tubes vortexed for 1 min, and incubated for 10 min on ice. The samples were centrifuged at 25,000×*g* for 10 min at 4 °C after which 500 μL of each supernatant was transferred to a clean GC vial and dried under a gentle stream of nitrogen at 37 °C.

Oximation and Silylation

Oximation reagent was prepared by dissolving 200 mg methoxyamine in 10 mL pyridine. The dried samples received 50 μL of the oximation reagent. The samples were vortexed for 1 min and incubated for 60 min at 60 °C. Silylation followed with the addition of 50 μL BSTFA (containing 1 % TMCS) to the samples. The samples were vortexed again for 1 min and incubated for 60 min at 60 °C. Lastly, 50 μL of the external standard (methyl tricosanoate in trimethylpentane with a final concentration of 50 μg/mL) was added to the sample and vortexed prior to GC-MS analysis (Lindeque et al. 2013).

GC-TOF-MS Parameters

The GC-TOF-MS-system consisted of an Agilent 7890 GC system coupled with a Leco Pegasus HT mass analyzer. An Agilent 7693 auto sampler was used for sample introduction. Chromatography was performed on a Restek RXi®-5 column (10 m×0.2 mm×0.18 μm). A sample volume of 1 μL was injected (using a split/split less injector) per run with a 1:10 split ratio. The front inlet temperature was kept at 250 °C throughout the entire run. An initial oven temperature of 70 °C was maintained for 0.5 min and then increased at a rate of 40 °C per min to 110 °C where it was kept constant for 0.5 min. Temperature was then subsequently ramped as follows: 10 °C/min to 125 °C, 15 °C/min to 140 °C, 25 °C/min to 185, 12 °C/min to 200, and 30 °C/min to 300 °C, where it was maintained for 1 min equating to a total run time of ~12 min per sample. Helium was used as carrier gas at a constant flow of 1 mL/min. The transfer line was maintained at 225 °C and the ion source temperature at 200 °C for the entire run. Acquisition was delayed for the first 110 s which served as a solvent delay. Data were captured with an acquisition rate of 20 spectra (50–950 m/z) per second.

Data Processing

Data extraction, in terms of baseline subtraction, peak detection, and deconvolution, was performed using ChromaTOF (Leco). The "span" baseline tracking mode was selected with offset of 1. The program was allowed to automatically select smoothing parameters. Peaks were detected using an expected peak width of 3 s and signal-to-noise ratio of 20. Also, only masses between 100 and 800 m/z were used as model ions, and any true peak had to contain five apexing masses. Compounds were identified via spectral matching to the NIST11 commercial library and an in-house created library (Reinecke et al. 2012). A spectral match of 80 % similarity (similar to 800 in ChromaTOF) was needed before a compound could be given an identity. Also, only identities which contain at least one Si element in its formula were allowed to eliminate spectral matching of non-derivatized compounds or incorrect derivatives.

Statistical Analyses

The LOD for each of the 10 standard compounds was calculated as the average integrated noise signal in the blank samples plus three times the standard deviation of the integrated noise signal. This intensity value was converted to concentration using the internal standards. The LOQ was determined in similar fashion except that 10 times the standard deviation was added to the blank values (González and Herrador 2007). The CV for all repeated measures were determined and given as a percentage, as a means to illustrate precision. Accuracy was determined in two ways. Firstly, a 10 μg/mL sample of the standard compound mixture was analyzed and the calibration curves were used to determine the calculated concentration. Accuracy was then illustrated by determining the absolute error (subtracting the calculated concentration from the theoretical concentration). The second method for evaluating accuracy entailed the analysis of 100 μg/mL standards at increasing split ratios (1:20, 1:40, and 1:80) to simulate dilution effects or sample loss during sample preparation. Absolute errors in concentration were also determined as mentioned above. The abalone data were log-transformed and auto-scaled before multivariate analysis.

Results and Discussion

As mentioned earlier, it is impractical to perform calibration curves of all anticipated compounds in a biological sample when the goal is to perform untargeted metabolite profiling. It is common to see 300 (or more) compounds per sample analyzed, and a further hindrance to this is the limited availability of commercial standards for many of the metabolites. Moreover, it is also impossible to include an internal standard (stable isotope) for every metabolite in the sample which is also a requirement for absolute quantification. Several authors have therefore suggested a two-part evaluation and verification strategy to illustrate that a proposed untargeted screening method derives meaningful biological information despite the known shortcomings.

The proposed method was first evaluated using 10 standard compounds prepared in increasing concentrations. The overall satisfactory coefficients of determination (r^2) and linear regions of these standards (Fig. 1) indicate that the method is suitable to derive meaningful information from the measured compounds, each of which represents various compound classes expected in the biological sample. While no reference concentration values for these standard compounds exist for abalone (according to our knowledge), the results from several different animals showed that many of the primary metabolites fall within the selected concentration range (albeit with the assumption that there is no metabolite loss or bias). It is therefore possible to determine the relative quantity of most of the detected compounds without adapting the proposed method to either concentrate or dilute the sample prior to analysis. Also, a linear calibration model was used on all of the abovementioned standards, with the assumption that responses are linear in nature, especially in an untargeted approach (Koek et al. 2011). It should be noted that not all of the measured standards adhered to linear responses, for example, cysteine (detected as cystine) showed a non-linear (two-order polynomial) response with goodness-of-fit r^2>0.98 and for this reason was not include as part of Fig. 1. This will be described in greater detail below.

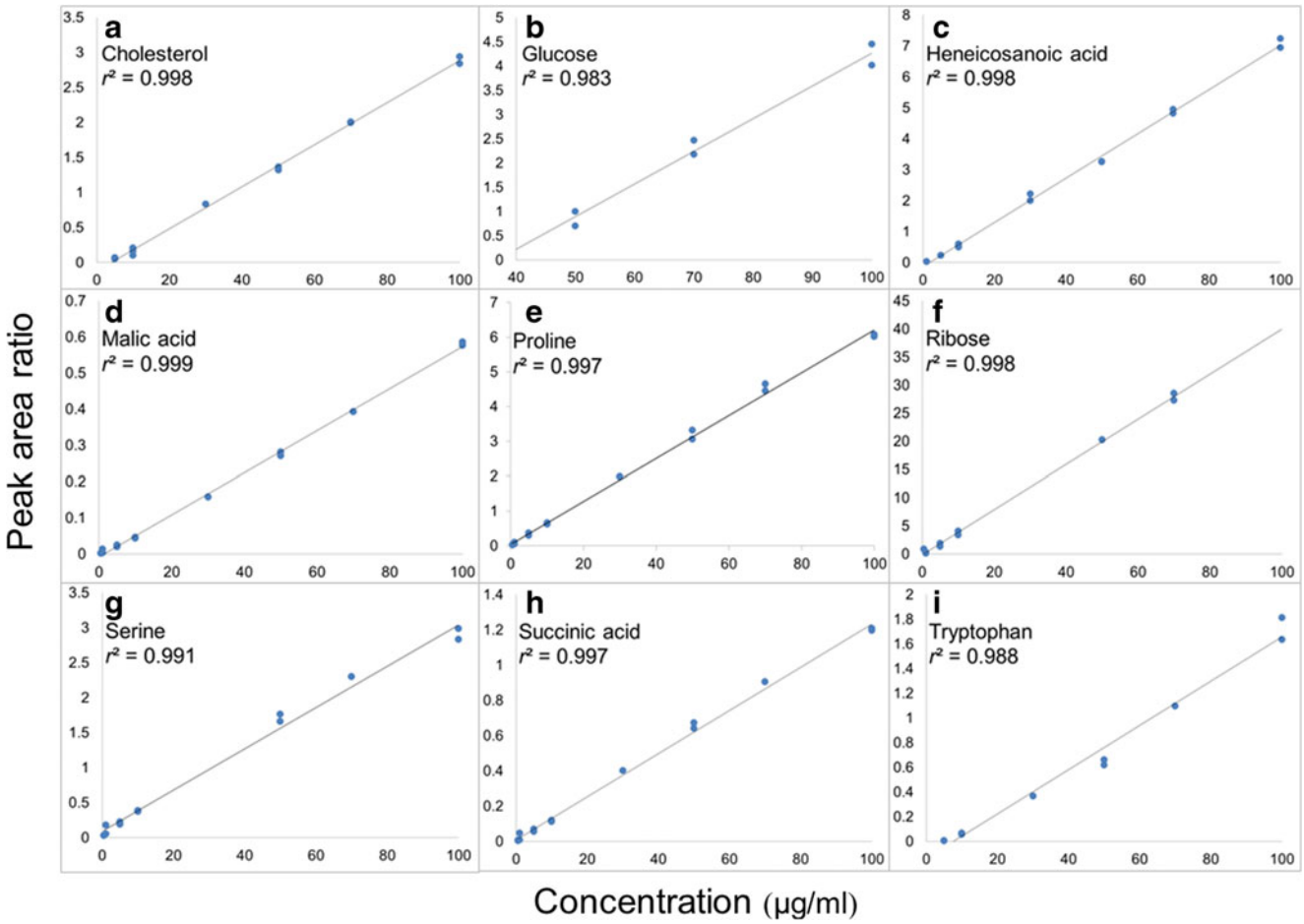

Fig. 1 Calibration curves of standards representing various compound classes expected in the biological matrix. The coefficients of determination (r^2) are indicated for **a** cholesterol, **b** glucose, **c** heneicosanoic acid, **d** malic acid, **e** proline, **f** ribose, **g** serine, **h** succinic acid, and **i** tryptophan

Linearity, LOD and LOQ of Standards

The calibration curves for those standards representing compounds from specific metabolite classes in the biological sample (Fig. 1) were constructed to evaluate the proposed extraction, derivatization, and analytical method. The LOD, LOQ, linear range, precision, and accuracy within their respective linear regions were determined (Table 1).

The r^2 of all compounds were generally 0.99 for their respective linear ranges (with the exception of glucose being 0.98). Most of the reference compounds showed linearity in response between 1 and 100 μg/mL except again for glucose which only gave a linear response between 50 and 100 μg/mL. As anticipated, these linear ranges are influenced by the internal standards used for normalization (relative quantification), their concentrations, as well as the calibration model. The use of isotopes could further improve these reported ranges; however, this was not done as isotopes are not available for all compounds extracted and measured in an untargeted manner. Moreover, these calibrations were also created with the assumption that there is no error in the response vector (*x*-axis), in other words, that no error occurred during the preparation of the different concentrations. With the selected internal standards and method, it appeared that the glucose response, similar to that of cysteine was also more non-linear in nature.

The lowest detectable concentration distinguishable from zero (or systemic noise) is considered the LOD. The LOD determined for the metabolites present in the standard compound mixture ranged from 0.01 to 3.30 μg/mL (Table 1). The LOQ is considered the lowest concentration at which a compound can be quantified with an acceptable level of precision. A LOQ range from 0.02 to 9.49 μg/mL was determined for the compounds used in the standard compound mixture (González and Herrador 2007; Naz et al. 2014). Qi et al. (2011) reported a metabolomic procedure using GC-TOF-MS to measure small metabolites found in hemodialysate. By using 21 standard compounds representing a number of chemical classes, their method displayed linearity ranging from 0.15 to 150 μg/mL. In their study, the amino acids proline and tryptophan showed linear ranges between 0.15 and 150 μg/mL (r^2=0.998) and 0.75 and 150 μg/mL (r^2=0.997), respectively (Qi et al. 2011). In the present study, proline showed linearity in response between 0 and 100 μg/mL (r^2= 0.997) and tryptophan between 10 and 100 μg/mL (r^2= 0.997). Based on findings like this, the present method compares well with other such approaches.

Precision and Accuracy of the Standard Compound Mixture

Precision of the standard compound mixture within their respective linear regions were determined, in terms of average CV. The average CV of the standard compounds ranged between 3.66 % (proline) and 23.78 % (succinic acid) (Table 1). Accuracy was determined firstly by using the standard compound mixture with a concentration determined from the average working range of the biological samples (10 μg/mL). The calibration curves were used to determine the calculated concentration. The absolute error values are shown in Table 1. From this data, it is evident that malic acid shows the smallest error (0.002 μg/mL) and proline the largest (1.52 μg/mL). Secondly, accuracy of the method after simulated sample loss or variation was determined by subtracting the obtained concentration from the theoretical concentration (results not shown). Generally, the results indicated good accuracy with most determinations being less than 1.5 μg/mL deviation. In terms of the results found with precision and accuracy based on the standard compound mixture, the method shows promise for the analysis of biological samples.

Table 1 Analytical parameters for the verification of the GC-TOF-MS method using standard compounds

Compound	Linear range (μg/mL)	r^2	LOD (μg/mL)	LOQ (μg/mL)	Precision (%)	Accuracy (μg/mL)
Cholesterol	1–100	0.998	0.43	1.24	12.69	−0.13
Glucose	50–100	0.983	3.30	9.49	13.62	−1.18
Heneicosanoic acid	0–100	0.998	0.20	0.57	4.83	−0.21
Malic acid	0–100	0.999	0.01	0.04	21.58	0.002
Proline	0–100	0.997	0.01	0.02	3.66	−1.52
Ribose	0–70	0.998	0.04	0.13	22.78	−0.35
Serine	0–100	0.991	0.09	0.26	16.89	−0.90
Succinic acid	0–100	0.997	0.01	0.02	23.78	−0.12
Tryptophan	10–100	0.998	0.06	0.16	6.54	0.20
Cystine[a]	10–100	0.999	2.99	8.62	12.70	0.28

[a] Cysteine was measured in the oxidized form cystine

Repeatability and Intermediate Precision of Biological Replicates

A key step in the proposed method is the homogenization step, where most of the variation could occur when, for example, one sample is fully homogenized while another is barely disrupted. The use of an automated system such as a vibration mill is highly recommended for studies where tissue samples have to be disrupted and homogenized in order to extract metabolites from it. The use of Potter-Elvehjem style tissue grinders in analytical (metabolic) studies is not recommended unless it can be automated so that every sample is homogenized to the same extent without carryover. Even though the standards were subjected to a homogenization step, their precision results do not really portray the variance that could infiltrate the method at this step. For this reason, the actual biological samples were used to evaluate this step.

Overall repeatability (intra-day precision) of the homogenization, extraction, derivatization, and analytical methods were also evaluated using the abalone muscle samples collected. Five replicate samples (from the same abalone group A and group B from a second abalone) were prepared and analyzed as described above. CVs of the 199 compounds detected in at least 4 of the 5 replicates were determined (Fig. 2). About 60 % of the detected compounds had a CV <25 % while about 80 % of the measured compounds had a CV <50 %. The Food and Drug Administration (FDA) recommends a CV value of between 15 % and 20 % for targeted analysis of compounds (t'Kindt et al. 2009). However, more variation is expected when doing untargeted analysis; thus, a higher CV value is considered acceptable for metabolomic purposes data generation, which has various data cleanup steps post-analysis to correct for this (Schoeman et al. 2012). A CV of more than 50 % normally indicates that a compound is unreliably measured due to factors like degradation, production, or evaporation of the compound during preparation and analysis. For example, thiols such as cysteine are rapidly oxidized during sample preparation resulting in increased cystine levels (Bouatra et al. 2013). The CV values of several selected compounds from different metabolic classes as analyzed in the biological sample are presented in Table 2 (this is only a subset of the compounds found in the biological samples).

Abalone tissue from groups A and B were taken and prepared the following day to determine intermediate (or inter-day) precision. More often than not, tens to hundreds of samples could potentially be analyzed over several days (depending on the analysis time per sample). Ideally, the time-related differences in signal (technical variance) should be as small as possible and never exceed the relevant biological variation (van den Berg et al. 2006). The use of a quality control sample analyzed and injected at regular intervals within and between batches is highly recommended as this can be used to assess the variation and correct for this. While inter-day variation can be determined over several days or weeks, we have decided on two consecutive days as this corresponds to procedures in our own studies. CVs of all the detected compounds were determined similar to the day 1 samples. The CV distributions of the samples analyzed on the second day are also shown in Fig. 2. The precision statistics were very similar with about 80 % of the detected compounds having a CV <50 %. This similarity is also evident in the listed CV values in Table 2. In addition to the similarity in precision, most compounds also gave the same response (or relative concentration) on the second day of analysis. The absolute error in concentration of several selected compounds from different metabolite classes were determined by subtracting the day 1 concentrations from that obtained on day 2. These errors are listed in Table 2. On

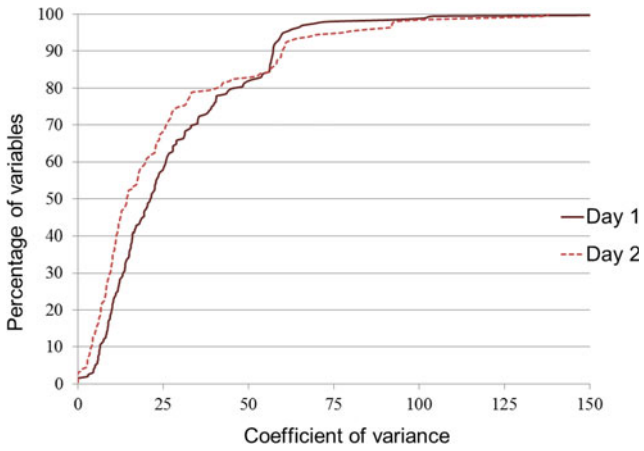

Fig. 2 Coefficient of variation distribution. CV values for compounds detected in abalone muscle tissue of five repeats over 2 days using the same extraction method

Table 2 Intra- and inter-day precision and error of various compounds detected in abalone muscle tissue

Compound	CV day 1 (%)	CV day 2 (%)	Absolute error (μg/mL)
Aminomalonic acid	10.31	10.14	0.67
Succinic acid	6.47	6.97	0.20
Galactose	21.53	5.01	0.50
Glucose	8.41	2.78	−1.61
Glycine	9.67	3.53	3.85
Inositol	4.35	4.38	0.48
Lyxofuranose	16.00	6.26	2.03
Pentanoic acid	5.05	2.90	0.77
Pinitol	6.96	3.70	0.02
Phenylalanine	8.79	11.01	−1.95
Proline	12.04	11.04	3.98
Isonicotinic acid	7.48	3.44	0.06
Threonine	11.73	18.11	0.55

average, an absolute error of 1 μg/mL was seen for the same compound detected over the two consecutive days. Most of the compounds showed almost identical results; however, those compounds at lower concentrations and close to the detection limit showed comparatively more deviation, as can be expected (Schoeman et al. 2012).

These results clearly indicate that the proposed method provides repeatable results over two consecutive days. Arguably, the small variation observed may be a result of non-analytical factors such as freeze-thawing or minor variations to room temperature.

Inter- vs. Intra-Group Variance of Biological Replicates

While the CV values indicate that the proposed method is highly precise and reliable, it should also be put in perspective of the ultimate goal of finding relevant biological information. One way to evaluate whether the observed precision is fit for purpose is to compare the inter- and intra-group variance of two simulated experimental groups. For the methodology to give any relevant information, it is important that the intra-group (technical) variance is smaller than the inter-group (biological) variance as visualized with multivariate statistics, using the unsupervised technique known as principle component analysis (PCA). The use of PCA enables one to ascertain whether or not a natural grouping between the various samples exists based on their detected metabolite profiles (du Preez and Loots 2013). This test assesses the total variance in the samples and groups the samples accordingly. It is commonly used in metabolomics studies, and therefore, a perfect way to evaluate the efficacy of the proposed method for generating accurate biological results. Five replicates of a second abalone sample were prepared to simulate two experimental groups (A and B). Despite the low variance between the two "control" homogeneous abalone sample sets, the very low technical variance between the repeats should result in them separating when the data is analyzed using PCA analysis.

The PCA score plot in Fig. 3 shows close grouping of the respective repeats and clear separation between the two simulated groups, A and B, respectively. PC 1 shows the largest variation in the data which in this case is also the relevant biological (inter-group) variance between the simulated groups. PC 2 explains the second largest variation in the data which appears to be mainly technical (intra-group) variance. This clearly illustrates the repeatability of proposed method and its capacity to generate meaningful biological information from abalone tissue samples, especially since these animals can be regarded as highly homogeneous seeing that both abalone experienced the same stressors and handling procedures.

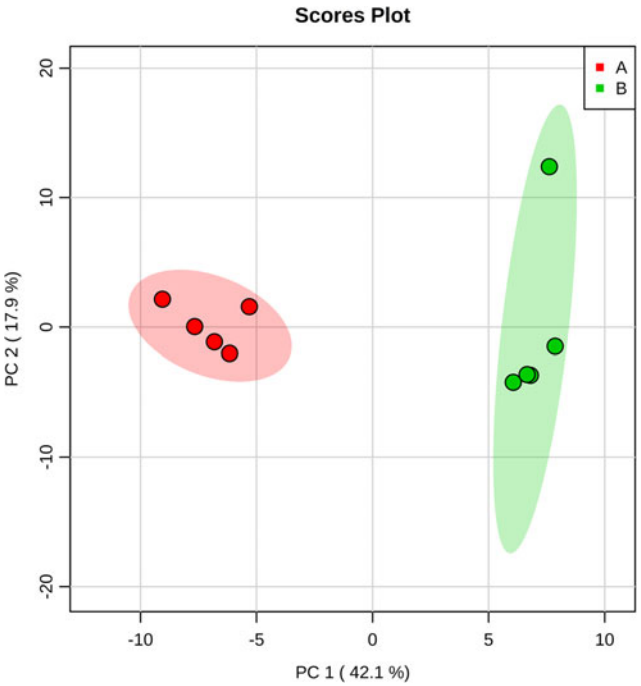

Fig. 3 Inter- and intra-group variation based on principle component analysis separation. Evaluation of the inter- and intra-group variation of two abalone replicates by using PCA separation

Conclusion

Here, we presented a GC-MS-based global metabolite profiling method for screening abalone that includes conditions for homogenization, metabolite extraction, derivatization, and GC-MS analysis. Naz et al. (2014) states that: "If a method is validated in terms of linearity, accuracy and precision for the selected compounds, it can be considered that the non-targeted approach will generate reliable and acceptable data sets for further evaluation". The reported analytical method showed good linearity, accuracy, and precision, which makes this method suitable for the proposed applications. In the aquaculture context, the strategy applied here for untargeted metabolomic analysis on abalone muscle may also be applicable to other abalone tissues, e.g., gills, digestive gland, or gonads. We anticipate that the proposed method can be deployed on a subject group with the purpose to infer biological meaning to metabolites that differ between sample groups. In addition, this method would also be capable of detecting even subtle changes in the metabolic composition of abalone tissue and differentiate slow and fast-growing abalone, healthy and diseased animals, those with good and poor quality meat, and ultimately answer specified biological questions. Subsequently, those compounds best describing this variation can be identified as markers for these differences, better explaining these circumstances and subsequently leading to improved production and quality.

Acknowledgments We are grateful for the donation of samples made by HIK Abalone Farm (Pty) Ltd., Hermanus, South Africa. We acknowledge the North-West University for financial support.

Compliance with Ethical Standards

Funding All funds were provided by the North-West University.

Conflict of Interest Leonie Venter, Peet Jansen van Rensburg, Du Toit Loots, Andre Vosloo and Jeremie Zander Lindeque declare that they have no conflict of interest.

Ethical Approval All institutional and national guidelines for the care and use of laboratory animals were followed.

References

Bouatra S, Aziat F, Mandal R, Guo AC, Wilson MR, Knox C, Bjorndahl TC, Krishnamurthy R, Saleem F, Liu P (2013) The human urine metabolome. PLoS ONE 8:e73076

Brown MR, Sikes AL, Elliott NG, Tume RK (2008) Physicochemical factors of abalone quality: a review. J Shellfish Res 27:835–842

Chiou T-K, Lai M-M (2002) Comparison of taste components in cooked meats of small abalone fed different diets. Fish Sci 68:388–394

du Preez I, Loots DT (2013) Detection limit for differentiating between various *Mycobacterium* species and *Pseudomonas aeruginosa* using gas chromatography-mass spectrometry (GC-MS) metabolomics: a comparison of two extraction methods. Afr J Microbiol Res 7:797–801

González AG, Herrador MÁ (2007) A practical guide to analytical method validation, including measurement uncertainty and accuracy profiles. Trends Anal Chem 26:227–238

Kanani H, Chrysanthopoulos PK, Klapa MI (2008) Standardizing GC-MS metabolomics. J Chromatogr B 871:191–201

Koek MM, Jellema RH, van der Greef J, Tas AC, Hankemeier T (2011) Quantitative metabolomics based on gas chromatography mass spectrometry: status and perspectives. Metabolomics 7:307–328

Laas A, Vosloo A (2010) Exploring basic biochemical constituents in the body tissues of South African abalone *Haliotis midae* reared in shore-based mariculture systems. Afr J Mar Sci 32:55–63

Lankadurai BP, Nagato EG, Simpson MJ (2013) Environmental metabolomics: an emerging approach to study organism responses to environmental stressors. Environ Rev 21:180–205

Lindeque JZ, Hidalgo J, Louw R, van der Westhuizen FH (2013) Systemic and organ specific metabolic variation in metallothionein knockout mice challenged with swimming exercise. Metabolomics 9:418–432

Naz S, Vallejo M, García A, Barbas C (2014) Method validation strategies involved in non-targeted metabolomics. J Chromatogr A 1353: 99–105

Qi X, Zhang Y, Gao J, Chen T, Zhao A, Yan Y, Jia W (2011) Metabolite profiling of hemodialysate using gas chromatography time-of-flight mass spectrometry. J Pharm Biomed Anal 55:1142–1147

Rammouz RE, Létisse F, Durand S, Portais J-C, Moussa ZW, Fernandez X (2010) Analysis of skeletal muscle metabolome: evaluation of extraction methods for targeted metabolite quantification using liquid chromatography tandem mass spectrometry. Anal Biochem 398: 169–177

Reinecke CJ, Koekemoer G, van der Westhuizen FH, Louw R, Lindeque JZ, Mienie LJ, Smuts I (2012) Metabolomics of urinary organic acids in respiratory chain deficiencies in children. Metabolomics 8: 264–283

Roodt-Wilding R (2007) Abalone ranching: a review on genetic considerations. Aquac Res 38:1229–1241

Saric J, Want EJ, Duthaler U, Lewis M, Keiser J, Shockcor JP, Ross GA, Nicholson JK, Holmes E, Tavares MF (2012) Systematic evaluation of extraction methods for multiplatform-based metabotyping: application to the *Fasciola hepatica* metabolome. Anal Chem 84:6963–6972

Schoeman JC, du Preez I, Loots DT (2012) A comparison of four sputum pre-extraction preparation methods for identifying and characterising *Mycobacterium tuberculosis* using GCxGC-TOFMS metabolomics. J Microbiol Methods 91:301–311

t'Kindt R, Morreel K, Deforce D, Boerjan W, Van Bocxlaer J (2009) Joint GC-MS and LC-MS platforms for comprehensive plant metabolomics: repeatability and sample pre-treatment. J Chromatogr B 877: 3572–3580

Troell M, Robertson-Andersson D, Anderson R, Bolton J, Maneveldt G, Halling C, Probyn T (2006) Abalone farming in South Africa: an overview with perspectives on kelp resources, abalone feed, potential for on-farm seaweed production and socio-economic importance. Aquaculture 257:266–281

van den Berg RA, Hoefsloot HC, Westerhuis JA, Smilde AK, van der Werf MJ (2006) Centering, scaling, and transformations: improving the biological information content of metabolomics data. BMC Genomics 7:142

Verpoorte R, Choi Y, Mustafa N, Kim H (2008) Metabolomics: back to basics. Phytochem Rev 7:525–537

Viant MR, Sommer U (2013) Mass spectrometry based environmental metabolomics: a primer and review. Metabolomics 9:144–158

Vosloo A, Vosloo D (2006) Routes of water loss in South African abalone *Haliotis midae* during aerial exposure. Aquaculture 261:670–677

Xu F, Zou L, Ong CN, Zou L, Ong CN, Ong CN (2010) Experiment-originated variations, and multi-peak and multi-origination phenomena in derivatization-based GC-MS metabolomics. Trends Anal Chem 29:269–280

REVIEWS IN Aquaculture

Reviews in Aquaculture (2016) **0**, 1–23 doi: 10.1111/raq.12181

Abalone growth and associated aspects: now from a metabolic perspective

Leonie Venter[1], Du Toit Loots[1], Andre Vosloo[2], Peet Jansen van Rensburg[1] and Jeremie Zander Lindeque[1]

1 Human Metabolomics, North-West University, Potchefstroom, South Africa
2 School of Life Sciences, University of KwaZulu-Natal, KwaZulu-Natal, South Africa

Correspondence
Leonie Venter, Human Metabolomics, North-West University, Potchefstroom 2520, South Africa. Email: 21834350@nwu.ac.za

Received 2 June 2016; accepted 7 September 2016.

Abstract

Worldwide, there are approximately 100 Haliotis species, more commonly known as abalone or 'Paua' in New Zealand, 'Venus's-ears' in Greece, 'Awabi' in Japan, 'Perlemoen' in South Africa and 'Ormers' in Europe. Regardless of what they are called in any part of the world, a high monetary value is coupled to this animal, because it is largely considered a seafood delicacy. Subsequently, a great deal of research primarily focused on improving the health and growth rates of abalone were carried out to maximise productivity of the commercial farming efforts in various countries. In this review, we comprehensively describe the most recent available scientific literature on abalone biology, and those aspects related to the growth of this organism; more specifically, those factors related to the uptake and breakdown of metabolic products which ensures long-term growth. We subsequently discuss this in terms of basic animal design, farming outcomes, feeding, cellular growth mechanisms and the unique metabolic processes that exist in these species. Using this information and the knowledge of the metabolic processes in other organisms, we additionally make a number of new hypotheses regarding how these metabolic processes may function in terms of abalone growth. Based on the information presented in this review, we also identify major research opportunities and gaps in the existing knowledge of abalone metabolism, which when elucidated may not only serve the purpose of better understanding these organisms growth but also could potentially lead to increased productivity of the abalone commercial farming sector.

Key words: abalone, aquaculture, artificial feeds, growth, metabolism, metabolomics.

Introduction

To date, the methods for cultivating abalone, a marine invertebrate mollusc, have been investigated to such an extent that most factors concerning abalone farming (e.g. spawning, water temperature, formulated diets) are generally considered to be well understood. Despite this however, knowledge of abalone metabolism and the biochemical processes associated with growth, development and feeding are not. This fact becomes evident when reviewing the existing scientific literature and is further substantiated by Morash and Alter (2015): 'We are at a crucial time where understanding the mechanistic physiology of abalone will give us an advantage as the climate continues to change and farming practices become more industrialised.', Laas and Vosloo (2010): 'Knowledge of the basic biochemical constituents of abalone under culture conditions would be a very useful tool in their management in aquaculture systems.', and Sales and Janssens (2004): 'Evaluation of the effective use of feed ingredients in abalone feeds is not only hampered by a lack of knowledge on nutrient requirements and possible anti-nutritional factors present in some feed ingredients, but also by an effective measurement of the response to these.' As the future of sustainable abalone aquaculture depends on optimal growth rates, the various growth mechanisms involved has become a popular research topic.

In their natural habitat, abalone are classified as opportunistic herbivorous deposit scrapers, inhabiting subtidal zones with rocky shores or kelp forests (Vosloo & Vosloo

2006). Wild abalone populations are globally under pressure through overfishing, disease (Chang *et al.* 2005; Wetchateng *et al.* 2010; Macey *et al.* 2011), ocean acidification (Byrne *et al.* 2011) and poaching. For example, abalone populations along the coast of South Africa have been in decline since the early 1990s and are classified as depleted, mainly due to a highly organised poaching network involving divers, local middlemen and foreign syndicates (Raemaekers & Britz 2009; De Greef & Raemaekers 2014).

Abalone farming on the other hand serve to supply to the growing demand, without depleting the natural abalone reserves, and have shown exponential growth since the mid-1990s. South African abalone are now successfully cultured in man-made, shore-based systems, where they are increasingly grown on formulated artificial feeds (Laas & Vosloo 2010). Due to its unique gustatory properties, special nutritional value and the safety standards that this food has to comply with, for commerce, these abalone are in high demand and of high monetary value (Øiseth *et al.* 2013; Latuihamallo & Apituley 2015).

To successfully culture abalone, an understanding of its physiology and the effects of various biotic and abiotic factors on the organisms growth and health are essential (Hahn 1989). Furthermore, a better understanding of abalone metabolism could also assist in identifying potential additional strategies to optimise growth, identify markers for monitoring health and growth rates and subsequently improve abalone farm productivity.

This review summarises the current literature with regard to the various aspects relating to basic abalone biology, feeding and nutrition, in addition to describing the present commercial value of abalone farms. However, to better understand the limitations or deficiencies in current farming practices, feeding and growth, it is necessary to understand the basic biology and structure, driven by cellular processes like metabolism. So, perhaps of even more importance is the comprehensive overview in this review, of this organism's metabolome, which not only describes links and summarises the metabolism-related research to date, but also exposes the missing pieces to this puzzle. Subsequently, the lack of a definite abalone metabolic design will be discussed in the concluding paragraphs, together with the potential use of information attained through abalone metabolomics driven research, in the context of commercial abalone farms.

The interrelationship between structure, function and metabolism

Abalone are single-shelled marine molluscs that belong to the phylum Mollusca, the class Gastropoda, family Haliotidae and the single genus *Haliotis* (Denny & Gaines 2007). Abalone are possibly best known for their unusual flattened shell, with the mother-of-pearl lining and the row of respiratory pores extending from the left anterior margin of the shell, closing posteriorly as growth proceeds (Kilburn & Rippey 1982). Abalone have the typical molluscan body plan, consisting of a head-foot portion and a visceral mass portion, displaying ~180° torsion (Hickman *et al.* 2006).

Head-foot portion

The head-foot section of abalone is characterised by a muscular foot structure containing a haemolymph cavity, which functions as a hydrostatic skeleton (Kilburn & Rippey 1982; Payne & Crawford 1989; Mgaya & Mercer 1994; Hickman *et al.* 2006). The large muscular foot, which fills the shell opening, functions in attachment and locomotion (Leighton 2008). From a metabolic perspective, it is interesting to note that although the foot region comprises approximately 66% of the body mass, it receives only 27% of the cardiac output (Jorgensen *et al.* 1984). Poor perfusion, high glycogen reserves (Laas & Vosloo 2010) and the diversity in anaerobic enzymes (Gäde 1988; O'omolo *et al.* 2003) suggest that the foot muscle relies primarily on anaerobic glycolysis for energy generation.

Visceral mass portion

The visceral mass is the nonmuscular metabolic region of the abalone and contains the digestive, respiratory, circulatory and reproductive organs (Kilburn & Rippey 1982; Hickman *et al.* 2006).

The abalone digestive system consists of a mouth, a buccal region and an oesophagus that extend posteriorly to the crop and terminate in the anus which, due to torsion, is situated dorsally to the gills. The digestive gland is closely associated with the intestine and functions in energy storage (in the form of lipids and glycogen), metabolic transformation, enzyme synthesis, gametogenesis and a protective role via antioxidant production (Carefoot *et al.* 2000). Due to these dynamic functions, biochemical constituents of the digestive gland tissue are highly variable (Laas & Vosloo 2010), and there have been conflicting reports of digestive gland glycogen decreasing (Carefoot *et al.* 1993) or remaining unchanged (Sheedy *et al.* 2015) in a response to starvation.

Aerobic metabolism of abalone is supported by gas exchange through a pair of bipectinate gills located below the shell pores. Due to shell asymmetry, the left gill is bigger than the right (Wells *et al.* 1998a; Ragg & Taylor 2006; Leighton 2008). During resting conditions, the right gill is continuously perfused, and this adequately supplies to the oxygen demand. However, when oxygen demand increases, abalone are able to divert more haemolymph towards the

left gill also, subsequently increasing oxygen uptake (Ragg & Taylor 2006).

A circulatory system containing a heart, arteries, veins and various sinuses throughout the body is found in abalone, allowing haemolymph to fill and circulate through the spaces surrounding its internal organs (Hickman *et al.* 2006; Morash & Alter 2015). Haemocyanin of gastropods displays a reverse Bohr effect, where oxygen binds tighter at a low pH or high carbon dioxide (CO_2) partial pressure, enabling abalone to maintain oxygen saturation when clamping to surfaces (Wells *et al.* 1998a; Morash & Alter 2015). The structural and functional limitations of the oxygen supply system may partly explain the enhanced anaerobic capacity and diversity of the anaerobic pathways (D-lactate, opine and glucose/aspartate–succinate pathways) in abalone. As a result of the oxygen binding properties of haemocyanin, it has been suggested that the abalone circulatory system has a bias for oxygen storage instead of oxygen delivery, in scenarios where muscles are actively working (Donovan *et al.* 1999).

It is clear that the evolutionary history of abalone has endowed them with adaptations, some quite unique, at the morphological, anatomical, biochemical and metabolic levels to suit their biology and ecology. We require a good understanding of these features as the characteristics of the farming environment may be complementary, or at odds with, the basic biology of abalone.

Abalone biology vs. growth in the farming context

Abalone have a number of traits that contribute to successful farming including: the relatively small number of adults required as broodstock, which relieves pressure on wild stocks, they have a nonfeeding planktonic larval stage, they consume a relatively nonfouling algal food supply as juveniles, they have high survival rates under crowded conditions, they are relatively sedentary (hence use minimal energy for movement), and they eat plant-based food which is relatively cheap (Hahn 1989; Fallu 1991). Considering all of these characteristics, abalone can be considered as a model farm animal, supporting expanding industries in China, Korea, South Africa, Chile, Australia and the USA (all producing >200 metric tonnes per annum) (Cook 2014).

Abalone farms are found in regions with coastal water temperatures that coincide with optimal growth temperatures. Many farms have both hatcheries and on-growing facilities. The hatchery is typically divided into four divisions, each specialised to the different life cycle phases of the abalone, and includes the (i) broodstock, (ii) larvae, (iii) settlement and (iv) weaning phase. Once the abalone have completed these development stages, they are moved to the farms' grow-out facility where they are tended and cared for until they reach market size (Hahn 1989; Fallu 1991; Troell *et al.* 2006).

As abalone grow only two to three centimetres per year, it takes approximately 4 years for abalone to reach a market size of approximately 80 g/90 mm, in these intensive culture systems (Fallu 1991; Troell *et al.* 2006). Freezing, canning or live export to Eastern markets are the destined outcome for most farm grown abalone, ultimately contributing significantly to the country's exports and economy per annum (Vosloo & Vosloo 2006).

To optimise growth, strict control of the farming growth environment is maintained, including water temperature (due to site selection), oxygen supply, food availability and water circulation rates (Denny & Gaines 2007). Despite this however, and the fact that all abalone in a basket are typically the offspring of a small number of parents with very little genetic variation, individual abalone growth performance (based on size) in a hatchery is difficult to predict between the individuals (Heath & Moss 2009). Although regular size grading and sorting into size classes assist in better growth performance, variation in growth rates still occurs. In the end, slow-growing animals will never really catch up and fail to reach their potential maximum size, despite optimising the growth environment (Steinarsson & Imsland 2003). Even in a good growth performing abalone group, slow growers are always present, which contribute to an increased average age of the population (Mouton & Gummow 2011). Fallu (1991) reported that slow growth, coinciding with a decreased food utilisation, and reduced rates of meat protein and glycogen synthesis, could be reversed by treating these slow growers with insulin. A study investigating the genetic growth aspects of tropical abalone *Haliotis asinina* revealed upregulated ferritin and metallothionein in the fast-growing animals. Consequently, it was speculated that fast-growing animals have a different metabolic rate and/or a differential ingestion of copper containing feeds, making ferritin and metallothionein possible markers of improved growth in abalone (Lucas 2007).

It can be expected that the way abalone utilise available energy strongly influences the degree of growth achieved by the end of the farming period. Abalone are known to be poikilotherms and subsequently do not utilise energy to maintain body temperature, and generally, their metabolic rate can be predicted by body size and ambient water temperatures (Fallu 1991; Britz *et al.* 1997). Barkai and Griffiths (1988) used a standard energy budget equation (consumption = growth rate + reproductive output + respiration + faecal losses + excretion), to determine the energy allocation pattern of *Haliotis midae*. From this study, it was found that approximately 63% of the energy content of the consumed food is lost as faeces; 32% expended on respiration; less than 1% lost as excreted ammonia (NH_3); and only about 5% of energy intake is

used for growth and reproductive output (Barkai & Griffiths 1988; Sales & Britz 2001).

The concept of growth can be crudely summarised as the process by which ingested food gets converted to body tissue. Optimising maximum growth is top priority in the abalone farming sector (Lee 2004; Naidoo *et al.* 2006) and is typically measured as a correlation between shell length and live weight (Sales & Janssens 2004). On a typical abalone farm, the grow-out phase is usually the most expensive and the longest of all the development phases, making it a priority for the farmer to get the maximum growth and hence, return on the investment spent during this phase (Fallu 1991). Subsequently, a great deal of research has gone into the feeding of abalone, for the purpose of manufacturing high-quality feed necessary for increasing farm productivity.

Feeding of abalone in the farming context

Although abalone are generally nocturnal feeders (Fallu 1991; Knauer *et al.* 1995), it was reported that *H. midae* prefer to feed in the early hours of the morning, rather than at dusk (Wood & Buxton 1996). Due to their nocturnal feeding pattern, abalone are relatively sedentary during the day, and active at night (Barkai & Griffiths 1988). Furthermore, vigorously moving water was also reported to stimulate abalone to feed (Fallu 1991). A feeding frequency of once a day was found sufficient when using formulated feeds (Sales & Britz 2001), due to the fact that these foods can remain in the crop and stomach of abalone for up to 12 h after ingestion, and subsequently released as needed (Wood & Buxton 1996).

Abalone can be classified as opportunistic herbivores and subsequently feed on a variety of different plant-based foods, which changes throughout their development, that is their diets progress from planktonic diatoms, to sessile diatoms/algae, to attached seaweeds, etc. as they develop from free-swimming larvae, to attached, to juveniles, to adults, respectively (Sales & Britz 2001; Troell *et al.* 2006). When deciding on which feed best suits the farm (kelp, seaweed and/or artificial feeds), various factors are considered and include the price of the specific feed, its conversion ratio, its freshness and its accessibility. Farms are constantly investigating suitable feeding combinations and feeding formulas that will significantly improve growth rates of abalone (Troell *et al.* 2006). To achieve maximum growth rates, the type of feed that is utilised in culture systems needs to complement the abalone digestive system (Bansemer *et al.* 2014). Tamayo *et al.* (2011) found that in clams, high growth rates are typically achieved through a combination of faster feeding and higher digestive performance, this may be true for abalone as well.

Research carried out for the purpose of determining the exact nutrient requirements, and subsequently, optimal feed ingredients of formulated abalone feeds are complicated by the slow-feeding behaviour and growth rates of abalone (Sales 2004). Despite this however, extensive research regarding the best feeding strategy for abalone is widely available. As the scope of this study is not to review all these findings, dietary research carried out on especially *H. midae* serve well to illustrate this point (Day & Cook 1995; Britz 1996a; Sales & Britz 2001; Day & Branch 2002; Macey & Coyne 2005; Naidoo *et al.* 2006; Ten Doeschate & Coyne 2008; Robertson-Andersson *et al.* 2011; Huddy & Coyne 2014).

Formulated feeds as main diet for growing abalone

Pelletized or extruded abalone feed is usually formulated from proteins, carbohydrates, lipids, minerals and vitamins, which are held together by an alginate binder (Fallu 1991). Abfeed™ (Marifeed Pty Ltd, Hermanus, South Africa), for instance, is formulated using fishmeal, soya bean meal, starch, vitamins and minerals consisting of about 43% carbohydrates, 35% protein, 10% moisture, 6% ash, 5% fat and 1% crude fibre (Troell *et al.* 2006). A review performed by Bansemer *et al.* (2014) gives comprehensive insights into macroalgae used as abalone feed. The benefits of using formulated abalone feeds over that of fresh seaweed, macroalgae or kelp include the following: being more readily available, ease of use, easily manufactured, optimised to achieve high growth rates, has a low food conversion ratio, easily stored and transported, and its composition is not varied or dependant on a geographical location (Fallu 1991; Fleming *et al.* 1996). Optimising the percentage of proteins, carbohydrates, lipids and other additives in formulated abalone feed is the subject of numerous complementary, and contradictory studies, and will subsequently be briefly discussed below.

Proteins

Protein is regarded as an important dietary component in abalone feed, as this is the anabolic substrate which is considered to mostly influence growth (Lee 2004). Apart from using protein-rich ingredients including fish and abalone viscera silage, *Spirdina* spp., additional amino acids such as methionine, arginine, lysine or threonine are also added. Although sufficient amounts of protein are essential for optimum growth, amounts above a certain threshold hold no additional value (Fleming *et al.* 1996) and simply get catabolised to free amino acids not utilised for growth (Dunstan 2010). That said, there are, however, large discrepancies in the literature regarding the optimal levels for dietary protein intake in abalone, with the amounts reported in scientific literature to vary between 20% and

50% of the total nutrient intake (Fallu 1991; Fleming *et al.* 1996; Bautista-Teruel & Millamena 1999; Angell *et al.* 2012). This variation could be species dependent, and the optimal dietary protein intake for *H. midae* largely considered to be 36% of the total nutrient intake (Robertson-Andersson *et al.* 2011), derived mainly from fishmeal and *Spirulina* spp. (Britz 1996b).

Carbohydrates
Research on the composition of *Haliotis* digestive enzymes revealed high concentrations of not only protease but also amylase, cellulase and alginase accompanied by comparatively low amounts of lipases, and subsequently, the conclusion was made that carbohydrates are the most important energy source for these animals (Lee 2004). Consequently, formulated abalone feeds contain carbohydrate contents varying anything between 30% and 60% (Fallu 1991; Fleming *et al.* 1996; Sales 2004), derived from low cost raw materials such as wheat flour, maize flour, sodium alginate, dextrin, starch and bran (Sales 2004). When abalone are fed a diet with insufficient amounts of carbohydrates, they utilise mostly protein, as a source, for *de novo* carbohydrate synthesis, reducing the amounts of available protein for muscle anabolism and growth (Fallu 1991).

Lipids
Dietary lipids play an important role in the provision of energy, essential fatty acids and fat-soluble nutrients, for optimal abalone growth. The lipids in formulated abalone feeds are typically derived from fish oil, vegetable oil, lipids bound in fishmeal or a combination of these ingredients. As abalone have low dietary lipid requirements (5%), substantiated by their low lipase activity, it is likely that lipids are still oversupplied in some formulated feeds on the market (Fallu 1991; Fleming *et al.* 1996; Lee 2004).

Minerals & vitamins
In general, research on the optimal composition and levels of vitamins and minerals in abalone feed are scarce (Fleming *et al.* 1996); however, overtime an approximation of 5% of the total nutrient contents of formulated abalone feed was deemed sufficient to make up minerals, vitamins and other trace elements in abalone feed (Fallu 1991). Some examples of the vitamins found in formulated abalone feeds are vitamin E (Bansemer *et al.* 2016), vitamin A, vitamin-B12, vitamin-C, vitamin-D, riboflavin and biotin (Mai 1998). Minerals used to enhance abalone feeds may include sodium, calcium (Bansemer *et al.* 2016), sodium chloride, zinc and potassium iodide (Tan & Mai 2001). Many of these minerals added to the diet are considered unnecessary as abalone absorbed some of these components directly from the surrounding water (Fleming *et al.* 1996; Sales 2004).

Binders
Apart from the added starch which can serve as a binding agent, other binding agents are also added to formulated abalone feeds, which not only allow for the food pellets to remain intact but also serve to stabilise and prevent loss of the water soluble nutrients (Fleming *et al.* 1996; Sales 2004). Typically, sodium alginate is used in amounts ranging from 20% to 45% of the total feed weight (Fallu 1991).

Interindividual variation despite identical feeding strategies

Interindividual variation in energy acquisition and growth exists in the same population of abalone despite similar or identical environmental conditions. These interindividual differences, although being problematic from a farming productivity perspective, do create new opportunities for understanding the energetics involved in growth variability, which surely is a necessity in aquaculture (Tamayo *et al.* 2014). As previously mentioned, growth can be summarised as the conversion of ingested food to body tissue, that is the relationship between anabolism (biosynthesis) and catabolism (biodegrading) which is important for growth, and a better understanding thereof could assist in determining the optimal nutrient requirements and also possibly those factors related to abalone growth rates. In a spat of clams for instance, it was found that faster growth was related to increased energy acquisition, reduced metabolic maintenance costs and reduced growth costs in terms of the metabolism used to sustain biosynthesis (Tamayo *et al.* 2011). The evaluation of normal metabolism includes scenarios from adaptation to starvation periods, exercise and pregnancy. Abnormal metabolism may be a consequence of abnormal hormone secretion, enzyme deficiencies, nutrient deficiencies or the actions of drugs and toxins (Murray *et al.* 2003). However, before one can assess or measure abnormal metabolism due to any stressors, an adequate knowledge of 'normal' abalone metabolism is first required.

Basic metabolism and how we apply it to abalone

Metabolism can be seen as the sum total of all chemical changes that convert nutrients to energy and the chemical end products of cells. The synthesis of biological macromolecules and the generation of energy to drive vital functions are regarded as the two main purposes of metabolism. To achieve this balance, contrasting metabolic pathways are required as depicted in Fig. 1. These pathways are typically divided into three categories: (i) Catabolism, (ii) Anabolism and (iii) Amphibolism. Catabolism can be broadly defined as the oxidation of complex nutrient molecules, through mostly exergonic reactions, resulting in the

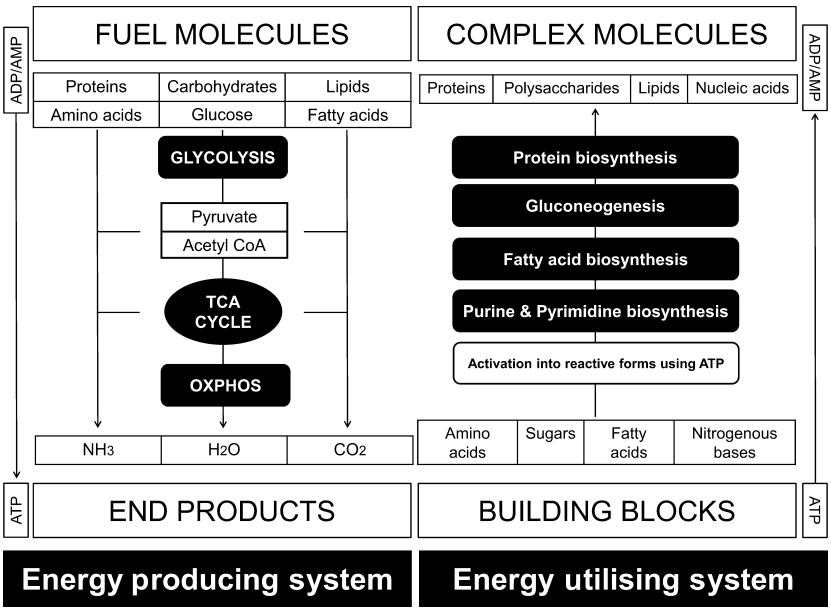

Figure 1 Overview of metabolism highlighting the energy producing and utilising systems.

production of energy in the form of adenosine triphosphate (ATP). In this instance, carbohydrates, lipids and proteins are metabolised to a common intermediate molecule known as acetyl coenzyme A (acetyl CoA). Acetyl CoA subsequently serves as a substrate for the tricarboxylic acid (TCA) cycle, which in turn generates reduced electron carriers for ATP production via the oxidative phosphorylation (OXPHOS) system and the end products of catabolism, namely water, CO_2 and NH_3 (Murray *et al.* 2003; Garrett & Grisham 2010). Anabolism on the other hand is the synthesis of complex biomolecules from simple precursors. These reactions involve the formation of new covalent bonds and an input of chemical energy to drive endergonic processes. Hence, the ATP generated during catabolism is used together with nicotinamide adenine dinucleotide phosphate (NADP) for the reductive reactions required during this process. Anabolic processes subsequently allow for the synthesis of various macromolecules including polysaccharides, lipids, proteins and nucleic acids from their sugar, fatty acid, amino acid and nitrogenous base precursors, respectively. In essence, these metabolic processes are used to build genetic material, cells and muscle and are essential for the development, growth and maintenance thereof (Garrett & Grisham 2010). Amphibolism is the process or those pathways that act as both catabolic and anabolic, as many metabolic intermediates are shared between the two processes (Murray *et al.* 2003; Whitney & Rolfes 2008; Garrett & Grisham 2010).

One of the unifying principles of biology is the profound similarities that exist in the major metabolic pathways when comparing different species and organisms (Garrett & Grisham 2010). A result of this phenomenon is the scientific practises of gene prediction, functional genomics and associated software. Also, large similarities between molluscan metabolism and that of vertebrates have been reported (Ballantyne 2004). Subsequently, it is advisable to investigate abalone metabolism in the context of what is already known from other organisms, to predict the missing puzzle pieces in abalone metabolism.

Large differences in energy expenditure associated with the metabolism of proteins, carbohydrates and lipids are found in tissues. These changes are due to the different ways proteins, carbohydrates and lipids are handled by cells and their function in cellular metabolism. Generally, proteins act as structural and functional elements in cellular metabolism, carbohydrates are used primarily for energy production, and lipids serve as the major structural elements of cell membranes (Lawrence 2013). Abalone are capable of catabolising proteins, carbohydrates and lipids, as these are all prominently found in their diet. As a rule, abalone tissue has a low lipid content, and therefore, proteins and carbohydrates are mainly used to fuel metabolism resulting in reduced lipid metabolism (Vosloo & Vosloo 2010). This phenomenon, and many other unique metabolic processes identified in abalone, will be discussed below in the context of the summary given in Table 1.

Protein metabolism

The primary physiological purpose of amino acids is to serve as the building blocks for proteins. Amino acid biosynthesis requires firstly the synthesis of the correct

Table 1 Summary of biomolecules associated with different abalone-based studies

Abalone species	Tissue studied	Biomolecule detected or analysed	Metabolic pathways involved	Methods used	Perturbation, stressor or measurand	Reference
Haliotis lamellosa	Adductor and foot muscle	Tauropine, and D-lactate	Opine metabolism	Spectrophotometer and enzyme analysis	Experimental anoxia and exercise induced scenarios	Gäde (1988)
		ATP, ADP, AMP, Arg phosphate and succinate	Energy metabolism			
		Arg, taurine, Ala and Asp	Amino acid (AA) metabolism			
Haliotis iris and *Haliotis australis*	Adductor and foot muscle	Tauropine, taurine dehydrogenase, lactate dehydrogenase and D-lactate	Opine metabolism	Enzyme analysis	Stress handling and air exposure periods	Wells and Baldwin (1995)
		ATP, ADP and AMP	Energy metabolism			
Haliotis midae	Tissue and shell	Ala, Arg, Asp, Cys, Glu, Gly, His, Ile, Leu, Lys, Met, Phe, Pro, Ser, Thr, Trp and Val	Amino acid metabolism	LC techniques, GC with flame ionisation detector (FID), spectrophotometer and flame emission analysis	Optimisation experiments for *H. midae* diet	Knauer *et al.* (1995)
		C16:0, C18:1, C18:2, C19:0 and C20:5	Fatty acid metabolism			
		Calcium, cadmium, cobalt, copper, iron, sodium, magnesium, manganese, nickel, zinc and chromium	Mineral metabolism			
Haliotis laevigata	Foot muscle	C16:0, C18:0, C18:1n-7, C18:1n-9, C20:4n-6, C20:5n-3 and C22:5n-3	Fatty acid metabolism	GC – FID	Lipid investigations into different diets	Dunstan *et al.* (1996)
		Cholesterol	Sterol metabolism			
Haliotis rufescens	Soft body parts	Abalone nonessential AA: Ala, Asp, Cys, Glu, Gly, Pro and Ser Abalone essential AA: Arg, His, Ile, Leu, Lys, Met, Phe, Thr, Trp and Val	Amino acid metabolism	Radio assayed methods	Abalone amino acids classification study	Fleming *et al.* (1996)
Haliotis rufescens	Foot muscle	AMP, ATP, ADP and $NADH/NAD^+$	Energy metabolism	High performance liquid chromatography (HPLC)	Hypoxia and toxicant exposure	Shofer & Tjeerdema (1998)
Haliotis iris	Adductor and foot muscles	Tauropine dehydrogenase	Opine metabolism	Spectrophotometer and kinetic software	Abalone exposed to wave action	Wells *et al.* (1998b)
		ATP, IMP, D-lactate, glycogen and glucose	Energy metabolism			
		Homarine	Organic osmolytes			

Table 1 (continued)

Abalone species	Tissue studied	Biomolecule detected or analysed	Metabolic pathways involved	Methods used	Perturbation, stressor or measurand	Reference
Haliotis kamtschatkana	Adductor and foot muscles	Tauropine dehydrogenase, octopine dehydrogenase, strombine dehydrogenase, alanopine dehydrogenase, lysopine dehydrogenase and tauropine	Opine metabolism	Enzyme assays	Abalone crawling in water and air exposure	Donovan *et al.* (1999)
		D-lactate dehydrogenase, D-lactate, arginine and arginine phosphate	Energy metabolism			
Haliotis kamtschatkana	Digestive gland	Glucose	Energy metabolism	Gilson oxygen-cell fitted with a Clark-type O_2 electrode	Measuring metabolic activity of digestive gland cells	Carefoot *et al.* (2000)
Haliotis rufescens	Adductor muscle	Phosphoarginine	Energy metabolism	HPLC	Validation of a phosphoarginine HPLC method	Viant *et al.* (2001)
Haliotis tuberculata	Haemolymph	Noradrenaline and dopamine	Catecholamine metabolism	HPLC with electrochemical detection	Mechanical stressor exposure	Malham *et al.* (2003)
Haliotis fulgens	Eggs and larvae	Triacylglycerol and phospholipids	Lipid metabolism	Latroscan MK-5 flame ionisation detector	Metabolic rate and biochemical reserve investigation	Moran & Manahan (2003)
Haliotis midae	Adductor and foot muscle	Tauropine and D-lactate	Opine metabolism	Anion exchange chromatography on DEAE-Sephacel	Exposure to extreme anaerobic conditions and incubation under simulated transport conditions	O'omolo *et al.* (2003)
Haliotis fulgens	Muscle	C14:0, C16:0, C16:1n-7, C16:4, C17:0,C17:1n-7, C18:0, C18:1n-7, C18:1n-9, C18:2n-4, C18:2n-6, C18:3n-3, C18:4n-3, C18:3n-6, C20:0, C20:1n-7, C20:1n-9, C20:1n-11,C 20:2n-6, C20:4n-3, C20:4n-6, C20:5n-3, C21:5n-3, C22:1n-9, C22:1n-11, C22:5n-3, C22:5n-6, and C22:6n-3	Fatty acid metabolism	GC-FID	Starvation and dietary lipid differences	Durazo-Beltrán *et al.* (2004)

Table 1 (continued)

Abalone species	Tissue studied	Biomolecule detected or analysed	Metabolic pathways involved	Methods used	Perturbation, stressor or measurand	Reference
Haliotis rubra and *Haliotis laevigata*	Digestive gland, gonads and foot muscle	Saturated -, monounsaturated -, and polyunsaturated fatty acids, n-3:n-6 polyunsaturated fatty acid ratio and arachidonic acid:eicosapentaenoic acid ratio	Lipid/fatty acid metabolism	GC-FID	Examining the lipid and fatty acid composition of tissues and the effect of different conditioning temperatures	Grubert *et al.* (2004)
Haliotis rufescens	Digestive gland and foot muscle	Glycogen	Energy metabolism	Spectrophotometric analysis	Examination of the effect of reduced food supply, elevated temperature and WS exposure on abalone health	Braid *et al.* (2005)
Haliotis rufescens	Digestive gland and foot muscle	Ala, Asp, Glu, Gln, Gly, Ile, Leu, Lys, Pro, Thr, Val, Tyr, Trp, Phe and taurine	Amino acid metabolism	NMR	Investigation into the effects of elevated water temperature, reduced food availability and WS-RLP presence and abalone metabolic profiles	Rosenblum *et al.* (2005)
		α- and β-glucose, phosphagens, TCA cycle intermediates, carnitine, nucleotides, glycolytic products and homarine	Energy metabolism			
Haliotis rufescens	Foot muscle	Various amino acids, taurine and hypotaurine	Amino acid metabolism	NMR	Antibiotic oxytetracycline therapy during a metabolic recovery period after WS-RLP elimination	Rosenblum *et al.* (2006)
		Carbohydrates, glycogen and phosphoarginine	Energy metabolism			
		Glycine-betadine and homarine	Organic osmolytes			
Haliotis midae	Haemolymph	Chlorine, sodium, potassium, magnesium, calcium and copper	Mineral metabolism	Inductively coupled plasma mass spectrometry	Extreme dehydration stress as a result of air exposure	Vosloo and Vosloo (2006)
Haliotis fulgens	Plasma and muscle	Abalone essential AA: Arg, His, Ile, Leu, Lys, Met, Phe, Thr and Val Abalone nonessential AA: Ala, Asn, Glu, Gly, Pro, Ser, taurine and Tyr	Amino acid metabolism	HPLC analysis	A 27 day starvation period	Viana *et al.* (2007)
Haliotis diversicolor	Muscle	Glycine, and glutamate AMP	Amino acid metabolism Energy metabolism	Omission tests	Characterisation of the taste of abalone meat	Brown *et al.* (2008)

Table 1 (continued)

Abalone species	Tissue studied	Biomolecule detected or analysed	Metabolic pathways involved	Methods used	Perturbation, stressor or measurand	Reference
Haliotis midae	Digestive gland and muscle	Glucose and glycogen Proteins Lipids	Energy metabolism Amino acid metabolism Lipid/fatty acid metabolism	Enzyme colorimetric reactions, enzyme analysis, Western blot immunodetection, and a lipid extraction method	Age differences, seasonal changes, natural and artificial feed and supplementation of natural and artificial feeds	Laas and Vosloo (2010)
Haliotis discus and *Haliotis discus hannai*	Muscle	Cadmium, lead and mercury C14:0, C16:0, C16:1n-7, C18:0, C18:1n-9, C18:1n-7, C18:2n-6, C18:3n-3, C20:0, C20:1n-9, C20:4n-6, C20:5n-3, C22:1n-9, C22:4n-6, C22:5n-3, C22:6n-3 and C24:1n-9 Ala, Arg, Asp, Glu, Gly, His, Ile, Leu, Lys, Met, Phe, Pro, Ser, Thr, Tyr and Val	Mineral metabolism Fatty acid metabolism Amino acid metabolism	Inductive coupling to plasma and mercury analyser GC-FID	Heavy metal contents and biochemical characteristic comparisons of two abalone species	Bae *et al.* (2011)
Haliotis fulgens	Muscle	Saturated fatty acids, monounsaturated fatty acids, polyunsaturated fatty acids and long-chain polyunsaturated fatty acids	Fatty acid metabolism	GC	Long period starvation	Durazo and Viana (2013)
Haliotis tuberculata	Muscle	Saturated, unsaturated, monounsaturated and long-chain polyunsaturated fatty acids	Fatty acid metabolism	GC-FID	Evaluation of the growth performance, appearance and fatty acids in abalone fed different diets	Hernández *et al.* (2013)
Haliotis rubra × *laevigata* hybrid	Haemolymph	Proteins, phosphate, magnesium, sodium, chloride, calcium and potassium	Various metabolic pathways	Biochemistry multichannel analyser	Elevated water temperature exposure	Hooper *et al.* (2014)
Haliotis discus hannai Ino	Muscle	Saturated, monounsaturated and polyunsaturated fatty acids Volatile compounds: aldehydes, aromatic compounds, alkanes, alcohols, ketones and furans Betaine, dimethylamine and homarine	Fatty acid metabolism Various metabolic pathways Organic osmolytes	GC-MS and solid-phase micro-extraction gas chromatography–mass spectrometry	Investigations into different heating conditions	Wang *et al.* (2014)
Haliotis squamata	Muscle and gonads	Essential AA: Arg, His, Ile, Leu, Lys, Met, Phe, Thr and Val Nonessential AA: Ala, Asp, Glu, Gly and Ser Saturated and unsaturated fatty acids	Amino acid metabolism Fatty acid metabolism	Kjeldahl protein establishing method and lipid extraction followed by calculation method	Abalone cultured in different aquaculture systems	Latuihamallo and Apituley (2015)

Table 1 (continued)

Abalone species	Tissue studied	Biomolecule detected or analysed	Metabolic pathways involved	Methods used	Perturbation, stressor or measurand	Reference
Haliotis rubra × *Haliotis laevigata*	Digestive gland	Ala, Arg, Asp, Glu, Gln, Gly, His, inosine, Ile, Leu, Lys, Met, *N,N*-dimethylglycine, Phe, Ser, taurine, Thr, Trp, Tyr, uracil and Val	Amino acid metabolism	NMR	Short-term feeding and starvation experiments	Sheedy *et al.* (2015)
		Betaine and homarine	Organic osmolytes			
		Acetate, Glucose, succinate, and D-lactate	Energy metabolism			
		O-phosphocholine	Lipid biosynthesis			
Haliotis diversicolor supertexta	Haemolymph and muscle	Alan, Glu and Leu	Amino acid metabolism	NMR	Abalone exposed to dibutyl phthalate	Zhou *et al.* (2015)
		Acetate, ATP/ADP, glucose, succinate and D-lactate	Energy metabolism			
Haliotis midae	Muscle	Aminomalonic acid, glycine, phenylalanine, proline and threonine	Amino acid metabolism	GC-MS	Establishment of an untargeted GC-MS metabolite profiling method	Venter *et al.* (2016)
		Galactose, glucose	Energy metabolism			
		Pinitol, inositol and isonicotinic acid	Various metabolic pathways			
		Pentanoic acid	Fatty acid metabolism			

alpha (α)-keto acid carbon skeleton for the amino acid, followed by transamination of the α-keto acid with glutamic acid serving as the amino donor via an aminotransferase reaction (Garrett & Grisham 2010). Abalone essential amino acids (Arg – arginine, His – histidine, Ile – isoleucine, Leu – leucine, Lys – lysine, Met – methionine, Phe – phenylalanine, Thr – threonine, Trp – tryptophan and Val – valine) and nonessential amino acids (Ala – alanine, Asp – aspartic acid, Cys – cystine, Glu – glutamic acid, Gly – glycine, Pro – proline, Ser – serine and Tyr – tyrosine) have been confirmed in a number of studies as summarised in Table 1 (Fleming *et al.* 1996; Viana *et al.* 2007; Bae *et al.* 2011; Latuihamallo & Apituley 2015). Rosenblum *et al.* (2005) reported that the less metabolically active nonessential amino acids of abalone are used to maintain osmoregulation, when the levels of free amino acids are depleted. The fact that taurine has a well-established role in osmoregulation of marine invertebrate tissues (Welborn & Manahan 1995; Fasulo *et al.* 2012; Cappello *et al.* 2013) further supports this observation. Apart from their possible role in osmoregulation, these essential and nonessential amino acids are typically degraded by different pathways, subsequently forming succinyl CoA, acetyl CoA, acetoacetate, pyruvate, α-ketoglutarate, fumarate and oxaloacetate, all of which feed into the energy production pathways (Whitney & Rolfes 2008; Garrett & Grisham 2010).

It is generally considered that energy production from proteins is energy expensive, and less optimal than energy acquisition from carbohydrates. To favour carbohydrates as the preferred energy source, various organisms, including abalone and catabolise, ingested proteins into their respective amino acids, peptides or protein pools (Lawrence 2013). However, in times when energy levels are low, or carbohydrate intake is restricted, or when there is surplus of protein or amino acids in the system, protein is used as an energy source. For this to occur, protein is catabolised into two end products: the carbon structure (without an amino group) and ammonia (Whitney & Rolfes 2008; Garrett & Grisham 2010). The carbon structure feeds directly into the energy generating metabolic pathways, and in aquatic animals, the ammonia is excreted, due to its toxicity (Morash & Alter 2015). It has additionally been reported that especially during the early development phase of marine animals, protein is more readily used as an energy source (Latuihamallo & Apituley 2015).

Carbohydrate metabolism

In most organisms, a large amount of cellular energy is derived from the oxidation of carbohydrates via glycolysis and the TCA cycle (Lawrence 2013). Glycolysis consists of two phases: (i) glucose breakdown to glyceraldehyde-3-phosphate (G-3-P) molecules and (ii) the conversion of G-3-P to eventually produce two pyruvate molecules. During this process, two ATP and two nicotinamide adenine dinucleotide (NADH) molecules are the result (Garrett & Grisham 2010). Enough evidence exists to suggest that glucose in abalone follows the traditional glycolysis route used in other organisms. A number of studies have focused on the quantification of glucose in abalone as summarised in Table 1 (Carefoot *et al.* 2000; Braid *et al.* 2005; Rosenblum *et al.* 2005, 2006; Laas & Vosloo 2010; Sheedy *et al.* 2015; Zhou *et al.* 2015; Venter *et al.* 2016). Also, glucose-6-phosphate was successfully measured in the shell adductor and foot muscle of *Haliotis lamellose* (Gäde 1988), supporting glucose breakdown via glycolysis. That said, it should also be noted that no studies have been carried out to date proving the presence of the other metabolites of glycolysis, for example fructose-6-phosphate, fructose-1.6-diphosphate and dihydroxyacetone phosphate in abalone. Regardless of this shortcoming, the well-known end product of glycolysis, pyruvate (essential for opine formation, as will be discussed later), has been successfully measured in abalone (Zhou *et al.* 2015), further supporting this suggested metabolic pathway exists in this animal.

During conditions when insufficient carbohydrates are consumed and glycogen is depleted, most organisms have the capacity for *de novo* glucose synthesis, from nonsugar carbon substrates, through a process known as gluconeogenesis (Salway 2004). Gluconeogenesis can be seen as the reversal of glycolysis, with a few deviations. Glycolysis and gluconeogenesis are under reciprocal control, thus when the one is active, the other is inhibited (Garrett & Grisham 2010). As glycogen has also been measured on a number of occasions in abalone (Carefoot *et al.* 2000; Braid *et al.* 2005; Rosenblum *et al.* 2005, 2006; Laas & Vosloo 2010; Zhou *et al.* 2015) as indicated in Table 1, it leads us to believe that the same, or a similar metabolic pathway exists in abalone metabolism. Metazoans are known to synthesise glycogen from glucose, as a mean to store carbohydrates, resulting in a lower energy cost for glycogen synthesis when compared to protein synthesis (Lawrence 2013).

Lipid metabolism

Lipids primarily play a role in growth and gonad maturation in abalone (Durazo & Viana 2013). The synthesis of fatty acids and other lipid components in many living organisms starts with malonyl CoA, a four carbon molecule synthesised using two acetyl CoA's, at the expense of one ATP molecule. As mentioned earlier, abalone have low lipid concentrations in their tissues, which is most likely due to a lower dependence on these compounds as an energy source, driven by the low amounts of lipid compounds present in their diets, and subsequently less lipase in their digestive tract (Laas & Vosloo 2010). Interestingly, the

primary function of n-3 and n-6 polyunsaturated fatty acids in abalone is to serve as substrates for structural components (Durazo-Beltrán *et al.* 2003). Generally, the neutral lipids of abalone are only metabolised as an energy source, when protein and carbohydrates are depleted, during extended periods of fasting (Durazo & Viana 2013).

The portion of cellular energy, utilised for lipid metabolism, is relatively low when compared to the overall costs of carbohydrates and proteins, because only a fraction of the fatty acids and sterols absorbed from the diet, undergo *de novo* lipid synthesis (Lawrence 2013). Nonetheless, when lipids are required as an energy source, they are typically metabolised to glycerol and fatty acids in the cytoplasm, and eventually form glycolysis substrate intermediates (Murray *et al.* 2003; Whitney & Rolfes 2008; Garrett & Grisham 2010). The catabolism of fatty acids can proceed via a number of routes depending on the length of the acid, the number of carbons and whether they are saturated or unsaturated via a process named beta (β)-oxidation. Most important to know is that the products of β-oxidation are acetyl CoA, NADH and flavin adenine dinucleotides ($FADH_2$). Equally important to note is that acetyl CoA enters the TCA cycle, and NADH and $FADH_2$ will be used by the electron transport chain (ETC) to produce ATP (Lopaschuk *et al.* 2010). Fatty acids ranging from C14 to C24 have been detected abalone (Table 1). Studies investigating the effect of starvation, dietary composition, water temperature variation, and pre- and post-spawning cycles on abalone lipid and/or fatty acid content are present in the literature. Very few mechanistic studies investigating the breakdown of these lipids, however, have been performed, with most of the research to date focused more towards describing the varying compositions of the fatty acids during such conditions (Durazo-Beltrán *et al.* 2004; Grubert *et al.* 2004; Durazo & Viana 2013; Hernández *et al.* 2013; Wang *et al.* 2014).

Nucleic acid biosynthesis

Nucleic acids (deoxyribonucleic (DNA)–ribonucleic acid (RNA)) are complex polymeric molecules, with a sequence of nitrogenous bases (or nucleotides) which encodes the genetic information necessary for biological inheritance as well as having other functions, like coding for both structural and functional proteins (Hickman *et al.* 2006). Nucleotides (purine: adenine and guanine and pyrimidine: thymine, cytosine and uracil) play a central role in metabolism, because they carry energy (in the form of high-energy phosphate bonds), combine cofactors of enzymes and participate in cell signalling (Salway 2004; Garrett & Grisham 2010). When energy levels are low, most of the ATP is in the form of adenosine monophosphate (AMP), and AMP-activated protein kinase (AMPK) is allosterically activated. Activation of AMPK signals the breakdown of proteins and lipids and shuts down biosynthesis and cell growth pathways (Garrett & Grisham 2010). From a farming productivity perspective, it would make sense to keep the AMP levels to a minimum, ensuring AMPK is inactive and anabolic pathways function as normal. However, from a culinary point of view, it has been reported that higher AMP levels play a key role in the desired taste of abalone (Brown *et al.* 2008). This may be a point of further investigation as both a high or low AMP content can be justified for increased productivity, and these ratios can easily be altered during stress. However, it was indicated that changes in adenylate concentrations can be detected rather rapidly following application of a stressor. In the short time, it took to remove *Haliotis iris* from substratum and freeze clamp the tissue samples, changes in adenylate muscle concentrations could already be detected and it was found that inosine monophosphate (IMP) concentrations increased due to AMP degradation (Wells *et al.* 1998b).

Energy metabolism

Cellular respiration is the process whereby cells manufacture energy (ATP) using intermediates produced during catabolism. Two types of respiration occur namely: (i) aerobic (requiring oxygen) and (ii) anaerobic (absence of oxygen) respiration. In terms of the amounts of ATP produced, aerobic respiration is far more efficient than anaerobic respiration. Respiration can roughly be divided into three stages consisting of: (i) glycolysis (aerobic and anaerobic), (ii) tricarboxylic acid cycle (aerobic) and (iii) oxidative phosphorylation (aerobic) (Wardlaw & Insel 2006), which will be discussed briefly below in the context of abalone metabolism.

Aerobic glycolysis

As described above, glycolysis is the process by which 1× glucose molecule is metabolised into 2× pyruvate molecules, 2× ATP molecules, 2× coenzyme molecules, 2× hydrogen ions (which enter the ETC) and 2× water molecules. In animals, the pyruvate produced is generally converted to acetyl CoA during aerobic conditions, by means of the enzyme pyruvate dehydrogenase, and then further metabolised in the TCA cycle to produce NADH, $FADH_2$ and CO_2. Acetyl CoA can also be used for the synthesis of fatty acids and lipids when the energy demand is met and glycogen stores are well stocked (Wardlaw & Insel 2006; Garrett & Grisham 2010).

As a general observation, abalone adductor–foot muscle are poorly perfused and subsequently abalone are thought to depend more strongly on anaerobic glycolysis to synthesise the required energy for this organs function of clamping to surfaces and movement (Hickey & Wells 2003).

As these animals are considered to be rather sedentary by nature, the proposed anaerobic glycolysis pathway can easily meet the lower energy demand required by the foot muscle, despite it producing comparatively less ATP than aerobic glycolysis.

Anaerobic glycolysis

Anaerobic metabolism is initiated whenever the oxygen demand exceeds the supply (Wardlaw & Insel 2006). In abalone, anaerobic glycolysis occurs due to the adequate muscle glycogen reserves available, high activities of pyruvate reductase for generating NAD^+ and the high concentrations of arginine phosphate (Donovan *et al.* 1999). During anaerobic conditions, such as hypoxia, the adductor muscle, mantle, digestive glands and gills of mussels have been reported to switch to anaerobic respiration in an attempt to generate ATP (Stefano *et al.* 2015). A similar mechanism of energy production is thought to take place in abalone, because its adductor muscle, foot muscle and haemolymph (Gäde 1988; Wells & Baldwin 1995; Donovan *et al.* 1999; Vosloo & Vosloo 2006) have been reported to respond to hypoxic conditions. However, during prolonged exercise or rapid movement through well-oxygenated water, anaerobic glycolysis is localised to the foot muscle only (Donovan *et al.* 1999). In survival scenarios where the whole animal needs to deal with anoxic (or hypoxic) situations, both the shell adductor and foot muscle were shown to uphold anaerobic metabolism (Gäde 1988).

Three main pathways are said to be responsible for energy production in marine invertebrates (including abalone) during anaerobic conditions (Fig. 2), namely (i) the lactate pathway, responsible for medium rates of energy production and used to maintain or increase metabolic activity; (ii) the opine pathway, which has the same function as the lactate pathway but occurs exclusively in invertebrates; and (iii) the glucose/aspartate–succinate pathway, which is used primarily for survival during anoxia (Livingstone 1983; Lee & Lee 2011; Harcet *et al.* 2013).

Lactate pathway. Mitochondrial respiration actively consumes electrons from NADH, produced from the oxidation of carbohydrates and other substrates (amino acids and to a lesser extent fatty acids in abalone). When mitochondrial respiration is low (due to low bioenergetics or an oxygen shortage), the ETC can no longer function optimally, and subsequently, NADH accumulates. This in turn results in a rate reduction in other important metabolic pathways due to a consequential NAD^+ shortage. It is during such times that the lactate pathway comes into play to avoid total metabolic shutdown during anaerobic conditions. Accumulating pyruvate is converted to lactate (by means of lactate dehydrogenase and coenzymes) simultaneously oxidising NADH to NAD^+, allowing the anaerobic glycolysis pathway to function (Murray *et al.* 2003; Whitney & Rolfes 2008; Garrett & Grisham 2010). Numerous mollusc (including abalone) species produce the D-isomer of lactate (and not L-lactate as in vertebrate organisms) which is said to play an important role in anaerobic energy metabolism (Cristescu *et al.* 2008). Due to abalone's reportedly low mitochondrial activity (see Tricarboxylic acid cycle), it can be assumed that this pathway is extremely important to this species in order to regulate NAD^+ concentrations, and to produce much needed ATP. This hypothesis is also supported by the relatively high D-lactate levels commonly found in abalone muscle samples when analysed with gas chromatography–mass spectrometry (GC-MS). However, the opine pathway is perhaps a better means for supplying to the required energy demand during anaerobic conditions, as it does not result in an acidic end product.

Opine pathway. In addition to D-lactate, molluscs accumulate a multitude of end products of anaerobic glycolysis (O'omolo *et al.* 2003), for example octopine, strombine, alanopine, tauropine, lysopine and β-alanopine (collectively known as opines). Opine formation in invertebrates (like abalone) takes place via a cytosolic fermentation pathway, where pyruvate is coupled to an amino acid (most popularly arginine, glycine, alanine, taurine, lysine and β-alanine) using a very specific dehydrogenase, resulting in an imino acid derivative (octopine, strombine, alanopine tauropine, lysopine and β-alanopine, respectively) as an energy metabolism end product (Fig. 3) (O'omolo *et al.* 2003; Baldwin *et al.* 2007; Müller *et al.* 2012; Harcet *et al.* 2013). The imino acid dehydrogenase in molluscs functions in a similar fashion to that of lactate dehydrogenase, resulting in the regeneration of cytoplasmic NAD^+ for usage in the G-3-P dehydrogenase reaction of glycolysis. Regardless of this substitution, the proton stoichiometry and the ATP yields remain the same (Gäde 1988; Prosser 1991; O'omolo *et al.* 2003), with the synthesis of two molecules of ATP per one molecule of glucose (Livingstone 1983; Müller *et al.* 2012). The main advantage of the opine pathway, however, over that of the lactate dehydrogenase reaction is that the opine end products are less acidic than D-lactate, which subsequently allows for better intracellular pH regulation and osmotic pressure (Harcet *et al.* 2013). As one amino acid is required for each opine synthesised (Müller *et al.* 2012), a large amino acid pool in molluscs is crucial for sustaining the lower NADH:NAD^+ ratio required (Gäde 1988).

Gäde (1988), Wells *et al.* (1998b) and O'omolo *et al.* (2003) investigated opine metabolism in the adductor and foot muscles of various abalone species during anaerobic conditions, and observed an accumulation of tauropine in the adductor muscle and D-lactate in the foot muscle.

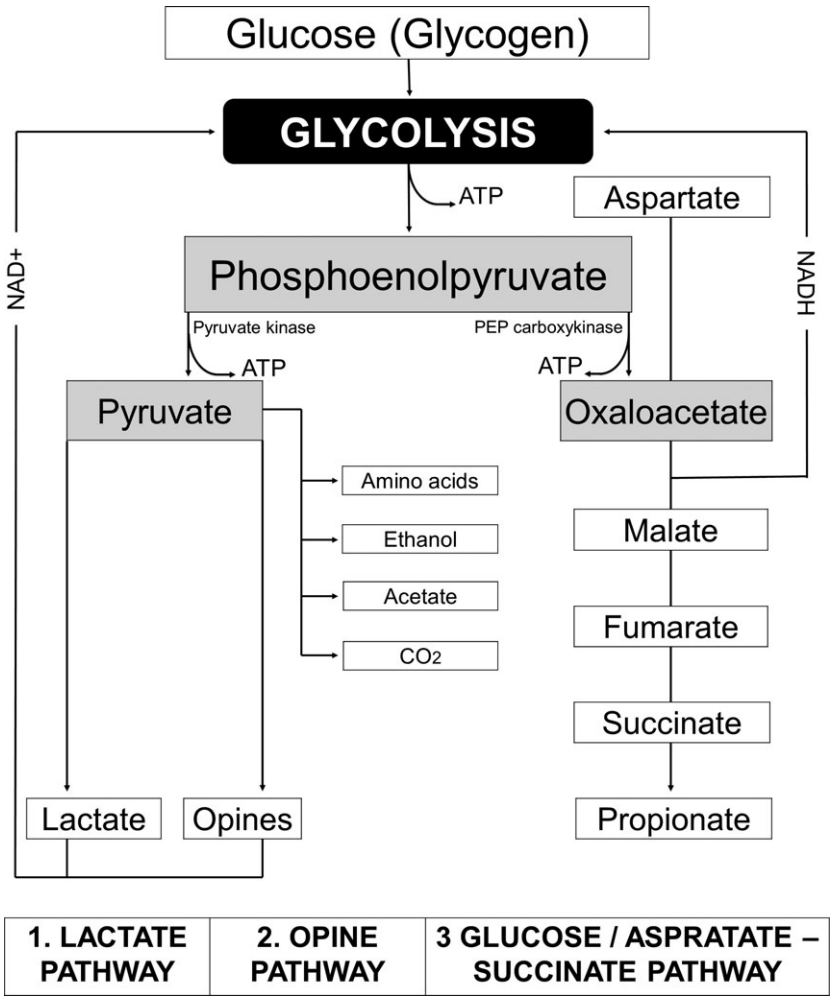

Figure 2 Different anaerobic glycolytic routes followed in marine invertebrates like abalone.

$$\text{Pyruvate} + \text{amino acid} + \text{NADH} + \text{H}^{+} \xrightarrow{\text{Imino acid dehydrogenase}} \text{Imino acid} + \text{NAD}^{+} + \text{H}_2\text{O}$$

Figure 3 General opine formation reaction. See text for more detail on opines found in abalone.

The presence of tauropine dehydrogenase in the shell adductor muscle is most likely due to this muscle being more metabolically active (when compared with the foot muscle) and largely dependent on anaerobic metabolism. As the foot muscle is responsible for the slower gliding movements, it requires less energy comparatively, and hence, D-lactate dehydrogenase alone is sufficient. Predominately, tauropine is produced during functional hypoxia and D-lactate seems to be formed during environmental hypoxia (Gäde 1988). On the basis of these findings, it was suggested using D-lactate dehydrogenase and tauropine dehydrogenase, as indicators of anaerobic stress, rather than the measurement of glycogen reserves, which are generally more difficult to quantify accurately (Wells & Baldwin 1995).

Glucose/aspartate–succinate pathway. This pathway is conventionally divided into (i) the glucose–succinate pathway and (ii) the aspartate–succinate pathway (with succinate being the end product of both). In essence, this pathway involves the reversal of the second half of the TCA cycle, as a mean to use accumulating reduced equivalents for the synthesis of NAD^+ and FAD. Both of these pathways are advantageous to cells rich in amino acids, typically those of marine invertebrates (Harcet *et al.* 2013) like abalone (as seen in Table 1).

Generally, the catabolism of glucose via glycolysis produces phosphoenolpyruvate (PEP), which in turn can be metabolised to pyruvate via pyruvate kinase, or to oxaloacetate by means PEP carboxykinase (Fig. 2) (the ratio of which varies in different species and tissues). In the presence of high amounts of reduced equivalents such as NADH and FADH, oxaloacetate can be converted to succinate and propionate through a reversed TCA cycle. The conversion of succinate to propionate results in approximately five ATP molecules, allowing the organism to survive in a lower energy state, with comparatively lower free radical production (Stefano *et al.* 2015). Amino acids (such as aspartate) can also be used in this process, by feeding directly into the cycle via oxaloacetate. In tissues where low PEP carboxykinase activity occurs, the main precursor of succinate or propionate is aspartate. The result of these reactions is an increased ATP yield from glucose, as extra substrate-level phosphorylation reactions and an electron-transfer-coupled phosphorylation involving fumarate as the electron acceptor take place. The primary function of the glucose–succinate pathway is survival during anoxia, even though the energy efficiency of this pathway is twice that of the D-lactate or opine pathways (Livingstone 1983; Prosser 1991). Before the glucose–succinate pathway can become operational in marine molluscs however, a reduction in pH is required and subsequently inhibition of PEP carboxykinase and pyruvate kinase activities. This pH reduction is made possible by the accumulation of acidic end products, largely brought about by the aspartate–succinate pathway (Livingstone 1983) as well as lactate.

Equally important to this process is the aspartate–succinate pathway, operating during the early stages of anaerobic metabolism which requires NADH (from carbohydrates) and produces alanine (Livingstone 1983). In addition to the breakdown of glycogen and arginine phosphate, the amino acid aspartate is also able to serve as a substrate for energy production during anoxia in abalone. Co-fermentation of glycogen and aspartate during anaerobic conditions are indicated by the synchronised depletion of aspartate and accumulation of alanine and succinate in the foot and adductor muscles of abalone. However, Gäde (1988) further speculates that the lack of propionate and acetate found in abalone is an indication that abalone can tolerate anoxic conditions less well as compared to other species like blue mussels or oysters. Confirmation of this is the fact that *H. lamellose* cannot survive anoxia experiments exceeding 8 h (Gäde 1988).

Tricarboxylic acid cycle

The final pathway required for the oxidation of carbohydrates, proteins and lipids is the TCA cycle, which is a series of reactions that oxidises acetyl CoA and reduce coenzymes, that upon re-oxidation, are linked to ATP formation (in the presence of oxygen). Briefly, the binding of oxaloacetate with a 2-carbon length acetyl CoA molecule results in a 6-carbon compound called citrate, which initiates this process. By releasing carbons (as CO_2) during a range of reactions, the 4-carbon compound oxaloacetate forms and the process repeats itself, subsequently releasing hydrogen ions along with electrons, which are carried by the electron carriers NADH and $FADH_2$ to the ETC (Murray *et al.* 2003; Whitney & Rolfes 2008; Garrett & Grisham 2010).

When investigating the effect of food restrictions on withering syndrome Rickettsiales-like prokaryote (WS-RLP) infected abalone, reduced TCA cycle intermediates were detected in the foot muscle of *Haliotis rufescens* (Rosenblum *et al.* 2005). Succinate was also found in elevated concentrations in abalone muscle in response to toxic exposure. The conversion of α-ketoglutarate to succinate is associated with aerobic respiration, resulting in an indirect increase in reactive oxygen species (ROS), and subsequently oxidative stress (Zhou *et al.* 2015). Succinate is actually the most commonly found TCA cycle intermediate in abalone metabolism-based studies (Gäde 1988; Sheedy *et al.* 2015; Zhou *et al.* 2015), which can be expected considering it presents as an anaerobic end product. It is important to note that the TCA cycle of abalone has as yet not been fully characterised, making this an important point for future research. Interestingly, a study performed by Venter *et al.* (2016) showed comparatively low organic acids to be present in various GC-MS analysed tissue samples of abalone, in comparison with their amino acid content, which is a rather unique occurrence, because these levels are usually very similar in other animal tissue samples analysed via the same approach (Lindeque *et al.* 2013). The fact that the TCA cycle intermediates in abalone are often below the detection limits of such analytical approaches supports the hypothesis that these animals make little use of mitochondrial metabolism and most likely have fewer than expected mitochondria per cell.

Oxidative phosphorylation

During aerobic metabolism, almost all of the energy released from the oxidation of proteins, lipids and carbohydrates are made available as reducing equivalents (hydrogen ions and electrons) in the mitochondria which subsequently feeds into the ETC where they move along a redox gradient, with oxygen ultimately acting as the final electron acceptor, with the production of water and ATP (Murray *et al.* 2003; Whitney & Rolfes 2008; Garrett & Grisham 2010). As a by-product of OXPHOS, mitochondria generate ROS, which is a highly regulated procedure under normal physiological conditions. Excessive mitochondrial ROS production, during conditions of stress, or disease, or anoxia or toxin exposure, may overwhelm the repair rates,

radical scavenging capacity and detoxification mechanisms of the cell, eventually causing damage to proteins, lipids and DNA, and potentially also mitochondrial defects (Wallace & Fan 2010; Vosloo *et al.* 2013a).

Vosloo and colleagues did extensive studies in this regard on abalone. They determined that the mitochondrial respiration efficiency was optimal at 19°C with a 98% oxygen exposure. This was measured by an increase in cytochrome *c* oxidase subunits 1 and 2 (*cox*1 and *cox*2) transcripts level, proposing a change in the efficiency of complex IV for preventing ROS formation. A lowered metabolic rate, however, was found at 19°C and 126% oxygen exposure, which is most likely due to an improvement in gaseous exchange (Vosloo *et al.* 2013c). Furthermore, antioxidant enzyme activity (superoxide dismutase and glutathione peroxidise, specifically) was also found to be upregulated at elevated temperatures (Vosloo *et al.* 2013b), subsequently resulting in a reduction in DNA fragmentation and protein damage at elevated oxygen consumption rates. However, at lowered oxygen consumption rates, DNA damage occurred under hypoxic and hyperoxic conditions, suggesting that the antioxidant enzymes did not prevent oxidative damage during these conditions (Vosloo *et al.* 2013a). This shows not only the importance of oxygen control but also that of temperature in the farming scenario.

Phosphagens

Phosphagens store energy in the form of high-energy phosphate bonds, for rapid use when necessary, or for the maintenance of a favourable ATP:adenosine diphosphate (ADP) ratio (Prosser 1991; Murray *et al.* 2003). In vertebrates, the only available phosphagen is in the form of creatine phosphate (phosphocreatine) while in invertebrate muscle tissue, such as that of abalone, arginine phosphate (phospho-L-arginine) is the primary phosphogen used. During prolonged conditions of hypoxia, it was determined that abalone use phosphoarginine as a phosphate reservoir for ATP synthesis (Morash & Alter 2015). Evidence also exists that abalone depend on phosphoarginine as an energy source during both environmental and functional anoxia. During periods of increased energy requirements (such as during hypoxia), energy stored in phosphoarginine is released to acceptors such as ADP, resulting in free arginine. Considering that octopine is the combination of arginine and pyruvate (in the opine pathway), it can be hypothesised that the released arginine binds pyruvate to restore NAD^+ levels for glycolysis, thereby acting in two important energy preservation pathways. Considering the importance of phosphoarginine in abalone's energy metabolism, it was proposed using the phosphoarginine:inorganic phosphate ratio, as an indicator of the energy status of the organism, rather than the change in adenylate energy charge (Viant *et al.* 2001). Interestingly, we have observed relatively high concentrations creatine in abalone muscle samples analysed with nuclear magnetic resonance spectroscopy (NMR) and liquid chromatography–tandem mass spectrometry (LC-MS/MS). The latter suggests that abalone might also use creatine to store high-energy phosphates in addition to arginine. In the context of the abalone farm, it might be worthwhile to monitor the levels of these phosphagens, as a mean to ascertain how the energy levels in abalone vary in different farming conditions, for maximising abalone growth.

Where to from here?

Due to their relatively low energy requirements, and their hypothetically low mitochondrial activity, a number of compounds traditionally used for anabolism are also being used for energy production or to maintain NAD^+ levels in abalone. Despite the fact that in recent years there has been an increased effort to better characterise abalone metabolism, there is still much that is largely unexplained. Considering that abalone growth rates are the primary point of interest to the abalone farmer (van der Merwe *et al.* 2011), a better understanding of abalone genetics, transcriptomics, proteomics and metabolomics would undoubtedly give clues to interventions which could optimise growth. This can be achieved through omics experiments comparing fast and slow growers, an approach previously used in oysters (Tamayo *et al.* 2014). Considering the abalone omics research to date, van der Merwe *et al.* (2011), using transcriptomics and quantitative real-time polymerase chain reaction experiments, indicated that the genes associated with the insulin signalling pathway explain the growth variation of farmed *H. midae*. An Illumina Genome Analyzer was used to generate high-quality DNA, in order to characterise the *H. midae* transcriptome, and identified the expressed genes associated with important traits, like improved growth and disease resistance (Franchini *et al.* 2011). Proteomic analysis carried out on the eggs produced from a hybrid abalone (*Haliotis discus hannai* Ino and *Haliotis gigantea*), and its parental lines identified 59 abalone proteins involved in energy metabolism, lipid metabolism, protein biosynthesis, electron carrier proteins, proliferation, apoptosis, signal transduction, immunity, decomposition and cytoskeletal structure (Di *et al.* 2015).

The total number of primary metabolites found in all organisms is far less than the total number of genes, RNA transcripts and proteins present, and thus, an investigation of the genome, transcriptome and proteome alone is not considered sufficient as they do not necessarily accurately reflect the phenotype. As metabolomics is at the endpoint of the omics cascade, and the closest to the cells functional phenotype, it not only links the genotype and phenotype, but it is regarded as the final recipient of genetic

information, as gene expression is ultimately reflected in changes of metabolite concentrations (Dettmer *et al.* 2007; Tugizimana *et al.* 2013).

Metabolomics can be defined as the nonbiased identification and quantification of metabolites in a biological system using highly selective and sensitive analytical techniques (Dunn *et al.* 2005). Metabolites or small molecules within a cell, tissue, organ, biological fluid or the entire organism constitute the metabolome (Lankadurai *et al.* 2013) and are likely to contribute to the functional state of cells and serve as a direct signature of biochemical activity (Patti *et al.* 2012). Considering this, using such an approach for investigating abalone growth patterns would undoubtedly result in a better understanding of the effects of various stressors or interventions on the abalone metabolome, and possible metabolic pathways that are linked to growth, and the polymorphisms influencing this. Depending on the aim of the study, a number of different metabolomics approaches using a multitude of analytical techniques can be used to conduct metabolomics research, and a review by Young & Alfaro 2016 can be viewed for detailed explanations.

In 2006, Rosenblum *et al.* speculated that metabolomics should be further developed and integrated as a complementary tool for characterising and identifying pathological events affecting various aquatic species. It was further suggested that metabolomics could be useful to better understand drug–host–pathogen interactions and the outcome of drug treatments in these aquatic species. Now 10 years later, it is still believed that the potential of metabolomics research with regard to aquaculture has yet to be realised (Alfaro & Young 2016). Although metabolomics as a research field are still in its infancy, the use of metabolomics for aquaculture application is highly relevant (Young & Alfaro 2016), considering that a well-established value chain for aquaculture products (especially abalone) is in place, with the potential to expand as the market grows, and the recent advancements in metabolomics.

In this review, we amongst other things summarised metabolism-related data reported for abalone to date, in order to get a better understanding of its metabolome and how this influences its growth. However, based on this, and what we already know from other organisms, a number of hypotheses where additionally made. As metabolism consists of a series of metabolites which are dependent on enzymes, co-factors and intermediates, it would not make sense to follow a single end point approach (such as measuring only glucose for instance, and subsequently making conclusions on the glycolysis pathway). Thus, pathway-specific abalone studies are needed to confirm the presence of hypothetical compounds X, Y and Z. Figure 4 is a representation of a metabolic map using the typical mammalian design. To emphasise how little we really know of abalone metabolism, all of the compounds found in abalone associated studies are plotted as nodes throughout this map

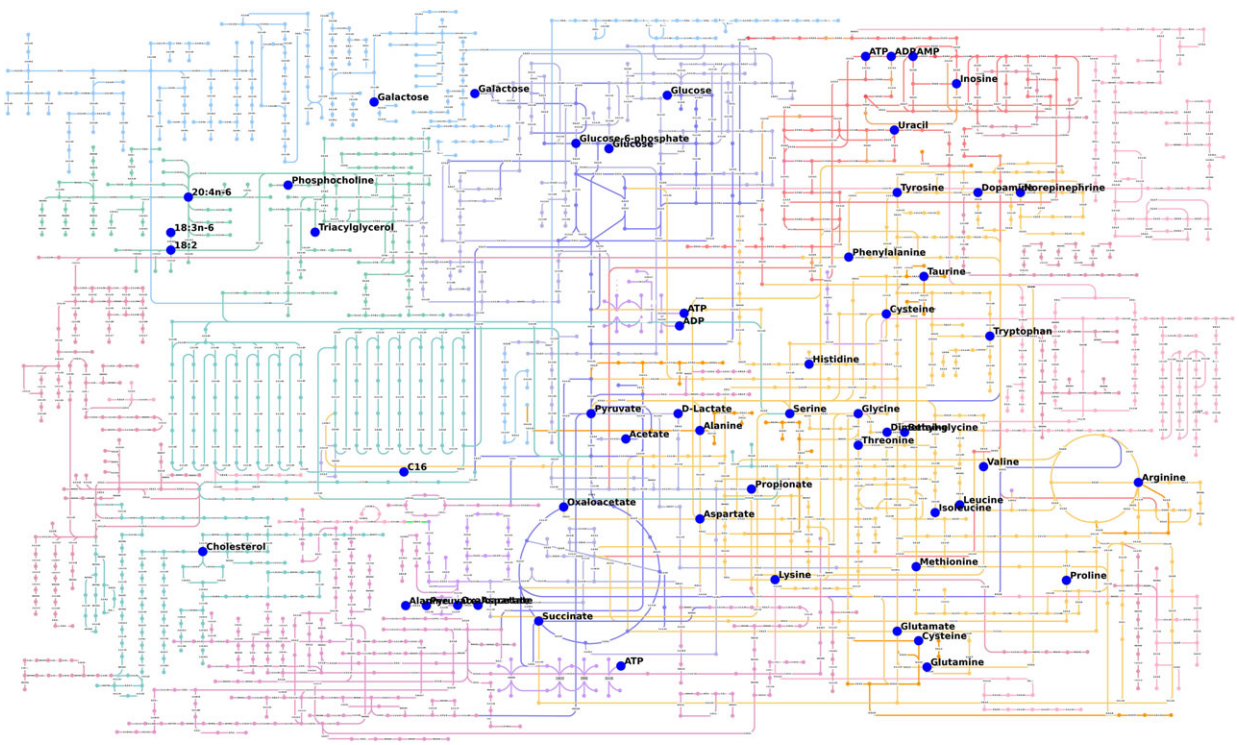

Figure 4 Metabolic map displaying specific abalone associated metabolites.

using the web-based program Pathway Projector (Kono *et al.* 2009). What is important to mention regarding this figure, is that the requirements for the compounds found in abalone to be mapped to this scheme were strict: (i) the compound had to be measured or identified in an abalone specific study (in this figure no speculations of what we think will result in the specific conversion was included), (ii) the compound had to have a Kyoto Encyclopaedia of Genes and Genomes (KEGG) compound identification (e.g. even though homarine has been found in abalone, this compound lacks a KEGG number and is hence excluded), (iii) only compounds previously described in the organisms listed online could be included (although octopine contains a KEGG number, Pathway Projector could not assign a pathway position for the compound). Considering the lack of nodes and the multitude of untouched pathways, it is evident that more research still needs to be performed in order to fully understand the metabolism of abalone.

Conclusion

In *H. midae,* as is the case in most other commercially important abalone species, slow growth rates are the biggest obstacle for achieving profitability and global competitiveness of this species. Ongoing research into the intricate and somewhat unique biochemical processes of abalone is needed to better understand growth, which ultimately includes a better understanding of their metabolism, and those factors influencing this. After a thorough study of the literature, it was determined that little is really known about the metabolism of abalone. Some important theories arose from this study which could actually impact the farming industry considerably – such as the hypothesis that abalone have very few mitochondria and thus low respiration rates. Subsequently, abalone rely comparatively more on other metabolic pathways for energy production, which in turn may give clue to better feeding approaches. In that respect, a global picture of abalone metabolism under normal and stressed conditions is needed to predict the physiological traits associated with growth rates, body weight, food conversion efficiency, disease resistance and flesh quality, and also to optimise nutrient supply and other farming conditions. Systems biology studies such as metabolomics on *H. midae* are generally scarce and would greatly contribute to the elucidation of these metabolic processes. Clarification of the abalone metabolome would also be considered a valuable approach to identifying biomarkers of growth, stress and health.

Acknowledgements

The financial assistance of the North-West University and the Technology Innovation Agency is hereby acknowledged.

References

Alfaro AC, Young T (2016) Showcasing metabolomic applications in aquaculture: a review. *Reviews in Aquaculture*. doi: 10.1111/raq.12152.

Angell AR, Pirozzi I, De Nys R, Paul NA (2012) Feeding preferences and the nutritional value of tropical algae for the abalone *Haliotis asinina*. *PLoS One* **7**: e38857.

Bae JH, Yoon SH, Lim SY (2011) A comparative of heavy metal contents and biochemical characteristics of Japanese (*Haliotis discus*) and Korean abalone (*Haliotis discus hannai*). *Food Science and Biotechnology* **20**: 273–276.

Baldwin J, Elias J, Wells R, Donovan D (2007) Energy metabolism in the tropical abalone, *Haliotis asinina* Linné: comparisons with temperate abalone species. *Journal of Experimental Marine Biology and Ecology* **342**: 213–225.

Ballantyne JS (2004) Mitochondria: aerobic and anaerobic design—lessons from molluscs and fishes. *Comparative Biochemistry and Physiology Part B: Biochemistry and Molecular Biology* **139**: 461–467.

Bansemer MS, Qin JG, Harris JO, Howarth GS, Stone DA (2014) Nutritional requirements and use of macroalgae as ingredients in abalone feed. *Reviews in Aquaculture* **5**: 1–15.

Bansemer MS, Qin JG, Harris JO, Duong DN, Currie K-L, Howarth GS *et al.* (2016) Dietary inclusions of dried macroalgae meal in formulated diets improve the growth of greenlip abalone (*Haliotis laevigata*). *Journal of Applied Phycology*. doi: 10.1007/s10811-10016-10829-10810.

Barkai R, Griffiths C (1988) An energy budget for the South African abalone *Haliotis midae* Linnaeus. *Journal of Molluscan Studies* **54**: 43–51.

Bautista-Teruel MN, Millamena OM (1999) Diet development and evaluation for juvenile abalone, *Haliotis asinina*: protein/energy levels. *Aquaculture* **178**: 117–126.

Braid BA, Moore JD, Robbins TT, Hedrick RP, Tjeerdema RS, Friedman CS (2005) Health and survival of red abalone, *Haliotis rufescens*, under varying temperature, food supply, and exposure to the agent of withering syndrome. *Journal of Invertebrate Pathology* **89**: 219–231.

Britz PJ (1996a) Effect of dietary protein level on growth performance of South African abalone, *Haliotis midae*, fed fishmeal-based semi-purified diets. *Aquaculture* **140**: 55–61.

Britz PJ (1996b) The suitability of selected protein sources for inclusion in formulated diets for the South African abalone, *Haliotis midae*. *Aquaculture* **140**: 63–73.

Britz PJ, Hecht T, Mangold S (1997) Effect of temperature on growth, feed consumption and nutritional indices of *Haliotis midae* fed a formulated diet. *Aquaculture* **152**: 191–203.

Brown MR, Sikes AL, Elliott NG, Tume RK (2008) Physicochemical factors of abalone quality: a review. *Journal of Shellfish Research* **27**: 835–842.

Byrne M, Ho M, Wong E, Soars NA, Selvakumaraswamy P, Shepard-Brennand H *et al.* (2011) Unshelled abalone and corrupted urchins: development of marine calcifiers in a

changing ocean. *Proceedings of the Royal Society of London B: Biological Sciences* **278**: 2376–2383.

Cappello T, Mauceri A, Corsaro C, Maisano M, Parrino V, Paro GL *et al.* (2013) Impact of environmental pollution on caged mussels *Mytilus galloprovincialis* using NMR-based metabolomics. *Marine Pollution Bulletin* **77**: 132–139.

Carefoot TH, Qian P-Y, Taylor BE, West T, Osborne J (1993) Effect of starvation on energy reserves and metabolism in the Northern abalone, *Haliotis kamtschatkana*. *Aquaculture* **118**: 315–325.

Carefoot TH, Taylor BE, Land S (2000) Use of isolated digestive-gland cells in the study of biochemical and physiological processes in gastropod molluscs. *Comparative Biochemistry and Physiology Part A: Molecular & Integrative Physiology* **125**: 497–502.

Chang PH, Kuo ST, Lai SH, Yang HS, Ting YY, Hsu CL *et al.* (2005) Herpes-like virus infection causing mortality of cultured abalone *Haliotis diversicolor supertexta* in Taiwan. *Diseases of Aquatic Organisms* **65**: 23–27.

Cook PA (2014) The worldwide abalone industry. *Modern Economy* **5**: 1181–1186.

Cristescu ME, Innes DJ, Stillman JH, Crease TJ (2008) D-and L-lactate dehydrogenases during invertebrate evolution. *BMC Evolutionary Biology* **8**: 1–10.

Day EG, Branch GM (2002) Influences of the sea urchin *Parechinus angulosus* (Leske) on the feeding behaviour and activity rhythms of juveniles of the South African abalone *Haliotis midae* Linn. *Journal of Experimental Marine Biology and Ecology* **276**: 1–17.

Day RW, Cook P (1995) Bias towards brown algae in determining diet and food preferences: the South African abalone *Haliotis midae*. *Marine and Freshwater Research* **46**: 623–627.

De Greef K, Raemaekers S (2014) *South Africa's Illicit Abalone Trade: An Updated Overview and Knowledge Gap Analysis*. TRAFFIC, Cambridge, UK.

Denny MW, Gaines SD (2007) *Encyclopedia of Tidepools and Rocky Shores*. University of California Press, London.

Dettmer K, Aronov PA, Hammock BD (2007) Mass spectrometry-based metabolomics. *Mass Spectrometry Reviews* **26**: 51–78.

Di G, Luo X, Huang M, Chen J, Kong X, Miao X *et al.* (2015) Proteomic profiling of eggs from a hybrid abalone and its parental lines: *Haliotis discus hannai* Ino and *Haliotis gigantea*. *Animal Genetics* **46**: 646–654.

Donovan D, Baldwin J, Carefoot T (1999) The contribution of anaerobic energy to gastropod crawling and a re-estimation of minimum cost of transport in the abalone, *Haliotis kamtschatkana* (Jonas). *Journal of Experimental Marine Biology and Ecology* **235**: 273–284.

Dunn WB, Bailey NJ, Johnson HE (2005) Measuring the metabolome: current analytical technologies. *Analyst* **130**: 606–625.

Dunstan GA, Baillie HJ, Barrett SM, Volkman JK (1996) Effect of diet on the lipid composition of wild and cultured abalone. *Aquaculture* **140**: 115–127.

Dunstan G (2010) A simple model for the determination of the relative utilization efficiency of protein by blacklip abalone *(Haliotis rubra* Leach). *Aquaculture Nutrition* **16**: 1–12.

Durazo E, Viana MT (2013) Fatty acid profile of cultured green abalone (*Haliotis fulgens*) exposed to lipid restriction and long-term starvation. *Ciencias Marinas* **39**: 363–370.

Durazo-Beltrán E, D'Abramo LR, Toro-Vazquez JF, Vasquez-Peláez C, MaT V (2003) Effect of triacylglycerols in formulated diets on growth and fatty acid composition in tissue of green abalone (*Haliotis fulgens*). *Aquaculture* **224**: 257–270.

Durazo-Beltrán E, Viana MT, D'Abramo LR, Toro-Vazquez JF (2004) Effects of starvation and dietary lipid on the lipid and fatty acid composition of muscle tissue of juvenile green abalone (*Haliotis fulgens*). *Aquaculture* **238**: 329–341.

Fallu R (1991) *Abalone Farming*. Fishing News Books, Oxford.

Fasulo S, Iacono F, Cappello T, Corsaro C, Maisano M, D'Agata A *et al.* (2012) Metabolomic investigation of *Mytilus galloprovincialis* (Lamarck 1819) caged in aquatic environments. *Ecotoxicology and Environmental Safety* **84**: 139–146.

Fleming AE, Van Barneveld RJ, Hone PW (1996) The development of artificial diets for abalone: a review and future directions. *Aquaculture* **140**: 5–53.

Franchini P, Van der Merwe M, Roodt-Wilding R (2011) Transcriptome characterization of the South African abalone *Haliotis midae* using sequencing-by-synthesis. *BMC Research Notes* **4**: 59.

Gäde G (1988) Energy metabolism during anoxia and recovery in shell adductor and foot muscle of the gastropod mollusc *Haliotis lamellosa*: formation of the novel anaerobic end product tauropine. *The Biological Bulletin* **175**: 122–131.

Garrett R, Grisham C (2010) *Biochemistry*. Brooks Cole, Cengage Learning, Belmont, CA.

Grubert MA, Dunstan GA, Ritar AJ (2004) Lipid and fatty acid composition of pre-and post-spawning blacklip (*Haliotis rubra*) and greenlip *(Haliotis laevigata*) abalone conditioned at two temperatures on a formulated feed. *Aquaculture* **242**: 297–311.

Hahn KO (1989) *Handbook of Culture of Abalone and Other Marine Gastropods*. CRC Press, Inc., Boca Raton, FL.

Harcet M, Perina D, Pleše B (2013) Opine dehydrogenases in marine invertebrates. *Biochemical Genetics* **51**: 666–676.

Heath P, Moss G (2009) Is size grading important for farming the abalone *Haliotis iris*? *Aquaculture* **290**: 80–86.

Hernández J, de la Parra AM, Lastra M, Viana MT (2013) Effect of lipid composition of diets and environmental temperature on the performance and fatty acid composition of juvenile European abalone (*Haliotis tuberculata* L. 1758). *Aquaculture* **412**: 34–40.

Hickey AJ, Wells RM (2003) Thermal constraints on glycolytic metabolism in the New Zealand abalone, *Haliotis iris*: the role of tauropine dehydrogenase. *New Zealand Journal of Marine and Freshwater Research* **37**: 723–731.

Hickman CP, Roberts LS, Larson A, Ober WC, Garrison C (2006) *Integrated Principles of Zoology*. McGraw-Hill International, New York.

Hooper C, Day R, Slocombe R, Benkendorff K, Handlinger J (2014) Histopathology and haemolymph biochemistry following anaesthesia and movement in farmed Australian abalone (*Haliotis rubra* × *Haliotis laevigata*). *Aquaculture* **422**: 202–210.

Huddy RJ, Coyne VE (2014) Detection and localisation of the abalone probiotic *Vibrio midae* SY9 and its extracellular protease, VmproA, within the digestive tract of the South African abalone, *Haliotis midae*. *PLoS One* **9**: e86623.

Jorgensen D, Ware S, Redmond J (1984) Cardiac output and tissue blood flow in the abalone, *Haliotis cracherodii* (Mollusca, Gastropoda). *Journal of Experimental Zoology* **231**: 309–324.

Kilburn R, Rippey E (1982) *Sea Shells of Southern Africa*. Macmillan South Africa, Johannesburg.

Knauer J, Hecht T, Britz P (1995) A note on the feeding behaviour and growth of juvenile South African abalone, *Haliotis midae*, fed on an artificial weaning diet. *South African Journal of Science* **91**: 91–93.

Kono N, Arakawa K, Ogawa R, Kido N, Oshita K, Ikegami K *et al.* (2009) Pathway projector: web-based zoomable pathway browser using KEGG atlas and Google Maps API. *PLoS One* **4**: e7710.

Laas A, Vosloo A (2010) Exploring basic biochemical constituents in the body tissues of South African abalone *Haliotis midae* reared in shore-based mariculture systems. *African Journal of Marine Science* **32**: 55–63.

Lankadurai BP, Nagato EG, Simpson MJ (2013) Environmental metabolomics: an emerging approach to study organism responses to environmental stressors. *Environmental Reviews* **21**: 180–205.

Latuihamallo M, Apituley D (2015) Amino acid and fatty acid of abalone *Haliotis Squamata* cultured in different aquaculture systems. *Procedia Food Science* **3**: 174–181.

Lawrence JM (2013) *Sea Urchins: Biology and Ecology*. Academic Press, Elsevier, London.

Lee S-M (2004) Utilization of dietary protein, lipid, and carbohydrate by abalone *Haliotis discus hannai*: a review. *Journal of Shellfish Research* **23**: 1027–1030.

Lee A-C, Lee K-T (2011) The enzyme activities of opine and lactate dehydrogenase in the gills, mantle, foot, and adductor of the hard clam *Meretrix lusoria*. *Journal of Marine Science and Technology* **19**: 361–367.

Leighton P (2008) Abalone hatchery manual. In: Robinson G, McGowan N (eds) *Aquaculture Explained*, pp. 2–5. Aquaculture Technical Section, Aquaculture Development Division, Bord Iascaigh Mhara, Dun Laoghaire.

Lindeque JZ, Hidalgo J, Louw R, van der Westhuizen FH (2013) Systemic and organ specific metabolic variation in metallothionein knockout mice challenged with swimming exercise. *Metabolomics* **9**: 418–432.

Livingstone D (1983) Invertebrate and vertebrate pathways of anaerobic metabolism: evolutionary considerations. *Journal of the Geological Society* **140**: 27–37.

Lopaschuk GD, Ussher JR, Folmes CD, Jaswal JS, Stanley WC (2010) Myocardial fatty acid metabolism in health and disease. *Physiological Reviews* **90**: 207–258.

Lucas T (2007) Investigating genetic and molecular aspects of growth of the tropical abalone *Haliotis asinina*. School of Integrative Biology, PhD Thesis. The University of Queensland Brisbane, Queensland, Australia.

Macey B, Coyne V (2005) Improved growth rate and disease resistance in farmed *Haliotis midae* through probiotic treatment. *Aquaculture* **245**: 249–261.

Macey B, Christison K, Mouton A (2011) *Halioticida noduliformans* isolated from cultured abalone (*Haliotis midae*) in South Africa. *Aquaculture* **315**: 187–195.

Mai K (1998) Comparative studies on the nutrition of two species of abalone, *Haliotis tuberculata* L. and *Haliotis discus hannai* Ino.: VII. Effects of dietary vitamin C on survival, growth and tissue concentration of ascorbic acid. *Aquaculture* **161**: 383–392.

Malham SK, Lacoste A, Gelebart F, Cueff A, Poulet SA (2003) Evidence for a direct link between stress and immunity in the mollusc *Haliotis tuberculata*. *Journal of Experimental Zoology Part A: Comparative Experimental Biology* **295**: 136–144.

van der Merwe M, Franchini P, Roodt-Wilding R (2011) Differential growth-related gene expression in abalone (*Haliotis midae*). *Marine Biotechnology* **13**: 1125–1139.

Mgaya YD, Mercer JP (1994) A review of the biology, ecology, fisheries and mariculture of the European abalone *Haliotis tuberculata* Linnaeus 1758 (Gastropoda: Haliotidae). *Biology and Environment: Proceedings of the Royal Irish Academy* **94B**: 285–304.

Moran AL, Manahan DT (2003) Energy metabolism during larval development of green and white abalone, *Haliotis fulgens* and *H. sorenseni*. *The Biological Bulletin* **204**: 270–277.

Morash AJ, Alter K (2015) Effects of environmental and farm stress on abalone physiology: perspectives for abalone aquaculture in the face of global climate change. *Reviews in Aquaculture* **7**: 1–27.

Mouton A, Gummow B (2011) The occurrence of gut associated parasites in the South African abalone, *Haliotis midae*, in Western Cape aquaculture facilities. *Aquaculture* **313**: 1–6.

Müller M, Mentel M, van Hellemond JJ, Henze K, Woehle C, Gould SB *et al.* (2012) Biochemistry and evolution of anaerobic energy metabolism in eukaryotes. *Microbiology and Molecular Biology Reviews* **76**: 444–495.

Murray R, Granner DK, Mayes P, Rodwell V (2003) *Harper's Illustrated Biochemistry*. McGraw-Hill, New York, NY.

Naidoo K, Maneveldt G, Ruck K, Bolton JJ (2006) A comparison of various seaweed-based diets and formulated feed on growth rate of abalone in a land-based aquaculture system. *Journal of Applied Phycology* **18**: 437–443.

Øiseth SK, Delahunty C, Cochet M, Lundin L (2013) Why is abalone so chewy? Structural characterization and relationship to textural attributes. *Journal of Shellfish Research* **32**: 73–79.

O'omolo S, Gäde G, Cook P, Brown A (2003) Can the end products of anaerobic metabolism, tauropine and D-lactate, be used as metabolic stress indicators during transport of live South African abalone *Haliotis midae*? *African Journal of Marine Science* **25**: 301–309.

Patti GJ, Yanes O, Siuzdak G (2012) Innovation: metabolomics: the apogee of the omics trilogy. *Nature Reviews Molecular Cell Biology* **13**: 263–269.

Payne AI, Crawford RJ (1989) *Oceans of Life: Off Southern Africa*. Vlaeberg Publishers, Cape Town.

Prosser CL (1991) *Comparative Animal Physiology, Environmental and Metabolic Animal Physiology*. John Wiley & Sons, Hoboken, NJ.

Raemaekers SJPN, Britz PJ (2009) Profile of the illegal abalone fishery (*Haliotis midae*) in the Eastern Cape Province, South Africa: organised pillage and management failure. *Fisheries Research* **97**: 183–195.

Ragg NL, Taylor HH (2006) Heterogeneous perfusion of the paired gills of the abalone *Haliotis iris* Martyn 1784: an unusual mechanism for respiratory control. *Journal of Experimental Biology* **209**: 475–483.

Robertson-Andersson D, Maneveldt G, Naidoo K (2011) Effects of wild and farm-grown macroalgae on the growth of juvenile South African abalone *Haliotis midae* Linnaeus. *African Journal of Aquatic Science* **36**: 331–337.

Rosenblum E, Viant M, Braid B, Moore J, Friedman C, Tjeerdema R (2005) Characterizing the metabolic actions of natural stresses in the California red abalone, *Haliotis rufescens* using 1H NMR metabolomics. *Metabolomics* **1**: 199–209.

Rosenblum ES, Tjeerdema RS, Viant MR (2006) Effects of temperature on host-pathogen-drug interactions in red abalone, *Haliotis rufescens,* determined by 1H NMR metabolomics. *Environmental Science & Technology* **40**: 7077–7084.

Sales J (2004) Abalone. *Aquafeeds: Formulation and Beyond* **1**: 23–26.

Sales J, Britz P (2001) Research on abalone (*Haliotis midae* L.) cultivation in South Africa. *Aquaculture Research* **32**: 863–874.

Sales J, Janssens G (2004) Use of feed ingredients in artificial diets for abalone: a brief update. *Nutrition Abstracts and Reviews: Series B* **74**: 13–21.

Salway JG (2004) *Metabolism at a Glance*. John Wiley & Sons, Guildford.

Sheedy JR, Lachambre S, Gardner DK, Day RW (2015) 1H-NMR metabolite profiling of abalone digestive gland in response to short-term starvation. *Aquaculture International* **24**: 503–521.

Shofer SL, Tjeerdema RS (1998) Effects of hypoxia and toxicant exposure on adenylate energy charge and cytosolic ADP concentrations in abalone. *Comparative Biochemistry and Physiology Part C: Pharmacology, Toxicology and Endocrinology* **119**: 51–57.

Stefano G, Mantione K, Casares F, Kream R (2015) Anaerobically functioning mitochondria: evolutionary perspective on modulation of energy metabolism in *Mytilus edulis*. *Invertebrate Survival Journal* **12**: 22–28.

Steinarsson A, Imsland AK (2003) Size dependent variation in optimum growth temperature of red abalone (*Haliotis rufescens*). *Aquaculture* **224**: 353–362.

Tamayo D, Ibarrola I, Urrutia MB, Navarro E (2011) The physiological basis for inter-individual growth variability in the spat of clams (*Ruditapes philippinarum*). *Aquaculture* **321**: 113–120.

Tamayo D, Ibarrola I, Urrutxurtu I, Navarro E (2014) Physiological basis of extreme growth rate differences in the spat of oyster (*Crassostrea gigas*). *Marine Biology* **161**: 1627–1637.

Tan B, Mai K (2001) Zinc methionine and zinc sulfate as sources of dietary zinc for juvenile abalone, *Haliotis discus hannai* Ino. *Aquaculture* **192**: 67–84.

Ten Doeschate K, Coyne V (2008) Improved growth rate in farmed *Haliotis midae* through probiotic treatment. *Aquaculture* **284**: 174–179.

Troell M, Robertson-Andersson D, Anderson RJ, Bolton JJ, Maneveldt G, Halling C *et al.* (2006) Abalone farming in South Africa: an overview with perspectives on kelp resources, abalone feed, potential for on-farm seaweed production and socio-economic importance. *Aquaculture* **257**: 266–281.

Tugizimana F, Piater L, Dubery I (2013) Plant metabolomics: a new frontier in phytochemical analysis. *South African Journal of Science* **109**: 01–11.

Venter L, Jansen van Rensburg P, Loots DT, Vosloo A, Lindeque JZ (2016) Untargeted metabolite profiling of abalone using gas chromatography mass spectrometry. *Food Analytical Methods* **9**: 1254–1261.

Viana MT, D'Abramo LR, Gonzalez MA, García-Suárez JV, Shimada A, Vásquez-Peláez C (2007) Energy and nutrient utilization of juvenile green abalone (*Haliotis fulgens*) during starvation. *Aquaculture* **264**: 323–329.

Viant MR, Rosenblum ES, Tjeerdema RS (2001) Optimized method for the determination of phosphoarginine in abalone tissue by high-performance liquid chromatography. *Journal of Chromatography B: Biomedical Sciences and Applications* **765**: 107–111.

Vosloo A, Vosloo D (2006) Routes of water loss in South African abalone (*Haliotis midae*) during aerial exposure. *Aquaculture* **261**: 670–677.

Vosloo D, Vosloo A (2010) Response of cold-acclimated, farmed South African abalone (*Haliotis midae*) to short-term and long-term changes in temperature. *Journal of Thermal Biology* **35**: 317–323.

Vosloo A, Laas A, Vosloo D (2013a) Differential responses of juvenile and adult South African abalone (*Haliotis midae* Linnaeus) to low and high oxygen levels. *Comparative Biochemistry and Physiology Part A: Molecular & Integrative Physiology* **164**: 192–199.

Vosloo D, van Rensburg L, Vosloo A (2013b) Oxidative stress in abalone: the role of temperature, oxygen and L-proline supplementation. *Aquaculture* **416**: 265–271.

Vosloo D, Vosloo A, Morillion EJ, Samuels JN, Sommer P (2013c) Metabolic readjustment in juvenile South African abalone (*Haliotis midae*) acclimated to combinations of temperature and dissolved oxygen levels. *Journal of Thermal Biology* **38**: 458–466.

Wallace DC, Fan W (2010) Energetics, epigenetics, mitochondrial genetics. *Mitochondrion* **10**: 12–31.

Wang H-X, Qin L, Wang Y, Zhou D-Y, Song S, Wang X-S *et al.* (2014) Effects of heating conditions on fatty acids and volatile compounds in foot muscle of abalone *Haliotis discus hannai* Ino. *Fisheries Science* **80**: 1097–1107.

Wardlaw GM, Insel PM (2006) *Perspectives in Nutrition*. McGraw-Hill Higher Education, New York.

Welborn J, Manahan D (1995) Taurine metabolism in larvae of marine invertebrate molluscs (Bilvalvia, Gastropoda). *Journal of Experimental Biology* **198**: 1791–1799.

Wells RM, Baldwin J (1995) A comparison of metabolic stress during air exposure in two species of New Zealand abalone, *Haliotis iris* and *Haliotis australis*: implications for the handling and shipping of live animals. *Aquaculture* **134**: 361–370.

Wells RM, Baldwin J, Speed SR, Weber RE (1998a) Haemocyanin function in the New Zealand abalones *Haliotis iris* and *H. australis*: relationships between oxygen-binding properties, muscle metabolism and habitat. *Marine and Freshwater Research* **49**: 143–149.

Wells RM, McShane PE, Ling N, Wong RJ, Lee TO, Baldwin J (1998b) Effect of wave action on muscle composition, metabolites and growth indices in the New Zealand abalone, Paua (*Haliotis iris*), with implications for harvesting and aquaculture. *Comparative Biochemistry and Physiology Part B: Biochemistry and Molecular Biology* **119**: 129–136.

Wetchateng T, Friedman CS, Wight NA, Lee P-Y, Teng PH, Sriurairattana S *et al.* (2010) Withering syndrome in the abalone *Haliotis diversicolor supertexta*. *Diseases of Aquatic Organisms* **90**: 69–76.

Whitney E, Rolfes SR (2008) *Understanding Nutrition*. Thomson Wadsworth, Belmont, CA.

Wood A, Buxton C (1996) Aspects of the biology of the abalone *Haliotis midae* (Linne, 1758) on the east coast of South Africa. Feeding biology. *South African Journal of Marine Science* **17**: 61–68.

Young T, Alfaro AC (2016) Metabolomic strategies for aquaculture research: a primer. *Reviews in Aquaculture*. doi: 10.1111/raq.12146.

Zhou J, Chen B, Cai Z (2015) Metabolomics-based approach for assessing the toxicity mechanisms of dibutyl phthalate to abalone (*Haliotis diversicolor supertexta*). *Environmental Science and Pollution Research* **22**: 5092–5099.

Journal of Chromatography B, 1071 (2017) 44–48

Contents lists available at ScienceDirect

Journal of Chromatography B

journal homepage: www.elsevier.com/locate/chromb

From untargeted LC-QTOF analysis to characterisation of opines in abalone adductor muscle: Theory meets practice

Leonie Venter[a,*], Peet J. Jansen van Rensburg[a], Du Toit Loots[a], Andre Vosloo[b], Jeremie Zander Lindeque[a]

[a] Human Metabolomics, North-West University, Potchefstroom Campus, Private Bag X6001, Potchefstroom 2520, South Africa
[b] School of Life Sciences, University of KwaZulu-Natal, Westville Campus, Private Bag X54001, Durban 4000, South Africa

ARTICLE INFO

Article history:
Received 28 October 2016
Accepted 18 January 2017
Available online 24 February 2017

Keywords:
Abalone
Alanopine
Mass spectrometry
Opines

ABSTRACT

Abalone have a unique ability to use pyruvate, various amino acids and dehydrogenases, to produce opines as means to prevent the accumulation of NADH during anaerobic conditions. In this study, the theoretical masses, formulae and fragment patterns of butylated opines were used to predict which of these compounds could be found in the abalone adductor muscle using untargeted liquid chromatography quadrupole time-of flight-mass spectrometry. These findings were validated using synthesised opine standards. In essence alanopine, lysopine, strombine and tauropine produced in abalone adductor muscle could be characterised using the highest identification confidence levels.

1. Introduction

The greatest challenge in untargeted metabolomics research is undoubtedly the confident identification of metabolites [1]. Frequently a large number of mass spectrometry (MS) detected signals remain unidentified [2], or are annotated with low confidence. This problem escalates when one works with organisms for which dedicated databases (like the Human Metabolome Database) do not exist. As, many of the available databases have limited information on derivatised compounds, theoretical derivatised mass and/or fragmentation spectra are used for annotating the identified features. This is the case when identifying butylated compounds analysed in an untargeted manner, using liquid chromatography quadrupole time-of flight-mass spectrometry (LC-QTOF).

Our own research on abalone includes targeted amino acid analysis and untargeted LC-QTOF analysis of abalone muscle samples subjected to butylation. Prior to the analysis of these samples, abalone were exposed to hypoxic conditions in an attempt to elucidate their metabolic response during anaerobic conditions. A specific mass repeatedly observed in data obtained by untargeted LC-QTOF analysis resulted in a closer investigation of the fragments produced from this compound, shown to be alanine. It is known that amino acids act as osmo-effectors in abalone during anaerobic conditions. Alanopine (opine) and NAD^+ are produced in invertebrates such as abalone, by means of a specific opine dehydrogenase that condensates pyruvate and alanine (amino acid) in the presence of nicotinamide adenine dinucleotide (NADH) + H^+ [3]. Based on this theoretical knowledge the unknown feature was hypothesised to be alanopine. Alanopine, produced from alanine, is one of the opines described in abalone. Other opines include: lysopine, octopine, strombine, tauropine, and ß-alanopine produced from the amino acids: lysine, arginine, glycine, taurine and ß-alanine respectively [4]. Opines are the collective name given to a group of anaerobic end products found in several marine invertebrate phyla, but widely prevalent in marine molluscs [3]. No opine detection in abalone by means of MS has been reported to date. The presence of alanopine leads one to believe that the other opines known to occur in these marine invertebrates would most likely also be present in the untargeted LC-QTOF data collected.

The aim of this communication, is to describe the approach used to confirm the presence of butylated opines in abalone muscle samples, by following the identification confidence levels described by Schymanski et al. [5] and Summer et al. [6].

2. Material and methods

2.1. Chemicals and reagents

Acetonitrile (BJ017), chloroform (BJ049), methanol (BJ230) and water (BJ365) purchased from Anatech Instruments (Pty) Ltd.

* Corresponding author at: North–West University, Potchefstroom Campus, Private Bag X6001, Potchefstroom, 2520, Building F3–G119, South Africa.
E-mail address: Leonie.Venter@nwu.ac.za (L. Venter).

http://dx.doi.org/10.1016/j.jchromb.2017.01.025
1570-0232/

(Olivedale, South Africa) and acetyl chloride (00990), 1-butanol (281549), formic acid (14265) and 3-phenylbutyric acid (116807) from Sigma-Aldrich (Kempton Park, South Africa) were used during metabolite extraction, sample derivatisation and LC-QTOF analysis. Alanine (A7627), arginine (A5006), glycine (G7126), lysine (L5501) taurine (T0625), sodium pyruvate (P2256) and sodium cyanohydridborate ($NaBH_3CN$) (156159) were used for opine synthesis (Sigma-Aldrich).

2.2. Abalone sample preparation

Juvenile abalone from HIK Abalone Farm (Pty) Ltd (Hermanus, South Africa) subjected to hypoxic incubation [7] were dissected for adductor muscle tissue samples after shucking the animals. Using our standard metabolomics samples extraction method [8], ten milligrams of abalone muscle tissue was homogenised in an Eppendorf tube containing 40 μL of water, 100 μL of methanol, 50 μL of 3-phenylbutyric acid internal standard (50 μg/mL) and a 3 mm stainless steel bead, in a vibration mill for 4 min at 30 Hz. Subsequently, the samples were vigorously mixed for 1 min, after the addition of chloroform (100 μL) and water (50 μL), and then allowed to stand on ice for an additional 10 min. The samples were then centrifuged at 25 000 × *g* for 10 min at 4 °C, and 60 μL of the upper polar phase and 30 μL of the lower apolar chloroform phase, transferred to a glass screw top vial and dried under a gentle stream of nitrogen at 37 °C.

2.3. Opine synthesis

Opines were synthesised individually by mixing equal amounts of sodium pyruvate (100 μg/mL) and the respective amino acid stock solutions (100 μg/mL previously prepared), followed by drying of the mixture under a light stream of nitrogen gas at 37 °C. Once fully dried, 100 μL of $NaBH_3CN$ (1 mg/mL) and 900 μL of methanol were added to each tube [9], followed by incubation at 25 °C for 60 min. The mixture was once again dried under a nitrogen gas stream at 37 °C.

2.4. Butylation

To the dried residue, 100 μL of 3N butanolic hydrogen chloride (prepared by adding 25% acetyl chloride to the final volume of 1-butanol on ice) was added, where after the samples were capped and incubated at 60 °C for 60 min. The butylated samples were evaporated to dryness under a gentle stream of nitrogen gas at 60 °C and reconstituted in 200 μL water:acetonitrile (50:50) containing 0.1% formic acid.

2.5. LC-QTOF parameters

An Agilent 1200 LC system using an injection volume of 5 μL was used for analysis. Butylated samples were separated on an Agilent ZORBAX SB-Aq C18 column (2.1 × 150 mm, 3.5 μm), at 30 °C. The mobile phases consisted of (A) water and (B) acetonitrile both containing 0.1% formic acid. The separation was performed using the following gradient: 0–3 min 0% (B); 3–11 min 25% (B); 11–30 min 100% (B) at a flowrate of 0.25 mL/min; where after the flowrate was increased to 0.5 mL/min to 32 min 100% (B), and ending at 33 min 100% (B) 0.25 mL/min along with a 10 min post-run at this condition. Mass spectrometry detection was performed on an Agilent 6510 QTOF mass analyser using positive electrospray ionization, a drying gas temperature of 300 °C, a drying gas flow of 7.5 L/min and nebulizer pressure of 30 psi. All ions MS/MS experiments were setup with multiple collision energies: 0, 10, 20 and 40 V. A reference solution containing masses 121.050873 $[M+H]^+$ and 922.009798 $[M+H]^+$ were constantly infused as accurate mass reference.

2.6. Data analysis

Data extraction and visualisation were performed using Agilent's MassHunter Qualitative software (B.06). The find by formula function (FbF) in MassHunter was used to find features with high resolution masses and isotope patterns corresponding to the theoretical chemical formula of butylated opines. The METLIN database

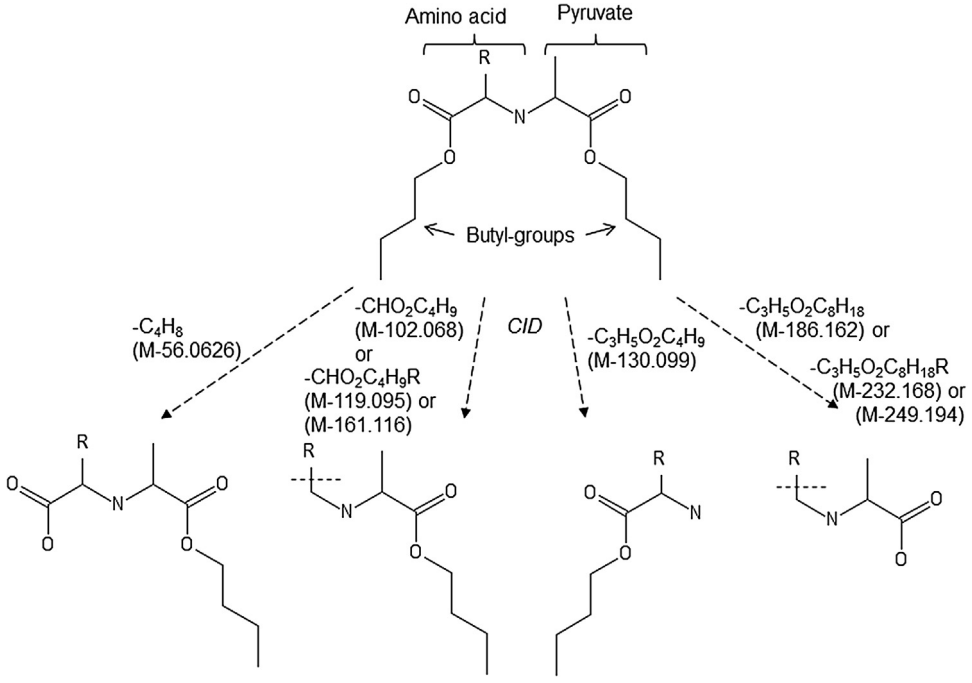

Fig. 1. Predicted collision induced dissociation (CID) pattern of butylated opines.

(http://metlin.scripps.edu) was used to match accurate mass and fragmentation data of synthesised compounds.

2.7. Predicting and confirming intact and fragment masses of butylated opines

Derivatisation adds selectivity to a method, as only compounds with specific functional groups undergo the process and as a result the analytical characteristics (such as compound mass, and retention time) of the derivative become more unique, which ultimately assists with the identification thereof [6]. Derivatisation was used to identify opines in our untargeted butylated data, utilising the fact that when butylating, the active hydrogen(s) of opine carboxylic acid group(s) is replaced with a butyl group (M + 56.063 m/z) [7]. Most opines (except tauropine) contain two carboxylic acid groups and subsequently two butyl groups are added (M + 112.125 m/z) during the derivatisation thereof. In this study, the theoretical chemical formulae and masses of butylated opines were determined and used to find features in the data with corresponding high resolution masses and isotope patterns. Moreover fragmentation patterns of butylated opines were predicted to assist with comparisons of MS/MS spectra.

Based on theory, as shown in Fig. 1, butylated opines would be expected to show a dominant $[M+H-102.068]^+$ neutral loss ion when neutral or acidic amino acids are used for synthesis, and $[M+H-119.095]^+$ or $[M+H-161.116]^+$ neutral loss when basic amino acids are used. According to prediction the pyruvate entity could be lost during fragmentation, resulting in a $[M+H-130.099]^+$ neutral loss ion, subsequently leaving only the

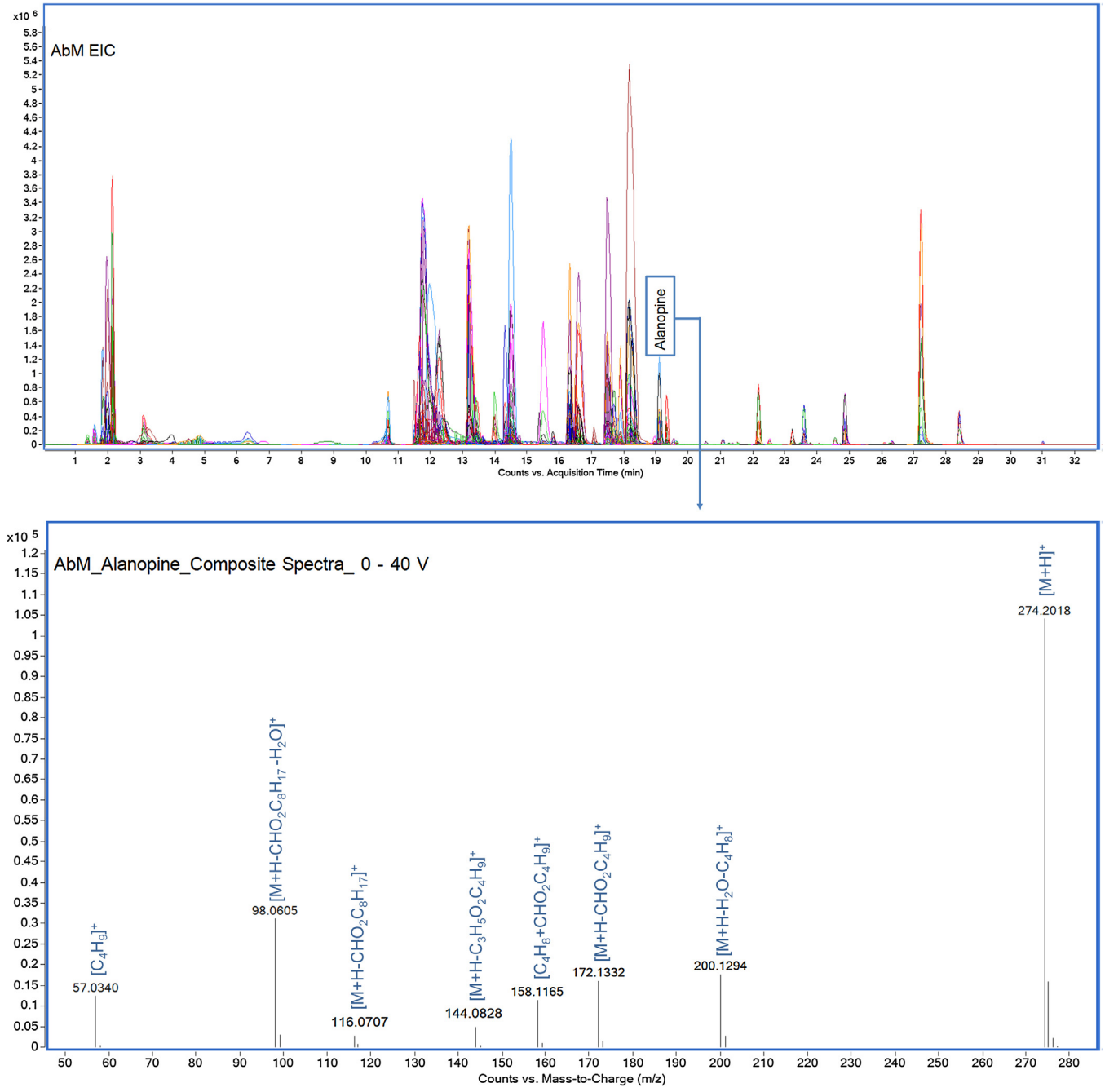

Fig. 2. Extracted ion chromatogram of abalone abductor muscle and composite MS/MS spectra of postulated alanopine.

amino acid backbone. Other potential fragments also predicted are shown in Fig. 1.

3. Results and discussion

3.1. Identification of alanopine in abalone based on theoretical information

Using the FbF function in MassHunter to search for the theoretical determined mass (274.2019 m/z) and molecular formula ($C_{14}H_{27}NO_4$) of butylated alanopine a match was found at 19.0 min as indicated in the extracted ion chromatogram (EIC) of abalone muscle (AbM) in Fig. 2. Next the characteristic accurate mass fragments produced from alanopine in the muscle sample, were matched to the theoretically determined fragments, to confirm probable structure. As shown in Fig. 2, the feature tentatively identified as alanopine displayed fragments which matched the predicted ions of 172.1339 m/z (274.2019 m/z minus the 102.0680 neutral loss); 98.0560 m/z (274.2019 m/z minus the 102.0680 neutral loss of the butylated carboxylate group, minus the 56.0626 neutral loss of the pyruvate butyl group, minus the 18.0153 of water) and 57.0705 (56.0626 + H).

The results presented to this point indicate a level 3 identity for alanopine, as described by Schymanski et al. [5]. Although the inclusion of theoretical fragmentation matching in the identification process adds confidence, it still remained unconfirmed identities without the inclusion of orthogonal information such as retention time matching [5,6]. To achieve the highest level of confidence, it is required to match the analytical characteristics of the annotated features with that of a reference standard. For this purpose, an alanopine reference standard was synthesised and analysed. Furthermore, reference standards for other opines, including: lysopine, octopine, strombine and tauropine, were additionally synthesised in order generate reference information (retention time and accurate mass spectra) for opine confirmation in abalone.

3.2. Confirmation of successful opine synthesis

In order to evaluate the success of each synthesis, the aforementioned synthesised opines were analysed, using the LC-QTOF method described above, prior to and after butylation. Using the METLIN database, it was possible to match the accurate mass, chemical formula and fragmentation data of the unbutylated synthesised opine standards to that in the library (Table 1). The retention time (RT) of these unbutylated standards were between 1.6 and 1.7 min, indicative of the poor retention of unbutylated opines. Evaluation of the natural isotope distribution patterns, showed relative intensities in accordance to the mass of interest. Based on comparisons of the mass, formula and fragmentation data (ions and intensity ratios) between the database and data obtained, alanopine, lysopine, octopine, strombine and tauropine were successfully synthesised.

As summarised in Table 1, the accurate masses, formulae and fragmentation data obtained after LC-QTOF analysis of butylated synthesised standards, were matched with that theoretically determined, using the fact that during butylation every OH group would result in a mass gain of 56.0626 due to the addition of C_4H_8. Using this and the unbutylated fragments of the METLIN database the butylated parameters for the standards of alanopine, lysopine, octopine, strombine and tauropine were determined. The retention

Table 1
Predicted and confirmed analytical characteristics of the unbutylated and butylated opines in synthesised standards and abalone muscle tissue samples.

Unbutylated synthesised opine standards

Opine	Alanopine		Lysopine		Octopine		Strombine		Tauropine	
	MID 65929	Synthesised	MID 89468	Synthesised	MID 3377	Synthesised	MID 66046	Synthesised	MID 65620	Synthesised
Formula	$C_6H_{11}NO_4$		$C_9H_{18}N_2O_4$		$C_9H_{18}N_4O_4$		$C_5H_9NO_4$		$C_5H_{11}NO_5S$	
Accurate mass	161.0688		218.1267		246.1328		147.0532		197.0358	
Precursor ion $[M+H]^+$ (m/z)	162.0760	162.0798	219.1340	219.1332	247.1451	247.1401	148.0600	148.0525	198.0430	198.0431
Product ions $[M+H]^+$ (m/z)	116.0710	116.0697	173.1280	173.1275	230.1184	230.1158	102.0550	102.0558	152.0380	152.0377
	114.0550	114.0555	156.1020	156.1013	188.0952	188.0922	76.0393	76.0401	126.0220	126.0216
	70.0651	70.0655	147.1130	147.1124	142.0888	142.0861	56.0495	56.0499	108.9950	108.0116
RT (min)	–	1.7	–	1.6	–	1.7	–	1.6	–	1.7

Butylated synthesised opine standards

Opine	Alanopine		Lysopine		Octopine		Strombine		Tauropine	
	Theory	Synthesised	Theory	Synthesised	Theory	Synthesised	Theory	Synthesised	Theory	Synthesised
Formula	$C_{14}H_{27}NO_4$		$C_{17}H_{34}N_2O_4$		$C_{17}H_{34}N_4O_4$		$C_{13}H_{25}NO_4$		$C_9H_{19}NO_5S$	
Accurate mass	273.1940		330.3754		358.2580		259.1784		253.0984	
Precursor ion $[M+H]^+$ (m/z)	274.2019	274.2013	331.3834	331.3834	359.2659	359.2651	260.1863	260.1858	254.1063	254.1059
Product ions $[M+H]^+$ (m/z)	218.1393	218.1389	229.3153	229.3012	303.2034	303.2024	158.1182	158.1182	222.1707	222.1706
	172.1338	172.1332	173.2523	173.2503	247.1408	247.1396	130.0869	130.0869	198.0437	198.0437
	116.0712	116.0708	156.2262	156.2260	201.1352	201.1353	102.0680	102.0553	152.0382	152.0376
	70.0657	70.0661	130.0994	130.0862	142.0869	142.0870	56.0626	56.0503	108.9950	108.0117
RT (min)	–	19.2	–	13.9	–	16.7	–	18.1	–	11.7

Butylated opines detected in abalone muscle tissue samples

Opine	Alanopine		Lysopine		Octopine		Strombine		Tauropine	
	Synthesised	Abalone	Synthesised	Abalone	Synthesised	Abalone	Synthesised	Abalone	Synthesised	Abalone
Formula	$C_{14}H_{27}NO_4$		$C_{17}H_{34}N_2O_4$		$C_{17}H_{34}N_4O_4$		$C_{13}H_{25}NO_4$		$C_9H_{19}NO_5S$	
Accurate mass	273.1940		330.3754		358.2580		259.1784		253.0984	
Precursor ion $[M+H]^+$ (m/z)	274.2013	274.2018	331.3834	331.3788	359.2651		260.1858	260.1868	254.1059	254.1058
Product ions $[M+H]^+$ (m/z)	172.1332	172.1332	275.2997	275.2977	303.2024		158.1182	158.1179	198.0437	198.0422
	116.0708	116.0707	173.2503	173.2527	247.1396		148.0611	148.0611	152.0376	152.0371
	57.0709	57.0370	156.2260	156.2226	142.0870		102.0553	102.0555	108.0117	108.0110
RT (min)	19.2	19.0	13.9	14.1	16.7	–	18.1	18.0	11.7	11.8

times for these butylated standards serve as proof that butylation results in better retention of highly polar compounds like opines. These retention times were subsequently used to achieve a level 1 identification for these compounds in the analysed abalone muscle tissue samples.

3.3. Confirmed opines detected in abalone adductor muscle

For final confidence in the identification process the butylated synthesised opine standards were compared to the data collected when analysing abalone. A retention time match of 19.0 and 19.2 min for the tentatively identified alanopine feature from abalone and the synthesised alanopine standard, together with mass and formula data, resulted in confirmation of this feature. Subsequently, the other opines thought to occur in abalone were also searched for, starting with the FbF algorithm (based on theoretically determined butylated information), which resulted in a mass and formula match for lysopine, strombine and tauropine. The search for octopine however yielded no results. In order to achieve a higher level of confidence in the identification of these features, the characteristic fragmentation data for these opines detected in abalone muscle tissue samples were matched to that of synthesised opines (see supplementary material for spectra), resulting in MS/MS spectra matches for lysopine, strombine and tauropine. Final confirmation for the presence of lysopine, strombine and tauropine in abalone muscle tissue, were achieved by comparison of their retention times to that of the lysopine, strombine and tauropine synthesised standards.

4. Conclusions

The ability of opines to form butyl esters were used in an attempt to detect and identify these compounds found in abalone muscle data obtained by untargeted analysis. Due to the lack of available standards for these compounds, and the fact that no butylated opine MS/MS spectra and retention time information was available in commercially available databases, we had to rely on theoretical fragmentation patterns and synthesised standards to confirm the identities of these compounds. By using the 1) accurate mass of the precursor ions, 2) unequivocal monoisotopic mass, 3) isotopic distribution of precursor ions, 4) accurate mass MS/MS fragment ions, and 5) MS spectra and retention time comparisons to the in-house synthesised opine compounds, the presence of alanopine, lysopine, strombine and tauropine were confirmed in abalone muscle tissue. Although octopine was not present in the abalone muscle tissue analysed, this methodology can be used for searching for octopine in other abalone tissues, or for opines in general in other organisms. Next a targeted method to quantitate opines, predefined and selected for their relevance should be set up. The quantitative monitoring of opines produced in abalone subjected to functional and/or environmental hypoxia scenarios, as typically experienced on abalone farms or for the purpose of investigating anaerobic responses from a purely academic perspective will ultimately complete the metabolomics research cycle.

Acknowledgements

This work was supported by the North-West University and the Technology Innovation Agency. The authors thank HIK Abalone Farm (Pty) Ltd., South Africa for the donation of abalone samples. The authors are grateful to Dr C.J.F. Taute for his advice with regards to compound synthesis.

Appendix A. Supplementary data

Supplementary data associated with this article can be found, in the online version, at http://dx.doi.org/10.1016/j.jchromb.2017.01.025.

References

[1] J.F. Xiao, B. Zhou, H.W. Ressom, Metabolite identification and quantitation in LC-MS/MS-based metabolomics, TrAC Trends Anal. Chem. 32 (2012) 1–14.
[2] E. Werner, J.-F. Heilier, C. Ducruix, E. Ezan, C. Junot, J.-C. Tabet, Mass spectrometry for the identification of the discriminating signals from metabolomics: current status and future trends, J. Chromatogr. B 871 (2008) 143–163.
[3] L. Venter, D.T. Loots, A. Vosloo, P. Jansen van Rensburg, J.Z. Lindeque, Abalone growth and associated aspects: now from a metabolic perspective, Rev. Aquacult. (2016), http://dx.doi.org/10.1111/raq.12181.
[4] J. Baldwin, J. Elias, R. Wells, D. Donovan, Energy metabolism in the tropical abalone, Haliotis asinina Linné: comparisons with temperate abalone species, J. Exp. Mar. Biol. Ecol. 342 (2007) 213–225.
[5] E.L. Schymanski, J. Jeon, R. Gulde, K. Fenner, M. Ruff, H.P. Singer, J. Hollender, Identifying small molecules via high resolution mass spectrometry: communicating confidence, Environ. Sci. Technol. 48 (2014) 2097–2098.
[6] L.W. Sumner, Z. Lei, B.J. Nikolau, K. Saito, U. Roessner, R. Trengove, Proposed quantitative and alphanumeric metabolite identification metrics, Metabolomics 10 (2014) 1047.
[7] S. O'omolo, G. Gäde, P. Cook, A. Brown, Can the end products of anaerobic metabolism tauropine and D-lactate, be used as metabolic stress indicators during transport of live South African abalone *Haliotis midae*? Afr. J. Mar. Sci. 25 (2003) 301–309.
[8] L. Venter, P. Jansen van Rensburg, D.T. Loots, A. Vosloo, J.Z. Lindeque, Untargeted metabolite profiling of abalone using gas chromatography mass spectrometry, Food Anal. Methods 9 (2016) 1254–1261.
[9] R.F. Borch, M.D. Bernstein, H.D. Durst, Cyanohydridoborate anion as a selective reducing agent, J. Am. Chem. Soc. 93 (1971) 2897–2904.

Metabolomics (2018) 14:49
https://doi.org/10.1007/s11306-018-1346-8

ORIGINAL ARTICLE

Uncovering the metabolic response of abalone (*Haliotis midae*) to environmental hypoxia through metabolomics

Leonie Venter[1] · Du Toit Loots[1] · Lodewyk Japie Mienie[1] · Peet J. Jansen van Rensburg[1] · Shayne Mason[1] · Andre Vosloo[2] · Jeremie Zander Lindeque[1]

Received: 17 November 2017 / Accepted: 3 March 2018

Abstract

Introduction Oxygen is essential for metabolic processes and in the absence thereof alternative metabolic pathways are required for energy production, as seen in marine invertebrates like abalone. Even though hypoxia has been responsible for significant losses to the aquaculture industry, the overall metabolic adaptations of abalone in response to environmental hypoxia are as yet, not fully elucidated.

Objective To use a multiplatform metabolomics approach to characterize the metabolic changes associated with energy production in abalone (*Haliotis midae)* when exposed to environmental hypoxia.

Methods Metabolomics analysis of abalone adductor and foot muscle, left and right gill, hemolymph, and epipodial tissue samples were conducted using a multiplatform approach, which included untargeted NMR spectroscopy, untargeted and targeted LC–MS spectrometry, and untargeted and semi-targeted GC-MS spectrometric analyses.

Results Increased levels of anaerobic end-products specific to marine animals were found which include alanopine, strombine, tauropine and octopine. These were accompanied by elevated lactate, succinate and arginine, of which the latter is a product of phosphoarginine breakdown in abalone. Primarily amino acid metabolism was affected, with carbohydrate and lipid metabolism assisting with anaerobic energy production to a lesser extent. Different tissues showed varied metabolic responses to hypoxia, with the largest metabolic changes in the adductor muscle.

Conclusions From this investigation, it becomes evident that abalone have well-developed (yet understudied) metabolic mechanisms for surviving hypoxic periods. Furthermore, metabolomics serves as a powerful tool for investigating the altered metabolic processes in abalone.

Keywords Abalone · Aquaculture · Environmental hypoxia · Metabolism · Metabolomics

1 Introduction

The key goal of intermediary metabolism is to uphold adenosine triphosphate (ATP) supply to ensure that living cells can grow, reproduce, and respond to stresses (Salway 2004). In unstressed circumstances, basal metabolism is dominated by anabolic activity that synthesizes macromolecules leading to cell growth, division and repair (Garrett and Grisham 2010). However, during hypoxic conditions, catabolic processes are activated to ensure the availability of energy for mechanisms related to survival, recovery and maintenance of cell homeostasis (Sokolova et al. 2012). Energy levels are partially managed through suppression of energy consuming reactions (oxy-conforming) and activation of oxygen-independent metabolic pathways, like phosphagen breakdown and anaerobic glycolysis (Storey 2005). Invertebrates

Electronic supplementary material The online version of this article (https://doi.org/10.1007/s11306-018-1346-8) contains supplementary material, which is available to authorized users.

✉ Jeremie Zander Lindeque
Zander.Lindeque@nwu.ac.za

[1] Human Metabolomics, North-West University, Potchefstroom Campus, Private Bag X6001, Potchefstroom 2520, South Africa

[2] School of Life Sciences, University of KwaZulu-Natal, Westville Campus, Private Bag X54001, Durban 4000, South Africa

Published online: 12 March 2018

have well defined anaerobic metabolic pathways capable of energy production during hypoxia (Gäde et al. 1984; Gäde and Grieshaber 1986; Fields and Storey 1987; Gäde 1988; Grieshaber et al. 1993; Carroll and Wells 1995; O'omolo et al. 2003; Storey 2004; Müller et al. 2012; Liu et al. 2014). Despite this, knowledge on the holistic metabolic response of abalone during hypoxic conditions is scarce. The interplay of anaerobic pathways and the mechanisms behind the many accumulated anaerobic end-products in marine invertebrates are understudied, not to mention the interplay between different tissues.

Abalone are single-shelled, marine mollusks, which have large commercial value and in South Africa, *Haliotis midae* farming generates the largest aquaculture-based income (Britz and Venter 2016). Consequently, abalone aquaculture is an important research field, with a central focus on increasing farming outputs and reducing animal losses. Hypoxia is responsible for significant losses to the aquaculture industry as it not only results in animal mortalities, but also causes a significant decline in growth (in surviving animals). Environmental hypoxia is typically experienced on abalone farms when animals are transported out of water for an extended period of time, such as during size grading procedures (Hooper et al. 2014), or during periods of reduced water flow or higher water temperatures. Moreover, hypoxia also occurs in the natural marine environment, which severely impacts growth and survival. This was previously demonstrated when harmful algal blooms caused massive abalone stock losses in South Africa, attributed to anoxia (Pitcher and Calder 2000; Mouton 2017). Considering this, a better understanding of the biochemical responses of abalone is crucial to assist with recovery or to prevent metabolic resource depletion when abalone are subjected to hypoxic episodes (Cook 2014).

The aim of this study was to elucidate the metabolic response of *H. midae* subjected to environmental hypoxia; and to study the interplay of different abalone tissues using metabolomics. A multiplatform metabolomics approach (Fig. 1) was used to investigate the metabolite profiles in adductor muscle, foot muscle, epipodial tissue, hemolymph, left and right gill samples, and included the use of: untargeted nuclear magnetic resonance (NMR) spectroscopy;

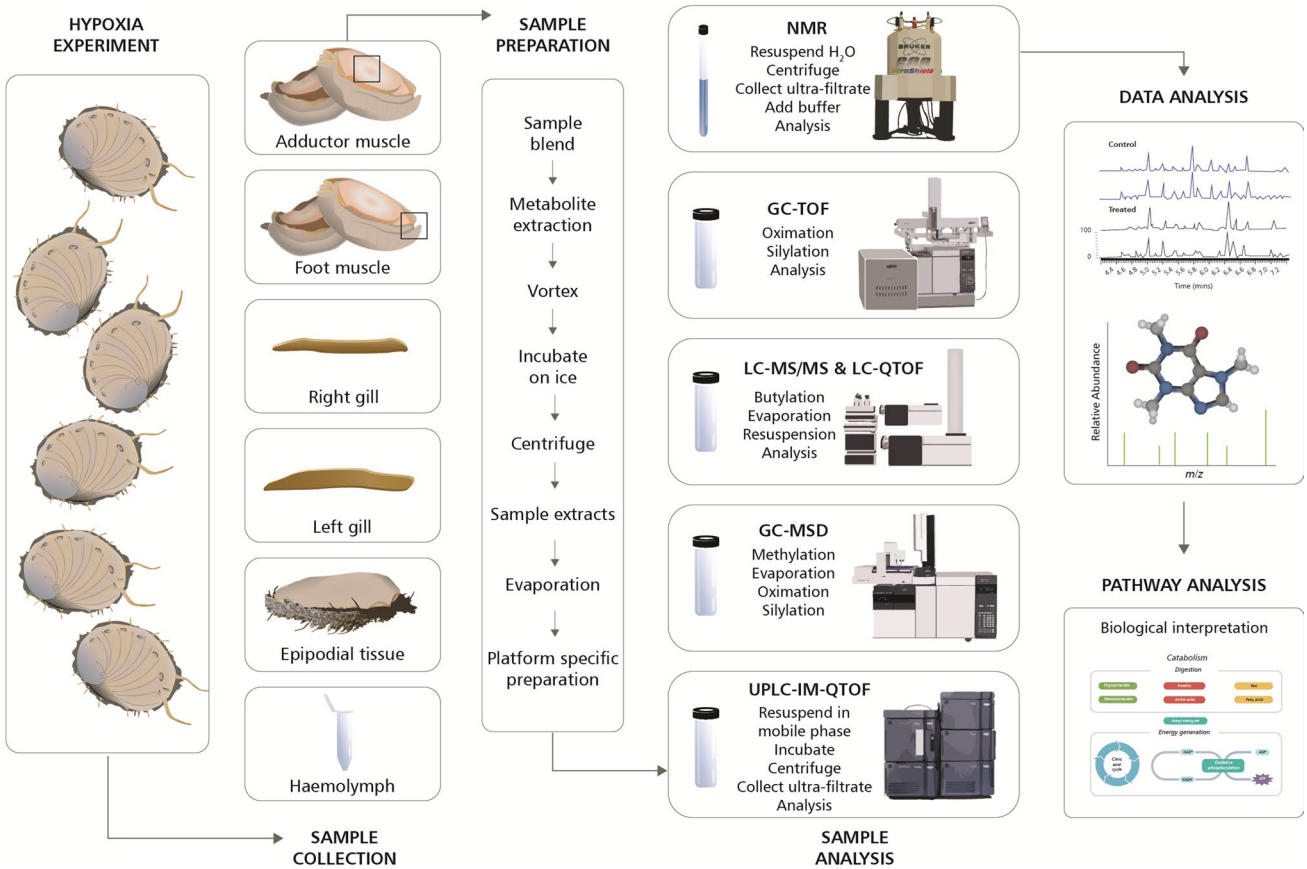

Fig. 1 Summary of the experimental workflow. Adductor and foot muscle, right and left gill, epipodial tissue and hemolymph samples were collected after a hypoxia experiment and prepared for analysis with multiple analytical techniques. The results were processed and pathway interpretation performed to highlight the most affected metabolic pathways

untargeted ultra-performance liquid chromatography–ion mobility-quadrupole time of flight spectrometry (UPLC–IM-QTOF); untargeted gas chromatography–time of flight spectrometry (GC–TOF); semi-targeted liquid chromatography–quadrupole time of flight mass spectrometry (LC–QTOF) analyses of butylated esters; semi-targeted gas chromatography–mass spectrometry-detector (GC–MSD) analyses of methylated fatty acids (FAMEs) and targeted liquid chromatography–tandem mass spectrometry (LC–MS/MS).

2 Materials and methods

Detailed information regarding the abalone dissection procedure, chemicals and reagents, preparation of standards and solutions, sample preparation for specific platform analysis, sample analysis, data extraction processes and the procedures followed to identify detected compounds can be found in the online supplementary material.

2.1 Experimental setup and animals

Adult abalone, *H. midae* (n = 12) were collected during the winter season from a single raceway at HIK Abalone Farm (Pty) Ltd situated in Hermanus, South Africa. Animals of interest were transferred to a portable aquarium tank in circulating seawater as used by the farm. Following an acclimation period, control animals (n = 6) were removed and dissected. The remaining animals were exposed to environmental hypoxia, by covering the water surface area with a polystyrene sheet containing a small opening, through which 100% nitrogen was flushed slowly into the system (O'omolo et al. 2003). Abalone were removed after 6 h, at which point no attachment behavior was seen. These animals were dissected in the same manner as the control group to sample adductor and foot muscle, left and right gill, epipodial tissue and hemolymph samples, following the procedures stated in the online supplementary material (S.1).

2.2 Metabolite extraction

A subsection of each sampled tissue was removed with a scalpel (while on ice), transferred to a new tube and weighed for the purpose of pre-analysis normalization (Lindeque et al. 2013). Each sample was homogenized in bulk whereafter it was divided into five tubes for analysis on five different analytical platforms. A target sample weight of 100 mg for the right gill tissue, 200 mg for the left gill tissue, 150 mg for the epipodial tissue and 300 mg for the adductor and foot muscle tissue were used throughout the extraction process.

For every 10 mg of abalone tissue, 20 µL water, 50 µL methanol and 20 µL internal standard (2-acetamidophenol and 3-phenylbutyric acid, with a final concentration of 50 µg/mL) was added along with both a 3 and a 7-mm stainless steel bead to micro-centrifuge tubes. Samples were homogenized for 4 min at 30 Hz, using a Retch M400 vibration mill, whereafter 20 µL chloroform and 10 µL water were added to the homogenate. The samples were vortexed for 1 min and incubated on ice for 10 min, before they were centrifuged at 25,000×*g* for 10 min at 4 °C to give phase separation. Selected volumes of the aqueous and organic phases were transferred to a screw top vial (depending on the analytical platform) and dried under a gentle stream of nitrogen at 37 °C, together with an additional 100 µL platform-specific internal standard: for NMR analysis, 100 µL of the polar phase and 50 µL of the a-polar phase was transferred with nor-leucine internal standard (100 µg/mL). For UPLC–IM-QTOF and LC–QTOF analyses, 70 µL of the polar phase and 35 µL of the a-polar phase was transferred with nor-leucine internal standard (100 µg/mL). For GC–QTOF analysis 70 µL of the polar phase and 35 µL of the a-polar phase was transferred with nonadecanoic acid internal standard (100 µg/mL). For LC–MS/MS analysis 10 µL of the polar phase and 5 µL of the a-polar phase was transferred with nor-leucine internal standard (10 µg/mL). For GC–MSD analysis, nonadecanoic acid internal standard (100 µg/mL) and 150 µL of the a-polar phase of the tissue homogenate was transferred.

Hemolymph samples were prepared by adding 500 µL of the collected hemolymph to 1500 µL cold acetonitrile in micro-centrifuge tubes. The samples were vortexed and incubated on ice for 30 min, followed by centrifugation at 25,000×*g* for 10 min at 4 °C. The supernatant was aliquoted into several screw top vials (one for each analytical platform). All hemolymph samples were dried under a gentle stream of nitrogen at 37 °C after the addition of 100 µL instrument specific internal standards.

2.3 Sample preparation

For NMR spectroscopy analysis, dried sample extracts were re-dissolved in 500 µL ultra-pure water and centrifuged at 12,000×*g* for 10 min, whereafter the ultra-filtrate was transferred together with 50 µL 1.5 M potassium phosphate monobasic deuterated NMR buffer solution at pH 7.4 (Dona et al. 2014) to 5 mm NMR glass tubes. Sample preparation for compatibility with GC–TOF (Venter et al. 2016a), LC–MS/MS, LC–QTOF (Venter et al. 2017), GC–MSD (Willers et al. 2016) platforms were conducted as previously described. Extracts used for UPLC–IM-QTOF analysis were re-suspended in 110 µL water:acetonitrile (50:50), whereafter the samples were vortexed and incubated at room temperature for 30 min and centrifuged at 25,000×*g* for 10 min, after which the supernatant (100 µL) was transferred to vials

for analysis. Details regarding the preparation methods can be found in the online supplementary material (S.1).

2.4 Sample analysis

Elaboration on the methods can be found in online supplementary material (S.1).

NMR spectroscopy analyses were performed on a Bruker Advance III HD NMR spectrometer following the parameters described previously (Irwin et al. 2016).

GC–TOF analyses were performed on a LECO Pegasus HT mass analyzer coupled to an Agilent 7890A GC in accordance to an in-house method.

LC–MS/MS analyses were performed in positive ion mode using an Agilent 1200 LC system coupled to an Agilent 6410 Triple Quadrupole. Selected metabolites were analyzed in multiple reaction monitoring (MRM) mode as described in the supplementary material (Table S.1).

LC–QTOF analyses were conducted using an Agilent 1200 LC system coupled to an Agilent 6510 QTOF mass analyzer operated in accordance to the method used by Venter et al. (2017).

GC–MSD analyses of FAMEs were performed with an Agilent GC–MSD instrument as described by Willers et al. (2016).

UPLC–IM-QTOF analyses were performed in accordance to an in-house method, using a Waters Acquity UPLC system coupled via an ESI interface to a Synapt G2-Si hybrid ion mobility-MS system.

2.5 Data analysis and processing

The raw data files of each platform were processed with their corresponding software to create a data matrix. Software and processing details are given in the online supplementary material (S.1). Supervised zero filtering was performed (Venter et al. 2015) so that features (unidentified chromatographic or NMR signals) detected in all the samples of at least one experimental group remained in the data matrix. The NMR data was normalized with the internal standard, 2-acetamidophenol, while GC–TOF data was normalized with 3-phenylbutyric acid. Mass spectrometry total useful signal (MSTUS) normalization (Warrack et al. 2009) was the preferred normalization method for the data acquired by UPLC–IM-QTOF, LC–QTOF, GC–MSD and LC–MS/MS analysis. Missing or zero values were replaced with half of the minimum positive value in the data, within MetaboAnalyst (Xia et al. 2015).

2.6 Data pre-treatment and statistical analysis

Data pre-treatment and statistical analyses were performed with the webserver MetaboAnalyst and MS Excel. The generalized logarithm (glog) was used to transform the data before statistical analysis (Lindeque et al. 2015). Univariate analyses were used to identify features that differed markedly between the control and experimental group. A feature was considered significant when it had a Student's t test p value < 0.05 (FDR corrected) and effect size d value > 0.8 (Ellis and Steyn 2003). Effect size can be regarded as a scaled fold change, where the difference between the means of the two groups is divided by the maximum standard deviation of the two groups. The Pearson correlation of selected metabolites in different tissues was investigated in MetaboAnalyst. The list of metabolites used in this test is given in the online supplementary material (S.1).

2.7 Compound identification and pathway analysis

Features that differed markedly between the control and experimental group were identified by comparing the metadata provided by each analytical platform (such as accurate mass, fragmentation spectra, retention time, chemical shifts and collision cross section values) to several in-house, commercial and public libraries/databases. The online supplementary material (S.1) can be viewed for guidelines followed for instrument specific compound identifications. The important metabolites identified were ranked with the classification system previously published (Schymanski et al. 2014). Those metabolites that were confidently identified (Level 1–3) were used for pathway interpretation. Some metabolites were detected on more than one analytical platform, and when this occurred, the platform with the highest identification confidence level received preference, and if a duplicate metabolite still existed the metabolite with the best (smallest) p value was selected.

A metabolic map of the metabolic response of *H. midae* to environmental hypoxia was created. The metabolites are reported as relative compound intensities based on the tissue in which the findings were made. Manual pathway analysis was performed, where a pathway was considered important when most of the metabolites in the pathway were affected, and/or when shared metabolites in the pathway (i.e. metabolites connected with other pathways) were also considerably altered.

3 Results and discussion

Farmed abalone are rather homogeneous and have a very uniform genetic background enabling one to use limited numbers in experiments (as supported by power analysis). The number of animals analyzed in this study also agreed with the proposed sampling measures of the Metabolomics standards initiative (Sumner et al. 2007).

Those metabolites which differed significantly between the control and experimental group, and which were confidently identified, are listed in Table S.2 (Supplementary material—Table 2). Metabolites detected with elevated (↑) or decreased (↓) relative abundances (compared to the control group) were subsequently mapped (Fig. 2) and interpreted. The pathways that were affected by environmental hypoxia include: [A] carbohydrate metabolism (Glycolysis); [B] oxaloacetate–succinate pathway; [C] threonine–serine–glycine metabolism; [D] sulphur containing amino acid metabolism; [E] cysteine–taurine metabolism; [F] pyruvate–lactate/alanine pathway; [G] aspartate–succinate pathway; [H] pyruvate–opine pathway; [I] lysine–tryptophan metabolism; [J] glutaryl–CoA pathway; [K] branched chain amino acid metabolism; [L] ketone body metabolism; [M] propionyl–CoA pathway; [N] tricarboxylic acid (TCA) cycle; [O] alternative aspartate pathway; [P] purine and pyrimidine metabolism; [Q] urea cycle; [R] proline metabolism; [S] electron transport chain (ETC); [T] phenylalanine–tyrosine metabolism; [U] beta(ß)–oxidation; [V] fatty acid transport pathway; and [W] fatty acid synthesis. Significant metabolite concentration differences found in abalone adductor muscle (AM), foot muscle (FM), left gill (LG), right gill (RG), hemolymph (H) and epipodial tissue (E) samples after hypoxia are indicated in Fig. 2 where relative abundance are indicated as elevated (blue) or decreased (red).

3.1 ATP production and NAD$^+$ recovery during environmental hypoxia

Evidence of phosphagen breakdown [Q] and anaerobic glycolysis [B, F and H] were found (Fig. 2) in most of the investigated tissues. Phosphagens and anaerobic metabolic pathways are responsible to uphold energy levels during hypoxia, through a process referred to as substrate-level-phosphorylation (Feala et al. 2009). Abalone typically use phosphoarginine as primary phosphagen for instant energy liberation (Grieshaber et al. 1993), which resulted in accumulated arginine in most tissues (epipodial tissue, adductor muscle and the gills). However, the presence of creatine in the foot muscle of hypoxic abalone suggests that energy is also maintained with phosphocreatine metabolism. Exposing abalone to environmental hypoxia resulted in reduced levels of arginine and creatine in the foot muscle samples, which is most likely due to the further breakdown pathways being up-regulated, or metabolic shuttles between tissues.

Initial energy replenishment through phosphagen breakdown is short-lived, and subsequently assisted by anaerobic pathways. As mitochondrial respiration and ATP production

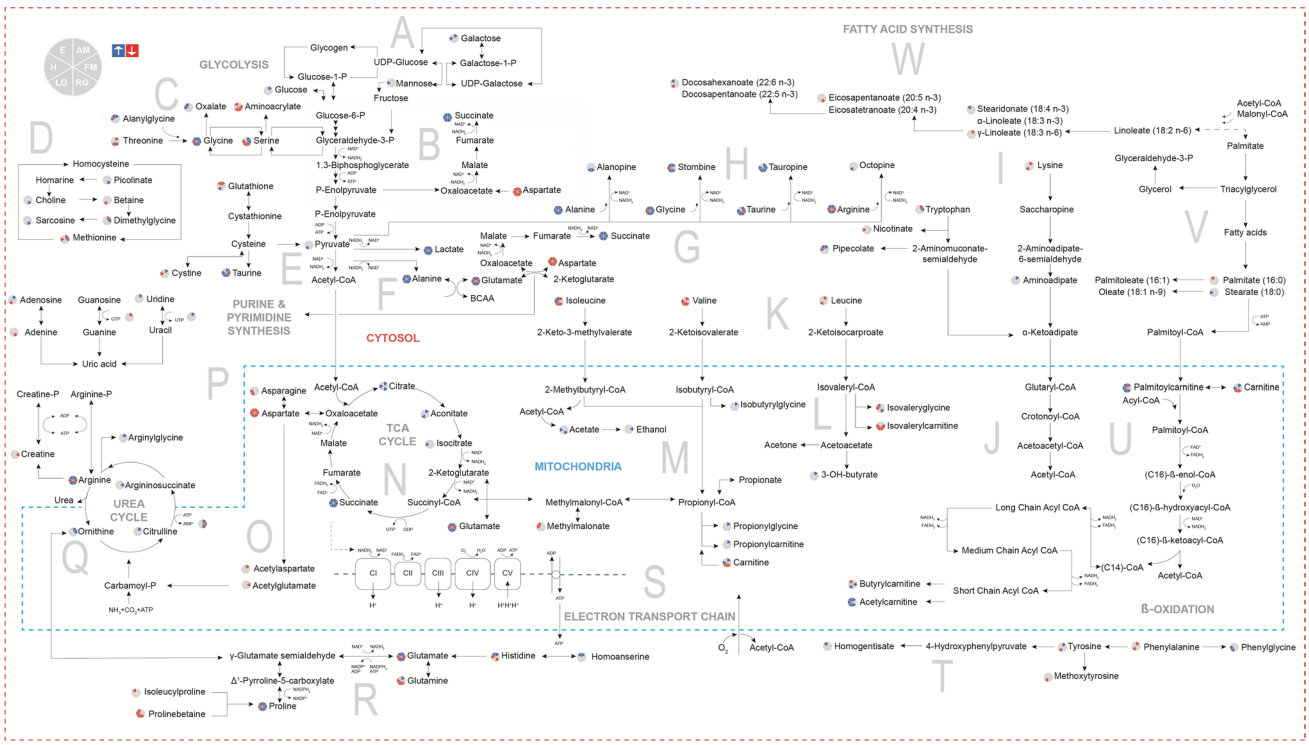

Fig. 2 The holistic metabolic response of *Haliotis midae* following environmental hypoxia. Elevated (blue) and decreased (red) metabolite findings in abalone adductor muscle (AM), foot muscle (FM), left gill (LG), right gill (RG), hemolymph (H) and epipodial tissue (E) following environmental hypoxia

slow with reduced oxygen levels, anaerobic pathways are activated to counter the energy and redox ($NADH:NAD^+$) imbalance, which is supported by the elevated levels of lactate, several opines, succinate and alanine. During prolonged hypoxia, the majority of ATP is produced by the phosphoglycerate kinase and pyruvate kinase reactions in the glycolysis pathway [B], which is only possible as long as cytoplasmic nicotinamide adenine dinucleotide (NAD^+) levels are sustained. Three complementary glycolytic pathways are involved in NAD^+ recovery during hypoxia in abalone, which are the: (1) glucose–lactate pathway [F], (2) glucose–opine pathway [H] and (3) glucose/aspartate–succinate pathway [G].

In an attempt to avoid metabolic shutdown and allow continued glycolysis during hypoxia, pyruvate is converted to lactate by oxidizing NADH to NAD^+ (Whitney and Rolfes 2008), which is supported by the elevated lactate levels found in all of the abalone tissues investigated. During prolonged anaerobic metabolism, lactate synthesis will eventually exceed the clearance thereof, resulting in a reduction in intracellular pH (Green and Storey 2016), which in turn further limits ATP production over long periods of anaerobic stress. In order to prevent acidotic shock, an increase in cell buffer capacity is subsequently required, which is partially accomplished in *H. midae* by the production of alanine and opines.

Opines are anaerobic end-products, produced in *H. midae* through the condensation of pyruvate and several amino acids which converts NADH to NAD^+ (Sato et al. 1993). A connection between the specific opines formed, and their associated amino acids, can be seen following environmental hypoxia [H]. Elevated levels of alanine were accompanied by an elevation in alanopine in the left and right gill samples. Reduced levels of glycine were accompanied by a reduction in strombine in the hemolymph. Elevated taurine in the adductor muscle, gills and hemolymph samples were also accompanied by elevated tauropine in the same tissue samples. Finally, octopine was elevated only in the left gill samples, which corresponded with elevated arginine. Similar associations were also recognized in other animals exposed to environmental hypoxia (Kreutzer et al. 1989). These results not only indicate the extent of the hypoxic stress induced during the environmental hypoxia experiment, but also the animal's dependence on the opine metabolic pathway to sustain NAD^+ levels and limit lactate-induced acidosis.

Reduced aspartate, accompanied by elevated concentrations of alanine and succinate in all of the tissues investigated, imply activation of the glucose/aspartate–succinate pathway [B] to sustain NAD^+ levels. A synchronized depletion of aspartate accompanied by elevations in alanine and succinate in the foot and adductor muscles of other abalone were also previously reported in response to anoxia (Gäde 1988), confirming our findings. Succinate is the end product of the glucose–succinate pathway [B], the aspartate–succinate pathway [G] and the TCA cycle [N], during conditions of anaerobic ATP production in abalone.

3.2 Central carbon metabolism during environmental hypoxia

Several sugar-based metabolites (such as galactose, mannose and glucose) were generally elevated in *H. midae*, following hypoxic exposure (Fig. 2). As mentioned, glycolysis and interconnected carbohydrate pathways [A] become more important during hypoxia when anaerobic energy production is required, which result in the release of carbohydrates from glycogen stores and glycoproteins, and the up-regulation of gluconeogenesis (Roznere et al. 2014). This may lead to elevated carbohydrate metabolites, as seen in the abalone. Elevated TCA cycle [N] intermediates (citrate, aconitate, isocitrate and succinate) were detected possibly due to impaired mitochondrial respiration and down-regulation of the TCA cycle via isocitrate dehydrogenase, as a means to prevent metabolic energy waste as typically experienced in vertebrates (Garrett and Grisham 2010). The aforementioned redox imbalance is a major contributor to this down-regulation and the accumulation of the TCA cycle intermediates. Fortunately, however, alternative substrates, such as glutamate, can still be used to synthesize the much needed α-ketoglutarate and down-stream TCA cycle intermediates very effectively (Boardman et al. 2016) during hypoxia, preventing total TCA cycle shutdown.

3.3 Up-regulated protein and amino acid catabolism

The concentrations of numerous amino acids were significantly affected by environmental hypoxia (Table S.2). It is known that, during low energy states, the adenosine monophosphate (AMP) to ATP ratio increases, which subsequently allosterically activates AMP activated protein kinase (AMPK). AMPK signals the catabolism of proteins (and lipids), and inhibits anabolism and cell growth (Venter et al. 2016b). Considering the elevated levels of AMP detected in both the right gill and adductor muscle samples [Q], in addition to the elevated amino acid concentrations in these and other tissues, it becomes apparent that hypoxia results in pronounced protein catabolism (Fields 1983).

3.3.1 The role of ketogenic- and glucogenic amino acids

The glucogenic amino acids (arginine, glutamate, glutamine, glycine, histidine, methionine, proline and serine) were predominantly elevated in the adductor muscle of abalone during environmental hypoxia (Fig. 2). Typically, during

stressed conditions, glucogenic amino acids are converted to alanine via the transamination of pyruvate [F] (Salway 2004). The detection of elevated alanine and pyruvate attests to this, as well as the elevated glutamate, synthesized by transamination of α-ketoglutarate. Elevated alanine is a key survival response as it assists in: the buffering of H^+ ions, regulation of intracellular osmotic pressure, and serves as a substrate for alanopine production (Fujimori and Abe 2002; Garrett and Grisham 2010; Müller et al. 2012). Elevated concentrations of alanine were also seen in *H. diversicolor*, after exposure to a toxin stressor that induced an anaerobic state (Lu et al. 2017), supporting our results. Elevated concentrations of glycine and methionine detected in the adductor muscle samples as a result of hypoxia, were also previously reported (Lu et al. 2016). We additionally detected elevated serine concentrations, not previously reported, which is also an important energy substrate (for gluconeogenesis) as serine can be deaminated to form pyruvate (Salway 2004).

Aspartate, asparagine, glutamate and glutamine are well known metabolic fuels during anaerobic conditions (Storey 2005). Environmental hypoxia additionally resulted in reduced concentrations of both aspartate (all tissues investigated) and asparagine (hemolymph and left gill). In contrast, glutamate was increased in the epipodial tissue, adductor muscle and both gill samples. The reduced aspartate levels can be linked to its role in replenishing oxaloacetate during hypoxia [O], as was previously indicated for *Apostichopus japonicus* (Prathomya et al. 2017). Glutamate is an active intermediate of amino acid metabolism [N and R], and closely associated with the TCA cycle. As mentioned, amination of α-ketoglutarate produces glutamate, which in turn can be further aminated to yield glutamine. Glutamine in turn may serve as a nitrogen store, lowering ammonia toxicity during hypoxia (Venter et al. 2016b). Reduced histidine concentrations were also detected in the hemolymph samples of hypoxic *H. midae*, corresponding to the reduction of glutamate in the hemolymph. Histidine is metabolized to glutamate with the removal of one carbon group (Salway 2004), which links this also to the one-carbon metabolism and elevated methionine.

As seen in Fig. 2, environmental hypoxia resulted in significantly increased proline concentrations in the adductor muscle, left gill, right gill and epipodial tissue samples of *H. midae* (Table S.2) which is likely a result of reduced proline catabolism [R and Q] due to the redox imbalance. However, proline synthesis cannot be excluded as was previously seen in plants. During periods of dehydration, the proline anabolic pathways in plants are activated while the proline catabolic pathways are repressed (Hayat et al. 2012). Proline is thought to prevent dehydration, function as a molecular chaperon stabilizing the structure of proteins, maintain protein integrity and enhance the activities of different enzymes. It can be speculated that proline plays a similar role in marine animals. Furthermore, accumulated proline, buffer cytosolic pH and protects against the damaging effects of reactive oxygen species (Hochachka et al. 1973; Hayat et al. 2012; Vosloo et al. 2013). Evidence for this was found in green-lipped mussel subjected to temperature stress (Dunphy et al. 2015). Moreover, *H. midae* that were fed a L-proline supplemented feed for 1 month, and subjected to oxygen and temperatures stress, still displayed an increase in mass, suggesting some benefit for the animal despite the stressed conditions (Vosloo et al. 2013).

The levels of the ketogenic amino acids, leucine and lysine, were lower in the adductor muscle and left gill after exposure to environmental hypoxia. Both leucine and lysine are considered essential amino acids for vertebrate species, and can only be assumed to be the same for invertebrates. The results of this investigation support this hypothesis, as the concentrations of these, and other essential amino acids, were depleted after the prolonged hypoxia. Considering the up-regulated fatty acid oxidation and increased use of carnitine (Li et al. 2009) during hypoxic conditions, it is also reasonable to assume that lysine [I] was actively used to synthesize carnitine [J], which may contribute to the reduced lysine detected. Furthermore, leucine [K] and the other branched-chain amino acids are substrates for gluconeogenesis under conditions of high ATP demand (Mason et al. 2015).

3.3.2 Pathways preventing ammonia/nitrogen toxicity

The involvement of arginine and phosphoarginine in ATP production during hypoxia (Morash and Alter 2016) has already been discussed. However, since arginine showed the most significant increase in concentration in the adductor muscle of *H. midae* after exposure to environmental hypoxia (Table S.2), its involvement in connected pathways cannot be ignored. Significantly elevated concentrations of ornithine and citrulline were also found in the adductor muscle following environmental hypoxia, while elevated argininosuccinate was found in the foot muscle. This result implicates the urea cycle [Q] in maintaining the nitrogen/ammonia balance with increased amino acid catabolism. Only a small portion of the ammonia released from amino acid catabolism is used for the synthesis of non-essential amino acids (like alanine and glutamate), while the majority of the ammonia is excreted, either as pure ammonia or as urea (Nollens et al. 2004; Schmidt-Nielsen 2007). Previous literature on *H. laevigata* indicated that these organisms are extremely sensitive to ammonia exposure, which results in dramatically reduced growth and nutrient uptake (Harris et al. 1998). Thus the urea cycle in abalone plays an important role during stressed conditions such as hypoxia. In standard farming conditions, it was reported that energy loss in the form of ammonia excretion is negligible in *H.*

midae, accounting for less than 1% of consumption (Barkai and Griffiths 1988). However, this is likely to be significantly more during hypoxia.

3.3.3 Detoxification through glycine conjugation

Several dipeptides (arginylglycine, alanylglycine, alanyllysine, cysteinylcysteine, isoleucylthreonine, valylglycine) were drastically increased in the hypoxic animals (Table S.2). The occurrence of dipeptides in cellular fluids can be largely ascribed to incomplete protein breakdown (Shen et al. 2008; Wishart et al. 2012). These peptides also play a key role in cell signaling, which may further modulate specific metabolic reactions. Interestingly, elevated alanylglycine and arginylglycine correlated with elevated alanine and arginine levels, hinting to possible phase II detoxification (specifically glycine conjugation). Alanine levels in the epipodial tissue (for example) correlated with alanylglycine levels ($r = 0.9$) in the environmental hypoxia group while they did not correlate in the control group. Similarly, arginine levels in the adductor muscle moderately correlated ($r = 0.6$) with arginylglycine levels in the hypoxic animals while no correlation was found in the controls. Also, lower isovalerylglycine levels corresponded to lower branched-chain amino acid levels.

In humans, it is well known that various states of organic aciduria produce large amounts of different acyl-CoAs, which in turn serve as substrates for glycine *N*-acyltransferase (GLYAT), and subsequently the synthesis of glycine conjugates (Loots et al. 2005). Considering that acyl-transferase enzymes can conjugate glycine to a variety of different accumulated amino acids (Badenhorst et al. 2014), the role of glycine conjugation in detoxifying accumulating intermediates and maintaining coenzyme A (CoA) levels seem highly probable in abalone based on our findings [L and M]; although additional evidence to confirm such activities in abalone is needed.

3.3.4 Amino acids as osmolytes

The osmolytes altered by environmental hypoxia included various non-essential amino acids (alanine, arginine, asparagine, aspartate, cysteine, glutamate, glutamine, glycine, proline, serine and tyrosine), opines, taurine, choline, betaine, dimethylglycine and sarcosine (Table S.2). This suggests a change in the osmotic regulation of abalone when exposed to oxygen poor environments. Taurine for example has been reported to be more related to osmoregulation than to energetics (Tripp-Valdez et al. 2017). Likewise, the elevated concentrations of the less metabolically active non-essential amino acids are believed to maintain osmoregulation in abalone (Rosenblum et al. 2005). Moreover, elevated opine levels also ensure that the intracellular osmotic pressure is maintained, via pH regulation (Harcet et al. 2013). A combination of trimethylamine oxide, betaine and sarcosine was also reported to contribute to intracellular osmolarity in marine invertebrates (Wilbur and Hochachka 2016). Considering this, the elevated levels of the aforementioned osmolytes in *H. midae* following hypoxic exposure, are most likely produced for the purpose to maintain intracellular osmolarity (in addition to energy production).

3.4 Lipid metabolism during environmental hypoxia

Very few lipid metabolites were altered after environmental hypoxia, suggesting that cellular energy production via lipid metabolism was limited. This was expected, since only a fraction of the fatty acids and sterols absorbed from the diet undergo de novo lipid synthesis in abalone (Venter et al. 2016b). The total lipid profiles (FAMEs analyses) did not show significant differences in the ratios of fatty acids within structural and store lipids after hypoxia; which can also be expected given the homogenous (pre-hypoxic) farming conditions during which lipid synthesis was most active. Moreover, the concentration of lipids (estimated from the FAMEs) were unchanged after hypoxia, which was rather surprising, but highly likely due to the relatively low lipid stores in abalone tissue previously reported (Vosloo and Vosloo 2010).

The types and amounts of free and bound fatty acids detected in the different tissues varied, similar to observations in *H. rubra* and *H. laevigata* (Grubert et al. 2004). Reduced concentrations of bound docosahexaenoate (22:6 n-3), eicosapentaenoate (20:5 n-3) and octadecatrienoate (18:3 n-6) were found in the left gill, right gill and adductor muscle, respectively (Table S.2). This suggests a higher fatty acid release rate (lipolysis) during hypoxia, specifically for the long chain fatty acids. On the other hand, the epipodial tissues contained higher amounts of bound docosahexaenoate and stearidonate (18:4 n-3) fatty acids, accompanied by lower levels of free palmitate, suggesting a lack of lipolysis activity. This contradicting finding was also seen in *H. fulgens*, where elevated concentrations of docosahexaenoate and eicosapentaenoate were detected in the muscle tissue following starvation stress (Durazo-Beltrán et al. 2004).

The fatty acylcarnitines in *H. midae* that were most affected included free carnitine, acetylcarnitine, butyrylcarnitine and palmitoylcarnitine, which were predominantly elevated (Table S.2). This can be explained by the inhibition of ß-oxidation [U], by the redox imbalance, resulting in elevated levels of fatty acids (such as palmitoleate) and their associated fatty acylcarnitines. Furthermore, it should be mentioned that carnitine conjugation of these accumulating fatty acids also plays a role in detoxification.

3.5 Interplay and cooperation of the different tissues

The largest metabolic effects were seen in the adductor muscle, followed by the epipodial tissue, then the left and right gill, the foot muscle and lastly, the hemolymph samples (Fig. 2). This diverse response to hypoxia can be attributed to the varying functionality and metabolism associated with the various organs from which the tissue was sampled. Additionally, much like higher organisms, we believe that metabolites are shuttled between various different organs (e.g. from hypoxic tissue to regions that have access to oxygen) where they can be more appropriately utilized. An example of this in higher-order animals is the lactate shuttle between fatigued muscles and liver.

The left gill of abalone is only used during hypoxic conditions to enhance surface area and oxygen uptake (Ragg and Taylor 2006). This is shown very aptly during this investigation, as comparison of the left gill of hypoxic animals to the inactive left gill in the control group resulted in numerous metabolic differences (not seen when the right gills were compared). With the accumulation of metabolites in the muscles during environmental hypoxia, it can be speculated that the left gill was recruited to assist with energy production and clearance of some accumulated metabolites. Since the gills are proximal to the immediate environment (and remaining oxygen) it can be reasoned that oxygen-dependent pathways are still partially functional. Thus the elevated metabolites detected in the gills may be a consequence of a combination of shuttled metabolites and their own metabolic shutdown. The idea that metabolites are shuttled to and from the gills are supported by the correlation of specific metabolites found in the gills (especially the left gill) and other tissues: for example, in the environmental hypoxic group, alanine levels in the left gill correlated with the levels in the hemolymph ($r = 0.82$), which was not the case in the control group. The same correlation was also found for lactate ($r = 0.80$) and several other accumulated metabolites.

Prior literature pertaining to the biochemistry and physiology of abalone epipodial tissue is rather scarce, but the results of this study showed that the epipodial tissue has similar metabolic profiles to the other muscles. It has been hypothesized that the epipodial tissue plays a role in oxygen uptake (Taylor and Ragg 2005). Hence, it might be possible that metabolites from the muscles are shuttled to the epipodial tissue during hypoxia, similar to the gills. Again this theory is supported by the correlation of metabolite levels between the tissues. Leucine and alanopine levels in the epipodial tissue and hemolymph correlated ($r = 0.83$ and 0.78 respectively) in the environmental hypoxic group while these metabolites did not correlate in the control group. Alanopine in the epipodial tissue also correlated moderately with that in the foot muscle ($r = 0.73$). Although it is possible that other factors contribute to this covariance, the involvement of metabolite shuttles cannot be dismissed. The aforementioned metabolic similarity of epipodial tissue to the muscle tissue also allows for an important opportunity for non-destructive sampling for health screening, without critical damage to the animal (Wasko et al. 2003; Slabbert and Roodt-Wilding 2006).

Of all the samples studied, the least number of significant differences were detected in the hemolymph during hypoxia. During extreme hypoxia, such as the environmental hypoxia, cellular metabolites may become depleted, resulting in reduced metabolite concentrations in the systemic fluid. Additionally, reduced pH and/or increased free ammonia could also influence metabolite channels and pumps. Considering this, the role of hemolymph as a sample for analyzing metabolic end-products, like ammonia for instance, becomes apparent. Metabolic end products produced during hypoxic conditions may be released into the hemolymph and absorbed by other tissues (organs) which are able to oxidize these products (metabolic shuttle), e.g. the metabolic profiles detected in the hepatopancreas (which receives large hemolymph volumes) of *H. fulgens* confirms the transport function of hemolymph (Tripp-Valdez et al. 2017). This was also the case according to the correlation analysis we performed. As in the previous sections, the concentrations of many compounds in the different tissues correlate with the hemolymph concentrations which highlight its transport/shuttle function that links the different tissues. Consequently, hemolymph represents the exo-metabolome since it contains metabolite information of how the intracellular metabolic network influences its external environment (by the uptake of extracellular metabolites and secretion of intracellular metabolites) (Dunn 2008). One of the end products of anaerobic respiration is lactate, which is known to cause a drop in extracellular and intracellular pH, resulting in a disturbed acid–base balance during hypoxia. It has been suggested that abalone hemolymph has very limited pH buffering capacity, and is consequently prone to metabolic acidosis during hypoxia (Morash and Alter 2016). However, it is important to note that hemocyanin of gastropod hemolymph displays a reverse Bohr Effect, where oxygen binds tighter at a low pH or higher carbon dioxide (CO_2) partial pressure. This enables abalone to maintain oxygen saturation when clamping to surfaces during hypoxic conditions (Wells et al. 1998).

4 Conclusions

This is the first study to comprehensively describe the metabolic response of *H. midae* exposed to environmental hypoxia, using six complementary analytical platforms. The results demonstrate that environmental hypoxia created a metabolic imbalance in *H. midae*, with compromised energy

levels, skewed NADH:NAD^+ ratio and the accumulation of metabolites and toxic end products, such as ammonia. In response to the imbalances, the metabolism shifted to more catabolic processes in order to correct the energy and redox imbalances. Due to the large amounts of arginine detected, it can be deducted that these animals have large phosphoarginine pools able to regenerate ATP at the onset of hypoxia. Thereafter, energy production continued via anaerobic metabolic pathways associated with the breakdown of glycogen, proteins and lipids. For efficient anaerobic metabolism and energy production, recovery of NAD^+ is crucial, which is predominantly achieved by the conversion of pyruvate to lactate, the conversion of pyruvate to opines, and the conversion of glucose and aspartate to succinate. It is apparent from the results that different tissues undergo different metabolic changes during hypoxia, which is likely linked to their metabolic activity (as seen with comparison to the left and right gills) and their proximity to the environment. We hypothesize that accumulated muscle metabolites are shuttled (via hemolymph) to the gills and epipodial tissue where available oxygen allows further breakdown of the metabolites or excretion into the environment. With these findings, it is now possible to predict metabolic responses in hypoxic conditions and intervene accordingly, by recovery diets or supplements.

Acknowledgements We gratefully acknowledge the North-West University and the Technology Innovation Agency of the Department of Science and Technology of South Africa for financial support. We also thank HIK Abalone Farm (Pty) Ltd, South Africa for supplying experimental animals and welcoming us to your farm.

Compliance with Ethical Standards

Conflict of interest All authors declare that they have no conflict of interest.

Ethical approval All of the research pertaining to the perturbations and abalone collection was done in accordance with institutional guidelines of the relevant institutional committees and granted Aquaculture Research Permit.

References

Badenhorst, C. P. S., Erasmus, E., Van der Sluis, R., Nortje, C., & Van Dijk, A. A. (2014). A new perspective on the importance of glycine conjugation in the metabolism of aromatic acids. *Drug Metabolism Reviews, 46*(3), 343–361.

Barkai, R., & Griffiths, C. (1988). An energy budget for the South African abalone *Haliotis midae* Linnaeus. *Journal of Molluscan Studies, 54*(1), 43–51.

Boardman, L., Sørensen, J. G., Koštál, V., Šimek, P., & Terblanche, J. S. (2016). Chilling slows anaerobic metabolism to improve anoxia tolerance of insects. *Metabolomics, 12*(12), 176.

Britz, P., & Venter, S. (2016). Aquaculture review: South Africa. *World Aquaculture*, *47*(4), 19–28.

Carroll, J. L., & Wells, R. M. (1995). Strategies of anaerobiosis in New Zealand infaunal bivalves: Adaptations to environmental and functional hypoxia. *New Zealand Journal of Marine and Freshwater Research, 29*(2), 137–146.

Cook, P. A. (2014). The worldwide abalone industry. *Modern Economy, 5*(13), 1181–1186.

Dona, A. C., Jiménez, B., Schäfer, H., Humpfer, E., Spraul, M., Lewis, M. R., et al. (2014). Precision high-throughput proton NMR spectroscopy of human urine, serum, and plasma for large-scale metabolic phenotyping. *Analytical Chemistry, 86*(19), 9887–9894.

Dunn, W. B. (2008). Current trends and future requirements for the mass spectrometric investigation of microbial, mammalian and plant metabolomes. *Physical Biology, 5*(1), 011001.

Dunphy, B. J., Watts, E., & Ragg, N. L. (2015). Identifying thermally-stressed adult green-lipped mussels (*Perna canaliculus* Gmelin, 1791) via metabolomic profiling. *American Malacological Bulletin, 33*(1), 127–135.

Durazo-Beltrán, E., Viana, M. A. T., D'Abramo, L. R., & Toro-Vazquez, J. F. (2004). Effects of starvation and dietary lipid on the lipid and fatty acid composition of muscle tissue of juvenile green abalone (*Haliotis fulgens*). *Aquaculture, 238*(1), 329–341.

Ellis, S., & Steyn, H. (2003). Practical significance (effect sizes) versus or in combination with statistical significance (*p* values): Research note. *Management Dynamics: Journal of the Southern African Institute for Management Scientists, 12*(4), 51–53.

Feala, J. D., Coquin, L., Zhou, D., Haddad, G. G., Paternostro, G., & McCulloch, A. D. (2009). Metabolism as means for hypoxia adaptation: Metabolic profiling and flux balance analysis. *BMC Systems Biology, 3*(1), 91.

Fields, J. H. (1983). Alternatives to lactic acid: Possible advantages. *Journal of Experimental Zoology Part A: Ecological Genetics and Physiology, 228*(3), 445–457.

Fields, J. H., & Storey, K. B. (1987). Tissue-specific alanopine dehydrogenase from the gill and strombine dehydrogenase from the foot muscle of the cherrystone clam *Mercenaria mercenaria* (Linn.). *Journal of Experimental Marine Biology and Ecology, 105*(2–3), 175–185.

Fujimori, T., & Abe, H. (2002). Physiological roles of free D-and L-alanine in the crayfish *Procambarus clarkii* with special reference to osmotic and anoxic stress responses. *Comparative Biochemistry and Physiology Part A: Molecular & Integrative Physiology, 131*(4), 893–900.

Gäde, G. (1988). Energy metabolism during anoxia and recovery in shell adductor and foot muscle of the gastropod mollusc *Haliotis lamellosa*: Formation of the novel anaerobic end product tauropine. *The Biological Bulletin, 175*(1), 122–131.

Gäde, G., Carlsson, K.-H., & Meinardus, G. (1984). Energy metabolism in the foot of the marine gastropod *Nassa mutabilis* during environmental and functional anaerobiosis. *Marine Biology, 80*(1), 49–56.

Gäde, G., & Grieshaber, M. K. (1986). Pyruvate reductases catalyze the formation of lactate and opines in anaerobic invertebrates. *Comparative Biochemistry and Physiology Part B: Comparative Biochemistry, 83*(2), 255–272.

Garrett, R., & Grisham, C. (2010). Biochemistry, Brooks. (4th ed., pp. 511–812). Belmont, CA: Brooks Cole, Cengage Learning.

Green, S. R., & Storey, K. B. (2016). Regulation of crayfish, *Orconectes virilis*, tail muscle lactate dehydrogenase (LDH) in response to anoxic conditions is associated with alterations in phosphorylation patterns. *Comparative Biochemistry and Physiology Part B: Biochemistry and Molecular Biology, 202*, 67–74.

Grieshaber, M., Hardewig, I., Kreutzer, U., & Pörtner, H.-O. (1993). Physiological and metabolic responses to hypoxia in invertebrates. In *Reviews of physiology, biochemistry and pharmacology* (Vol. 125, pp. 43–147). Berlin: Springer.

Grubert, M. A., Dunstan, G. A., & Ritar, A. J. (2004). Lipid and fatty acid composition of pre-and post-spawning blacklip (*Haliotis rubra*) and greenlip *(Haliotis laevigata*) abalone conditioned at two temperatures on a formulated feed. *Aquaculture, 242*(1), 297–311.

Harcet, M., Perina, D., & Pleše, B. (2013). Opine dehydrogenases in marine invertebrates. *Biochemical Genetics, 51*(9–10), 666–676.

Harris, J. O., Maguire, G. B., Edwards, S., & Hindrum, S. M. (1998). Effect of ammonia on the growth rate and oxygen consumption of juvenile greenlip abalone, *Haliotis laevigata* Donovan. *Aquaculture, 160*(3), 259–272.

Hayat, S., Hayat, Q., Alyemeni, M. N., Wani, A. S., Pichtel, J., & Ahmad, A. (2012). Role of proline under changing environments: A review. *Plant Signaling & Behavior, 7*(11), 1456–1466.

Hochachka, P. W., Fields, J., & Mustafa, T. (1973). Animal life without oxygen: Basic biochemical mechanisms. *American Zoologist, 13*(2), 543–555.

Hooper, C., Day, R., Slocombe, R., Benkendorff, K., & Handlinger, J. (2014). Histopathology and haemolymph biochemistry following anaesthesia and movement in farmed Australian abalone (*Haliotis rubra* × *Haliotis laevigata*). *Aquaculture, 422*, 202–210.

Irwin, C., van Reenen, M., Mason, S., Mienie, L. J., Westerhuis, J. A., & Reinecke, C. J. (2016). Contribution towards a metabolite profile of the detoxification of benzoic acid through glycine conjugation: An intervention study. *PLoS ONE*, 11(12), e0167309.

Kreutzer, U., Siegmund, B. R., & Grieshaber, M. K. (1989). Parameters controlling opine formation during muscular activity and environmental hypoxia. *Journal of Comparative Physiology B: Biochemical, Systemic, and Environmental Physiology, 159*(5), 617–628.

Li, P., Mai, K., Trushenski, J., & Wu, G. (2009). New developments in fish amino acid nutrition: Towards functional and environmentally oriented aquafeeds. *Amino Acids, 37*(1), 43–53.

Lindeque, J. Z., Hidalgo, J., Louw, R., & van der Westhuizen, F. H. (2013). Systemic and organ specific metabolic variation in metallothionein knockout mice challenged with swimming exercise. *Metabolomics, 9*(2), 418–432.

Lindeque, J. Z., van Rensburg, P. J. J., Louw, R., van der Westhuizen, F. H., Florit, S., Ramírez, L., et al. (2015). Obesity and metabolomics: Metallothioneins protect against high-fat diet-induced consequences in metallothionein knockout mice. *Omics: A Journal of Integrative Biology, 19*(2), 92–103.

Liu, C., Shin, P., & Cheung, S. (2014). Comparisons of the metabolic responses of two subtidal nassariid gastropods to hypoxia and reoxygenation. *Marine Pollution Bulletin, 82*(1), 109–116.

Loots, D. T., Erasmus, E., & Mienie, L. J. (2005). Identification of 19 new metabolites induced by ab normal amino acid conjugation in isovaleric acidemia. *Clinical Chemistry, 51*(8), 1510–1512.

Lu, J., Feng, J., Cai, S., & Chen, Z. (2017). Metabolomic responses of *Haliotis diversicolor* to organotin compounds. *Chemosphere, 168*, 860–869.

Lu, J., Shi, Y., Wang, S., Chen, H., Cai, S., & Feng, J. (2016). NMR-based metabolomic analysis of *Haliotis diversicolor* exposed to thermal and hypoxic stresses. *Science of The Total Environment, 545*, 280–288.

Mason, S., van Furth, A. M., Mienie, L. J., Engelke, U. F., Wevers, R. A., Solomons, R., et al. (2015). A hypothetical astrocyte–microglia lactate shuttle derived from a 1H NMR metabolomics analysis of cerebrospinal fluid from a cohort of South African children with tuberculous meningitis. *Metabolomics, 11*(4), 822–837.

Morash, A. J., & Alter, K. (2016). Effects of environmental and farm stress on abalone physiology: Perspectives for abalone aquaculture in the face of global climate change. *Reviews in Aquaculture, 8*(4), 342–368.

Mouton, A. (2017). Red tide devastates South African abalone farms. *Aquaculture Magazine, 31*, 32–35.

Müller, M., Mentel, M., van Hellemond, J. J., Henze, K., Woehle, C., Gould, S. B., et al. (2012). Biochemistry and evolution of anaerobic energy metabolism in eukaryotes. *Microbiology and Molecular Biology Reviews, 76*(2), 444–495.

Nollens, H. H., Keogh, J. A., & Probert, P. K. (2004). Haematological pathology of shell lesions in the New Zealand abalone, *Haliotis iris* (Mollusca: Gastropoda). *Comparative Clinical Pathology, 12*(4), 211–216.

O'omolo, S., Gäde, G., Cook, P., & Brown, A. (2003). Can the end products of anaerobic metabolism, tauropine and D-lactate, be used as metabolic stress indicators during transport of live South African abalone *Haliotis midae*. *African Journal of Marine Science, 25*(1), 301–309.

Pitcher, G., & Calder, D. (2000). Harmful algal blooms of the southern Benguela current: A review and appraisal of monitoring from 1989 to 1997. *African Journal of Marine Science, 22*, 255–271.

Prathomya, P., Prisingkorn, W., Jakovlić, I., Deng, F.-Y., Zhao, Y.-H., & Wang, W.-M. (2017). 1H NMR-based metabolomics approach reveals metabolic alterations in response to dietary imbalances in *Megalobrama amblycephala*. *Metabolomics, 13*(2), 17.

Ragg, N. L., & Taylor, H. H. (2006). Heterogeneous perfusion of the paired gills of the abalone *Haliotis iris* Martyn 1784: An unusual mechanism for respiratory control. *Journal of Experimental Biology, 209*(3), 475–483.

Rosenblum, E., Viant, M., Braid, B., Moore, J., Friedman, C., & Tjeerdema, R. (2005). Characterizing the metabolic actions of natural stresses in the California red abalone, *Haliotis rufescens* using 1H NMR metabolomics. *Metabolomics, 1*(2), 199–209.

Roznere, I., Watters, G. T., Wolfe, B. A., & Daly, M. (2014). Non-targeted metabolomics reveals biochemical pathways altered in response to captivity and food limitation in the freshwater mussel *Amblema plicata*. *Comparative Biochemistry and Physiology Part D: Genomics and Proteomics, 12*, 53–60.

Salway, J. G. (2004). *Metabolism at a glance*. Guildford: Wiley.

Sato, M., Takeuchi, M., Kanno, N., Nagahisa, E., & Sato, Y. (1993). Distribution of opine dehydrogenases and lactate dehydrogenase activities in marine animals. *Comparative Biochemistry and Physiology Part B: Comparative Biochemistry, 106*(4), 955–960.

Schmidt-Nielsen, K. (2007). *Animal physiology: Adaptation and environment*. New York: Cambridge University Press.

Schymanski, E. L., Jeon, J., Gulde, R., Fenner, K., Ruff, M., Singer, H. P., et al. (2014). Identifying small molecules via high resolution mass spectrometry: Communicating confidence. *Environmental Science and Technology, 48*(4), 2097–2098.

Shen, Y., Hixson, K. K., Tolic, N., Camp, D. G., Purvine, S. O., Moore, R. J., et al. (2008). Mass spectrometry analysis of proteome-wide proteolytic post-translational degradation of proteins. *Analytical Chemistry, 80*(15), 5819–5828.

Slabbert, R., & Roodt-Wilding, R. (2006). Non-destructive sampling of juvenile abalone using epipodial tentacles and mucus: Method and application. *African Journal of Marine Science, 28*(3–4), 719–721.

Sokolova, I. M., Frederich, M., Bagwe, R., Lannig, G., & Sukhotin, A. A. (2012). Energy homeostasis as an integrative tool for assessing limits of environmental stress tolerance in aquatic invertebrates. *Marine Environmental Research, 79*, 1–15.

Storey, K. B. (2004). Adventures in oxygen metabolism. *Comparative Biochemistry and Physiology Part B: Biochemistry and Molecular Biology, 139*(3), 359–369.

Storey, K. B. (2005). *Functional metabolism: Regulation and adaptation*. Hoboeken: Wiley.

Sumner, L. W., Amberg, A., Barrett, D., Beale, M. H., Beger, R., Daykin, C. A., et al. (2007). Proposed minimum reporting standards for chemical analysis. *Metabolomics, 3*(3), 211–221.

Taylor, H., & Ragg, N. (2005). The role of body surfaces and ventilation in gas exchange of the abalone, *Haliotis iris. Journal of Comparative Physiology B, 175*(7), 463–478.

Tripp-Valdez, M. A., Bock, C., Lucassen, M., Lluch-Cota, S. E., Sicard, M. T., Lannig, G., et al. (2017). Metabolic response and thermal tolerance of green abalone juveniles (*Haliotis fulgens*: Gastropoda) under acute hypoxia and hypercapnia. *Journal of Experimental Marine Biology and Ecology, 497*, 11–18.

Venter, L., van Rensburg, P. J. J., Loots, D. T., Vosloo, A., & Lindeque, J. Z. (2016a). Untargeted metabolite profiling of abalone using gas chromatography mass spectrometry. *Food Analytical Methods, 9*(5), 1254–1261.

Venter, L., Lindeque, Z., van Rensburg, P. J. J., Van der Westhuizen, F., Smuts, I., & Louw, R. (2015). Untargeted urine metabolomics reveals a biosignature for muscle respiratory chain deficiencies. *Metabolomics, 11*(1), 111–121.

Venter, L., Loots, D. T., Vosloo, A., Jansen van Rensburg, P., & Lindeque, J. Z. (2016b). Abalone growth and associated aspects: Now from a metabolic perspective. *Reviews in Aquaculture, 2*, 2016.

Venter, L., van Rensburg, P. J. J. , Loots, D. T., Vosloo, A., & Lindeque, J. Z. (2017). From untargeted LC–QTOF analysis to characterisation of opines in abalone adductor muscle: Theory meets practice. *Journal of Chromatography B, 1071*, 44–48.

Vosloo, D., van Rensburg, L., & Vosloo, A. (2013). Oxidative stress in abalone: The role of temperature, oxygen and L-proline supplementation. *Aquaculture, 416*, 265–271.

Vosloo, D., & Vosloo, A. (2010). Response of cold-acclimated, farmed South African abalone (*Haliotis midae*) to short-term and long-term changes in temperature. *Journal of Thermal Biology, 35*(7), 317–323.

Warrack, B. M., Hnatyshyn, S., Ott, K.-H., Reily, M. D., Sanders, M., Zhang, H., et al. (2009). Normalization strategies for metabonomic analysis of urine samples. *Journal of Chromatography B, 877*(5), 547–552.

Wasko, A. P., Martins, C., Oliveira, C., & Foresti, F. (2003). Non-destructive genetic sampling in fish. An improved method for DNA extraction from fish fins and scales. *Hereditas, 138*(3), 161–165.

Wells, R. M., Baldwin, J., Speed, S. R., & Weber, R. E. (1998). Haemocyanin function in the New Zealand abalones *Haliotis iris* and *H. australis*: Relationships between oxygen-binding properties, muscle metabolism and habitat. *Marine and Freshwater Research, 49*(2), 143–149.

Whitney, E., & Rolfes, S. R. (2008). *Understanding nutrition*. Belmont: Cengage Learning.

Wilbur, K. M., & Hochachka, P. W. (2016). *The Mollusca: Environmental biochemistry and physiology* (Vol. 2). New York: Academic Press.

Willers, C., van Rensburg, P. J. J., & Claassens, S. (2016). Can a metabolomics-based approach be used as alternative to analyse fatty acid methyl esters from soil microbial communities? *Soil Biology and Biochemistry, 103*, 417–428.

Wishart, D. S., Jewison, T., Guo, A. C., Wilson, M., Knox, C., Liu, Y., et al. (2012). HMDB 3.0—the human metabolome database in 2013. *Nucleic Acids Research, 41*(D1), D801–D807.

Xia, J., Sinelnikov, I. V., Han, B., & Wishart, D. S. (2015). MetaboAnalyst 3.0—making metabolomics more meaningful. *Nucleic Acids Research, 43*(W1), 251–257.

© 2018. Published by The Company of Biologists Ltd | Biology Open (2018) 7, bio031070. doi:10.1242/bio.031070

RESEARCH ARTICLE

The cross-tissue metabolic response of abalone (*Haliotis midae*) to functional hypoxia

Leonie Venter[1], Du Toit Loots[1], Lodewyk J. Mienie[1], Peet J. Jansen van Rensburg[1], Shayne Mason[1], Andre Vosloo[2] and Jeremie Z. Lindeque[1,*]

ABSTRACT

Functional hypoxia is a stress condition caused by the abalone itself as a result of increased muscle activity, which generally necessitates the employment of anaerobic metabolism if the activity is sustained for prolonged periods. With that being said, abalone are highly reliant on anaerobic metabolism to provide partial compensation for energy production during oxygen-deprived episodes. However, current knowledge on the holistic metabolic response for energy metabolism during functional hypoxia, and the contribution of different metabolic pathways and various abalone tissues towards the overall accumulation of anaerobic end-products in abalone are scarce. Metabolomics analysis of adductor muscle, foot muscle, left gill, right gill, haemolymph and epipodial tissue samples indicated that South African abalone (*Haliotis midae)* subjected to functional hypoxia utilises predominantly anaerobic metabolism, and depends on all of the main metabolite classes (proteins, carbohydrates and lipids) for energy supply. Functional hypoxia caused increased levels of anaerobic end-products: lactate, alanopine, tauropine, succinate and alanine. Also, elevation in arginine levels was detected, confirming that abalone use phosphoarginine to generate energy during functional hypoxia. Different tissues showed varied metabolic responses to hypoxia, with functional hypoxia showing excessive changes in the adductor muscle and gills. From this metabolomics investigation, it becomes evident that abalone are metabolically able to produce sufficient amounts of energy when functional hypoxia is experienced. Also, tissue interplay enables the adjustment of *H. midae* energy requirements as their metabolism shifts from aerobic to anaerobic respiration during functional hypoxia.

This article has an associated First Person interview with the first author of the paper.

KEY WORDS: Abalone, Functional hypoxia, Metabolism, Metabolomics

INTRODUCTION

Muscle performance is essential to the lifestyle of animals (Pörtner, 2002). Typically, intense bouts of muscle activity deplete cellular energetic reserves, resulting in increased oxygen demand beyond the rate of uptake (Morash and Alter, 2016), which limits adenosine triphosphate (ATP) production via muscle oxidative metabolism (Storey, 2005). During such burst contractile muscle activity, organisms are generally fuelled by anaerobic metabolism where ATP production is made possible from substrate-level phosphorylation via the breakdown of phosphagens, but also due to glycolytic degradation of, predominantly, carbohydrates (Baldwin and England, 1982; Ellington, 1983). While lipids and proteins are more ideally used for structural elements of cells, they can also assist with ATP supply to working tissues (Venter et al., 2016b). The ability of organisms to use alternative metabolic ways to meet metabolic demand when aerobic respiration is compromised, ensure survival until recovery from the anaerobic episode is possible, whereafter normal aerobic respiration can continue (Fields, 1983).

Abalone, single-shelled marine molluscs, are highly dependent on anaerobic metabolism during episodes of unfavourable oxidation (Morash and Alter, 2016), like functional hypoxia. Functional hypoxia occurs when the internal oxygen pressure in an organism falls due to intensive muscular activity (Liu et al., 2014). In natural environments this type of muscle activity is likely to occur when animals are trying to escape from predators, or are in the pursuit of prey. In such scenarios, the rate of ATP use by muscles is too high to be met by aerobic respiration, forcing the organism to rapidly switch to anaerobic respiration for ATP production in contracting muscles (Müller et al., 2012). In a typical abalone farming environment, extreme functional hypoxia scenarios are less common but can be induced when abalone climb and crawl for feeding purposes; or as a result of shell adhesion or righting after being dislodged (Morash and Alter, 2016). Increased single end-point metabolites of functional hypoxia in abalone are well known and attest to the fact that abalone breakdown phosphagens (like phosphoarginine) and utilise anaerobic glycolysis for energy production (Gäde and Grieshaber, 1986; O'omolo et al., 2003). However, current knowledge on the holistic metabolic response for energy metabolism during functional hypoxia, and the contribution of different metabolic pathways towards the overall accumulation of anaerobic end-products in abalone are far from clear. Furthermore, the organismal response associated with functional hypoxia has not been investigated in different abalone tissues, allowing for more uncertainty of how various tissues work together to ensure energy production and/or survival of abalone.

To this end, knowledge of the basic biochemical constituents of abalone under culture conditions would be a very useful tool in their management in aquaculture systems (Laas and Vosloo, 2010). Considering that *Haliotis midae* is an important aquaculture species in South Africa and the largest generator of revenue for the mariculture sector (Dale-Kuys et al., 2017), insights into the metabolic alterations to external stressors are crucial for optimising farming strategies. With this being said, metabolomics research in

[1]Human Metabolomics, North-West University, Potchefstroom Campus, Private Bag X6001, Potchefstroom 2520, South Africa. [2]School of Life Sciences, University of KwaZulu-Natal, Westville Campus, Private Bag X54001, Durban 4000, South Africa.

*Author for correspondence (Zander.Lindeque@nwu.ac.za)

J.Z.L., 0000-0001-8017-4278

Received 6 November 2017; Accepted 27 February 2018

Biology Open (2018) 7, bio031070. doi:10.1242/bio.031070

aquaculture is proving extremely valuable for generating novel information into the mechanisms implemented by aquatic organisms (Young et al., 2017). Metabolomics can be defined as the nonbiased identification and quantification of metabolites in a biological system, using highly selective and sensitive analytical techniques (Dunn et al., 2005). Metabolites, or small molecules within a cell, tissue, organ, biological fluid or the entire organism, constitute the metabolome (Lankadurai et al., 2013), and are likely to contribute to the functional state of cells and serve as a direct signature of biochemical activity (Patti et al., 2012). Considering this, using such an approach for investigating abalones response to hypoxia might result in a better understanding of the biochemical responses and altered metabolites induced by hypoxia.

The aim of this study was to use a multiplatform metabolomics approach, utilising untargeted nuclear magnetic resonance (NMR) spectroscopy, untargeted gas chromatography-time of flight spectrometry (GC-TOF), semi-targeted liquid chromatography-quadrupole time of flight mass spectrometry (LC-QTOF) analyses of butylated esters, semi-targeted gas chromatography-mass spectrometry-detector (GC-MSD) analyses of fatty acid methyl esters (FAMEs) and targeted liquid chromatography-tandem mass spectrometry (LC-MS/MS), to generate a holistic view of the metabolic pathways affected by functional hypoxia, in order to characterise the bioenergetics of abalone metabolism, and to evaluate the interplay of various hypoxic tissues (adductor muscle, foot muscle, epipodial tissue, haemolymph, left gill and right gill) in *H. midae*.

RESULTS

Heatmap visualisation of data

The metabolites that differed significantly between the control and functional hypoxia group ($P<0.05$ and $d>0.8$) are shown in the heatmap presented in Fig. 1. Each row represents the metabolite detected in adductor muscle (AM), foot muscle (FM), left gill (LG), right gill (RG), haemolymph (H) and epipodial tissue (E) samples, and each column represents the samples of control (C) and functional hypoxia (FH) groups, respectively.

Tissue-specific metabolite findings of *H. midae* subjected to functional hypoxia

Additionally the significant metabolites are listed in Table 1. Starting with the findings of the adductor muscle sample, information on the metabolite of interest in terms of P-value (classified only as $P<0.05$, $P<0.001$ or $P<0.0001$), d-value, an increase (↑) or decrease (↓) in relative intensity, the identification level (ID) assigned, the analytical platform on which the metabolite was detected and the metabolite class best describing the finding are shown. Next, information on the metabolites detected in the foot muscle, epipodial tissue, haemolymph, left gill and right gill samples can be found.

Metabolic map of *H. midae* metabolic response following functional hypoxia

Subsequently the data presented in Fig. 1 and Table 1 were mapped on a metabolic chart as depicted in Fig. 2. Metabolites affected by hypoxia are indicated as elevated (blue) or decreased (red) metabolite abundance when directly compared to the findings of the control group. Findings are represented by the tissue [adductor muscle (AM), foot muscle (FM), left gill (LG), right gill (RG), haemolymph (H) and epipodial tissue (E)] in which the finding was made when viewing the key next to the metabolite. Manual pathway analysis was done by focussing on those pathways that showed significant change during hypoxia. A pathway was considered important when most of the metabolites in the pathway were affected, and/or when the shared metabolites in the pathway (i.e. metabolites connected with other pathways) were also considerably altered. The pathways affected by functional hypoxia (Fig. 2) included: (A) sugar metabolism (glycolysis); (B) oxaloacetate-succinate pathway; (C) threonine-serine-glycine metabolism; (D) sulphur-containing amino acid metabolism; (E) cysteine-taurine-cysteine metabolism; (F) pyruvate-lactate/alanine pathway; (G) aspartate-succinate pathway; (H) pyruvate-opine pathway; (I) lysine-tryptophan metabolism; (J) glutaryl-CoA pathway; (K) branched chain amino acid metabolism; (L) ketone body metabolism; (M) propionyl-CoA pathway; (N) tricarboxylic acid (TCA) cycle; (O) alternative aspartate pathway; (P) purine and pyrimidine metabolism; (Q) urea cycle; (R) proline metabolism; (S) electron transport chain (ETC); (T) phenylalanine-tyrosine metabolism; (U) beta(β)-oxidation; (V) fatty acid transport pathway; and (W) fatty acid synthesis.

DISCUSSION

An average of 2036 features was reliably detected for each tissue (after data clean-up). From this, the metabolites that differed markedly between the groups were identified (Table 1) and visualised (Fig. 1).

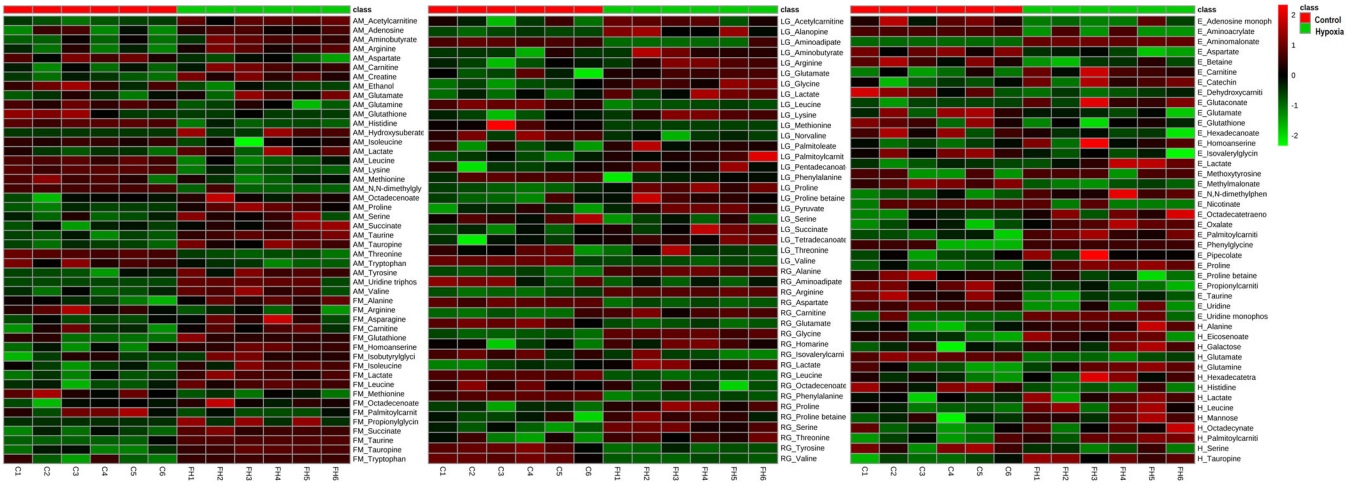

Fig. 1. Heatmap visualisation of metabolomics data generated from *H. midae* following functional hypoxia. Each row represents a significant ($P<0.05$) metabolite detected in abalone adductor muscle (AM), foot muscle (FM), left gill (LG), right gill (RG), haemolymph (H) and epipodial tissue (E) samples, and each column represents the samples of control (C) and functional hypoxia (FH) groups, respectively.

Biology Open (2018) 7, bio031070. doi:10.1242/bio.031070

Table 1. Tissue-specific metabolite findings of *H. midae* subjected to functional hypoxia

Compound	*P*-value	*d*-value	↑/↓	ID	Platform	Group	Compound	*P*-value	*d*-value	↑/↓	ID	Platform	Group
Adductor muscle													
Threonine	<0.001	9.06	↓	1	LC-MS/MS	AA	Butyrylcarnitine	<0.01	2.15	↑	3	LC-QTOF	FA
Lysine	<0.001	5.87	↓	1	LC-MS/MS	AA	Valine	<0.01	1.65	↑	1	LC-MS/MS	AA
Isoleucine	<0.001	5.45	↓	1	LC-MS/MS	AA	Succinate	<0.01	1.69	↑	1	GC-TOF	CHO
Taurine	<0.001	4.74	↑	1	LC-MS/MS	AA	Ethanol	<0.01	1.76	↓	1	NMR	O
Acetylcarnitine	<0.001	3.88	↑	1	LC-MS/MS	FA	Hydroxysuberate	<0.05	1.26	↑	3	LC-QTOF	CHO
Creatine	<0.001	3.38	↑	1	LC-MS/MS	CHO	Uridine triphosphate	<0.05	1.11	↑	3	LC-QTOF	O
Tauropine	<0.001	2.80	↑	1	LC-MS/MS	AA	Serine	<0.05	1.26	↑	1	LC-MS/MS	AA
Proline	<0.001	2.78	↑	1	LC-MS/MS	AA	Lactate	<0.05	1.23	↑	1	GC-TOF	CHO
N,N-dimethylglycine	<0.001	2.53	↓	1	LC-MS/MS	AA	Aminobutyrate	<0.05	1.20	↑	1	GC-TOF	O
Tryptophan	<0.001	2.84	↓	1	LC-MS/MS	AA	Adenosine	<0.05	0.99	↑	3	LC-QTOF	O
Tyrosine	<0.001	2.65	↑	1	LC-MS/MS	AA	Glutathione	<0.05	0.96	↓	3	LC-QTOF	CHO
Aspartate	<0.001	2.34	↓	1	LC-MS/MS	AA	Octadecenoate	<0.05	1.29	↑	1	GC-MSD	FA
Carnitine	<0.01	2.33	↑	1	LC-MS/MS	FA	Methionine	<0.05	1.14	↓	3	LC-QTOF	AA
Arginine	<0.01	1.96	↑	1	LC-MS/MS	AA	Leucine	<0.05	0.85	↓	1	LC-MS/MS	AA
Histidine	<0.01	2.03	↓	1	LC-MS/MS	AA	Glutamate	<0.05	1.07	↑	1	LC-MS/MS	AA
Glutamine	<0.01	1.69	↓	1	LC-MS/MS	AA							
Foot muscle													
Tauropine	<0.001	2.99	↑	1	LC-MS/MS	AA	Alanine	<0.01	1.72	↑	1	LC-MS/MS	AA
Succinate	<0.001	3.20	↑	1	GC-TOF	CHO	Methionine	<0.01	1.87	↓	1	LC-MS/MS	AA
Leucine	<0.001	2.60	↑	1	LC-MS/MS	AA	Isobutyrylglycine	<0.01	1.89	↑	3	LC-QTOF	AA
Taurine	<0.001	2.10	↑	3	LC-QTOF	AA	Arginine	<0.05	1.82	↓	1	LC-MS/MS	AA
Propionylglycine	<0.001	1.98	↑	3	LC-QTOF	AA	Palmitoylcarnitine	<0.05	1.26	↓	1	LC-MS/MS	FA
Homoanserine	<0.001	1.99	↑	3	LC-QTOF	AA	Isoleucine	<0.05	2.03	↑	1	NMR	AA
Carnitine	<0.01	0.80	↑	1	LC-MS/MS	FA	Tryptophan	<0.05	0.80	↑	1	LC-MS/MS	AA
Lactate	<0.01	2.55	↑	1	NMR	CHO	Asparagine	<0.05	1.32	↑	1	LC-MS/MS	AA
Glutathione	<0.01	2.09	↑	3	LC-QTOF	CHO	Octadecenoate	<0.05	1.29	↑	1	GC-MSD	FA
Epipodial tissue													
Aminomalonate	<0.001	10.61	↑	3	LC-QTOF	CHO	Catechin	<0.01	1.51	↑	3	LC-QTOF	O
Proline	<0.001	3.19	↑	1	LC-MS/MS	AA	Oxalate	<0.01	1.99	↑	1	GC-TOF	CHO
Methylmalonate	<0.001	4.90	↓	1	NMR	CHO	Uridine	<0.01	1.03	↓	3	LC-QTOF	O
Homogentisate	<0.001	1.86	↑	3	LC-QTOF	O	Homoanserine	<0.01	1.22	↑	3	LC-QTOF	AA
Uridine monophosphate	<0.001	2.05	↑	3	LC-QTOF	CHO	Octadecatetraenoate	<0.01	1.41	↑	1	GC-MSD	FA
Palmitoylcarnitine	<0.001	2.73	↑	1	LC-MS/MS	FA	Glutamate	<0.05	1.32	↓	1	LC-MS/MS	AA
Glutaconate	<0.001	1.91	↑	3	LC-QTOF	O	Phenylglycine	<0.05	0.89	↑	3	LC-QTOF	AA
Proline betaine	<0.001	2.05	↓	3	LC-QTOF	AA	Nicotinate	<0.05	1.18	↓	3	LC-QTOF	O
Propionylcarnitine	<0.001	1.88	↓	3	LC-QTOF	FA	Betaine	<0.05	1.77	↓	1	NMR	AA
Aminoacrylate	<0.001	1.83	↓	3	LC-QTOF	O	Hexadecanoate	<0.05	1.44	↓	1	GC-MSD	FA
Aspartate	<0.001	2.23	↓	1	LC-MS/MS	AA	Pipecolate	<0.05	0.95	↑	3	LC-QTOF	O
Dehydroxycarnitine	<0.001	1.75	↓	3	LC-QTOF	FA	Rigin	<0.05	0.88	↓	3	LC-QTOF	O
Isovalerylglycine	<0.01	1.65	↓	3	LC-QTOF	AA	Lactate	<0.05	1.13	↑	1	GC-TOF	CHO
Taurine	<0.01	2.79	↓	1	NMR	AA	Glutathione	<0.05	1.17	↓	3	LC-QTOF	CHO
N,N-dimethylphenylalanine	<0.01	2.10	↑	1	GC-TOF	AA	Adenosine monophosphate	<0.05	1.57	↓	1	NMR	O
Carnitine	<0.01	2.07	↑	1	LC-MS/MS	FA	Methoxytyrosine	<0.05	1.05	↑	3	LC-QTOF	O
Haemolymph													
Glutamate	<0.001	7.28	↓	1	LC-MS/MS	AA	Serine	<0.05	1.14	↓	1	LC-MS/MS	AA
Tauropine	<0.001	1.80	↑	3	LC-QTOF	AA	Mannose	<0.05	1.20	↑	1	GC-TOF	CHO
Alanine	<0.01	1.91	↑	1	LC-MS/MS	AA	Octadecynoic acid	<0.05	0.89	↑	2	GC-MSD	FA
Histidine	<0.01	2.14	↓	1	LC-MS/MS	AA	Galactose	<0.05	1.22	↑	1	GC-TOF	CHO
Leucine	<0.01	1.39	↑	1	LC-MS/MS	AA	Lactate	<0.05	0.80	↑	1	GC-TOF	CHO
Palmitoylcarnitine	<0.05	1.46	↑	1	LC-MS/MS	FA	Eicosenoate	<0.05	0.98	↑	2	GC-MSD	FA
Glutamine	<0.05	1.40	↑	1	LC-MS/MS	AA	Hexadecatetraenoate	<0.05	0.81	↑	1	GC-MSD	FA
Left gill													
Leucine	<0.001	5.09	↓	1	LC-MS/MS	AA	Lactate	<0.05	1.33	↑	1	GC-TOF	CHO
Proline	<0.001	2.86	↑	1	LC-MS/MS	AA	Aminobutyrate	<0.05	1.56	↑	3	LC-QTOF	O
Glycine	<0.001	2.92	↑	1	LC-MS/MS	AA	Arginine	<0.05	1.68	↑	1	NMR	AA
Valine	<0.001	2.27	↓	1	LC-MS/MS	AA	Lysine	<0.05	1.68	↑	1	NMR	AA
Aminoadipate	<0.001	2.15	↓	3	LC-QTOF	CHO	Proline betaine	<0.05	1.50	↑	3	LC-QTOF	AA
Alanopine	<0.01	1.75	↑	1	LC-MS/MS	AA	Pyruvate	<0.05	1.29	↑	3	LC-QTOF	CHO
Palmitoylcarnitine	<0.01	1.62	↑	1	LC-MS/MS	FA	Succinate	<0.05	1.22	↑	1	GC-TOF	CHO
Serine	<0.01	1.89	↓	1	LC-MS/MS	AA	Threonine	<0.05	1.07	↓	3	LC-QTOF	AA
Norvaline	<0.01	1.83	↓	1	GC-TOF	AA	Glutamate	<0.05	0.99	↑	1	LC-MS/MS	AA
Tetradecanoate	<0.01	1.34	↑	2	GC-MSD	FA	Pentadecanoate	<0.05	1.10	↑	1	GC-MSD	FA
Phenylalanine	<0.01	1.41	↓	1	LC-MS/MS	AA	Palmitoleate	<0.05	1.16	↑	1	GC-MSD	FA
Methionine	<0.01	1.25	↓	3	LC-QTOF	AA	Acetylcarnitine	<0.05	1.15	↑	3	LC-MS/MS	FA
Right gill													
Leucine	<0.001	9.71	↓	1	LC-MS/MS	AA	Proline	<0.001	2.49	↑	1	LC-MS/MS	AA

Continued

Biology Open (2018) 7, bio031070. doi:10.1242/bio.031070

Table 1. Continued

Compound	*P*-value	*d*-value	↑/↓	ID	Platform	Group	Compound	*P*-value	*d*-value	↑/↓	ID	Platform	Group
Glycine	<0.001	8.55	↑	1	LC-MS/MS	AA	Carnitine	<0.01	2.26	↑	1	LC-MS/MS	FA
Aspartate	<0.001	10.06	↓	1	LC-MS/MS	AA	Lactate	<0.01	2.33	↑	1	GC-TOF	CHO
Arginine	<0.001	12.32	↑	1	LC-MS/MS	AA	Aminoadipate	<0.01	1.33	↓	3	LC-QTOF	O
Phenylalanine	<0.001	8.79	↓	1	LC-MS/MS	AA	Proline betaine	<0.05	1.32	↑	3	LC-QTOF	AA
Alanine	<0.001	7.57	↑	1	LC-MS/MS	AA	Isovalerylcarnitine	<0.05	1.21	↓	3	LC-QTOF	FA
Valine	<0.001	3.71	↓	1	LC-MS/MS	AA	Aminoacrylate	<0.05	1.13	↓	3	LC-QTOF	O
Glutamate	<0.001	3.49	↓	1	LC-MS/MS	AA	Octadecenoate	<0.05	1.09	↓	1	GC-MSD	FA
Tyrosine	<0.001	2.78	↓	1	LC-MS/MS	AA	Threonine	<0.05	1.14	↑	1	NMR	AA
Serine	<0.001	2.95	↑	1	LC-MS/MS	AA	Homarine	<0.05	1.20	↑	1	NMR	CHO

These findings were assessed in a holistic manner by using a metabolic map (Fig. 2) uniquely designed for abalone metabolism, highlighting the anaerobic energy producing systems and the contribution of various macromolecules (carbohydrates, proteins and lipids) as energy substrates for survival during hypoxia.

Substrate-level phosphorylation for ATP production during functional hypoxia

It is already well known that substrate-level phosphorylation serves as an alternative route for ATP production when mitochondrial respiratory activity becomes inadequate (Feala et al., 2009). Based on the findings of Table 1 (Fig. 1), this study confirms that *H. midae* utilise substrate-level phosphorylation in terms of phosphagen breakdown (Pathway Q) to ensure that energy is instantaneously available (Grieshaber et al., 1993) during the initial phase of functional hypoxia. The presence of creatine in the adductor muscle of the hypoxic abalone suggests that energy is maintained with phosphocreatine metabolism in addition of phosphoarginine, which is more commonly used in marine invertebrates. Based on Fig. 2 (Pathway Q), the contribution of phosphoarginine and phosphocreatine for the production of arginine and creatine during ATP replenishment in the adductor muscle is strongly suggested, considering the elevated levels of these metabolites detected during functional hypoxia.

When oxygen availability is compromised to the level where aerobic ATP production cannot meet the increased demand (fast enough), anaerobic glycolysis becomes the main way to rapidly produce ATP (Garrett and Grisham, 2010), as demonstrated by the elevated levels of lactate, several opines, succinate and alanine detected in selected tissues of *H. midae* (Table 1). Altogether Pathways B, F and H allowed for the regeneration of cytoplasmic nicotinamide adenine dinucleotide (NAD^+) for usage in the glyceraldehyde-3-phosphate dehydrogenase reaction of glycolysis (Fig. 2). Consequently NAD^+ feeds into the glycolytic pathway, and enables phosphoglycerate kinase and pyruvate kinase to synthesis ATP directly from the phosphorylation of adenosine diphosphate (ADP) (Garrett and Grisham, 2010). Abundant amounts of pyruvate is produced which is converted to lactate (and opines) while co-enzymes are released to allow glycolysis to continue (Whitney and Rolfes, 2008). This production of predominantly lactate during

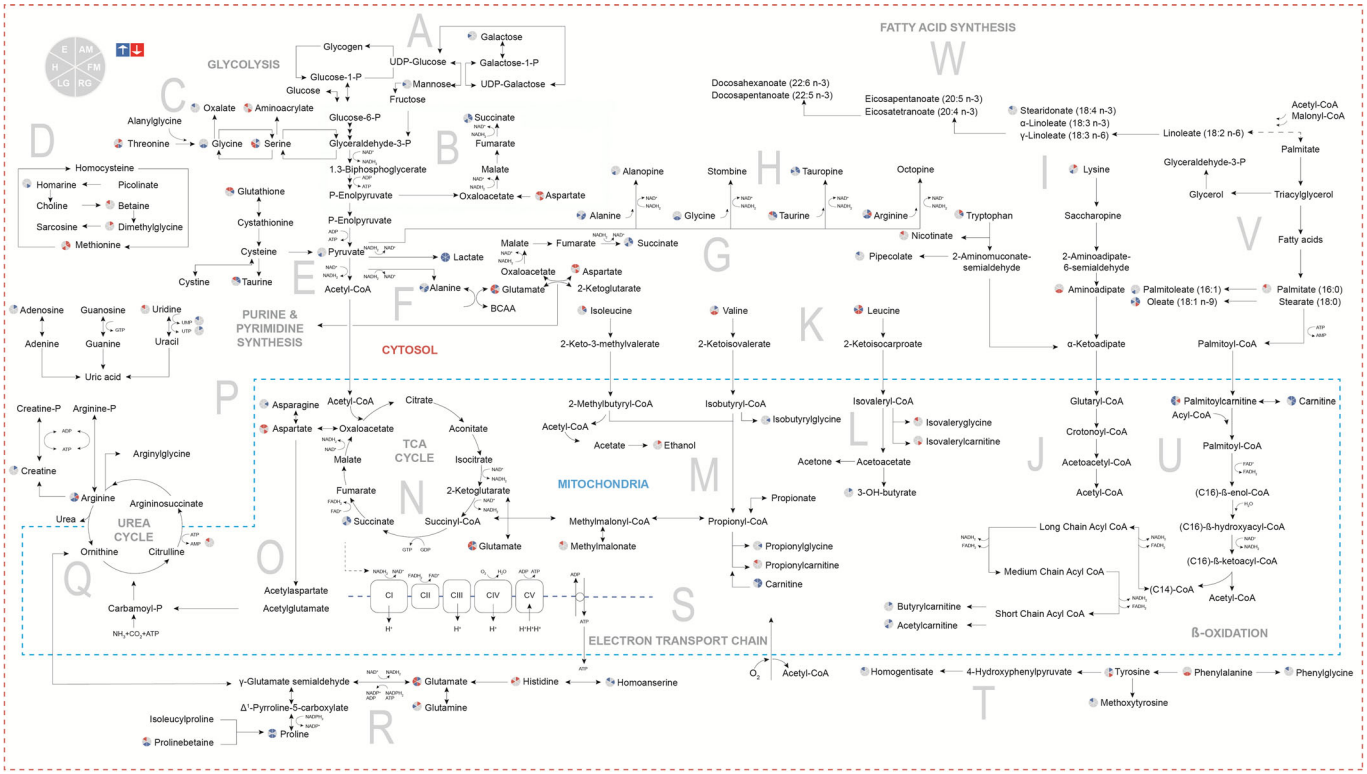

Fig. 2. Metabolic map of *H. midae* metabolic response following functional hypoxia. Elevated (blue) and decreased (red) metabolite findings in abalone adductor muscle (AM), foot muscle (FM), left gill (LG), right gill (RG), haemolymph (H) and epipodial tissue (E) following functional hypoxia.

Biology Open (2018) 7, bio031070. doi:10.1242/bio.031070

functional hypoxia is clearly demonstrated in Fig. 2, where lactate was found elevated in all of the tissues investigated (Pathway F). The most notable differences in lactate levels were found in the foot muscle, followed by the right gill, left gill, adductor muscle, epipodial tissue and lastly the haemolymph samples. Another class of end-products of anaerobic glycolysis, called opines, also contributed to the replenishment of NAD^+ levels during functional hypoxia. Tauropine was predominantly produced by *H. midae* following functional hypoxia (Pathway H), detected in highest levels in the foot muscle, adductor muscle and then haemolymph samples. Alanopine was also detected as elevated in the left gill sample (Table 1). Interestingly, no octopine (formed from the condensation of pyruvate and arginine) was detected in *H. midae* exposed to functional hypoxia (Pathway H), despite arginine availability in these tissues. This is most likely due to the low enzyme activity of octopine dehydrogenase in this species (O'omolo et al., 2003). These results might also indicate that functional hypoxia (Fig. 2) is not severe enough for *H. midae* to require octopine synthesis. It has previously been reported, that octopine formation only occurs during recovery from functional anaerobiosis in most *Pecten* species (Gäde et al., 1984). Following physical activity, octopine dehydrogenase was however detected in *H. kamtschatkana* (Donovan et al., 1999) and *H. midae* (O'omolo et al., 2003) without allowing some time for recovery. Contradictory to previous research reporting elevated concentrations of lactate and tauropine in both the adductor and foot muscles in the abalone *H. lamellosa* (Gäde, 1988), *H. discus hannai* (Sato et al., 1991), *H. iris* (Baldwin et al., 1992) and *H. midae* (O'omolo et al., 2003) after functional hypoxia, we indicate the highest levels of lactate and tauropine in the foot muscle samples analysed (Fig. 2). Previous reports speculate that the shell adductor muscle is the main source of tauropine production during exercise, as it enables the animal to re-attach itself after becoming dislodged. In *H. kamtschatkana*, in fact, a fivefold increase in the adductor muscle tauropine was reported, leading to the argument that anaerobic glycolysis supplies some of the much needed energy required in the adductor muscle, in contrast to that of the foot muscle, which primarily produces energy aerobically (Donovan et al., 1999). Seeing that lactate was elevated in all of the tissues investigated in our study, while tauropine was only elevated in half of the investigated tissues, following functional hypoxia (Table 1), it suggests a gradual and progressive requirement to correct the redox imbalance during prolonged exposure to hypoxia. As functional hypoxia persists, replenishment of NAD^+ via lactate alone becomes insufficient, leading to the synthesis of opines. Also the release of NAD^+ via the production of succinate (Pathway B) assists with substrate availability for ATP production during functional hypoxia. Increased adductor muscle and foot muscle succinate in *H. midae* corresponds to findings in *H. lamellose* where a synchronised depletion of aspartate accompanied by elevations in alanine and succinate in the foot and adductor muscles were reported in response to anoxia (Gäde, 1988).

Response of protein metabolism to functional hypoxia

Of all the detected compounds classes, proteins (amino acid subgroup) are the group of metabolites most changed by functional hypoxia (Table 1). Considering Fig. 2, it becomes apparent that proteins are used for energy production during functional hypoxia. Abalone [marine invertebrates in general (Fields, 1983)] tissue are noted for high concentrations of amino acids, thus the use of protein for energy metabolism directly foreseeing the conversion to other amino acids or to glucose (Shao et al., 2015) is possible in this functional hypoxic scenario.

Several glucogenic amino acids (alanine, arginine, glycine, proline and serine) were elevated in the right gill tissue samples analysed from the functional hypoxic group (Fig. 2, Table 1). Amino acids, threonine, glycine and serine, feed into the glyceraldehyde-3-phosphate reaction of the glycolysis pathway (pathway E), adding to energy production in especially the right gill, which was severely affected by functional hypoxia (Fig. 1). Typically, during stressed conditions (like functional hypoxia) glucogenic amino acids are converted to alanine via the transamination of pyruvate (Pathway F) (Salway, 2004). Increased alanine was observed in the right gill, foot muscle and haemolymph samples, largely due to the fact that alanine is in equilibrium with pyruvate, which is oxidatively decarboxylated to carbon dioxide (CO_2) and acetyl coenzyme A (CoA) in aerobic conditions (Salway, 2004). However, in anaerobic conditions, abalone can also use the increased alanine for alanopine production.

Functional hypoxia resulted in elevated asparagine in the foot muscle and reduced levels of aspartate in epipodial tissue, adductor muscle and the right gill samples analysed (Pathway O), supporting the fact that anaerobic catabolism of aspartate is commonly implemented by marine invertebrates. Aspartate in particular is catabolised by reactions of the TCA cycle running from oxaloacetate to succinate (Storey, 2005). Thus, the decrease in aspartate can be ascribed to the replenishment of the TCA intermediate, oxaloacetate. Alternatively, it can also be a result of the apparent unchanged TCA cycle, which does not lead to accumulation of connecting compounds. Aspartate is also used for the synthesis of glutamate via the aspartate aminotransferase reaction, and serves as the precursor for the biosynthesis of a number of other amino acids (Shao et al., 2015). The amino acid glutamate (Pathway G and R) was increased in the left gill and adductor muscle samples, but decreased in the right gill, haemolymph and epipodial tissue samples. Glutamate not only plays a vital role as amino donor via aminotransferase reactions enabling amino acid biosynthesis (Venter et al., 2016b), but also serves as a precursor for glutamine synthesis, and is overall involved in cellular metabolism (Shao et al., 2015). Glutamine (Pathway R) was increased in the haemolymph sample and decreased in the adductor muscle tissue (the exact opposite of glutamate) demonstrating interplay with glutamate.

The branched-chain amino acids (BCAA) leucine and isoleucine were reduced in the adductor muscle samples (Pathway K), while valine was elevated, following functional hypoxia (Fig. 2). During periods of extended exercise (functional hypoxia), BCAAs are used as carbon skeletons in gluconeogenesis and alanine synthesis in order to prevent lactate accumulation (Layman, 2002). Conversely, elevated BCCAs were also reported in the gills of *H. diversicolor* (Lu et al., 2016) and *H. fugens* (Tripp-Valdez et al., 2017) following hypoxia and thermal stress.

Some amino acids, like glycine and taurine, feed into the glycolysis pathway, eventually assisting with glycolytic ATP production, and are termed osmolytes. Generally, the osmolytes of marine invertebrates are present at higher concentrations due to their importance in the regulation of osmosis (Zhou et al., 2015). However, the osmolytes betaine and dimethylglycine (Pathway D) were lower as a result of functional hypoxia, which might have drained these compounds in an attempt to regulate the osmotic pressure. Then again, increases in alanine, taurine, alanopine, tauropine and other non-essential amino acids detected in this study complies with maintenance of intracellular osmotic pressure in abalone (Rosenblum et al., 2005; Tripp-Valdez et al., 2017). An increased presence of the osmolyte homarine (an endogenously synthesised hetero-aromatic quaternary ammonium compound) was

Biology Open (2018) 7, bio031070. doi:10.1242/bio.031070

detected in the right gill of abalone subjected to functional hypoxia (Pathway D), which is most likely synthesised via methylation of picolinate or via the metabolism of glycine and succinyl-CoA (Netherton and Gurin, 1982). The exact role of hormarine in abalone metabolism is not yet known despite it being elevated in *H. iris* muscle tissue after exposure to wave action (Wells et al., 1998), the foot muscle tissue and digestive glands of stunted and diseased *H. rufescens* (Viant et al., 2003), and digestive gland and foot muscle tissue of Rickettsiales-like prokaryote-infected *H. rufescens* (Rosenblum et al., 2005). Homarine has previously been implicated to assist with osmoregulation and trans-methylation, and exhibits morphogenetic activity which may influence cell proliferation and differentiation (Rosenblum et al., 2005). The elevated levels of homarine detected in the right gill of *H. midae* after exposure to functional hypoxia in this experiment (Fig. 2) support its osmoregulatory function, since this tissue will be the first to be influenced by oxygen deprivation. Proline-betaine, another osmolyte (Hayat et al., 2012), was detected in elevated levels in the gills of the abalone after functional hypoxia (Table 1), and can in effect be used to produce proline (Pathway R) also elevated in the gill samples. Furthermore, proline resulted in significant increases in the adductor muscle and epipodial tissue samples of *H. midae*. Typically, proline acts as an osmolyte to balance water stress and possesses protective mechanisms for the stabilising of proteins and antioxidant enzymes. The scavenging of reactive oxygen species and balancing of redox homeostasis are also promoted by proline metabolism (Liang et al., 2013).

Response of carbohydrate and lipid metabolism to functional hypoxia

Carbohydrates are deemed as the most important energy source for abalone and therefore are supplied in bulk to abalone formulated feeds (Lee, 2004). When ATP is required quickly, during episodes of intense exercise, carbohydrates are primarily utilised as they support maximal rates of ATP production (Weber, 2011). During physical activities, glycogen (the stored form of glucose) is broken down to supply glucose (Whitney and Rolfes, 2008). Based on the findings, the glycolysis pathway in Fig. 2 and Table 1 suggests that carbohydrates were metabolised for anaerobic energy production. When evaluating the presence of substrates for glycolytic use, only galactose and mannose (Pathway A) were elevated in the haemolymph samples. Also the intermediates of the TCA cycle (with succinate being the exception) did not vary significantly between the experimental groups, suggesting that the TCA cycle functioned adequately despite a redox imbalance (skewed NAD^+: NADH ratio). However, the presence of lactate, alanopine and tauropine indicates the use of anaerobic rather than aerobic carbohydrate metabolism following functional hypoxia. Furthermore, the accumulation of these anaerobic end products demonstrate that the rate of pyruvate production exceeded the rate of pyruvate clearance, which creates a view that functional hypoxia resulted in a rapid decrease in cellular ATP, which was compensated for by anaerobic ATP production.

The most apparent changes in the fatty acid profile of *H. midae* after the functional hypoxia experiment (Table 1), were the elevated levels of palmitoleate (C16:1) in the left gill, and oleate (C18:1 n-9) in the muscle and haemolymph samples (Pathway V). In *H. discus hannai* and *H. diversicolor*, oleate was also reported to be the predominant fatty acid released from lipids for β-oxidation (Lou et al., 2013; Li et al., 2015). A few fatty acids and carnitines were affected by functional hypoxia (Fig. 2), corresponding to the relatively low lipid stores previously reported to occur in abalone tissue (Vosloo and Vosloo, 2010). An increase in palmitoleate supports the increases observed in palmitoylcarnitine, carnitine and acetylcarnitine, which demonstrates compromised β-oxidation (Pathway U), despite fatty acid release from lipids through activated lipase action.

Abalone tissue-specific responses and interplay

A general observation was that the largest number of significantly changed metabolites was detected in the adductor muscle, followed by the gills, the foot muscle, epipodial tissue and lastly the haemolymph, which displayed the least number of significant metabolites between experimental groups (Fig. 1, Fig. 2 and Table 1). The results indicated that *H. midae* tissues display a diverse response to hypoxia, most likely attributed to the varying functionality and metabolism associated with the various organs from which the tissue was sampled. Additionally, much like higher organisms, certain metabolites are shuttled between various different organs and tissues (e.g. from hypoxic tissue to regions that have access to oxygen) where they can be more appropriately utilised. An example of this in higher animals is the lactate shuttle between fatigued muscles and the liver. Each tissue function, in terms of the hypoxia, will subsequently briefly be discussed.

Gills

Seeing that environmental oxygen levels did not change, the fact that the gills displayed alterations following functional hypoxia are likely attributed to the shuttle of accumulated products from systemic circulation. Hence, it can be reasoned that aerobic metabolism in the gills still function adequately. Because of this, the gills might be a site where accumulated products in the circulation are further catabolised (like NADH), which is shuttled through increased perfusion. The gills can be regarded as the first line of physiological mechanism that enable abalone to cope with variation in oxygen levels (Ragg and Taylor, 2006; Morash and Alter, 2016). The right gill, which is generally perfused, serves as sole handler to the initial change in internal oxygen levels, explaining why large metabolic changes were detected in the right gill. After a period of increased oxygen demand, more haemolymph can be diverted to the left gill for increased oxygen uptake (Ragg and Taylor, 2006). The metabolite arginine, detected in the right gill, displayed the largest increase in metabolic activity (Table 1), possibly due rapid energy production via phosphoarginine. It is also likely a result of shuttled arginine as the gills can either release or use this product. Then again, aspartate, measured in the right gill, showed the largest decrease in metabolic response. Considering the involvement of aspartate in the synthesis of TCA cycle intermediates, lower levels are expected in scenarios where oxygen supply is still adequate for aerobic metabolism. In the abalone *H. diversicolor* the gills were also reported as easily affected following hypoxic stress (Lu et al., 2016).

Haemolymph

During intense activity, the abalone circulatory system is known to favour oxygen storage instead of oxygen delivery resulting in insufficient haemolymph gas transport and in effect isolation of general circulation (Donovan et al., 1999). Of all the samples studied, the least number of metabolites were detected in the haemolymph (Table 1) and of the detected metabolites, most were elevated (Fig. 2). During functional hypoxia, elevated energy demand results in the elevated release of metabolites from cellular stores that are shuttled between various organs. Metabolic end products produced during functional hypoxia may be released into the haemolymph and absorbed by other tissues (organs), which are

Biology Open (2018) 7, bio031070. doi:10.1242/bio.031070

able to oxidise these products (metabolic shuttle). Haemolymph also represents the exo-metabolome since it contains metabolite information of how the intracellular metabolic network influences its external environment (Dunn, 2008). Furthermore, the haemolymph of abalone utilise a reverse Bohr shift mechanism which utilises the decrease in pH during anaerobic conditions to ensure survival for longer in the absence of oxygen (Venter et al., 2016b).

Muscle

Energy production via both substrate-level phosphorylation and the glycolysis pathway (Venter et al., 2016b) require metabolic fuel, and as abalone muscle has the ability to store large amounts of amino acids and phosphoarginine (more than the other tissues), carbohydrates and proteins are rapidly broken down to serve as substrates for energy production. The abundance of affected muscle metabolites is an expected outcome following functional hypoxia, considering the reduced oxygen supply to the muscle, forcing the muscle to switch to anaerobic metabolism as activity endures. The findings of both adductor and foot muscle predominantly displayed changes in metabolites detected in the functional hypoxia group most likely due to inhibition of mitochondrial metabolism and fatigue following functional hypoxia. This demonstrates the reliance of abalone muscle on oxygen for energy metabolism, despite its capacity for anaerobic metabolism, as confirmed in previous experiments on *H. lamellose* (Gäde, 1988).

Epipodial tissue

Unique findings made by observations in the epipodial tissue include betaine, uridine, adenosine monophosphate, oxalate and nicotinate, which amongst other functions support pyrimidine nucleotide synthesis and participate in redox reactions (Young et al., 2017). However, most of the metabolite results of the epipodial tissue, such as aspartate and carnitine, are similar to those in other tissues, suggesting that the epipodial tissue has similar metabolic profiles to the adductor muscle and right gill. This presents an important opportunity for non-destructive sampling for health screening, without critical damage to the animal (Wasko et al., 2003; Slabbert and Roodt-Wilding, 2006). Also, the role of epipodial tissue as a means to shuttle metabolites cannot be dismissed based on the findings made here.

H. midae tissue display a diverse response to functional hypoxia, most likely attributed to the varying functionality and metabolism associated with the various organs from which the tissue was sampled. Additionally, much like higher organisms, certain metabolites are shuttled between various different organs and tissues (e.g. from hypoxic tissue to regions that have access to oxygen) where they can be more appropriately utilised (Brooks, 1986; Proia et al., 2016).

CONCLUSIONS

Taken together, this study brings to front the metabolic response of *H. midae* after subjection to functional hypoxia, demonstrating how abalone can cope with episodes of burst activity (functional hypoxia), by continuing to drive the metabolic needs via anaerobic metabolism. Energy is initially produced by means of phosphoarginine breakdown, followed by anaerobic central carbon metabolism, with the production of lactate, opines (tauropine and alanopine) and succinate. It is also clear that *H. midae* used all of the main metabolite classes, e.g. proteins (amino acids), carbohydrates (glucose) and lipids (fatty acids), to contribute to ATP production when exercise is induced. By performing cross-tissue analysis it becomes evident that all of the investigated tissues are not affected to the same extent following functional hypoxia. The gills and haemolymph manage oxygen delivery based on oxygen demand. The haemolymph also shuttles metabolites between tissues where some metabolites are further metabolised. Both adductor and foot muscle produced anaerobic end-products releasing NAD^+ for glycolytic ATP production, making it possible to say that *H. midae* is more dependent on anaerobic metabolism after a period of induced functional hypoxia. No special metabolic function apart from metabolite shuttling was observed in the epipodial tissue, but it does correlate well with other tissues making this an important tissue for non-destructive research purposes.

Functional hypoxia can be seen as a self-inflicted stressor, but *H. midae* has shown to have well-developed metabolic capabilities to withstand the exercise-induced episode, whereafter normal aerobic metabolism will likely continue once oxygen availability returns. Ideally in an aquatic system, stress should be limited to ensure that metabolic energetics are used for anabolic processes resulting in growing organisms, and not catabolic processes aimed at energy production for survival, like typically experienced in this metabolomics study. The use of metabolomics enabled a global view of the metabolic response implemented by *H. midae* adductor muscle, foot muscle, left gill, right gill, haemolymph and epipodial tissue samples, following exposure to functional hypoxia. With this in mind, it is important to next focus on certain metabolic intermediates and/or end-products (e.g. arginine, lactate, opines) and establish defined concentration ranges for normality and certain stressors. This may serve well to monitor and assess abalone health on abalone farms, which is still lacking in the aquaculture industry (Fasulo et al., 2012; Alfaro and Young, 2016).

MATERIALS AND METHODS

Experimental setup and animals

Adult abalone were collected during the winter season from the grow-out platform at HIK Abalone Farm (Pty) Ltd, situated in Hermanus, South Africa. As part of day-to-day farming activities, the tanks were cleaned weekly and animals were provided with standard artificial abalone feed (Vosloo et al., 2013). All of the research pertaining to the perturbations and abalone collection was done in accordance with institutional guidelines of the relevant institutional committees and granted Aquaculture Research Permit. Animals (n=12) were removed from the same raceway and placed into a large aquarium tank with flowing seawater. The control animals (n=6) were removed and dissected for sampling of adductor muscle, foot muscle, left gill, right gill, epipodial tissue and haemolymph samples. In order to induce functional hypoxia, the remaining animals were placed upside-down on their shells (O'omolo et al., 2003). After relatively vigorous contractions of the shell adductor muscle, the animals eventually regained their normal posture, and were immediately inverted again; this was repeated to the point where the animals were unable to upright themselves. After 18 min the abalone were considered exhausted and were removed from the system and dissected in the same manner as the control group. Prior to dissection, the animals were weighed to the nearest 0.01 g and the shell lengths were measured to the nearest 0.10 mm, along the longest axis, using callipers. Additionally, abalone gender was assessed by observing the gonad colour, which is green in females and cream in males. The control group had an average wet weight of 83.00±8.27 g and shell length of 75.53±2.05 mm, and consisted of four males and two females. The functional hypoxia group had an average wet weight of 94.33±11.13 g and shell length of 79.00±2.76 mm and consisted of two males and four females.

Sample dissection

All abalone were collected, dissected and snap frozen within a standardised time period (Hernandes et al., 2017), accumulating to approximately 10 min per animal. Abalone were shucked individually with a scalpel, working rapidly from the anterior to posterior axis, cutting longitudinally through the

Biology Open (2018) 7, bio031070. doi:10.1242/bio.031070

foot between the mantle and the distal surface of the foot. Haemolymph was collected from the pedal sinus using a 1 ml syringe with a 27-gauge needle and immediately transferred and stored in micro-centrifuge tubes. Epipodial tissue was cut from the left anterior of the area surrounding the abalone foot muscle using dissection scissors. Both the left and the right gill were collected, by making an incision in the mantle situated to the left side of the animal, located directly under the shell pores. The gills were carefully removed with dissection forceps, from the left and right walls of the mantle cavity. A sample of the shell adductor muscle was removed using a scalpel, from the ventral surface towards the central point where the muscle attaches to the shell. The foot muscle samples were collected from the posterior side of the ventral surface, excluding sole epithelium and majority of the mucus glands. Muscle samples to the equivalent of the volume of a micro-centrifuge tube were sampled in small blocks using a scalpel. As soon as the sample of interest was removed, it was immediately placed into a micro-centrifuge tube and snap frozen using dry ice.

Metabolite extraction

Tissue homogenisation was performed using the two-step method described by Venter et al. (2016a), using a sample weight of 20 mg for the right gill tissue, 40 mg for the left gill tissue, 30 mg for the epipodial tissue and 60 mg for the adductor and foot muscle tissue.

For every 10 mg of abalone tissue, 20 µl water, 50 µl methanol and 20 µl internal standard (2-acetamidophenol and 3-phenylbutyric acid, with a final concentration of 50 µg/ml) was added along with both a 3- and a 7-mm stainless steel bead to micro-centrifuge tubes. Samples were homogenised for 4 min at 30 Hz using a Retch M400 vibration mill, whereafter 20 µl chloroform and 10 µl water were added to the homogenate. The samples were vortexed for 1 min and incubated on ice for 10 min, before they were centrifuged at 25,000×***g*** for 10 min at 4°C to induce phase separation. Selected volumes of the aqueous and organic phases were transferred to a screw-top vial (depending on the analytical platform) and dried under a gentle stream of nitrogen at 37°C, together with an additional 100 µl platform-specific internal standard. For NMR analysis, 100 µl of the polar phase and 50 µl of the a-polar phase were transferred, and dried together with nor-leucine internal standard (100 µg/ml). For LC-QTOF analysis, 70 µl of the polar phase and 35 µl of the a-polar phase were transferred, and dried together with nor-leucine internal standard (100 µg/ml). For GC-QTOF analysis, 70 µl of the polar phase and 35 µl of the a-polar phase were transferred, and dried together with nonadecanoic acid internal standard (100 µg/ml). For LC-MS/MS analysis, 10 µl of the polar phase and 5 µl of the a-polar phase were transferred, and dried together with nor-leucine internal standard (10 µg/ml). For GC-MSD analysis, nonadecanoic acid internal standard (100 µg/mL) and 150 µl of the a-polar phase of the tissue homogenate were dried. All samples were dried under a gentle stream of nitrogen at 37°C.

Haemolymph samples were prepared by adding 500 µl of the collected haemolymph to 1500 µl cold acetonitrile in micro-centrifuge tubes. The samples were vortexed and incubated on ice for 30 min, followed by centrifugation at 25,000×***g*** for 10 min at 4°C. The supernatant was aliquoted into various screw-top vials (one for each analytical platform). After the addition of 100 µl instrument specific internal standard, all samples were dried under a gentle stream of nitrogen at 37°C.

Sample preparation

Dried sample extracts for NMR spectroscopy analyses were re-dissolved in 500 µl ultra-pure water and centrifuged at 12,000×***g*** for 10 min, whereafter the ultra-filtrate was transferred together with 50 µl 1.5 M potassium phosphate monobasic deuterated NMR buffer solution at pH 7.4 (Dona et al., 2014) to 5 mm NMR glass tubes.

The sample extracts prepared for untargeted GC-TOF analyses were removed from the freezer and dried under a nitrogen stream at 60°C for 5 min, prior to oximation and silylation. A volume of 50 µl of the oximation reagent (200 mg methoxyamine dissolved in 10 ml pyridine) was added to the samples, whereafter the samples were capped, vortexed for 1 min and incubated for 60 min at 60°C. Once oximation was completed, the samples were cooled prior to adding 100 µl O-bis(trimethylsilyl)trifluoro acetamide (BSTFA), containing 1% trimethylchlorosilane (TMCS). The samples were then vortexed for 1 min and incubated for 60 min at 60°C and transferred to glass GC vials for analyses (Venter et al., 2016a).

Samples prepared for LC-MS/MS and LC-QTOF analyses were butylated once the dried residue (stored at −80°C) was dried again, using nitrogen at 60°C for 5 min. To the dried residue, 100 µl 3 N butanolic hydrogen chloride (HCl) was added and the samples were incubated at 60°C for 60 min. Butanolic HCl (3 N) was prepared by creating a 1:4 ratio of acetyl chloride and 1-butanol solution. The butylated samples were then evaporated to dryness again under a stream of nitrogen at 60°C. The dried residue was reconstituted in 200 µl water:acetonitrile (50:50) containing 0.1% formic acid (Venter et al., 2017).

The GC-MSD-analyses-prepared dried extracts were removed from the freezer and dried again using a stream of nitrogen at 60°C for 5 min. The samples were suspended in 500 µl chloroform and 500 µl methanol, followed by the addition of 1 ml of methanolic potassium hydroxide (KOH), and incubated for 30 min at 40°C. Methanolic KOH was prepared daily before analysis of the batch, by dissolving 280 mg of potassium hydroxide pellets in 25 ml methanol (Lindeque et al., 2013). Once the samples were cooled to room temperature, FAMEs were extracted with the addition of 2 ml hexane, 200 µl acetic acid (1 N) and 2 ml water. The samples were centrifuged for 5 min at 2000×***g*** in order to separate the organic and water phases. The upper organic phase was recovered using a clean tube with a rubber suction teat, and the lower phase was re-extracted with 2 ml hexane, for another three cycles as described above. The pooled organic solvent phases collected were evaporated under a gentle stream of nitrogen at 37°C. Following the drying step, 50 µl oximation reagent (200 mg methoxyamine dissolved in 10 ml pyridine) was added, then vortexed for 1 min and incubated for 60 min at 60°C. After cooling, silylation was performed by adding 50 µl BSTFA (containing 1% TMCS) to the samples and incubated for 60 min at 60°C and transferred to glass GC vials for analyses (Willers et al., 2016).

Sample analysis

Samples collected from the same tissue were assigned to the same batch using a randomisation equation to allocate these to the respective batches for analysis (Dunn et al., 2012), with quality control samples included amongst the batch which was injected at regular intervals throughout the analytical run of the analysed batch. Thus, six batches (adductor muscle, foot muscle, left gill, right gill, haemolymph and epipodial tissue) were analysed over 6 days on all of the analytical platforms described below.

NMR spectroscopy analyses were performed on a Bruker Advance III HD NMR spectrometer operating at 500 MHz ^{1}H, equipped with a triple-resonance inverse (TXI) ^{1}H(^{15}N, ^{13}C) probe head and x, y, z gradient coils. Automated tuning and matching, locking and shimming using the standard Bruker routines ATMA, LOCK, and TopShim were used to optimise the NMR conditions daily. The NMR spectra were acquired as 128 transients in 32,000 data points with a spectral width of 6002 Hz. The sample temperature was maintained at 27°C and the water resonance was pre-saturated by single-frequency irradiation during a relaxation delay of 4 s, with a 90° excitation pulse of 8 µs, acquiring spectra at 64 scans per sample (~runtime of 8 min per sample). Shimming of the sample was performed automatically on the deuterium signal. The resonance line widths for trimethylsilyl-tetradeuteropropionic acid and metabolites were <1 Hz (measurements at half the height of the peak). Fourier transformation and phase and baseline correction were done automatically. Bruker Topspin (Version 3.1) software was used for spectral data processing and Bruker AMIX (Version 3.9.12) software was used to distinguish and identify metabolites (Ellinger et al., 2013; Irwin et al., 2016).

GC-TOF analyses were executed on a LECO Pegasus HT mass analyser coupled to an Agilent 7890A GC. Chromatographic separation was performed on a Restek RXi-1MS column (30 m×0.32 mm×0.25 µm). A sample volume of 1 µl was injected (using a split/split-less injector) per run with a 1:20 split ratio. The front inlet temperature was kept at 250°C. An initial oven temperature of 80°C was maintained for 1 min and then increased as follows: 10°C/min to 150°C at 1.50 min, 14°C/min to 230°C, 18°C/min to 300°C where it was maintained for 2 min equating to a total run time of ~20 min per sample. Hydrogen was used as carrier gas at a constant flow of 3.2 ml/min. The transfer line temperature was maintained at 225°C and the ion source temperature at 200°C for the entire run. Acquisition was

Biology Open (2018) 7, bio031070. doi:10.1242/bio.031070

delayed for the first 1.9 min which served as a solvent delay. Data were captured with an acquisition rate of 20 spectra (40–950 m/z) per second, with a detector voltage of 50 V over the daily tune voltage and electron energy of -70 V.

LC-MS/MS analyses were performed in positive ion mode using an Agilent 1200 LC system coupled to an Agilent 6410 Triple Quadrupole. A sample injection volume of 0.5 µl was separated chromatographically on an Agilent SB-Aq column (2.1×100 mm×1.8 µm) at 45°C. The mobile phases consisted of (A) water and (B) acetonitrile both with 0.1% formic acid. The gradient separation conditions included: 0 min 5% (B); 0-0.2 min 5% (B); 0.2-2 min 25% (B); 2-7 min 25% (B); 7-7.5 min 90% (B); 7.5-9 min 90% (B) all using a flowrate of 0.4 ml/min; 9-9.1 min 90% (B); 9.1-12 min 95% (B) and 12-12.5 min 5% (B) using a flowrate of 0.5 ml/min, with a post-run step of 4 min at this condition, resulting in a run time of 16.5 min per sample. The drying gas temperature was set at 300°C with a drying gas flow of 7.5 l/min and nebuliser pressure of 30 psi. Selected metabolites (Table S1) were analysed in multiple reaction monitoring (MRM) mode with a dwell time of 45 ms and enhanced sensitivity at an electron multiplier voltage of 400 above tune voltage.

LC-QTOF analyses were conducted using an Agilent 1200 LC system using an injection volume of 5 µl for chromatographic separation. Butylated samples were separated on an Agilent ZORBAX SB-Aq C18 column (2.1×150 mm×3.5 µm) fitted with a guard pre-column at 30°C. The mobile phases consisted of (A) water and (B) acetonitrile, both containing 0.1% formic acid. The separation was performed using the following gradient: 0-3 min 0% (B), 3-11 min 25% (B), 11-30 min 100% (B) at a flowrate of 0.25 ml/min, whereafter the flowrate was increased to 0.5 ml/min to 32 min 100% (B), and ending at 33 min 100% (B) 0.25 ml/min along with a 10 min post-run at this condition, resulting in a runtime of 43 min per sample. Mass spectrometry detection was performed on an Agilent 6510 QTOF mass analyser using positive electrospray ionisation with a drying gas temperature of 300°C, a drying gas flow of 7.5 l/min and nebuliser pressure of 30 psi. The Q-TOF was set to scan from 50 to 1 000 m/z. Both centroid and profile data were stored and the instrument set to extended dynamic range (2 GHz). The all ions MS/MS functionality was used with the following collision energies: 0, 10, 20 and 40 V using nitrogen collision gas. A reference solution containing masses 121.050873 $[M+H]^+$ and 922.009798 $[M+H]^+$ were constantly infused as accurate mass reference. Furthermore the instrument was calibrated with Agilent ESI-L low concentration tuning mix before the analysis of each batch of samples (Venter et al., 2017).

GC-MSD analyses of FAMEs were performed with an Agilent GC-MSD instrument consisting of a gas chromatograph with a split/split-less injector (250°C) equipped with an auto sampler coupled to an inert XL mass selective detector. The gas chromatograph was equipped with a SPB-1 column (60 m×0.25 mm×0.250 µm film thickness) using helium as the carrier gas at a flow rate of 1.0 ml/min. A sample volume of 2 µl was injected per run with a 1:2 split ratio. The front inlet temperature was kept at 250°C throughout the entire run. The initial oven temperature was 150°C for 4 min, ramping to 200°C at 4°C/min to 250°C at 2°C/min, and then to 295°C at 10°C/min followed by a hold for 2 min, resulting in a runtime of 48 min per sample. The transfer line temperature was set to 280°C and the source temperature at 230°C. Acquisition was delayed for the first 5 min serving as a solvent delay. Data were captured with an acquisition rate of 3.58 spectra (40-450 m/z) per second, with electron energy of 70 eV (Willers et al., 2016).

Data analysis

NMR data were extracted and pre-processed using Bruker's Topspin NMR software (Version 3.1) as previously described (Irwin et al., 2016). GC-TOF data were extracted using ChromaTOF (Version 4.50.8) as previously described (Venter et al., 2016a). LC-MS/MS data were quantified using Agilent's MassHunter Quantitative software (Version B.06). LC-QTOF data extraction was performed using Agilent's MassHunter Qualitative software (Version B.06) utilising the molecular feature extraction algorithm and find by formula function corresponding to theoretical chemical formula of butylated metabolites listed in an in-house butyl ester library. Agilent's MassHunter Mass Profiler Professional (Version B.02.02) was used to align the data. GC-MSD data were extracted as previously described (Willers et al., 2016). The GC-MSD compound list was then used in MET-IDEA (METabolomics Ion-based Data Extraction Algorithm) (Lindeque et al., 2013) to reintegrate target peaks, to yield a data matrix with no missing values.

Data pre-processing in the form of zero filtering was performed (Venter et al., 2015) to ensure a more complete dataset. The NMR data were normalised as a relative concentration by using the internal standard 2-acetamidophenol. GC-TOF data were normalised relative to the internal standard 3-phenylbutyric acid (Luier and Loots, 2016). Mass spectrometry total useful signal (MSTUS) was the preferred normalisation method for the data acquired by LC-QTOF, GC-MSD and LC-MS/MS analysis (Venter et al., 2015). Data pre-treatment steps were completed by using the webserver MetaboAnalyst (3.0) (Xia et al., 2015). Missing values (or zeros) were replaced by half of the minimum positive value in the original data. Next, data were transformed using generalised logarithm (glog) (Lindeque et al., 2015). Principal component analysis (PCA) was used to determine whether a natural grouping in the data exists when considering this from a multivariate perspective (Lindeque et al., 2015). Gender was investigated using this approach in order to confirm that the relevant biological variance in the compared groups was not influenced by this confounder. As a result, the grouping displayed visually on the PCAs did not display any favour towards possible confounding factors within the groups of interest.

Univariate statistical analyses were performed with MetaboAnalyst (3.0) (Xia et al., 2015) and MS Excel. Student's *t*-test was used to find significant differences in metabolite levels between the experimental groups. Features with a *P*-value <0.05 (false discovery rate corrected *P*-value) indicated that the features differed significantly between the groups and were labelled as important and not removed from the data (Lindeque et al., 2013). Effect size was calculated (on the remaining features) to ensure practical significance, by determining the absolute difference between the means of the two groups divided by the maximum standard deviation of the two groups. Features with a *d*-value >0.8 were labelled as important and remained in the data matrix for further analysis (Ellis and Steyn, 2003). Effect size is similar to fold change (i.e. the absolute difference between the group means) but scaled to the highest standard deviation instead of the control group mean. The important features were visualised with a heatmap (using auto-scaled data) to show concentration variance between samples and groups.

Following a comparison to several in-house, commercial and public libraries/databases, compiled by injection and analysis of previously purchased or synthesised standards, practical and statistical significant features were given identities (where possible). Each identification was ranked using the identification confidence levels previously described (Schymanski et al., 2014), whereafter the important metabolites were used for pathway analysis. If metabolites were detected on more than one analytical platform, the platform with the highest identification confidence level received preference, and if a duplicate metabolite still existed the metabolite with the best (smallest) *P*-value was selected. A metabolic map of the metabolic response of *H. midae* to functional hypoxia was compiled manually, using previous knowledge, relevant literature and online servers like Kyoto Encyclopaedia of Genes and Genomes (KEGG) and International Union of Biochemistry and Molecular Biology (IUBMB)-Nicholson, where possible. The metabolites are reported as relative compound intensities based on the tissue in which the findings were made represented by adductor muscle, foot muscle, epipodial tissue, haemolymph, left gill and right gill samples.

Acknowledgements

We are thankful to HIK Abalone Farm (Pty) Ltd for the donation of abalone samples.

Competing interests

The authors declare no competing or financial interests.

Author contributions

Conceptualization: D.T.L., A.V., J.Z.L.; Methodology: L.V., P.J.J.v.R., S.M., J.Z.L.; Software: J.Z.L.; Validation: P.J.J.v.R.; Formal analysis: L.V., P.J.J.v.R., S.M.; Investigation: L.J.M.; Resources: L.J.M.; Data curation: L.V.; Writing - original draft: L.V.; Writing - review & editing: L.V., D.T.L., L.J.M., P.J.J.v.R., S.M., A.V., J.Z.L.; Visualization: L.V., L.J.M.; Supervision: D.T.L., A.V., J.Z.L.; Project administration: A.V., J.Z.L.

Funding
Funding was supplied by the North-West University (NWU) and the Technology Innovation Agency (TIA) of the Department of Science and Technology, Republic of South Africa.

Supplementary information
Supplementary information available online at
http://bio.biologists.org/lookup/doi/10.1242/bio.031070.supplemental

References

Alfaro, A. C. and Young, T. (2016). Showcasing metabolomic applications in aquaculture: A review. *Rev. Aquacult*. doi:10.1111/raq.12152.
Baldwin, J. and England, W. (1982). The properties and functions of alanopine dehydogenase and octopine dehydrogenase from the pedal retractor muscle of Strombidae (Class Gastropoda). *Pac. Sci.* **36**, 381-394.
Baldwin, J., Wells, R., Low, M. and Ryder, J. (1992). Tauropine and D-lactate as metabolic stress indicators during transport and storage of live paua, (New Zealand Abalone) (*Haliotis iris*). *J. Food Sci.* **57**, 280-282.
Brooks, G. A. (1986). The lactate shuttle during exercise and recovery. *Med. Sci. Sports Exerc.* **18**, 360-368.
Dale-Kuys, R., Vervalle, J., Roodt-Wilding, R. and Rhode, C. (2017). Genetic association analysis of candidate loci under selection with size in the South African abalone. *Aquac. Int.* **25**, 1197-1214.
Dona, A. C., Jiménez, B., SchäFer, H., Humpfer, E., Spraul, M., Lewis, M. R., Pearce, J. T. M., Holmes, E., Lindon, J. C. and Nicholson, J. K. (2014). Precision high-throughput proton NMR spectroscopy of human urine, serum, and plasma for large-scale metabolic phenotyping. *Anal. Chem.* **86**, 9887-9894.
Donovan, D., Baldwin, J. and Carefoot, T. (1999). The contribution of anaerobic energy to gastropod crawling and a re-estimation of minimum cost of transport in the abalone, *Haliotis kamtschatkana* (Jonas). *J. Exp. Mar. Biol. Ecol.* **235**, 273-284.
Dunn, W. B. (2008). Current trends and future requirements for the mass spectrometric investigation of microbial, mammalian and plant metabolomes. *Phys. Biol.* **5**, 011001.
Dunn, W. B., Bailey, N. J. and Johnson, H. E. (2005). Measuring the metabolome: Current analytical technologies. *Analyst* **130**, 606-625.
Dunn, W. B., Wilson, I. D., Nicholls, A. W. and Broadhurst, D. (2012). The importance of experimental design and QC samples in large-scale and MS-driven untargeted metabolomic studies of humans. *Bioanalysis* **4**, 2249-2264.
Ellinger, J. J., Chylla, R. A., Ulrich, E. L. and Markley, J. L. (2013). Databases and software for NMR-based metabolomics. *Curr. Metabolomics* **1**, 28-40.
Ellington, W. R. (1983). The recovery from anaerobic metabolism in invertebrates. *J. Exp. Zool.* **228**, 431-444.
Ellis, S. and Steyn, H. (2003). Practical significance (effect sizes) versus or in combination with statistical significance (*P*-values): research note. *Manage. Dynam.* **12**, 51-53.
Fasulo, S., Iacono, F., Cappello, T., Corsaro, C., Maisano, M., D'agata, A., Giannetto, A., De Domenico, E., Parrino, V. and Paro, G. L. (2012). Metabolomic investigation of *Mytilus galloprovincialis* (Lamarck 1819) caged in aquatic environments. *Ecotoxicol. Environ. Saf.* **84**, 139-146.
Feala, J. D., Coquin, L., Zhou, D., Haddad, G. G., Paternostro, G. and Mcculloch, A. D. (2009). Metabolism as means for hypoxia adaptation: metabolic profiling and flux balance analysis. *BMC Syst. Biol.* **3**, 91.
Fields, J. H. (1983). Alternatives to lactic acid: possible advantages. *J. Exp. Zool. A Ecol. Genet. Physiol.* **228**, 445-457.
Gäde, G. (1988). Energy metabolism during anoxia and recovery in shell adductor and foot muscle of the gastropod mollusc *Haliotis lamellosa*: formation of the novel anaerobic end product tauropine. *Biol. Bull.* **175**, 122-131.
Gäde, G. and Grieshaber, M. K. (1986). Pyruvate reductases catalyze the formation of lactate and opines in anaerobic invertebrates. *Comp. Biochem. Physiol. B Comp. Biochem.* **83**, 255-272.
Gäde, G., Carlsson, K.-H. and Meinardus, G. (1984). Energy metabolism in the foot of the marine gastropod *Nassa mutabilis* during environmental and functional anaerobiosis. *Mar. Biol.* **80**, 49-56.
Garrett, R. and Grisham, C. (2010). *Biochemistry. Brooks Cole Cengage Learning, Boston USA*. Belmont: Brooks Cole, Cengage Learning.
Grieshaber, M., Hardewig, I., Kreutzer, U. and Pörtner, H.-O. (1994). Physiological and metabolic responses to hypoxia in invertebrates. *Rev. Physiol. Biochem. Pharmacol.* **125**, 43-147.
Hayat, S., Hayat, Q., Alyemeni, M. N., Wani, A. S., Pichtel, J. and Ahmad, A. (2012). Role of proline under changing environments: a review. *Plant Signal. Behav.* **7**, 1456-1466.
Hernandes, V. V., Barbas, C. and Dudzik, D. (2017). A review of blood sample handling and pre-processing for metabolomics studies. *Electrophoresis* **38**, 2232-2241.
Irwin, C., Van Reenen, M., Mason, S., Mienie, L. J., Westerhuis, J. A. and Reinecke, C. J. (2016). Contribution towards a metabolite profile of the detoxification of benzoic acid through glycine conjugation: An intervention study. *PLoS ONE* **11**, e0167309.
Laas, A. and Vosloo, A. (2010). Exploring basic biochemical constituents in the body tissues of South African abalone *Haliotis midae* reared in shore-based mariculture systems. *Afr. J. Mar. Sci.* **32**, 55-63.
Lankadurai, B. P., Nagato, E. G. and Simpson, M. J. (2013). Environmental metabolomics: An emerging approach to study organism responses to environmental stressors. *Environ. Rev.* **21**, 180-205.
Layman, D. K. (2002). Role of leucine in protein metabolism during exercise and recovery. *Can. J. Appl. Physiol.* **27**, 646-662.
Lee, S.-M. (2004). Utilization of dietary protein, lipid, and carbohydrate by abalone *Haliotis discus hannai*: A review. *J. Shellfish Res.* **23**, 1027-1030.
Li, M., Mai, K., Ai, Q., He, G., Xu, W., Zhang, W., Zhang, Y., Zhou, H. and Liufu, Z. (2015). Effect of dietary lipid on the growth, fatty acid composition and Δ5 *Fads* expression of abalone (*Haliotis discus hannai* Ino) hepatopancreas. *J. Ocean University of China* **14**, 317-324.
Liang, X., Zhang, L., Natarajan, S. K. and Becker, D. F. (2013). Proline mechanisms of stress survival. *Antioxid Redox Signal.* **19**, 998-1011.
Lindeque, J. Z., Hidalgo, J., Louw, R. and Van Der Westhuizen, F. H. (2013). Systemic and organ specific metabolic variation in metallothionein knockout mice challenged with swimming exercise. *Metabolomics* **9**, 418-432.
Lindeque, J. Z., Jansen Van Rensburg, P. J., Louw, R., Van Der Westhuizen, F. H., Florit, S., Ramírez, L., Giralt, M. and Hidalgo, J. (2015). Obesity and metabolomics: Metallothioneins protect against high-fat diet-induced consequences in metallothionein knockout mice. *OMICS* **19**, 92-103.
Liu, C., Shin, P. and Cheung, S. (2014). Comparisons of the metabolic responses of two subtidal nassariid gastropods to hypoxia and re-oxygenation. *Mar. Pollut. Bull.* **82**, 109-116.
Lou, Q. M., Wang, Y. M. and Xue, C. H. (2013). Lipid and fatty acid composition of two species of abalone, *Haliotis discus hannai* Ino and *Haliotis diversicolor* Reeve. *J. Food Biochem.* **37**, 296-301.
Lu, J., Shi, Y., Wang, S., Chen, H., Cai, S. and Feng, J. (2016). NMR-based metabolomic analysis of *Haliotis diversicolor* exposed to thermal and hypoxic stresses. *Sci. Total Environ.* **545-546**, 280-288.
Luier, L. and Loots, D. T. (2016). Tuberculosis metabolomics reveals adaptations of man and microbe in order to outcompete and survive. *Metabolomics* **12**, 40.
Morash, A. J. and Alter, K. (2016). Effects of environmental and farm stress on abalone physiology: Perspectives for abalone aquaculture in the face of global climate change. *Rev. Aquacult.* **8**, 342-368.
Müller, M., Mentel, M., van Hellemond, J. J., Henze, K., Woehle, C., Gould, S. B., Yu, R.-Y., van der Giezen, M., Tielens, A. G. and Martin, W. F. (2012). Biochemistry and evolution of anaerobic energy metabolism in eukaryotes. *Microbiol. Mol. Biol. Rev.* **76**, 444-495.
Netherton, J. and Gurin, S. (1982). Biosynthesis and physiological role of homarine in marine shrimp. *J. Biol. Chem.* **257**, 11971-11975.
O'omolo, S., Gäde, G., Cook, P. A. and Brown, A. C. (2003). Can the end products of anaerobic metabolism, tauropine and D-lactate, be used as metabolic stress indicators during transport of live South African abalone *Haliotis midae*. *Afr. J. Mar. Sci.* **25**, 301-309.
Patti, G. J., Yanes, O. and Siuzdak, G. (2012). Innovation: metabolomics: the apogee of the omics trilogy. *Nat. Rev. Mol. Cell Biol.* **13**, 263-269.
Pörtner, H. O. (2002). Environmental and functional limits to muscular exercise and body size in marine invertebrate athletes. *Comp. Biochem. Physiol. A Mol. Integr. Physiol.* **133**, 303-321.
Proia, P., Di Liegro, C. M., Schiera, G., Fricano, A. and Di Liegro, I. (2016). Lactate as a metabolite and a regulator in the central nervous system. *Int. J. Mol. Sci.* **17**, 1450.
Ragg, N. L. and Taylor, H. H. (2006). Heterogeneous perfusion of the paired gills of the abalone *Haliotis iris* Martyn 1784: An unusual mechanism for respiratory control. *J. Exp. Biol.* **209**, 475-483.
Rosenblum, E., Viant, M., Braid, B., Moore, J., Friedman, C. and Tjeerdema, R. (2005). Characterizing the metabolic actions of natural stresses in the California red abalone, *Haliotis rufescens* using 1H NMR metabolomics. *Metabolomics* **1**, 199-209.
Salway, J. G. (2004). *Metabolism at a Glance*. Guildford: John Wiley & Sons.
Sato, M., Takeuchi, M., Kanno, N., Nagahisa, E. and Sato, Y. (1991). Characterization and physiological role of tauropine dehydrogenase and lactate dehydrogenase from muscle of abalone, *Haliotis discus hannai*. *Tohoku J. Agric. Res.* **41**, 83-95.
Schymanski, E. L., Jeon, J., Gulde, R., Fenner, K., Ruff, M., Singer, H. P. and Hollender, J. (2014). Identifying small molecules via high resolution mass spectrometry: Communicating confidence. *Environ. Sci. Technol.* **48**, 2097-2098.
Shao, Y., Li, C., Chen, X., Zhang, P., Li, Y., Li, T. and Jiang, J. (2015). Metabolomic responses of sea cucumber *Apostichopus japonicus* to thermal stresses. *Aquaculture* **435**, 390-397.
Slabbert, R. and Roodt-Wilding, R. (2006). Non-destructive sampling of juvenile abalone using epipodial tentacles and mucus: Method and application. *Afr. J. Mar. Sci.* **28**, 719-721.
Storey, K. B. (2005). *Functional Metabolism: Regulation and Adaptation*. Hoboeken, New Jersey. John Wiley & Sons.
Tripp-Valdez, M. A., Bock, C., Lucassen, M., Lluch-Cota, S. E., Sicard, M. T., Lannig, G. and Pörtner, H. O. (2017). Metabolic response and thermal tolerance

of green abalone juveniles (*Haliotis fulgens:* Gastropoda) under acute hypoxia and hypercapnia. *J. Exp. Mar. Biol. Ecol.* **497**, 11-18.

Venter, L., Lindeque, Z., van Rensburg, P. J., van der Westhuizen, F., Smuts, I. and Louw, R. (2015). Untargeted urine metabolomics reveals a biosignature for muscle respiratory chain deficiencies. *Metabolomics* **11**, 111-121.

Venter, L., Jansen Van Rensburg, P., Loots, D. T., Vosloo, A. and Lindeque, J. Z. (2016a). Untargeted metabolite profiling of abalone using gas chromatography mass spectrometry. *Food Anal. Method.* **9**, 1254-1261.

Venter, L., Loots, D. T., Vosloo, A., Jansen Van Rensburg, P. and Lindeque, J. Z. (2016b). Abalone growth and associated aspects: now from a metabolic perspective. *Rev. Aquacult.* doi:10.1111/raq.12181.

Venter, L., Jansen Van Rensburg, P. J., Loots, D. T., Vosloo, A. and Lindeque, J. Z. (2017). From untargeted LC-QTOF analysis to characterisation of opines in abalone adductor muscle: Theory meets practice. *J. Chromatogr. B* **1071**, 44-48.

Viant, M. R., Rosenblum, E. S. and Tjeerdema, R. S. (2003). NMR-based metabolomics: a powerful approach for characterizing the effects of environmental stressors on organism health. *Environ. Sci. Technol.* **37**, 4982-4989.

Vosloo, D. and Vosloo, A. (2010). Response of cold-acclimated, farmed South African abalone (*Haliotis midae*) to short-term and long-term changes in temperature. *J. Therm. Biol.* **35**, 317-323.

Vosloo, D., Van Rensburg, L. and Vosloo, A. (2013). Oxidative stress in abalone: the role of temperature, oxygen and L-proline supplementation. *Aquaculture* **416**, 265-271.

Wasko, A. P., Martins, C., Oliveira, C. and Foresti, F. (2003). Non-destructive genetic sampling in fish. An improved method for DNA extraction from fish fins and scales. *Hereditas* **138**, 161-165.

Weber, J.-M. (2011). Metabolic fuels: regulating fluxes to select mix. *J. Exp. Biol.* **214**, 286-294.

Wells, R. M., Mcshane, P. E., Ling, N., Wong, R. J., Lee, T. O. and Baldwin, J. (1998). Effect of wave action on muscle composition, metabolites and growth indices in the New Zealand abalone, Paua (*Haliotis iris*), with implications for harvesting and aquaculture. *Comp. Biochem. Physiol. B Biochem. Mol. Biol.* **119**, 129-136.

Whitney, E. and Rolfes, S. R. (2008). *Understanding Nutrition*. Belmont, California: Cengage Learning.

Willers, C., Van Rensburg, P. J. J. and Claassens, S. (2016). Can a metabolomics-based approach be used as alternative to analyse fatty acid methyl esters from soil microbial communities? *Soil Biol. Biochem.* **103**, 417-428.

Xia, J., Sinelnikov, I. V., Han, B. and Wishart, D. S. (2015). MetaboAnalyst 3.0—making metabolomics more meaningful. *Nucleic Acids Res.* **43**, W251-W257.

Young, T., Kesarcodi-Watson, A., Alfaro, A. C., Merien, F., Nguyen, T. V., Mae, H., Le, D. V. and Villas-Bôas, S. (2017). Differential expression of novel metabolic and immunological biomarkers in oysters challenged with a virulent strain of OsHV-1. *Dev. Comp. Immunol.* **73**, 229-245.

Zhou, J., Chen, B. and Cai, Z. (2015). Metabolomics-based approach for assessing the toxicity mechanisms of dibutyl phthalate to abalone (*Haliotis diversicolor supertexta*). *Environ. Sci. Pollut. Res.* **22**, 5092-5099.

FIRST PERSON

First person – Leonie Venter

First Person is a series of interviews with the first authors of a selection of papers published in Biology Open, helping early-career researchers promote themselves alongside their papers. Leonie Venter is first author on 'The cross-tissue metabolic response of abalone (*Haliotis midae*) to functional hypoxia', published in BiO. Leonie is a PhD student in the lab of Dr Zander Lindeque in the Human Metabolomics Department at North-West University, Potchefstroom Campus, South Africa, investigating metabolic-driven processes, primarily with the use of metabolomics and their application to answer everyday aquaculture questions.

What is your scientific background and the general focus of your lab?

My academic background is in biochemistry, with my postgraduate studies focused on the application of metabolomics methods to research questions concerning energy-driven metabolism processes, as is the general focus of the lab. My PhD project involved researching abalone metabolic processes, and expanded my scientific background to aquaculture in the process.

How would you explain the main findings of your paper to non-scientific family and friends?

Metabolism depends on the building and breaking of cellular processes to ensure that energy is created and available for everyday life. Imagine a seesaw on a playground with balanced metabolism in the middle, and building (anabolism) processes on the one side and breaking (catabolism) processes on the other end; whenever the one side of metabolism is high, the other is low. In the context of abalone farming, farmers prefer anabolic reactions to be high, resulting in larger abalone with a higher worth. As soon as a stressor like oxygen shortage (hypoxia) comes into the mix, catabolic reactions start to dominate as other mechanisms now require activation for protection from the stressor. Hypoxia is an episodic occurrence on abalone farms, during which abalone are able to produce energy by using oxygen-independent mechanisms. This is achieved by protein (amino acid), carbohydrate (glucose) and lipid (fatty acid) subunits predominantly stored in the muscle sample of abalone. Additionally, abalone blood proved to function as a shuttle between tissues, transporting metabolites to where they are required for energy production. Metabolic results from abalone gills support oxygen delivery based on demand. Together, tissue interplay enables abalone to manage their energy requirements when hypoxia causes a metabolic imbalance. This is not ideal from a farming perspective but is somewhat reassuring as abalone have well-developed metabolic capabilities to withstand exercise-induced hypoxia, after which balanced metabolism is likely to continue once oxygen availability returns.

Leonie Venter's contact details: North-West University, Potchefstroom Campus, Private Bag X6001, Potchefstroom 2520, South Africa.

E-mail: leonie.venter@nwu.ac.za

Leonie Venter

What are the potential implications of these results for your field of research?

Now that a metabolic response to functional hypoxia for abalone has been defined, it would make sense to get an idea of what metabolite concentrations would be during standard farming conditions. Following the acquisition of this knowledge, a list of biomarkers needs to be established for use as part of regular health monitoring programmes. Ultimately, the biomarkers of interest should be refined to a point-of-use test that can be used on-farm by general farm personnel. In effect, it would be possible to determine if the metabolism of farmed animals uses the resources supplied for production value, or if these animals are using their metabolic energy to counter stressors, resulting in negative animal growth.

"The compact and clever physical design of abalone came as a total surprise to me. If you think invertebrates can't be that complicated, think again."

What has surprised you the most while conducting your research?

The compact and clever physical design of abalone came as a total surprise to me. If you think invertebrates can't be that complicated, think again. Not only do abalone have well-developed capacities for survival in the absence of oxygen (abalone circulation favours oxygen storage instead of delivery during intense physical activity), but they also implement physiological, cellular and metabolic alterations to

Biology Open (2018): doi:10.1242/bio.031070: Supplementary information

An abalone in the process of regaining normal posture after being placed upside-down on its shell to induce functional hypoxia.

counter hypoxic episodes. The in-depth metabolic changes that they can initiate go beyond what vertebrates are capable of; this is perfectly demonstrated when anaerobic respiration is activated and the production of lactate, multiple opines and succinate ensures energy production. Additionally, their extensive use of amino acids to power multiple metabolic reactions makes you rethink the dietary importance of amino acids in feeds formulated for abalone.

What, in your opinion, are some of the greatest achievements in your field and how has this influenced your research?

The rapidly expanding capabilities and diversity of metabolomics analytical platforms and biostatistics are currently influencing all fields of biology, and their potential in aquaculture is also receiving more attention, placing the research performed in our paper in the spotlight. The fact that compounds can be accurately identified using high-end analytical platforms enabled us to detect opine metabolites in this study, filling some crucial gaps in the abalone metabolic plan. Additionally, the commercial growth achieved by the South African abalone industry is beneficial to research aimed at maximising abalone growth and health. The study serves to address the lack of knowledge of abalone metabolism and determine potential strategies to optimise their metabolism to favour growth.

What changes do you think could improve the professional lives of early-career scientists?

In many countries, there is growing pressure on universities to increase numbers of postgraduate students. This is often detrimental to the mentoring process. Early-career scientists need mentors to invest in their scientific and personal development beyond the project at hand. Only then, the building of your own research prestige becomes more probable, taking pride in doing things well becomes the norm and nurturing of great but realistic research ambitions becomes the goal.

What's next for you?

A postdoctoral position in a new lab as part of a new research team in a new environment is the next step for me. I believe I am now equipped to transfer the skills obtained as part of my PhD to the industry, using metabolomics in association with other omics techniques to assist with biomarker development and/or general health monitoring.

Reference

Venter, L., Loots, D. T., Mienie, L. J., Jansen van Rensburg, P. J., Mason, S., Vosloo, A. and Lindeque, J. Z. (2018). The cross-tissue metabolic response of abalone (*Haliotis midae*) to functional hypoxia. *Biol. Open* **7:** bio031070.

APPENDIX D

CONFERENCE CONTRIBUTIONS

“We’re here to put a dent in the universe.”

–Steve Jobs

Untargeted metabolite profiling of abalone using gas chromatography mass spectrometry

Leonie Venter[1], Peet Jansen van Rensburg[1], Du Toit Loots[1], Andre Vosloo[2], Jeremie Zander Lindeque[1]

(1) Human Metabolomics, North-West University, Potchefstroom Campus, Potchefstroom, South Africa.
(2) School of Life Sciences, University of KwaZulu-Natal, Durban, South Africa.

INTRODUCTION

Abalone meat is a delicacy in many parts of the world, fetching high prices and a valuable source of income for countries, farming and exporting this commodity. The quality of abalone is based on its unique sensory properties including texture, flavour and appearance. An analytical method for determining the metabolite profile of abalone, would serve as a valuable tool for monitoring quality and add to consumer satisfaction. Gas chromatography mass spectrometry (GC-MS) is a popular and suitable metabolomics technique, due to its high separation power, reproducible retention times and selective mass detection. Despite the recent advances in metabolomics and associated analytical instruments, there is still no information to date describing the use of GC with MS for monitoring the primary metabolism of abalone, especially not in the context of a global or untargeted approach.

AIM

The aim of this study was to establish a reliable untargeted GC-MS method for analysing, firstly, a standard compound mixture consisting of 10 compounds representing various compound classes, secondly, to apply the method in an untargeted manner to abalone muscle samples and, thirdly, this method was applied to two groups of abalone on different diets.

METHODOLOGY

SAMPLES
- Standard compounds
- Abalone dissections

EXTRACTION
- Homogenisation
- Centrifuging
- Evaporation

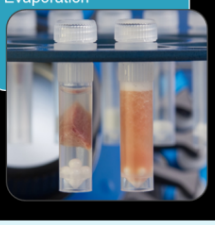

DERIVATISATION
- Oximation
- Silylation

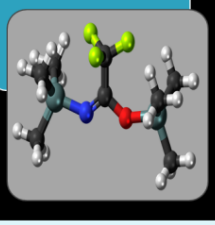

GC-TOF-MS
- Agilent 7890 GC system
- Leco Pegasus HT mass analyser

DATA ANALYSIS
- Data processing
- Statistical tests

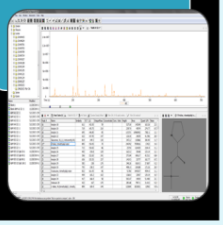

RESULTS & DISCUSSION

METHOD VALIDATION

Table 1: Analytical parameters for the verification of the GC-TOF-MS method using standard compounds

Compound	Linear range (µg/mL)	r^2	LOD (µg/mL)	LOQ (µg/mL)	Precision (%)	Accuracy (µg/mL)
Cholesterol	1 – 100	0.998	0.43	1.24	12.69	-0.13
Glucose	50 - 100	0.983	3.30	9.49	13.62	-1.18
Heneicosanoic acid	0 - 100	0.998	0.20	0.57	4.83	-0.21
Malic acid	0 - 100	0.999	0.01	0.04	21.58	0.002
Proline	0 - 100	0.997	0.01	0.02	3.66	-1.52
Ribose	0 - 70	0.998	0.04	0.13	22.78	-0.35
Serine	0 - 100	0.991	0.09	0.26	16.89	-0.90
Succinic acid	0 - 100	0.997	0.01	0.02	23.78	-0.12
Tryptophan	10 - 100	0.998	0.06	0.16	6.54	0.20
Cystine	10 – 100	0.999	2.99	8.62	12.70	0.28

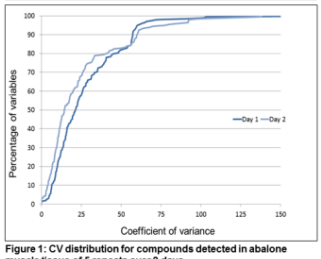

Figure 1: CV distribution for compounds detected in abalone muscle tissue of 5 repeats over 2 days

Considering the impracticality of calibration curves for all anticipated compounds in a biological sample, a two-part evaluation and verification strategy was used to illustrate that the proposed untargeted method derives meaningful biological information despite the known shortcomings.

Calibration curves with a concentration range of 1 to 100 µg/mL for the standards representing compounds from specific metabolite classes in the biological sample were constructed to evaluate the proposed extraction, derivatisation and analytical method.

From these curves it was evident that the r^2 of all compounds were generally 0.99 for their respective linear ranges, the limit of detection (LOD) ranged between 0.01 - 3.30 µg/mL, the limit of quantification (LOQ) resulted in values between 0.02 - 9.49 µg/mL, the accuracy determined was less than 1.5 ppm and the precision displayed a coefficient of variance (CV) <25% (Table 1). Based on the standard compound mixture, the method shows promise for the analysis of biological samples.

When evaluating the method in terms of biological samples harvested, the repeatability and intermediate precision showed CV values <50% for most compounds measured over 2 days (Fig. 1). Generally when a CV value is more than 50% it shows that a compound cannot be measured reliable.

BIOLOGICAL APPLICATION

This untargeted GC-MS method was further applied to *Haliotis midae* (45-73 g, 62-74 mm) which received two different formulated feeds. The goal was to determine if this method could detect metabolic difference in abalone muscle samples, between abalone fed Abfeed and AbfeedX.

By using *t*-test as an univariate statistical analysis, it was possible to determine if a statistical significance between the two experimental groups existed by determining a *P*-value. The *P*-value is considered statistical significant whenever the value is less than 0.05. Table 2 summarises the *P*-values associated with the compounds found as statistical significant between the two groups.

Furthermore pathway analysis were used to pinpoint these significant compounds metabolic status using Metaboanalyst webserver.

The preliminary results indicate that a number of different carbohydrate (sugar) metabolic pathways (Fig. 2) are affected between abalone feeding on Abfeed and AbfeedX.

Table 2: *P*-values of statistical significant compounds

Compound	*P*-value	Compound	*P*-value
Erythrose	0.0263	Glucose	0.0002
Fructose	0.0294	Glycerol	0.0178
Galactose	0.0136	C18:1n-5	0.0362
Glucopyranose	0.0035	Pinitol	0.0400

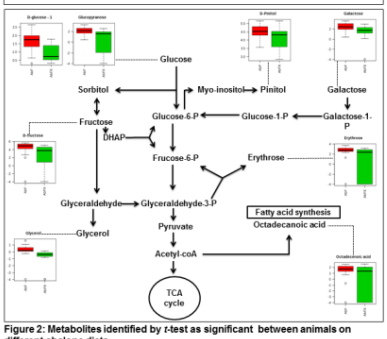

Figure 2: Metabolites identified by *t*-test as significant between animals on different abalone diets

CONCLUSION

We conclude that the proposed method can be deployed for metabolite profiling of abalone to answer important biological questions. By evaluating the linearity, accuracy and precision of selected compounds, the untargeted approach generated reliable and acceptable data based on the conditions set for homogenisation, metabolite extraction, derivatisation and GC-MS analysis. In addition we anticipate that this method would also be capable of detecting even subtle changes in the metabolic composition of abalone tissue, and differentiate healthy and diseased animals, those with good and poor quality meat and ultimately assist in explaining the mechanisms involved in the changes. Subsequently, the compounds best describing this variation can be identified as markers for these differences, better explaining these circumstances and subsequently leading to improved production and quality of abalone.

For elaboration see paper titled: "Untargeted metabolite profiling of abalone using gas chromatography mass spectrometry" in Food Analytical Methods (in press)

METABOLOME TEMPERATURE STRESS RESPONSE IN ABALONE

Leonie Venter[1], Peet Jansen van Rensburg[1], Du Toit Loots[1], Andre Vosloo[2], Jeremie Zander Lindeque[1]

(1) Human Metabolomics, North-West University, Potchefstroom, South Africa.
(2) School of Life Sciences, University of KwaZulu-Natal, Durban, South Africa.

INTRODUCTION

Studies have shown that abalone exposed to higher temperatures within their optimal growth range were able to adjust to these variations by altering their biological processes in an attempt to adapt their physiological requirements. In order to better understand the biochemical mechanisms associated with temperature stress response in abalone, metabolomics can be used. Metabolomic analyses provide a snapshot of a biological system, supplying information of the metabolites present at a given time as a result of a perturbation.

AIM

The aim of this study was to use an untargeted gas chromatography-mass spectrometry metabolomics approach to identify compounds and related metabolic pathways associated with *Haliotis midae* (63.8 ± 1.56 g) muscle tissue after exposure to varying water temperature for two weeks.

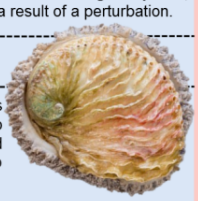

EXPERIMENTAL DESIGN & APPROACH

GROUP 1: N = 24 at 16 °C (control)

GROUP 2: N = 24 at 19 °C

GROUP 3: N = 24 at 22 °C

Sampled on day 1, 3, 7 and 14 followed by snap freezing and -80 °C storage.

Oxygen consumption and ammonia excretion rates were determined and revealed constant values for control group at 16 °C suggesting that experimental holding conditions did not affect the animals.

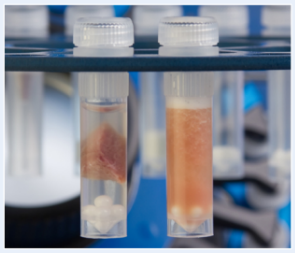

1. SAMPLE PREPARATION

Homogenisation, Centrifuging, Evaporation, Derivatisation

2. GC-TOF-MS ANALYSIS

Agilent 7890 GC system
Leco Pegasus HT mass analyser

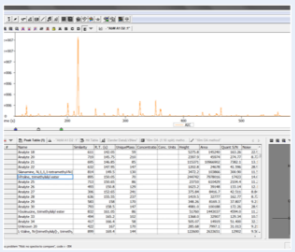

3. DATA ANALYSIS

Data processing
Statistical tests

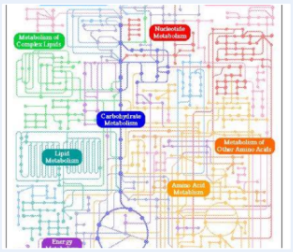

4. PATHWAY ANALYSIS

MetaboAnalst WebServer
KEGG Pathway finder

RESULTS & DISCUSSION

Two-way statistical analyses indicated that time (days) opposed to temperature resulted in more statistically relevant features. Considering that temperatures between 12 °C and 20 °C are physiologically optimal for *H. midae* the current experiment housed abalone close to its natural range. When displaying the features found per day, it is clear (Fig. 1) that on day 7 the most statistical significant features (*P*-value < 0.05) were found, indicating that the biggest metabolic changes occurred on day 7. This finding adds to the observation that a process of adaptation to thermal stress occurs in abalone, as on day 14 less statistical significant features emerged.

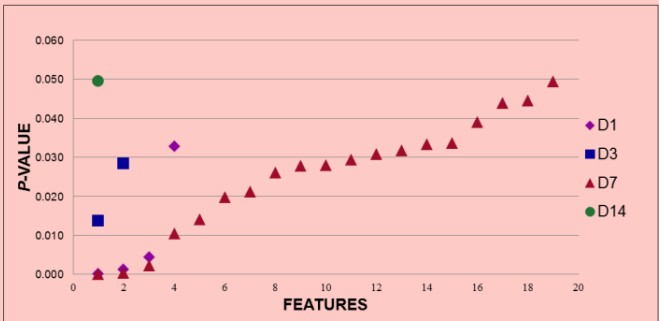

Figure 1: Statistical significant features measured over 14 days

One-way univariate analyses were used to evaluate the features found on day 7. After pathway analysis the results indicate a number of different metabolic pathways are influenced by different holding temperatures (Fig. 2). Of the 11 pathways affected, the glycine, serine and threonine metabolic way displayed the biggest Pathway impact value.

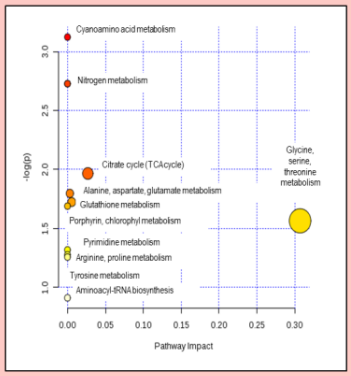

Figure 2: Summary of pathway analysis

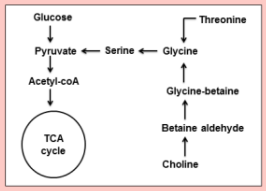

Figure 3: Basic glycine, serine and threonine metabolism

Previous temperature studies done on NMR found glycine-betaine as abundant peak in abalone foot muscle. This intermediate of the glycine, serine and threonine metabolism confirms the observation, that this pathway (Fig. 3) is involved in abalone metabolome temperature stress response.

CONCLUSION

- Significant different metabolic patterns occur over 14 days
- Preliminary results indicate that a process of adaptation to thermal stress occur in abalone
- Day 7 displayed the most significant features
- Glycine, serine and threonine metabolism tends to the main affected metabolic pathway

Future work on this topic will include cross-platform metabolic profiling on complementary analytical platforms to increase metabolite coverage, resulting in greater insight into affected metabolic pathways. Ultimately we aim to use this knowledge to better understand the metabolic mechanisms involved when abalone are subjected to temperature stressors. The possibility to develop biomarkers to monitor animal health and screen compounds associated with thermal stress also exists.

UNIVERSITY OF KWAZULU-NATAL ™ INYUVESI YAKWAZULU-NATALI

HIK·ABALONE·FARM

technology innovation AGENCY

NORTH-WEST UNIVERSITY ® YUNIBESITI YA BOKONE-BOPHIRIMA NOORDWES-UNIVERSITEIT POTCHEFSTROOM CAMPUS

World Aquaculture 2017

June 26-30, Cape Town, South Africa

International Conference & Exposition

WORLD AQUACULTURE Society

Certificate of Participation

Leonie Venter

Peet J. Jansen van Rensburg, Du Toit Loots, Andre Vosloo, Jeremie Zander Lindeque

for Oral Presentation of

APPLICATION OF FUNCTIONAL METABOLOMICS TO IDENTIFY KEY METABOLIC CHANGES IN Haliotis midae DUE TO ENVIRONMENTAL HYPOXIA

Marta Haws
Program Co-Chair

Peter Britz
Program Co-Chair

Michael Schwarz
Program Co-Chair